Université de La Réunion
Centre d'Économie et de Management de l'Océan Indien

Rapport d'activité final
2019-2023

porteur de projet :

Sabine Garabedian

ReNovRisk-Impact : Evaluation des dommages des risques cycloniques dans le bassin de l'Océan Indien

---

Table des matières

Première partie

Introduction générale

Chapitre 1

Éléments contextuels

1.1 Changement climatique

Le réchauffement climatique d'origine anthropique est estimé à +1 °C depuis la période "pré-industrielle" [1] et devrait atteindre un niveau de +1,5 °C entre 2030 et 2052 environ s'il se poursuit au rythme actuel (+0,2 °C par décennie depuis 30 ans) selon le GIEC (voir figure 1.1). Les impacts d'un réchauffement climatique de cette ampleur et les conditions de stabilisation à ce niveau ont fait l'objet du premier rapport spécial (SR15) [2] publié par le 6e cycle d'évaluation en 2018, entrepris à la suite de l'invitation à la COP21 en 2015. La première condition clé est une forte baisse des émissions mondiales de CO2, qui sont passées de 15 milliards de tonnes en 1970 à 40 milliards de tonnes aujourd'hui. Cette baisse devra se poursuivre jusqu'à atteindre le *net zéro*, c'est-à-dire la situation pour laquelle les émissions anthropiques résiduelles seront compensées par des éliminations anthropiques. La seconde condition est la stabilisation ou la réduction du forçage radiatif due aux facteurs non CO2 (autres gaz à effet de serre, aérosols, usage des terres), c'est-à-dire tendre vers un retour à l'équilibre entre le rayonnement solaire entrant dans l'atmosphère et les émissions de rayonnements infrarouges en sortant.

Ce rapport ainsi que les deux suivants [3] mettent en avant que chaque demi-degré compte. Le niveau de risque lié au climat augmente ainsi nettement pour un certain nombre de systèmes naturels et humains pour chaque demi-degré supplémentaire (Masson-Delmotte, 2020). Ce constat est illustré par une représentation synthétique de l'évolution du niveau de risque d'impacts en fonction du niveau de réchauffement climatique pour une augmentation de 1 °C, 1,5 °C ou 2 °C en tenant compte des aléas climatiques mais également des expositions, des vulnérabilités et des options d'adaptation.

Par ailleurs, ce rapport insiste sur le fait que les risques ne sont pas équitablement répartis. En effet, certains territoires sont exposés de façon disproportionnée aux conséquences néfastes du changement climatique. C'est notamment le cas pour l'Arctique, les zones semi-arides et de climat méditerranéen, les pays les moins avancés et les petits États insulaires en développement. Ce n'est pas la première fois que le GIEC souligne dans ses rapports l'hétérogénéité des territoires devant le risque climatique et le caractère particulièrement vulnérable des petites économies insulaires au changement climatique. Depuis

1. La période "pré-industrielle" est définie par le GIEC (Groupe d'experts intergouvernemental sur l'évolution du climat) comme la période de référence 1850-1900 (Masson-Delmotte et al., 2018).
2. www.ipcc.ch/report/SR15
3. Le SRCCL (août 2019) qui porte sur le changement climatique et l'utilisation des terres et le SROCC (septembre 2019) qui porte sur l'océan et la cryosphère dans un climat qui change.

FIGURE 1.1 – Variation de la température mondiale observée et réponses modélisées à des trajectoires stylisées des émissions et du forçage anthropiques

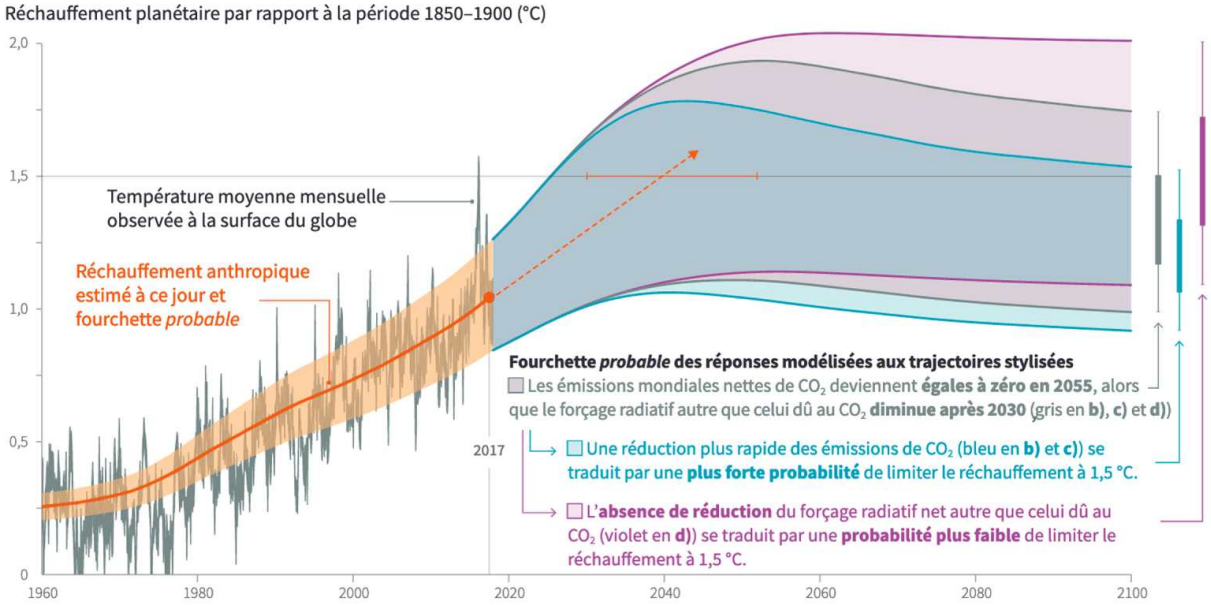

Source : (Masson-Delmotte et al., 2018)

2001, un chapitre leur est spécialement consacré, notamment du fait de leur exposition à la hausse du niveau des mers et à l'intensification des phénomènes météorologiques extrêmes (Field & Barros, 2014; Parry et al., 2007; McCarthy et al., 2001).

Les négociations internationales visant à lutter contre ce changement climatique ont réellement débuté avec l'instauration des COP (Conferences of the Parties) lors du sommet de la terre à Rio en 1992 et ont connu depuis de multiples péripéties [4]. Lors des derniers accords de Paris en 2015 dans le cadre de la COP21, les 195 pays présents se sont engagés à maintenir le réchauffement climatique en dessous de 1,5 °C. Pour cela, ils disposent de deux grandes stratégies de gestion du risque liées au changement climatique : des politiques d'atténuation visant à limiter les causes et des politiques d'adaptation visant à gérer les conséquences (Van Gameren et al., 2014).

Plus précisément, les politiques d'atténuation se concentrent sur les facteurs du changement climatique et se définissent selon le GIEC comme des "*interventions humaines visant à réduire les sources de gaz à effet de serre ou à augmenter les puits de carbone*" (Pachauri et al., 2014a, p.125). Il s'agit principalement de définir des engagements au niveau international pour atténuer les causes du changement climatique, c'est-à-dire limiter les émissions de gaz à effet de serre (GES). Ce fut l'objectif premier des différentes COP qui se sont tenues depuis 1995 avec l'adoption du protocole de Kyoto (signé en 1997 et prolongé en 2012) et des accords de Paris en 2015. Malgré ces engagements, la hausse des émissions de GES a perduré puisque celles-ci ont augmenté de 2,2 % par an entre 2000 et 2010 alors qu'elles n'avaient augmenté que de 1,3 % par an entre 1970-2000 (Pachauri et al., 2014b). Ces politiques d'atténuation portent une attention particulière aux systèmes énergétiques puisque l'usage de combustibles fossiles produit 78 % de la hausse des

4. Pour une revue de la littérature sur l'historique des négociations internationales sur le changement climatique, voir Bodansky (2001); Gupta (2010), et pour la place de l'Europe dans ces négociations, voir Afionis (2017).

émissions anthropiques totales de GES sur la période 1970-2010.

Les politiques d'adaptation sont, quant à elles, définies par le GIEC comme les "*démarches d'ajustement au climat actuel ou attendu, ainsi qu'à ses conséquences, de manière à en atténuer les effets préjudiciables et à en exploiter les effets bénéfiques*" (Pachauri et al., 2014a, p.118). Cette adaptation doit donc être anticipée et planifiée en amont de l'avènement du risque. Les politiques d'adaptation sont entrées sur la scène des négociations internationales bien plus tardivement car elles étaient perçues initialement de manière négative, véhiculant l'idée d'un renoncement ou d'une passivité face à l'enjeu de la limitation des émissions de GES (Van Gameren et al., 2014). Il y a deux raisons pour que les acteurs internationaux aient finalement intégré cette dimension d'adaptation dans les négociations : la première est d'ordre politique, l'autre d'ordre physique. Sur le plan politique, dans les années 2002-2007, les pays en développement unis au sein du G77 + Chine ont largement œuvré à faire reconnaître l'adaptation comme un thème important des négociations climatiques (Aykut & Dahan, 2011). Cette reconnaissance (ainsi que l'accès au fond financier qui l'accompagne) avait un double objectif : reconnaître l'injustice climatique de la responsabilité historique des pays du Nord et reconnaître une plus grande vulnérabilité des pays en développement au changement climatique. Sur le plan physique, l'échec des stratégies d'atténuation, avec la non-tenue des engagements de réduction des émissions de Kyoto et le blocage des négociations à Copenhague en 2009, a modifié les trajectoires climatiques potentielles de telle sorte que le réchauffement climatique perdurera, du fait de la concentration actuelle de GES, quelle que soit l'ampleur des efforts entrepris en termes d'atténuation jusqu'en 2040 environ. Durant cette période, les politiques d'adaptation deviennent alors essentielles pour réduire le risque climatique.

Bien que le but ultime de ces deux types de stratégie politique soit de minimiser les conséquences indésirables du changement climatique (Ayers & Huq, 2009), elles ont longtemps été (et le sont encore parfois) présentées comme distinctes, voire opposées, du fait de leurs caractéristiques différentes en termes d'objectif et d'échelle spatio-temporelle (Sharifi, 2020; Swart & Raes, 2007). En effet, les politiques d'atténuation ont une dimension globale, dont la réalisation aura des effets à long terme, alors que les politiques d'adaptation ont une dimension le plus souvent locale, dont la réalisation est attendue à court terme[5]. Cependant, ces deux stratégies sont moins indépendantes qu'elles n'en ont l'air. En effet, les mesures d'atténuation peuvent réduire les besoins d'adaptation à long terme et les mesures d'adaptation peuvent réduire les coûts d'atténuation en améliorant les capacités d'adaptation (Sharifi, 2020; Endo et al., 2017; Swart & Raes, 2007).

1.2 Vulnérabilité

L'introduction de la notion d'adaptation a également fait apparaître la notion de vulnérabilité au changement climatique, ainsi que celle d'exposition ou encore de résilience (Van Gameren et al., 2014). Le GIEC a considérablement contribué à l'usage du concept de vulnérabilité dans les questions du changement climatique. Présente depuis la publication du premier rapport d'évaluation, il met d'autant plus l'accent sur cette notion depuis son troisième rapport en 2001. La définition de la vulnérabilité a évolué au cours du temps et des rapports pour se stabiliser en 2014 comme "*la propension ou la prédisposition à être affecté négativement. La vulnérabilité englobe une variété de concepts et d'éléments, y compris la sensibilité ou la susceptibilité au préjudice et le manque de capacité à faire*

5. Pour d'autres points de différentiation voir Füssel & Klein (2006).

face et à s'adapter" (Pachauri et al., 2014a, p.128).

Sur le plan académique, la définition est plus confuse. En effet, l'émergence du concept de vulnérabilité dans la littérature, antérieure aux questions de changement climatique, est issue de deux traditions de recherche divergentes, chacune explorant des facettes différentes de cette notion (Lin et al., 2017) : d'une part, la littérature sur la sécurité alimentaire (Bohle et al., 1994; Kasperson & Kasperson, 2005), d'autre part, celle sur les risques associés aux catastrophes naturelles (Adger, 2006; Cutter et al., 2003; Füssel & Klein, 2006; Gallopín, 2006). C'est néanmoins l'intégration de la notion de vulnérabilité dans les questions de changement climatique qui a véritablement démultiplié la littérature sur le sujet. Les approches sur le changement climatique en termes de vulnérabilité se sont progressivement substituées aux approches traditionnelles en termes d'impact (McCarthy et al., 2001; Turner et al., 2003; Schröter et al., 2005; Polsky et al., 2007). Cependant, si cette littérature sur la vulnérabilité au changement climatique s'accorde avec les différentes dimensions définies par le GIEC que sont l'exposition, la sensibilité et la résilience, celle-ci peine à trouver un consensus autour de sa délimitation, de sa mesure et donc du périmètre d'intervention des politiques publiques. De nombreux articles cherchent à définir une grille de lecture et d'analyse qui soit commune aux différentes perceptions (Alwang et al., 2001; Adger, 2006; Füssel, 2007). Plusieurs distinctions ont été apportées que l'on retrouve sous différentes appellations (Füssel, 2010; Wolf et al., 2013) : "interne" vs "externe" (Turner et al., 2003; Bohle, 2001), "biophysique" (ou "naturelle") vs "sociale" (ou "socio-économique") (Cutter, 1996; Brooks, 2003; Adger, 2006; Füssel, 2007), "top-down" vs "bottom-up" (Dessai & Hulme, 2004), "end-point" vs "starting-point" (Kelly & Adger, 2000), ou encore "outcome" vs "context" (O'Brien et al., 2007). Pour Füssel (2007, 2010), la principale raison de cette confusion vient de l'absence de distinction entre deux dimensions largement indépendantes des facteurs de vulnérabilité : la sphère (interne ou externe) et le domaine de la connaissance (socio-économique ou biophysique). Une autre source de confusion vient également de l'héritage historique de la littérature sur le risque naturel pour laquelle la vulnérabilité est l'un des facteurs de risque. En effet, dans ce cadre, le risque est défini comme une fonction de l'aléa, de l'exposition et de la vulnérabilité (Pachauri et al., 2014b) lorsque la vulnérabilité est elle-même définie comme une fonction de l'exposition, de la sensibilité et de la résilience dans la littérature sur le changement climatique (Kasperson & Kasperson, 2005; Gallopín, 2006; Adger, 2006).

Dans la lignée de travaux cherchant à lier les différents aspects de la vulnérabilité (Lin et al., 2017; Brooks, 2003; Brooks et al., 2005), nous proposons dans ce projet, une évaluation des risques liés au changement climatique qui fusionne les différentes définitions de la vulnérabilité au changement climatique et du risque naturel. La figure 1.2 présente une articulation de ces définitions ainsi que le champ d'influence des stratégies d'atténuation et d'adaptation sur chacune de ces notions. En effet, en limitant les émissions de GES, les stratégies d'atténuation vont influencer la fréquence et l'intensité des aléas (ou chocs) alors que les stratégies d'adaptation vont, quant à elles, venir modifier la vulnérabilité face à ces aléas en modifiant l'exposition, la sensibilité ou la résilience des territoires et des populations (Martens et al., 2009).

1.3 Les petites économies insulaires

Les petites économies insulaires (PEI) sont particulièrement exposées aux risques liés au changement climatique, notamment à l'élévation du niveau des mers et à la multiplication des événements extrêmes (Nurse et al., 2014). Cela a amené 43 pays à faible

FIGURE 1.2 – Cadre conceptuel : Politiques climatiques et Vulnérabilité(s)

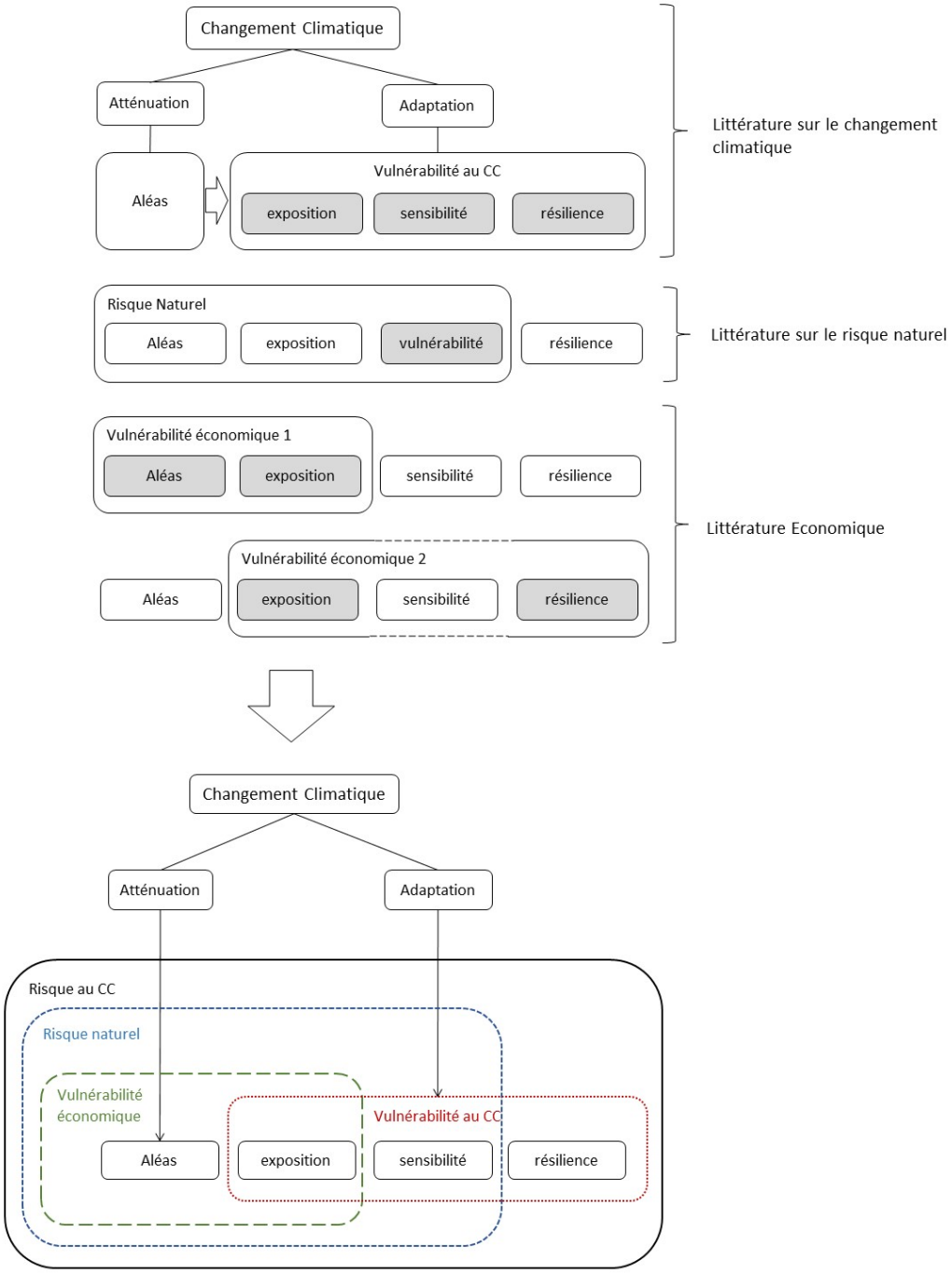

Source : auteure

élévation côtière et petites îles à fonder une coalition en 1990, l'Alliance des petits États insulaires (AOSIS [6], afin de faire pression au sein des négociations internationales pour demander des mesures plus radicales en termes d'engagement à la communauté internationale. L'AOSIS s'est également engagée lors de la COP22 à Marrakech puis à la COP23 à Bonn à atteindre *au plus vite* 100 % d'énergies renouvelables dans leur mix énergétique.

Cependant, compte tenu du faible poids des émissions de gaz à effet de serre des PEI dans les émissions mondiales (moins de 1 %), la problématique du changement climatique se pose principalement en termes d'adaptation et non d'atténuation. De ce fait, hormis quelques exceptions, la littérature concernant l'impact du changement climatique s'est assez peu intéressée aux stratégies d'atténuation dans les territoires insulaires. Ces rares travaux traitent cette question à travers des analyses sur le secteur énergétique soit pour répondre aux engagements de réduction d'émissions (Chen et al., 2020), soit parce qu'un territoire est un acteur majeur dans le secteur de l'énergie mondiale (Blechinger & Shah, 2011), soit pour garantir une certaine sécurité énergétique (Dornan & Jotzo, 2015). En revanche, les travaux sur les stratégies d'adaptation sont plus fréquents (Robinson, 2020; Klöck & Nunn, 2019; Petzold & Magnan, 2019; Robinson, 2018) et, généralement, ils lient cette question à la problématique de la vulnérabilité (Scandurra et al., 2018).

En parallèle de la littérature sur la vulnérabilité présentée précédemment, la théorie économique a également développé son propre concept de vulnérabilité qui a émergé autour des faiblesses spécifiques des petits États insulaires (Briguglio, 1995; Atkins et al., 2000; Cordina et al., 2004; Briguglio et al., 2009). Cependant, la crise asiatique a mis en évidence que cette vulnérabilité avait une portée plus large et qu'elle concernait également les pays émergents (Guillaumont, 2004). Cette littérature est plus consensuelle quant à sa définition mais elle rencontre des divergences sur son évaluation. Guillaumont (2009) la définit comme le risque pour un pays de voir son développement entravé par les chocs exogènes qu'il subit, chocs à la fois naturels (tremblements de terre, éruptions volcaniques, typhons, ouragans, inondations, etc.) et économiques (chutes de la demande extérieure, instabilité des prix mondiaux des produits de base, fluctuations internationales des termes de l'échange, etc.). Il existe deux courants principaux concernant son évaluation. Celui porté par Briguglio et al. (2009) pour qui la vulnérabilité correspond à l'exposition et doit être traité conjointement avec la résilience pour évaluer le risque. Ce courant a donné lieu à l'Indicateur Net de Vulnérabilité et de Résilience (NVRI) [7]. Un autre courant est porté par Guillaumont (2009) pour qui la vulnérabilité est composée des chocs, de l'exposition et de la résilience. Cependant, l'objectif de ces recherches étant de définir des politiques publiques susceptibles de réduire cette vulnérabilité, elles ne s'intéressent qu'à la dimension structurelle de la vulnérabilité, l'Indice de Vulnérabilité Économique (EVI) [8] ne prend donc en compte que les deux premières dimensions (Closset et al., 2017).

En tant que région d'outre-mer française, La Réunion est incluse dans les engagements nationaux tout en ayant un profil proche des membres de l'AOSIS [9]. Parmi les régions d'outre-mer, La Réunion a affiché une forte volonté politique d'être un acteur majeur dans la lutte contre le changement climatique en termes d'atténuation. Dès 2008, La Réunion

6. http ://www.aosis.org/about/

7. Initialement l'Indice de Vulnérabilité Économique (EcVI).

8. Celui-ci couvre 145 pays en développement sur la période 1975 à 2018(https ://ferdi.fr/donnees/un-indicateur-de-vulnerabilite-economique-evi-retrospectif).

9. Les autres îles de l'océan Indien (Comores, les Maldives, Maurice, les Seychelles) font partie de cette alliance.

avait fixé à travers le programme Gerri [10] l'objectif d'atteindre l'autonomie énergétique en 2025. Cet objectif ambitieux a été revu en 2013 dans le SRCAE [11] et concorde aujourd'hui avec celui de la loi transition énergétique pour une croissance verte dans les outre-mer de 2015 c'est-à-dire, produire 50 % de l'énergie consommée à partir de sources renouvelables en 2020 et atteindre l'autonomie énergétique à l'horizon 2030. Or, contrairement aux objectifs affichés, cette part a une tendance plutôt décroissante depuis 2000 et oscille entre 30 % et 35 % depuis une dizaine d'années [12] (OER, 2020). Concernant les questions d'adaptation, si le terme apparaît depuis quelques années dans les discours institutionnels, il n'existe à ma connaissance ni de directive en ce sens, ni d'étude économique sur le sujet. Cependant, la vulnérabilité économique a, elle, été mise en évidence dans quelques travaux qui calculent l'EVI, notamment Goavec & Hoarau (2015) qui obtiennent un EVI pour La Réunion de 48,14 contre 55,74 pour les SIDS et 40,20 pour les pays en développement non SIDS.

Ce constat sur les stratégies d'adaptation, ou plutôt leurs absences, nous a amenée à proposer le projet RenovRisk-Impacts visant à apporter des outils d'aide à la décision dans le cas des risques cycloniques pour des territoires tels que La Réunion. L'insertion de cette problématique spécifique dans le cadre conceptuel des stratégies face au changement climatique de la figure 1.2 et la façon dont elles peuvent les influencer est présentée sur la figure 1.3.

FIGURE 1.3 – Cadre conceptuel 2

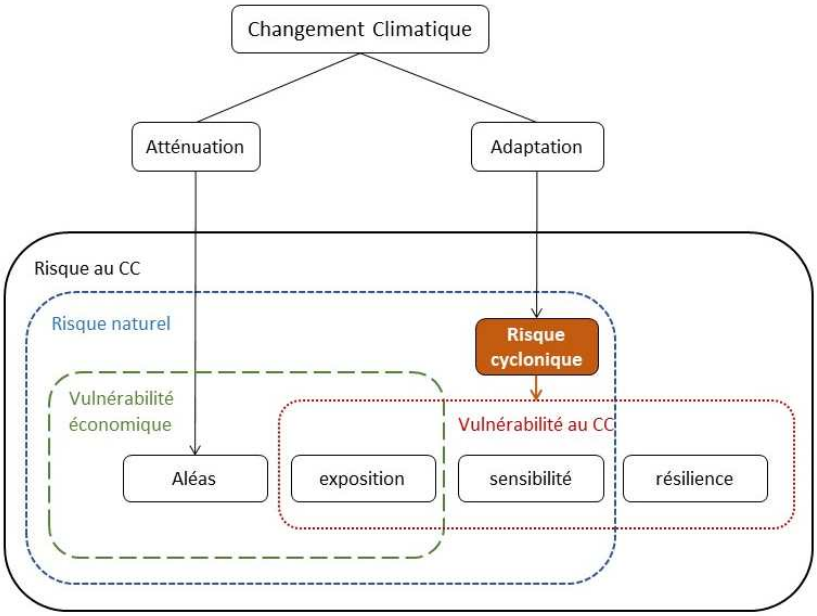

Source : auteure

10. Grenelle Environnement à La Réunion, Réussir l'Innovation.
11. Schéma Régional Climat Air Énergie.
12. En 2019, cette part était de 31,2 % contre 46,7 % en 2000.

Chapitre 2

ReNovRisk : REunion NOVative research on cyclonic Risk

Les stratégies d'adaptation ont pour objectif de limiter les effets des aléas engendrés par le changement climatique. Or, les PIE sont plus exposés aux conséquences du réchauffement climatique et plus spécifiquement à deux principaux aléas (Field & Barros, 2014) : l'élévation du niveau des eaux et les événements climatiques extrêmes.

Or, La Réunion est particulièrement concernée par le risque cyclonique puisqu'elle se situe dans le sud-ouest de l'océan Indien qui représente 10 % de l'activité globale et le changement climatique va entraîner des modifications dans la cyclogenèse de telle sorte que s'ils ne devraient pas être plus nombreux, les cyclones devraient en revanche être plus intenses. Face à cette problématique, nous avons construit en 2015 projet pluridisciplinaire sur l'analyse du risque cyclonique dans la zone sud-ouest de l'océan Indien avec des chercheurs de l'Université de La Réunion et du BRGM [1]-Réunion. Cette impulsion a donné lieu aux projets *ReNovRisk* dont le projet *ReNovRisk-Impacts* (2019-2023).

En effet, le bassin sud-ouest de l'océan Indien (SWIO) rassemble 10 à 12 % de l'activité cyclonique dans le monde avec deux régions qui sont particulièrement exposées : le canal du Mozambique et l'océan ouvert à l'est de Madagascar (Neumann, 1993). Cette forte activité a été confirmée plus récemment par Mavume (2008) et Leroux et al. (2018) qui montrent que le bassin SWIO a une moyenne de 9 à 10 tempêtes tropicales par an dont la moitié se transforme en cyclones tropicaux (CT). De plus, on a pu observer dans cette région des systèmes particulièrement intenses. Par exemple, Idai et Kenneth en 2019 ont atteint le stade de cyclone tropical intense (maximum de la vitesse moyenne du vent entre 46 et 59 m/s) (Mawren et al., 2020), et Gafilo en 2004 et Hellen en 2014, le stade de cyclone tropical très intense (maximum de la vitesse moyenne du vent supérieur à 60 m/s) (WMO, 2016; Colomb et al., 2019).

Or, l'intensité des cyclones tropicaux augmente avec le réchauffement climatique (Knutson et al., 2010; Walsh et al., 2016; Bindoff et al., 2019; Knutson et al., 2020). Mavume et al. (2009) montrent que le nombre de cyclones tropicaux intenses est passé de 36 entre 1980-1993 à 56 entre 1994-2007 soit une augmentation de 55 % lorsque la température moyenne de la surface de la mer augmentait de 0,12 °C. Et cette augmentation de température des océans va se poursuivre pendant des siècles après la stabilisation du forçage anthropique (Collins et al., 2013; Bindoff et al., 2019).

L'importance de la question de l'intensification des cyclones dans cette région est renforcée par deux points. Premièrement, le bassin SWIO comprend un nombre important

1. Bureau de recherches géologiques et minières.

d'îles d'origine volcanique dont la topographie particulière influe, d'une part, sur la trajectoire et l'intensité des cyclones tropicaux ce qui crée des trajectoires sinueuses plus difficiles à prévoir et, d'autre part, rend les atterrissages plus complexes à simuler puisque les reliefs créent des murs et des couloirs d'accélération modifiant les champs de vent en altitude (Terry et al., 2013; Barbary et al., 2019; Tulet et al., 2021) et renforcent localement la convection, la canalisation du vent et les précipitations [2]. Ces difficultés de prévisions augmentent les risques et les dommages potentiels dans ces territoires. Deuxièmement, ces îles sont sous la souveraineté de cinq États distincts [3] et comptent un grand nombre de pays en développement dotés d'infrastructures et de systèmes d'approvisionnement en eau et en nourriture fragiles, et où une proportion importante de la population vit dans l'extrême pauvreté (Alex et al., 2019; Tulet et al., 2021). Ces territoires économiquement vulnérables ont également une forte croissance démographique, ce qui va augmenter la population exposée. Cependant, ces territoires sont très hétérogènes avec un niveau de PIB par habitant à La Réunion qui atteint près de 56 fois celui de Madagascar et des niveaux d'IDH compris entre 0,480 (Madacascar) et 0,774 (La Réunion) [4].

2.1 Les projets *ReNovRisk*

En 2015, un groupe de réflexion pluridisciplinaire s'est organisé sous l'impulsion de Pierre Tulet (ex. Lacy, Université de La Réunion) et Séverine Bes-de-Berc (ex. BRGM-Réunion) dont l'objectif était de construire un programme intégré sur l'analyse du risque cyclonique dans le bassin sud-ouest de l'océan Indien (SWIO). Nous avons alors conçu le projet *ReNovRisk* (REunion NOVative research on cyclonic RISK) qui comportait quatre parties visant à couvrir l'ensemble des maillons des risques cycloniques en mobilisant des compétences physiques, météorologiques, géologiques, géographiques, hydrologiques et économiques. Ce programme sur quatre ans, avec un budget global de près de six millions d'euros, a été proposé à la région Réunion. Cependant, étant donné l'ampleur du projet, nous avons dû scinder le projet en quatre projets correspondant aux quatre parties initiales. Ainsi, les quatre volets de *ReNovRisk* ont été proposés indépendamment et sont financés par différents fonds de l'Union européenne (FEDER, FEDER-Interreg), du gouvernement français (Fonds CPER), du BRGM (Service Géologique Français), du CNRS (National Centre de recherche scientifique) et de la Région de La Réunion. *ReNovRisk* rassemble également un grand consortium de laboratoires de recherche et des instituts scientifiques de plusieurs pays de l'océan Indien occidental, notamment en France, à Madagascar, aux Seychelles, au Mozambique et à Maurice. Le premier projet a débuté en 2017 et, malgré des calendriers différents, les quatre projets conservent une interaction forte comme le présente la figure 2.1.

Ainsi, le projet *ReNovRisk-Cyclones* (composé également de deux sous-projets) a pour objectif, d'une part, d'améliorer la couverture des observations des cyclones tropicaux (CT) sur la zone SWIO et, d'autre part, de développer des modèles de prévision haute résolution des CT pour analyser les activités futures à partir de simulations de climat et de méso-échelle, à l'échelle du bassin et à l'échelle locale. Les résultats de *ReNovRisk-Cyclones*

2. La Réunion, par exemple, détient plusieurs records du monde de précipitations cumulées : 1,1 m et 1,8 m sur respectivement 12 h et 24 h, pour le CT Denise en 1966 (Holland, 1993), et 3,9 m et 4,9 m sur respectivement 72 h et 96 h, pour le CT Gamède en 2007 (Quetelard et al., 2007).

3. La République de Madagascar, la république de Maurice, la république des Seychelles, l'Union des Comores et la France avec La Réunion, Mayotte et les Iles Éparses.

4. Données de 2010.

FIGURE 2.1 – Articulation des quatre projets *ReNovRisk*

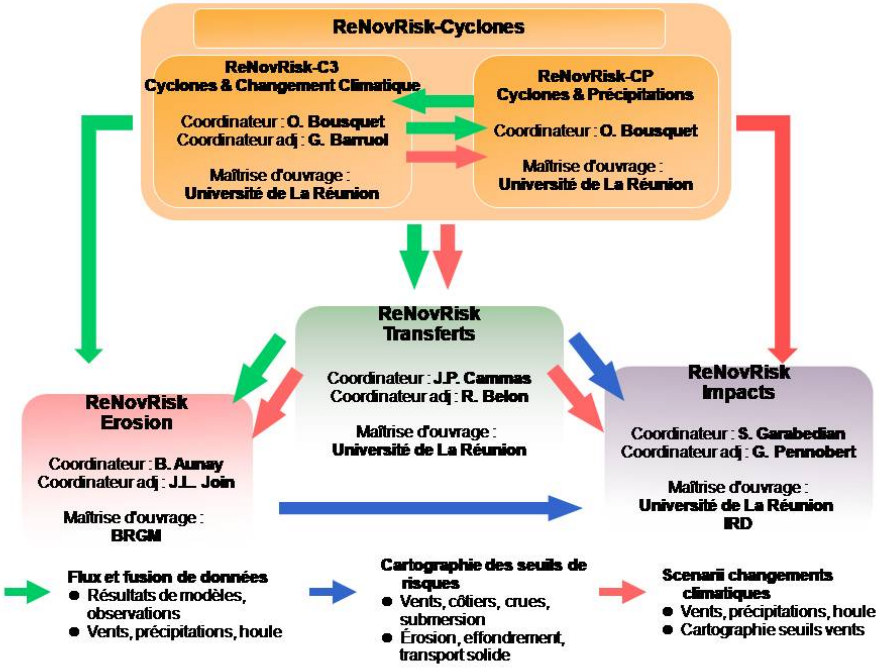

Source : Tulet, doc interne

alimentent les autres projets *ReNovRisk* avec des données de vents, de précipitations et des champs de houle, ainsi que des données sur l'intensité et l'occurrence des cyclones. Le projet *ReNovRisk-Erosion* étudie les glissements de terrain, les inondations et les transports solides dans deux bassins versants sensibles de La Réunion. *ReNovRisk-Transfert* analyse le transfert et la connexion des risques cycloniques sur le plateau volcanique occidental de La Réunion, qui descend à travers des ravines semi-urbanisées temporaires (risques d'inondation) jusqu'au littoral de l'océan ou le lagon de l'arrière-récif (risques de transport de sédiments, d'érosion et de submersion). Il fournit aussi aux autres programmes *ReNovRisk* des cartes haute résolution des champs de vent à travers le modèle BOGUS sur La Réunion. Enfin, *ReNovRisk-Impacts*, dont je suis le porteur et qui est le volet socio-économique du programme, vise à cartographier et analyser la vulnérabilité aux risques cycloniques et d'évaluer les coûts des dommages causés par les CT à La Réunion et à Madagascar. Par ailleurs, il aborde également les impacts sociaux des CT. Une présentation détaillée des projets, de leurs interactions ainsi que les premiers résultats a été publiée dans Tulet et al. (2021).

2.2 Le projet *ReNovRisk-Impacts*

Le projet "*ReNovRisk-Impacts : évaluations économiques du risque cyclonique : le cas de La Réunion et de Madagascar*" a débuté en septembre 2019 avec l'obtention d'un financement FEDER-Interreg d'un montant de 446 220 euros pour une durée initiale de 30 mois. Suite à une demande de dérogation du fait de la situation sanitaire, cette durée à été porté à 42 mois pour une fin de projet en mars 2023.

L'équipe

Pour réaliser ce projet, j'ai constitué une équipe rattachée à l'Université de La Réunion dont la composition est présenté dans le tableau suivant :

Nom	Contrat	Période
Idriss Fontaine	ingénieurs de recherche	01/09/2019 à 31/08/2021
David Nortes Martinez	ingénieurs de recherche	01/09/2019 à 31/08/2021
Pierre Mandboundou	ingénieurs de recherche	01/09/2021 à 31/08/2022
Mamoudou Ba	ingénieurs de recherche	01/02/2022 à 31/01/2023
Jessica Galais	responsable administrative	01/09/2020 à 31/08/2022

J'ai également proposé plusieurs stages de recherche dans le cadre de ce programme de recherche

- 01/05/2020 au 31/08/2020 : Fabien Girard, Master 2 Économie Appliquée de l'Université de La Réunion : "Les conséquences socio-démographiques des passages des cyclones tropicaux : le cas de Madagascar" ;
- 03/05/2021 au 09/07/2021 : Maël Jammes, Master 1 Analyse et Politique Économique, Université de Lyon 2 : "Impact des cyclones sur l'activité économique de Madagascar" ;
- 03/05/2021 au 09/07/2021 : Hugo Girousse, Master 1 Économie du Développement, Université de Grenoble : "Création d'un indice d'exposition aux cyclones sur l'île de La Réunion" ;
- 03/05/2021 au 09/07/2021 : Philomène Roche, année de césure après une licence d'Économie de Toulouse School of Economics : "Construction d'un indice de soutenabilité environnementale intégré à l'Indice de Développement Humain" ;
- 01/09/2021 au 30/11/2021 et du 02/05/2022 au 30/06/2022 : Ramilimanitra Tsiory Maminiaina Andrianavalona, Master 2 Master Macro-économie et Économie Publique, Université Catholique de Madagascar : "Vulnérabilité Éeconomique et estimation du coût direct associée au passage des cyclones tropicaux à Madagascar" ;
- 01/03/2022 au 15/07/2022 : Sandhya Apaya, Master 2 Économie Appliquée de l'Université de La Réunion : "Indice de risque cyclonique à La Réunion selon la méthode BOD" ;

Enfin une thèse que je codirige (codirecteur : Yves Croissant, CEMOI, Université de La Réunion) est rattachée au projet sur les "*conséquences économiques et risques sociaux associés aux passages des cyclones tropicaux : approches empiriques*". Elle est réalisé par Éric Kulanthaivelu depuis le 01/10/2020.

Le projet étant en collaboration avec Madagascar, j'ai également été amenée à établir un partenariat avec le Bureau national de la gestion des risques et des catastrophes de Madagascar (BNGRC) et avec l'Université Catholique de Madagascar (UCM).

J'ai par ailleurs effectué différentes démarches afin d'obtenir des données avec

— l'Agence de l'urbanisme de La Réunion(Agorah) via un appel de marché ; ;
— la Caisse Centrale de Réassurance (CCR) via une convention ;
— l'INSEE via un abonnement au CASD ouvert sous le nom de *Cyclori*.

Le programme de recherche

En termes de gestion du risque, la réduction des impacts négatifs des événements cycloniques suppose, d'une part, une meilleure prévision des cyclones eux-mêmes d'un point de vue météorologique (*RNR-cyclone*) et de leur atterrissage (*RNR-Erosion* et *RNR-Transfert*), mais également une meilleure connaissance des conséquences économiques de ces événements. En effet, les territoires du bassin ne pourront pas éviter le passage des cyclones, il convient alors de définir les mesures permettant de limiter les coûts de ces dommages. Dans ce but, le projet *RNR-Impacts* a pour objectif d'évaluer différents aspects du risque cyclonique sur le bassin SWIO dans le cas de La Réunion et de Madagascar à travers trois actions, comme le présente la figure 2.2.

Une première action (A1) a pour objectif de définir une situation de référence à travers l'analyse du risque cyclonique des zones. Cette étude se consacre pour l'instant à la zone de La Réunion avec le développement d'indice d'exposition et d'un indice de risque. Les actions suivantes visent alors à évaluer les impacts après un événement cyclonique en opérant la distinction communément admise dans la littérature sur les risques naturels entre les dommages directs et indirects (Cavallo et al., 2010; Kousky, 2014).

Les dommages directs sont généralement définis comme les dommages immédiats de destruction lors de l'aléa naturel et sont traités dans une deuxième action (A2). Il s'agit d'évaluer à travers des fonctions de dommage le coût de destruction engendré par le passage d'un cyclone. Cet exercice est mené à deux niveaux. Le premier niveau a pour objectif d'évaluer le coût de destruction pour des cyclones actuels. Le second niveau a pour objectif d'évaluer les surcoûts engendrés par les futurs cyclones en prenant en compte la variation de leur intensité due au changement climatique. En ce qui concerne les dommages indirects, la littérature est moins établie même si, globalement, il s'agit des répercussions ou des conséquences de l'aléa naturel.

Nous avons donc choisi de traiter dans une troisième action (A3) plusieurs de ces dimensions indirectes. Un premier travail traite de l'impact des événements cycloniques sur des déterminants socioéconomiques comme la fécondité à Madagascar ou l'age du mariage dans les pays en développement. Un second travail consiste à évaluer le coût macroéconomique des événements cycloniques en prenant en compte les répercussions intersectorielles à travers un MEGC ainsi que la comparaison des effets de différentes politiques d'ajustement.

Enfin, la thèse entreprise par Éric Kulanthaivelu s'est intéressée dans un premier temps à l'impact des événements cycloniques sur la croissance économique d'après une base de données mondiale, et elle cherche à présent l'existence potentielle d'impact sur les inégalités en se basant sur le territoire états-unien.

Les publications

Ce travail a donné lieu à plusieurs articles qui sont publiés, en cours de publication ou en cours de rédaction. Ces articles sont présentés à la partie 3 de ce rapport (p. 69).

Articles publiés ou en cours de publication :

FIGURE 2.2 – Présentation des actions du projet *ReNovRisk-Impacts*

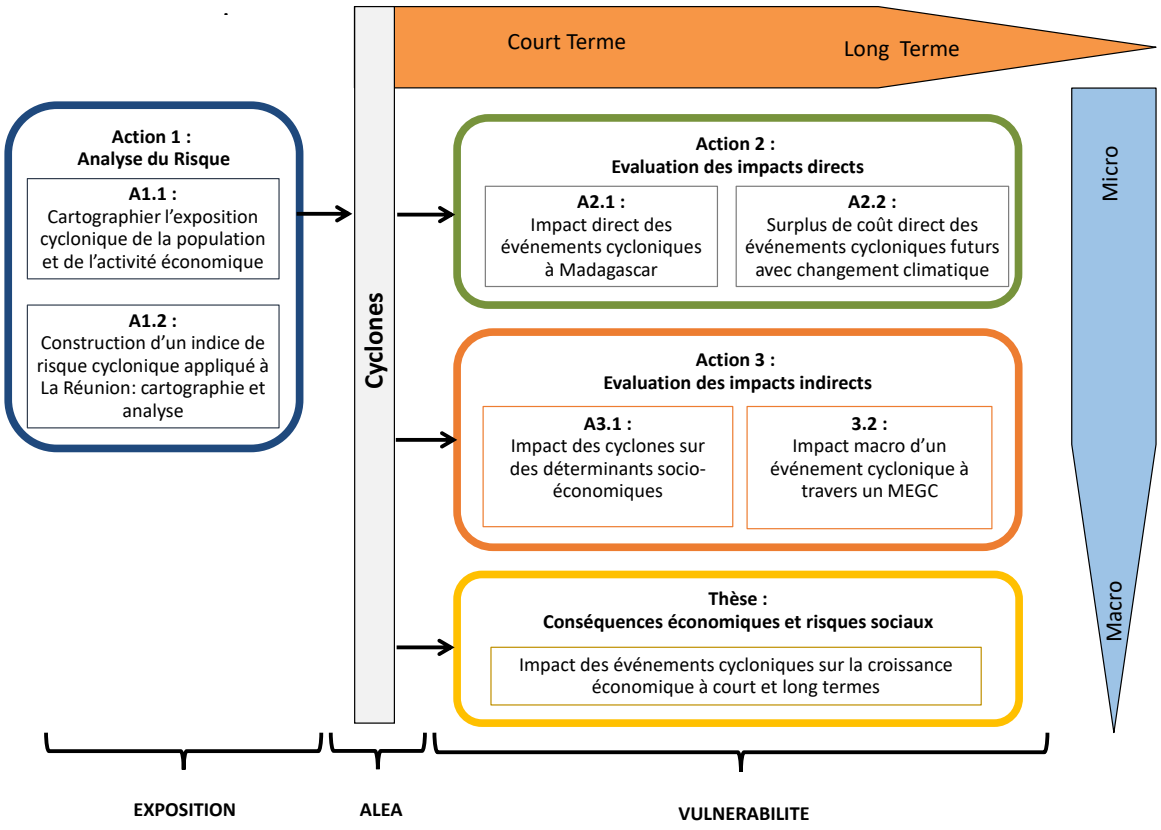

Source : auteure

- Tullet P., *et al.*, "ReNovRisk : a multidisciplinary program to study the cyclonic risks in the South West Indian Ocean", *Natural Hazards*, 2021, Springer Verlag.
- Fontaine I., Garabedian S., Jammes M., "The short term impact of tropical cyclones in Madagascar : Evidence from night light data", a paraître à *Applied economics.*
- Fontaine I., Garabedian S., Vérèmes H., "Tropical Cyclones and Fertility : New Evidence from developing countries", en révision à *Ecological economics.*
- Fontaine I., Garabedian S., Vérèmes H., "The current and future costs of tropical cyclones : a case study of La Réunion", en soumission à *La Revue Economique.*
- Mamboundou P., Garabedian S., Fontaine I., "Effets économiques d'un choc spatialisé et évaluation des politiques de compensation : le cas d'un MEGC appliqué au cyclone tropical Dina à La Réunion", en soumission à *La Revue Economique*,
- Ba M., Fontaine I., Garabedian S., "Does cyclone shocks affect child marriage ?", en soumission à *World Developement.*

Article en cours de rédaction :

- Garabedian S., Apaya S., Fontaine I., "A composite indicator for assessing tropical cyclone risk : sub-regional analysis for La Réunion".

Les formations

Durant ce projet, nous avons pu effectuer du transfert de compétence à travers plusieurs séances de travail à destinations d'étudiants ou de collègues d'autres champs disciplinaire. Nous avons particulièrement travaillé avec équipes du projet RNR-Transfert et plus particulièrement SEAS-OI (4 ingénieurs et chercheurs). De plus, les différents travaux ont été présentés lors de colloques tel que l'AFSE qui regroupe environ 300 participants, permettant la diffusion des principaux résultats. Enfin, des présentations ont été faite avec Madagascar notamment lors du colloque sur les grands enjeux du développement dans l'Agenda 2030 pour l'Afrique et Madagascar à l'Université Catholique de Madagascar en 2022 qui comptait environ 50 participants. Cependant la crise Covid étant intervenu lors de la phase concernant Madagascar, cela a considérablement limitée ces échanges par rapport à ce que nous avions prévu lors du dépôt du projet.

Deuxième partie

Synthèse des travaux de RNR-Impacts

Chapitre 3

Indice de risque au cyclone (A1)

Le GIEC comme le programme des Nation-Unis présente le risque comme une fonction de l'aléa, de l'exposition et de la vulnérabilité (Field & Barros, 2014; Pelling et al., 2004). Cependant comme nous l'avons mentionné en introduction, la littérature sur le risque naturel peine à trouver un consensus sur les définitions conceptuelles comme sur les articulations entre ces notions ce qui rend la comparabilité des analyses complexe. Dans cette action, nous avons construit un indice d'exposition et un indice de risque. Cependant, nous avons cherché au préalable, à définir un cadre d'analyse qui puisse guider pour l'ensemble du projet. nous. Cela a nécessité de mobiliser deux type de jeux de donnée : l'un relatif aux aléas, l'autre à la valeur économique.

Concernant les données relatives aux aléas, les cyclones sont généralement approximés dans la littérature par la force des vents du système malgré la nature multi-aléas qui caractérise, puisque l'ampleur des dommages dus aux autres aléas est corrélés à la force du vent du système (Jiang et al., 2008; Jordan & Clayson, 2008). Nous avons donc recours à la base de données TCE-DAT (Geiger et al., 2018) qui recense les vitesses de vents maximales pour 2 700 cyclones sur la période 1950-2015 à une résolution de 0,1 °. Cependant, lorsque l'on s'intéresse aux coûts des cyclones et de leur évolution, ces données posent un double problème sur le plan spatial et sur le plan temporel. Sur le plan spatial, les observations de hautes résolutions sont assez récentes (image Pleiade depuis 2011 et Sentinel depuis 2014) et ne couvrent pas l'ensemble des territoires. Ce problème est d'autant plus important lorsqu'on s'intéresse à un petit territoire avec une topographie escarpée (qui vient modifier les champs de vents) comme dans le cas de La Réunion. Dans ces situations, une descente d'échelle plus fine permet de mieux appréhender la réalité du territoire. C'est le travail qui a été réalisé par Hélène Vérèmes dans le cadre de *RNR-Transfert* avec le développement du modèle BOGUS (Vérèmes, 2020) qui permet une descente d'échelle à une résolution de 2,5 km^2 qui tient compte de la topographie. Sur le plan temporel, les données historiques ne peuvent pas nous renseigner sur les caractéristiques des cyclones tropicaux futurs dans un environnement climatique modifié. Nous devons dans ce cas faire appel à des cyclones synthétiques générés à l'aide de la méthodologie d'Emanuel (2008) et développés par le WindRiskTech [1] pour des conditions climatiques actuelles et futures (Bertinelli et al., 2016; Emanuel, 2011; Hallegatte, 2007).

Ensuite, les données relatives à la valeur économique du territoire qui est susceptible de subir des dommages doivent être spatialisées (Bertinelli et al., 2016). Or, à un niveau

1. http ://www.windrisktech.com/index.html

microéconomique, cette spatialisation nécessite des informations sur l'occupation des sols et la valeur des actifs. Si nous avons réalisé dans l'action 1 de ce projet une cartographie de l'occupation des sols, l'attribution d'une valeur monétaire n'est pas évidente. En effet, nous avons recours à des données de déclaration de sinistre et à des données foncières afin de procéder à une telle attribution, mais celles-ci restent encore actuellement insuffisantes compte tenu de la finesse de notre désagrégation. Á un niveau macroéconomique, nous avons retenu une méthode novatrice et en pleine expansion dans la littérature qui utilise les lumières nocturnes comme mesure de la répartition de l'activité économique. Cette méthodologie est utilisée pour les pays en développement (Chen & Nordhaus, 2011; Henderson et al., 2012; Chen & Nordhaus, 2015; Pinkovskiy & Sala-i Martin, 2016), pour mesurer l'impact des catastrophes naturelles sur la croissance (Bertinelli & Strobl, 2013; Elliott et al., 2015) ou encore pour mesurer la période de reprise après une catastrophe (Heger & Neumayer, 2019; Kocornik-Mina et al., 2020; Nguyen & Noy, 2020) [2].

Á partir de ces éléments, nous avons établi une grille d'analyse pour calculer d'une part, les indices (d'exposition et de risque) et d'autre part les fonction de dommages. Les fonction de dommage non linéaire dérivée des travaux d'Emanuel (2011) peuvent alors traiter le problème de l'évaluation des coûts des événements cycloniques de façon plus ou moins agrégée, comme cela apparaît sur la figure 3.1. Ainsi, les données de vents peuvent être traitées de façon macro à travers les données de TCE-DAT pour les cyclones observés (Macro observés 2) et des cyclones synthétiques du WindRiskTech pour une comparaison entre une climatologie contemporaine et future (Macro Synthétiques 2). Á l'échelle micro, nous utilisons les données de vents issus du BOGUS pour des événements historiques (Micro 2). Concernant la valeur économique, nous utilisons la méthode des lumières nocturnes pour distribuer le PIB pour une approche macro (Macro 1). Á l'échelle micro, nous utilisons la cartographie de l'occupation des sols et des valeurs économiques qui y sont associées (Micro 1). Plusieurs croisements sont alors possibles. enfin, ces fonction de dommage seront également intégré dans le MEGC présenté dans la partie 5.2

3.1 Cadre d'analyse

3.1.1 Les éléments du risque

La littérature concernant les indices de mesure du risques est abondante [3]. La notion de risque fait l'objet de nombreuses définitions mais celles-ci semblent obéir à une logique sous-jacente commune quant à ses constituants. Conformément à la définition de l'UNDRO (1979), le risque est traditionnellement considéré comme résultant de trois composantes : l'occurrence de l'aléa, l'exposition (éléments ou valeur à risque) et la vulnérabilité (Dao & Peduzzi, 2004; Binita et al., 2021). L'occurrence des dangers et l'exposition ont tendance à être agrégées dans un indicateur d'exposition physique (Garlatti, 2013; Welle & Birkmann, 2015; Peduzzi et al., 2012). La multiplication est utilisée pour agréger les 3 composantes (Peduzzi et al., 2009; Welle & Birkmann, 2015; Binita et al., 2021; Feindouno et al., 2017). Ce principe suit une logique simple selon laquelle une probabilité d'occurrence d'un aléa de 0 conduit à une absence de risque, tout comme le font l'absence de valeur à risque ou l'absence de vulnérabilité face à un événement.

2. Pour une revue de la littérature récente sur les lumières nocturnes, voir, Gibson et al. (2020).
3. Pour une revue de la littérature sur les indices de risque voir Ramli et al. (2020)

FIGURE 3.1 – Fonction de dommage

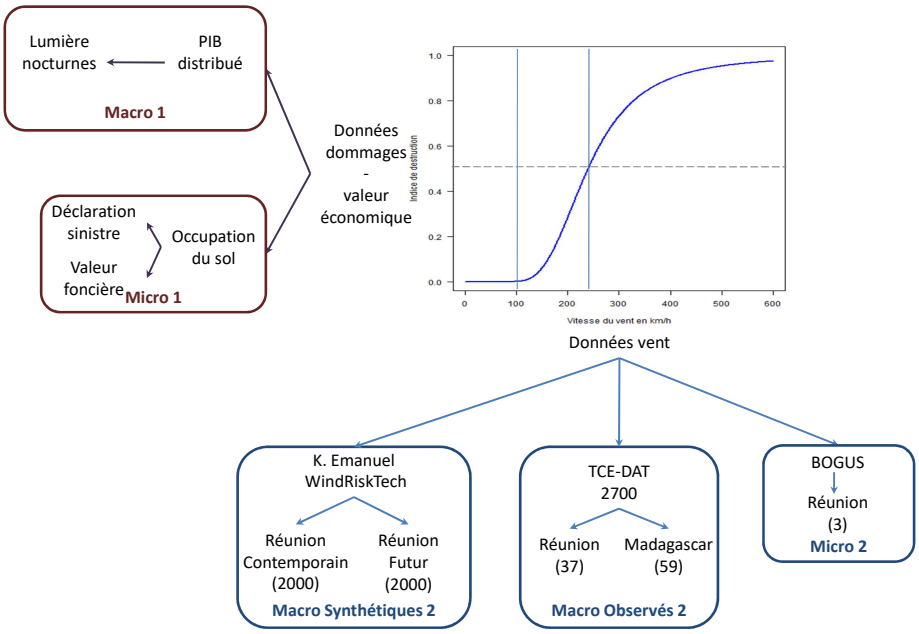

Source : auteure

la formalisation du risque peut alors prendre différente forme selon les critères considérés. Ainsi Dewan (2013); Khalid & Babb (2008); Li & Li (2013) et Poompavai & Ramalingam (2013) utilise une fonction du risque composé de l'aléa (H) et de la vulnérabilité (V) comme dans l'équation 3.1

$$R = H * V \tag{3.1}$$

D'autres travaux dans la ligné des travaux de Davidson & Lambert (2001) intègrent la dimension exposition (E) que l'on peut écrire de façon générale comme l'équation 3.2

$$R = H^{\alpha} * E^{\beta} * V^{\gamma} \tag{3.2}$$

α, β, γ peuvent selon les travaux prendre les valeurs de 1 (Kc et al., 2021), de 1/3, ou encore des valeurs spécifiées par des processus de hiérarchie analytique (AHP) qui permet de transférer l'expérience des experts en une valeur pondérée objective (Zhang et al., 2017; Chen, 2007; LI et al., 2006).

Enfin, il est également possible de trouver des spécifications qui intègrent la résilience (Rs) que ce soit en divisant la valeur de l'indice comme dans l'équation 3.3 (Hoque et al., 2017) ou en venant ajuster l'exposition comme dans l'équation 3.4 .

$$R = H * V * E/Rs \tag{3.3}$$
$$R = H * V * E(1 - Rs) \tag{3.4}$$

3.1.2 Quelques indices existant

Ainsi, de nombreux indice de risque ont été développés au cours du temps, qu'il s'agisse d'indices de risque au changement climatiques ou au catastrophes naturelles. Nous présentons ici trois des plus connus, à savoir le Disaster Risk Index (DRI), le Disaster Exposure Index (DEI) et le World Risk Index (WRI).

Le Disaster Risk Index (DRI) : Le Disaster Risk Index (DRI), basé sur un modèle économétrique, mesure le risque de mort moyen par pays sur des catastrophes de moyenne et grande échelle (tremblements de terre, cyclones, inondations, etc.). Les pays sont indexés pour chaque type de danger en fonction de leur degré d'exposition physique, de leur degré de vulnérabilité relative et de leur degré de risque. Le DRI utilise des parcelles de 5*5km et 32 indicateurs socioéconomiques et environnementaux (Peduzzi et al., 2009). Néanmoins, deux limites de l'indice apparaissent rapidement :

- Le risque de mort n'est qu'une petite partie des catastrophes naturelles et est rarement le plus significatif.
- Le DRI est confronté à une difficulté d'utilisation des données depuis qu'EM-DAT ne garde les données que pour les aléas engendrant plus de 100 000$ de pertes et plus de 10 morts (ignorant donc de nombreux petits aléas).

Disaster Exposure Index (DEI) : Le Disaster Exposure Index est un indice innovant, flexible, fiable et simple (Garlatti, 2013) ne mesurant que les événements météorologiques extrême et classifiant les régions en fonction de l'impact humain et physique des aléas à partir des bases de données DesInventar. Cet indice est décomposable par type de catastrophes et par type d'impact et mesure à un niveau national et sous-national les régions d'Amérique latine. Ici, l'exposition diffère du sens qu'on lui donne généralement dans la littérature puisqu'il correspond plutôt à l'impact immédiat d'après aléa. Le DEI est donc un indicateur des pertes directes et immédiates d'un événement. Il établit les mêmes indicateurs d'impacts (humains et physiques) pour toutes les zones étudiées en écartant seulement les pertes monétaires au vu du manque de précision de leurs estimations. Les indicateurs d'impacts humains peuvent être directs (morts, disparus, blessés, malades) ou indirects (victimesaffectés, évacués, relocalisés) tandis que les indicateurs d'impacts physiques concernent les maisons (détruites, affectées), les infrastructures (routes, transport, communications, aqueducs, égouts) ou encore le capital (économie, services). Le DEI mesure la moyenne de tous les sous-indicateurs pour chaque catastrophe, chaque région et sous-région. Le score de toutes les catastrophes a été agrégée en utilisant comme pondération la probabilité de l'aléa, ce qui nous permet d'obtenir une seule mesure de DEI pour chaque pays. Afin de mesurer au mieux l'exposition réel des plus petites régions, l'impact par aléa a été préféré comme indicateur à l'impact total. Enfin, l'indice a été normalisé pour qu'il soit compris entre 0 et 1, le 1 représentant la région la plus exposée.

World Risk Index (WRI) : Les Nations Unies ont défini un indice mondial d'exposition humaine aux risques liés aux catastrophes naturelles (Welle & Birkmann, 2015) : le World Risk Index (WRI). Selon l'IDMC [4], on estime que plus de 42 millions de personnes sont des réfugiées climatiques en 2010. Le WRI est publié chaque année depuis 2011 où il indique les pays ayant le plus besoin de renforcer ses mesures pour faire face et s'adapter aux événements naturels extrêmes. Il est calculé pays par pays, par la multiplication

4. Internal Displacement Monitoring Centre

de l'exposition et de la vulnérabilité et décrit le risque de catastrophe pour divers pays et régions. Diverses pondérations sont réalisées. Par exemple, au niveau de l'exposition, la sécheresse et la montée des eaux ont un coefficient de 0,5 tandis que les tempêtes, les tremblements de terre et les inondations ont un coefficient de 1. Cet indice nécessite un minimum de données (certaines données étant indisponibles dans de nombreux pays d'Afrique, il couvre 173 pays) et prend en compte plusieurs paramètres :

- L'exposition à un risque naturel (tremblements de terre, tempêtes, inondations, sécheresses, montée des eaux, etc. . .).
- La prédisposition, ou la probabilité, qu'une société ou un écosystème donné soit affecté en cas d'aléa naturel. Sont alors observées les conditions économiques et nutritionnelles des pays ainsi que les logements et les infrastructures préexistantes.
- La capacité à faire face en fonction du type de gouvernance, du niveau de préparation, du degré d'anticipation des systèmes d'alerte, des services médicaux et du niveau de sécurité sociale et matérielle.
- Les stratégies d'adaptations impliquant les mesures envisagées et les capacités aidant les communautés à faire face aux conséquences négatives probables de catastrophes naturelles et du changement climatique.

3.2 Construction d'indices

3.2.1 L'indice d'exposition (A1.1)

D'après le travail d'Hugo Girousse, sous la direction de Sabine Garabedian (CEMOI, Université de la Réunion) et d'Idriss Fontaine (CEMOI, Université de la Réunion), 2021.

Concernant la construction d'indice, un premier travail qui a été mené dans le cadre du stage d'Hugo Girousse sous la direction d'Idriss Fontaine et Sabine Garabedian, porte sur la construction et l'analyse d'un indice d'exposition au risque cyclonique appliqué à La Réunion. Cet indice regroupe les deux premières dimensions du risque, à savoir l'aléa à travers la probabilité d'occurrence et l'intensité de l'aléa et l'exposition à travers la population et l'activité économique.

En pratique, la composante d'aléa peut être égale à la probabilité de l'aléa d'intérêt, calculée comme le nombre d'événements par an pendant une période donnée (Dao & Peduzzi, 2004) ou le nombre d'événements de la catastrophe considérée sur le nombre d'événements globaux . catastrophes affectant la zone étudiée sur une période de temps donnée (Garlatti, 2013). En ce qui concerne les cyclones tropicaux, en plus de la fréquence, d'autres indicateurs peuvent prendre en compte le calcul global de l'aléa, tels que l'onde de tempête, la vitesse du vent et les précipitations du cyclone (Hoque et al., 2018), la pression du vent (Peduzzi et al., 2012), ou catégorie (sur l'échelle de Saffir-Simpson), durée de l'événement et pourcentage de pays touchés (Feindouno et al., 2017).

L'exposition est définie par l'UNISDR (2009) comme "*la présence de personnes, de moyens de subsistance, de services et de ressources environnementaux, d'infrastructures ou d'actifs économiques, sociaux ou culturels dans des endroits qui pourraient être affectés négativement*" (Welle & Birkmann, 2015). Cependant, les auteurs donnent au concept d'exposition des significations différentes. Il peut se référer uniquement à la population exposée à un aléa donné comme pour Peduzzi et al. (2012) ou Dao & Peduzzi (2004), ou

une combinaison de différents indicateurs sur la population et la zone affectée tels que la densité de logement de la population, les infrastructures basses comme pour Binita et al. (2021). Différents types d'exposition peuvent être calculés comme des impacts humains (direct et indirect), des impacts physiques (maisons, infrastructures) des impacts sur le capital (cultures, bétail, etc.) (Garlatti, 2013).

Nous nous concentrons sur le vent dans un premier temps pour deux raisons. La première est que les cyclones sont souvent caractérisés par la force de leurs vents. La seconde est plus opérationnelle puisqu'il s'agit de pallier l'absence d'information concernant le risque lié aux vents forts alors qu'il existe des plans de prévention des risques (PPR) concernant les inondations et les mouvements de terrain. Pour mener cette analyse, nous avons construit différents indices au niveau des IRIS [5].

- Un indice d'exposition physique I_{ph} qui nous permet de faire des analyses de caractérisation de la population
- Un indice d'exposition I_{pp} qui est la moyenne des données physique et de la population
- Un indice d'exposition I_{pe} qui est la moyenne des données physique et de l'activité économique.

Nous avons alors appliqué cet indice sur les 3 jeux de données sur les vents :

- BOGUS
- TCE-DAT
- WinRiskTech

Une synthèse est présentée dans le tableau 3.2. Cela nous permet d'avoir plusieurs cartes d'exposition que nous pouvons comparer comme le montre la figure 3.3 :

- Soit avec deux jeux de donnée de vent pour un même évènement ;
- Soit pour comparer un événement en particulier par rapport à l'ensemble des événements ;
- Soit pour étudier le contenu informationnel de chacun des indices ;
- Ou encore comparer l'évolution de l'exposition dans le futur.

L'indice d'exposition physique (I_{ph}) nous permet de mener une étude sur la caractérisons les actifs exposés afin de définir le profil des actifs exposés afin de voir si le risque cyclonique (vent fort) vient s'ajouter à une fragilité pré-existante au niveau des ménages comme au niveau de structures productives.

Des résultats sur la caractérisation de la population exposée montrent une corrélation positive avec le taux de chômage et de pauvreté et négative avec le revenu médian comme le montre le tableau 3.1. La population la plus fragile économiquement serait donc également la plus exposée aux cyclones.

3.2.2 L'indice de risque (A1.2)

D'après le travail de Sandhya Apaya sous la direction de Sabine Garabedian (CEMOI, Université de la Réunion) et d'Idriss Fontaine (CEMOI, Université de la Réunion), 2022

5. L'IRIS est un "Ilots Regroupés pour l'Information Statistique" permettant un découpage infracommunal qui fait référence à la taille visée de 2 000 habitants par maille élémentaire (INSEE).

FIGURE 3.2 – Exposition : Indice

	Événement Dina 2002, Bejisa 2014, Berguita 2018		1950-2020	CA : 1984-2014	CF : 2070-2100
données / Indices	*BOGUS*	*TCE-DAT*		*WRT-C*	*WRT-F*
I_{ph}	$I_{VentMax}$		$\frac{Pr + I_{VentMax}}{2}$		
Caractérisation population	Revenu médian / Taux de pauvreté / Taux de chômage				
I_{pp}	$\frac{I_{VentMax} + I_{Pop}}{2}$		$\frac{I_{hp} + I_{Pop}}{2}$		
I_{pe}	$\frac{I_{VentMax} + I_{LN}}{2}$		$\frac{I_{ph} + I_{LN}}{2}$		

Source : auteure

FIGURE 3.3 – Exposition : Carte

	Événement (Dina)		1950-2020	Présent	Futur
données / Indices	*BOGUS*	*TCE-DAT*		*WRT-C*	*WRT-F*
I_{ph}	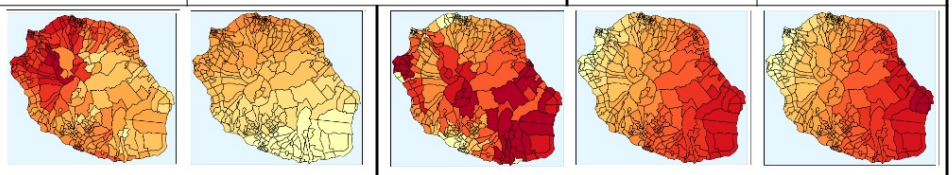				
I_{pp}	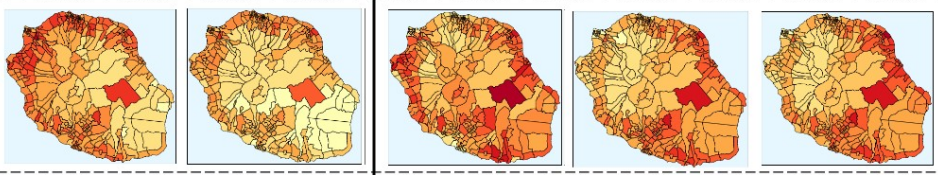				
I_{pe}	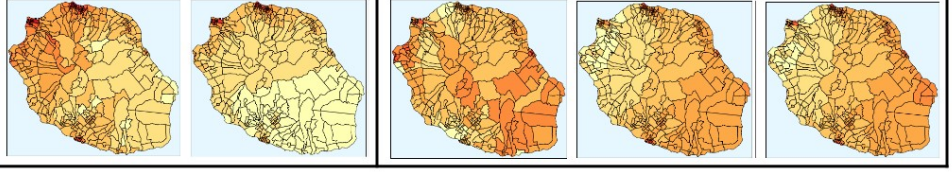				

Source : auteure

Tableau 3.1 – Caractérisation de la population exposée

table de corrélation	Test de Pearson
Taux de pauvreté	0,190***
Taux de chômage	0,176***
Revenu médian	-0,166***

L'extension de l'analyse de l'exposition à celle de risque est mené dans le cadre du stage de Sandhya Apaya sous la direction d'Idriss Fontaine et Sabine Garabedian, qui a pour but d'associé les dimensions d'aléas et d'exposition à celle de vulnérabilité.

Dans la littérature, le terme vulnérabilité est utilisé pour décrire divers concepts, issus de diverses disciplines (Kappes et al., 2012). Cette variété de définitions de la vulnérabilité pourrait provenir des objectifs variés de l'étude de la vulnérabilité (Adger, 2006). La vulnérabilité peut être décrite comme "*le concept expliquant pourquoi, avec un niveau donné d'exposition physique, les gens sont plus ou moins à risque*" (PNUD, 2004).

En pratique, la vulnérabilité peut être décrite comme une fonction de la susceptibilité, de la capacité de faire face et des capacités d'adaptation (Welle & Birkmann, 2015), la susceptibilité étant comprise comme la probabilité de subir des préjudices et des dommages en cas de survenance d'un aléa naturel et de faire face (CC) et adaptatives (AC) correspondant aux capacités de réponse sociétale aux aléas naturels (Welle & Birkmann, 2015).

Une des méthodes pour sélectionner des indicateurs pertinents de vulnérabilité dans une zone étudiée (pays, région,..) est l'utilisation de la régression linéaire (Peduzzi et al., 2009; Brooks et al., 2005; Kappes et al., 2012; Peduzzi et al., 2012). En utilisant le nombre de personnes tuées par des catastrophes liées au climat comme approximation de la mortalité par risque, des indicateurs clés tels que les populations ayant accès à l'assainissement, le taux d'alphabétisation, la mortalité maternelle, l'apport calorique, la voix et la responsabilité, les libertés civiles, les droits politiques, l'efficacité du gouvernement, le taux d'alphabétisation (femmes/hommes) et l'espérance de vie à la naissance peuvent être identifiés (Brooks et al., 2005). Dans le cas du cyclone tropical, des corrélations significatives sont établies au niveau national entre la mortalité par risque et l'exposition physique, le pourcentage de terres arables et l'indice de développement humain (Dao & Peduzzi, 2004). Des résultats de régression significatifs montrent une corrélation positive entre le nombre de tués et la distance à la capitale, et une corrélation négative avec le produit intérieur brut mesuré en parité de pouvoir d'achat par habitant (PPA/hab), ce qui suggère que les pays pauvres, avec une forte population vivant dans les zones côtières, sont les plus à risque, faisant écho aux PEID. Enfin, le PIB PPA/hab peut être remplacé par l'IDH ou des indicateurs de gouvernance (Peduzzi *et al.* 2012).

Les indicateurs peuvent également être sélectionnés en s'appuyant sur l'évaluation d'experts par le biais de groupes de discussion (Brooks et al., 2005; Kappes et al., 2012). L'agrégation des classements des indicateurs effectués par les experts pour 3 catégories (santé, gouvernance, éducation) a mis en évidence l'assainissement, l'espérance de vie, l'efficacité du gouvernement et l'alphabétisation comme des indicateurs clés.

Les variables socio-économiques peuvent être sélectionnées en fonction de ce qui est

FIGURE 3.4 – Décomposition de l'indice de risque

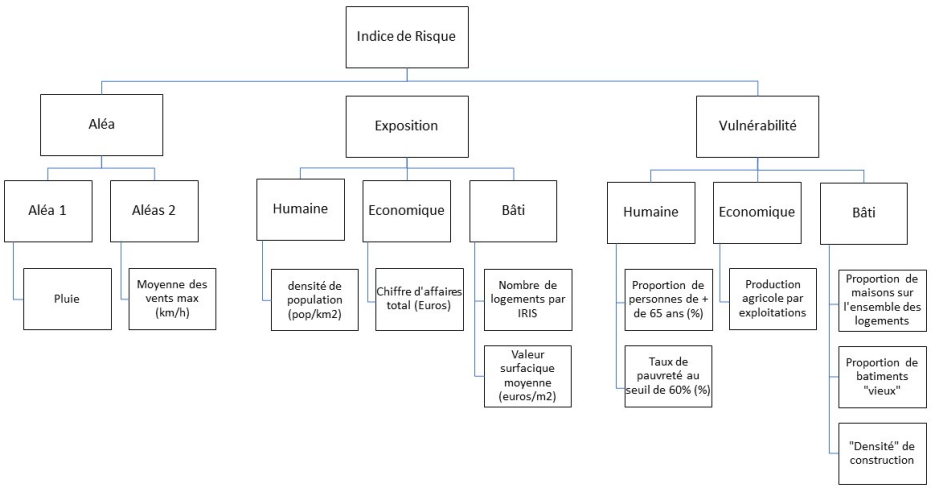

Source : auteure

jugé perspicace par les organisations internationales telles que les objectifs du millénaire pour le développement et le cadre d'action Hyogo des Nations Unies (Welle & Birkmann, 2015), conduisant à la sélection de variables appartenant à un éventail de sous-catégories comprenant : les infrastructures publiques, les conditions de logement, la nutrition, la pauvreté et les dépendances et les capacités économiques et les revenus pour évaluer la susceptibilité ainsi que les indices de corruption, la préparation aux catastrophes, les services médicaux, l'équité entre les sexes, l'état environnemental pour faire face ou encore les capacités d'adaptation. La sélection peut également s'appuyer sur l'examen de la littérature et des données (Hoque et al., 2018) ou sur les connaissances courantes (Marzocchi et al., 2012).

Nous avons donc proposé un indice de risque cyclonique qui fait une décomposition entre différentes couche comme le présente la figure 3.4.

La question de l'agrégation des indicateurs revêt également une importance majeur. Nous avons proposé ici d'appliquer la méthode Multi Layer Benefit-Of-Doubt (MLBoD) qui est une extension de la méthode BOD (Benefit-Of-Doubt). Ces méthodes permettent alors de calculer des poids associés aux indicateurs de façon endogène afin de maximiser le niveau de risque dans le but de faire apparaître le plus fort niveau de risque possible par rapport à un référentiel étant le maximum de risque atteins par un IRIS sur le territoire.

En effet, BOD est une application de l'approche DEA (Data Enveloppement Analysis), qui consiste à construire, à partir des performances meilleures, une frontière d'efficacité ou courbe des possibilités puis à déterminer les performances relatives des autres individus participant à l'étude par rapport à ce cadre de référence (benchmark) établi (OCDE, 2008). Ainsi, la méthode BOD permet d'attribuer un poids relatif à un IRIS i au regard des scores obtenus par ceux parmi le groupe qui sont les plus risqués. En associant le score de 1 au risque le plus élevé sur le territoire, les IRIS les moins risqués auront logiquement un score inférieur à l'unité mais strictement positif. Ainsi défini, le poids relatif de chaque IRIS

i dépend de son niveau de risque comparativement à la situation "maximale" observée qui représente le benchmark c'est-à-dire la pire des situation possible. Comme il s'agit dans ce cas d'un indice sur deux niveaux, nous devons utiliser un modèle Multi Layer Benefit-Of-Doubt (MLBoD) qui rend compte de la structure hiérarchique de l'indice.

Le double avantage de cette méthode, est de permettre, en plus de la classification des IRIS en fonction de leur degré de risque, de mener des analyses des indicateurs qui pèsent le plus dans la construction de l'indice, dû fait de la pondération endogène, et donc d'identifier les dimensions qui doivent en priorité faire l'objet de politiques publiques.

Chapitre 4

Évaluation des coûts des cyclones (A2)

Les cyclones tropicaux sont souvent considérés comme l'un des phénomènes naturels les plus destructeurs auxquels une économie peut être confrontée (Camargo & Hsiang, 2016). Actuellement, les dégâts mondiaux des cyclones tropicaux sont estimés à 26 milliards de dollars américains par an, soit 0,04 % du produit mondial brut (Mendelsohn et al., 2012; EM-DAT, 2020).

L'estimation de ces impacts en termes de coût est à la croisée de deux champs disciplinaires. Ainsi, un pan de la littérature plutôt économique s'intéresse à l'impact des catastrophes naturelles sur la croissance économique à court terme (Felbermayr & Gröschl, 2014; Noy, 2009; Raddatz, 2005) et plus récemment à long terme (Krichene et al., 2021; Berlemann & Wenzel, 2018; Hsiang & Jina, 2014). Un autre pan de cette littérature, plutôt issue des questions de gestion des risques naturels, cherche à quantifier un coût à travers la construction d'une fonction de dommage (Hsiang et al., 2017; Mendelsohn et al., 2012; Nordhaus, 2010).

Sur le plan méthodologique, la forme de la fonction de dommage a longtemps été discutée (Pielke & Roger, 2007) avant qu'un relatif consensus ne s'établisse autour d'une forme non linéaire. De façon générale, cette fonction peut être empirique c'est-à-dire construite sur des observations ex post ou synthétique, à savoir construites ex ante sur des considérations d'experts. Elle peut également être absolue, autrement dit renvoyer la valeur absolue de la destruction ou relative, soit renvoyer un pourcentage que l'on applique sur une valeur maximale. La construction d'une fonction de dommage nécessite un double jeu de données : d'une part, des données relatives aux aléas cycloniques (vent, pluie, houle) et, d'autre part, des données relatives à la valeur économique du territoire (globale ou spécifique à chaque entité présente sur le territoire). Or, ces deux jeux de données présentent des complexités qui leur sont propres.

4.1 L'impact direct des cyclones à Madagascar (A2.1)

4.1.1 Analyse à travers les lumières nocturnes

D'après le travail de Maël Jammes, sous la direction de Sabine Garabedian (CEMOI, Université de la Réunion) et d'Idriss Fontaine (CEMOI, Université de la Réunion), 2021.

Dans le cadre de cette deuxième action, un premier travail a été mené sur Madagascar

afin d'évaluer l'impact des cyclone sur l'activité économique mesuré à travers la méthode des lumières nocturne. Ce travail mené dans le cadre du stage de Maël Jammes sous la direction d'Idriss Fontaine et Sabine Garabedian, a donnée lieu à un article "*Short-term impact of tropical cyclones in Madagascar : Evidence from nightlight data*" actuellement en révison à *Applied Economics* et qui a été présenté lors du colloque annuel de l'AFSE (French Economic Association) en 2022 (Dijon, France). Cet article est présenté dans la chapitre 8 des publications.

En effet, les conséquences macroéconomiques des cyclones tropicaux, et des catastrophes naturelles plus généralement, ont fait l'objet de débats intenses. Certains travaux suggèrent que les catastrophes naturelles ont un effet macroéconomique globalement positif tandis que d'autres trouvent l'inverse. Ce manque de consensus s'explique en partie par une controverse sur la manière dont l'exposition à ces catastrophes est mesurée. En ce qui concerne les cyclones tropicaux, toutes les études empiriques mesurant l'exposition par l'intensité « physique » du phénomène associé trouve qu'ils engendrent une diminution du Produit Intérieur Brut à court voire à long terme. Cependant, si la littérature contemporaine dispose de plusieurs contributions mesurant les effets macroéconomiques des cyclones, elle dispose en revanche de moins de travaux étudiant l'effet de l'exposition aux cyclones à un niveau plus fin. Or, l'exposition à des vents cycloniques est principalement local, et en raison d'un effet « taille », il est rare qu'un pays soit exposé dans sa globalité à un cyclone tropical. Le but de cette étude est de combler ce manque dans le cas d'un pays régulièrement exposé : Madagascar.

Comme évoqué précédemment, les études empiriques sur les effets des cyclones tropicaux exploitent principalement des données agrégées à l'échelle des pays. Cette agrégation au niveau pays pose parfois problème car il s'agit aussi de ramener l'exposition cyclonique à l'échelle du pays. De plus, les données agrégées ne sont disponibles qu'annuellement, ce qui peut poser problème car la fréquence annuelle peut masquer les effets et la trajectoire infra-annuelle des conséquences liées à l'évènement. Partant de ce constant, le choix que nous faisons est différent. En effet, nous exploitons des données de lumières nocturnes, connues comme étant une bonne approximation de l'activité économique au niveau local, disponibles mensuellement à un niveau de résolution géographique extrêmement élevé. En effet, chacune des images de luminosité que nous exploitons correspond à une grille dont le maillage est de 0,004° ce qui représente des carreaux de 250 m2. Partant de cette première donnée d'entrée, nous ramenons le niveau de notre analyse à l'échelle du « Fokontany » correspondant à l'échelon administrative le plus fin à Madagascar. Nous disposons ainsi de données de lumières nocturnes mensuelles couvrant la période allant de janvier 2012 à avril 2020. Nous combinons ensuite ces données à un jeu de données renseignant de l'exposition cyclonique mesuré en termes de vents maximums estimés. Ce dernier jeu de données est également disponible pour un haut niveau de résolution géographique. Une fois les traitements/fusions de données effectués, nous nous retrouvons avec un jeu de données en panel renseignant si un « Fokontany » donné a été exposé à des vents cycloniques durant un mois donné.

Nous employons ensuite les outils techniques de l'économétrie des données de panel. Cette stratégie, par l'ajout d'effets fixes, possède l'avantage de pouvoir contrôler de l'hétérogénéité inobservée invariante dans le temps des « Fokontany ». Le modèle que nous estimons cherche à expliquer le niveau des lumières nocturnes en fonction de l'exposition

cyclonique des mois précédents (jusqu'à 24 mois). Les résultats principaux de notre étude sont les suivants. Tout d'abord, l'effet d'un choc cyclonique est ambigu durant les 12 mois qui suivent l'exposition. Cependant, passé ce délai, l'effet mesuré est clairement positif. Plus précisément Méthodologie : une augmentation d'un km/h de la vitesse du vent entraîne très léger impact négatif le 4e mois, puis un impact cumulé positif les mois suivants comme le montre la figure 1.

Dit autrement, l'intensité lumineuse au niveau local est supérieure à ce qu'elle aurait été en l'absence de l'évènement cyclonique. Ensuite, en incluant de l'hétérogénéité à notre modèle empirique de base, nous montrons que l'effet de court-terme est négatif dans certains cas. En particulier, l'effet du cyclone est significativement négatif pour les zones régulièrement exposées et celles où l'activité économique pré-évènement est plus élevée. En revanche, peu importe le cas particulier considéré, passée la première année, l'activité économique devient supérieure à son niveau d'avant choc, et, l'exposition cyclonique génère globalement un surcroit de lumières nocturnes. Dans l'ensemble, notre papier est dans la lignée des contributions suggérant que les chocs cycloniques peuvent engendre un surcroit d'activité économique.

4.1.2 Évaluation économique des coûts directs associés au passage du cyclone tropical Enawo en 2017 à Madagascar

D'après le travail de Tsiory Maminiaina Andrianavalona Ramilimanitra sous la direction de Sabine Garabedian (CEMOI, Université de la Réunion) et d'Idriss Fontaine (CEMOI, Université de la Réunion), 2021-2022.

Un deuxième travail a été mené sur Madagascar afin d'évaluer l'impact des cyclone sur l'activité économique mesuré à travers la méthode des lumières nocturne pour le cyclone Enawo. Ce travail a été mené dans la cadre du stage de recherche réalisé par Tsiorymaminiaina Ramilimanitra de l'Université Catholique de Madagascar, sous la direction de Sabine Garabedian et d'Idriss Fontaine. Il a donné lieux à un article : "*Évaluation économique des coûts directs associés au passage du cyclone tropical Enawo en 2017 : cas de Madagascar*" qui a été présenté au colloque sur "Les Grands enjeux du Développement dans l'agenda 2030 pour l'Afrique et Madagascar" en 2022 (Antananarivo, Madagascar). Cet article est présenté dans la chapitre 9 des publications.

Cette étude repose sur l'utilisation des données sur les lumières nocturnes afin répartir de manière plus objective les activités économiques (valeurs économiques) à un niveau spatial plus désagrégé (régional). Cette méthode novatrice en pleine expansion dans la littérature permet de de mesurer les activités économiques dans les pays en développement où les données historiques (conventionnelles) sont réputées être parfois incomplètes (Chen & Nordhaus, 2011; Henderson et al., 2012; Chen & Nordhaus, 2015). Cette méthode a été utilisé pour améliorer des indicateurs économiques déjà existants (Henderson et al., 2012) ou encore pour étudier l'impact des catastrophes naturelles sur la croissance économique (Mohan & Strobl, 2017) mais également dans le cadre d'une étude qui utilise une fonction de dommage (Bertinelli & Strobl, 2013; Elliott et al., 2015). La méthode proposée dans mon étude utilise à la fois les lumières nocturnes et la fonction de dommage.

Nous avons procédé en deux étapes. Dans un premier temps, il s'agit de répartir et de

distribuer le PIB au sein du territoire de Madagascar en utilisant la méthode des Lumières Nocturnes qui est une méthode novatrice et en pleine expansion dans la littérature. Pour ce faire, nous avons mobilisé les images nocturnes à haute résolution issues des observations Visible Infrared Imaging Radiometer (VIIRS) à bord du Suomi-National Polar-Orbiting Partnership. Dans un deuxième temps, les informations sur les cyclones sont obtenues à partir de la base de données TCE-DAT (Tropical-Cyclone Exposure-Data) de Geiger et al. (2018) qui contient des données mondiales à haute résolution sur les vitesses de vents maximales pour 2 700 systèmes cycloniques dont 59 ont touchés Madagascar. A partir de la superposition de ces deux bases de données, nous appliquons une Fonction de Dommage (Emanuel, 2011).

L'analyse des champs de vents montrent que les régions de la partie Nord-Est de Madagascar étant les plus touchées par les vents cycloniques de Enawo ; cela implique que les pixels les plus touchés seront dans cette zone et que vraisemblablement le montant des dommages sera le plus important. En appliquant une fonction de dommage (Emanuel, 2011), nous avons pu simuler quelques situations hypothétiques sur les dommages avec des seuils de vents adéquats au contexte de Madagascar. Les résultats de l'analyse montrent que plus on diminue la valeur des seuils de vents, plus les pertes seront considérables, soient des pertes pouvant aller de 22% à 32% de la valeur économique totale.

4.2 Une évaluation des surcoûts des cyclones futurs (A2.2)

D'après le travail d'Idriss Fontaine (CEMOI, Université de la Réunion), Sabine Garabedian (CEMOI, Université de la Réunion) et Hélène Vérèmes (LACy, OSU-Réunion, Université de La Réunion), 2020-2021.

Enfin, concernant les conséquence dû au changement climatique, nous avons effectué une étude agrégée afin de mener une évaluation du surplus de coût engendré par les cyclones futurs dans le cas de La Réunion. Ce travail à donné lieu à un article "The current and future costs of tropical cyclones : a case study of La Réunion", actuellement en soumission à *La Revue Economique* qui est présenté dans la chapitre 10 des publications.

En effet, les pertes économiques dues aux événements cycloniques augmentent régulièrement depuis plusieurs décennies (Grinsted et al., 2019) et cette augmentation devrait perdurer dans les années à venir. Or, comme cela a été dit en préambule, les cyclones devraient, d'une part, s'intensifier du fait du changement climatique (Knutson et al., 2010; Bindoff et al., 2019; Knutson et al., 2020) et, d'autre part, la croissance démographique et économique risque d'entraîner une augmentation des personnes et des actifs exposés. Et la zone SWOI, dont La Réunion, est particulièrement exposée à ce type d'événements extrêmes. Pourtant, il n'existe pas d'études approfondies sur les coûts engendrés par les cyclones actuels ou futurs, alors que ce type d'informations permettrait d'éclairer les politiques publiques sur les mesures d'adaptation à mettre en place.

Pour réaliser cette étude, nous avons utilisé les données de vents pour 4 000 cyclones synthétiques du WinRiskTech avec la méthode des lumières nocturnes. Concernant les données relatives aux cyclones, nous avons utilisé 2 000 cyclones à climatologie actuelle

(CA) c'est-à-dire sur la période 1984-2014 et 2 000 cyclones à climatologie future (CF) c'est-à-dire à l'horizon 2070-2100. La climatologie actuelle et future s'appuie sur le modèle CNRM-6 issu du Centre National de Recherches Météorologiques (Météo-France/CNRS) qui correspond au scénario médian du GIEC. Concernant les données des lumières nocturnes, nous avons utilisé des images satellites nocturnes des capteurs Day/Night Band (DNB) des observations Visible Infrared Imaging Radiometer (VIIRS), à bord du Suomi-National Polar-Orbiting Partnership (S-NPP) [1]. La Réunion est couverte par 10 000 pixels dont l'intensité lumineuse permet de capturer la distribution spatiale de l'activité économique à travers la pondération du PIB. En effet, de nombreuses études soulignent une relation forte entre le logarithme du PIB et le logarithme des lumières nocturnes (Chen & Nordhaus, 2011; Henderson et al., 2012; Bertinelli & Strobl, 2013; Li et al., 2013). En appliquant la fonction de dommage sur la valeur attribuée aux différents pixels, nous pouvons alors calculer un coût global ou annualisé.

Concernant les coûts globaux, parmi les 2 000 cyclones à CA circulant dans un rayon de 150 km autour de La Réunion, 48,88 % n'engendrent aucun dommage. Ce pourcentage passe à 42,88 % lorsque l'on considère les cyclones à CF, soit une diminution de 6 points. Autrement dit, la probabilité qu'un cyclone engendre des dommages est effectivement plus élevée dans le futur. De plus, les cyclones les plus extrêmes (100^{e} percentile) engendrent une perte de 40,26 % de la valeur économique à CA contre 67,75 % à CF. Enfin, les pertes sont plus importantes pour chaque percentile de la distribution de l'intensité des cyclones à CF par rapport à la CA, ce qui nous donne une moyenne des pertes économiques par cyclone de 0,76 % en CA contre 1,43 % en CF, soit presque le double. Avec un PIB constant à celui de 2018 de 19,2 milliard d'euros, cela représenterait une valeur moyenne des pertes qui passerait de 146 millions d'euros à CA à 278 millions d'euros à CF. Or, la valeur du PIB étant amenée à croître d'ici 2070-2100, nous pouvons considérer ce montant comme une valeur plancher. Nous pouvons également représenter la répartition spatiale de ces pertes économiques comme sur la figure 4.1 où la carte de gauche représente les pertes de production [2] à CA et celle de droite à CF. Il en ressort que les pixels les plus éclairés sont susceptibles de souffrir des dommages économiques les plus importants (les pertes économiques moyennes par pixel supérieures à 100 000 euros sont plus fréquentes autour de Saint-Denis et dans la zone industrielle du Port). De plus, ici aussi, nous pouvons observer que les pertes économiques par pixel sont plus élevées pour les cyclones à CF qu'à CA.

Cette analyse globale permet de mettre en évidence les surcoûts engendrés par les cyclones futurs, ainsi que l'hétérogénéité spatiale de ces surcoûts. En revanche, elle ne tient pas compte du nombre de cyclones par an. L'annualisation de nos résultats [3] montre que la probabilité de subir un cyclone engendrant des dommages passe de 0,215 à CA à 0,237 à CF, soit une période de retour qui passe de 5 ans à 4 ans. Autrement dit, La

1. Au lieu des données de veilleuses du programme de satellites météorologiques de défense (DMSP) qui sont traditionnellement utilisées. Ce choix s'explique par une meilleure qualité et disponibilité des données VIIRS.

2. Nous parlons ici de perte de production car il s'agit de multiplier le poids de chaque pixel par le PIB total.

3. Á travers une année hypothétique échantillonnée selon une loi de Poisson corrigée du paramètre 0,475 correspondant au nombre moyen de cyclones circulant dans un rayon de 150 km autour de La Réunion sur la période 1979-2017, pour laquelle nous calculons les pertes économiques totales. Puis nous répétons 100 000 fois l'expérience pour les deux scénarios climatiques.

FIGURE 4.1 – Coût moyen contemporain et futur par pixel

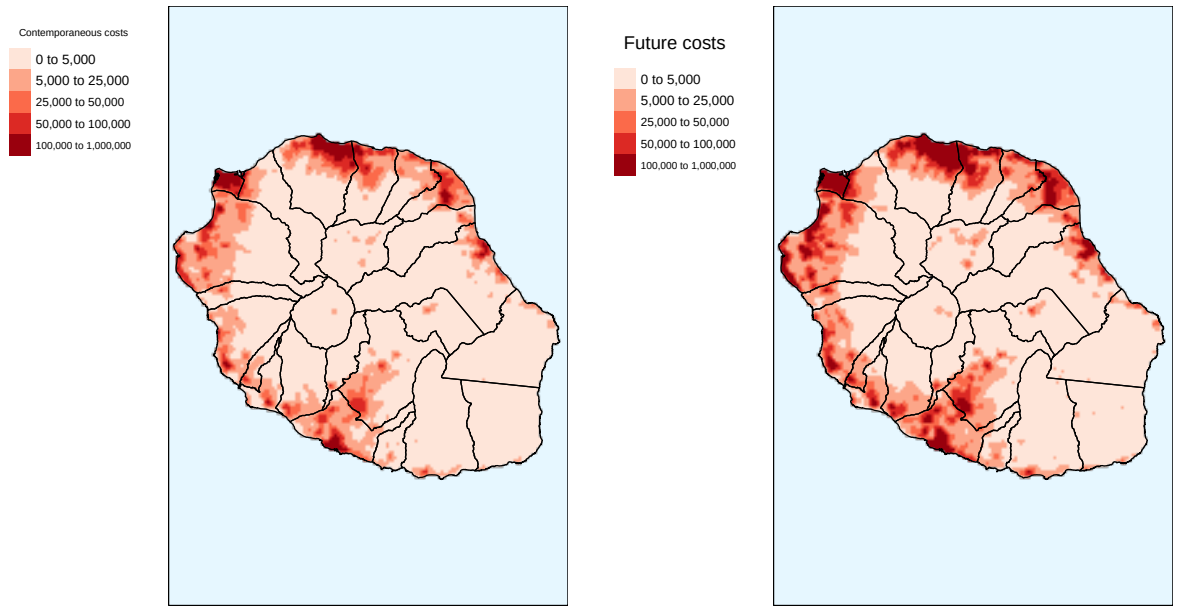

Sources : Black marble night light data (Román et al., 2018), synthetic tropical cyclones (Emanuel, 2011) et calcul des auteurs

Réunion peut s'attendre à subir un cyclone créant des dommages tous les 4 ans dans le futur contre tous les 5 ans actuellement. De plus, comme précédemment, on observe des pertes annuelles moyennes supérieures à CF avec 0,69 % contre 0,36 % à CA.

Chapitre 5

Évaluation des impacts indirects (A3)

Au-delà des coûts économiques directs, les cyclones ont également des impacts indirects. Parmi les impacts indirects, nous faisons la distinction entre les impacts sur des déterminant socio-économiques et les impacts provenant des effets de rétroaction dans l'économie et notamment des politiques d'ajustement visant à amoindrir ces effets négatifs des événements cycloniques. Concernant les déterminants socio-économiques, il existe encore peu d'études sur les conséquences de ces événements au niveau individuel (Anttila-Hughes & Hsiang, 2013) du fait probablement, d'une forte exigence en données.

Nous nous sommes donc intéressé dans un premier temps, à la façon dont les ménages modifient leurs décisions après avoir été touchés par un cyclone, notamment celle de se marier ou encore d'avoir des enfants. Or, étant probable que ces modifications soient plus importantes dans le cas de pays où les moyens institutionnels pour faire face à ces événements sont limités, notre cas d'étude porte sur les pays en développement en général et sur Madagascar en particulier. En effet, si le changement climatique et ses conséquences, figure désormais en tête des priorités des pays à tous les niveaux de développement, il est généralement admis que les populations des pays en développement sont les plus vulnérables à ces menaces climatiques. Les conditions climatiques sont d'autant plus importantes dans ces pays que leurs économies sont fortement dépendantes de l'agriculture, qui est la principale source de revenus, de nourriture et d'emplois. Les conséquences des chocs climatique peuvent donc avoir une influence particulière sur les modification des comportements post-catastrophe.

Dans un second temps, nous avons cherché à évaluer les répercussions économiques des dommage direct à travers un MEGC. Pour cela, nous avons proposé une méthode visant à spécialiser l'activité économique retranscrit dans la MCS. A partir de ce modèle, nous avons donc cherché à évaluer le montant des effets de rétroaction dans le cas d'un cyclone de forte intensité (le cyclone Dina faisant office de référence) et dans le cas de cyclones de plus faibles intensités mais récurrents. Á partir de l'analyse de ces répercussions naturelles, nous avons étudier l'impact de différentes politiques d'investissement public visant à limiter les impacts indirects de la catastrophe.

5.1 Les impacts sur les déterminants socio-économiques (A3.1)

5.1.1 L'impact des cyclones sur les mariage précoces

D'après le travail de Mamoudou Ba (CEMOI, Université de La Réunion), Idriss Fontaine (CEMOI, Université de La Réunion) et Sabine Garabedian (CEMOI, Université de La Réunion), 2022.

Concernant les impacts sur les déterminants socio-économiques, nous nous sommes intéressé dans un premier travail aux impacts des événements cycloniques sur la décision mariage. Ce travail à donné lieu à un article "Does cyclone shocks affect child marriage ?" qui est en soumission à *World Developement* et qui est présenté dans la chapitre 12 des publications.

Dans le cas du choix du mariage, les conditions climatiques extrêmes peuvent conduire les familles à accepter des propositions de mariage moins souhaitables pour leurs filles en raison de la pauvreté ou de la recherche d'un statut social plus élevé. Le mariage des jeunes filles peut constituer une sécurité économique pour elles-mêmes et leurs parents, car il représente une part importante des finances des ménages engagés dans cette pratique. Le marché du mariage est basé sur des pratiques coutumières traditionnelles qui diffèrent d'une région à l'autre. Selon le marché, la dot peut être utilisée comme un legs dans certains ménages et comme un prix dans d'autres. Dans le premier cas, elle est considérée comme un mécanisme par lequel les mariées attirent de bons maris. Dans le second cas, elle est considérée comme un héritage par lequel les parents transfèrent leur richesse à leurs filles lors du mariage. Bien que les conséquences du mariage précoce soient largement documentées dans la littérature économique, comme la mortalité infantile, la violence domestique, la santé de la mère ou du nouveau-né, il existe peu de preuves empiriques sur les déterminants du mariage. Les chocs économiques à court terme peuvent influencer les décisions de mariage selon la direction des paiements.

L'objectif de cette étude est de faire la lumière sur les déterminants du mariage des enfants et comment les chocs cycloniques affectent le comportement de mariage. Pour ce faire, nous utilisons un échantillon de données géocodées sur les vitesses des vents cycloniques, les précipitations et les informations sur les températures couplées à des données de cohorte sur les femmes âgées de plus de 24 ans provenant des enquêtes démographiques et sanitaires (EDS) sur la période 1981-2015 pour sept pays fréquemment touchés par des chocs cycloniques. Pour examiner l'impact des chocs cycloniques sur le risque de mariage des enfants, nous estimons un modèle à proportion de risque de Currie et Neidell (2005) ou Corno *et al.* (2020). Notre principale variable d'intérêt est l'âge de la femme au premier mariage, nous définissons le mariage précoce comme ayant lieu avant l'âge de 18 ans. Nous discutons des biais de sélection et des canaux de canalisation possibles qui peuvent influencer la relation.

Nos résultats montrent que les événements cyclonique n'impacte la décision de mariage que pour des phénomènes extrême c'est-à-dire avec des vents supérieur à 190km/h. De plus, lors des événements cycloniques, la vitesse du vent n'affecte pas significativement la probabilité de mariage pour les filles âgées de 12 à 24 ans. Cela suggère que les ménages ne

comptent pas sur le mariage des filles de l'âge du mariage dans le cadre de leurs stratégies d'adaptation à court terme pour faire face à un événement cyclone. Cependant, la vitesse du vent a des effets négatifs et significatifs sur la probabilité de mariage pour les filles de 12 à 17 ans. Il est possible que les ménages agricoles en difficulté retardent le mariage de leur fille afin de respecter les délais de paiement de la dot pour protéger leur consommation après un événement Cyclone.

5.1.2 L'impact des cyclones sur la fécondité dans les pays en développement

D'après le travail d'Idriss Fontaine (CEMOI, Université de La Réunion), Sabine Garabedian (CEMOI, Université de La Réunion) et Hélène Vérèmes (LACy, OSU-Réunion, Université de La Réunion), 2019-2021.

Dans un second travail concernant les impacts sur les déterminants socio-économiques, nous nous sommes intéressé aux impacts des événements cycloniques sur la décision de faire un enfants. Ce travail à donné lieu à l'article "Tropical cyclones and Fertility : New Evidence from Developing countries", qui est actuellement en révision à *Ecological Economics* et qui est présenté dans la chapitre 11 des publications.

Dans la littérature sur les relations entre la fécondité et les désastres naturels, les réponses varient considérablement, avec des augmentations (Nobles et al., 2015; Nandi et al., 2018; Finlay, 2009) ou des diminutions (Davis, 2017; Evans et al., 2010; Poertner, 2008) des naissances, en fonction des contextes sociaux et environnementaux locaux (Sellers & Gray, 2019). Il nous a paru intéressant, dans le cadre de l'étude des impacts des événements cycloniques, de chercher à apporter des éléments de réponses en examinant les effets du passage des cyclones sur la fécondité dans 6 pays en développement : Banglasdeh, Cambodge, République Dominicaine, Haïti, Madagascar et Philippines sur la période 1985-2015.

Pour répondre à cette problématique, nous avons mobilisé deux bases de données. La première base est la version malgache de l'enquête démographique et de santé (EDS ou DHS) qui fournit l'historique de la fécondité de chaque femme interrogée, ainsi que des informations détaillées sur leur localisation géographique. La seconde est la base de données (TCE-DAT) de Geiger et al. (2018) concernant l'exposition aux cyclones tropicaux. Ces données mondiales à haute résolution fournissent des informations sur le profil du champ de vent de plus de 2 700 systèmes cycloniques sur la période 1950-2015. En effet, comme cela a été mentionné dans la section 3, les cyclones tropicaux sont généralement approximés la force du vent du système. En fusionnant les informations géographiques de ces deux bases de données ainsi que l'historique de fécondité de EDS, nous construisons un panel de données qui fait apparaître, pour la période 1985-2015, l'exposition aux cyclones tropicaux d'une mère donnée au cours d'une année donnée. La relation entre les variations de l'exposition à la vitesse du vent des cyclones tropicaux et la probabilité d'accouchement des femmes est ensuite examinée au moyen de régressions à effets fixes.

Nous obtenons deux principaux résultats de cette étude.

Premièrement, nos modèles montrent un impact négatif des chocs de vitesse du vent des cyclones tropicaux sur la probabilité d'accouchement des mères. La relation esti-

mée est systématiquement négative, indépendamment de l'inclusion de contrôles pour la température et les précipitations. Par exemple dans le modèle incluant les variables de contrôle mais pas de variable d'interaction, l'exposition à un choc dont la vitesse du vent en t est de 38,8 km/h (équivalent à un écart type) induit une baisse de $2,6$ points de la probabilité d'accoucher en $t+1$. Les spécifications alternatives du modèle empirique de base, consistant à modifier notre restriction d'échantillon en incluant les mères qui migrent ou à diviser l'échantillon pour considérer deux sous-périodes, ne modifient pas le modèle qualitatif ni quantitatif de nos résultats de base.

Deuxièmement, l'analyse des régressions par pays montrent que si le schéma qualitatif est le même pour les six pays étudiés, les schémas quantitatifs sont quant à eux considérablement différents. Ainsi, des pays comme Madagascar ou les Philippines sont ceux qui ont le moins d'effet. Par exemple, une exposition supplémentaire à la vitesse du vent réduit la probabilité de maternité en $t+1$ de $0,0452$ aux Philippines et de $0,0271$ à Madagascar alors que en Haïti, cette baisse de la probabilité est de $0,231$. Nous avons donc approfondit le lien entre le degré d'exposition associé au cyclone et la fertilité. Pour cela, nous introduisons une variable d'interaction entre l'exposition à la vitesse du vent et une variable fictive égale à un si le village a été exposé plus de neuf fois à des systèmes cycloniques au cours de la période d'échantillonnage de notre étude. Il en ressort que la réponse de la fertilité aux chocs cycloniques dépend du degré d'exposition associé au milieu de vie de la mère : dans les zones sujettes aux cyclones, la probabilité d'accoucher diminue moins.

5.2 Effets d'entrainement et politiques d'ajustement (A3.2)

D'après le travail de Pierre Nziengui Mamboundou (CEMOI, Université de La Réunion), Sabine Garabedian (CEMOI, Université de La Réunion) et Idriss Fontaine (CEMOI, Université de La Réunion), 2021-2022.

Concernant les effets de rétroactions des impacts directs des événements cycloniques sur l'ensemble de l'économie et l'analyse des politiques d'ajustements, nous avons construit un Modèle d'Equilibre général calculable spatialisé permettant de tester différents types de cyclone et différentes politiques d'ajustement. Ce travail à donné lieu à un article "Effets économiques d'un choc spatialisé et évaluation des politiques de compensation : le cas d'un MEGC appliqué au cyclone tropical Dina à La Réunion" qui est actuellement en soumission à *La Revue Economique* et qui est présenté dans la chapitre 13 des publications.

L'évaluation des impacts socioéconomiques des cyclones à La Réunion nous a conduit à considérer ceux résultants directement de l'activité cyclonique et ceux découlant indirectement des cyclones. En effet, la littérature économique en la matière renseigne que l'évaluation des dommages des phénomènes naturels extrêmes de types cyclones, sécheresse, tremblement de terre, doit nécessairement prendre en compte les dommages directs qui portent généralement sur les dégradations observées après la catastrophe ; et les dommages indirects liés, entre autres, aux interruptions d'activités, aux impacts sur les agents économiques (Kousky, 2014). L'intérêt de cette démarche est d'aboutir à une évaluation complète des dommages de ces phénomènes d'une part, et d'autre part de proposer des scénarii de politiques publiques permettant de les atténuer.

Concernant l'identification de l'outil le plus adapté pour mener l'étude, la littérature renseigne la possibilité de recourir à un modèle Input-Output ou à un modèle d'équilibre

général calculable (MEGC) (Botzen et al., 2020). Toutefois, elle met aussi en évidence le fait que les résultats des modèles Input-Output peuvent être sensibles à la façon avec laquelle le phénomène climatique est introduit (Rose & Wei, 2013). Par ailleurs, ces modèles ne permettent pas de modéliser des politiques d'atténuation. Les MEGC quant à eux permettent de faire l'impasse sur les limites des modèles Input-Output ce qui a légitimé leur adoption pour mener ce travail.

Dans la littérature, il existe deux approches pour appréhender un choc naturel au sein des MEGC. La première repose sur une réduction de la valeur ajoutée au travers d'un coefficient de dommage (Narita et al., 2010; Sassi, 2011; Washida et al., 2014). La deuxième postule quant à elle postule une réduction du stock de capital disponible pour produire (Xie et al., 2014; Rose & Wei, 2013; Wittwer & Griffith, 2011). Considérant le fait que les dommages liés aux cyclones sont majoritairement des destructions physiques des actifs, nous avons adopté pour suivre la seconde approche dans la modélisation du choc cyclonique. En outre, l'analyse de la littérature a révélé l'importance qu'occupe la spatialisation des effets d'un choc naturel dans ce type d'analyse. En effet, les chocs naturels n'impactent pas de façon homogène les territoires. Il est donc nécessaire d'intégrer la dimension spatiale dans la spécification des chocs naturels, en l'occurrence du choc cyclonique dans notre analyse. A partir de ces différentes informations, un MEGC intégrant les dommages sectoriels à partir de la commune d'exercice de l'activité économique a été construit. Ce dernier a été calibré pour évaluer les impacts d'un cyclone de type Dina (2002), considéré ici comme le cyclone de référence eu égard au fait que c'est le cyclone le plus destructeur qui a touché La Réunion ces 20 dernières années.

De façon pratique, l'analyse admet deux scénarii de choc. Un choc d'intensité qui correspond à la survenue d'un cyclone unique de type Dina, et un choc de récurrence illustré par quatre cyclones de moindre intensité dont la somme des dommages directs est similaire au cyclone unique Les résultats de l'étude montrent que les chocs cycloniques se diffusent à l'économie par le canal des prix. On relève une hausse de ces derniers qui entraine une contraction de l'activité productive. Cette diminution de l'activité productive résulte de la raréfaction de l'offre de capital qui pénalise la dynamique des secteurs et, est intensifiée par la hausse des prix qui induit une baisse de la demande domestique. Cette situation entraine une hausse du chômage et une détérioration de la situation des ménages. Pour atténuer ces effets négatifs, différentes politiques économiques ont été explorées. Elles reposent sur un réinvestissement en capital au prorata des dommages de chaque secteur, sur un réinvestissement axé sur les secteurs à forte valeur ajoutée et sur les secteurs intensifs en consommations intermédiaires. A cet effet, il apparait qu'un réinvestissement tourné vers les secteurs intensifs en valeur ajoutée est la seule politique à même de redynamiser l'économie après un choc cyclonique intense alors qu'aucune des politiques envisagées ne permet d'inverser la tendance négative qui prévaut dans le choc de récurrence. Ces résultats témoignent qu'il faut à la fois accorder un intérêt particulier aux secteurs intensifs en valeur ajoutée dans le cadre des chocs intense mais aussi qu'il faut envisager des politiques d'atténuation dont le montant est supérieur à celui des dommages observés lors des chocs récurrents. En outre, cette étude offre aux pouvoirs publics un levier d'appréciation des impacts potentiels des chocs cycloniques et des politiques d'atténuation dans les territoires ultramarins qui ont des structures économiques et des contraintes naturelles relativement similaires.

Chapitre 6

Thèse

6.1 Impact macroéconomique des cyclones

D'après le travail de Eric Kulanthaivelu sous la direction de Sabine Garabedian (CEMOI, Université de La Réunion), d'Yves Croissant (CEMOI, Université de La Réunion) et d'Idriss Fontaine (CEMOI, Université de La Réunion), 2019-2023.

La question de l'impact économique des cyclones tropicaux peut également s'analyser à travers des indicateur plus macroéconomique. C'est l'objectif de la thèse d'Eric Kulanthaivelu qui a débuté en octobre 2020 financé sur un contrat doctoral. Dans le cadre de cette thèse, un premier travail a consisté à analyser l'impact des cyclones sur la croissance économique pour l'ensemble des pays. Ce travail à donné lieu à un article "Tropical Cyclones and Economic Growth : The Importance of Considering Small Island Developing States" qui est actuellement en révision à la *Revue d'Economie Politique* et qui a été présenté lors du colloque annuel de l'AFSE (French Economic Association) en 2022 (Dijon, France). Cet article est présenté dans la chapitre 14 des publications. Un deuxième travail consiste à étudier l'impact des cyclones sur les inégalités en prenant les Etat-Unis comme terrain d'étude afin de descendre au niveau des comtés. Ce travail à donné lieu à un article "The impact of tropical cyclones on income inequality in the U.S. : an empirical analysis" qui est en soumission à *Ecological Economics* et qui est présenté dans la chapitre 15 des publications.

La littérature sur les cyclones tropicaux constitue un sous-ensemble de la catégorie de l'économie des catastrophes naturelles. Au sein de cette plus large thématique des catastrophes naturelles, la question des conséquences économiques engendrées par ces chocs reste ouverte et indécise. Lorsque les travaux de Noy (2009) ou Felbermayr & Gröschl (2014) démontrent l'impact négatif de ces phénomènes météorologiques extrêmes, d'autres études comme celles de Caballero & Hammour (1994), Skidmore & Toya (2002) ou encore Crespo Cuaresma et al. (2008) soutiennent l'hypothèse d'un impact positif, induit par les relances budgétaires et autres programmes d'aides subséquents aux catastrophes. Cette soudaine augmentation des dépenses relatives aux reconstructions est alors analysée comme une opportunité pour les territoires de remplacer le stock de capital détruit par des infrastructures et équipements plus efficients, ce qui entraîne in fine, une forme de destruction créatrice. Les résultats portant spécifiquement sur les cyclones tropicaux semblent plus univoques : Hsiang & Jina (2014), et plus récemment Kunze (2021) et Krichene et al. (2021) corroborent un impact négatif et persistant sur la croissance

économique des pays touchés.

Toutefois, ces effets causaux obtenus sur base monde semblent dissimuler de l'hétérogénéité, et suggèrent l'existence d'axes permettant d'atténuer voire d'annihiler les pertes de croissance économique. Tout d'abord, Strobl (2012), montre la présence d'effets négatifs à l'échelle cantonale ou régionale, mais une absence d'effet sur la croissance économique à l'échelle nationale dans le cas états-unien. Zhou & Zhang (2021) estiment que les pertes de croissance observées à Hong-Kong ne sont pas imputables aux dégâts générés par les cyclones en tant que phénomènes météorologiques, mais plutôt à l'interruption des activités dans le cadre des systèmes d'alertes gouvernementaux.

Afin d'apporter des éclairages complémentaires sur cette question, le premier chapitre de la thèse vise à retrouver les résultats obtenus par ailleurs sur base monde, et scinde l'échantillon mondial en considérant deux paramètres structurels de vulnérabilité : la taille des pays, ainsi que leur niveau de développement. En effet, les cyclones tropicaux étant principalement des phénomènes côtiers, il est probable que les pertes économiques soient observables seulement au sein des régions touchées, et non pas forcément à l'échelle nationale. D'autre part, la vulnérabilité des pays en développement semble être plus grande comparée à celle des pays développés, du fait notamment d'infrastructures de moindre qualité ou d'absence de systèmes préventifs mis en place par les pouvoirs publics. La conjonction de ces deux paramètres met en lumière une catégorie de pays faisant l'objet d'un intérêt grandissant dans les milieux académiques et institutionnels, notamment à l'aune de leur destin face au dérèglement climatique et des bouleversements attendus dans la fréquence des catastrophes naturelles : les Petits Etats Insulaires en Développement (PEID). Les PEID semblent être particulièrement vulnérables aux cyclones tropicaux, et plus généralement aux catastrophes naturelles, du fait de leur faible superficie, leur caractère insulaire, leur niveau de production locale limitée et leur éloignement par rapport aux principaux axes commerciaux et/ou grandes puissances économiques.

En adoptant une méthode de régression linéaire en données de panel avec prise en compte des effets fixes, le premier chapitre estime les liens entre l'exposition cyclonique, défini à l'aide d'un indicateur physique basé sur la vitesse des vents cycloniques à l'instar de Hsiang & Jina (2014), et le taux de croissance du Produit Intérieur Brut par habitant. Les données sur l'exposition cyclonique sont fournies par Geiger et al. (2018), et celles sur le PIB par habitant proviennent de l'United Nations Statistics Division (UNSD, 2020). La distinction de l'échantillon entre PEID et non PEID forme l'originalité et la contribution de ce travail. Des pertes de points de croissance quasiment constantes se cumulent jusqu'à 15 ans après un épisode cyclonique chez les PEID, lorsque l'analyse dans les non PEID demeure non conclusive, et ce, indépendamment du niveau de développement. Une analyse complémentaire viserait à analyser les canaux de transmission derrière ces effets négatifs chez les PEID afin d'identifier la spécificité de ces territoires.

Cette première série de résultats caractérise donc la vulnérabilité des PEID face aux évènements cycloniques, et ce, en termes de pertes intertemporelles de croissance économique. Cependant, le taux de croissance du PIB par habitant ne permet totalement de rendre compte des conditions de vie des populations, de leur bien-être. Cet indicateur est sujet à de nombreuses critiques, notamment du fait qu'il ne tienne pas compte du stock de ressources naturelles présent sur les territoires. A cet égard, le second chapitre explore l'impact des cyclones tropicaux sur les inégalités de revenus aux Etats-Unis.

Le deuxième chapitre de la thèse s'intéresse donc aux effets des cyclones tropicaux sur l'inégalité des revenus. Pour cela, cette étude utilise un ensemble de données de panel des comtés américains touchés au cours de la période 2010 - 2019. Il exploite les informations géophysiques pour construire le prédicteur d'intensité de catastrophe et montre que les chocs de tempête réduisent considérablement les niveaux d'inégalité des revenus locaux au cours de l'année où ils se produisent . Une étude étroite des effets de composition révèle plusieurs modèles intéressants. Premièrement, l'impact immédiat est tiré par les deux quintiles les plus bas et, dans une moindre mesure, le quintile supérieur de la distribution des revenus. Deuxièmement, les effets bénéfiques sur l'inégalité des revenus sont stabilisés à court terme et la fréquence des événements est un paramètre crucial à considérer comme les comtés exposés à plusieurs reprises présentent des réponses plus importantes après une grève du cyclone que leurs homologues rarement exposés. Enfin, entre autres, cette étude souligne l'importance des filets de sécurité sociale dans les effets de répartition défavorable des cyclones tropicaux.

6.2 Évaluations économiques des impacts cycloniques : Cas de Madagascar

D'après le travail de Tsiory Maminiaina Andrianavalona Ramilimanitra, sous la direction de Sabine Garabedian d'Yves Croissant (CEMOI, Université de La Réunion) et de Pierre Lazamanana (Université d'Antananarivo), 2023-2026.

Madagascar, un Etat insulaire se situant dans le Bassin Sud-Ouest de l'Océan Indien (SWIO ou South Western Indian Ocean) est caractérisée par un fort degré d'exposition au passage de l'évènement météorologique extrême qu'est le cyclone. Le bassin SWIO est classée troisième comme étant le bassin cyclonique tropical le plus actif dans le monde (Tulet *et al.*, 2021) dont environ 11% (Leroux *et al.*, 2018) voire 15% (Héron *et al.*, 2020) des activités cycloniques globaux y sont observées, avec une moyenne annuelle de 9 à 10 tempêtes tropicales (Neumann., 1993 ; Mavume, 2008 ; Leroux *et al.* ,2018). A Madagascar, le EMDAT (Emergency Events Database) estime que le passage des cyclones tropicaux entre 2000 et 2021 a causé plus de 1500 morts et 744 275 personnes considérées comme sans abris. Madagascar n'a pas été en effet épargné du passage de plusieurs systèmes tropicaux atteignant le stade de Cyclone tropical Intense avec une vitesse de vent moyen soutenu de 166 à 212km/h (équivalent à un cyclone de catégorie 4 selon l'échelle de Saffir-Simpson) entre 2000 et 2017 selon le rapport du Joint Research Centre ou JRC (2017). Entre autres le cyclone Gafilo (2004) qui a été le plus destructeur causant 363 morts et affectant 990.000 personnes et le cyclone Enawo (2017) qui a entrainé plus de 80 morts et affectant plus de 430 000 personnes.

De plus, la faible compétitivité de l'économie malgache représente entre autres un des facteurs accentuant sa vulnérabilité au passage des cyclones tropicaux. Sur le plan socio-économique, le rapport du PNUD (2018) met en évidence que derrières les améliorations sur plusieurs années observées en termes de croissance économique pour le pays se cachait un PIB par habitant qui n'a cessé de décroitre. Le dernier Diagnostic réalisé par la Banque Mondiale (2022) pour Madagascar souligne que le pays est l'un des seuls pays à avoir connu une dégradation du revenu moyen par habitant sur une très longue période (1960-2020). Ce même diagnostic renforce la liaison étroite du revenu des plus pauvres avec le revenu moyen par habitant où une part très importante de la population (environ

80%) contre 68% au début de l'année 2000 ; vit encore dans une situation d'extrême pauvreté, avec un revenu journalier inférieur à 2,15 dollars (1,90 dollars par jour en Parité de Pouvoir d'achat de 2011).

L'intensification des cyclones représente donc un enjeu majeur pour Madagascar. Cependant, il existe peu de littérature sur l'évaluation économique des cyclones pour le cas de Madagascar, d'où l'intérêt de cette thèse qui viendrait couvrir cette problématique. L'objectif principal serait donc d'évaluer économiquement les impacts potentiels directs et indirects des cyclones tropicaux pour le territoire de Madagascar en prenant en compte le changement climatique. Pour ce faire, trois chapitres seront abordés successivement.

Le premier chapitre s'intéresse à l'évaluation des impacts macroéconomiques (impacts indirects) des cyclones sur les grands agrégats économiques comme le PIB par tête, l'investissement, la consommation, le taux d'inflation, les dépenses gouvernementales, les exportations et les importations. Les approches et méthodologies utilisées dans le cadre de l'évaluation des impacts indirects face aux chocs naturels ont évolué rapidement dans la littérature. Nous utilisons un modèle (régression standard) de panel à Vecteur Auto-Regressif (VAR) en considérant le PIB par tête comme variable d'intérêt et où les autres variables seront exogènes au modèles comme dans la plupart des études dans la littérature. Cette étude sera complétée par la suite par une évaluation d'impact sur le long-terme en utilisant la méthode de la Double Différence qui consiste d'une part à construire les agrégats contre-factuels afin de dégager la tendance des différents agrégats économiques sur le long-terme en fonction des quatre hypothèses proposées par la littérature : pas de reprise (no recovery) , retour à la tendance (recovery) , retour au-delà de la tendance ou mieux reconstruire (build-back-better) , destruction créatrice (creative destruction).

Le second chapitre vise à évaluer l'impact des cyclones à travers l'utilisation d'une fonction de dommage empirique à partir des données de vents (paramètre unique) en vue d'évaluer les coûts des dommages (pertes économiques) occasionnés par le passage des cyclones tropicaux à Madagascar. Ce chapitre vient en prolongement de l'étude réalisé durant le stage et la méthodologie sera donc celle utilisée dans le travail sur La Réunion (section 4.2) qui met en relation le profil de champ de vents cycloniques (vitesses maximales de vents en km/h) et la valeur économique (exprimé par l'intensité lumineuse des lumières nocturnes) détruit par les vents (Emmanuel K, 2011). Les informations sur les cyclones pour Madagascar pourraient être obtenues à partir de la base de données TCE-DAT (Tropical-Cyclone Exposure-Data) de Geiger *et al.* (2018) qui contient des données mondiales à haute résolution sur les vitesses de vents maximales pour 2 700 systèmes cycloniques. Nous mobiliserons par ailleurs les images nocturnes à haute résolution issues des observations Visible Infrared Imaging Radiometer (VIIRS) à bord du Suomi-National Polar-Orbiting Partnership pour répartir et distribuer le PIB au sein du territoire de Madagascar. Les informations qui permettraient de calibrer de manière empirique la fonction de dommage pour Madagascar peuvent être obtenues auprès du Bureau National pour la Gestion des Risque et des Catastrophe (BNGRC) à Madagascar. En plus du calibrage empirique d'une fonction de dommage pour le territoire, valider empiriquement la corrélation entre les lumières nocturnes et les activités économiques à Madagascar pourrait être également une piste d'approfondissement de ce chapitre (Bhandari et Roychowdhury 2011 ; Henderson *et al.*, 2012 ; Chen et Nordhaus, 2015 ; McCord et Rodriguez-Heredia, 2022).

Finalement, le dernier chapitre consisterait à évaluer l'impact des cyclones futurs en prenant en compte le phénomène de changement climatique par fonction de dommage en couplant ce modèle à la méthode des lumières nocturnes a été réalisée précédemment avec des modèles de prévision à haute résolution de l'activité cyclonique actuelle et future dans un contexte de changement climatique issus du WinRiskTech. Il s'agira alors de comparer des coûts de dommages actuel et futur ce qui permettra de dégager les surplus de coûts par rapport aux coûts actuels calculés. Ce dernier chapitre représente également un intérêt crucial en termes de politique publique sachant que pour Madagascar, le passage des cyclones tropicaux est inévitable et qu'une augmentation de 50% de l'intensité des activités cycloniques serait attendu pour l'année 2100 en raison du phénomène de changement climatique (USAID, 2018). A cet égard, pour un évènement météorologique extrême comme le cyclone tropical, la mise en place de politiques d'adaptation forte s'impose. La connaissance des surplus de coûts dans ce chapitre pourraient dans un premier temps éclairer les décideurs publics sur les politiques d'aménagements du territoire de Madagascar, de prendre les mesures adéquats afin de réduire ces surplus de coûts, de réduire la vulnérabilité des entités dans les localités les plus exposées mais également de renforcer la capacité de résilience et d'adaptation de ces dernières. Sarkissian *et al.* (2021) soulignent également une possibilité d'amélioration de la situation socio-économique post-cyclonique sur le long-terme par rapport à la tendance avant le passage du cyclone en mettant en place une politique basée sur la notion de « Build-Back-better ou BBB» (mieux reconstruire ou retour au-delà de la tendance). Les auteurs affirment que le renforcement lors des reconstructions des infrastructures dites « critiques » comme les réseaux électriques, les réseaux d'eaux potables, les réseaux d'égouts, les réseaux de télécommunications, les réseaux de transport amélioreraient davantage la capacité de réponse des habitants face aux risques cycloniques dans le futur.

Conclusion

Durant ce projet, les études réalisées ont permis d'amener un éclairage sur la dimension économique de l'évaluation du risque cyclonique dans le bassin sud-ouest de l'océan indien et plus particulièrement sur les territoires de La Réunion et de Madagascar. En effet, dans le cadre de la mise en place de politiques publiques, nécessite plusieurs étapes : faire un diagnostic, définir des objectifs et choisir le type de politiques publiques permettant d'atteindre ces objectifs. En effet, dans un premier temps, il est nécessaire d'identifier les territoires et/ou les dimensions d'une économie qui doivent être visés par les politiques publiques. Dans un deuxième temps, il faut définir les objectifs des politiques publiques. Enfin, dans un troisième temps, il convient d'analyser les impacts des différentes politiques potentielles à mettre en place pour atteindre ces objectifs.

Concernant La Réunion nous avons pu mettre en évidences des résultats relatifs à ces trois points.

Premièrement, concernant le diagnostic, nous avons pu mettre en évidence que le risque cyclonique est inégalement répartie sur le territoire à travers la construction d'un indice composite. Cet indice agrégeant une dimension d'aléa (moyenne des vents par évènement cyclonique et pluviométrie), exposition (densité de population, chiffre d'affaire, valeur agricole, valeur locative surfacique), et vulnérabilité (proportion de population de plus de 65 ans, taux de pauvreté, proportion de maisons anciennes) à travers la méthode du MLBOD, à permis de cartographier le risque par IRIS comme présenté sur la figure 6.1.

Deuxièmement, nous avons pu mettre en évidence des trajectoires d'évolution des coûts des dommages relatifs aux chocs cycloniques qui tiennent compte du changement climatique. En comparant l'impact de cyclones synthétiques simulés à climatologie actuelle et à climatologie future sur l'économie de La Réunion spatialisée avec les lumières nocturne, nous avons estimé que les pertes devrait doubler en moyenne d'ici 2100 passant d'une destruction en moyenne de 0,76 % du PIB à 1,43 %.

Troisièmement, l'analyse de l'efficacité comparée des politiques d'adaptation en utilisant un MEGC spécialisé, a montré que seul un investissement au prorata des dégâts permettrait d'atténuer les effets négatifs observés. Néanmoins, cette atténuation ne serait pas de nature à rattraper la tendance du BAU. Pour les pouvoirs publics, l'enseignement majeur à tirer de cette analyse porte sur le fait que face à des cyclones intenses ou récurrents, la stratégie de réponse à adopter pour relancer l'économie peut se baser sur des politiques d'investissement tournées vers les secteurs les plus impactés. Il faut toutefois que les ressources mobilisées soient supérieures aux coûts des dommages pour relancer durablement l'activité économique.

Concernant Madagascar, malgré la crise de la Covid nous ayant empêché de réaliser le travail initialement prévu, nous avons néanmoins mener des analyses en ayant recours à un certains nombres d'enquête couplées aux données météorologues. Cependant, ces

FIGURE 6.1 – Indice de Risque composite par IRIS de La Réunion

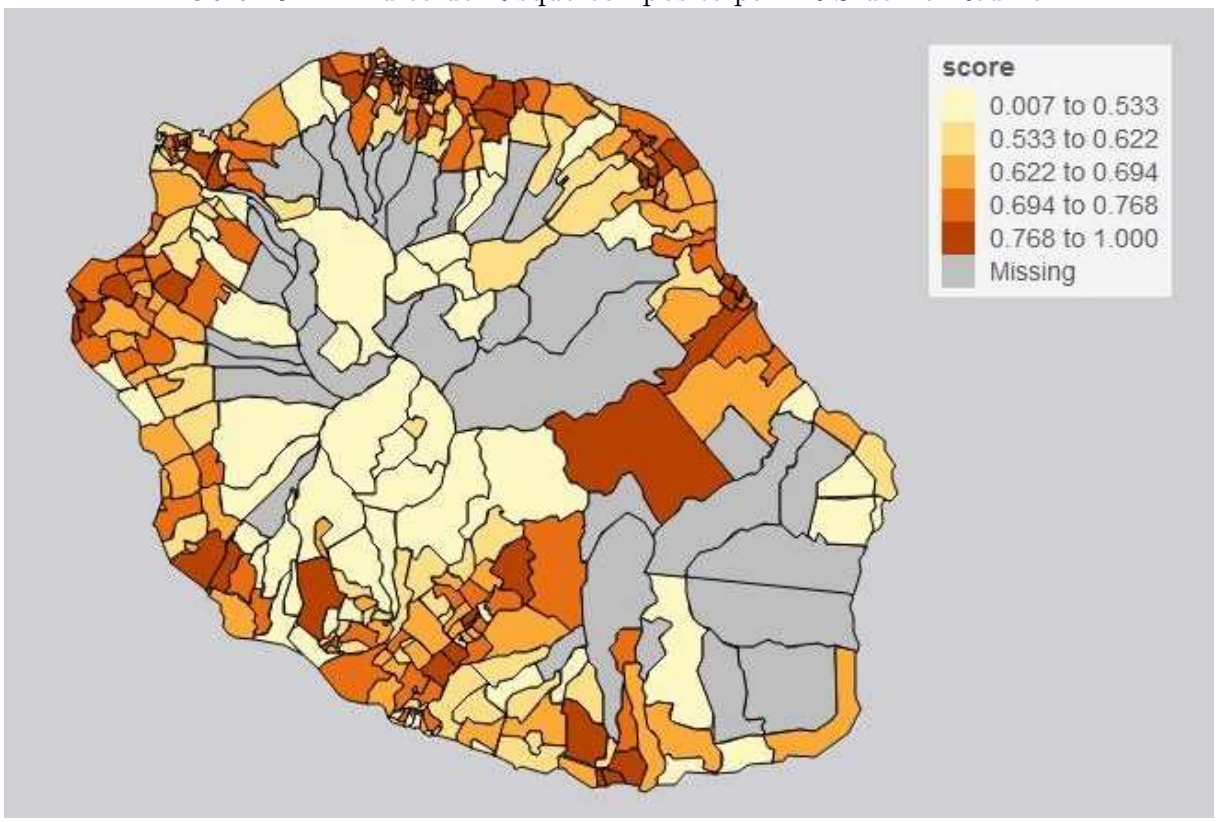

Source : Apaya, Garabedian, Fontaine (2023)

travaux ne se concentre que sur l'aspect diagnostic dans un premier temps même si ceux-ci permettent d'apporter des éclairages aux politiques publiques sur les impacts des chocs cycloniques.

Ainsi, un premier travail à permis de mettre en évidence que pour les Fokontany partageant des caractéristiques spécifiques, les chocs cycloniques ont un effet négatif mesuré par la variation des lumières nocturnes, durant les quatre premiers mois suivant l'événement. Cependant, un effet positif apparaît par la suite et se poursuit jusqu'à deux ans après l'événement. Cela conforte l'idée des mécanismes économiques suggérant qu'après une période de contraction, l'économie impactée rebondit au-delà de la tendance contre-factuelle (tendance en l'absence de choc) tout en soulignant l'importance du temps d'intervention suite à une telle catastrophe.

Un second travail visant à mesure l'impact du cyclone Enawo toujours à travers las variation de lumière nocturne, montre que les pertes pourraient constituer entre 22% à 32% de la valeur économique totale.

Un troisième travail sur données d'enquête (DSH) met en évidence un effet négatif sur la fécondité. En particulier, être exposé à des vents de 100 km/h diminue la probabilité d'accoucher de 24,6 points dans l'année en cours avec une nouvelle baisse de 5,6 et 1,9 points respectivement 1 et 2 ans après l'exposition. Nous constatons également que l'effet causal négatif est amplifié dans les zones rurales et non éclairées par rapport aux zones éclairées ainsi que pour les mères ayant un faible niveau d'éducation. Combiné avec des preuves transversales indiquant que la décision post-cyclone d'avoir des enfants est délibérée, nous pensons que les cyclones tropicaux agissent comme un choc négatif qui augmente le coût d'opportunité d'avoir des enfants.

Enfin, certains de nos travaux ont été menés dans un cadre plus large que les territoires initialement visés afin de mieux appréhender l'impact des cyclones dans leur ensemble.

Ainsi, nous avons chercher à tester l'impact des cyclones sur la croissance économique pour l'ensemble des pays exposés. Il s'avère qu'il n'existe des effets négatifs significatifs que dans les PEID. Cet impact est estimé à -0,016 point de pourcentage sur la croissance du PIB par habitant pour un km/h supplémentaire de vent. Cela semble être dû à une dépendance accrue vis-à-vis des conditions économiques étrangères, à des capacités de reconstruction insuffisantes et à des difficultés à mettre en oeuvre des politiques d'adaptation. Ce résultat souligne la particularité des PEID face au risque cyclonique ainsi que leur plus forte vulnérabilité qui invite à un traitement différencié dans les politiques d'adaptation.

Ensuite, nous nous sont intéressé à l'impact des cyclones sur les inégalité de revenu mais à un niveau plus fin, soit au niveau des contés américains. Cette analyse montre un impact négatif immédiat des cyclones tropicaux sur l'inégalité des revenus, qui semble être tiré par les quintiles les plus pauvres pour lesquels la part du revenu global augmente par rapport à ceux au sommet de la distribution. La part des 60% inférieurs augmente de 0,006 point de pourcentage pour chaque km/h supplémentaire d'intensité cyclonique, tandis que la part des 40% inférieurs de la distribution augmente de 0,004 point de pourcentage.

Enfin, afin d'étendre l'analyse de l'impact sur les déterminants socio-économiques, nous avons étudié l'impact des cyclones sur les mariages précoces pour six pays en voie de développement (Bangladesh, Cambodge, Haiti, Madagascar, Philippines et Timor-Leste) exposés à travers des données d'enquête (DHS). Les analyses montrent dans un premier temps que seul les cyclones intenses (vent supérieur à 190km/h) ont un impact. Dans un second temps, elles montrent que pour ces cyclones intenses, il y a un effet négatif sur les mariages précoces, c'est à dire pour les mariages des filles âgées de 12 à 17 ans alors qu'aucun impact significatif n'est observé sur les mariages des filles entre 12 et 24 ans.

Ces travaux, de part leur diversité, ont permis d'ouvrir la voie à de nombreuse réflexion concernant les impacts des cyclones sur le tissu économique et social d'un territoire.

Bibliographie

Adger, W. N. (2006). Vulnerability. *Global environmental change*, 16(3), 268–281.

Afionis, S. (2017). *The European Union in international climate change negotiations*. Taylor & Francis.

Alex, b., Baillat, A., & Gemenne, F. (2019). Rapport d'etude n9 : Prospective ocean indien occidental.

Alwang, J., Siegel, P. B., Jorgensen, S. L., et al. (2001). *Vulnerability : a view from different disciplines*. Technical report, Citeseer.

Anttila-Hughes, J. & Hsiang, S. (2013). Destruction, disinvestment, and death : Economic and human losses following environmental disaster. *SSRN Electronic Journal*.

Atkins, J. P., Mazzi, S., & Easter, C. D. (2000). A commonwealth vulnerability index for developing countries : The position of small states.

Ayers, J. M. & Huq, S. (2009). The value of linking mitigation and adaptation : a case study of bangladesh. *Environmental Management*, 43(5), 753–764.

Aykut, S. & Dahan, A. (2011). Le régime climatique avant et après copenhague : sciences, politiques et l'objectif des deux degrès. *Natures Sciences Sociétés*, 19(2), 144–157.

Barbary, D., Leroux, M.-D., & Bousquet, O. (2019). The orographic effect of reunion island on tropical cyclone track and intensity. *Atmospheric Science Letters*, 20(2), e882.

Berlemann, M. & Wenzel, D. (2018). Hurricanes, economic growth and transmission channels : Empirical evidence for countries on differing levels of development. *World Development*, 105, 231–247.

Bertinelli, L., Mohan, P., & Strobl, E. (2016). Hurricane damage risk assessment in the caribbean : An analysis using synthetic hurricane events and nightlight imagery. *Ecological Economics*, 124, 135–144.

Bertinelli, L. & Strobl, E. (2013). Quantifying the local economic growth impact of hurricane strikes : An analysis from outer space for the caribbean. *Journal of Applied Meteorology and Climatology*, 52(8), 1688–1697.

Bindoff, N., Cheung, W., Kairo, J., Arístegui, J., Guinder, V., Hallberg, R., Hilmi, N., Jiao, N., Karim, M., Levin, L., O'Donoghue, S., Purca Cuicapusa, S., Rinkevich, B., Suga, T., Tagliabue, A., & Williamson, P. (2019). Changing ocean, marine ecosystems, and dependent communities. in : Ipcc special report on the ocean and cryosphere in a changing climate.

Binita, K., Shepherd, J., King, A. W., & Gaither, C. J. (2021). Multi-hazard climate risk projections for the united states. *Natural Hazards*, 105(2), 1963–1976.

Blechinger, P. F. H. & Shah, K. U. (2011). A multi-criteria evaluation of policy instruments for climate change mitigation in the power generation sector of trinidad and tobago. *Energy Policy*, 39(10), 6331–6343.

Bodansky, D. (2001). The history of the global climate change regime. *International relations and global climate change*, 23(23), 505.

Bohle, H.-G. (2001). Vulnerability and criticality : perspectives from social geography. *IHDP update*, 2(01), 3–5.

Bohle, H. G., Downing, T. E., & Watts, M. J. (1994). Climate change and social vulnerability : toward a sociology and geography of food insecurity. *Global environmental change*, 4(1), 37–48.

Botzen, W. W., Deschenes, O., & Sanders, M. (2020). The economic impacts of natural disasters : A review of models and empirical studies. *Review of Environmental Economics and Policy*.

Briguglio, L. (1995). Small island developing states and their economic vulnerabilities. *World Development*, 23(9), 1615 – 1632.

Briguglio, L., Cordina, G., Farrugia, N., & Vella, S. (2009). Economic vulnerability and resilience : Concepts and measurements. *Oxford Development Studies*, 37(3), 229–247.

Brooks, N. (2003). Vulnerability, risk and adaptation : A conceptual framework. *Tyndall Centre for Climate Change Research Working Paper*, 38(38), 1–16.

Brooks, N., Adger, W. N., & Kelly, P. M. (2005). The determinants of vulnerability and adaptive capacity at the national level and the implications for adaptation. *Global environmental change*, 15(2), 151–163.

Caballero, R. & Hammour, M. (1994). The cleansing effect of recessions american economic review 84 (5).

Camargo, S. J. & Hsiang, S. M. (2016). Tropical cyclones : From the influence of climate to their socioeconomic impacts. *Extreme Events : Observations, Modeling, and Economics*, (pp. 303–42).

Cavallo, E., Powell, A., & Becerra, O. (2010). Estimating the direct economic damages of the earthquake in haiti. *The Economic Journal*, 120(546), F298–F312.

Chen, A., Stephens, A., Koon, R. K., Ashtine, M., & Koon, K. M.-K. (2020). Pathways to climate change mitigation and stable energy by 100% renewable for a small island : Jamaica as an example. *Renewable and Sustainable Energy Reviews*, 121, 109671.

Chen, X. (2007). Risk assessment and zonation of typhoon disasters in fujian province. *Chinese journal of ecology*, 26(6), 961–966.

Chen, X. & Nordhaus, W. (2015). A test of the new viirs lights data set : Population and economic output in africa. *Remote Sensing*, 7(4), 4937–4947.

Chen, X. & Nordhaus, W. D. (2011). Using luminosity data as a proxy for economic statistics. *Proceedings of the National Academy of Sciences*, 108(21), 8589–8594.

Closset, M., Feindouno, S., Guillaumont, P., & Simonet, C. (2017). A physical vulnerability to climate change index : Which are the most vulnerable developing countries ?

Collins, M., Knutti, R., Arblaster, J., Dufresne, J.-L., Fichefet, T., Friedlingstein, P., Gao, X., Gutowski, W. J., Johns, T., Krinner, G., et al. (2013). Long-term climate change : projections, commitments and irreversibility. In *Climate Change 2013-The Physical Science Basis : Contribution of Working Group I to the Fifth Assessment Report of the Intergovernmental Panel on Climate Change* (pp. 1029–1136). Cambridge University Press.

Colomb, A., Kriat, T., & Leroux, M.-D. (2019). On the rapid weakening of very intense tropical cyclone hellen (2014). *Monthly Weather Review*, 147(8), 2717–2737.

Cordina, G. et al. (2004). Economic vulnerability and economic growth : some results from a neo-classical growth modelling approach. *Journal of Economic Development*, 29(2), 21–39.

Crespo Cuaresma, J., Hlouskova, J., & Obersteiner, M. (2008). Natural disasters as creative destruction ? evidence from developing countries. *Economic Inquiry*, 46(2), 214–226.

Cutter, S. L. (1996). Vulnerability to environmental hazards. *Progress in human geography*, 20(4), 529–539.

Cutter, S. L., Boruff, B. J., & Shirley, W. L. (2003). Social vulnerability to environmental hazards. *Social science quarterly*, 84(2), 242–261.

Dao, Q.-H. & Peduzzi, P. (2004). Global evaluation of human risk and vulnerability to natural hazards. *Enviro-info 2004, Sh@ ring*, (pp. 435–446).

Davidson, R. A. & Lambert, K. B. (2001). Comparing the hurricane disaster risk of us coastal counties. *Natural Hazards Review*, 2(3), 132–142.

Davis, J. (2017). Fertility after natural disaster : Hurricane mitch in nicaragua. *Population and environment*, 38(4), 448–464.

Dessai, S. & Hulme, M. (2004). Does climate adaptation policy need probabilities ? *Climate policy*, 4(2), 107–128.

Dewan, A. (2013). *Floods in a megacity : geospatial techniques in assessing hazards, risk and vulnerability*. Springer.

Dornan, M. & Jotzo, F. (2015). Renewable technologies and risk mitigation in small island developing states : Fiji's electricity sector. *Renewable and Sustainable Energy Reviews*, 48, 35–48.

Elliott, R. J., Strobl, E., & Sun, P. (2015). The local impact of typhoons on economic activity in china : A view from outer space. *Journal of Urban Economics*, 88, 50–66.

EM-DAT, C. (2020). Em-dat : The ofda/cred international disaster database. *Centre for Research on the Epidemiology of Disasters, Universidad Católic a de Lovaina, Bruselas*.

Emanuel, K. (2008). The hurricane - climate connection. *Bulletin of the American Meteorological Society*, 89(5), ES10–ES20.

Emanuel, K. (2011). Global warming effects on us hurricane damage. *Weather, Climate, and Society*, 3(4), 261–268.

Endo, I., Magcale-Macandog, D. B., Kojima, S., Johnson, B. A., Bragais, M. A., Macandog, P. B. M., & Scheyvens, H. (2017). Participatory land-use approach for integrating climate change adaptation and mitigation into basin-scale local planning. *Sustainable cities and society*, 35, 47–56.

Evans, R. W., Hu, Y., & Zhao, Z. (2010). The fertility effect of catastrophe : Us hurricane births. *Journal of Population Economics*, 23(1), 1–36.

Feindouno, S., Goujon, M., & Santoni, O. (2017). Un indicateur d ?intensité cyclonique au niveau pays.

Felbermayr, G. & Gröschl, J. (2014). Naturally negative : The growth effects of natural disasters. *Journal of development economics*, 111, 92–106.

Field, C. B. & Barros, V. R. (2014). *Climate change 2014–Impacts, adaptation and vulnerability : Regional aspects*. Cambridge University Press.

Finlay, J. E. (2009). *Fertility response to natural disasters : the case of three high mortality earthquakes*. The World Bank.

Füssel, H.-M. (2007). Vulnerability : A generally applicable conceptual framework for climate change research. *Global environmental change*, 17(2), 155–167.

Füssel, H.-M. (2010). Review and quantitative analysis of indices of climate change exposure, adaptive capacity, sensitivity, and impacts.

Füssel, H.-M. & Klein, R. J. (2006). Climate change vulnerability assessments : an evolution of conceptual thinking. *Climatic change*, 75(3), 301–329.

Gallopín, G. C. (2006). Linkages between vulnerability, resilience, and adaptive capacity. *Global environmental change*, 16(3), 293–303.

Garlatti, A. (2013). Climate change and extreme weather events in latin america. *Inter-American Development Bank. Research Dept. II. Title. III. Series IDB-TN-490*.

Geiger, T., Frieler, K., & Bresch, D. N. (2018). A global historical data set of tropical cyclone exposure (tce-dat). *Earth System Science Data*, 10(1), 185–194.

Gibson, J., Olivia, S., & Boe-Gibson, G. (2020). Night lights in economics : Sources and uses 1. *Journal of Economic Surveys*, 34(5), 955–980.

Goavec, C. & Hoarau, J.-F. (2015). Une mesure de la vulnérabilité économique structurelle pour une économie ultrapériphérique européenne : le cas de la réunion. *Géographie, économie, société*, 17(2), 177–200.

Grinsted, A., Ditlevsen, P., & Christensen, J. H. (2019). Normalized us hurricane damage estimates using area of total destruction, 1900- 2018. *Proceedings of the National Academy of Sciences*, 116(48), 23942–23946.

Guillaumont, P. (2004). On the economic vulnerability of low-income countries.

Guillaumont, P. (2009). An economic vulnerability index : its design and use for international development policy. *Oxford Development Studies*, 37(3), 193–228.

Gupta, J. (2010). A history of international climate change policy. *Wiley Interdisciplinary Reviews : Climate Change*, 1(5), 636–653.

Hallegatte, S. (2007). The use of synthetic hurricane tracks in risk analysis and climate change damage assessment. *Journal of applied meteorology and climatology*, 46(11), 1956–1966.

Heger, M. P. & Neumayer, E. (2019). The impact of the indian ocean tsunami on aceh ?s long-term economic growth. *Journal of Development Economics*, 141, 102365.

Henderson, J. V., Storeygard, A., & Weil, D. N. (2012). Measuring economic growth from outer space. *American economic review*, 102(2), 994–1028.

Holland, G. (1993). Wmo/tc-no. 560, report no. tcp-31.

Hoque, M. A.-A., Phinn, S., Roelfsema, C., & Childs, I. (2017). Tropical cyclone disaster management using remote sensing and spatial analysis : A review. *International journal of disaster risk reduction*, 22, 345–354.

Hoque, M. A.-A., Phinn, S., Roelfsema, C., & Childs, I. (2018). Assessing tropical cyclone risks using geospatial techniques. *Applied Geography*, 98, 22–33.

Hsiang, S., Kopp, R., Jina, A., Rising, J., Delgado, M., Mohan, S., Rasmussen, D., Muir-Wood, R., Wilson, P., Oppenheimer, M., et al. (2017). Estimating economic damage from climate change in the united states. *Science*, 356(6345), 1362–1369.

Hsiang, S. M. & Jina, A. S. (2014). *The causal effect of environmental catastrophe on long-run economic growth : Evidence from 6,700 cyclones*. Technical report, National Bureau of Economic Research.

Jiang, H., Halverson, J. B., Simpson, J., & Zipser, E. J. (2008). Hurricane ?rainfall potential ? derived from satellite observations aids overland rainfall prediction. *Journal of Applied Meteorology and Climatology*, 47(4), 944–959.

Jordan, M. R. & Clayson, C. A. (2008). A new approach to using wind speed for prediction of tropical cyclone generated storm surge. *Geophysical research letters*, 35(13).

Kappes, M. S., Keiler, M., von Elverfeldt, K., & Glade, T. (2012). Challenges of analyzing multi-hazard risk : a review. *Natural hazards*, 64(2), 1925–1958.

Kasperson, J. X. & Kasperson, R. E. (2005). *The Social Contours of Risk : Risk analysis, corporations & the globalization of risk*, volume 2. Earthscan.

Kc, B., Shepherd, J., King, A. W., & Johnson Gaither, C. (2021). Multi-hazard climate risk projections for the united states. *Natural Hazards*, 105(2), 1963–1976.

Kelly, P. M. & Adger, W. N. (2000). Theory and practice in assessing vulnerability to climate change andfacilitating adaptation. *Climatic change*, 47(4), 325–352.

Khalid, F. & Babb, R. (2008). Hazard and risk assessment from hurricane ivan (2004) in grenada using geographical information systems and remote sensing. *Journal of maps*, 4(sup1), 4–10.

Klöck, C. & Nunn, P. D. (2019). Adaptation to climate change in small island developing states : a systematic literature review of academic research. *The Journal of Environment & Development*, 28(2), 196–218.

Knutson, T., Camargo, S. J., Chan, J. C., Emanuel, K., Ho, C.-H., Kossin, J., Mohapatra, M., Satoh, M., Sugi, M., Walsh, K., et al. (2020). Tropical cyclones and climate change assessment : Part ii : Projected response to anthropogenic warming. *Bulletin of the American Meteorological Society*, 101(3), E303–E322.

Knutson, T. R., McBride, J. L., Chan, J., Emanuel, K., Holland, G., Landsea, C., Held, I., Kossin, J. P., Srivastava, A., & Sugi, M. (2010). Tropical cyclones and climate change. *Nature geoscience*, 3(3), 157–163.

Kocornik-Mina, A., McDermott, T. K., Michaels, G., & Rauch, F. (2020). Flooded cities. *American Economic Journal : Applied Economics*, 12(2), 35–66.

Kousky, C. (2014). Informing climate adaptation : A review of the economic costs of natural disasters. *Energy economics*, 46, 576–592.

Krichene, H., Geiger, T., Frieler, K., Willner, S., Sauer, I., & Otto, C. (2021). Long-term impacts of tropical cyclones and fluvial floods on economic growth–empirical evidence on transmission channels at different levels of development. *World Development*, 144, 105475.

Kunze, S. (2021). Unraveling the effects of tropical cyclones on economic sectors worldwide : direct and indirect impacts. *Environmental and Resource Economics*, 78(4), 545–569.

Leroux, M.-D., Meister, J., Mekies, D., Dorla, A.-L., & Caroff, P. (2018). A climatology of southwest indian ocean tropical systems : Their number, tracks, impacts, sizes, empirical maximum potential intensity, and intensity changes. *Journal of Applied Meteorology and Climatology*, 57(4), 1021–1041.

LI, C.-m., LUO, X.-l., LIU, J.-l., & HE, J. (2006). Application of analytical hierarchy process in the assessment model on tropical cyclone disaster ?s influence. *Journal of tropical meteorology*, 3.

Li, K. & Li, G. S. (2013). Risk assessment on storm surges in the coastal area of guangdong province. *Natural Hazards*, 68(2), 1129–1139.

Li, X., Xu, H., Chen, X., & Li, C. (2013). Potential of npp-viirs nighttime light imagery for modeling the regional economy of china. *Remote Sensing*, 5(6), 3057–3081.

Lin, K.-H. E., Lee, H.-C., & Lin, T.-H. (2017). How does resilience matter ? an empirical verification of the relationships between resilience and vulnerability. *Natural Hazards*, 88(2), 1229–1250.

Martens, P., McEvoy, D., & Chang, C. (2009). The climate change challenge : linking vulnerability, adaptation, and mitigation. *Current opinion in environmental sustainability*, 1(1), 14–18.

Marzocchi, W., Garcia-Aristizabal, A., Gasparini, P., Mastellone, M. L., & Di Ruocco, A. (2012). Basic principles of multi-risk assessment : a case study in italy. *Natural hazards*, 62(2), 551–573.

Masson-Delmotte, V. (2020). Réchauffement climatique : état des connaissances scientifiques, enjeux, risques et options d ?action. *Comptes Rendus. Géoscience*, 352(4-5), 251–277.

Masson-Delmotte, V., Zhai, Z., Pörtner, H., Roberts, D., Skea, J., Shukla, P., Pirani, A., Moufouma-Okia, W., Péan, C., Pidcock, R., S, C., Matthews, J., Chen, Y., Zhou, X., Gomis, M., Lonnoy, E., Maycock, T., Tignor, M., & Waterfield, T. (2018). Global warming of 1.5°c : An ipcc special report on the impacts of global warming of 1.5°c above pre-industrial levels and related global greenhouse gas emission pathways, in the context of strengthening the global response to the threat of climate change.

Mavume, A. F. (2008). Tropical cyclones in the south-west indian ocean : intensity changes, oceanic interaction and impacts.

Mavume, A. F., Rydberg, L., Rouault, M., & Lutjeharms, J. R. (2009). Climatology and landfall of tropical cyclones in the south-west indian ocean. *Western Indian Ocean Journal of Marine Science*, 8(1).

Mawren, D., Hermes, J., & Reason, C. (2020). Exceptional tropical cyclone kenneth in the far northern mozambique channel and ocean eddy influences. *Geophysical Research Letters*, 47(16), e2020GL088715.

McCarthy, J. J., Canziani, O. F., Leary, N. A., Dokken, D. J., White, K. S., et al. (2001). *Climate change 2001 : impacts, adaptation, and vulnerability : contribution of Working Group II to the third assessment report of the Intergovernmental Panel on Climate Change*, volume 2. Cambridge University Press.

Mendelsohn, R., Emanuel, K., Chonabayashi, S., & Bakkensen, L. (2012). The impact of climate change on global tropical cyclone damage. *Nature climate change*, 2(3), 205–209.

Mohan, P. & Strobl, E. (2017). The short-term economic impact of tropical cyclone pam : An analysis using viirs nightlight satellite imagery. *International journal of remote sensing*, 38(21), 5992–6006.

Nandi, A., Mazumdar, S., & Behrman, J. R. (2018). The effect of natural disaster on fertility, birth spacing, and child sex ratio : evidence from a major earthquake in india. *Journal of Population Economics*, 31(1), 267–293.

Narita, D., Tol, R. S., & Anthoff, D. (2010). Economic costs of extratropical storms under climate change : an application of fund. *Journal of Environmental Planning and Management*, 53(3), 371–384.

Neumann, C. J. (1993). Global overview. *Global guide to tropical cyclone forecasting.*

Nguyen, C. N. & Noy, I. (2020). Measuring the impact of insurance on urban earthquake recovery using nightlights. *Journal of Economic Geography*, 20(3), 857–877.

Nobles, J., Frankenberg, E., & Thomas, D. (2015). The effects of mortality on fertility : population dynamics after a natural disaster. *Demography*, 52(1), 15–38.

Nordhaus, W. D. (2010). The economics of hurricanes and implications of global warming. *Climate Change Economics*, 1(01), 1–20.

Noy, I. (2009). The macroeconomic consequences of disasters. *Journal of Development economics*, 88(2), 221–231.

Nurse, L. A., McLean, R. F., Agard, J., Briguglio, L., Duvat-Magnan, V., Pelesikoti, N., Tompkins, E., & Webb, A. (2014). Small islands.

O'Brien, K. L., Eriksen, S., Nygaard, L. P., & Schjolden, A. (2007). Why different interpretations of vulnerability matter in climate change discourses. *Climate policy*, 7(1), 73–88.

OCDE (2008). *Handbook on constructing composite indicators : methodology and user guide*. OECD publishing.

OER (2020). Bilan énergétique de la réunion.

Pachauri, R., Meyer, L., & Team, C. W. (2014a). Annex ii : Glossary [mach, kj, s. planton and c. von stechow (eds.)].

Pachauri, R., Meyer, L., & Team, C. W. (2014b). *Climate Change 2014 : Synthesis Report. Contribution of Working Groups I, II and III to the Fifth Assessment Report of the Intergovernmental Panel on Climate Change*. IPCC, Geneva, Switzerland.

Parry, M., Parry, M. L., Canziani, O., Palutikof, J., Van der Linden, P., Hanson, C., et al. (2007). *Climate change 2007-impacts, adaptation and vulnerability : Working group II contribution to the fourth assessment report of the IPCC*, volume 4. Cambridge University Press.

Peduzzi, P., Chatenoux, B., Dao, H., De Bono, A., Herold, C., Kossin, J., Mouton, F., & Nordbeck, O. (2012). Global trends in tropical cyclone risk. *Nature climate change*, 2(4), 289–294.

Peduzzi, P., Dao, H., Herold, C., & Mouton, F. (2009). Assessing global exposure and vulnerability towards natural hazards : the disaster risk index. *Natural hazards and earth system sciences*, 9(4), 1149–1159.

Pelling, M., Maskrey, A., Ruiz, P., Hall, P., Peduzzi, P., Dao, Q.-H., Mouton, F., Herold, C., & Kluser, S. (2004). Reducing disaster risk : a challenge for development.

Petzold, J. & Magnan, A. K. (2019). Climate change : thinking small islands beyond small island developing states (sids). *Climatic Change*, 152(1), 145–165.

Pielke, J. & Roger, A. (2007). Future economic damage from tropical cyclones : sensitivities to societal and climate changes. *Philosophical Transactions of the Royal Society A : Mathematical, Physical and Engineering Sciences*, 365(1860), 2717–2729.

Pinkovskiy, M. & Sala-i Martin, X. (2016). Lights, camera ? income ! illuminating the national accounts-household surveys debate. *The Quarterly Journal of Economics*, 131(2), 579–631.

Poertner, C. C. (2008). Gone with the wind ? hurricane risk, fertility and education. *Hurricane Risk, Fertility and Education (February 2008)*.

Polsky, C., Neff, R., & Yarnal, B. (2007). Building comparable global change vulnerability assessments : The vulnerability scoping diagram. *Global environmental change*, 17(3-4), 472–485.

Poompavai, V. & Ramalingam, M. (2013). Geospatial analysis for coastal risk assessment to cyclones. *Journal of the Indian Society of Remote Sensing*, 41(1), 157–176.

Quetelard, H., Bessemoulin, P., Peterson, T., Burton, A., Boodhoo, Y., & Cerveny, R. (2007). Wmo ccl rapporteur for climate extremes decision. *World Meteorological Organization*.

Raddatz, C. (2005). *Are external shocks responsible for the instability of output in low income countries ?* The World Bank.

Ramli, M., Alias, N., Yusop, Z., & Taib, S. (2020). Disaster risk index : A review of local scale concept and methodologies. In *IOP Conference Series : Earth and Environmental Science*, volume 479 (pp. 012023). : IOP Publishing.

Robinson, S. (2018). Climate change adaptation in small island developing states : Insights and lessons from a meta-paradigmatic study. *Environmental Science & Policy*, 85, 172–181.

Robinson, S.-a. (2020). Climate change adaptation in sids : A systematic review of the literature pre and post the ipcc fifth assessment report. *Wiley Interdisciplinary Reviews : Climate Change*, 11(4), e653.

Román, M. O., Wang, Z., Sun, Q., Kalb, V., Miller, S. D., Molthan, A., Schultz, L., Bell, J., Stokes, E. C., Pandey, B., et al. (2018). Nasa's black marble nighttime lights product suite. *Remote Sensing of Environment*, 210, 113–143.

Rose, A. & Wei, D. (2013). Estimating the economic consequences of a port shutdown : the special role of resilience. *Economic Systems Research*, 25(2), 212–232.

Sassi, M. (2011). L'évaluation monétaire des dommages du risque naturel d'inondation en région paca : une analyse à l'aide d'un modèle d'équilibre général calculable. *Revue d'Economie Regionale Urbaine*, (4), 627–650.

Scandurra, G., Romano, A., Ronghi, M., & Carfora, A. (2018). On the vulnerability of small island developing states : A dynamic analysis. *Ecological Indicators*, 84, 382–392.

Schröter, D., Polsky, C., & Patt, A. G. (2005). Assessing vulnerabilities to the effects of global change : an eight step approach. *Mitigation and Adaptation Strategies for Global Change*, 10(4), 573–595.

Sellers, S. & Gray, C. (2019). Climate shocks constrain human fertility in indonesia. *World development*, 117, 357–369.

Sharifi, A. (2020). Trade-offs and conflicts between urban climate change mitigation and adaptation measures : A literature review. *Journal of Cleaner Production*, (pp. 122813).

Skidmore, M. & Toya, H. (2002). Do natural disasters promote long-run growth ? *Economic inquiry*, 40(4), 664–687.

Strobl, E. (2012). The economic growth impact of natural disasters in developing countries : Evidence from hurricane strikes in the central american and caribbean regions. *Journal of Development economics*, 97(1), 130–141.

Swart, R. & Raes, F. (2007). Making integration of adaptation and mitigation work : mainstreaming into sustainable development policies ? *Climate policy*, 7(4), 288–303.

Terry, J. P., Kim, I.-H., & Jolivet, S. (2013). Sinuosity of tropical cyclone tracks in the south west indian ocean : Spatio-temporal patterns and relationships with fundamental storm attributes. *Applied Geography*, 45, 29–40.

Tulet, P., Aunay, B., Barruol, G., Barthe, C., Belon, R., Bielli, S., Bonnardot, F., Bousquet, O., Cammas, J.-P., Cattiaux, J., Chauvin, F., Fontaine, I., Fontaine, F., Gabarrot, F., Garabedian, S., Gonzalez, A., Join, J.-L., Jouvenot, F., Nortes-Martinez, D., Mékiès, D., Mouquet, P., Payen, G., Pennober, G., Pianezze, J., Rault, C., Révillion, C., Rindraharisaona, E., Samyn, K., Thompson, C., & Vérèmes, H. (2021). ReNovRisk : a multidisciplinary programme to study the cyclonic risks in the South-West Indian Ocean. *Natural Hazards*.

Turner, B. L., Kasperson, R. E., Matson, P. A., McCarthy, J. J., Corell, R. W., Christensen, L., Eckley, N., Kasperson, J. X., Luers, A., Martello, M. L., et al. (2003). A framework for vulnerability analysis in sustainability science. *Proceedings of the national academy of sciences*, 100(14), 8074–8079.

Van Gameren, V., Weikmans, R., & Zaccai, E. (2014). *L'adaptation au changement climatique*. La découverte Paris.

Vérèmes, H. (2020). Application de la méthode dite «de bogus» dans le programme renovrisk-transferts.

Walsh, K. J., McBride, J. L., Klotzbach, P. J., Balachandran, S., Camargo, S. J., Holland, G., Knutson, T. R., Kossin, J. P., Lee, T.-c., Sobel, A., et al. (2016). Tropical cyclones and climate change. *Wiley Interdisciplinary Reviews : Climate Change*, 7(1), 65–89.

Washida, T., Yamaura, K., & Sakaue, S. (2014). Computable general equilibrium analyses of global economic impacts and adaptation for climate change : the case of tropical cyclones. *International Journal of Global Warming*, 6(4), 466–499.

Welle, T. & Birkmann, J. (2015). The world risk index–an approach to assess risk and vulnerability on a global scale. *Journal of Extreme Events*, 2(01), 1550003.

Wittwer, G. & Griffith, M. (2011). Modelling drought and recovery in the southern murray-darling basin. *Australian Journal of Agricultural and Resource Economics*, 55(3), 342–359.

WMO (2016). Tropical cyclone programme, regional association i ?tropical cyclone operational plan for the south-west indian ocean.

Wolf, S., Hinkel, J., Hallier, M., Bisaro, A., Lincke, D., Ionescu, C., & Klein, R. J. (2013). Clarifying vulnerability definitions and assessments using formalisation. *International Journal of Climate Change Strategies and Management*.

Xie, W., Li, N., Wu, J.-D., & Hao, X.-L. (2014). Modeling the economic costs of disasters and recovery : analysis using a dynamic computable general equilibrium model. *Natural Hazards and Earth System Sciences*, 14(4), 757–772.

Zhang, Y., Fan, G., He, Y., & Cao, L. (2017). Risk assessment of typhoon disaster for the yangtze river delta of china. *Geomatics, Natural Hazards and Risk*, 8(2), 1580–1591.

Zhou, Z. & Zhang, L. (2021). Destructive destruction or creative destruction ? unraveling the effects of tropical cyclones on economic growth. *Economic Analysis and Policy*, 70, 380–393.

Troisième partie

Publication

Chapitre 7

ReNovRisk : a multidisciplinary programme to study the cyclonic risks in the South West Indian Ocean

Tulet, Aunay, Barruol, Barthe, Belon, Bielli, Bonnardot, Bousquet, Cammas, Cattiaux, Chauvin, Fontaine, Fontaine, Gabarrot, Garabedian, Gonzalez, Join, Jouvenot, Nortes Martinez, Mékiès, Mouquet, Payen, Pennober, Pianezze, Rault, Revillion, Rindraharisaona, Samyn, Thompson, Vérèmes

- ***Natural Hazard***, 2021

Natural Hazards
https://doi.org/10.1007/s11069-021-04624-w

ORIGINAL PAPER

ReNovRisk: a multidisciplinary programme to study the cyclonic risks in the South-West Indian Ocean

Pierre Tulet[1] · Bertrand Aunay[2] · Guilhem Barruol[3,4] · Christelle Barthe[1] · Remi Belon[2] · Soline Bielli[1] · François Bonnardot[5] · Olivier Bousquet[1] · Jean-Pierre Cammas[1,6] · Julien Cattiaux[7] · Fabrice Chauvin[7] · Idriss Fontaine[8] · Fabrice R. Fontaine[3,9] · Franck Gabarrot[6] · Sabine Garabedian[8] · Alicia Gonzalez[3,4] · Jean-Lambert Join[3] · Florian Jouvenot[10] · David Nortes-Martinez[8] · Dominique Mékiès[1] · Pascal Mouquet[10] · Guillaume Payen[6] · Gwenaelle Pennober[10] · Joris Pianezze[1] · Claire Rault[2] · Christophe Revillion[10] · Elisa J. Rindraharisaona[3,4] · Kevin Samyn[2] · Callum Thompson[1] · Hélène Vérèmes[1,6]

Received: 13 October 2020 / Accepted: 3 February 2021

Abstract
Today, resilience in the face of cyclone risks has become a crucial issue for our societies. With climate change, the risk of strong cyclones occurring is expected to intensify significantly and to impact the way of life in many countries. To meet some of the associated challenges, the interdisciplinary ReNovRisk programme aims to study tropical cyclones and their impacts on the South-West Indian Ocean basin. This article is a presentation of the ReNovRisk programme, which is divided into four areas: study of cyclonic hazards, study of erosion and solid transport processes, study of water transfer and swell impacts on the coast, and studies of socio-economic impacts. The first transdisciplinary results of the programme are presented together with the database, which will be open access from mid-2021.

Keywords Tropical cyclone · Cyclonic hazards · Interdisciplinary programme · Indian Ocean

1 Introduction

The South-West Indian Ocean (SWIO) is the second-to-third most active tropical cyclone basin in the world. Approximately 10%–12% of the world's total cyclonic activity takes place in the SWIO, where two regions are particularly involved: the Mozambique Channel and the open ocean east of Madagascar (Neumann et al. 1993). Mavume et al. (2008) and Leroux et al. (2018) confirmed this high activity and showed that the basin has an annual average of 9 to 10 tropical storms, half of which develop into

✉ Pierre Tulet
pierre.tulet@univ-reunion.fr

Extended author information available on the last page of the article

Published online: 10 March 2021

tropical cyclones (TC). Particularly intense TCs have developed in this part of the world recently. Very Intense Tropical Cyclone (VITC, WMO (2016), maximum of the average wind speed greater than 60 m s^{-1}; Hellen (2014)) and Intense Tropical Cyclone (ITC, maximum of the average wind speed between 46 and 59 m s^{-1}); Kenneth (2020)) were the two most intense tropical cyclones ever observed in the Mozambique Channel. More recently, ITC Idai (2019) caused more than 1000 deaths in Mozambique. VITC Fantala (2016) was the second most intense tropical cyclone ever recorded in the whole basin and devastated the Farquhar archipelago of the Seychelles. VITC Gafilo (2004) made landfall first on the north-eastern region of Madagascar and then on its south-western part, affecting more than 200 000 people and killing more than 350. In 2017, ITC Enawo also landed in North-East Madagascar and killed ~ 50 people (more than 300 000 people affected).

Two essential elements make the SWIO particularly sensitive to cyclonic risks. The first is large number of developing countries with fragile infrastructures and food and water supply systems, where a significant proportion of the population is living in extreme poverty. The second is due to the topography of some regions in the basin. Several islands of volcanic origin have steep slopes that locally reinforce convection, wind channelling effects and precipitation. Reunion Island, for instance, lays claim to several world records for cumulative rainfall: 1.1 m and 1.8 m over 12 h and 24 h, respectively, for TC Denise in 1966 (Holland 1993), and 3.9 m and 4.9 m over 72 h and 96 h, respectively, for TC Gamède in 2007 (Quetelard et al. 2007). Its orography has been shown to significantly influence the track and intensity of TCs passing nearby (Barbary et al. 2019). Terry et al (2013) also showed that in January and February a large proportion of storms in the SWIO had curving and sinuously moving trajectories. This track sinuosity is found to increase the storm longevity and the difficulties in forecasting, which reinforce the exposure of the territories.

Such intense precipitation generates landslides, ground movements and flash floods. In general, following the passage of a cyclone, several hundreds of landslides can impact the infrastructures (more than 200 landslides, rock falls or erosion phenomena were counted during TC Berguitta (2018) in Reunion Island (Aunay et al. 2018)). Sudden slope collapses and accelerations of slow-moving landslides are driven by the duration and intensity of precipitation (e.g. Caine 1980; Iverson 2000). Beyond the number of landslides, the moving masses involved can be considerable: two landslides of over 350 Mm^3 each, in the Salazie area of Reunion Island, move up to 1 m per year and more than 1,000 people live directly on their surfaces (Belle et al. 2014).

In some regions of Mozambique and Madagascar, which have vast plains or highlands as well as catchment areas sensitive to flooding, the impact of cyclonic rainfall can be particularly tragic. In 2019, for instance, floods caused by the landfall of TC Idai affected more than 2.6 million people in Mozambique, Malawi and Zimbabwe, with a devastating cost in human lives (more than 1000 deaths and 2450 persons declared missing), as well as significant economic damage (2 billion dollars estimated in 2019). Furthermore, TCs induce indirect economic impacts—both in time and space, and throughout the different levels of the economic fabric—whose magnitudes may compete with direct ones (Camargo and Hsiang 2015; Meyer et al. 2013). Such phenomena are especially relevant in the context of the SWIO insofar as the combination of both kinds of economic impacts has the potential to compromise a given country's long-term capacity to grow and develop (Hsiang and Jina 2014).

Regarding the strong impact of cyclonic hazards on lives and territories of the SWIO, a crucial question arises concerning the evolution of this risk with climate change. One

key aspect is the expected increase in ocean temperatures, future projections for which are described by the Intergovernmental Panel for Climate Change (IPCC). According to their scenario RCP8.5 describing "business-as-usual" high emissions, CMIP5 and CMIP6 climate models (i.e. those in the Coupled Model Intercomparison Project Phases 5 and 6) predict a global average increase in ocean surface temperatures of 2.6 °C–4.8 °C by 2100 (ICCP, 2013). In the SWIO basin, this increase could exceed 4 °C in the northern Mozambique Channel and have the direct consequence of significantly increasing the energy available for TCs. Associated with this temperature evolution, the tropical band delineated by the seasonal displacement of the inter-tropical convergence zone is expanding by 0.25°–0.5° latitude per decade (Lu et al. 2009; Staten et al. 2018, 2020). This expansion significantly widens the geographical zones conducive to cyclogenesis and thus increases the potential for cyclonic impacts on territories that are currently at low risk. It also affects the evolution of cyclone intensity. Kosin et al. (2014) highlight a year-on-year poleward shift in the latitude at which cyclones reach their lifetime maximum intensity. More recently, based on an analysis of 39 years of data, Kosin et al. (2020) have shown an 8% increase per decade in the occurrence of the most intense cyclones (categories 3–5 on the Saffir–Simpson scale).

High-resolution numerical modelling studies that re-simulate historical cyclones using projected future climates also point to an increase in cyclone risk. Most studies highlight an increase in intensity of the order of 10 hPa and an increase in precipitation of 15%–27% (Lackmann 2015; Parker et al. 2018; Mittal et al. 2019). However, to date, no regional or mesoscale studies have been carried out to study the climatic evolution of cyclone hazard in the SWIO basin.

With regard to future cyclone risk, in its AR5 report of 2014 (Impacts, Adaptation and Vulnerability, https://www.ipcc.ch/report/ar5/wg2/), the IPCC recommends (i) strengthening early warning capabilities, (ii) developing cyclone and flood shelters, (iii) improving building codes and practices, (iv) strengthening transport systems and road infrastructure, and (v) developing rainwater and wastewater management.

In response to some of these challenges, the ReNovRisk programme (REunion NOVative research on cyclonic RISKs, € 6 M) was launched in 2017. It is funded by the European Union (FEDER and INTER-REG5 funds), Région Reunion, the French government (CPER funds), the BRGM (French Geological Survey), and the CNRS (French National Centre for Scientific Research). ReNovRisk is developing an integrated study of the various risks associated with tropical cyclones in the SWIO basin by integrating mapping and economic analysis of the damage.

Coordinated by the Université de La Reunion, BRGM and IRD (French Research Institute for Development), ReNovRisk brings together a large consortium of research laboratories and scientific institutes from several countries in the western Indian Ocean, including France, Madagascar, the Seychelles, Mozambique, and Mauritius. Drawing on this wide pool of resources and expertise, the objectives of the ReNovRisk programme are multiple: (i) to improve observations and numerical forecasting systems for tropical cyclones in the SWIO, (ii) to study the cyclonic risks associated with winds, rainfall, ground movements, floods, submersion and swell over several target regions, and (iii) to develop a methodology suited to the SWIO that can estimate the direct and indirect economic costs associated with cyclonic damage.

This article is intended to present an overview of the ReNovRisk programme by detailing the presentation and strategy of its sub-programmes (Sect. 2). Some preliminary results from the various sub-programmes are presented in Sect. 3, and the ReNovRisk open databases are described in Sect. 5.

2 Organization and strategy of ReNovRisk programmes

The ReNovRisk programme is divided into four interactive sub-programmes (Fig. 1). ReNovRisk-Cyclone (RNR-C) is divided into two components referred to as "Cyclones and Climate Change" and "Cyclones and Precipitation". It aims to (i) improve the spatial coverage of TC observations over the SWIO, (ii) develop high-resolution TC forecasting models and (ii) analyse future TC activity at both basin and local scale from high-resolution climate and mesoscale simulations. The RNR-C outputs feed the other ReNovRisk programmes with swell fields, high-resolution winds and precipitation and also climate projections on the intensity and occurrence of cyclones. The aim of ReNovRisk-Erosion (RNR-E) is to study landslides, floods and solid transport in two sensitive catchment areas of Reunion Island. ReNovRisk-Transfer (RNR-T) analyses the transfer and connection of cyclonic risks across the western volcanic plateau of Reunion Island, which slopes down through temporary semi-urbanized ravines (flood risks) to the coastline of either the ocean or the back reef lagoon (risks of sediment transport, erosion, and submersion). RNR-T also provides other ReNovRisk programmes with high-resolution maps of rainfall over Reunion Island. ReNovRisk-Impacts (RNR-I) aims at mapping and analysing the economic vulnerability of, and the damage caused by TC in Reunion Island and Madagascar. Furthermore, RNR-I also approaches societal impacts of TC. The geographic area of the ReNovRisk programmes is shown in Fig. 2.

2.1 ReNovRisk-cyclone (RNR-C)

Given the colossal impact of TCs on local populations, infrastructures and economic development in the SWIO, it is essential to improve the prediction of cyclonic events at all spatial and temporal scales in order to adapt public development policies to the present and future risks faced by the territories. In this respect, research work carried out in recent decades has significantly improved the prediction of TCs at all time scales (DeMaria et al. 2014). The advent of coupled ocean–atmosphere models, in particular, constitutes a major step forward in assessing the impact of cyclonic activity at the

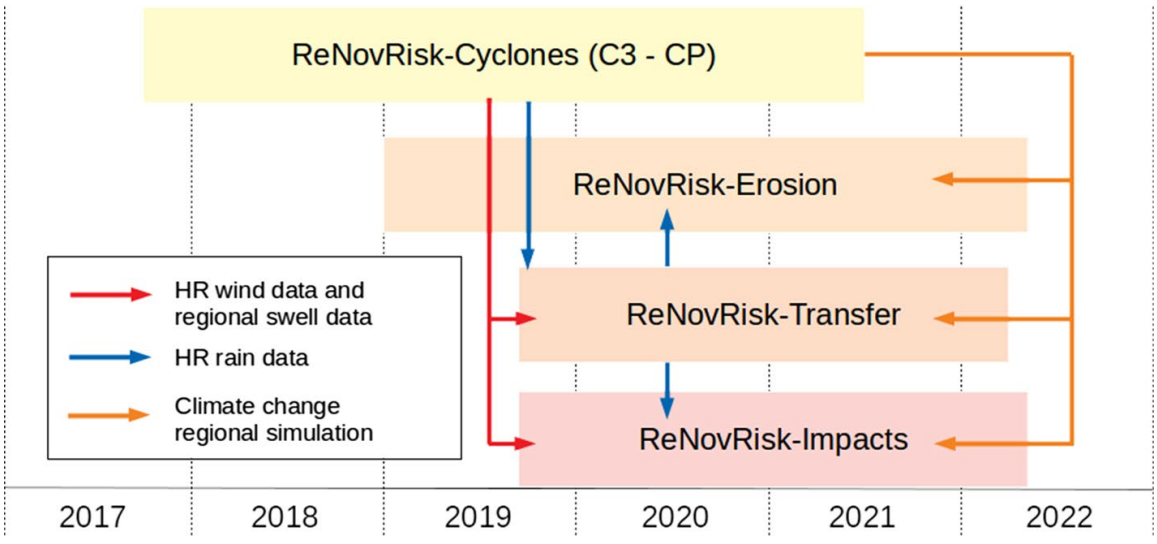

Fig. 1 Scheme of development times of the various ReNovRisk sub-programmes and data-feeding links between them

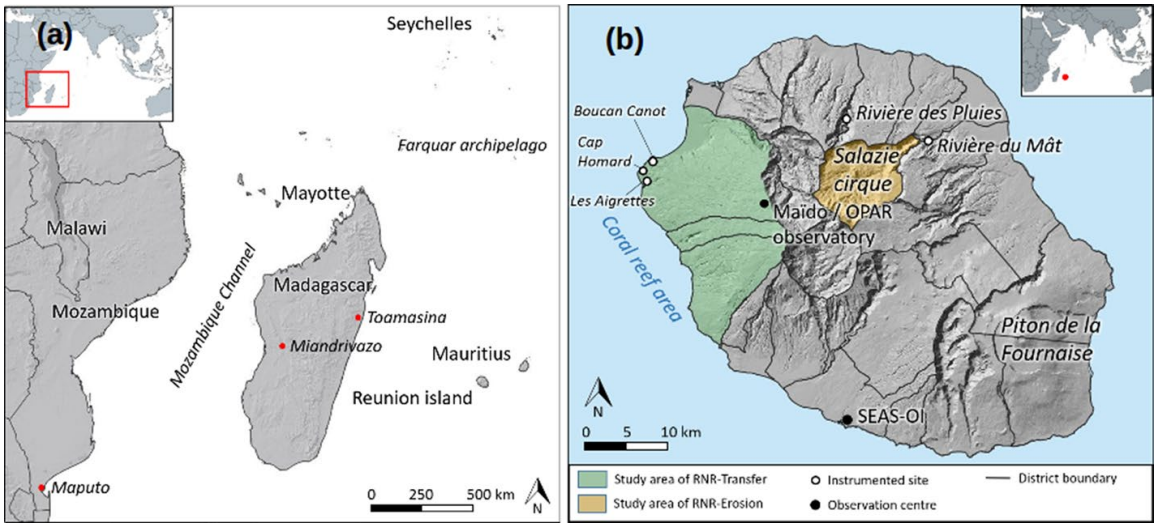

Fig. 2 Geographic area of the ReNovRisk programmes. **a** SWIO domain of ReNovRisk. **b** Reunion Island map and locations cited in the text

regional level (e.g. Eyring et al. 2016; Vitart et al. 2017). Nevertheless, it is commonly agreed that current models do not yet have the technicality and sophistication required to accurately assess the impact of TCs at the local scale.

Coupled numerical weather prediction (NWP) and climate models also require extensive observations to constrain and thoroughly assess the performance of their atmospheric and oceanic components. Because TCs develop, evolve and propagate primarily over oceanic areas, which are generally poorly equipped with conventional observing systems, collecting observations in TC basins can be extremely difficult. Due to the small proportion of land masses and also to the difficulties of sustainably operating observation systems in this poor area, the SWIO is the least instrumented of the six TC basins. Although satellite imagery has now made it possible to track the trajectories and general evolution of TCs all around the world, additional measurements are still urgently needed to study the mechanisms governing the evolution and impacts of low-pressure tropical systems in this particularly active basin.

In this respect, RNR-C has been built along three principal lines:

- An observation component, aimed at providing additional TC observations to calibrate, initialize and evaluate the performance of coupled models in this particularly under-instrumented region;
- A modelling component, aiming at developing a coupled, high-resolution (0.5 km–2 km), ocean–wave–atmosphere modelling system to represent the interactions between a TC and its environment as exhaustively as possible;
- A climate component, aiming at assessing the consequences of climate change on the properties (trajectories, intensity and structure) and potential impacts of tropical cyclones at both local and basin scales.

2.1.1 Observations

The observation component of RNR-C aims to provide accurate observations of TCs and their environments by reinforcing regional- and local-scale observing capabilities in the SWIO. To achieve this objective, RNR-C was built around three approaches.

The first is a conventional and ideally sustainable approach, based on the deployment of regional observation networks and the acquisition of new satellite observations of wind and sea swell in the SWIO. Regarding ground-based observations, a water vapour observing network composed of Ground-based Navigation Satellite System (GNSS) receivers and weather stations was deployed throughout the western part of the basin from November 2017 to September 2020 within the framework of the RNR-C's sub-programme "Indian Ocean GNSS Applications for Meteorology" (IOGA^{4}MET). This important achievement has significantly enhanced water vapour observation capabilities in the SWIO and provides a new tool to thoroughly investigate the water vapour cycle in this area (Lees et al. 2020; Bousquet et al. 2020a).

Regarding space-borne observations, a collaboration with ESA (European Space Agency) and IFREMER (Institut Français de Recherche pour l'Exploitation de la MER) has enabled a unique set of high-resolution (1 km) satellite images of sea surface wind and roughness to be collected from synthetic aperture radars (SAR) deployed onboard the Sentinel 1A/1B satellites of the European Earth Observation programme Copernicus. Throughout 2018 to 2020, SAR data have been acquired on demand (with 48 h notice) for about two-thirds of the TCs that developed in the basin over this period. (About one hundred images were collected, nearly half of which were acquired in the eye-wall regions of TCs and tropical storms.)

The second, an experimental approach, is based on the temporary deployment of various atmospheric and oceanic observation systems at different points in the basin. Several temporary atmospheric and oceanographic observing campaigns have been organized to validate the performance of coupled ocean–wave–atmosphere systems developed within the RNR-C programme (Sect. 2.1.2) the main achievement of which has been the organization of a regional field campaign that took place in various places of the SWIO from January 21 to April 8, 2019. During this field experiment, various sensors were deployed in and around Reunion Island, and in Madagascar, Mozambique, and Mayotte, to sample atmospheric and oceanic environmental conditions during the 2018–2019 TC season. A regional radiosonde network (RS) was deployed in Mayotte (France), Toamasina (Madagascar), and Maputo (Mozambique), enabling 700 soundings to be collected over this 2 ½-month period. Two ocean gliders were launched from Reunion Island to sample the thermodynamic properties of the tropical Indian Ocean up to 500 km from the island. An unmanned airborne system (UAS https://www.boreal-uas.com/), equipped with high-frequency aerosol, wind, and temperature sensors, was deployed for several weeks to measure ocean–atmosphere fluxes and aerosol concentrations in the immediate environment of TCs up to several hundred km from Reunion Island.

The third, an exploratory approach, is based on the deployment and evaluation of new and original methods of investigation to collect oceanic observations in the SWIO from biologging and seismic observations. A particularly original approach, based on biologging technology, has been explored to collect oceanic data from sea turtles equipped with autonomous environmental tags. A first experiment was carried out from January 2019 to September 2020 in the western part of the tropical Indian Ocean, with

the aim of assessing the relevance of low-cost sea turtle borne observations for ocean monitoring and modelling (Bousquet et al. 2020c). Another original approach, based on previous work by Davy et al. (2014, 2016) and Barruol et al. (2016), was also further investigated to evaluate and quantify extreme swell events from microseismic noise measurements recorded by ground-based and underwater seismometers. The analysis of data collected in RNR-C (Rindraharisaona et al. 2020) has demonstrated that terrestrial seismic stations could also be a great alternative for sampling Austral swell events by behaving as ground-based wave gauges.

2.1.2 Mesoscale modelling: improvement of mesoscale numerical models for TC forecasting

An important objective of RNR-C is to design, develop, and evaluate a high-resolution (0.5 km– 2 km) integrated modelling system based on the coupling of state-of-the-art atmosphere, ocean, and wave models. This tool, intended to prefigure fine-scale operational NWP systems to be used by WMO/RSMC Reunion (http://severeweather.wmo.int) in the medium term, will, in particular, investigate the internal physical processes responsible for TC intensification and produce realistic TC simulations over the most densely populated regions of the SWIO basin.

Based on the conceptual model of a tropical cyclone as a Carnot heat engine, the theory formulated by Emanuel (1986, 1988) predicts that the maximum potential intensity depends on the sea surface temperature and the outflow layer air temperature (Bister and Emanuel, 2002). In this context, an ocean–wave–atmosphere (OWA) coupled system has been developed for high-resolution modelling of tropical cyclones in the SWIO (Fig. 3). The coupling between the atmospheric model Meso-NH (http://mesonh.aero.obs-mip.fr/, Lac et al. 2018), the surface model SurfEX (https://www.umr-cnrm.fr/surfex/, Masson

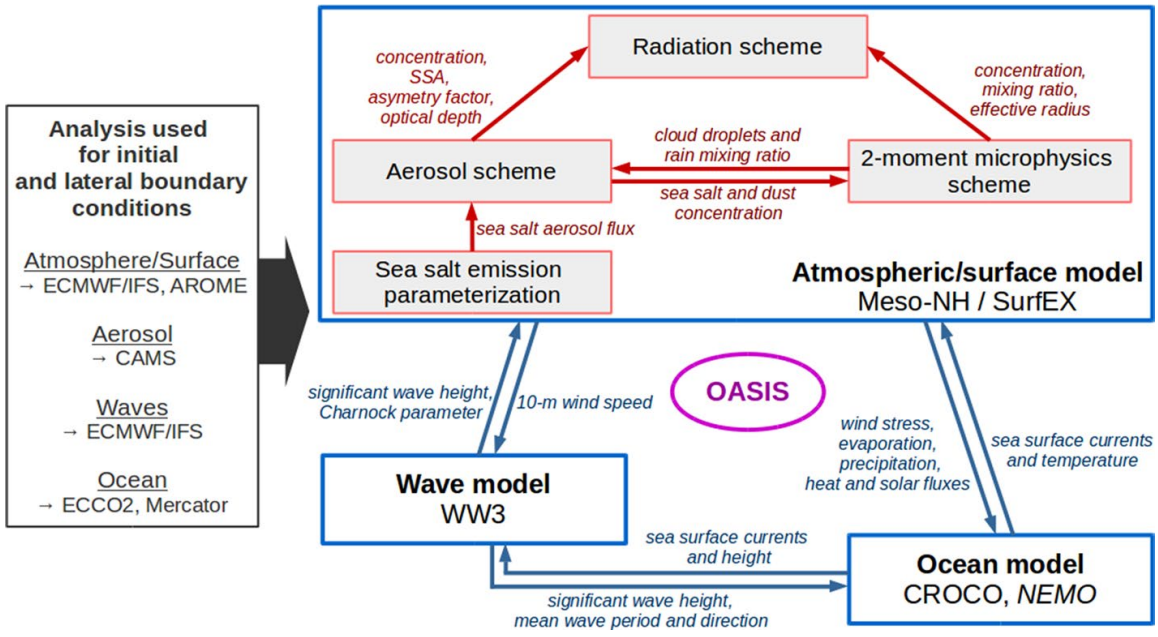

Fig. 3 Schematic diagram of the coupling systems in cyclone numerical modelling. The OWA coupling is shown in blue while the coupling inside the atmosphere/surface model is shown in red. Fields exchanged among the atmospheric, wave, and oceanic models are shown in blue italics; they are exchanged at intervals defined by the user (typically ~ 10 min). Fields exchanged among the atmospheric schemes are shown in red italics; they are exchanged at each time step

et al. 2013), the wave model WaveWatch III (http://polar.ncep.noaa.gov/waves/wavewatch/) and the ocean model CROCO (http://www.croco-ocean.orgref) was realized through the OASIS coupler (https://portal.enes.org/oasis, Craig et al. 2017) as described by Voldoire et al. (2017) and Pianezze et al. (2018). This coupled system is particularly innovative since it enables the user to represent (i) the air–sea interactions, which have long been recognized as a key issue in improving the accuracy of tropical cyclone intensity (e.g. Rotunno and Emanuel, 1987), (ii) the swell generated by the strong winds, and (iii) the sea salt aerosol emissions induced by the combined effects of strong winds and waves (Andreas et al. 1995). In non-polluted environments, these sea salt aerosols are the main source of condensation nuclei for cloud formation. A parameterization of such aerosol emission as a function of atmospheric, oceanic, and wave parameters (Ovadnevaite et al. 2014) has been introduced in the atmospheric/surface model. Once emitted, these aerosols are integrated in the ORILAM aerosol scheme (Tulet et al. 2005): they are transported by advection and turbulence and can be lost by sedimentation, and dry or wet deposition. The aerosol scheme was then coupled with the two-moment bulk microphysics scheme LIMA (Vié et al. 2016) as described in Hoarau et al. (2018a). Since cloud–radiation interactions are suspected to influence the track (Fovell et al. 2016), the structure (Bu et al. 2014) and the intensity (Trabing et al. 2019) of a tropical cyclone, specific developments on the secondary formation, and habits of ice crystals (Hoarau et al. 2018b) in the LIMA microphysics scheme are in progress. This will enable a better description of the ice water content, the ice crystal effective radius and the ice crystal shape, which are used as input for the radiation scheme. Attention has also been paid to initial and lateral boundary conditions for each component (atmosphere, surface, aerosol, wave and ocean) of the coupled system (see the box on the left in Fig. 3). This coupled system can be viewed as a prototype for the French operational model AROME. It has been run on several tropical cyclones (Bejisa, 2014; Fantala, 2016; Berguitta, 2018; Idai, 2019) to produce high-resolution precipitation, wind and wave fields all over the SWIO, and deliver some of these fields to the other sub-programmes.

2.1.3 Climate modelling

While it is generally accepted that global warming will have a significant impact on ocean surface temperatures, which is a factor favouring the development of TCs, no one really knows how the other ingredients involved in the formation of tropical low-pressure systems will evolve in the future. While disaster scenarios suggest an increase in intense events, some scenarios also suggest a "benevolent nature" that could counteract this pessimistic trend. In this respect, a key objective of RNR-C is to assess the consequences of climate change on the properties and potential impacts of tropical cyclones in the SWIO basin. The experimental strategy is based on two complementary approaches: (i) the use of high-resolution global and regional climate simulations to estimate the evolution of cyclonic activity at basin scale (changes in TC trajectory, intensity and structure; impact on water resources) and (ii) the use of high-resolution mesoscale coupled simulations to assess the potential impact of climate change on the structure and the impacts of TC in specific target areas such as Reunion Island.

To address this issue, high-resolution (~20 km–25 km) global climate simulations found with the French climate model ARPEGE-Climat (https://www.umr-cnrm.fr/spip.php?article124&lang=en) have been run to assess the impact of climate change on the frequency, distribution and, to a lesser extent, intensity of future tropical cyclones (Cattiaux et al. 2020). Higher-resolution simulations have also been carried out using the limited-area

climate model ALADIN-Climat and the integrated OWA model developed in the programme (Fig. 3) to analyse the response of TC to climate change in terms of structural development and determine whether changes in storm activity and/or structure will pose an additional threat to coastal areas and islands of the SWIO basin in the future (Thompson et al. submitted). The first results obtained from the analysis of the various simulations carried out in the programme are presented in Sect. 3.5.

2.2 ReNovRisk-erosion (RNR-E)

Among the impacts of cyclones landing on Reunion Island, hydrological floods, sediment fluxes and erosional processes are causes of major concern to population and infrastructures. The hydrological regime of the island's rivers stands out for the coexistence of several major parameters that predispose it to extreme vulnerability. Holding almost all the world records for rainfall between 12 h (1170 mm) and 15 days (6083 mm), the island presents a very marked relief with a peak at 3,069 m, exceptional escarpments up to 1500 m in height and having an average slope of over 70°, and very steep natural valleys and cirques. As a result, all the processes that can lead to erosion and ground movements are particularly active in Reunion Island.

The objective of the sub-programme RNR-E falls within this major issue regarding forecasting of and protection against torrential floods. Liébault et al. (2010) point out that the characterization of erosion and sediment transport in Reunion Island rivers requires better knowledge of the hydrological-hydraulic and geomorphological processes that control the production and transfer of liquid and solid flows.

To meet this target, RNR-E involves the monitoring and data acquisition at various scales of two representative hydrological catchment areas on Reunion Island: Salazie cirque and Rivière des pluies (Fig. 2b). New instrumentation has been set up in the aim of analysing and quantifying the interactions between upstream and downstream in the following processes:

- Formation of the sedimentary stock: this is linked to erosion phenomena in the upstream parts of the catchment areas and to gravity destabilization (in particular rampart collapses and landslides). GNSS, a network of geodetic markers, LiDAR and seismic surveys are being implemented on the six major large-scale landslides in the Salazie cirque and in the Rivière des Pluies watershed. We are also carrying out hydrological, hydrogeological and geochemical monitoring of groundwater and surface water at the level of these landslides. In addition, the structure from motion technique has been applied using historical aerial images, image correlation techniques and SAR interferometry to characterize landslide dynamics.
- Flow processes: completing the hydrological monitoring equipment of the experimental catchment "La Rivière des Pluies", which is part of the French OZCAR network (https://www.ozcar-ri.org/observatories/the-network/), RNR-E proposes to detail the variability of the contribution of tributaries to the flash flood processes. Specific photogrammetric discharge monitoring stations are used in order to document an accurate rainfall–runoff model (Stumpf et al. 2016).
- Bedload transport: as direct measurements of the bedload transport are extremely difficult to make during a tropical cyclone, RNE-E uses the high-frequency seismic noise generated by the rivers as a proxy for the sediment transport. Eleven broadband seismometers have been deployed along two rivers, both located in the northern side of the

island (Rivière des Pluies and Rivière du Mât, Fig. 2b), in the framework of the "Rivière des Pluies" temporary seismic network (Fontaine et al. 2015). This has allowed us to analyse the spatial and temporal variations of the seismic noise along these rivers with respect to the rainfall and hydrological data, and to characterize the bedload variations during tropical storms and cyclones (Gonzalez et al. 2017; Gonzalez 2019; Gonzalez et al. submitted). A very good correlation was obtained between the seismic noise amplitude and the water level during the river flood related to TC Dumazile in March 2018 (Gonzalez 2019; Gonzalez et al. submitted). Preliminary results show that the amplitude of the high-frequency seismic signal (> 1 Hz) recorded at the seismometers may be used as a proxy for the water level during a cyclone. Spectral and polarization analyses of seismic data were also used in order to decipher the seismic signature of water flow and bedload transport.

Firstly, it was shown that the behaviour of landslides can be modelled by inverse models with a bimodal transfer function using a Gaussian-exponential impulse response, linked to the rain and piezometric level (Belle et al. 2014). Then, the recharge of the large Grand Ilet landslide (350 Mm^3) in the humid tropical season was characterized through a robust, multidisciplinary hydrological approach, notably comprising a precise water budget of the landslide. It appears that surface processes play a major role in the landslide recharge regime (Belle et al. 2018).

Then, landslide displacement mapping based on ALOS-2/PALSAR-2 data using image correlation techniques and SAR interferometry was applied to the Hell-Bourg landslide (Raucoules et al. 2018). The capability of space-borne high-resolution L-band synthetic aperture radar (SAR) images (ALOS-2/PALSAR2 data in StripMap SM1 mode) for deriving and mapping two components of the deformation of slow landslides has been investigated. The deformation was characterized on the basis of sub-pixel correlation offset tracking techniques and differential SAR interferometry. On the Hell-Bourg landslide (Fig. 2b, with displacements up to about 1 m $year^{-1}$), the deformation maps produced performed significantly better than the C-band or lower-resolution SAR data used in previous studies. A comparison was carried out with GNSS data acquired on the test site. Even with a reduced image set (seven acquisitions), detailed deformation maps and information on deformation evolution during 2014–2016 could be generated.

Finally, RNR-E has implemented a new methodology based on structure-from-motion processing of archive aerial photographs to quantify geomorphological changes in Reunion Island since 1978 (Rault et al. 2020). Photographic archives indeed hold a decades-long 3D history and, for the first time, our measurements reveal the cumulated signature of landslides on the Cirque de Salazie from 13 cyclones over the 37 years investigated. Such an approach demonstrates that the structure-from-motion technique is a game changer for landslide risk mitigation planning.

Most of the acquisition of the data presented above is still ongoing (as of September 2020) and is ready for the next cyclonic event in Reunion Island.

2.3 ReNovRisk-transfer (RNR-T)

RNR-T focuses specifically on the study of cyclonic hazard transfer in natural environments. It focuses on the natural risks associated with cyclones landing on Reunion Island and more specifically on the western micro-region, taking its workshop area as the Maïdo massif, the coastal strip between Saint-Paul and Saint-Leu, the back reef lagoon and the

open ocean, depending on the position along the coast (green area in Fig. 2b). The general objective is to analyse how cyclonic hazards are transferred between the natural environments of the atmosphere, the hydrosphere, the littoral zone and the open ocean. With regard to the transfer from the atmosphere to the hydrosphere and the coastline, the atmospheric hazards are the wind gusts and precipitation associated with cyclonic events. These hazards depend on many factors intrinsic to the cyclone and other factors in relation with the landfall area. Cyclonic winds are, by nature, the most intense in the upper reaches of Reunion Island, an area where the most intense cyclonic precipitation is generally also found. The scientific questions associated with these themes arise at the interfaces of the natural environments.

Between the atmosphere and the hydrosphere, the challenge concerns the quality of the precipitation data that are delivered to hydrologists to initialize hydrological models. Whether the issue is the rainfall observations or the forecasts by numerical models, the difficulties lie in the validation of the quality of the data. The spatial representativeness of rainfall and wind observations is a key factor for studying natural hazards, especially in the complex topographical context of Reunion Island. These scientific questions are being attacked by meteorological observations at the OPAR observatory (https://opar.univ-reunion.fr/) using new data fusion and numerical modelling methodologies to produce high-resolution rain and wind data of landfalling TCs over Reunion Island, with a focus on the Maïdo massif.

For this purpose, a numerical modelling method to produce low-cost high-resolution wind fields of landfalling TCs has been developed. To produce wind fields consistent with both the position and intensity of the system, the large-scale environment and the topography of the targeted region, the Meso-NH atmospheric model was implemented with Holland's parametric approach (Holland 1980) coupled with the use of meteorological analysis from the IFS (Integrated Forecasting System) model of ECMWF (European Centre for Medium-Range Weather Forecasts). The parameters used in the Holland formulation are deduced from the RSMC Reunion Island best-track. This so-called bogus method was set up within the framework of the SPICy programme (Système de Prévision des Inondations en contexte Cyclonique, http://spicy.brgm.fr/fr) and tested on 5 historical cyclones that affected Reunion Island (Bejisa, Dumile, Felleng, Gamède and Dina). The structure reproduced was shown to be realistic as long as the information on the radius of the maximum winds injected into the bogus was relevant. The wind fields reconstructed by the bogus method showed good agreement with in situ observations as soon as the orography of the island was well reproduced. This method was deployed in the framework of the ReNovRisk programme (Vérèmes 2020, Technical Report). To date, high-resolution wind fields of 6 tropical cyclones at landfall on Madagascar and Reunion Island have been produced. 10 m wind gusts were provided at a horizontal resolution of 500 m on Reunion Island for Dina (2002), Berguitta (2018) and Bejisa (2014), and on Madagascar for Enawo (2017). A horizontal resolution of 2 km was used on Madagascar for Gafilo (2004) and Ava (2018). This approach enables us to produce high-resolution wind fields at low numerical cost. It should be noted that this tool does not permit the precipitation fields to be produced since the rainbands are not reproduced by the bogus method.

Additionally, the operational product ANTILOPE (ANalyse par spaTIaLisation hOraire des PrEcipitations) archived by the French meteorological office (Météo-France) has been implemented over Reunion Island. ANTILOPE estimates the quantity of rainfall at the scale of a 1 km^2-grid from radar data corrected by rainfall data (Laurantin 2008). The archived product is calculated for a 1-h time step. It is a hybrid product of the PANTHERE quantitative precipitation estimate (QPE) (Parent du Châtelet et al. 2005) and a kriging

interpolation of the rain gauges available at the time of QPE (Pauthier et al. 2016). The variation of the radar reflectivity over the hour is analysed for each pixel of 1 km^2 and in steps of 5 min. This variation automatically associates a fraction of the current hour with a convective rainfall (between 0 and 60 min) and its complementary fraction to a stratiform rainfall. The stratiform part is obtained by kriging the large-scale rainfall values, whereas the convective part is obtained by detecting cells on the radar images and is corrected using the convective accumulations of the rain gauges located under these cells. The ANTILOPE data were not produced and archived by Météo-France until 2016. However, for Reunion Island, the PANTHERE rain data have been available since the end of 2013, so a reprocessing of the ANTILOPE data over the 2014–2019 period for Reunion Island is possible. ANTILOPE almost fully corrects the underestimation of the precipitation obtained from PANTHERE (Fig. 4). Within the framework of RNR-T, an external service was therefore entrusted to Météo-France to reprocess the entire database for the Reunion Island area. The 15-min time-step ANTILOPE dataset has been generated for the 2014–2019 period with a horizontal resolution of 1 km^2. It provides a view not only of cyclonic rains but of all rainfall on Reunion Island and will thus make it possible to assess the exceptional nature of past or future events. The ANTILOPE database is also expected to provide input data for econometric models developed by RNR-I.

Along the western slopes of the Maïdo massif, the challenge in the hydrosphere stems from a lack of knowledge of the behaviour of temporary ravines of the Maïdo massif, in particular their disconnection from the underground reservoirs and their very large infiltration capacities at the beginning of the rainy season. Time series of stream flows in these ravines are very sparse and most often uncorrelated with the simultaneous availability of good rainfall series. RNR-T will attack these obstacles, firstly by setting up hydrological instrumentation along two ravines in almost ungauged catchments and, secondly, by using a semi-distributed rainfall–runoff model (Rojas-Serna et al. 2016; De Lavenne et al. 2019). This model has fine spatial resolution (square kilometre) and hourly time steps, suited to the nonlinear behaviour of this type of ravines, and is sequentially calibrated considering

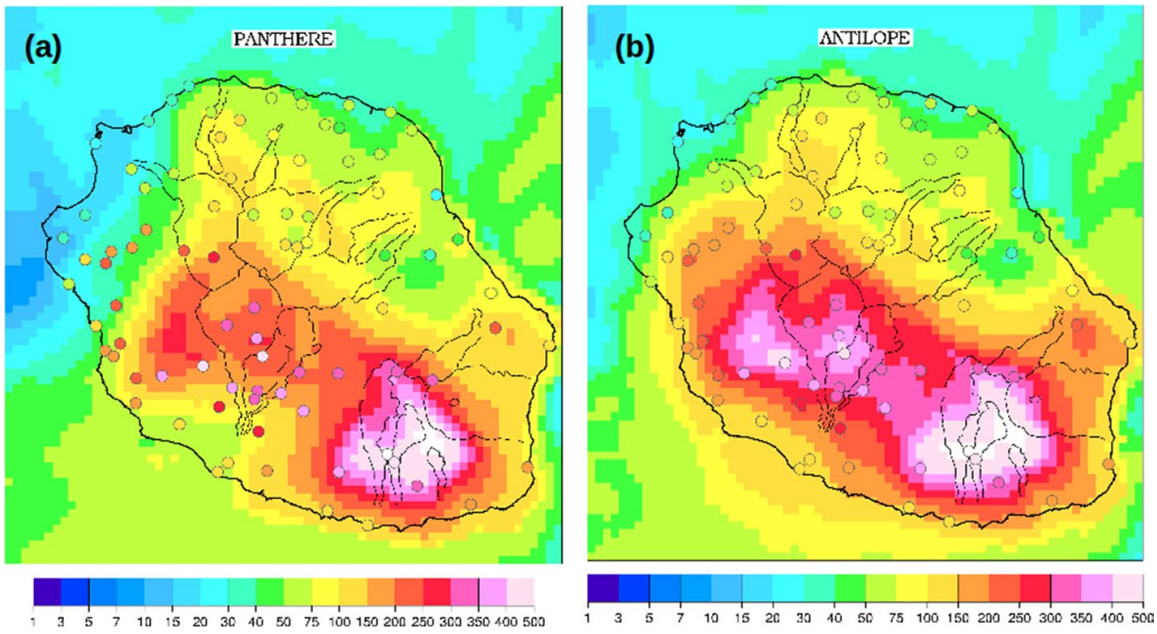

Fig. 4 Cumulative rainfall (mm.day-1) observed on January 1, 2018 during TC Beguitta with PANTHERE **a** and ANTILOPE **b**. Rain gauge data are superimposed (coloured circles)

the observations available at the outlet of the catchment and at different gauging points inside the catchment (De Lavenne et al. 2019).

The Maïdo watershed is characterized on the sea side by the largest fringing reef of Reunion Island (400 m wide). Although the contributions of the watershed are weak on a yearly scale, allowing the development of the reef life, in a cyclonic context the forcing of the watershed, is not negligible. The inputs of fresh water loaded with suspension and nutrients modify the reef environment and can alter the calcification and therefore the growth of the coral. Oceanic forcings (swell) on the reef barrier remove pieces of coral, which can feed the beaches with coral debris. Water masses that submerge the reef barrier and pass through the reef system are the vector of a strong littoral drift. The instrumented site of "La Passe de l'Hermitage" (coral reef area on Fig. 2b) has been set up to quantify the processes and impacts of cyclonic events. The interdisciplinary scientific team in charge of this site is developing tools and indicators to observe, monitor and model the impacts of climate change in the coastal reef zone, and the possible synergy with local anthropogenic pressures. The measurement activity includes (1) monitoring global and local anthropogenic pressures (ocean acidification, freshwater groundwater flow, beach frequentation), and (2) monitoring indicators of beach morphological dynamics and loss of resistance and/or resilience (reproduction and recruitment of scleractinian corals and millepores, carbonate balance), and mapping the trajectories of benthic communities in response to disturbances. These activities are partially approved at the national or international level (SNO Dynalit; https://www.dynalit.fr/).

2.4 ReNovRisk-impacts (RNR-I)

The main goal of RNR-I is to assess both the economic vulnerability and the potential economic impacts of cyclones. Such evaluations are intended to serve as decision support tools in policy- and decision-making.

Among the impacts of natural hazards (see, for example Hallegate (2014)), RNR-I will pay special attention to two distinct effects. On the one hand, immediate direct effects, namely the direct monetary costs of destruction/reconstruction due to the damage caused by a TC event, will be considered. On the other hand, indirect long-term effects (belated observable effects caused by the consequences of a TC over the territory) will be studied focusing on i) the macroeconomic repercussions of the aforementioned damage throughout the territory (cross-sectoral effects) and ii) the consequences on socio-economic determinants (e.g. fertility or education).

For direct effects, RNR-I seeks to develop a general protocol largely based on spatialized analysis, which can include bottom-up (Reunion Island) as well as top-down (Madagascar) cases. At the core of this protocol is the idea that impacts are a combination of hazard, exposure and vulnerability. Regarding hazard, a TC presents particularities that should be taken into account, as characteristic rainfall and high-speed winds of TCs (multi hazard-inputs) can induce storm surges, flooding events and landslides (cascading hazard outputs), which are also likely to significantly amplify the vulnerability of the territory. Intersecting hazard maps with land-cover information, RNR-I produces exposure maps (of entities likely to be impacted by the hazards-output). Building from these maps, we will focus on the physical and economic dimensions of vulnerability evaluated by means of damage functions. The physical vulnerability approaches the variable degrees of individual damage that, e.g. buildings, infrastructures or crops, suffer depending on the intensity of the hazard

(confirmed by remote sensing). The economic valuation of the level of destruction, linked to the value of the land use, determines the economic vulnerability.

For the characterization of cascading output hazard, monitoring the spatial footprint of the TC impacts by remote sensing offers great potential for assessing the extent of impacted areas. For this purpose, RNR-I has developed two automated processing flows, based on high spatial resolution optical and radar satellite data (10 m), that detect changes between a reference image before the cyclone and post-event images. These two analyses are complementary. Changes detected with Sentinel-1 data, based on the normalized difference ratio, allows the extent of flooded areas to be monitored as close as possible to the cyclone event (Alexandre et al. 2020). Changes detected with Sentinel-2 data, based on the use of change vector analysis (CVA) (Mouquet et al. 2020), which has shown its potential for monitoring changes in surface states (Hussain et al. 2013), allow a better characterization of land-cover change over longer time periods. Various events in the SWIO have been processed, and the results have been made available to the public.

For indirect effects, the negative impacts are not as obvious, especially because propagation mechanisms within socio-economic dimensions remain mostly undisclosed. RNR-I tackles this issue through two complementary approaches. We first rely on modern econometric techniques (Dell et al. 2014 or Camargo and Hsiang, 2016) together with the opportunity of merging geolocated data on the magnitude of TCs, and also on both economic and social features. The econometric strategy enables us to focus on how households reorganize their lives in the aftermath of TCs. One innovation of RNR-I is to focus on the causal effect of TCs on birthrate. The second approach undertakes the construction of theoretical models (CGE), accounting for the interdependence among economic agents, to explain the transmission channels through which the indirect effects take place (Narayan (2003) or Botzen et al. (2019)).

The data of RNR-C and RNR-T will be used by RNR-I for direct comparisons with the outputs of the system detecting changes in satellite images following the passage of a tropical cyclone. Furthermore, the simulated wind fields will also be used by RNR-I as output-hazard data for the development of either simulation models—computational laboratories devoted to the ex-ante evaluation of shocks—or econometric models—statistical models based on ex-post data in the aim of uncovering relations between relevant variables—to evaluate the potential socio-economic impact of cyclones (see Sects. 3.1 and 3.4). In the particular case of TC Enawo, the cross-analysis of the modelled wind field with the results of the change detection algorithms on Sentinel 2 satellite images shows good correlations between the maximum winds and the decrease in vegetation cover over a hundred kilometres around the landfall point, despite the difference in resolution and the presence of numerous clouds at this period (not shown).

3 Presentation of cross-disciplinary results

3.1 Floods following TC Ava in the Miandrivazo region

Coming from the north-east of the island, TC Ava landed on 5 January 2018 near the city of Toamasina on the east coast of Madagascar, with sustained winds of more than 150 km h^{-1}. Overall, the cyclone severely hit and caused heavy rainfall throughout the central part of the country and particularly in the studied region of Miandrivazo (Fig. 2a). Rainfall image maps computed from RNR-C meteorological models showed that TC Ava

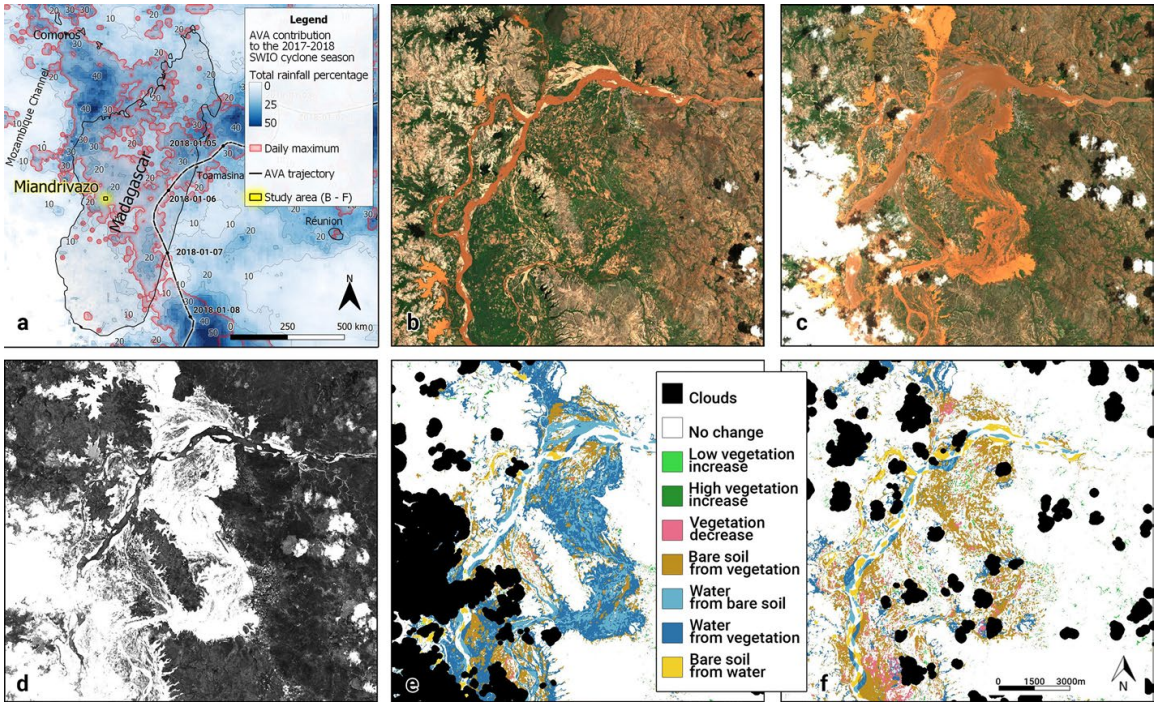

Fig. 5 Detection of changes between two remote-sensed images associated with TC Ava. **a** Location map of the Miandrivazo study site in Madagascar and meteorological conditions during TC Ava. **b** Sentinel-2 imagery of the region before the cyclone (25/12/2017) and **c** after cyclone Ava (09/01/2018). **d** Magnitude of changes between images (b) and (c) (the lighter the shade, the greater the change). **e** Classification of the main categories of changes just after the cyclone impact (09/01/2018) and **f** ten days later (19/01/2018)

brought about 20% of the total annual rains and reached the maximum daily precipitation for the whole 2017–2018 cyclone season in this area (Fig. 5a).

With the image of 25 December 2017 as a reference, we used the CVA algorithm to highlight areas of greatest change and compute classification maps of the impacts on two post-event images, 9 and 19 January 2018, respectively, 4 and 14 days after the event (Fig. 5b and c).

The results show a first rapid flooding of the entire floodplain, covering agricultural and forest plots, but sparing buildings and urban areas located on higher ground (day + 4, Fig. 5d and e). Two weeks after the event, most of the flooded areas were replaced by bare wet soils, mainly affecting the agricultural parcels, which suffered strong decreases in crop cover. The main riverbed was deeply and durably modified, with the appearance of sand-banks and new water bodies (Fig. 5f).

3.2 Cyclonic heavy precipitations on landslides

A forced atmospheric high-resolution (500 m) simulation of TC Bejisa initialized and coupled at the lateral boundaries by the ocean–wave–atmosphere system (Meso-NH-OVA described previously with a 2 km resolution) has been carried out in order to obtain higher-resolution wind and rainfall maps over Reunion Island. The 24-h cumulative rainfall on 1 January 2014 during TC Bejisa shows three zones with cumulative rainfall greater than 250 mm in both the observations and the simulation (Fig. 6). The rainfall observations are a merged product of rain gauges and radar data given by the ANTILOPE QPE product. The zone of heavy rainfall in the centre of the island is relatively well reproduced by the model,

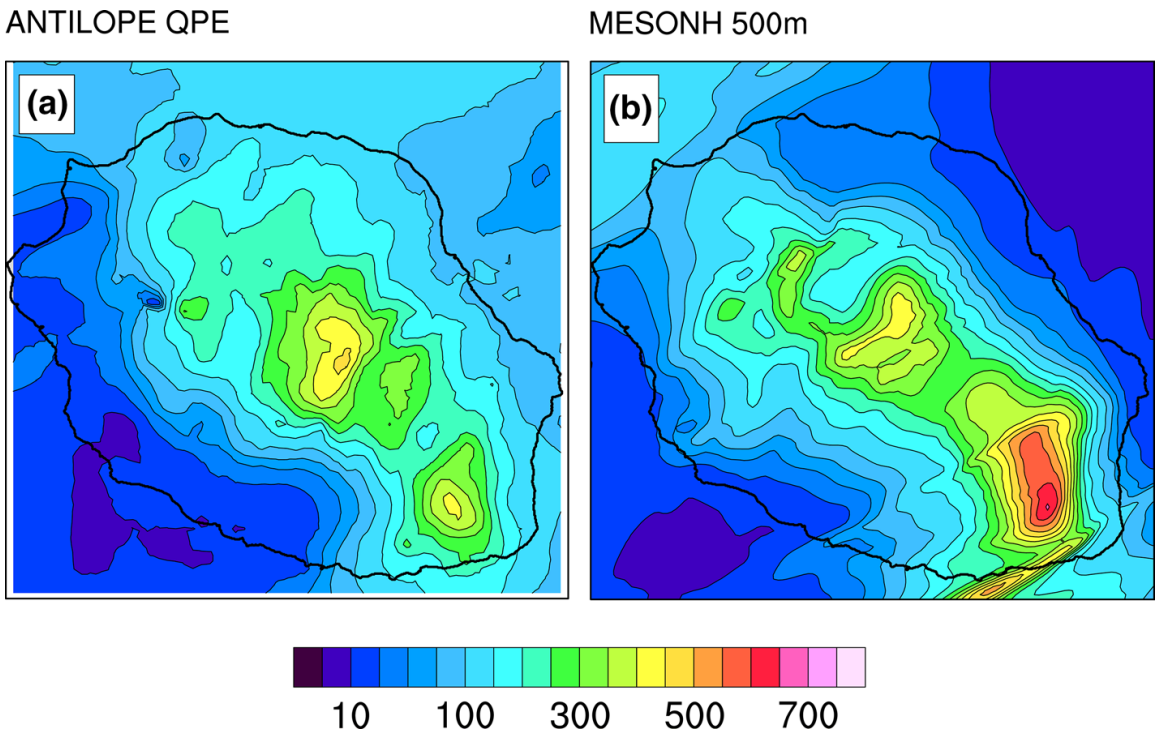

Fig. 6 Cumulative rainfall over 24 h for the day of January 1, 2014 (mm) given by ANTILOPE QPE (radar and rain gauge observations, (**a**) and modelled by Meso-NH with a horizontal resolution of 500 m (**b**)

although the simulation tends to give slightly higher maximum values (~500 mm) than the merged data (~450 mm). In the simulation, the maximum rainfall is located on the south-eastern flank of Piton de la Fournaise (Fig. 2b) with values greater than 700 mm, whereas they barely reach 400 mm in the observations. This tendency of the models to overestimate rainfall on the south-east flank of the volcano has been found in other simulations of intense precipitation events. It should be noted, however, that the density of rain gauges is quite low and that radar acquisition in this area is partially masked by the orography. The third, northernmost, zone of maximum cumulative rainfall is overestimated by the model. While the cumulative rainfall is relatively well represented by the model on the west coast of the island, with values between 10 and 100 mm, the model tends to underestimate the cumulative rainfall over the north-east and east. This may be due to the slight shift of the modelled TC to the west compared to observations. Even though the rainfall restitution is not perfect, and taking into account the uncertainties in the production of an observed 2D rainfall field (especially in areas with low coverage in observations such as the south-eastern flank of the volcano), using a resolution of 500 m significantly improves the spatial distribution of rainfall (not shown).

During TC Bejisa (January 2014), beyond many small "normal landslides", a significant one (1.1 million m^3) occurred in the centre of Reunion Island in the Salazie area (Fig. 2b and Fig. 7). After regular field observations, its volume was calculated by comparing two high-resolution DEM (LiDAR surveys). This landslide resulted in the accumulation of a large amount of various materials in the "Roche à Jacquot river" bed (Salazie cirque), most likely creating a temporary dam in the river. The dam vanished rapidly during Bejisa because of the strong river flow (a few tens of $m^3\ s^{-1}$). Fortunately, neither the landslide nor the rupture of the dam had an impact on infrastructure or people.

In the next step, rainfall data produced by ANTILOPE will be used to estimate the slope instabilities. Groundwater is one of the multiple and various factors that significantly

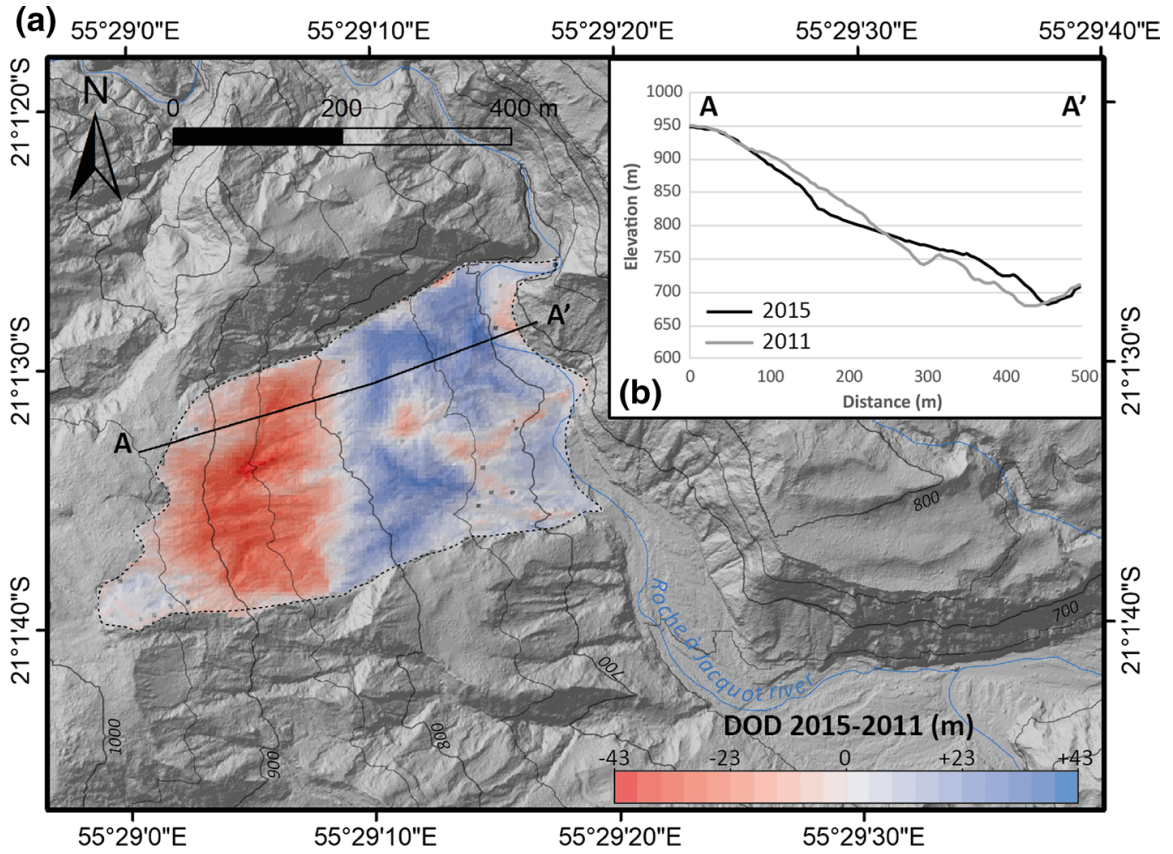

Fig. 7 1.1 Mm^3 landslide triggered by the cyclone Bejisa in 2014 in Salazie. (a) DEMs of Difference (DOD) at 5 m resolution in the area affected by the landslide, surrounded by the dotted line; the red (erosion) and blue (accumulation) zones reveal major topographic changes between 2011 and 2015 (acquisition years of the DEMs). The black line A–A' marks the ends of the 2011 and 2015 topographic profiles presented in (**b**) showing clear mass transfer

influence landslide displacement. A rise in water tables during aquifer recharge (e.g. after rainfalls) increases hydrostatic pressure in the media, which tends to decrease the landslide shear strength and cause the landslide to accelerate (Iverson and Major 1987; Baum and Reid 1992; Van Asch et al. 1999; Coe et al. 2003; Cappa et al. 2004; Corominas et al. 2005; Schulz et al. 2009).

The prediction of the movement pattern of landslides is assessed using physically based numerical modelling approaches (Corominas et al. 2005; Malet et al. 2005; Tacher et al. 2005; van Asch et al. 2007; Fernández-Merodo et al. 2012) or inverse numerical modelling that combines both numerical approaches and observations (Belle et al. 2014; Bernardie et al. 2015; Vallet et al. 2015). For both techniques, accurate spatial and temporal rainfall data are required.

3.3 Cyclonic swell impact on beach profile morphology

The ReNovRisk programme seeks to relate the evolution and distribution of cyclonic wave heights to the evolution of the coastline and the coastal sedimentary stock on Reunion Island. The first exploratory study was based on TC Bejisa.

The swell field was extracted from a simulation at 2 km horizontal resolution using the coupled ocean–waves–atmosphere system (CROCO, WW3 and Meso-NH) (Pianezze et al. 2018). The significant wave height and direction are shown in Fig. 8. On 1 January

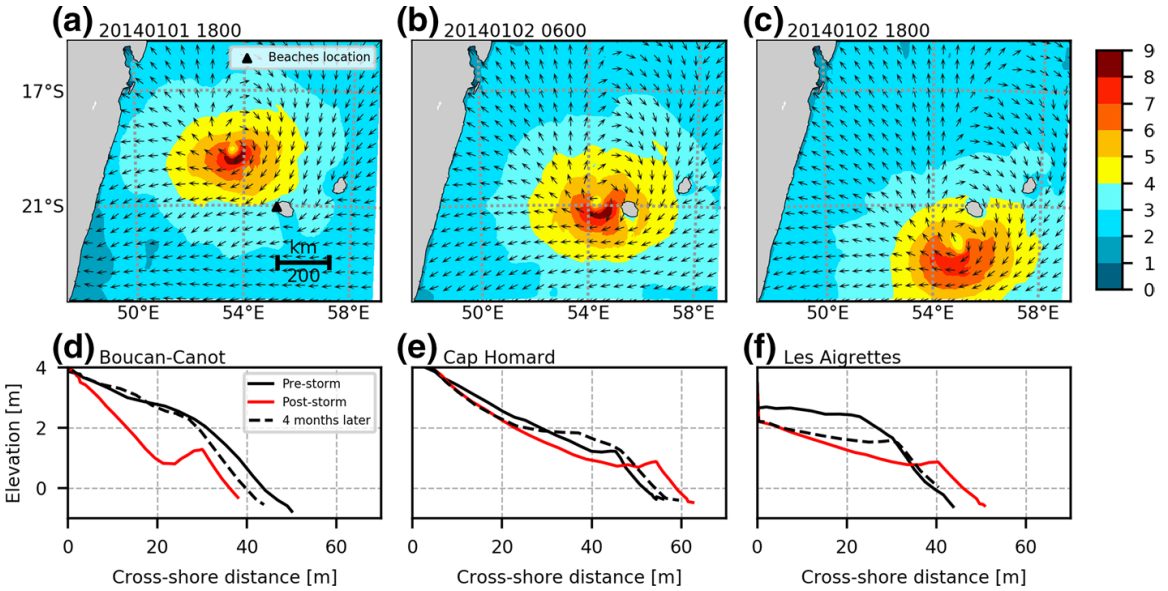

Fig. 8 Top: Significant wave height and direction simulated by Meso-NH-WW3-CrOCO during TC Bejisa. **a** 01 January 2014 at 18 UTC, **b** 02 January 2014 at 06 UTC, and **c** 02 January, 2014 at 18 UTC (Based on Pianezze et al. 2018). Bottom: Morphosedimentary evolution of beach topographic profiles caused by cyclone Bejisa at three sites:**d** Boucan Canot, **e** Cap Homard and **f** Les Aigrettes. Pre-storm topographic profiles (black lines) correspond to the date of 14 December 2013, post-storm (red lines)–17 January 2014 and the black dotted line corresponds to 4 months after Bejisa, that is, to 27 May 2014

at 18 UTC (Fig. 8a), the system was located north-west of Reunion Island and moving southwards, the maximum significant wave height, between 8 and 9 m, being concentrated under the wall of the system. When it passed closest to the island on 2 January at 06 UTC (Fig. 8b), the whole coastline was exposed to waves, and the maximum significant wave height of the cyclone was around 9 m. After Bejisa had passed close to the island's coasts, the south and west facades were still affected by strong swell as the wave fields also propagated northwards (Fig. 8c).

At the same time, within the framework of DYNALIT, the seasonal and paroxysmal morphosedimentary dynamics of beaches were monitored (Mahabot et al. 2017a, b) along three cross-shore profiles of the carbonate sandy beaches that were impacted by the cyclonic swell of TC Béjisa: "Boucan Canot", "Cap Homard" and "Les Aigrettes" (location on Fig. 2b).

Close to these three beaches, the temporal evolution of the cyclonic swell was characterized by a coupled simulation. The simulated significant wave height exceeded 3 m for 37 h from 1 January at 19 UTC to 3 January at 9 UTC. Since this swell was directly produced under the TC, as the TC passed along Reunion Island, the wave direction varied from south to east, affecting these beaches differently. To assess the impact of TC Bejisa on these three beaches, measurements by Differential Global Positioning System were made one month before the cyclone, two weeks after and 4 months after the cyclone. Profiles were established on a radial between the foreshore and backshore. The profile of Boucan Canot (Fig. 8d) presents the main morphological and volumetric change induced by Bejisa. The toe of beach retreat attained 7.5 m and very significant erosion can be observed along the profile, which reaches a thickness of 2 m between 20 and 25 m cross-shore distance. Along the profile, the volume change rate attained -42.53 ± 1.6 m^3. Four months after Bejisa, during fair-weather conditions, waves slowly carried material back on shore to rebuild–more or less–the original profile. However, the lower foreshore still retains the

after effects of the cyclonic swell and the head of the beach profile also shows a slight loss of sediment thickness, which can be expected to be perennial as there is no more dune recharge on this built-up coastline. After Bejisa, the Cap Homard (Fig. 8e) profile essentially shows a displacement of the beach berm by about 10 m, resulting in an advance of the beach profile of about + 7.2 m. In addition, the whole profile underwent a decrease in sedimentary thickness of about 40 cm on average. In addition to this transfer between the backshore and foreshore, the cumulative sediment loss was -6.76 ± 2.21 m^3. Four months later, the beach was rebuilt with a convex berm that was larger than before Bejisa hit. Finally, the Les Aigrettes profile (Fig. 8f) shows a sediment transfer from the backshore to the foreshore and the nearshore, resulting in an advance of the beach profile by about + 6.7 m. However, this advance was the result of the transfer from the backshore/foreshore to the nearshore zone. The volume change of -23.42 ± 1.71 m^3 after Bejisa is a good indicator of the lowering of the beach profile. Four months later, the profile had not recovered its initial morphology. Although beach recovery from severe storms has been shown to spread over years to decades (Dodet et al. 2018), in Reunion Island, on coral reef beaches, no long-term reconstruction of beach profiles has been demonstrated (Mahabot et al. 2017a, b).

3.4 Integration of simulated wind fields in the evaluation of direct economic impacts

Wind-induced physical damage to buildings and infrastructures can be very severe and increase their vulnerability—and the vulnerability of the assets they may contain—to TC induced hazards, such as floods. The identification of such damage, and its consequences in the socio-economic fabric, is therefore essential for the evaluation and quantification of TC impacts (Tamura 2009; Camargo and Hsiang 2015).

The simulations of high-resolution wind fields produced by ReNovRisk using the Bogus method (Sect. 3.2), given their dynamic character (output every 15 min), can be used to finely identify entities exposed to potentially damaging winds.

In the computational models for the ex-ante evaluation of economic impacts under development in RNR-I, the utilization of the high-resolution wind fields simulated enables both the entities exposed and the duration of the exposure to be identified. In turn, this thorough identification of exposed entities should allow fine estimations to be made of potential damage to buildings, infrastructures and plots. Figure 9 illustrates the potential of the simulated high-resolution wind fields in the analysis of exposure. The figure represents three snapshots of the simulation of cyclone Bejisa, over a layer of urban land use composed of buildings and infrastructures, in which the changes in wind speed can be appreciated as the cyclone moves southward (wind speeds represented have been limited to those that can cause damage, i.e. those higher than ~ 25 m s^{-1} (Tamura 2009)). As can be appreciated, the identification of entities exposed to damaging winds, together with an estimation of the duration of the exposition, is fairly straightforward with this method and highly valuable for a fine evaluation of potential direct damage.

3.5 Cyclonic impact on human reproduction in Madagascar

Estimated wind fields generated by TCs can be used within an econometric framework to investigate questions related to their impacts on social or economic characteristics (Dell et al. (2014), Hsiang and Jina (2014) or Strobl (2012)). As an example of TC social impact, RNR-I studies whether TCs may change parents' decisions

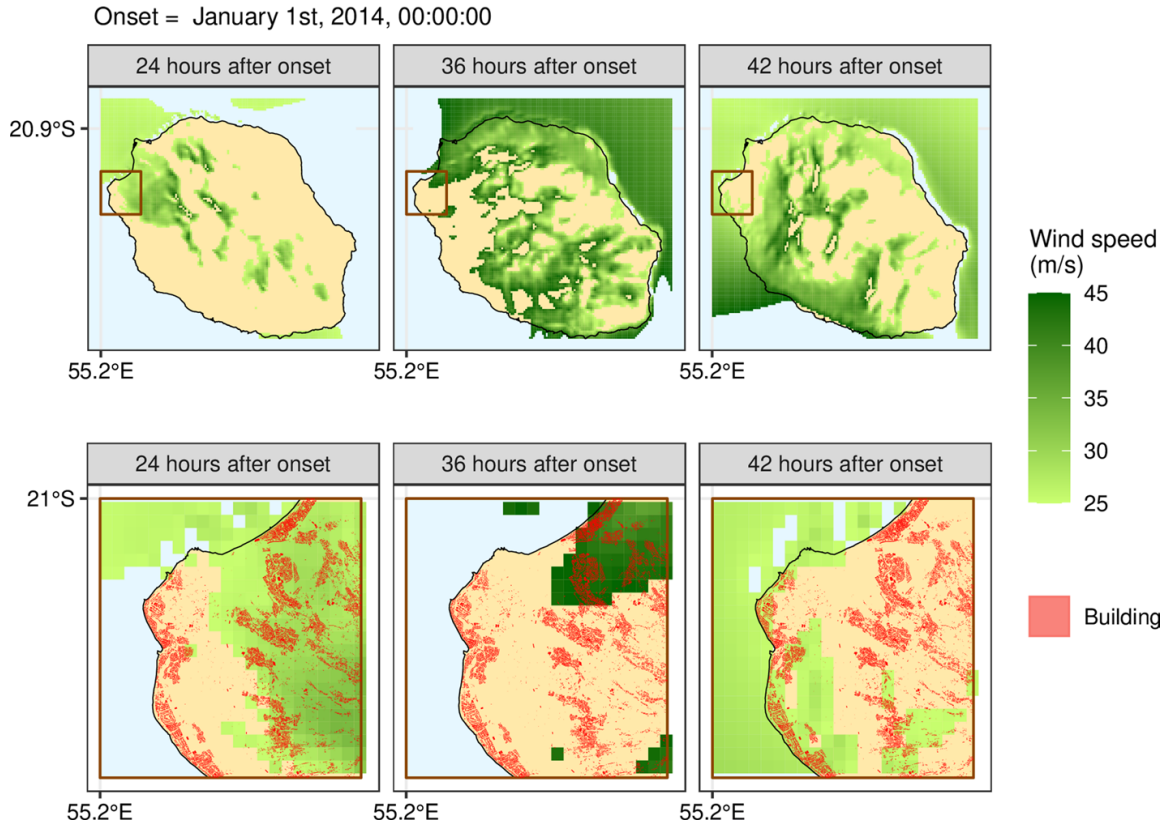

Fig. 9 Example of a GIS-based method for the evaluation of the dynamic exposure. Top from left to right: evolution of damaging wind fields (speed equal to or higher than 25 m s^{-1}) over Reunion Island taken from the simulation of TC Bejisa. Bottom from left to right: close-up maps (15 km × 15 km) enabling the identification of buildings and infrastructures exposed (location and duration) to damaging winds

about having children in Madagascar. This is being done by using geolocated microdata from the Malagasy Demographic and Health Survey, together with wind field data generated by tropical cyclones hitting Madagascar during the 1985–2009 period (Geiger et al. 2017). Merging geolocated data with the full fertility history of the women interviewed enables a unique dataset to be constructed, potentially emphasizing links between births and the mothers' TC experiences. RNR-I then applies panel econometric techniques, exploiting year-to-year variations in exposure to TCs, to estimate the causal effect of TCs on mothers' likelihood of giving birth. The main result of this study is that, on average and all other things being equal, exposure to wind speeds of 27.8 m s^{-1} (approximately 100 km h^{-1}) implies a total fall in the probability of giving birth of 25.6 points in the current year, together with a further decline of 5.9 and 2.0 points, respectively, one and two years after being exposed. Alternative estimations of the empirical model show that the adverse effect of TC exposure on the number of births is persistent. The estimated effect is shown to be robust to many alternative specifications of the econometric model. This new empirical evidence is consistent with economic mechanisms suggesting that TC exposure is perceived as an adverse shock—generating uncertainties in many aspects of daily life (loss of income, crops, livelihood)—that leads couples to postpone their decision to have children.

3.6 Evolution of TCs in the SWIO in the context of climate change

The evolution of tropical cyclones (frequency, intensity, trajectory, seasonality, etc.) in a warmer climate remains largely uncertain: the theory is poorly known, the series of observations are heterogeneous in time and space, and most of the multi-model climate projections available so far are too poorly resolved (100 km or more) to properly represent these phenomena. Nevertheless, two options are available: (i) to perform dedicated high-resolution simulations (50 km or less) and detect tropical cyclones using object tracking algorithms, or (ii) to exploit existing low-resolution climate projections by looking for links between cyclone activity (in monthly mean) and the large-scale environment (cyclogenesis indices).

In Cattiaux et al. (2020), we explored these two approaches, with a focus on the Southern Indian Ocean. On the one hand, we performed dedicated experiments with the CNRM-CM6-1 atmospheric model in a rotated-stretched configuration (resolution up to 12 km over the area of interest), capable of producing realistic cyclones. In a 2 K-warmer world, the model simulates a 20% decrease in the frequency of tropical cyclones in the basin, associated with a slight poleward shift in their trajectories (Fig. 10a), together with an increase in their maximum intensity and a reduction of about one month in the period of cyclonic activity (later onset, Fig. 10c). On the other hand, we calculated the cyclogenesis indices in these dedicated simulations and in the CMIP5 multi-model projections (lower resolution). The indices do not capture the decrease in frequency, but partially represent the changes in geographical (Fig. 10b) and seasonal (Fig. 10c) distribution.

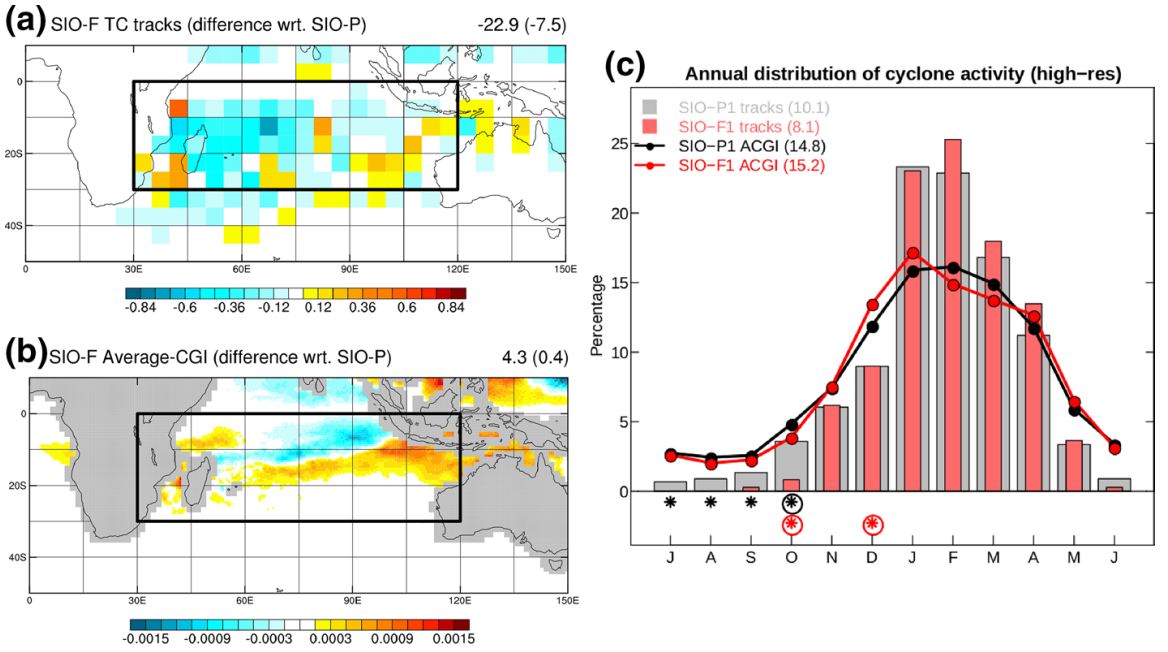

Fig. 10 Future evolution of TCs in the Indian Ocean. **a** Difference in track densities between future and present simulations. On average over the basin, we find a 20% decrease in the number of cyclone days (i.e. 7.5 days less). **b** Difference in cyclogenesis indices between present and future simulations. The indices miss the average decrease (they give + 0.4 days over the basin), but suggest the southward shift observed in a). **c** Annual distribution of cyclones (bars) and cyclogenesis indices (lines) for present (grey/black) and future (red) simulations. A significant decrease at the beginning of the season (October) and a significant increase at the end of the season (February to April) are visible

These results are consistent with a similar study on the North Atlantic (Chauvin et al. 2019), and, more generally, with the scientific literature (e.g. Camargo et al. 2014). The originality here lies in the focus on the South Indian Ocean (little studied so far) and the evidence of the reduction in the length of the cyclone season (important for monitoring and vigilance systems). Ongoing studies will give a better understanding the origins of the decrease in frequency projected by the model.

Further to the use of global climate models, another approach for evaluating future cyclonic risk is to estimate how damaging a recent historical cyclone could be if a similar one were to recur in the future (Schär 1996; Lackman 2015; Patricola 2018). In our case, we investigated Cyclone Bejisa, a climatologically typical cyclone that affected Reunion Island in early January 2014. Future environments for simulations of Bejisa-like cyclones were constructed using CMIP5 models to calculate changes in atmospheric and oceanic conditions, such as humidity and SST, between the recent climate and that of the end of the twenty-first century.

These changes were then added to ECMWF atmospheric and Mercator ocean analyses to create modified analyses of a future environment, thus permitting present versus future simulations. We conducted such simulations using the non-hydrostatic model Meso-NH with 3-km grid spacing, coupled to the ocean model CROCO for six different future environments derived from six different CMIP5 models.

Our findings suggest that future Bejisa-like cyclones will be 7% more intense, as measured by their maximum surface wind speed (Fig. 11a). Furthermore, the latitude at which future cyclones attain their lifetime maximum intensity will be displaced 2° further poleward, in line with an expansion of the tropics. In terms of trajectory, no substantial change was detected, as the present-day wind pattern was left unperturbed in order to maintain a north–south track that impacted Reunion Island. However, future cyclones were found to produce more intense rainfall, with the rainfall rates increasing by 29% on average (Fig. 11b). Additionally, future cyclones are predicted to be 9% smaller, as measured by the radius of their 17.5 m s^{-1} winds. However, further high-resolution studies are still needed to constrain this characteristic change, as large variability persists in the literature (Knutson

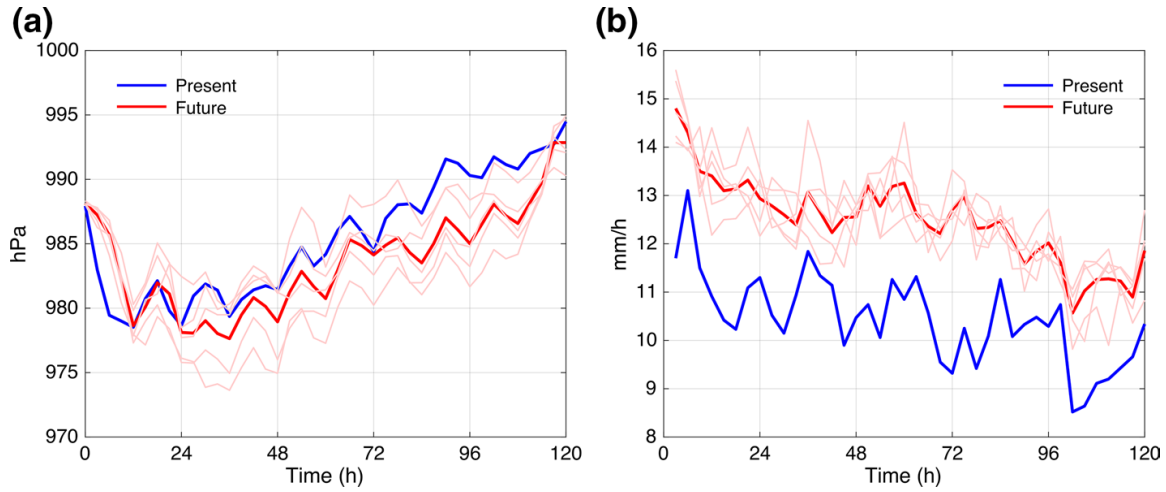

Fig. 11 Mean sea level pressure (**a**) and average rainfall rate within 100 km (**b**) of Bejisa-like cyclones simulated in Meso-NH coupled to the ocean model CROCO. A resimulation of Cyclone Bejisa in its historical environment (blue) is compared to Bejisa-like cyclones simulated in future environments derived from Coupled Model Intercomparison Project 5 (CMIP5) models (thin red lines) and their ensemble mean (red line). Projections indicate that such a typical cyclone could be characterized by significantly lower pressures and significantly heavier rainfalls in the future

2020). In addition to these atmospheric-related characteristics, we project a 0.2 m average increase in the significant ocean wave height, calculated by running the wave model WAVEWATCH III using hourly surface wind output. To the best of our knowledge, this is the first time that future changes in ocean waves have been projected for this basin. Although the change found here is modest, larger changes are anticipated for simulations based on stronger historical cyclones, with Cyclone Bejisa representing only a moderate-strength cyclone.

4 ReNovRisk database

The Sentinel remote sensing images produced during the RNR-I project have been processed and are stored on the servers and storage spaces of the SEAS-OI station, on which the project team relies (http://www.seas-oi.fr/en/web/guest/accueil). The SEAS-OI station is part of the French SEAS network of direct reception antennas for satellite data.

The SAR Sentinel-1 database is made up of data in the raw state or after different levels of pre-processing (spatial cropping and tiling, time filters) and processing (NDR, binary images, temporal summaries, etc.). Sentinel-2 optical data consist of raw L1C images, reflectance L2A images, cloud masks, multiple indices, and the results of change detection algorithms (classifications, temporal summaries, etc.). For each tile, covering an area of 100 km by 100 km, the entire time series (2015–2020) represents approximately 2 TB and more than 10,000 images. These numbers must be multiplied according to the geographical area and the number of S2 tiles monitored in the frame of the ReNovRisk programme.

These data from change detection chains therefore occupy very large volumes, which should be well organized to ensure a good perennial management. Work is underway to secure their storage and archiving, which currently rely mainly on the SEAS-OI infrastructure with a capacity of a few hundred TB. In addition, the metadata for each processing level is being produced to allow the harvesting of this image database. Finally, reflection is in progress to facilitate the availability of this data and, in particular, the final products (indices, change detection products), through a mapping web platform.

OSU-R (Observatoire des Sciences de l'Univers de la Reunion, CNRS, Météo-France and Université de la Reunion) organizes and supports transdisciplinary environmental research and operates a service unit (operation and maintenance of the stock of instruments, data analysis and processing). One goal of the services is the management of long-term observational data performed by its stations (that are part of European research infrastructures) and of measurement campaign datasets like the one produced in the framework of ReNovRisk. This data management is organized around 4 themes: data storage, metadata management, data processing, and data accessibility. The data storage provides long-term support and a backup guarantee, with an access by FTP for scientists and URL for data in open access. Metadata management is performed by means of OSU-R software, which allows information describing instrumentation and processing to be stored. The data processing is done through a data flow management service based on the Apache Airflow software (https://airflow.apache.org/), which pushes data to processing servers and data processing libraries, and classifies the data thus created. Finally, accessibility is achieved through the "GeOsur" tool (https://geosur.univ-reunion.fr), a web interface that aims to ensure the visibility of all the data produced. It is based on the open source software GeoNetwork (https://geonetwork-opensource.org) and allows the user to navigate easily through the database, using a search engine to visualize the different information on

the datasets, as well as the download links. This tool is based on standard data exchange protocols (ISO19139, OGC https://www.ogc.org), which allows it to be harvested to other institutional portals.

The ReNovRisk programme participates in an open science approach by making the data produced on cyclone risk available to the public. All this data management allows us to reference all the project data within the same catalogue. It will group together the data stored locally, and also data found in other databases. Finally, thanks to its interoperability, GeOsur will facilitate the transversal use of this data, both in the research field and for a wider audience. A demonstration of this interoperability is the harvesting of ReNovRisk data by another portal: PEIGO (http://peigeo.re), which is managed by AGORAH (http://www.agorah.com), the urban planning agency of Reunion Island, which aims to restore observational data in the form of cross-analyses to inform public policies.

5 Conclusions and perspectives

ReNovRisk is the first transdisciplinary programme dedicated to the study of cyclonic hazards in the Western Indian Ocean. It is composed of 4 different sub-programmes.

The first component, RNR-C, has enabled the development of new observation networks in the basin and numerical models for tropical cyclone modelling on the SWIO. The deployment of a GNSS network is intended to improve the state of the atmosphere in numerical weather prediction models through data assimilation. An intensive observation campaign was deployed in 2019 in the SWIO. New observation tools, in particular installed on marine and aerial drones, were tested in the environment of tropical cyclone Joaninha. Important numerical developments focused on the ocean–wave–atmosphere interactions, and on the representation of clouds and precipitation. The first studies have demonstrated the robustness of the modelling system, and a significant improvement in the track and intensity of the modelled tropical cyclones. ReNovRisk has also enabled high-resolution regional climate simulations for the SWIO, which have provided first answers to questions concerning the occurrence and geographical distribution of tropical cyclones in the coming decades. Moreover, high-resolution simulations of tropical cyclone Bejisa in a future climate have shown that its maximum intensity would be attained 2° further poleward, its intensity would increase by ~ 7%, and the precipitation rate would be strongly increased (~ 30%).

While RNR-C is planned to end in June 2021, the three other ReNovRisk sub-programmes are still in progress. Although they have not yet presented their final results, several scientific advances can be highlighted.

RNR-T is a first attempt to describe the integrated chain of tropical cyclone risks along a transect extending across the western volcanic plateau of Reunion Island (2000 m asl) and sloping down through ravines to the coastline. Infrastructures and preserved natural sites along the western coastal line of Reunion Island are particularly prone to overlapping cyclonic hazards (wind gusts, high precipitation, floods by ravines, transport of sediment, sea swell and submersion). A novel approach will involve cross-expertise in different domains (atmospheric physics, hydrology, sedimentology, geomorphology, coral reef growth, and ocean sciences). Complementary datasets will be required for calibrating model tools. Rainfall based on radar data corrected with rain gauge data will be estimated for catchments for which only a small number of point flow measurements are available.

RNR-E is a programme that focuses on the consequences of cyclones with the study, from upstream to downstream, of the sedimentary stock linked to ground movements and to flood-induced solid transport. The dynamics studied are characterized by different complementary methodologies. Thus, high-precision topographic surveys (GNSS network, geodetic marker, photogrammetry, and LiDAR) and seismological and electromagnetic measurement campaigns are being carried out on several landslides and rivers. Hydrological and geochemical monitoring of groundwater and surface water has also been implemented, and a broadband seismic network is monitoring the continuous transport of erosion products in rivers through the associated seismic noise. These data have made it possible to quantify, in particular with numerical modelling, precipitation and groundwater contributions to the acceleration of landslides during cyclonic events (Belle et al. 2014, 2018).

The remote sensing part of the RNR-I project has focused on the development of change detection algorithms to highlight the direct impacts of cyclones from satellite data. In order to promote their use by the largest possible number of interested parties, the processing chains developed are based on freely accessible Sentinel satellite data and are themselves published and open source. The data used come from the ESA Sentinel 1 and 2 satellites, acquired at high spatial (10 m) and temporal (5–10 day) resolutions with global coverage. Sen1Chain is the first processing chain developed that is based on SAR Sentinel 1 satellite data. It allows rapid detection of flooded areas by computing the normalized difference ratio (NDR) between two images, pre- and post-event. Based on radar data, Sen1Chain has the advantage of being insensitive to clouds, often numerous in a cyclonic context. The second processing chain developed, Sen2Chain, uses Sentinel 2 optical data to detect changes in land cover with a change vector analysis (CVA) method. As with Sen1Chain, Sen2Chain makes it possible to highlight floods linked to rainfall, but also modifications in plant cover under the action of the wind, or the appearance of bare ground. The greater sensitivity of this method to clouds is partly compensated by the high temporal acquisition frequency (5 days) increasing the probability of obtaining better quality images. Since 2015, the availability and historical depth of the Sentinel image database have allowed both processing chains to operate large time series of hundreds of images to place events in a seasonal context and highlight their exceptional nature. Several recent cyclonic events have been analysed in Madagascar (Enawo-2017 / Ava-2018), as have other events and geographical areas (Idai in Mozambique-2019, Dorian in the Bahamas—2019), on which the processing chains have demonstrated their effectiveness (Alexandre et al. 2020).

Beyond these thematic results, a significant contribution of ReNovRisk has been the networking of many scientists from different domains around collaborative programmes. ReNovRisk has brought together atmospheric physicists, hydrogeologists, geomorphologists, geophysicists, geomaticians, and economists to jointly analyse cyclonic hazards and impacts on Reunion Island and on the SWIO. These transdisciplinary collaborations have led to the development of a large set of tools to characterize the cyclonic hazards (wind, precipitation, swell) and their impacts after landfall (floods, landslides, coastline, sedimentary stock).

Furthermore, an important action of ReNovRisk is training and the communication of results. Two interoperable databases (GeOsur and Seas-OI) are under construction for free open access to the programme data with a horizon of mid-2021. Specific products developed for decision-makers and land-use planning institutes in Reunion Island will support adaptation to cyclonic hazards. Training activities are being carried out on the various scientific themes and on the tools deployed during ReNovRisk for students from SWIO countries (Mozambique and Madagascar).

ReNovRisk is intended to continue as the stakes are high for countries subject to cyclonic hazards, particularly in the SWIO, where the economic and health consequences of cyclones are significant in terms of poverty and infrastructure. As far as possible, ReNovRisk will be expanded more broadly into the fields of ecology, health, and social sciences, as the adaptation of territories to cyclone risks is a key element in building resilience to climate change.

Acknowledgements ReNovRisk was funded by the European Union through the ERDF and INTERREG5 programmes, the région Reunion, the French state through the CPER programme, the University of Reunion, the BRGM, the IRD and the CNRS. Numerical modelling was made possible thanks to the computer resources of Météo-France. The authors would like to thank all the participants of the ReNovRisk programme.

Author contributions All the authors made significant contributions to the document through their participation in the ReNovRisk programme, the exploitation of data or numerical tools and the production of results. All authors contributed to the writing of the paper.

Funding ReNovRisk was funded by the European Union through the ERDF and INTER-REG5 programmes, the Reunion region and the French state through the CPER programme, the University of Reunion, the BRGM, the IRD and the CNRS.

Data availability Data will be available on GeoSUR (https://geosur.univ-reunion.fr/web/) and Seas-Oi (http://www.seas-oi.fr/web/guest/acces-aux-donnees) web platform from mid-2021. Beforehand, the data used can be requested from the authors.

Code availability Numerical models are in open source and available on web platforms: http://mesonh.aero.obs-mip.fr/, https://www.umr-cnrm.fr/surfex/, http://polar.ncep.noaa.gov/waves/wavewatch/, http://www.croco-ocean.orgref and https://portal.enes.org/oasis

Compliance with ethical standards

Conflict of interest No conflict of interests.

Ethics approval All the authors assure to have respected the scientific standard ethics in accordance with the recommendations of the publisher.

Financial interests All authors certify that they have no affiliations with or involvement in any organization or entity with any financial interest or non-financial interest in the subject matter or materials discussed in this manuscript.

References

Alexandre C, Johary R, Catry T, Mouquet P, Révillion C, Srakotondraompiana S, Pennober G (2020) A sentinel-1 based processing chain for detection of cyclonic flood impacts. Remote Sens 12(2):252

Andreas EL, Edson JB, Monahan EC, Rouault MP, Smith SD (1995) The spray contribution to net evaporation from the sea: A review of recent progress. Boundary-Layer Meteorol 72:3–52. https://doi.org/10.1007/BF00712389

Aunay B, Rey A, Le Moigne B, Somoza K, Cance A, Salomero J (2018) Impacts de la tempête tropicale BERGUITTA sur La Reunion - Synthèse des investigations dans le cadre de la procédure de reconnaissance d'état de catastrophe naturelle. Rapport BRGM/RP-67604-FR

Baray JL, Courcoux Y, Keckhut P, Portafaix T, Tulet P, Cammas JP, Hauchecorne A, Godin Beekmann S, De Mazière M, Hermans C, Desmet F, Sellegri K, Colomb A, Ramonet M, Sciare J, Vuillemin C, Hoareau C, Dionisi D, Duflot V, Vérèmes H, Porteneuve J, Gabarrot F, Gaudo T, Metzger JM, Payen G, Leclair de Bellevue J, Barthe C, Posny F, Ricaud P, Abchiche A, Delmas R (2013) Maïdo observatory: a new high-altitude station facility at Reunion Island (21° S, 55° E) for long-term atmospheric remote sensing and in situ measurements. Atmos Meas Tech 6:2865–2877. https://doi.org/10.5194/amt-6-2865-2013

Barbary D, Leroux MD, Bousquet O (2019) The orographic effect of Reunion Island on tropical cyclone track and intensity. Atmos Sci Lett 20:e882. https://doi.org/10.1002/asl.882

Barruol G, Reymond D, Fontaine FR, Hyvernaud O, Maurer V, Maamaatuaiahutapu K (2006) Characterizing swells in the southern Pacific from seismic and infrasonic noise analyses. Geophys J Int 164:516–542. https://doi.org/10.1111/J.1365-246X.2006.02871.x

Barruol G, Davy C, Fontaine FR, Schlindwein V, Sigloch K (2016) Monitoring austral and cyclonic swells in the "Iles Eparses" (Mozambique Channel) from microseismic noise. Acta Oecologica 72:120–128. https://doi.org/10.1016/j.actao.2015.10.015

Baum RL, Reid ME (1992) Geology, Hydrology and Mechanics of the Alani-Paty Landslide, Manoa Valley, Oahu, Hawaii. USGS 92–501, 87

Bernardie S, Desramaut N, Malet JP, Gourlay M, Grandjean G (2015) Prediction of changes in landslide rates induced by rainfall. Landslides 12:481–494. https://doi.org/10.1007/s10346-014-0495-8

Belle P, Aunay B, Bernardie S, Grandjean G, Ladouche MR, Join JL (2014) The application of an innovative inverse model for understanding and predicting landslide movements (Salazie cirque landslides, Reunion Island). Landslides 11:343–355.

Belle P, Aunay B, Lachassagne P, Ladouche B, Join JL (2018) Control of tropical landcover and soil properties on landslides' aquifer recharge. Piezomet and Dyn Water. https://doi.org/10.3390/w10101491

Bister M, Emanuel KA (2002) Low frequency variability of tropical cyclone potential intensity 1 Interannual to interdecadal variability. J Geophys Res 107:4801. https://doi.org/10.1029/2001JD000776

Bordi I, Fraedrich K, Sutera A, Zhu X (2014) Ground-based GPS measurements: time behavior from half-hour to years. Theor and Appl Climatol 115:615–625

Botzen WJW, Deschenes O, Sanders M (2019) The economic impacts of natural disasters: a review of models and empirical studies. Rev Environ Econ and Policy 13(2):167–188.

Bousquet O, Lees E, Durand J, Peltier A, Duret A, Mekies D, Boissier P, Donal T, Fleischer-Dogley F, Zakariasy L (2020a) Densification of the ground-based GNSS observation network in the South-West Indian Ocean: current status, perspectives and examples of applications in meteorology and geodesy. Front Earth Sci 8:566105. https://doi.org/10.3389/feart.2020.566105

Bousquet O, Barbary D, Bielli S, Kebir S, Raynaud L, Malardel S, Faure G (2020b) An evaluation of tropical cyclone forecast in the Southwest Indian Ocean basin with AROME-Indian Ocean convection-permitting numerical weather predicting system. Atmos Sci Lett 21:e950. https://doi.org/10.1002/asl2.950

Bousquet O, Dalleau M, Bocquet M, Gaspar P, Bielli S, Ciccione S, Remy E, Vidard A (2020c) Sea turtles for ocean research and monitoring: overview and initial results of the STORM project in the Southwest Indian Ocean. Front Marine Sci 7:859 (**in press**)

Bu YP, Fovell RG, Corbosiero KL (2014) Influence of Cloud-Radiative Forcing on Tropical Cyclone Structure. J Atmos Sci 71:1644–1662.

Cattiaux J, Chauvin F, Bousquet O, Malardel S, Tsai CL (2020) Projected changes in the Southern Indian Ocean cyclone activity assessed from high-resolution experiments and CMIP5 models. J Clim 33(12):4975–4991. https://doi.org/10.1175/JCLI-D-19-0591.1

Camargo SJ, Tippett MK, Sobel AH, Vecchi GA, Zhao M (2014) Testing the performance of tropical cyclone genesis indices in future climates using the HiRAM model. J Climate 27:9171–9196. https://doi.org/10.1175/JCLI-D-13-00505.1

Camargo SJ, Hsiang SM (2015) Tropical cyclones: From the influence of climate to their socioeconomic impacts. In: M. Chavez, M. Ghil, and J. Urrutia-Fucugauchi, editors, Extreme Events Observations, Modeling, and Economics. Wiley, New York, ISBN 978–1–119–15701–4.

Caine N (1980) The rainfall intensity-duration control of shallow landslides and debris flows. Geografiska Ann: Series A, Phys Geograph 62(1–2):23–27

Cappa F, Guglielmi Y, Soukatchoff VM, Mudry J, Bertrand C, Charmoille A (2004) Hydromechanical modelling of a large moving rock slope inferred from slope levelling coupled to spring long-term hydrochemical monitoring: example of the La Clapière landslide (Southern Alps, France). J Hydrol 291:67–90.

Chauvin F, Pilon R, Palany P, Bel Madani A (2019) Future changes in Atlantic hurricanes with the rotated-stretched ARPEGE-Climat at very high resolution. Climate Dyn 54:947–972.

Coe JA, Ellis WL, Godt JW, Savage WZ, Savage JE, Michael JA, Kibler JD, Powers PS, Lidke DJ, Debray S (2003) Seasonal movement of the Slumgullion landslide determined from Global Positioning System surveys and filled instrumentation, July 1998-March 2002. Eng Geol 68:67–101.

Colomb A, Kriat T, Leroux MD (2018) The rapid weakening of very severe tropical cyclone hellen (2014). Month Weather Rev 147:2717–2737.

Corominas J, Moya J, Ledesma A, Lloret A, Gili JA (2005) Prediction of ground displacements and velocities from groundwater level changes at the Vallcebre landslide (Eastern Pyrenees, Spain). Landslides 2:83–96.

Craig A, Valcke S, Coquart L (2017) Development and performance of a new version of the OASIS coupler, OASIS3-MCT_3.0. Geoscientific Model Development 10:3297–3308.

Davy C, Barruol G, Fontaine FR, Stutzmann E, Sigloch K (2014) Tracking major storms from microseismic and hydroacoustic observations on the seafloor. Geophys Res Lett. https://doi.org/10.1002/2014GL062319

Davy C, Stutzmann E, Barruol G, Fontaine FR, Schimmel M (2015) Sources of secondary microseisms in the Indian Ocean. Geophys J Int 202:1180–1189.

Davy C, Barruol G, Fontaine FR, Cordier E (2016) Analyses of extreme swell events on La Reunion Island from microseismic noise. Geophys J Int 207:1767–1782.

De Lavenne A, Andréassian V, Thirel G, Ramos MH, Perrin C (2019) A regularization approach to improve the sequential calibration of a semidistributed hydrological model. Water Resour Res 55:8821–8839.

De Maria M, Sampson CR, Knaff JA, Musgrave KD (2014) Is tropical cyclone intensity guidance improving? Bull Amer Meteor Soc 95:387–398.

Dell M, Jones BF, Olken BA (2014) What do we learn from the weather? The new climate-economy literature. J Econ Lit 52(3):740–798

Dodet G, Castelle B, Masselink G, Scott T, Davidson M, Floc'h F, Jackson D, Suanez S (2018) Beach recovery from extreme storm activity during the 2013/14 winter along the Atlantic coast of Europe. Earth Surf Process Landforms. https://doi.org/10.1002/esp.4500

Dow JM, Neilan RE, Rizos C (2009) The International GNSS Service in a changing landscape of Global Navigation Satellite Systems. J Geodesy 83:191–198

Emanuel KA (1986) An air–sea interaction theory for tropical cyclones. part I: steady-state maintenance. J Atmos Sci 43:585–604. https://doi.org/10.1175/1520-0469(1986)043,0585:AASITF.2.0.CO;2

Emanuel KA (1988) The maximum intensity of hurricanes. J Atmos Sci 45:1143–1155. https://doi.org/10.1175/1520-0469(1988)045,1143:TMIOH.2.0.CO;2

Eyring V, Bony S, Meehl GA, Senior CA, Stevens B, Stouffer RJ, Taylor KE (2016) Overview of the design and experimental organization of the Coupled Model Intercomparison Project Phase 6 (CMIP6). Geosci Model Dev 9:1937–1958

Fernández-Merodo JA, García-Davalillo JC, Herrera G, Mira P, Pastor M (2012) 2D viscoplastic finite element modelling of slow landslides: the Portalet case study (Spain). Landslides. https://doi.org/10.1007/s10346-012-0370-4

Fontaine FR, Barruol G, Gonzalez A (2015) Rivière des Pluies Project, La Reunion Island, 2015–2018; RESIF - Réseau Sismologique et géodésique Français. http://dx.doi.org/https://doi.org/10.15778/RESIF.ZF2015

Fovell RG, Bu YP, Corbosiero KL, Tung W, Cao Y, Kuo H, Hsu L, Su H (2016) Influence of cloud microphysics and radiation on tropical cyclone structure and motion. Meteorol Monograph 56:11.1-11.27. https://doi.org/10.1175/AMSMONOGRAPHS-D-15-0006.1

Geiger T, Frieler K, Bresch DN (2017) A global data set of tropical cyclone exposure (TCE-DAT). GFZ Data Services. https://doi.org/10.5880/pik.2017.005

Gonzalez A, Fontaine FR, Barruol G, Recking A, Burtin A, Join JL, Delcher E, Michon L (2020) Seismic signature of a river flooding in La Reunion Island during the tropical cyclone Dumazile (March 2018), submitted to Geophysical Journal International

Gonzalez A (2019) Suivi sismologique de l'impact des cyclones sur la charge de fond de la Rivière des Pluies et de la Rivière du Mât à La Reunion, Ph. D. thesis, Université de La Reunion, 171 p.

Gonzalez A, Fontaine FR, Burtin A, Barruol G, Recking A, Join JL, Delcher E (2017) Seismic monitoring of the bedload transport in La Reunion Island rivers during tropical cyclones. EGU2017–5937, In, 19:14462. http://adsabs.harvard.edu/abs/2017EGUGA.1914462

Hoarau T, Barthe C, Tulet P, Claeys M, Pinty JP, Bousquet O, Delanoë J, Vié B (2018a) Impact of the generation and activation of sea salt aerosols on the evolution of Tropical Cyclone Dumile. J Geophys Res Atmos 123:8813–8831. https://doi.org/10.1029/2017JD028125

Hoarau T, Pinty JP, Barthe C (2018b) A representation of the collisional ice break-up process in the two-moment microphysics scheme LIMA v1.0 of Meso-NH. Geosci Model Dev 11:4269–4289. https://doi.org/10.5194/gmd-11-4269-2018

IPCC (2013) Climate Change 2013. The physical science basis. Contribution of Working Group I to the Fifth Assessment Report of the Intergovernmental Panel on Climate Change. In T. Stocker et al. (Eds.), (p. pp. 1535). Cambridge University Press. doi: https://doi.org/10.1017/CBO9781107415324

Iverson RM, Major JJ (1987) Rainfall, ground-water flow, and seasonal movement at Minor Creek landslide, northwestern California: physical interpretation of empirical relations. Bull Geol Soc Am 99:579–594. https://doi.org/10.1130/0016-7606(1987)99%3c579:RGFASM%3e2.0.CO;2

Iverson RM (2000) Landslide triggering by rain infiltration. Water Resour Res 36(7):1897–1910

Hallegate S (2014) Natural Disasters and Climate Change, Springer International Publishing, XXII, 194 pp, doi:https://doi.org/10.1007/978-3-319-08933-1__2

Holland GJ (1980) An analytic model of the wind and pressure profiles in hurricanes. Month Wea Rev 108:1212–1218

Holland G (1993) WMO/TC-No. 560, Report No. TCP-31, World Meterological Organization. Accessed: 17–03–2020, https://wmo.asu.edu/content/world-greatest-twenty-four-hour-1-day-rainfall.

Kossin J, Emanuel K, Vecchi G (2014) The poleward migration of the location of tropical cyclone maximum intensity. Nature 509:349–352. https://doi.org/10.1038/nature13278

Kossin J, Knapp KR, Olander TL, Velden CS (2020) Global increase in major tropical cyclone exceedance probability over the past four decades. Proceedings of the National Academy of Sciences May 2020, 201920849; DOI: https://doi.org/10.1073/pnas.1920849117

Hsiang SM, Jina AS (2014) The Causal Effect of Environmental Catastrophe on Long-Run Economic Growth: Evidence from 6,700 Cyclones. Working Paper 20352, National Bureau of Economic Research. https://www.nber.org/papers/w20352

Hussain M, Chen D, Cheng A, Wei H, Stanley D (2013) Change detection from remotely sensed images: from pixel-based to object-based approaches. ISPRS J Photogramm and Remote Sens 80:91–106

Knutson T, Camargo SJ, Chan JCL, Emanuel K, Ho CH, Kossin J, Mohapatra M, Satoh M, Sugi M, Walsh K, Wu L (2020) Tropical cyclones and climate change assessment: part ii: projected response to anthropogenic warming. Bull Am Meteorol Soc. https://doi.org/10.1175/BAMS-D-18-0194.1

Lac C, Chaboureau JP, Masson V, Pinty JP, Tulet P, Escobar J, Leriche M, Barthe C, Aouizerats B, Augros C, Aumond P, Auguste F, Bechtold P, Berthet S, Bielli S, Bosseur F, Caumont O, Cohard JM, Colin J, Couvreux F, Cuxart J, Delautier G, Dauhut T, Ducrocq V, Filippi JB, Gazen D, Geoffroy O, Gheusi F, Honnert R, Lafore JP, Lebeaupin Brossier C, Libois Q, Lunet T, Mari C, Maric T, Mascart P, Mogé M, Molinié G, Nuissier O, Pantillon F, Peyrillé P, Pergaud J, Perraud E, Pianezze J, Redelsperger JL, Ricard D, Richard E, Riette S, Rodier Q, Schoetter R, Seyfried L, Stein J, Suhre K, Taufour M, Thouron O, Turner S, Verrelle A, Vié B, Visentin F, Vionnet V, Wautelet P (2018) Overview of the Meso-NH model version 5.4 and its applications. Geosci Model Dev 11:1929–1969. https://doi.org/10.5194/gmd-11-1929-2018

Lackmann GM (2015) (2015), Hurricane Sandy before 1900 and after 2100. Bull Amer Meteor Soc 96(4):547–560. https://doi.org/10.1175/BAMS-D-14-00123.1

Lafore JP, Stein J, Asencio N, Bougeault P, Ducrocq V, Duron J, Fischer C, Héreil P, Mascart P, Masson V, Pinty JP, Redelsperger JL, Richard E, Vilà-Guerau de Arellano J (1998) The Meso-NH atmospheric simulation system. part I: adiabatic formulation and control simulations. Ann Geophys 16:90–109. https://doi.org/10.1007/s00585-997-0090-6

Laurantin O (2008) Antilope: Hourly rainfall analysis merging radar and rain gauge data. Proc. Int. Symp. on Weather Radar and Hydrology Conf. 2008, Grenoble, France, Laboratoire d'étude des Transferts en Hydrologie et Environnement (LTHE), 2–8

Lecacheux S, Bonnardot F, Rousseau M, Paris F, Pedreros R, Lerma NA, Quetelard H, Barbary D (2018) Probabilistic forecast of coastal waves for flood warning applications at Reunion Island (Indian Ocean). J Coastal Res 85:776–780. https://doi.org/10.2112/SI85-156.1

Lees E, Bousquet O, Roy D, Leclair J (2020) Analysis of diurnal to seasonal variability of integrated water vapour in the South Indian Ocean Basin using ground-based GNSS and 5th generation ECMWF Reanalysis (ERA5) data. Q. J. R. Meteorol, Soc (**In press**)

Leroux M, Meister J, Mekies D, Dorla A, Caroff P (2018) A climatology of Southwest Indian ocean tropical systems: their number, tracks, impacts, sizes, empirical maximum potential intensity, and intensity changes. J Appl Meteor Climatol 57:1021–1041. https://doi.org/10.1175/JAMC-D-17-0094.1

Liébault F, Peteuil C, Remaître A (2010) Approches géomorphologiques de la production sédimentaire des torrents. Sciences Eaux & Territoires, n°2: 128–35. https://doi.org/https://doi.org/10.14758/SET-REVUE.2010.2.15

Lu J, Deser C, Reichler T (2009) Cause of the widening of the tropical belt since 1958. Geophys Res Lett 36(3):L03803

Mahabot MM, Pennober G, Suanez S, Troadec R, Delacourt C (2017a) Effect of tropical cyclones on short-term evolution of carbonate sandy beaches on Reunion Island. Indian Ocean J Coast Res 33(4):839–853

Mahabot MM, Jaud M, Pennober G, Le Dantec N, Troadec R, Suanez S, Delacourt C (2017b) The basics for a permanent observatory of shoreline evolution in tropical environments; lessons from back-reef beaches in La Reunion Island, Comptes Rendus Geoscience, 349(6–7). ISSN. https://doi.org/10.1016/j.crte.2017.09.010

Malet JP, Van Asch ThWG, Van Beek R, Maquaire O (2005) Forecasting the behaviour of complex landslides with a spatially distributed hydrological model. Nat Hazards and Earth Syst Sci 5:71–85. https://doi.org/10.5194/nhess-5-71-2005

Masson V, Le Moigne P, Martin E, Faroux S, Alias A, Alkama R, Belamari S, Barbu A, Boone A, Bouyssel F, Brousseau P, Brun E, Calvet JC, Carrer D, Decharme B, Delire C, Donier S, Essaouini K, Gibelin AL, Giordani H, Habets F, Jidane M, Kerdraon G, Kourzeneva E, Lafaysse M, Lafont S, Lebeaupin Brossier C, Lemonsu A, Mahfouf JF, Marguinaud P, Mokhtari M, Morin S, Pigeon G, Salgado R, Seity Y, Taillefer F, Tanguy G, Tulet P, Vincendon B, Vionnet V, Voldoire A (2013) The SURFEXv7.2 land and ocean surface platform for coupled or offline simulation of earth surface variables and fluxes. Geosci Model Dev 6:929–960. https://doi.org/10.5194/gmd-6-929-2013

Mavume AF, Rydberg L, Lutjeharms JRE (2008) Climatology of tropical cyclones in the South-West Indian Ocean; landfall in Mozambique and Madagascar. West Indian Ocean J Mar Sci 8:15–36

Meyer V, Becker N, Markantonis V, Schwarze R, Van den Bergh JCJM, Bouwer LM, Bubeck P, Ciavola P, Genovese E, Green C, Hallegatte S, Kreibich H, Lequeux Q, Logar I, Papyrakis E, Pfurtscheller C, Poussin J, Przyluski V, Thieken AH, Viavattene C (2013) Review article: assessing the costs of natural hazards - state of the art and knowledge gaps. Nat Hazards and Earth Syst Sci 13(5):1351–1373

Mile M, Benácek P, Rózsa S (2019) The use of GNSS zenith total delays in operational arome/hungary 3d-var over a central European domain. Atmosp Measure Techniq 12(3):1569–1579

Mittal R, Tewari M, Radhakrishnan C, Ray P, Singh T, Nickerson AK (2019) Response of tropical cyclone Phailin (2013) in the Bay of Bengal to climate perturbations. Clim Dyn 53:2013–2030. https://doi.org/10.1007/s00382-019-04761-w

Mouquet P, Alexandre C, Rasolomamonjy J, Rosa J, Catry T, Révillion C, Rakotondraompiana S, Pennober G (2020) SENTINEL-1 AND SENTINEL-2 time series processing chains for cyclone impact monitoring in South WestIndian Ocean. Int Arch Photogramm Remote Sens Spatial Inf Sci. https://doi.org/10.5194/isprs-archives-XLIII-B3-2020-1593-2020

Narayan PK (2003) Macroeconomic impact of natural disasters on a small island economy: evidence from a CGE model. Appl Econ Lett 10(11):721–723. https://doi.org/10.1080/1350485032000133372

Neumann CJ (1993) Global guide to tropical cyclone forecasting. Chap 1: Global overview. TD 560 - TCP 31, WMO, Genève, Suisse, 1.1–1.37

Ovadnevaite J, Manders A, de Leeuw G, Ceburnis D, Monahan C, Partanen AI, Korhonen H, O'Dowd CD (2014) A sea spray aerosol flux parameterization encapsulating wave state. Atmos Chem Phys 14(4):1837–1852. https://doi.org/10.5194/acp-14-1837-2014

Parent du Châtelet J, Tabary P, Guimera M (2005) The PANTHERE Project and the Evolution of the French Operational Radar Network and Products : Rain-estimation, Doppler winds, and Dual-Polarisation (Le projet PANTHERE), 32nd American Meteorological Society Radar Conference, Albuquerque, NM, http://ams.confex.com/ams/pdfpapers/96217.pdf

Parker CL, Bruyère CL, Mooney PA, Lynch AH (2018) The response of land-falling tropical cyclone characteristics to projected climate change in northeast Australia. Clim Dyn 51:3467–3485. https://doi.org/10.1007/s00382-018-4091-9

Patricola CM, Wehner MF (2018) Anthropogenic influences on major tropical cyclone events. Nature 563:339–346. https://doi.org/10.1038/s41586-018-0673-2

Pauthier B, Bois B, Castel T, Thévenin D, Smith CC, Richard Y (2016) Mesoscale and local scale evaluations of quantitative precipitation estimates by weather radar products during a heavy rainfall event, Advances in Meteorology, vol. 2016, Article ID 6089319, 9 pages

Pianezze J, Barthe C, Bielli S, Tulet P, Jullien S, Cambon G, Bousquet O, Claeys M, Cordier E (2018) A new coupled ocean-waves-atmosphere model designed for tropical storm studies: example of tropical cyclone Bejisa (2013–2014) in the south-west Indian ocean. J Adv Model Earth Syst. https://doi.org/10.1002/2017MS001177

Quetelard H, Bessemoulin P, Peterson TC, Burton A, Boodhoo Y, Cerveny RS (2007) WMO CCl Rapporteur for climate extremes decision, World Meteorological Organization. Accessed: 17–03–2020, https://wmo.asu.edu/content/

Raucoules D, de Michele M, Aunay B (2018) Landslide displacement mapping based on ALOS-2/PALSAR-2 data using image correlation techniques and SAR interferometry: application to the Hell-Bourg landslide (Salazie Circle, La Reunion Island). Geocarto Int. https://doi.org/10.1080/10106049.2018.1508311

Rault C, Dewez TJB, Aunay B (2020) Structure-from-motion processing of aerial archive photographs: sensitivity analyses pave the way for quantifying geomorphological changes since 1978 in La Reunion Island. ISPRS Ann. Photogramm Remote Sens Spatial Inf Sci 2:773–780. https://doi.org/10.5194/isprs-annals-V-2-2020-773-2020

Rotunno R, Emanuel KA (1987) An air-sea interaction theory for tropical cyclones. part II: evolutionary study using a nonhydrostatic axisymmetric numerical model. J Atmos Sci 44:542–561. https://doi.org/10.1175/1520-0469(1987)044%3c0542:AAITFT%3e2.0.CO;2

Rindraharisaona EJ, Cordier E, Barruol G, Fontaine FR, Singh M (2020) Assessing swells in La Reunion Island from terrestrial seismic observations, oceanographic records and offshore wave models. Geophys J Int 221:1883–1895. https://doi.org/10.1093/gji/ggaa117

Rojas-Serna C, Lebecherel L, Perrin C, Andreassian V, Oudin L (2016) How should a rainfall-runoff model be parameterized in an almost ungauged catchment? a methodology tested on 609 catchments, Water Resour. Res 52:4765–4784. https://doi.org/10.1002/2015WR018549

Schär C, Frei C, Lüthi D, Davies HC (1996) Surrogate climate-change scenarios for regional climate models. Geophys Res Lett. https://doi.org/10.1029/96GL00265

Schulz WH, McKenna JP, Kibler JD, Biavati G (2009) Relations between hydrology and velocity of a continuously moving landslide -evidence of pore-pressure feedback regulating landslide motion? Landslides 6:181–190. https://doi.org/10.1007/s10346-009-0157-4

SeityY BP, Malardel S, Hello G, Bénard P, Bouttier F, Lac C, Masson V (2011) The AROME-France convective-scale operational model. Mon Wea Rev 139:976–991. https://doi.org/10.1175/2010MWR3425.1

Staten PW, Lu J, Grise KM, Davis SM (2018) Birner T (2018) Re-examining tropical expansion. Nat Clim Change 8:768–775. https://doi.org/10.1038/s41558-018-0246-2

Staten PW, Grise KM, Davis SM, Karnauskas KB, Waugh DW, Maycock A, Fu Q, Cook K, Adam O, Simpson IR, Allen RJ, Rosenlof K, Chen G, Ummenhofer CC, Quan X, Kossin JP, Davis NA, Son S (2020) Tropical widening: From global variations to regional impacts. Bull Amer Meteor Soc 101(6):E897–E904. https://doi.org/10.1175/BAMS-D-19-0047.1

Strobl E (2012) The economic growth impact of natural disasters in developing countries: evidence from hurricane strikes in the Central American and Caribbean regions. J Dev Econ 97(1):130–141

Stumpf A, Augereau E, Delacourt C, Bonnier J (2016) Photogrammetric discharge monitoring of small tropical mountain rivers: a case study at Rivière Des Pluies, Reunion Island". Water Resour Res 52(6):4550–4570. https://doi.org/10.1002/2015WR018292

Tacher L, Bonnard C, Laloui L, Parriaux A (2005) Modelling the behaviour of a large landslide with respect to hydrogeological and geomechanical parameter heterogeneity. Landslides 2:3–14. https://doi.org/10.1007/s10346-004-0038-9

Tamura Y (2009) Wind-induced damage to buildings and disaster risk reduction. The Seventh Asia-Pacific Conference on Wind Engineering, November 8–12, 2009, Taipei, Taiwan

Terry J, Kim I-H, Jolivet S (2013) Sinuosity of tropical cyclone tracks in the South West Indian Ocean: spatio temporal patterns and relationships with fundamental storm attributes. Appl Geogr 45:29–40. https://doi.org/10.1016/j.apgeog.2013.08.006

Thompson C, Barthe C, Bielli S, Tulet P, Pianezze J Projecting Characteristic Changes of a Typical Tropical Cyclone under Climate Change in the South West Indian Ocean. Submitted to J. Geophys. Res.

Trabing BC, Bell MM, Brown BR (2019) Impacts of radiation and upper-tropospheric temperatures on tropical cyclone structure and intensity. J Atmos Sci 76:135–153. https://doi.org/10.1175/JAS-D-18-0165.1

Tulet P, Crassier V, Cousin F, Suhre K, Rosset R (2005) ORILAM, a three-moment lognormal aerosol scheme for mesoscale atmospheric model: online coupling into the Meso-NH-C model and validation on the Escompte campaign. J Geophys Res 110:D18201. https://doi.org/10.1029/2004JD005716

Vallet A, Charlier JB, Fabbri O, Bertrand C, Carry N, Mudry J (2016) Functioning and precipitation-displacement modelling of rainfall-induced deep-seated landslides subject to creep deformation. Landslides 13:653–670.

Van Asch TWJ, Buma J, Van Beek LPH (1999) A view on some hydrological triggering systems in landslides. Geomorphology 30:25–32.

Vérèmes H (2020) Application de la méthode dite « de bogus » dans le programme ReNovRisk-TRANSFERTS, Technical report, Université de La Reunion; Région Reunion. 2020. https://doi.org/10.26171/

Veron F (2015) Ocean sprays. Annu Rev Fluid Mech 47(1):507–538.

Vié B, Pinty JP, Berthet S, Leriche M (2016) LIMA (v10): a quasi two-moment microphysical scheme driven by a multimodal population of cloud condensation and ice freezing nuclei. Geosci Model Develop 9(2):567–586. https://doi.org/10.5194/gmd-9-567-2016

Vitart F, Ardilouze C, Bonet A, Brookshaw A, Chen M, Codorean C, Déqué M, Ferranti L, Fucile E, Fuentes M, Hendon H, Hodgson J, Kang HS, Kumar A, Lin H, Liu G, Liu X, Malguzzi P, Mallas I, Manoussakis M, Mastrangelo D, MacLachlan C, McLean P, Minami A, Mladek R, Nakazawa T, Najm S, Nie Y, Rixen M, Robertson AW, Ruti P, Sun C, Takaya Y, Tolstykh M, Venuti F, Waliser D, Woolnough S, Wu T, Won DJ, Xiao H, Zaripov R, Zhang L (2017) The seasonal to sub-seasonal forecast project database. Bull Am Meteor Soc 98:163–173. https://doi.org/10.1175/BAMS-D-16-0017.1

Voldoire A, Decharme B, Pianezze J, Lebeaupin Brossier C, Sevault F, Seyfried L, Garnier V, Bielli S, Valcke S, Alias A, Accensi M, Ardhuin F, Bouin MN, Ducrocq V, Faroux S, Giordani H, Léger F, Marsaleix P, Rainaud R, Redelsperger JL, Richard E, Riette S (2017) SURFEX v8.0 interface with OASIS3-MCT to couple atmosphere with hydrology, ocean, waves and sea-ice models, from coastal to global scales. Geosci Model Dev 10:4207–4227. https://doi.org/10.5194/gmd-10-4207-2017

WMO (2016) Tropical Cyclone Programme, Regional Association I –Tropical Cyclone Operational Plan for the South-West Indian Ocean. Report No. TCP-12, Report No. TCP-12, WMO-No. 1178, https://library.wmo.int/doc_num.php?explnum_id=4031

Authors and Affiliations

Pierre Tulet[1] · Bertrand Aunay[2] · Guilhem Barruol[3,4] · Christelle Barthe[1] · Remi Belon[2] · Soline Bielli[1] · François Bonnardot[5] · Olivier Bousquet[1] · Jean-Pierre Cammas[1,6] · Julien Cattiaux[7] · Fabrice Chauvin[7] · Idriss Fontaine[8] · Fabrice R. Fontaine[3,9] · Franck Gabarrot[6] · Sabine Garabedian[8] · Alicia Gonzalez[3,4] · Jean-Lambert Join[3] · Florian Jouvenot[10] · David Nortes-Martinez[8] · Dominique Mékiès[1] · Pascal Mouquet[10] · Guillaume Payen[6] · Gwenaelle Pennober[10] · Joris Pianezze[1] · Claire Rault[2] · Christophe Revillion[10] · Elisa J. Rindraharisaona[3,4] · Kevin Samyn[2] · Callum Thompson[1] · Hélène Vérèmes[1,6]

[1] LACy, Laboratoire de l'Atmosphère et des Cyclones (UMR 8105, Université de la Reunion, CNRS, Météo-France), Saint-Denis de La Reunion, France

[2] BRGM, Bureau de Recherches Géologiques et Minières, Saint-Denis de La Reunion, France

[3] LGSR, Laboratoire Géosciences Reunion (Université de La Reunion, IPGP), Saint-Denis de La Reunion, France

[4] Université de Paris, Institut de physique du globe de Paris, CNRS, Paris, France

[5] DIROI, Direction Interrégionale Océan Indien (Météo-France), Saint-Denis de la Reunion, France

[6] OSUR, Observatoire des Sciences de l'Univers de La Reunion (UMS 3365, Université de la Reunion, CNRS, Météo-France), Saint-Denis de la Reunion, France

[7] CNRM, Centre National de la Recherche Météorologique (UMR 3589, Météo-France, CNRS), Toulouse, France

[8] CEMOI, Centre d'Economie et de Management de l'Océan Indien (Université de la Reunion), Saint-Denis de La Reunion, France

[9] Université de Paris, Institut de physique du globe de Paris, CNRS F-75005 Paris, France. Observatoire volcanologique et sismologique de la Martinique, Institut de physique du globe de Paris, F-97250 Fonds Saint Denis, France

[10] Espace-Dev, Espace pour le Développement (UMR 228, IRD, Université de la Guyane, Université de La Reunion, Université des Antilles, Université de Montpellier), Montpellier, France

Chapitre 8

Short-term impact of tropical cyclones in Madagascar : Evidence from nightlight data

Fontaine, Garabedian, Jammes

- ***Applied Economics***, à paraître, 2023
- ***Présentation :***
  Colloque AFSE, 70e, Dijon, juin 2022
  Rencontre géomatique de la Réunion et de l?Océan Indien, Saint-leu (La Réunion), novembre 2021

Short-term impact of tropical cyclones in Madagascar: Evidence from nightlight data*

Idriss Fontaine† Sabine Garabedian‡ Maël Jammes§

Abstract

This paper explores the short-term effect of tropical cyclones on economic activity at a local level in Madagascar. To achieve this challenging task, we combine high-resolution spatial data about nightlight brightness and exposure to tropical cyclones with geographic information at the smallest administrative level in Madagascar, namely the Fokontany. With this panel dataset, we then run fixed effect regressions. Our findings reveal that exposure to tropical cyclones leads to an ambiguous economic response as proxied by nocturnal brightness during the first year after the shock. However, during the second year, nightlights clearly increase, leading to an overall beneficial effect of 5% just 2 years after the tropical cyclone. We then provide a finer analysis by interacting wind speed exposure with variables that capture many heterogenous dimensions of our data. This analysis shows that for Fokontany sharing specific characteristics, the short-run effect of tropical cyclones is negative. However, the positive effect of exposure in the second year emerges as a regular pattern in our analysis. Overall, our empirical study is in line with economic mechanisms suggesting that after a period of contraction, the impacted economy rebounds beyond the counterfactual trend that would otherwise be observed in the absence of a shock. Our results are shown to be robust to alternative specifications of our baseline model.

Keywords: Tropical cyclones, Nightlight data, Madagascar, High-resolution spatial data

JEL classifications: O44, Q54.

Corresponding author: Idriss Fontaine, idriss.fontaine@univ-reunion.fr

*{We gratefully acknowledge the financial support from the *Fond Européen de Développement Régional* (FEDER), the *Région Réunion*, and the *Observatoire des Sociétés de l'Océan Indien* (OSOI). For his insightful comments and research assistance, we thank Pascal Mouquet who helped us collect the nightlight data for Madagascar. We are also grateful to Thomas Vogt for providing us with an updated version of TCE-DAT for Madagascar.

†Université de La Réunion, Centre d'Economie et de Management de l'Océan Indien, France, idriss.fontaine@univ-reunion.fr

‡Université de La Réunion, Centre d'Economie et de Management de l'Océan Indien, France, sabine.garabedian@univ-reunion.fr

§Université de La Réunion, Centre d'Economie et de Management de l'Océan Indien, France, mael.jammes99@gmail.com

1 Introduction

The macroeconomic consequences of tropical cyclones, and natural disasters more generally, have been the subject of intense debates. Certain studies (Crespo Cuaresma et al., 2008; Hallegatte et al., 2007; Skidmore and Toya, 2002) find that natural disasters have a positive impact on national income, while others (Felbermayr and Gröschl, 2014; Noy, 2009) observe their negative impact on the economy. This lack of conclusive evidence partly derives from a controversy about the way in which exposure to natural disasters is measured (Cavallo et al., 2013; Noy, 2009).[1]. Regarding tropical cyclones, the studies measuring the exposure of a given spatial unit by the wind speed at the surface find a reduction in output in the short term (Elliott et al., 2015; Strobl, 2012, 2011) and even in the long term (Berlemann and Wenzel, 2018; Hsiang and Jina, 2014; Krichene et al., 2021). While the economic literature has many papers studying the effects of tropical cyclones at the country level, it recognizes that such a level of analysis may hide the true consequences of phenomena that ultimately occur at the local level (Strobl, 2011). The purpose of this paper is therefore to fill this void by studying the case of Madagascar, a developing country that is frequently exposed to tropical cyclones.

The economic literature provides explanations that favor both a net negative impact and a net positive impact of natural disasters. For the "pessimistic" perspective, natural disasters could have a negative impact on economic activity insofar as the destruction of productive capital induces expenditure reductions that push the consumption component of output down (Anttila-Hughes and Hsiang, 2013; Baez et al., 2010; Carter et al., 2007). Arguably, post-disaster preferences could be altered, thus leading individuals to consume more rather than invest in human or physical capital (Cameron and Shah, 2015). Consequently, the impact would become long-lasting if the marginal utility of consuming exceeds the marginal utility of investing (Anttila-Hughes and Hsiang, 2013). In addition, Field et al. (2012) suggest that in some contexts, the detrimental consequences of natural disasters could be magnified if the funds allocated to the reconstruction of old activities are not used to finance new activities. Regarding the "optimistic" perspective, Skidmore and Toya (2002) and Crespo Cuaresma et al. (2008) suggest that in the wake of a disaster, investments in human capital would be more attractive, ultimately leading to an improvement in total factor productivity along with a net positive impact on economic growth. The economic literature also suggests

[1]Many studies use economic and human damages related to disasters from the EM-DAT dataset. However, the use of this dataset has at least two limitations. First, data on economic damages are collected from different sources, while the quality of reporting changes over time (Strobl, 2012). Second, monetary damages are likely to be correlated with output, namely the dependent variable in growth regression models (Felbermayr and Gröschl, 2014)

that the cause of the positive effect of disasters on economic activity could be the influx of foreign aid as well as the organized and well-executed reconstruction activities (Heger and Neumayer, 2019; Horwich, 2000). In addition to the net effect of disasters on economic activity, the trajectory followed by the affected country is also of interest. Studies highlighting a net negative effect either find a permanent negative effect of natural disasters (Berlemann and Wenzel, 2018; Hsiang and Jina, 2014; Krichene et al., 2021) or only a short-term effect before recovery to the counterfactual trend that would have taken place in the absence of the event (Bertinelli and Strobl, 2013; Elliott et al., 2015; Strobl, 2011). By contrast, studies observed a globally positive effect indicate that either economic activity, after suffering from a contraction, rebounds beyond the counterfactual trend (the so-called "build back better" hypothesis) or that the replacement of old and inefficient assets by new ones that embody the most productive technology is immediately positive for economic growth (the so-called "Schumpetarian creative destruction" hypothesis).[2] In addition to investigating the net effect of tropical cyclones in the Malagasy context, we also explore how the impact of tropical cyclones materializes in the short run by exploiting high frequency data of economic activity.

Empirical research using high frequency data to explore the economic consequences of exposure to tropical cyclones is still uncommon. The lack of studies on the short-term impact of exposure to cyclonic systems on economic activity is partly explained by the difficulty of accessing high frequency economic data. A welcome alternative that has emerged in recent years is to proxy economic activity by nocturnal nightlight images observed by satellite (Chen and Nordhaus, 2011; Gibson et al., 2020; Henderson et al., 2012). In the specific context of Madagascar, Henderson et al. (2012) showed a sharp increase in nightlight luminosity in the vicinity of Llakaka between 1998 and 2003 following the discovery of gigantic sapphire and ruby deposits, which suggests that nocturnal brightness is indeed correlated with economic activity. In general, studies that undertake a more "macro" approach find that the correlation between economic activity and nighttime brightness is highly positive (Chen and Nordhaus, 2015; Chen and Nordhaus, 2011; Henderson et al., 2012). Here, after exploiting the gridded dataset of gross domestic product at 0.08° of horizontal resolution, we also observe that the quality of the positive association between nighttime luminosity and economic output holds true at a local level in the Malagasy context.

When measuring the short-run post-cyclone economic consequences, we mainly combine two kinds of input data. We first collect daily nightlight data produced according to the methodology of Román et al. (2018) for the 2012M1-2020M4 sample period. This collection of

[2]For more details about the economic mechanisms at play and the potential economic path followed after catastrophic natural events, the interested reader can refer to Hsiang and Jina (2014) or Heger and Neumayer (2019).

images, also known as black marble data, is then aggregated to obtain a measure of monthly nightlight brightness. The second set of data corresponds to the TCE-DAT produced by Geiger et al. (2018). Geiger et al. (2018) provide data for wind field exposure on the ground generated by each landfalling tropical cyclone observed since 1950. For our research, we obtained wind speed exposure at a higher degree of resolution than the original TCE-DAT (0.02° rather than 0.1°) and updated until 2020. In addition to these two data, we take advantage of the existence of geographic information about the finest administrative level in Madagascar, namely the Fokontany,[3] to construct a panel dataset indicating if a given spatial unit has been exposed to cyclonic wind speed during a given month. With this new dataset in hand, we then employ fixed effect regressions in the context of a distributed lag model to unveil the effect of a tropical cyclone shock on economic activity as proxied by nightlight brightness. The choice to use the Fokontany as our baseline spatial unit appears reasonable, as the associated fixed effects have a higher economic interpretation than those associated with a spatial unit based on an arbitrary grid of the Malagasy territory. The general message of this paper nevertheless remains robust to this choice.

The results of our paper are the following. First, the effect of a tropical cyclone strike is ambiguous for the first 12 months. However, after this time, notably during the second year, coefficients associated with wind speed are unambiguously positive. This pattern is then confirmed by the visual inspection of the cumulative marginal effect, which shows that 2 years after the strike, a cyclone shock that is one standard deviation above the sample means leads to an increase in nightlight of about 5%. Second, subsequent analyses that incorporate heterogeneity through the interaction of wind speed exposure with variables capturing the heterogeneity dimension of interest confirm that the positive effect observed during the second year after the shock is a regular pattern. However, the magnitude of the beneficial effect of tropical cyclone shocks varies with non-prone and lit-up Fokontany more likely to observe a strong recovery. In addition, these regression models suggest that depending on the heterogeneity dimension, the short-term effect could be negative. Thus, for cyclone-prone or the most lit-up villages, we find a peak with a significantly negative impact (in absolute values) equivalent to -0.90% and -1.30%, respectively. Overall, our empirical results are more line with the "optimistic" view, which suggests that tropical cyclones could induce the economy to grow at a higher level than what would otherwise be observed.

Our paper draws on several empirical works that examine the economic consequences of tropical cyclones (Berlemann and Wenzel, 2018; Bertinelli and Strobl, 2013; Elliott et al., 2015; Hsiang and Jina, 2014; Krichene et al., 2021; Mohan and Strobl, 2017; Strobl, 2011).

[3]In Madagascar, the spatial unit of the Fokontany broadly corresponds to a "village" or hamlet. Throughout the paper, we will interchangeably employ the terms of village and Fokontany.

However, to the best of our knowledge, it is the only study to systematically examine the case of Madagascar. Arguably, Madagascar provides an interesting case study for at least two reasons. First, the country is located in the South West Indian Ocean (SWIO), a basin that records 11% of global cyclonic activity according to Leroux et al. (2018). Its particular geographical location in the SWIO means that the country is regularly exposed to tropical cyclones. Thus, during the period 1950-2020, 147 cyclonic systems made landfall on the Malagasy territory (Geiger et al., 2018). Second, the "scientific" literature now contains much evidence suggesting that climate change is likely to modify the frequency, genesis, spatial extent, and characteristics of the most extreme cyclonic systems (IPCC, 2019; Knutson et al., 2020; Knutson et al., 2010). Combined with the fact that future economic and demographic growth will increase people and asset exposure (Botzen et al., 2019), this raises questions about the economic development of Madagascar as a whole but also about the welfare of Malagasy citizens. Our paper thus complements the aforementioned literature in the sense that we do not rely on annual data. Just as depending on a broader regional unit like a region or country could "aggregate out" the true impact of tropical cyclones (Elliott et al., 2019; Elliott et al., 2015), we argue that relying on low-frequency data may also "hide" the true trajectory of the impacted local economy. To overcome the shortcomings associated with these two methodological issues, we base our empirical work on a disaggregated and local spatial unit, namely the Fokontany, along with an observation of their economic activity every month between 2012M1 and 2020M4.

We organize the rest of this paper as follows. In section 2, we present the country studied in this paper and the spatial unit of reference. Section 3 provides details about the two types of input data used in this research, while section 4 focuses on the empirical model. In section 5 we present the main result of the paper, its robustness, and further analyses. Finally, section 6 presents the conclusions.

2 Madagascar and the spatial unit of interest

2.1 Madagascar and its economy

Madagascar remains one of the poorest countries in the world. According to data from the Penn World Table, its gross domestic product per capita was US$1595 purchasing power parity in 2017 (Feenstra et al., 2015). Data from the United Nations Development Program indicate that with a human development index of 0.51, the development level of the country is still low. A large proportion of Malagasy citizens could be defined as extremely poor, as they live under the poverty line.

Annual economic growth in Madagascar oscillated between 0.9% and 4.2% during the 2012-2020 period (INSTAT, 2021). The Malagasy economy is highly sensitive to external shocks such as exchange rate fluctuations or natural disasters (Nordman et al., 2016). In particular, its geographic location in the SWIO basin means that the island is a cyclone-prone territory. As an example, during the 1950-2020 sample period, 147 cyclonic systems made landfall on Madagascar, equivalent to two systems on average per year. In addition to external shocks, the country is also sensitive to internal turmoil such as political instability. Since its independence from France in the late 1950s, Madagascar has experienced many political crises, with the country undergoing four constitutional changes and four crisis of political nature (Fontaine and Razafindravaosolonirina, 2021).

2.2 Spatial unit of interest: Fokontany

The Fokontany is the smallest administrative subdivision in Madagascar. Its members constitute the Fokonolona. Depending on the urban/rural nature of the area, the Fokontany can be hamlets, villages, sectors, or even neighborhoods. Each Malagasy commune is comprised of a set of Fokontany. Choosing the head of the Fokontany is partly the responsibility of the mayor: at a general assembly, the inhabitants of the Fokontany nominate five members of the Fokonolona, and the mayor then chooses the head of the Fokontany from among the five nominations. The Fokontany committee is made up of the head of Fokontany as well as one or even two deputies. Their role is to participate in all kinds of activity in the Fokontany: environmental preservation, socioeconomic development of the territory, management of public infrastructure, or even implementation of the town's urban plan. The heads of Fokontany also contribute to the democratic life of the territory by calling general assemblies of Fokontany. Decisions concerning the Fokontany are deliberate and may lead to the formulation of a "Dina" (collective agreement, set of customary rules), the application of which is the responsibility of the head of Fokontany. Concretely, the Fokontany committee is also an essential link in delivering administrative services to the population of the Fokontany, carrying out the population census, ensuring the smooth running of elections at the local level, and transmitting useful information to inhabitants. It is also the task of the Fokontany committee to inform the population about the arrival of a cyclone or any other natural disaster and ensure the management of the resulting risks. The Fokontany, through the rules set out in the "Dina," are responsible for the management of their natural resources. These can have a real effect on the vulnerability of Fokonolona to cyclones. We collected official geographic information about the spatial extent of each Malagasy Fokontany from the following website https://data.humdata.org/dataset/madagascar-administrative-level-0-4-boundaries. The

resulting spatial data contain geographic information for 17,465 villages. Summary statistics about the surface area of the Fokontany are shown in Table 1, revealing that the Fokontany constitute a very local geographic unit with a mean surface of 33.91 km^2 and a median of 12.56 km^2. We believe that using the Fokontany as a spatial unit makes it possible to capture the effect of the quality of territorial management by the committee in terms of the locality's short-term risk management and degree of preparedness to weather shocks. In this sense, the fixed effects associated with Fokontany have more of an economic interpretation than pixel fixed effects, which are the spatial unit of an "arbitrary" grid of the Malagasy territory.

3 Data

3.1 Night light data

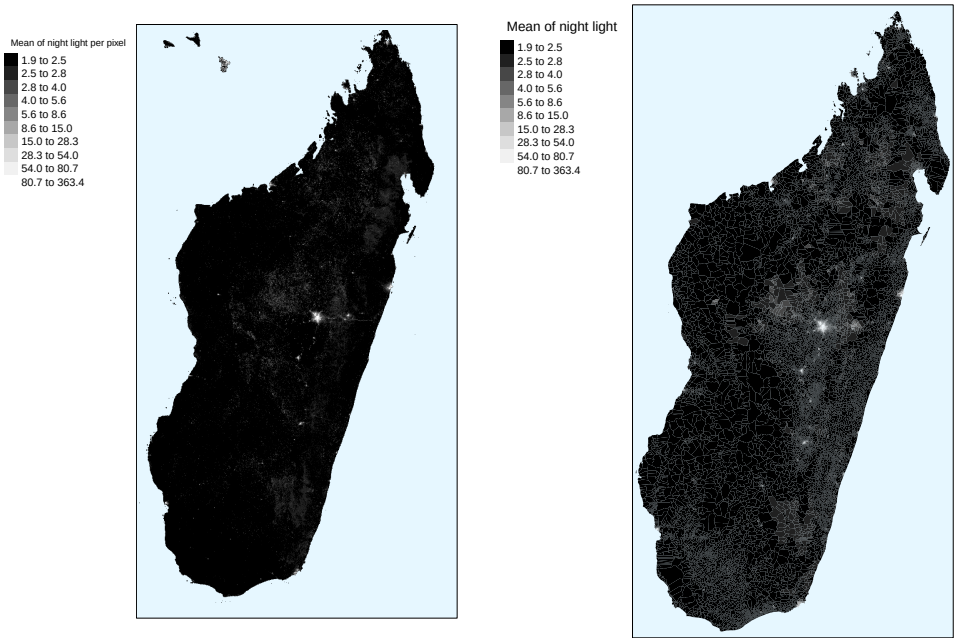

(a) Pixel level (b) Fokontany level

Figure 1: Mean nightlight brightness during the 2012M1-2020M4 period.

One prerequisite of our study is to objectively proxy economic activity at the local level. To do so, we follow an approach first used by Sutton and Costanza (2002) and later developed by Chen and Nordhaus (2011), Henderson et al. (2012), Chen and Nordhaus (2015), or Gibson (2021) (among others). We also rely on nightlight brightness observed from satellites. As stressed in Gibson et al. (2020), nightlight data are growing in popularity among economists, especially in contexts where other data sources are either non-existent or presumed to be of poor quality, as is probably the case for Madagascar.

In contrast to many economic papers (Bertinelli et al., 2016; Bertinelli and Strobl, 2013; Elliott et al., 2015) (among others), we use nighttime satellite images from the Day/Night Band (DNB) sensors of the Visible Infrared Imaging Radiometer Suite (VIIRS) on board of the Suomi-National Polar-orbiting Partnership (S-NPP) as opposed to nightlight data from the Defense Meteorological Satellite Program (DMSP). This choice is motivated by the shortcomings of DMSP data, especially the existence of blurred images, geolocation errors, and sensor saturation (Gibson et al., 2020). Furthermore, DMSP data are only available until 2013, and the original spatial resolution of the picture is lower than that of VIIRS.

For our study, our VIIRS input data are the daily nighttime data, also known as the "black marble" data produced following the methodology of Román et al. (2018).[4] More specifically, we use the raw images obtained from the satellite and aggregate daily data to obtain monthly data by employing a simple arithmetic average. However, the quality of satellite pictures depends on several factors such as cloud cover, moonlight characteristics, or other weather factors, which imply that for a given month and a given cell, the number of exploitable pictures during a month varies. To take this issue into account, we exploit information from the data producer, and for each pixel/month pair, we compute the average monthly brightness from daily observations recorded in "high quality."[5] The final resolution of cells of nocturnal brightness is 0.004° (approximately 500 meters of horizontal resolution), implying that the entire territory of Madagascar is represented by more than 2,000,000 pixels. Such high-resolution satellite images can be consuming when estimating econometric models. In particular, as our analysis is based on the 100 months from the 2012M1-2020M4 sample period, we have more than 200,000,000 observations in the final dataset. By considering the Fokontany as our spatial unit of reference and by computing the nightlight at the Fokontany level as the mean nightlight of pixels within them,[6] we avoid this issue. We nevertheless check

[4] "Black marble'' products are freely available on adsweb.modaps.eosdis.nasa.gov.

[5] In particular, we use the "BND_BRDF-Corrected_NL" nightlight data from the VNP46A2 collection. For this data, the data producer classifies each value for each pixel to be of "high quality," "poor quality," and "no retrieval." To compute our monthly average, we only keep high-quality pictures. Relying on all available pictures increases the variability of the time series of nightlight data, which can be imputed to data quality. We thank Pascal Mouquet for his research assistance during this step.

[6] To compute the mean nightlight brightness for the pixels of a given Fokontany, we use the `R` function

for the robustness of our choice by estimating the main baseline model from the pixel-level regression by aggregating the raw pixel by a factor of three and four.

Figure 1 shows the spatial distribution of nighttime brightness in Madagascar over the 2012M1-2020M4 sample period. In the figure, unlit areas are depicted in black, while the most lit areas change from gray to white depending on the radiance value. Figure 1 shows that the most lit areas correspond to the main cities of Madagascar, namely Antananarivo, Toamasina (on the east coast), Antsirabe (south of Antananarivo), and Antisiranana (on the north coast). Moreover, a large proportion of the Malagasy territory is unlit, especially along the west coast of the island. Given the nature of our input data, we implicitly assume, like Elliott et al. (2015), that unlit areas do not capture any economic activity. Table 1, which reports the summary statistics associated with average nightlight intensity during the 2012M1-2020M4 sample period, confirms the visual inspection of Figure 1. More than 90% of villages have a radiance value less than the average nightlight intensity of 4.82 (93% to be precise; statistic not shown in Table 1). The standard deviation of the distribution of nightlight intensity is almost three times greater than its mean and amounts to 13.75. The average total nightlight brightness over the studied sample is 7,099,715.

`exact_extract` from the package `exactextractr`

	Fokontany's area (in km^2)	Radiance value of nightlight (in nWatts.cm^{-2}sr.$^{-1}$)	Max. wind (in km/h)
Min.	0.01	1.91	0
Percentile 1%	0.12	2.04	5.45
Percentile 5%	0.74	2.11	5.96
Percentile 10%	1.74	2.15	6.34
Percentile 20%	3.87	2.21	6.84
Percentile 25%	4.97	2.23	7.02
Percentile 30%	6.10	2.26	7.27
Percentile 40%	8.94	2.30	7.69
Median	12.56	2.34	8.49
Percentile 60%	17.76	2.39	9.66
Percentile 70%	25.92	2.43	10.60
Percentile 75%	32.09	2.46	11.01
Percentile 80%	41.05	2.50	11.58
Percentile 90%	79.45	2.78	14.33
Percentile 95%	133.69	8.58	19.78
Percentile 99%	341.34	20.44	
Max.	1652.20	363.40	24.20
Mean	33.91	4.82	9.54
Standard deviation	71.50	13.75	3.44
$\frac{\text{Standard deviation}}{\text{Mean}}$	2.11	2.85	0.36

Table 1: Summary statistics of average nightlight intensity for the 2012M1-2020M4 period and mean maximum wind speed for the 1950-2020 period by Fokontany in Madagascar.
Sources: Black marble data of Roman et al. (2018), TCE-DAT of Geiger et al. (2018) and authors' own calculations.
Notes: Wind speed is expressed in kilometers per hours.

The appropriateness of nightlight data as a proxy for economic activity has been discussed in many studies. In general, a strong positive relationship between the economic output and nightlight brightness is found at the country level (Bertinelli and Strobl, 2013; Chen and Nordhaus, 2011; Henderson et al., 2012; Li et al., 2013). Against this background, it should be observed that nightlight data is not appropriate for capturing all types of economic activity. As observed in Gibson (2021), satellites are sometimes unable to capture the sort of lights used in rural areas. Concerning economic activities in rural areas, they are often associated by large unlit or low-lit areas. In a recent paper, Gibson et al. (2021) compares the

correlation of regional GDP with nightlight in Indonesia. Given the availability of regional GDP at a regional level in this country, they are able to consider both rural and urban areas when running regressions to estimate the elasticity of regional GDP with respect to nightlight. Their findings alleviate part of the concern about the use of nightlight data in rural areas. In particular, while a negative association is found when DMSP data is used, they find that nightlight from VIIRS is always positively associated with regional economic activity. As mentioned before, in the context of our paper, we only rely on the newer and more accurate nightlight data from VIIRS.

To delve further in this direction we aim to verify the existence of such a positive association between GDP and nighlight at a local level in Madagascar. To do so, we rely on the gridded gross domestic product (GDP) data of Kummu et al. (2018) which provide a pixel estimation of total GDP in a worldwide and consistent manner at a resolution level of approximately 0.08° over the 1990-2015 period.[7] As a result, for each Fokontany, we extract its corresponding GDP and level of nightlight brightness. Figure 2 shows the associated scatterplot of the logarithm of both indicators. An inspection of this figure indicates a strong positive relationship between the two indicators of economic activity. In particular, the linear regression line has a positive slope, and the correlation between village GDP and village nightlight level is 0.79.[8] Then, to go in a similar direction as Gibson et al. (2021), we split our sample of Fokontany into two subgroups according to the brightness measured at night. Fokontany with a radiance value lower than 5 correspond to unlit and mainly rural areas while the second group correspond to lit and mainly urban areas (see also section 5.3). Armed with these two datasets, we then estimate the elasticity of local GDP to nightlight brightness.[9] Each time, the coefficient associated to nightlight is significantly positive. In the urban sample, the elasticity is of 0.95 while in the rural areas the latter amounts to 2.66. It should however be observed that the estimated relationship is more noisy in the rural sample as the R-squared is of 0.08. In contrast, in the urban sample the share of regional GDP fluctuations explained by the regression is of 42%.[10] To further test the sensitivity of the main message of the paper to the existence of unlit Fokontany, in section 5.3 we will modify our baseline model by interacting the cyclonic exposure with a dummy that indicate if the

[7]For a detailed description of the data construction, the interested reader can refer to Kummu et al. (2018).

[8]We also checked for the existence of a positive relationship between GDP and nightlight at a local level without taking log into account. Furthermore, we also considered a less spatially disaggregated measure, namely the "commune" and found a similar positive association with a correlation of about 0.7.

[9]More specifically, the dependent variable of the regression is the log of local GDP and the independent variable is the log of the nightlight radiance value.

[10]For the global sample, we find an elasticity of local GDP to nightlight of 1.36 with a R-squared of 0.39. Complete regression results associated with this application for all samples are available upon request.

area is lit or not.

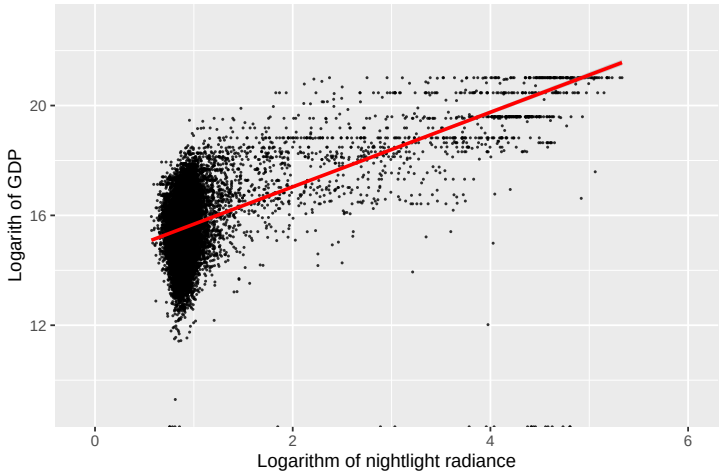

Figure 2: Scatter plot of the logarithm of nightlight brightness versus the logarithm of Gross Domestic Product.

3.2 Tropical cyclone data

A prerequisite for our empirical study is a measure of wind speed exposure at the local level. As it is not possible to rely on ground weather station data at a detailed level in Madagascar, we use an updated version of the TCE-DAT of Geiger et al. (2018). To produce the latter, Geiger et al. (2018) calculated an estimate of the lifetime's maximum surface wind speed at each spatial location (on a $0.02° \times 0.02°$ grid over land) for all landfalling cyclonic systems in Madagascar between 1950 and 2020. The computation is based on the International Best Track Archive for Climate Stewardship (IBTrACS) archive (Knapp et al., 2010), which contains all the information required for a wind field model like the Holland (1980) model that is widely used in studies evaluating the risks associated with the landfalling of tropical cyclones Peduzzi et al. (2012). Geiger et al. (2018) implemented the revised hurricane pressure-wind model of Holland (2008) in which the maximum surface wind speed W in $m.s^{-1}$ (for a given pixel)[11] at radial distance r of the center of a given cyclonic system is defined as follows:

$$W = \left(\frac{b_s}{\rho e} \Delta p \left(\frac{r}{r_m} \right) \right)^{0.5}, \tag{1}$$

where ρ is the surface air density in $kg.m^{-3}$, e the base of natural logarithms, and Δp the pressure drop at the cyclone center in hPa as a function of r and r_m (radius of maximum winds). The parameter b_s depends on Δp, the temporal intensity change in pressure, the

[11]For the sake of simplicity, we do not add an index to designate pixels.

absolute value of the latitude, and the tropical cyclone's translational speed. Further details on the development of the parametric equation of b_s can be found in Holland (2008). In addition to the wind field model in equation (1), Geiger et al. (2018) calculated a translational component multiplied by an attenuation factor (ratio between the tropical cyclone's center and the radius of maximum wind). The translational wind speed decrease in line with the distance from the cyclonic system's center is taken into account to provide more realistic estimates of wind exposure on the ground. To our knowledge, there is no other publicly available dataset for ground weather stations or remote sensing measurements covering the whole territory of Madagascar with a spatial resolution above $0.02° \times 0.02°$. This is the main reason why we decided to use the wind speed estimate calculated by Geiger et al. (2018).[12]

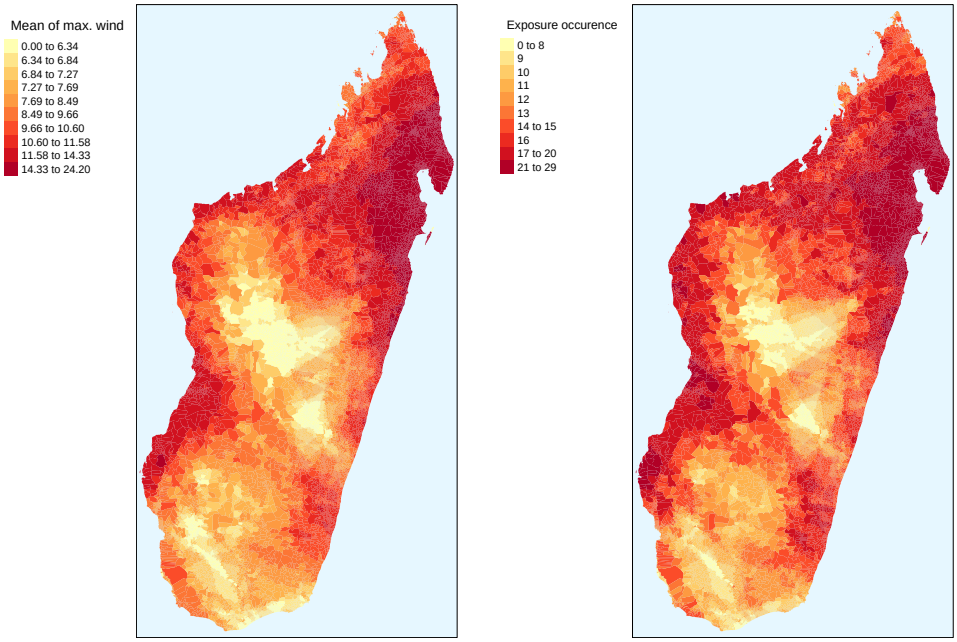

(a) Exposure measured by mean of max. wind speed (b) Exposure measured by occurence

Figure 3: Cyclone exposure in Madagascar between 1950 and 2020

Figure 3 depicts the observed exposure of Malagasy villages over the 1950-2020 period.

[12]The initial version of the dataset is referenced as Geiger et al. (2017) and is available in its initial form at https://dataservices.gfz-potsdam.de/pik/showshort.php?id=escidoc:2387904

This figure reports the average maximum wind speed experienced by each village (over the total number of landfalling cyclonic systems), while the latter depicts the exposure occurrence. The main difference between the two indicators of cyclonic exposure is that inland, when measured by the maximum wind speed, the windspeed intensity mechanically decreases, because the tropical cyclone wind speeds weaken once the system is not at sea. Consequently, by relying on dummies, panel (b) of Figure 3 provides a different picture to panel (a) and tends to slightly "overestimate" cyclonic exposure. Regardless of the indicator of exposure, the north-east coastline is the most exposed followed by villages along the west coast. This exposure at the village level is in line with the cyclogenesis of the SWIO. First, cyclonic systems form in the east of the SWIO basin before moving from east to west. Second, the Mozambique channel is the second area of cyclogenesis and sometimes cyclonic systems make landfall on the west coast of the island.

4 Empirical framework

The main purpose of the paper is to measure how exposure to wind speed induced by tropical cyclones impacts economic activity as measured by nightlight brightness intensity. To achieve this purpose, we estimate different versions of the following baseline model:

$$y_{ft} = \sum_{l=1}^{L=24} (\beta_l \times W_{f,t-l}) + \mu_f + \eta_t + \varepsilon_{ft} \tag{2}$$

In this regression model, y_{ft} is the logarithm of our dependent variable, namely mean nightlight intensity during month t for Fokontany f. As non-stationarity could be problematic in a panel framework, we conduct the unit root test of Im et al. (2003) on nightlight data. This test leads us to reject the null hypothesis of non-stationarity, and consequently, we include our dependent variable in the regression in (log-)level. Our main explanatory variable is the mean of maximum wind speed of pixels belonging to Fokontany f, and the set of β_l are estimated associated coefficients. It should be observed that in our baseline estimates, we include wind speed exposure from lag $t-1$ until lag $t-24$. Given that the monthly average of brightness intensity is computed using daily high-quality satellite imagery, we choose to exclude contemporaneous exposure in t to avoid having a tropical cyclone occur at the end of a given month, while daily observations of nightlight could be captured before exposure. The use of a distributed lag model allows us to unveil the dynamic effects of tropical cyclone exposure and focus on the cumulative effect of a tropical cyclone shock on the intensity of nightlight. The cutoff of 24 was chosen during the exploratory phase of this work and is consistent with empirical work using annual data (Bertinelli and Strobl, 2013; Elliott et

al., 2015). We nevertheless check for the robustness of this choice by either increasing or decreasing the number of lags. We include Fokontany fixed effects μ_f to control for unobserved and time-invariant characteristics that could potentially affect the brightness observed for a given spatial unit. These unobserved factors could be related to time-invariant heterogeneity among Fokontany. This individual fixed effect also accounts for the possibility that some Fokontany are more exposed to tropical cyclones and possibly implement mitigation measures (assumed to be time-invariant over our sample period), which could reduce the detrimental effects associated with tropical cyclone wind speed. Furthermore, it should be observed that choosing the Fokontany as our preferred spatial unit of interest has several implications, because we believe that the associated fixed effects have a greater economic interpretation than those related to a spatial unit based on an "arbitrary" grid of the Malagasy territory. We also flexibly account for month-specific components shared by all Fokontany using a month fixed effect η_t. The inclusion of such time fixed effects becomes even more relevant in our context, because some months are more cloudy than others, which impacts the number of valid daily observations obtained from the satellite. Moreover, the inclusion of these time fixed effects ensures that the relationship of interest is independent from idiosyncratic shocks. Finally, ε_{ft} is the standard error term.

In equation (2), the main coefficients of interest are the set of β_l. They are indicative of the effect of wind speed exposure in period $t-l$ on Fokontany's nightlight brightness intensity in the current period t. Existing evidence about the impact of tropical cyclone exposure on economic activity at the local level points mainly toward a negative effect that is mostly short-lived. Thus, using grid-level regressions for a sample of Caribbean islands, Bertinelli and Strobl (2013) found that the contemporaneous effect of hurricanes on nightlight is negative, while no significant effect is found for tropical cyclones occurring with a lag of 1 and 2 years. Likewise, Elliott et al. (2015) found similar results with Chinese data. These two papers use annual data for nightlight and cyclone exposure, which contrasts with our approach based on high-frequency monthly data.

A first option when estimating equation (2) is to use a standard ordinary least square (OLS) regression by pooling all cross-sections together and not transforming the data. Due to the exogenous nature of tropical cyclone wind speeds with regard to our dependent variable, it is unlikely that reverse causation is a concern. Arguably, exposure to wind speed could impact nightlight radiance, although the reverse effect appears impossible. However, a pooling model still suffers from the omitted variable bias.[13] In particular, if a correlation exists between the unobserved characteristics of a Fokontany and its nightlight intensity, putting the former into

[13] As recalled by Dell et al. (2014), in a pooling model context, increasing the number of control variables does not necessarily reduce the omitted variable bias.

the error term is problematic, as it may potentially lead to inconsistent estimates (Wooldridge, 2010). For this reason, our preferred specification throughout this paper includes both types of fixed effects.

Insofar as fixed effects are included in equation (2), variables are expressed in deviations from the individual and temporal sample means (Croissant and Millo, 2018). Our identification thus emphasizes month-to-month variations in levels from the observed means. As a consequence, the fixed effect coefficients associated with wind speed could be interpreted as the impact of tropical cyclone shocks on nightlight intensity. Given the nature of our estimated effect, it is legitimate to raise the question about the external validity of our study, especially in a context of anthropogenic warming. Indeed, one could argue that the effect of short-run changes of a given weather variable on some economic outcome differs from the effect of a long-run and gradual change in the same weather variable. In particular, economic agents (i.e., households, companies, or policymakers) may engage in actions to mitigate the negative effect of climate change or increase their coping capacity. Regarding tropical cyclones, it is expected that climate change will decrease their frequency but increase their average intensity along with the proportion of cyclonic systems reaching very intense levels (category 4-5 on the Saffir-Simpson scale) (Knutson et al., 2020). Consequently, it is likely that tropical cyclones will still act as a shock, and for this reason, focusing on annual variations remains a relevant departure point.

Our main assumption when identifying the causal effect of tropical cyclones on economic activity at the local level is randomness. Being exposed to cyclonic systems can be viewed as (quasi-)random insofar as the formation of cyclonic systems as well as their precise trajectories and magnitude are stochastic and difficult to predict. When they occur, tropical cyclones generate recognizable wind speeds of high magnitude that (quasi-)randomly hit large spatial units, thus leaving the inhabitants and assets on the ground impacted by the exposure. Given that month-to-month variations in the exposure to tropical cyclones shocks are (quasi-)random, our reduced-form panel framework imposes relatively few identifying assumptions, while ensuring a causative interpretation.

5 Results

This section presents the results obtained by estimating the econometric model detailed in the previous section with panel data techniques. It also provides additional analyses based on the interaction terms to unveil some heterogeneity in the effect along with several robustness checks of the baseline model. All estimations were done with the R software (R Core Team,

2019) using the tools provided by the "`fixest`" package.[14]

5.1 Main results

Table 2 reports the regression results of alternative estimations of equation (2). To observe how the inclusion of a Fokontany's fixed effects μ_f and time fixed effects η_t impact the estimated coefficients, we begin with a simple OLS regression in column (1) and then sequentially add fixed effects throughout columns (2) to (4).

	(1)	(2)	(3)	(4)
W_{t-1}	0.00239***	0.00188***	0.00110	0.00046***
	(0.00004)	(0.00002)	(0.00090)	(0.00002)
W_{t-2}	0.00096***	0.00043***	0.00039	−0.00023***
	(0.00004)	(0.00002)	(0.00088)	(0.00001)
W_{t-3}	−0.00063***	−0.00113***	0.00041	−0.00021***
	(0.00004)	(0.00002)	(0.00068)	(0.00002)
W_{t-4}	−0.00102***	−0.00152***	0.00047	−0.00015***
	(0.00004)	(0.00001)	(0.00089)	(0.00001)
W_{t-5}	−0.00063***	−0.00113***	0.00095	0.00027***
	(0.00005)	(0.00001)	(0.00076)	(0.00001)
W_{t-6}	0.00096***	0.00047***	0.00064	−0.00004*
	(0.00005)	(0.00002)	(0.00073)	(0.00002)
W_{t-7}	0.00215***	0.00166***	0.00068	−0.00000
	(0.00005)	(0.00002)	(0.00086)	(0.00002)
W_{t-8}	0.00166***	0.00116***	0.00084	0.00015***
	(0.00005)	(0.00001)	(0.00084)	(0.00002)
W_{t-9}	−0.00038***	−0.00088***	0.00157	0.00088***
	(0.00005)	(0.00002)	(0.00091)	(0.00003)
W_{t-10}	−0.00072***	−0.00122***	0.00020	−0.00048***
	(0.00005)	(0.00002)	(0.00078)	(0.00002)
W_{t-11}	−0.00128***	−0.00145***	0.00047	0.00016***
	(0.00004)	(0.00002)	(0.00083)	(0.00002)
W_{t-12}	0.00112***	0.00090***	0.00160	0.00120***
	(0.00004)	(0.00002)	(0.00137)	(0.00002)
W_{t-13}	0.00189***	0.00169***	0.00032	−0.00004*

[14] Details about the "`fixest`" package can be found via the following link: https://cran.r-project.org/web/packages/fixest/vignettes/fixest_walkthrough.html.

	(1)	(2)	(3)	(4)
	(0.00004)	(0.00002)	(0.00099)	(0.00002)
W_{t-14}	0.00177***	0.00152***	0.00076	0.00036***
	(0.00004)	(0.00001)	(0.00069)	(0.00001)
W_{t-15}	0.00054***	0.00016***	0.00049	0.00008***
	(0.00004)	(0.00001)	(0.00061)	(0.00001)
W_{t-16}	−0.00210***	−0.00248***	0.00066	0.00025***
	(0.00004)	(0.00002)	(0.00083)	(0.00001)
W_{t-17}	−0.00262***	−0.00300***	0.00086	0.00045***
	(0.00004)	(0.00002)	(0.00104)	(0.00002)
W_{t-18}	−0.00178***	−0.00215***	0.00088	0.00047***
	(0.00004)	(0.00002)	(0.00091)	(0.00002)
W_{t-19}	−0.00004	−0.00042***	0.00043	0.00002
	(0.00004)	(0.00002)	(0.00058)	(0.00002)
W_{t-20}	0.00144***	0.00106***	0.00121	0.00080***
	(0.00004)	(0.00002)	(0.00079)	(0.00002)
W_{t-21}	0.00020***	−0.00023***	0.00047	0.00005**
	(0.00004)	(0.00002)	(0.00101)	(0.00002)
W_{t-22}	−0.00213***	−0.00258***	0.00054	0.00010***
	(0.00004)	(0.00003)	(0.00058)	(0.00003)
W_{t-23}	−0.00187***	−0.00258***	0.00053	−0.00038***
	(0.00004)	(0.00002)	(0.00084)	(0.00002)
W_{t-24}	−0.00016***	−0.00084***	0.00106	0.00015***
	(0.00004)	(0.00002)	(0.00063)	(0.00002)
Fokontany fixed effects	NO	YES	NO	YES
Time fixed effects	NO	NO	YES	YES
adj. R^2	0.01927	0.80051	0.12626	0.90458
Obs.	1325586	1325586	1325586	1325586

$^{***}p < 0.001$; $^{**}p < 0.01$; $^{*}p < 0.05$

Table 2: Regression results with the logarithm of nightlight as dependent variable.
Sources: Black marble data of Roman et al. (2018), TCE-DAT of Geiger et al. (2018) and authors' own calculations.

The first column of Table 2 depicts the results of a model without any fixed effects. It thus corresponds to the "pooling" model. Quite surprisingly, this model suggests that wind speed experienced at the village level in $t-1$ and $t-2$ is positively associated with nightlight

radiance. However, from $t-3$ to $t-5$, wind speed is negatively associated with nightlight. Looking in detail at the other coefficients of wind speed exposure, we observe some erratic movements, since positive coefficients are followed by negative ones and so on. At first glance, the effect of wind speed exposure on local economic activity appears ambiguous.

In columns (2) and (3), we sequentially include Fokontany and time fixed effects. A closer inspection of these two columns reveals that the magnitude of the estimated coefficients β_l varies with the inclusion of the fixed effects. For instance, let us focus on β_1. From an estimate of β_1 of 0.00239 in model (1), the model of column (2) provides an estimate of 0.00188, while that of column (3) has $\beta_1 = 0.00110$. Such changes in the value of the coefficients indicate that correlations exist between fixed effects and economic activity as measured by nightlight, so that including them in the error term could induce bias in these estimations. Moreover, it is also noteworthy that coefficients associated with wind speed exposure are estimated with much less precision in the model that includes only time fixed effects, since each time the null hypothesis of $\beta_l = 0$ is not rejected. Overall, given the sensitivity of the results to the inclusion of fixed effects, our preferred specification controls for the Fokontany and time unobserved heterogeneity.[15]

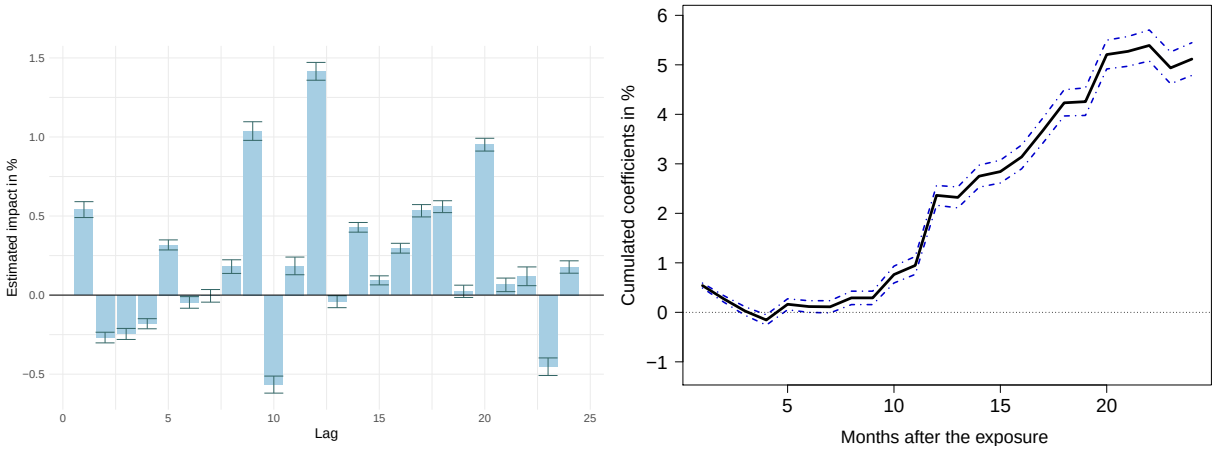

(a) Estimated impacts (b) Cumulative impacts

Figure 4: Effect of a one-standard deviation tropical cyclone shock in the baselin model.

Column (4) of Table 2 presents the results of the estimation of the complete version of equation (2), which incorporates both kinds of fixed effects. In accordance with what has been observed for the OLS model, it shows a positive effect of wind speed exposure in $t-1$

[15]To further strengthen this choice, we ran the Lagrange multiplier test. Specifically, we tested for the presence of village, time, and both kinds of fixed effects. Each time, the tests indicates the presence of fixed effects. As the presence of the Fokontany and time fixed effects is not rejected, the model with both of them is our preferred specification.

on the level of nightlight. However, for past wind speed exposure in $t-2$ to $t-4$, the estimated coefficients are significantly negative. Thus, the corresponding impact of a tropical cyclone strike to one standard deviation above its mean in t implies an increase in nightlight of 0.541% in $t+1$ but a decrease of 0.268%, 0.246%, and 0.181%, in $t+2$, $t+3$, and $t+4$, respectively. Over this period, the total effect amounts to -0.155% and significantly differs from zero. It should also be observed that during the first year after the exposure, half of the estimated coefficients are significantly negative, whereas the other half is significantly positive. By contrast, during the second year after a tropical cyclone strike, from month $t+13$ to month $t+24$, three quarters of the coefficients are significantly positive (see also panel (a) of Figure 4 who depicts the estimated impact to a cyclone shock of one-standard deviation) . To provide a better assessment of our findings, we display the cumulative marginal effects of a one-standard deviation tropical cyclone wind speed shock panel (b) of Figure 4. The visual inspection of the figure confirms what has been observed in analyzing the coefficients of Table 2. In particular, during the first year after the shock, the cumulative effect of wind speed on local economic activity is weak and oscillates around zero. For instance, in $t+8$, the cumulative effect is 0.292%. However, as coefficients are mainly positive during the second year after the tropical cyclone strike, we witness a strong and positively significant effect of wind speed on nightlight brightness. Thus, 15 months after the exposure, nightlight brightness is about 3% higher, while the gain reaches 5% after 2 years.

Overall, the results of the econometric model, including Fokontany and time fixed effects, suggest that the effect of tropical cyclone exposure on nightlight brightness is weak during the first year after the exposure and globally positive thereafter. In what follows, we will show that depending on the chosen specification, the short-term effect could be significantly negative. However, the net positive effect during the second year shows a strong and regular pattern in our estimations. As detailed by Hsiang and Jina (2014), economic activity follows four main trajectories after a disaster. Given the pattern observed from our regression, we interpret our results in accordance with the "build back better" hypothesis: after a period in which the economy suffers from the negative consequences associated with a disaster, the replacement of lost and "outdated" assets by new ones, which probably correspond to new and more efficient technologies, leads to a globally positive net effect (Crespo Cuaresma et al., 2008; Hsiang and Jina, 2014).[16] To our knowledge, we are the first authors to empirically document the existence of such an effect in the context of a developing country using detailed and spatial monthly data on nightlight data and cyclonic exposure. In particular, previous

[16]At this stage, it should be mentioned that we have no information about the true origin of the positive boosts in nightlight brightness unveiled by our regressions. The latter could come from either the private or the public sector (through specific reconstruction policy programs after the adverse shock) or from international aid.

studies, such as Bertinelli and Strobl (2013) and Elliott et al. (2015) (among others), using annual data find a negative and mainly short-lived effect. Mohan and Strobl (2017) and Skoufias et al. (2021) are probably the closest papers from ours in term of empirical approach. As in this paper, they employ high frequency nightlight data. However, they focus on a single particular cyclonic event while our regressions allow for a systematic study of several cyclonic events in Madagascar. Even with monthly data, these two papers find quite different and event-dependent results. While Mohan and Strobl (2017) findings are in line with ours, Skoufias et al. (2021) find either no significant effect or significant effect 7 months after the shock. Given these results, and combined with the new evidence provided in this paper, we believe that more empirical studies should be done to have a global perspective about the economic consequences of tropical cyclones at a local level in other regions of the world. In this respect, relying on high-frequency data is also needed because our baseline regressions show that the direction of the effect could take place and change within the year after the shock. This reinforces our initial conjecture that low-frequency data could hide the true trajectory of the impacted economy.

5.2 Robustness

Index of potential destruction

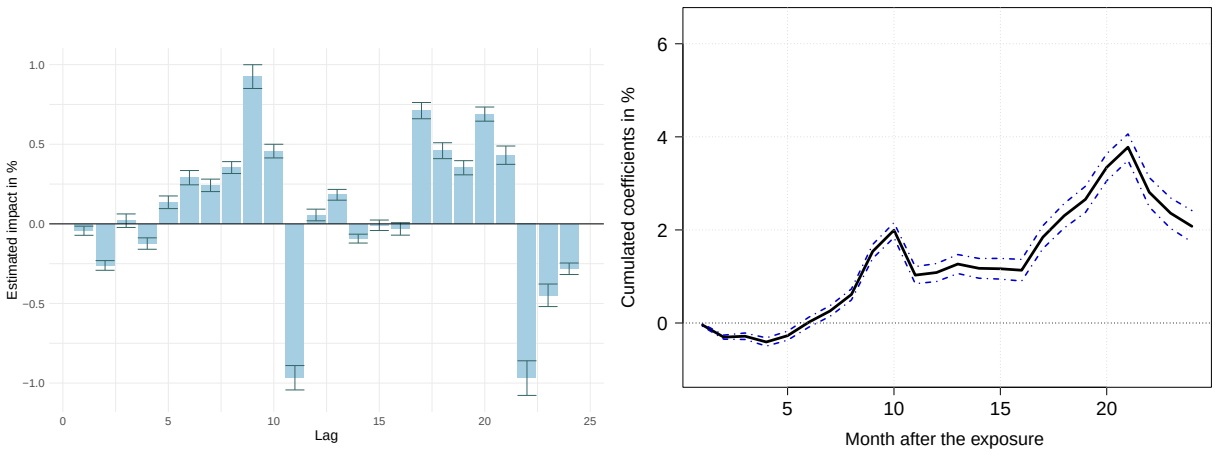

(a) Estimated impacts

(b) Cumulative impacts

Figure 5: Effect to a one-standard deviation tropical cyclone shock as measured by the index of potential destruction.

An important robustness check is to confirm whether the results are similar when an alternative formulation of our measure of tropical cyclone exposure is employed. We tackle

this issue by considering another measure of tropical cyclone incidence. Rather than using the wind speed experienced by a given spatial unit, many authors base their analysis on ad-hoc indices of potential destruction (also known as the damage function).[17] The impetus behind these indices follow Emanuel (2011). More specifically, below a certain threshold $\bar{W}$, it is unlikely that wind speed provokes substantial physical damage so that the level of physical destruction could be assumed to be zero. However, once the wind speed generated by the cyclonic system exceeds $\bar{W}$, the level of damage increases though in a non-linear fashion. Furthermore, to be appropriate, damage should not increase until infinity, and it is probably more realistic to propose an index that calibrates the proportion of economic loss between zero and one. Consequently, we follow Emanuel (2011) and construct the following index d_{ft} capturing the proportion of damaged property:

$$d_{ft} = \frac{v_{ft}^3}{1 + v_{ft}^3} \tag{3}$$

with

$$v_{ft} = \frac{MAX\left(W_{ft} - \bar{W}, 0\right)}{W^* - \bar{W}}. \tag{4}$$

Where W^* corresponds to the threshold at which half of buildings are damaged. We nevertheless lack strong empirical evidence when choosing appropriate values for $\bar{W}$ and W^*. Here, we fix $\bar{W}$ to 93 km/h as indicated by Emanuel (2011). We set W^* to 166 km/h, namely the threshold of wind speed at which the RSMC of La Réunion labels a tropical system as an "intense'' tropical cyclone. Corresponding results are reported in Figure 5 in forms of estimated impacts (estimated coefficients times a one-standard deviation cyclone shock), and cumulative marginal effects.

It appears that for a tropical cyclone shock of one standard deviation, the shape of the cumulative marginal effects is the same between our baseline estimate and the robustness check using d_{ft} instead of W. The quantitative nature of the impact is, however, slightly different. First, in the short term, during the first 5 months after the shock, the negative impact is significantly negative, though of weak magnitude, when the damage function is employed. Second, when the exposure is measured by wind speed, the net positive effect 20 months after the exposure is around 5% compared to 3.5% when the damage function is used.

Overall, the use of the damage function suggests that the main impetus of this paper does not depend on the choice of the wind speed variable. However, this alternative measure of exposure to cyclonic systems has an important limitation, since it relies on parameters,

[17] Examples include Strobl (2011), Bertinelli and Strobl (2013), Elliott et al. (2015), and Mohan and Strobl (2017)

namely $\bar{W}$ and W^*, for which evidence is scarce in the context of Madagascar. For this reason, our preferred specification directly uses wind speed experienced at the Fokontany level.

Using pixel rather than Fokontany

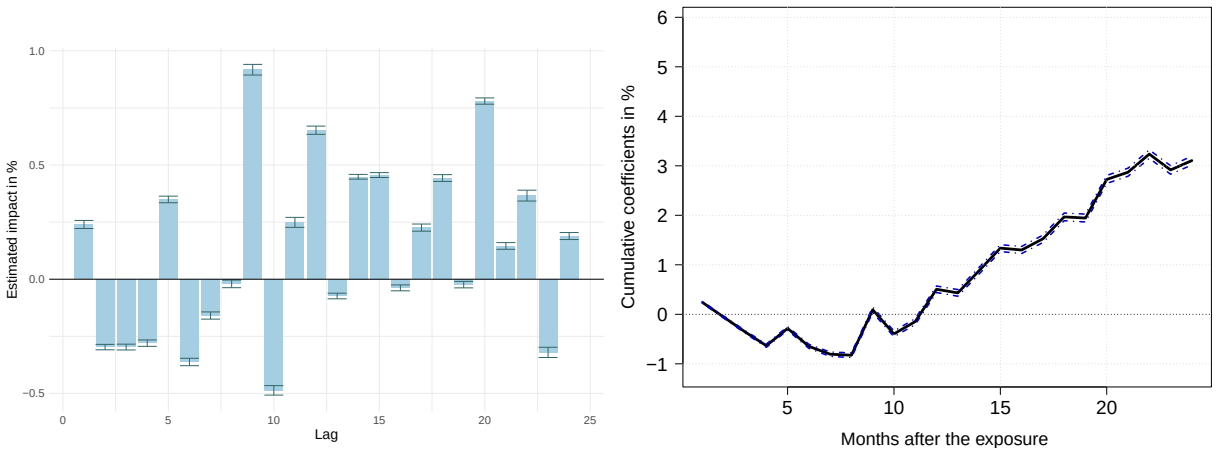

(a) Estimated impacts

(b) Cumulative impacts

Figure 6: Effect to a one-standard deviation tropical cyclone shock as measured by the index of potential destruction.

As explained previously, in our baseline estimation, we choose the Fokontany as our spatial unit of reference. This choice is motivated by the fact that i) the Fokontany constitute the smallest administrative level in Madagascar, ii) Fokontany fixed effects have probably more economic interpretatin and ii) pixel-level regressions are resource-consuming. Here, we reconsider our initial choice and estimate a pixel-level regression similar to the model of column (4) in Table 2. By showing the corresponding marginal cumulative effect to one standard deviation of wind speed shocks, Figure 6 shows the results. Two comments are in order here. First, and in contrast to the baseline case, the pixel-level regression shows the significantly negative impact of tropical cyclones on nightlights. Specifically, 9 months after the shock, the total nightlight loss is 0.9%. Second, we observe the same recovery pattern during the second year after the shock. After 2 years, the net effect of wind speed exposure is positive and amounts to 3% when the pixel is the spatial unit of reference (versus 5% when the village is the spatial unit of reference).

Again, the main message of our baseline model, namely the existence of a significant recovery during the second year after the impact, is insensitive to the spatial unit employed as the baseline. However, we believe that using the village in the baseline makes more economic

sense, since the associated fixed effects probably capture some unobserved components that cannot be controlled when using a cell based on an "arbitrary" cutting of Madagascar.

Changing the number of lags

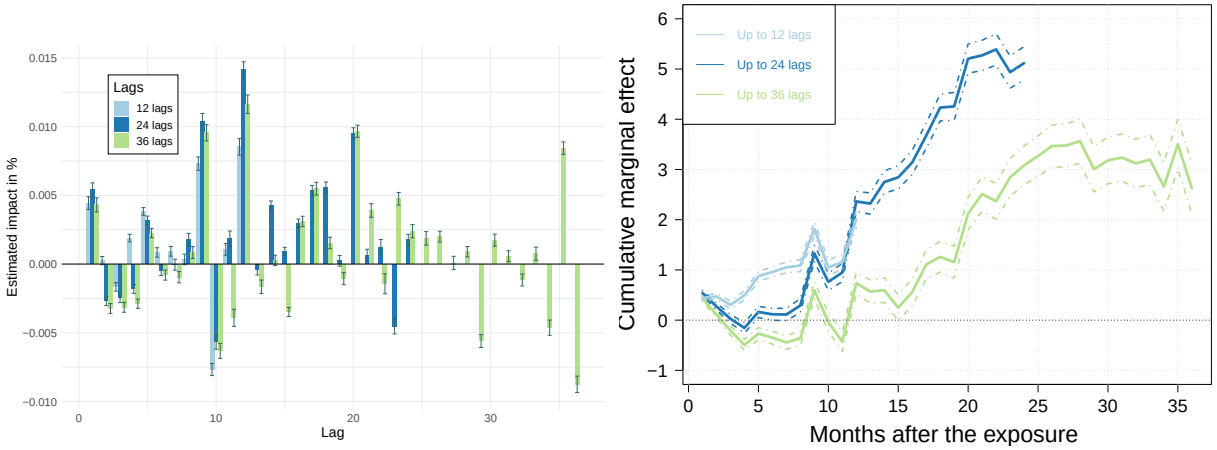

(a) Estimated impacts

(b) Cumulative impacts

Figure 7: Effects of a one-standard deviation tropical cyclone shock based on models including different number of lags.

In the baseline equation (2), we include up to 24 lags of maximum wind speed exposure in the econometric model. Here, we reconsider our main specification by changing the number of lags. We consider two alternatives: i) reducing the number of lags and only including up to 12 lags, and ii) increasing the number of lags and including up to 36 lags. The latter option enables us to investigate to what extent the positive effects due to wind speed persist over time.

As shown in Figure 7, the effect of tropical cyclone shocks is nearly the same for our baseline case and the case with only 12 lags. Despite the slightly higher short-term effect in the latter case, the effect is nearly identical 12 months after the impact. The comparison of the baseline estimates with the model with up to 36 lags shows some interesting features. First, when 36 lags are included, the short-term effect is slightly negative and significant. Second, and in line with the baseline case, a recovery is observed during the second year after the shock, although its magnitude is lower than what is observed in the model with 24 lags. Lastly, the increase in nightlights flattens 24 months after the Fokontany's exposure. In other words, in terms of the cumulative marginal effects, there are no significant differences between the point estimated in $t + 24$ and all the estimates associated with months $t + 25$ to $t + 36$.

Overall, even if the quantitative nature of the results slightly changes with the exclusion or inclusion of lags, the qualitative nature of the main significance of our baseline estimate is the same: a year after a tropical cyclone strike, economic activity as measured by nocturnal human lights recovers significantly.

5.3 Refinements of the results

Overall, the panel estimates of the last subsection reveal that a tropical cyclone shock leads to a significant increase in nocturnal economic activity 12 months after the impact. In this subsection, we propose an in-depth analysis by investigating three potential characteristics of the effect of wind speed exposure. First, we consider a specification to test the existence of non-linearities in the effect. Second, we test whether the causal effect depends on the degree of past exposure at the Fokontany level. Third, we question whether the effect is the same in terms of the average degree of brightness of villages. To deal with these three issues, we rely on either binary variables or interaction terms. To preserve parsimony and save some space, we present the corresponding estimated impacts together with the cumulative marginal effects. The former are easy to obtain, as they correspond to the product of the estimated coefficients and the standard deviation of tropical cyclone windspeed.

Using bins

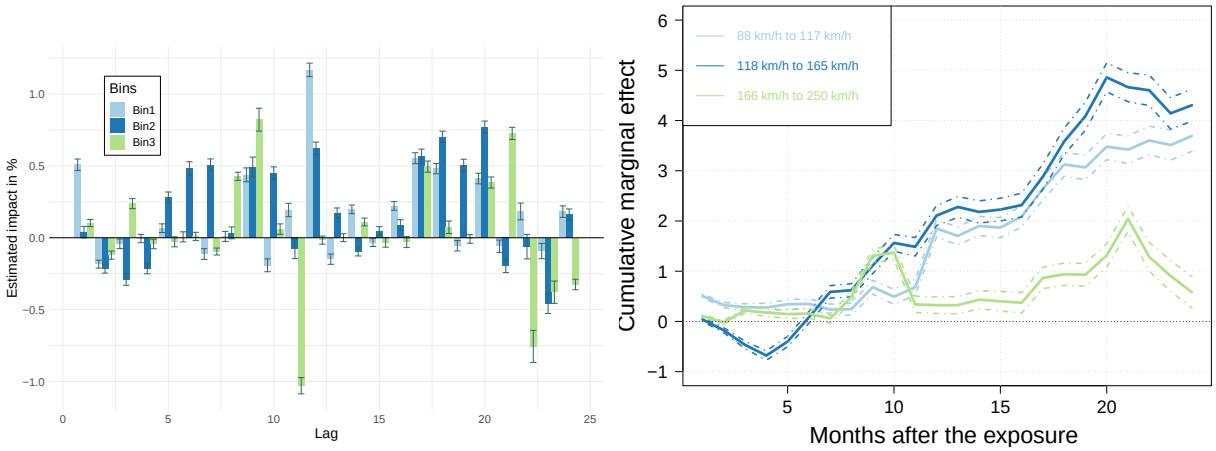

(a) Estimated impacts (b) Cumulative impacts

Figure 8: Effect to a one-standard deviation tropical cyclone shock for different bins.

Our baseline model implicitly assumes that the nightlight response to tropical cyclone shocks is linear in terms of wind speed exposure. However, the literature exploring the effect of

weather shocks on economic variables often indicates that effects are likely to be non-linear. In particular, Emanuel (2011) and Nordhaus (2010) suggest that damages exponentially increase with the level of wind speed experienced on the ground. In other papers, the non-linear nature of the response of economic activity to tropical cyclones is *a priori* imposed (Bertinelli and Strobl, 2013; Elliott et al., 2015; Mohan and Strobl, 2017; Strobl, 2011). Despite these proposals, in our baseline model, we depart from this "standard" practice by using a "raw" measure of wind speed exposure at the village level. Here, to reveal a possible non-linear relationship, we reconsider our baseline choice and employ a non-parametric approach by dividing wind speed into four bins. Such an approach has two main advantages. On the one hand, it is simple to implement, and on the other, it is flexible and does not impose any functional forms to our wind speed explanatory variable. We thus construct three dummies equal to one when wind speed falls within a given interval and otherwise zero. Specifically, $\tilde{w}_t^1 = 1(W_t \in]88; 117])$, $\tilde{w}_t^2 = 1(W_t \in]117; 165])$, and $\tilde{w}_t^3 = 1(W \in]165; 250])$.[18] Here, the chosen bins correspond to the classifications of cyclonic systems of the Regional Specialized Meteorological Center (RSMC) of La Réunion. The corresponding cumulative marginal effects are depicted in Figure 8.

Overall, the shapes of the cumulative marginal effects are similar to what we observed in our baseline. However, a thorough inspection of the three curves offers some nuanced results. More specifically, for wind speeds of intermediate magnitude, namely 118 km/h to 165 km/h, we observed a nil impact in $t-1$ along with a significantly negative impact in the short run (until 4 months). For this wind speed exposure, in $t-4$ the loss of nocturnal activities amounts to 0.680%. By contrast, for the two other bins, during the same timeframe, the cumulative marginal effect is weaker and fluctuates around zero. It is noteworthy that for intermediate wind speed exposure, the "recovery" is stronger than for low and high wind speed exposure. For example, 20 months after the exposure, the increase in nightlight activity is around 5% compared to 3.5% and 1.5% for low and high wind speed exposure, respectively. The shape of the cumulative marginal effect for intermediate wind speed exposure is consistent with the "build back better" hypothesis (Hsiang and Jina, 2014). Finally, another insight gained from Figure 8 is that for wind speed exposure of high magnitudes, the positive effect is significantly lower.

Cyclone prone Fokontany

The exposure of the Malagasy territory to tropical cyclones is quite heterogenous since 1950 (see panels of Figure 3). Specifically, during the 1950-2020 sample period, some villages were exposed to tropical cyclone wind speeds up to 20 times, while others were exposed

[18] Implicitly, the first bin $\tilde{w}_t^0 = 1(W_t \in [0; 88])$ serves as the reference in the regression.

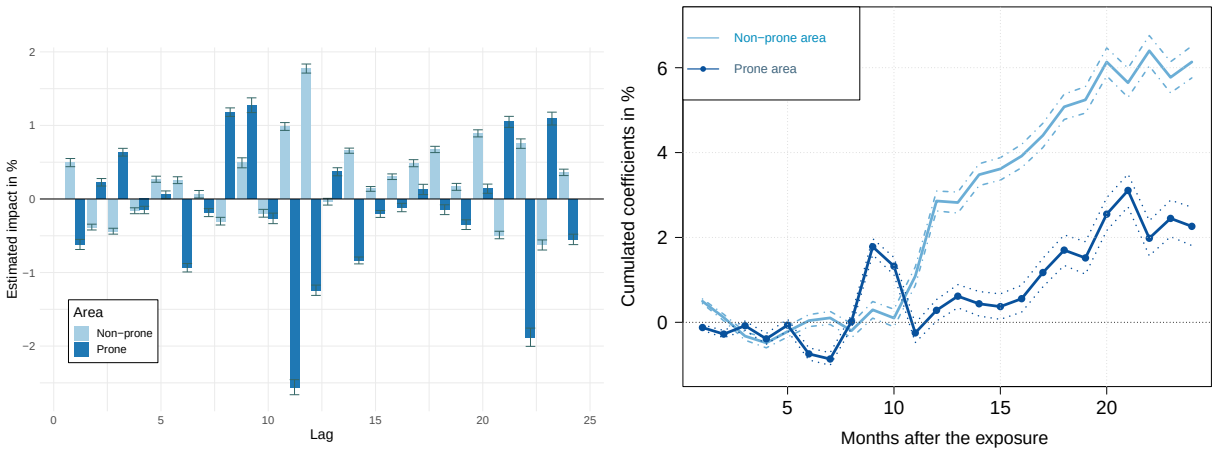

(a) Estimated impacts (b) Cumulative impacts

Figure 9: Effect to a one-standard deviation tropical cyclone shock for cyclone-prone Fokontany.

less than 10 times. Even after controlling for village fixed effects, it is still possible that the effect of tropical cyclone wind speeds depends on the degree of preparedness of people living in the most exposed village. Consequently, we could imagine that adaptation measures were implemented in the most exposed villages to lessen the detrimental effects of a tropical cyclone strike. To investigate this issue, we interact wind speed exposure with a dummy equal to one if the Fokontany were exposed more than 16 times to cyclonic systems during the 1950-2020 period. We refer to these villages as cyclone-prone areas. The corresponding results are shown in Figure 9. Unambiguously, our hypothesis regarding the effect of cyclonic wind speed depending on the level of exposure is invalidated. In particular, the estimated impacts are mainly negative and greater (in absolute values) for cyclone-prone areas than in non-prone areas. Thus, 7 months after the strike, the loss of nightlight in cyclone-prone villages is approximately 0.9%, while the corresponding effect is non-significant for non-prone areas. Thereafter, the beneficial effect revealed in our baseline estimate appears to be of a lower magnitude for cyclone-prone villages. At the end of the timeframe represented in Figure 9, non-cyclone prone villages experience an increase in nocturnal human activity of 6% compared to 2% for the villages that are more often exposed to cyclonic systems. We do not find any evidence that cyclone-prone areas in Madagascar use efficient adaptation measures that reduce the negative effect of tropical cyclones in the short term.

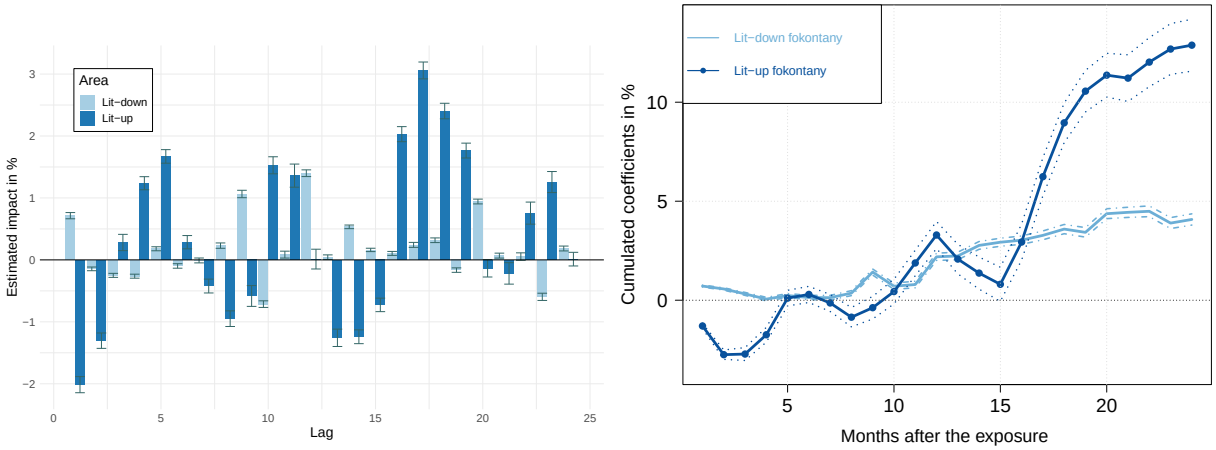

(a) Estimated impacts

(b) Cumulative impacts

Figure 10: Effect to a one-standard deviation tropical cyclone shock for lit and unlit Fokontany.

Lit Fokontany

In contrast to developed countries, a large proportion of the Malagasy territory is weakly lit. As shown in Figure 1, this is particularly true for the coastline of the island, especially the west coast. Furthermore, Table 1 indicates that more than 90% of Fokontany have a brightness level that is less than the mean of the corresponding distribution. We could conjecture that lit areas mainly correspond to urban areas, while poorly lit (or unlit) areas correspond more to rural areas. As stressed in Dessy et al. (2019), the characteristics of economic and human activity differ sharply in these two areas. In rural areas, agrarian activities are at the center of economic life. By contrast, in urban and "lit" areas, economic life is more diversified, and the share of the service sector is higher. Consequently, it is likely that the response to tropical cyclone shocks is heterogenous and depends on the characteristics of the area. For instance, we could imagine that the degree of sensitivity of agricultural areas to wind speed exposure is higher in the short term. To investigate this possibility, we interact wind speed exposure experienced at the Fokontany level with a dummy that indicates if the corresponding spatial unit is lit or not. We construct this dummy as follows. First, we inspected the monthly images of the Fokontany and selected the month with the highest record of good-quality images. This led us to select the month of October in 2013.[19] Based on this specific image, we classified villages as lit and "urban" areas when the observed radiance value exceeded 5 (corresponding to the rounded value of the mean of 4.82), and otherwise weakly lit. Figure 10 shows the estimated impacts together with the cumulative marginal effects.

[19]We also conducted a similar analysis based on other months. This had no impact on the qualitative or quantitative results.

The two curves of cumulative marginal effects of the panel (b) provide an interesting finding. For the Fokontany categorized as "lit," the short-term impact is unambiguously negative. At the time of the shock, nocturnal activities in "highly" lit Fokontany decrease by 1.301%. Two months after the shock, the total nightlight loss amounts to 2.750%. This short-term negative impact is not observed in unlit villages. Then, after the short-term negative effect, a recovery is quickly observable. In particular, from the fifth to the tenth month, the cumulative effect is non-significantly different from zero, suggesting that the loss observed during the first few months is later offset by some minor gains. However, during the second year after the shock, the recovery is evident, and at the end of the timeframe observed in the figure, the total nightlight gain reaches almost 13%, while for unlit areas, the same beneficial effect is around 4%. Overall, the estimation of the latter model indicates that the most lit areas suffer from a short-term detrimental effect of tropical cyclone shocks, although we did not find any evidence of such an effect for unlit and rural areas. For urban areas, we interpret the shape of the cumulative marginal effect as evidence supporting the "build back better" hypothesis, which indicates that a local economy initially suffers from tropical cyclone shocks. However, the gradual replacement of lost and probably outdated assets by more recent ones that use new and more efficient technologies induces a globally positive net effect. The novelty of our paper is to show that such transformations occur in the very short term, since the negative effect is only observed a few months after the disaster.

6 Conclusion

This paper investigates the local effect of tropical cyclones on economic activity in a developing country, namely Madagascar. We combine detailed spatial nightlight data with data on tropical cyclone exposure. Focusing on the smallest administrative subdivision in Madagascar rather than pixels obtained from a territorial grid, we find that wind speed exposure has an ambiguous effect on nightlight brightness up to 12 months after the shock. Thereafter, our regressions show that wind speed exposure actually increases the level of nightlight data. Further analyses indicate that depending on the heterogeneity dimensions considered, the short-run effect of wind speed exposure could be negative, although we can confirm that the overall beneficial effect on nightlight brightness is a regular pattern that emerges in our work. Alternative specifications of our baseline model, which involve changing the variable measuring the exposure, the spatial unit of interest, or the number of lags included in the model, do not alter the qualitative nature of our results.

We believe that the heterogeneity in the effects unveiled in our paper is key. We interpret it as a need to go further in this direction - namely employing high resolution spatial and

infra-annual data - for others cyclone-prone regions in the world because it is accompanied by specific messages in terms of policy design. In particular, as the short-term effects are effectively negative for lit-up and prone area and that positive effects are at work only during the second year, this indicates that the recovery process is long. In term of policy implications, this suggests that governments should be more reactive in assisting affected local populations who may initially be injured or homeless after the cyclone and subsequently find themselves in a precarious housing situation because of the destruction of assets. Such reactivity can be achieved through anticipation measures consisting for example in the *ex-ante* creation of funds dedicated to post-cyclone interventions, emergency response plans or the constitution of stocks of raw materials useful for reconstruction activities.

All in all, the results of this paper demonstrate that being hit by a tropical cyclone could induce an overall increase in nocturnal human activities. Even though this result provides an "optimistic" view about the consequences of natural disasters, two aspects should be kept in mind. On the one hand, by using such detailed geographic information on nightlights and cyclone exposure, we are able to provide information about the consequences of tropical cyclones without fully identifying the underlying mechanisms that lead to this post-cyclone trajectory. On the other hand, by questioning the consequences of tropical cyclones from a quantitative perspective, we probably neglect many non-tangible consequences of such weather events that could have a huge potential. In particular, the exposure to cyclonic systems also induces loss of life and assets, not to mention the emotional trauma and stress felt by inhabitants who are directly threatened by tropical cyclones. We are convinced that such aspects should occupy a greater place in the economic literature, because they have the potential to cause long-term disadvantages for the exposed population, especially for exposures that occur during infancy. Furthermore, given that the current predictions suggest that economic and demographic growth should increase population exposure worldwide, in a context where climate change will probably magnify the intensity of the most severe cyclonic events, we believe that the investigation of these issues is a promising avenue for future research.

References

Anttila-Hughes, J., Hsiang, S., 2013. Destruction, disinvestment, and death: Economic and human losses following environmental disaster. SSRN Electronic Journal. https://doi.org/10.2139/ssrn.2220501

Baez, J., De la Fuente, A., Santos, I.V., 2010. Do natural disasters affect human capital? An assessment based on existing empirical evidence.

Berlemann, M., Wenzel, D., 2018. Hurricanes, economic growth and transmission channels: Empirical evidence for countries on differing levels of development. World Development 105, 231–247. https://doi.org/https://doi.org/10.1016/j.worlddev.2017.12.020

Bertinelli, L., Mohan, P., Strobl, E., 2016. Hurricane damage risk assessment in the caribbean: An analysis using synthetic hurricane events and nightlight imagery. Ecological Economics 124, 135–144. https://doi.org/https://doi.org/10.1016/j.ecolecon.2016.02.004

Bertinelli, L., Strobl, E., 2013. Quantifying the local economic growth impact of hurricane strikes: An analysis from outer space for the caribbean. Journal of Applied Meteorology and Climatology 52, 1688–1697. https://doi.org/10.1175/JAMC-D-12-0258.1

Botzen, W.J.W., Deschenes, O., Sanders, M., 2019. The economic impacts of natural disasters: A review of models and empirical studies. Review of Environmental Economics and Policy 13, 167–188. https://doi.org/10.1093/reep/rez004

Cameron, L., Shah, M., 2015. Risk-taking behavior in the wake of natural disasters. Journal of Human Resources 50, 484–515.

Carter, M.R., Little, P.D., Mogues, T., Negatu, W., 2007. Poverty traps and natural disasters in ethiopia and honduras. World Development 35, 835–856. https://doi.org/https://doi.org/10.1016/j.worlddev.2006.09.010

Cavallo, E., Galiani, S., Noy, I., Pantano, J., 2013. Catastrophic natural disasters and economic growth. The Review of Economics and Statistics 95, 1549–1561. https://doi.org/10.1162/REST/_a/_00413

Chen, X., Nordhaus, W., 2015. A test of the new VIIRS lights data set: Population and economic output in africa. Remote Sensing 7, 4937–4947.

Chen, X., Nordhaus, W.D., 2011. Using luminosity data as a proxy for economic statistics. Proceedings of the National Academy of Sciences 108, 8589–8594. https://doi.org/10.1073/pnas.1017031108

Crespo Cuaresma, J., Hlouskova, J., Obersteiner, M., 2008. Natural disasters as creative destruction? Evidence from developing countries. Economic Inquiry 46, 214–226. https://doi.org/10.1111/j.1465-7295.2007.00063.x

Croissant, Y., Millo, G., 2018. Panel data econometrics with r. John Wiley & Sons, Ltd.

Dell, M., Jones, B.F., Olken, B.A., 2014. What do we learn from the weather? The new climate-economy literature. Journal of Economic Literature 52, 740–98. https://doi.org/10.1257/jel.52.3.740

Dessy, S., Marchetta, F., Pongou, R., Tiberti, L., 2019. Fertility response to climate shocks.

Elliott, R.J., Liu, Y., Strobl, E., Tong, M., 2019. Estimating the direct and indirect impact of typhoons on plant performance: Evidence from chinese manufacturers. Journal of environmental economics and management 98, 102252.

Elliott, R.J.R., Strobl, E., Sun, P., 2015. The local impact of typhoons on economic activity in china: A view from outer space. Journal of Urban Economics 88, 50–66. https://doi.org/https://doi.org/10.1016/j.jue.2015.05.001

Emanuel, K., 2011. Global warming effects on u.s. Hurricane damage. Weather, Climate, and Society 3, 261–268. https://doi.org/10.1175/WCAS-D-11-00007.1

Feenstra, R.C., Inklaar, R., Timmer, M.P., 2015. The Next Generation of the Penn World Table. American Economic Review 105, 3150–3182. https://doi.org/10.1257/aer.20130954

Felbermayr, G., Gröschl, J., 2014. Naturally negative: The growth effects of natural disasters. Journal of Development Economics 111, 92–106. https://doi.org/https://doi.org/10.1016/j.jdeveco.2014.07.004

Field, C.B., Barros, V., Stocker, T.F., Dahe, Q., 2012. Managing the risks of extreme events and disasters to advance climate change adaptation: Special report of the intergovernmental panel on climate change. Cambridge University Press.

Fontaine, I., Razafindravaosolonirina, J., 2021. The income loss of a political crisis: Evidence from madagascar (Working Paper), Document de travail. Centre d'Economie et de Management de l'Océan Indien.

Geiger, T., Frieler, K., Bresch, D.N., 2018. A global historical data set of tropical cyclone exposure (TCE-DAT). Earth System Science Data 10, 185–194. https://doi.org/10.5194/essd-10-185-2018

Geiger, T., Frieler, K., Bresch, D.N., 2017. A global data set of tropical cyclone exposure (TCE-DAT). GFZ Data Services. https://doi.org/http://doi.org/10.5880/pik.2017.005

Gibson, J., 2021. Better night lights data, for longer*. Oxford Bulletin of Economics and Statistics. https://doi.org/https://doi.org/10.1111/obes.12417

Gibson, J., Olivia, S., Boe-Gibson, G., 2020. NIGHT LIGHTS IN ECONOMICS: SOURCES AND USES1. Journal of Economic Surveys 34, 955–980. https://doi.org/https://doi.org/10.1111/joes.12387

Gibson, J., Olivia, S., Boe-Gibson, G., Li, C., 2021. Which night lights data should we use in economics, and where? Journal of Development Economics 149, 102602. https://doi.org/https://doi.org/10.1016/j.jdeveco.2020.102602

Hallegatte, S., Hourcade, J.-C., Dumas, P., 2007. Why economic dynamics matter in assessing climate change damages: Illustration on extreme events. Ecological Economics 62, 330–340. https://doi.org/https://doi.org/10.1016/j.ecolecon.2006.06.006

Heger, M.P., Neumayer, E., 2019. The impact of the indian ocean tsunami on aceh's long-term economic growth. Journal of Development Economics 141, 102365. https://doi.org/https://doi.org/10.1016/j.jdeveco.2019.06.008

Henderson, J.V., Storeygard, A., Weil, D.N., 2012. Measuring economic growth from outer space. American Economic Review 102, 994–1028. https://doi.org/10.1257/aer.102.2.994

Holland, G., 2008. A revised hurrican pressure-wind model. Monthly Weather Review 3432–3445.

Holland, G., 1980. An analytic model of the wind and pressure profiles in hurricanes. Monthly Weather Review 1212–1218.

Horwich, G., 2000. Economic lessons of the kobe earthquake. Economic development and cultural change 48, 521–542.

Hsiang, S.M., Jina, A.S., 2014. The causal effect of environmental catastrophe on long-run economic growth: Evidence from 6,700 cyclones (Working Paper No. 20352), Working paper series. National Bureau of Economic Research. https://doi.org/10.3386/w20352

Im, K.S., Pesaran, M.H., Shin, Y., 2003. Testing for unit roots in heterogeneous panels. Journal of econometrics 115, 53–74.

INSTAT, 2021. Tableau de bord économique (No. 45). Institut National de la Statistique.

IPCC, 2019. Special report on the ocean and cryosphere in a changing climate, in: Weyer, N.M. (Ed.), In It Together: Why Less Inequality Benefits All. In press.

Knapp, K.R., Kruk, M.C., Levinson, D.H., Diamond, H.J., Neumann, C.J., 2010. The international best track archive for climate stewardship (IBTrACS). Bulletin of the American Meteorological Society 91, 363–376. https://doi.org/10.1175/2009BAMS2755.1

Knutson, T., Camargo, S.J., Chan, J.C.L., Emanuel, K., Ho, C.-H., Kossin, J., Mohapatra, M., Satoh, M., Sugi, M., Walsh, K., Wu, L., 2020. Tropical cyclones and climate change assessment: Part II: Projected response to anthropogenic warming. Bulletin of the American Meteorological Society 101, E303–E322. https://doi.org/10.1175/BAMS-D-18-0194.1

Knutson, T., McBride, J., Chan, J., Emanuel, K., Holland, G., Landsea, C., Held, I., Kossin, J., Srivastava, A.K., Obersteiner, M., 2010. Tropical cyclones and climate change. Nature Geoscience 157–163. https://doi.org/https://doi.org/10.1038/ngeo779

Krichene, H., Geiger, T., Frieler, K., Willner, S.N., Sauer, I., Otto, C., 2021. Long-term impacts of tropical cyclones and fluvial floods on economic growth – empirical evidence on transmission channels at different levels of development. World Development 144, 105475.

https://doi.org/https://doi.org/10.1016/j.worlddev.2021.105475

Kummu, M., Taka, M., Guillaume, J.H., 2018. Gridded global datasets for gross domestic product and human development index over 1990–2015. Scientific data 5, 1–15.

Leroux, M.-D., Meister, J., Mekies, D., Dorla, A.-L., 2018. A climatolofy of southwest indian ocean tropical systems: Their number, tracks, impacts, sizes empirical maximum potential intensity, and intensity changes. Journal of Applied Meteorology and Climatology 57, 1021–1041.

Li, X., Xu, H., Chen, X., Li, C., 2013. Potential of NPP-VIIRS nighttime light imagery for modeling the regional economy of china. Remote Sensing 5, 3057–3081. https://doi.org/10.3390/rs5063057

Mohan, P., Strobl, E., 2017. The short-term economic impact of tropical cyclone pam: An analysis using VIIRS nightlight satellite imagery. International Journal of Remote Sensing 38, 5992–6006. https://doi.org/10.1080/01431161.2017.1323288

Nordhaus, W.D., 2010. THE ECONOMICS OF HURRICANES AND IMPLICATIONS OF GLOBAL WARMING. Climate Change Economics 01, 1–20.

Nordman, C., Rakotomanana, F., Roubaud, F., 2016. Informal *versus* formal: A panel data analysis of earnings gaps in madagascar. World Development 86, 1–17.

Noy, I., 2009. The macroeconomic consequences of disasters. Journal of Development Economics 88, 221–231. https://doi.org/https://doi.org/10.1016/j.jdeveco.2008.02.005

Peduzzi, P., Chatenoux, B., Dao, H., Bono, A.D., Herold, C., Kossin, J., Mouton, F., Nordbeck, O., 2012. Global trends in tropical cyclone risk. Nature Climate Change 2, 289–294.

R Core Team, 2019. R: A language and environment for statistical computing. R Foundation for Statistical Computing, Vienna, Austria.

Román, M.O., Wang, Z., Sun, Q., Kalb, V., Miller, S.D., Molthan, A., Schultz, L., Bell, J., Stokes, E.C., Pandey, B., Seto, K.C., Hall, D., Oda, T., Wolfe, R.E., Lin, G., Golpayegani, N., Devadiga, S., Davidson, C., Sarkar, S., Praderas, C., Schmaltz, J., Boller, R., Stevens, J., Ramos González, O.M., Padilla, E., Alonso, J., Detrés, Y., Armstrong, R., Miranda, I., Conte, Y., Marrero, N., MacManus, K., Esch, T., Masuoka, E.J., 2018. NASA's black marble nighttime lights product suite. Remote Sensing of Environment 210, 113–143. https://doi.org/https://doi.org/10.1016/j.rse.2018.03.017

Skidmore, M., Toya, H., 2002. Do natual disaster promote long-run growth? Economic Inquiry 40, 664–687. https://doi.org/10.1093/ei/40.4.664

Skoufias, E., Strobl, E., Tveit, T., 2021. Can we rely on VIIRS nightlights to estimate the short-term impacts of natural hazards? Evidence from five south east asian countries. Geomatics, Natural Hazards and Risk 12, 381–404. https://doi.org/10.1080/19475705.2021.1879943

Strobl, E., 2012. The economic growth impact of natural disasters in developing countries: Evidence from hurricane strikes in the central american and caribbean regions. Journal of Development Economics 97, 130–141. https://doi.org/https://doi.org/10.1016/j.jdeveco.2010.12.002

Strobl, E., 2011. The economic growth impact of hurricanes: Evidence from u.s. Coastal counties. The Review of Economics and Statistics 93, 575–589.

Sutton, P.C., Costanza, R., 2002. Global estimates of market and non-market values derived from nighttime satellite imagery, land cover, and ecosystem service valuation. Ecological Economics 41, 509–527. https://doi.org/https://doi.org/10.1016/S0921-8009(02)00097-6

Wooldridge, J.M., 2010. Econometric analysis of cross section and panel data. The MIT Press.

Chapitre 9

Evaluation économique des coûts directs associés au passage du cyclone tropical ENAWO en 2017 : le cas de Madagascar

Ramilimanitra Tsiory Maminiaina Andrianavalona

- ***Présentation :***
  Colloque sur les grands enjeux du développement dans l'Agenda 2030 pour l'Afrique et Madagascar, UCM, 2022

Evaluations économiques des coûts directs associés au passage du cyclone tropical Enawo en 2017 : Cas de Madagascar.

Economic assessment of the direct costs associated with the passage of tropical cyclone Enawo in 2017: The case of Madagascar.

Tsiory RAMILIMANITRA
Université de La Réunion-CEMOI
tsiory.ramilimanitra@univ-reunion.fr/ r.m.a.tsiory@gmail.com
N°ORCID : 0009-0009-4610-8774.

« Cette recherche a reçu le soutien financier de la Région Réunion et de l'Union Européenne – Programme FEDER INTERREG 2021-2027 ».

Mots-clés

Coûts ; cyclone tropical Enawo ; fonction de dommage ; lumières nocturnes ; Madagascar.

Keywords

Costs; Tropical cyclone Enawo; damage function; night lights; Madagascar

Classification JEL : A12, E23, O49, Q54, R12.

Résumé

L'évaluation des coûts des dommages et donc des pertes économiques qui sont associées au passage des catastrophes naturelles revêt une importance cruciale dans un contexte de réduction de vulnérabilité. En vue d'évaluer les coûts relatifs au passage du Cyclone Tropical Intense « Enawo » en 2017 à Madagascar, nous procéderons en deux étapes. Premièrement, il s'agit de répartir et de distribuer le PIB du pays en mobilisant les images nocturnes à haute résolution issues des observations *Visible Infrared Imaging Radiometer* (VIIRS) à bord du *Suomi-National Polar-Orbiting Partnership*. Deuxièmement, les informations sur les cyclones sont obtenues à partir de la base de données TCE-DAT (*Tropical-Cyclone Exposure-Data)* de Geiger & al (2018). En appliquant une fonction de dommage théorique (Emanuel, 2011), les résultats de l'analyse montrent que plus on diminue la valeur des seuils de vents, plus les pertes seront considérables ; allant de 22% à 32% de la valeur économique totale**.**

Abstract

Assessing the costs of damage and therefore the economic losses associated with the passage of natural disasters is important in a context of vulnerability reduction. In order to assess the

costs related to the passage of the Intense Tropical Cyclone "Enawo" in 2017 in Madagascar, we will proceed in two steps. First, we will allocate and distribute the country's GDP by mobilizing high-resolution nighttime imagery from the Visible Infrared Imaging Radiometer (VIIRS) observations aboard the Suomi-National Polar-Orbiting Partnership. Second, cyclone information is obtained from the Tropical-Cyclone Exposure-Data (TCE-DAT) database by Geiger & al (2018). Applying a theoretical damage function (Emanuel, 2011), the results of the analysis show that the lower the value of wind thresholds, the greater the losses will be; ranging from 22% to 32% of the total economic value.

Points clés

- Nous évaluons l'impact du passage du « cyclone tropical Intense Enawo » en 2017 sur l'économie de Madagascar.
- Les données sur l'intensité lumineuse des lumières nocturnes ont été mobilisées pour mesurer les activités (les valeurs) économiques par pixel du pays.
- Les régions de la partie Nord-Est de Madagascar ont été les plus affectées par les vents cycloniques d'Enawo; enregistrant par conséquent des coûts des dommages considérables.

1 -Introduction

Les cyclones tropicaux sont considérés comme l'un des phénomènes atmosphériques les plus destructeurs qu'un système socio-économique puisse faire face (Carmago et Hsiang, 2015). Selon Mendelsohn et *al.,* (2012), le coût des dommages mondial associé au choc cyclonique a été estimé à environ 26 milliards de dollars par an. A Madagascar, le EM-DAT (Emergency Events Database)[1] estime que le passage des cyclones tropicaux entre 2000 et 2021 a causé plus de 1 500 morts et environ 740 000 personnes sont considérées comme sans abris. L'île de Madagascar n'a pas été en effet épargnée du passage de plusieurs systèmes tropicaux atteignant le stade de Cyclone tropical Intense avec une vitesse de vent moyen soutenu de 166 à 212km/h (équivalent à un cyclone de catégorie 4 selon l'échelle de Saffir-Simpson-SS) depuis l'année 2000 à 2017 selon le rapport du Joint Research Centre ou JRC (2017). Entre autres le cyclone Gafilo en 2004 qui a été le plus destructeur, causant 363 morts et affectant 990 000 personnes, et le cyclone Enawo en 2017, qui a entrainé plus de 80 morts et affectant plus de 430 000 personnes ; plus récemment le cyclone Batsirai en 2022 qui a laissé un lourd bilan humain et cette année (2023) le cyclone Freddy qui a causé des dégâts matériels très importants.

De plus, les dommages directs (dégâts matériels et pertes humaines) dus aux catastrophes naturelles ont augmenté de façon spectaculaire au cours des dernières décennies (Hamid et *al.,* 2010 ; Ye et *al.,* 2020). Or, cette intensification des cyclones et les impacts qu'ils engendrent, tant au niveau de la société qu'au niveau de l'économie va perdurer dans un futur proche. En effet, d'une part, le changement climatique va continuer à affecter les activités cycloniques tant en termes de fréquence que d'intensité (Knutson et *al.,* 2010; IPCC, 2019; Knutson et *al.,* 2020) et d'une autre part, l'accumulation continue de la population et des actifs économiques dans les zones à risque va augmenter le nombre d'entités exposées (Freni et *al.,* 2010; Botzen et *al.,* 2019).

Madagascar, un Etat insulaire se situant dans le Bassin Sud-Ouest de l'Océan Indien (SWIO ou South Western Indian Ocean), est caractérisé par un fort degré d'exposition au passage de l'évènement météorologique extrême qu'est le cyclone. Le bassin SWIO est classé troisième

[1]Centre for Research on the Epidemiology of Disasters (CRED): http://www.emdat.be/

comme étant le bassin cyclonique tropical le plus actif dans le monde (Tulet et *al.*, 2021) dont environ 11% (Leroux et *al.,* 2018) voire 15% (Héron et *al.,* 2020) des activités cycloniques globales y sont observées. En effet, il est remarqué dans ce bassin une moyenne annuelle de 9 à 10 tempêtes tropicales (Neumann., 1993 ; Mavume, 2008 ; Leroux et *al.*, 2018). Le Rapport d'étude de l'Observatoire Défense et climat (2019) souligne également que 80% des catastrophes d'origine météorologique dans le pays sont représentées par des activités cycloniques. Dans cette logique, Madagascar serait particulièrement menacée par d'importantes pertes économiques ; les infrastructures de mauvaises qualités du pays le rendant en outre plus vulnérable aux chocs cycloniques (Tulet et *al.,* 2021).

Si l'évaluation des pertes économiques relatives aux activités cycloniques représentait depuis plusieurs décennies tant un intérêt académique que scientifique (Cf entre autres Strobl, 2011 ; Strobl, 2012 ; Bertineli et Strobl, 2013; Berlemann et Wenzel, 2018), il n'existe pas de méthode d'évaluation de coûts des dommages à partir des données de vents qui soit facilement réplicable. Or, dans ce contexte, il paraît important de quantifier les coûts des cyclones pour mener des analyses coûts-bénéfices des mesures d'adaptation (aménagement) à mettre en place. C'est ce que propose d'effectuer cet article à travers l'utilisation d'une méthodologie qui tente d'évaluer les pertes économiques associées au passage des cyclones en prenant comme cas pratique le cyclone Enawo qui a touché Madagascar en 2017 et qui a causé des dégâts considérables dans le pays.

Une distinction communément admise par la littérature entre dommages directs et dommages indirects associés aux risques naturels (Cf Kousky ; 2014) a conduit à l'utilisation de deux méthodes d'évaluations d'impacts différentes à la suite d'un évènement catastrophique naturel. D'une part, l'évaluation d'impact direct consistant à analyser et à estimer les coûts des dommages directs causés par l'aléa (Cf par exemple Mendelsohn et *al.,* 2012). Les dommages directs sont connus généralement par les destructions physiques (et humaines) observées immédiatement suite à un choc naturel. D'autre part, la méthode d'évaluation des impacts indirects qui consiste à examiner les répercussions des dommages directs sur les activités économiques du territoire exposé par l'évènement catastrophique (cf par exemple Felbermayr et Gröschl, 2014; Hsiang et Jina, 2014; Krichene et *al.,* 2021). Notre étude s'inscrit dans la première méthode d'évaluation d'impact.

L'étude repose sur l'utilisation des données sur les lumières nocturnes afin de répartir de manière plus objective les activités économiques (valeurs économiques) à un niveau spatial plus désagrégé (régional)[2]. Il s'agit d'une nouvelle méthode en pleine expansion dans la littérature, utilisée en vue de mesurer les activités économiques dans les pays en développement où les données historiques (conventionnelles) sont réputées être parfois incomplètes (Chen et Nordhaus, 2011; Henderson et *al.*, 2012; Chen et Nordhaus, 2015). Cette méthode a été utilisée pour améliorer des indicateurs économiques déjà existants (Cf Henderson et *al.,* 2012) ou encore pour étudier l'impact des catastrophes naturelles sur la croissance économique (Cf Mohan et Strobl, 2017) mais également dans le cadre d'une étude qui utilise une fonction de dommage (Cf Bertinelli et Strobl, 2013 ; Elliott et *al.,* 2015). La méthode proposée dans cet article utilise à la fois les lumières nocturnes et la fonction de dommage. Bien qu'il existe plusieurs procédures de quantifications des dommages directs, l'approche par la fonction de dommage est la méthode la plus courante et acceptée internationalement (Smith, 1994 ; Kreibich et Bubeck , 2013 ; Meyer et al, 2013 ; Pistrika et *al.,* 2013). Il est à savoir que la majorité des études utilisant les fonctions de dommages font appel aux données assurantielles (valeurs immobilières) et aux données foncières (Cf entre autres Apel et *al.,* 2008 ;Pistrika et

[2] Ce sont les régions de la partie Nord-Est de Madagascar qui ont été fortement exposées par le Cyclone Tropical Enawo en 2017.

al., 2013 ; Done et *al.*, 2018). Or, pour le cas particulier de Madagascar, ces données sont incomplètes voire inexistantes, d'où le choix des données sur les lumières nocturnes qui permettraient de détecter les valeurs économiques (par pixel) détruites par les vents cycloniques de Enawo. Ainsi, en appliquant une fonction de dommage (Emanuel, 2011), nous simulons quelques situations hypothétiques sur les dommages avec des seuils de vents adéquats au contexte de Madagascar. Les résultats de l'analyse montrent que plus on diminue la valeur des seuils de vents, plus les pertes seront considérables, soit une perte pouvant aller de 22% à 32% de la valeur économique totale.

La suite de l'article est organisée de la façon suivante. La deuxième partie présente le cadre contextuel de l'étude à travers la description des activités cycloniques dans le bassin SWIO ainsi que la situation économique de Madagascar. La troisième partie expose les données utilisées dans cette étude ; les lumières nocturnes et les cyclones tropicaux. La quatrième et la cinquième partie seront consacrées respectivement à la présentation méthodologique et aux principaux résultats d'analyses. Enfin, la dernière partie présentera la conclusion ainsi que les principales perspectives attribuées à l'étude.

2 -Cadre contextuel

Cette partie sera consacrée au cadrage général de l'étude. Elle expose d'une part la climatologie des cyclones tropicaux et d'une autre part le contexte économique de Madagascar.

2.1 La climatologie des cyclones tropicaux.

Les cyclones tropicaux font partis des évènements naturels catastrophiques les plus destructeurs auquel un système socio-économique puisse faire face (Carmago et Hsiang, 2015). Les cyclones tropicaux se forment et évoluent généralement au-dessus des eaux chaudes ; entre 5° et 20° de latitude (Emanuel K.A, 1987; Berlemann et Wenzel, 2018), dans les régions tropicales où il y a une poussée des vents de surface par convection avec une humidité relative de l'air supérieur à 70% (Gray, 1968). Ce type de choc est non seulement accompagné de vents violents, mais également de fortes précipitations entrainant des inondations et d'une onde de tempêtes causant une montée des eaux de surface de la mer (Elliot et *al.*, 2015).Cependant, les cyclones tropicaux sont généralement approximés par la force des vents ; sachant que l'ampleur des dommages dus aux deux autres aléas (inondations et montée des eaux de surface) est corrélées à la force du vent du système elle-même (Jordan et Clayson, 2008 ; Elliot et *al.*, 2015). D'où la notion de classification des cyclones tropicaux selon l'échelle de Saffir-Simpson[3] en fonction de l'intensité des vents : Catégorie 1 (119-153km/h) ; Catégorie 2 (154-177km/h) ; catégorie 3 (178-208km/h) ; catégorie 4 (209-251km/h) ; catégorie 5 (252km/h et plus).

Le bassin SWIO est classé troisième comme étant le bassin cyclonique tropical le plus actif dans le monde (Tulet et *al.*, 2021) dont environ 11% (Leroux et *al.*, 2018) voire 15% (Héron et *al.*, 2020) des activités cycloniques globaux y sont observées. Dans ce bassin, selon *World Meteorologique Organisation* ou WMO (2016), le système est baptisé Cyclone Tropical (CT) lorsqu'il atteint une vitesse de vent moyen soutenu compris entre 118 et 165km/h. A ce niveau, une distinction entre Cyclone Tropicale Intense ou CTI (166 à 212km/h) et un cyclone Tropicale Très Intense ou CTTI (vents moyen maximal supérieur à 212km/h) a été faite. En deçà de ces seuils, le système sera appelé dépression tropicale (51 et 62km/h) ou tempête tropicale modérée (63 et 88km/h) ou une forte tempête tropicale (89 et 117km/h).

En moyenne neuf cyclones par an au cours des six dernières décennies ont rendu les pays bordant le bassin SWIO particulièrement exposé à ce type de risque naturel (Mouquet et *al.*, 2020). A cela s'ajoute le fait que le bassin a été caractérisé plus récemment par des systèmes

[3] L'échelle ne tient pas en compte des impacts potentiels liés aux inondations et aux ondes de tempêtes.

tropicaux intenses, affectant de manière dramatique la vie de la communauté sur le plan économique, humain et matériel (Kuleshov, 2010). Entre autres, un cyclone tropical s'est développé à Madagascar durant la saison cyclonique[4] en 2017 dans le bassin SWIO et a atteint le stade de Cyclone Tropical Intense. Baptisé sous le nom de Enawo, ce dernier a touché terre dans la partie Nord-Est de Madagascar notamment dans la région de SAVA et d'Analanjirofo; avec une intensité de vent moyen soutenu de 230km/h (équivalent à une catégorie 4-5 de l'échelle SS) le 7 Mars 2017 ; avant que le glissement de terrain ait eu lieu (JRC, 2017). D'après les informations émises par le BNGRC (Bureau National pour la Gestion des Risques et des Catastrophes) de Madagascar, le cyclone Enawo a causé des dommages considérables détruisant et inondant des milliers de maisons; faisant plus de 80 morts, affectant plus de 430 000 personnes et environ 250 000 personnes ont été déplacées temporairement.

2.2 La situation économique de Madagascar.

En se basant sur les données de la banque mondiale, les chiffres montrent une croissance annuelle moyenne du PIB de 1,94% entre l'année 1961 et 2021. Malgré des diminutions importantes des taux de croissance économique (atteignant même des valeurs négatives) en 1991, 2002, 2009 ; qui sont imputable aux crises politiques qu'a connu le pays, l'économie Malgache a pu se relever après chaque crise avec des reprises économiques assez considérables[5]. Par ailleurs derrières les quelques améliorations observées en termes de croissance économique se cachait un PIB par habitant qui n'a cessé de décroitre (PNUD, 2018). Cela pourrait en effet expliquer en partie la part très importante de la population (ratio atteignant environ 80%) qui vit en dessous du seuil de pauvreté ; selon le rapport de la Banque Mondiale (2022).

En termes de contribution sectorielle[6], le secteur des services (47,62%) contribue en moyenne (sur la période 1984-2018) la part la plus importante à la croissance du PIB, le secteur agricole (27,54%) se place en deuxième position et où le secteur industriel se situe en dernier classement avec seulement 16% de contribution. Pour ce qui est de la part des emplois par secteur d'activité[7], C'est le secteur agricole qui emploie la part la plus importante de la population. Sachant aussi que 80% de la population Malgache vivent dans les milieux ruraux (Expansion, 2019). S'ensuit le secteur des biens dématérialisés et effectivement le secteur industriel se place en dernière position en termes de contribution sur le marché du travail.

Ces éléments révèlent ainsi la mauvaise posture de l'économie Malgache et que la faible compétitivité de l'économie pourrait expliquer en partie le classement du territoire de Madagascar en tant que PMA (Pays Moins Avancés) au niveau mondial.

3 -Données d'études

On s'intéressera ici aux données principales mobilisées dans le cadre de l'étude. Nous présenterons dans un premier temps les données sur les lumières nocturnes utilisées comme étant le proxy de mesure des activités économiques et les données sur les champs des vents comme mesure de l'intensité physique des cyclones tropicaux.

[4] Généralement allant de mi-novembre jusqu'en mi-avril.
[5] Banque Mondiale.
[6] Calcul de l'auteure ; Données Banque Mondiale.
[7] Calcul de l'auteure ; Données Banque Mondiale.

3.1 Les lumières nocturnes.

Etant donné que les données historiques (conventionnelles) sont réputées être parfois incomplètes au sein des pays en développement comme Madagascar (Chen et Nordhaus, 2011; Henderson et *al.,* 2012; Chen et Nordhaus, 2015), nous ferons appel aux données satellitaires sur les lumières nocturnes récemment usités par les économistes (Henderson et *al.,* 2012 ;Keola et *al.,* 2015 ;Gibson et *al.,* 2020 et tant d'autres). Ces données permettent de mesurer de manière plus objective les activités économiques du pays mais permettent également de spatialiser la valeur économique sachant que les données économiques régionales sont inexistantes dans le pays. Le principe général sur lequel la méthode des lumières nocturnes repose est que la somme des lumières observables dans l'espace correspondra à l'ensemble des activités des hommes. Ainsi, pour tous les pays où la majorité des données ne sont disponibles majoritairement qu'à une échelle nationale, ce type de données selon Henderson et *al.,* (2012) peut jouer un rôle crucial pour réaliser une analyse d'impact sur la croissance économique à un niveau spatial plus désagrégé (cf entre autres l'étude de Bertinelli et *al.,* 2016). En outre, la prise en considération de cette nouvelle mesure permettra aux gouvernements et aux analystes de situer la croissance économique des régions dans différentes unités économiques et de mettre en place les mesures et les politiques appropriées (Ghosh et *al.*,,2010).

Dans le cadre de notre étude, nous avons mobilisé les images nocturnes à haute résolution issues des observations *Visible Infrared Imaging Radiometer* (VIIRS) à bord du *Suomi-National Polar-Orbiting Partnership* utilisées dans des études plus récentes (entre autres Gibson, 2020) ; sachant qu'antérieurement les travaux (par exemple l'étude de Bertinelli et Strobl, 2013 ; Elliot et *al.,* 2015 ; Bertinelli et *al.,* 2016) faisaient appel aux données issues de la DMSP (*Defense Météorological Satellite Program*). Pour Madagascar, les données sur les lumières nocturnes (VIIRS) n'étant disponibles que pour une périodicité mensuelle, elles ont été agrégées[8] en utilisant une simple moyenne arithmétique.

La figure (Figure1) ci-dessous met en évidence l'intensité lumineuse moyenne des lumières nocturnes par pixel pour l'année précédant (2016)[9] le passage du cyclone Enawo. Sur la figure, la partie la moins éclairée dans le territoire de Madagascar fait référence à la couleur noire, tandis que la plus éclairée est représentée par le passage de la couleur grise vers la couleur blanche en fonction de la valeur de la radiance (c'est-à-dire de l'intensité lumineuse). La cellule la plus éclairée se situe dans le centre c'est-à-dire dans la capitale de Madagascar, à Antananarivo où on pourrait remarquer une forte concentration de diverses activités économiques. On constate également un éclairage dans la partie Nord-Est du pays mais avec une luminosité moins prononcée c'est-à-dire avec une valeur de la radiance moyenne (couleur grise). Par contre, il est remarquable que la partie Sud de Madagascar ne soit presque pas éclairée.

[9] Les lumières nocturnes de l'année 2016 ont été pris car elles reflètent pertinemment les activités économiques touchées par le cyclone Enawo.

Figure 1. Cartographie de la valeur moyenne de l'intensité lumineuse des lumières nocturnes par pixel pour Madagascar en 2016.

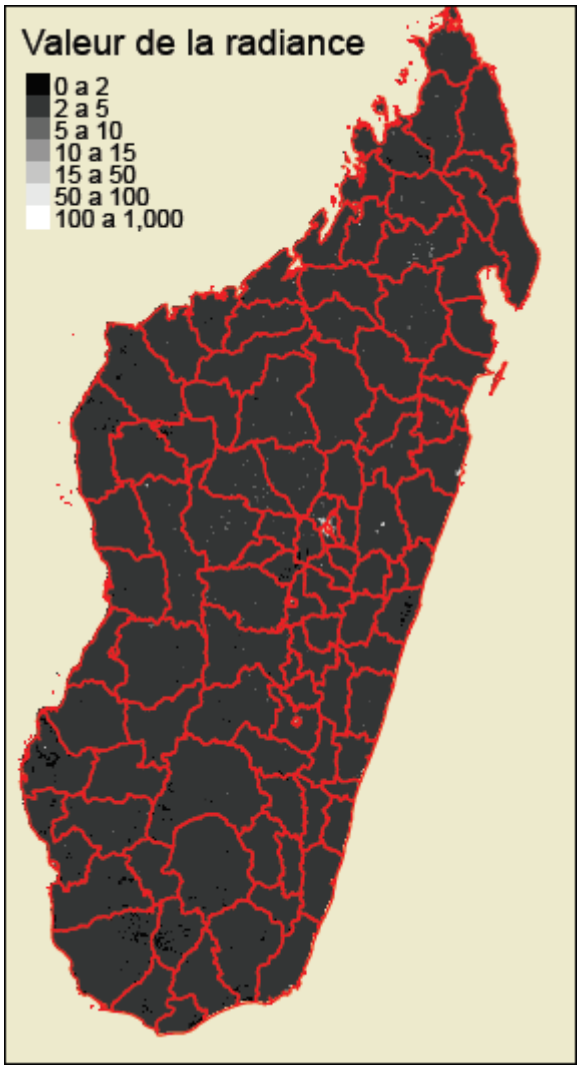

Source : Elaboration de l'auteure, données VIIRS (2016).

Par ailleurs, on remarque que le territoire de Madagascar dans son ensemble n'est presque pas éclairé la nuit. Rappelons aussi que l'essentiel des activités dans le pays sont des activités de jour que de nuit comme les activités agricoles, des activités qui émettent peu de lumières la nuit (Ghosh et *al.,* 2010 ; Keola et *al.,* 2015). Toutefois, cela ne nous empêcherait pas de réaliser des études préliminaires en utilisant ce type de données pour le cas de Madagascar. Sachant que pour cette dernière, la corrélation entre les lumières nocturnes et les activités économiques (PIB localisé) est clairement mise en évidence par Fontaine, Garabedian et Jammes (2022), avec une valeur positive qui s'élève à 0,79. Cette relation est autant vérifiée dans les pays caractérisé par un bon niveau de développement (Cf par exemple les études de Bhandari et Roychowdhury, 2011 ; Henderson et *al.*, 2012 ; Chen et Nordhaus, 2015 ; McCord et Rodriguez-Heredia, 2022). Soulignons maintes fois qu'il a été démontré dans plusieurs papiers (Henderson et *al.*, 2012 ; Chen et Nordhaus, 2015 ; Keola et *al.*, 2015 ; Gibson et *al.*, 2020) que les lumières nocturnes demeurent un bon proxy pour mesurer les activités économiques en général[10]. D'où, l'intérêt de réaliser une étude d'impact préalable avec ce type de données très novatrice pour le cas particulier de Madagascar.

[10] Les lumières nocturnes ne mesurent pas les activités économiques en tant que telles mais elles captent toute la dynamique autour que les activités génèrent et justement l'électrification de la zone ; non seulement au niveau des

3.2 Les vents cycloniques.

Bien que les cyclones tropicaux soient caractérisés par de multiples aléas d'après Elliot et *al.,* (2015), nous approximerons de manière générale le système tropical par la force du vent ; sachant que l'ampleur des dommages dus aux autres aléas est corrélée elle-même à la force du vent du système (Jordan et Clayson, 2008 ; Elliot et *al.,* 2015). En vue de réaliser l'évaluation proprement dite, nous aurons recours à la base de données TCE-DAT ou *Tropical-Cyclone Exposure-Data* de Geiger et *al.,* (2018) qui contient des données mondiales à haute résolution sur les vitesses de vents maximales pour 2700 systèmes cycloniques. A partir de la superposition de ces deux bases de données (données VIIRS et TCE-DAT) ; les coûts (pertes économiques) associés au passage du Cyclone Tropical Enawo en 2017 peuvent être obtenus.

Le Tableau 1 met en évidence que la vitesse de vent médiane associée à Enawo en 2017 a été environ à 201km/h et variant de 122km/h (valeur minimal) à 416km/h (Valeur maximal).

Tableau 1 : Résumé de la statistique descriptive des champs de vents cyclonique Enawo en 2017.

Champs des vents cycloniques : Enawo en 2017 (Km/h)	
Minimum	**122,40**
1er quantile	**156,60**
Médian	**201,24**
3ème quantile	**259,20**
Maximum	**416,52**

Source : Calcul de l'auteure, données TCE-DAT (2017).

L'exposition de Madagascar aux vents cycloniques associés à Enawo est illustrée par la Figure 2.

activités sectorielles mais à tous les niveaux comme dans les éclairages au niveau des hôpitaux, les éclairages publiques où on pourrait observer (ou) pas des petites activités.

Figure 2 : Cartographie de l'exposition de Madagascar aux vents cycloniques associés à Enawo en 2017 (en km/h)

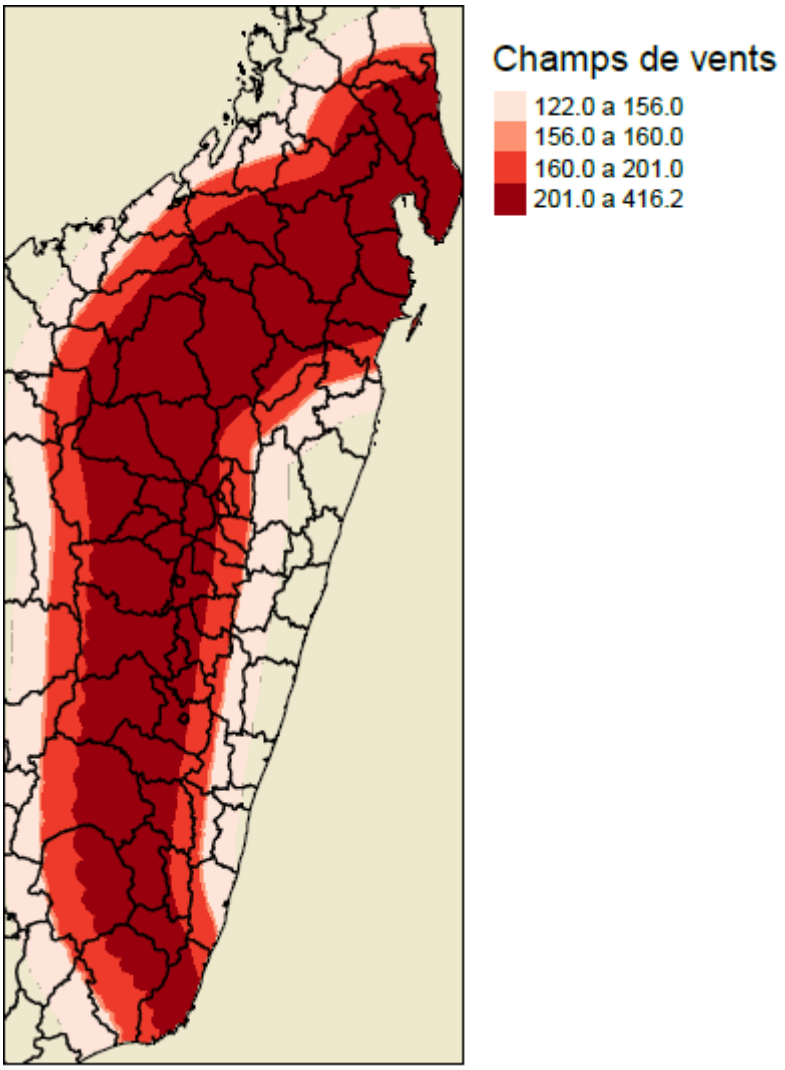

Source : Elaboration de l'auteure, Données TCE-DAT (2017).

En observant la trajectoire des vents, les régions de la partie Nord-Est de Madagascar sont les plus touchées par une intensité de vents très élevée (couleur grenat); avec un intervalle de vitesse de vents compris entre 201 à 416 km/h (équivalent à un cyclone de catégorie 4 à 5 selon l'échelle de Saffir-Simpson).

4 -Méthodologies

Cette partie méthodologique présente premièrement le cadre conceptuel sur lequel repose l'utilisation d'une fonction de dommage et développe deuxièmement les démarches d'analyses permettant d'évaluer les impacts économiques suite au passage du cyclone tropical Enawo à Madagascar en 2017.

4.1 Cadre conceptuel.

Plusieurs procédures de quantification des dommages ont été définies au cours de ces dernières décennies où les approches ainsi que les estimations économiques diffèrent considérablement (Jongman et *al.*, 2012). L'approche la plus couramment utilisée, et d'ailleurs la méthode internationalement acceptée pour évaluer les dommages directs pour tous aléas

considérés est la fonction (courbe) de dommage (Smith, 1994 ; Kreibich et Bubeck , 2013 ; Meyer et *al.,* 2013 ; Pistrika et *al.,* 2013). Elle peut prendre une appellation différente comme fonction de susceptibilité (Kreibich et Bubeck , 2013 ; Meyer et *al.,* 2013) ou aussi courbe de fragilité ou courbe de vulnérabilité (Masutomi et *al.,* 2012). De manière générale, une fonction de dommage décrit la relation entre un ou plusieurs paramètres d'aléas, avec les pertes monétaires qui en résulte pour une certaine utilisation d'un objet à risque (Kreibich et Bubeck ,2013 ; Meyer et *al.,* 2013).

Il est donc possible que la fonction soit mono-paramétrique ou multiparamétrique selon les facteurs à considérer dans le cadre de l'analyse. Outre le choix des paramètres à inclure, les analystes seront parallèlement confrontés entre le choix d'une fonction de type relative ou de type absolue (Jongman et *al.,* 2012 ; Pistrika et *al.,* 2013 **;** Romali et *al.,* 2015). Selon Pistrika et *al.,* (2013), les dommages sont dits relatifs lorsqu'ils sont exprimés en pourcentage de la valeur de remplacement totale des actifs endommagés, par contre ils sont absolus lorsqu'ils sont exprimés en valeur monétaire. Finalement, deux approches principales d'élaboration d'une fonction de dommage sont possibles : l'approche empirique et l'approche synthétique (Smith 1994 ; Freni et *al.,* 2010 ; Pistrika et *al.,* 2013). La distinction se situe au niveau du type d'information utilisé pour son élaboration. D'une part, les fonctions de dommages dérivées de manière empirique utilisent des données historiques (réelles) des dommages collectées après le passage d'un évènement naturel (Pistrika et *al.,* 2013). D'une autre part, cette approche empirique est à distinguer de l'approche synthétique alternativement appelée par approche théorique ou hypothétique[11]. Elle emploie des données théoriques sur les dommages qui peuvent être obtenues soient via des enquêtes (entretiens ou questionnaires) nécessitant un jugement des experts et des ingénieurs en sinistres, soient à travers les inventaires[12].

4.2 Application : Madagascar et le cyclone Tropical Enawo (2017).

La présente étude s'inscrit dans le cadre de l'application d'une fonction de dommage cyclonique (théorique) pour le territoire de Madagascar en vue d'estimer les coûts des dommages directs et donc les pertes économiques associées spécifiquement au passage du cyclone Enawo à l'année 2017. Le choix de l'approche est motivé par le manque d'informations et de données réelles complètes pour pouvoir calibrer de manière empirique une fonction de dommage spécifique pour Madagascar. Notre étude se base sur un travail récent déjà existant appliqué pour le cas de notre consœur, l'île de la Réunion (Cf Fontaine et *al.,* 2021). Fontaine et *al.,* (2021) ont fait appel à la fonction de dommage de Elliot et *al.,* (2015) qui calcul un indice de destruction potentiel (1) en vue de dégager la part de pixel détruite par les vents.

$$v_{ci} = \frac{MAX\left(W_{ci} - \bar{W}, 0\right)}{W^* - \bar{W}} \qquad (1)$$

Où v_{ci} est l'indice de destruction potentiel qui estime la valeur économique détruite pour un pixel ou une cellule c (unité géographique) donnée et pour un évènement cyclonique i. W_{ci} est le vent maximum estimé sur le pixel c pour un évènement cyclonique i. $\bar{W}$ est la vitesse minimale des vents correspondant à l'absence de dommages et W^* est le seuil correspondant à

[11] Simulation de quelques situations hypothétiques sur les dommages qu'une situation particulière peut causer à une utilisation de sol particulier

[12] Effectuer des enquêtes sur les différents types d'éléments à risque (par exemple les bâtiments et les routes) dans la zone étudiée.

une perte de la moitié (50%) des biens pour une cellule c. La fixation des seuils est la plus problématique et demeure une tâche difficile dans le cadre de l'utilisation d'une fonction de dommage étant donné les caractéristiques socio-économiques différentes des pays étudiés. En effet, il importe de souligner que comparativement à l'île de La Réunion, Madagascar ne possède pas d'infrastructures assez robustes pour faire face aux chocs de vents cycloniques. A cet égard, pour un niveau plus faible de seuil minimal et de seuil maximal que celui fixé pour l'île de la Réunion, des dégâts considérables pourraient être observables. Etant donné que notre état des connaissances sur la valeur réelle des seuils est encore limité, la meilleure stratégie est de réaliser de prime abord un test de robustesse des résultats en choisissant des valeurs de seuils moins élevées pour Madagascar par rapport à ceux de La Réunion (Voir Annexe 1 : Test de robustesses des résultats). Plus précisément, nous retenons des seuils inférieurs à 93 km/h et à 270 km/h (Seuil minimal et seuil maximal respectif pour La Réunion).

Les dommages physiques estimés à partir de la fonction de dommage d'Elliot et *al.*, (2015) seront donc convertis en perte monétaire en suivant théoriquement (hypothétiquement) la stratégie d'Emmanuel (2011) (2) :

$$f_{ci} = \frac{v_{ci}^3}{1+v_{ct}^3} \qquad (2)$$

Selon Emmanuel (2011), f_{ci} est un indice normalisé qui pour chaque pixel donne la part de valeur économique détruite. L'écriture de f_{ci} ici garantit que la part des destructions soit une fonction non linéaire du vent (exprimé par v_{ci}^3). Autrement dit, c'est le cube du vent maximum qui est retenu car généralement les dégâts générés par les cyclones augmentent de manière non linéaire avec l'intensité du vent (passé de 100 à 110km/h n'est pas similaire à passer de 220 à 230 km/h en termes de dégâts). L'indice (f_{ci}) impose que la proportion de la valeur économique détruite ne doit pas dépasser l'unité pour un niveau maximal de vents. En d'autres termes, les dégâts sont observés à partir d'un certain seuil et ensuite bornés à 100% des destructions.

En combinant les données des vents et les données sur les lumières nocturnes, il est possible d'estimer les pertes économiques totales au niveau global (F_i) pour un évènement cyclonique i, en utilisant la formule proposée d'abord par Bertinelli et *al.*, (2016), ensuite par Fontaine et *al.*, (2021) (3) :

$$F_i = \sum_{c=1}^{C} \frac{nl_c}{NL} \times f_{ci} \qquad (3)$$

Où C correspond au nombre total de pixel (cellules) caractérisant le pays d'étude en termes de lumières nocturnes, nl_c est la valeur moyenne des lumières nocturnes pour une cellule c pour une période donnée ; *NL* est la valeur totale des lumières nocturnes observées pour l'île d'étude à une année donnée.

Un lien étroit peut être établit entre les trois équations proposées dans le cadre de cette étude, les données sur les lumières nocturnes et les résultats obtenus dans l'article. D'abord, la distribution de la valeur moyenne du PIB pour l'année 2016 en fonction de l'intensité lumineuse a permis d'obtenir des valeurs économiques par pixel. Ensuite, l'utilisation de v_{ci} nous permet de dégager dans un premier temps un indice de destruction potentiel pour chaque pixel détruit (1). Plus l'indice est élevé, plus les pertes physiques à chaque pixel touché par les vents cycloniques seront importantes. Ces pertes physiques seront ensuite converties en pertes monétaires selon la stratégie d'Emanuel (2011) qui suppose qu'une augmentation des seuils de vents correspondra à des pertes par pixel considérables (2). Les pertes par pixel seront ensuite agréger pour obtenir les pertes économiques totales pour l'ensemble des pixels touchés par les

vents cycloniques (3). Soulignons que chaque pixel est associé à une valeur économique (valeur moyenne du PIB à l'année 2016) ; à cet effet, plus un pixel est exposé aux vents cycloniques, plus l'intensité lumineuse des lumières nocturnes pour ce pixel va diminuer (valeur du PIB diminue) et cela signifie implicitement l'existence de coût pour le pixel détruit. Les pertes économiques totales (coûts directs) pour la partie de Madagascar qui a été la plus exposée par les vents cycloniques de Enawo seront donc obtenues en additionnons les coûts par pixel.

5 -Résultats

Les régions de la partie Nord-Est de Madagascar étant les plus touchées par les vents cycloniques de Enawo (Voir Figure 2) ; cela implique que l'ensemble des coûts associés à ces vents (F_i dans 2) y seront observés incontestablement[13]. Soulignons par ailleurs que l'intérêt d'une spatialisation vient du fait qu'une région peut être beaucoup touchée par les vents, mais si elle a une faible valeur économique, cela ne sera pas très important en termes de coûts de dommages. En revanche, si une région est moyennement touchée mais qu'elle a une forte valeur économique, les coûts seront plus importants.

En vue de mieux choisir et d'avoir un aperçu général des seuils applicables au contexte de Madagascar, nous réalisons un test de robustesse des résultats (Voir Annexe/ tableau 2) en retenant comme seuils de références, ceux de La Réunion. En appliquant des seuils identiques pour Madagascar, nous obtenons une perte de 18,6% de la valeur économique totale pour la partie Nord-Est de Madagascar ; où le coût moyen ($f_{ci\ moyen}$) par pixel est évalué à 1060 dollars. Or, comme évoqué précédemment, en raison de la différence significative de la robustesse des infrastructures, il convient de diminuer la valeur des seuils. Etant donné que pour un niveau de seuil moins élevé, Madagascar pourrait subir de dégâts considérables.

Dans un premier temps, nous diminuons la valeur du seuil minimal ($\overline{W}$) respectivement à 80, 70, 60 km/h (SensMin1, SensMin2, SensMin3 respectivement dans le tableau 2) et en fixant la valeur du seuil maximal (W_{ci}) à 270 km/h (Seuil Maximal La Réunion). Et parallèlement, nous diminuons la valeur du seuil maximal respectivement à 250, 230,210 km/h (SensMax1, SensMax2, SensMax3 respectivement dans le tableau 2) et en fixant la valeur du seuil minimal à 93km/h (Seuil Minimal La Réunion). Remarquons qu'en diminuant la valeur du seuil minimal correspondant à l'absence du dommage, une augmentation peu significative est observée tant en termes de coût moyen par pixel qu'au niveau des pertes totales. Par contre, en modifiant la valeur du seuil maximal, on remarque que plus on diminue la valeur du seuil, plus il y a une augmentation conséquente des pertes, soit environ une hausse de 4 points de pourcentage des pertes totales et une hausse d'environ de 300 dollars du coût moyen par pixel après chaque diminution.

Dans un deuxième temps, pour vérifier davantage la robustesse des résultats dans le cadre de l'application d'une fonction de dommage pour le cas particulier de Madagascar, diminuons simultanément les deux valeurs des seuils (A partir de la ligne 4 du tableau 2 de l'annexe). Puisqu'il s'agit d'une approche théorique, nous allons simuler quelques situations hypothétiques sur les dommages qu'une situation particulière de champ de vent peut causer à la valeur économique. Globalement, l'analyse nous renvoie des pertes élevées comparativement aux pertes obtenues lorsque nous avons retenus l'un des seuils utilisés dans le contexte de La Réunion. Il est encore remarqué que la diminution du seuil minimal (pour une valeur fixée de

[13] Dans le cas où le cyclone a touché l'ensemble du territoire de Madagascar ou dans le cas où l'étude portait sur plusieurs cyclones ayant frappés plusieurs parties du pays, les pertes ne seraient observables qu'à partir de 50% comme indiqué dans la fonction de dommage d'Elliott & al (2015) (1). Autrement dit, les valeurs en dessous du seuil de 50% seraient nulles.

valeur maximal) entraine une hausse peu significative des pertes, tandis qu'une diminution du seuil maximal (pour une valeur fixée de valeur minimal) peut entrainer une hausse des pertes jusqu'à 10 points de pourcentage. Pour Madagascar, ces pertes pourraient passer de 22% à plus de 32% pour une vitesse de vent minimal et maximal allant de 80 à 60km/h et de 250 à 210 km/h, respectivement ; notamment pour un cyclone atteignant le stade de cyclone tropical intense comme Enawo. Ces éléments mettent davantage en évidence le fait que pour un pays ne possédant pas d'infrastructures adéquates pour faire face aux chocs cycloniques, des pertes considérables seraient constamment attendues.

Finalement, à partir du moment où les informations permettant de calibrer empiriquement une fonction de dommage pour Madagascar seraient disponibles, une distribution géographique des coûts cycloniques par le biais d'une cartographie se révèle cruciale de prime abord en vue d'attirer le regard des décideurs politiques sur les zones (districts, communes notamment dans la partie Nord-Est de Madagascar) nécessitant une intervention prioritaire en termes de réduction des risques cycloniques. Les pertes estimées dans le cadre de l'étude permettraient d'emblée au Gouvernement Malgache de revoir les priorités nationales en termes de budgétisation, de politique et de faire appel surtout à des financements post-catastrophiques auprès des partenaires extérieurs en cas de nécessité.

6 -Conclusion

En appliquant une fonction de dommage (Emanuel, 2011), nous avons pu simuler quelques situations hypothétiques sur les dommages avec des seuils de vents adéquats au contexte de Madagascar. Les résultats de l'analyse montrent que plus on diminue la valeur des seuils de vents, plus les pertes seront considérables, soient des pertes pouvant aller de 22% à 32% de la valeur économique totale.

Au moins quatre perspectives peuvent être attribuées à l'étude présentée dans cet article. D'abord, il est à déduire que les pertes estimées ici se révèlent comme très élevées connaissant l'importance des activités économiques en termes d'intensité lumineuses pour les régions de la partie Nord-Est de Madagascar. Pour cela, il est nécessaire dans les études futures d'affiner davantage ce résultat en faisant un calibrage empirique entre la valeur des lumières nocturnes et la valeur du PIB pour le cas particulier de Madagascar.

Ensuite, les données spatiales sur les lumières nocturnes, bien qu'elles soient une alternative pour les économistes pour mesurer les activités économiques à un niveau géographique plus détaillé, elles ont tendance à sous-estimer les activités économiques émettant moins voire presque pas de lumières comme les activités agricoles (Ghosh et *al.*, 2010 ; Keola et *al.*, 2015), les services écosystémiques (Sutton et Costanza, 2002). Or, comme souligné précédemment, Madagascar est composée d'une manière générale de populations vivant dans des milieux ruraux où les activités principales demeurent majoritairement les activités agricoles et dont les moyens d'éclairages sont peu existants. Dans cette logique, les imageries satellitaires nocturnes ne suffisent plus à elles seules à mesurer l'ensemble des activités économiques, d'où l'intérêt de recourir à d'autres sources de données complémentaires en vue d'une analyse plus complète plus tard (cf par exemple Keola et *al.*, 2015).

En outre, l'utilisation de la méthode par fonction de dommage a été surtout critiquée par l'accent qui est fortement mis sur l'évaluation des coûts associés aux dommages directs (Meyer et *al.*, 2013) ; ce dernier par contre n'est qu'une composante des dommages. En conséquence, cela pourrait conduire à des estimations de coûts incomplètes et donc, les décisions en termes de gestion des risques seraient biaisées en faveur de l'atténuation des coûts directs. Cela implique de réaliser dans l'avenir une évaluation des impacts indirects en supplément pour une analyse plus globale et plus complète.

Finalement, il a été remarqué dans plusieurs travaux récents que les phénomènes climatiques auraient pour conséquence l'intensification des activités cyclonique dans un futur proche. Ainsi, la connaissance des coûts associés aux dommages directs nous permettrait certes d'avoir d'emblée un aperçu de l'ampleur des pertes économiques. Par ailleurs, il importe de resituer plus tard l'étude dans un contexte de changement climatique en vue d'aider les décideurs publics pour une meilleure prise de décision sur la politique d'adaptation optimale face au risque cyclonique voire climatique.

Remerciements

Mes sincères remerciements vont tout d'abord à l'équipe organisatrice du colloque ASRDLF2023 afin que nous ; jeunes chercheurs ; puissions partager le fruit notre travail au grand public et de recevoir par conséquents des conseils, des remarques constructives auprès des experts en Recherches Scientifiques. Mes remerciements s'adressent ensuite à l'Université de La Réunion et à l'unité de recherche au sein de l'université connu sous le nom du CEMOI (Centre d'Economie et de Management de l'Océan Indien). Je tiens à adresser spécialement mes profondes gratitudes à Sabine Garabedian (MCF-HDR du CEMOI/ directrice de thèse) qui m'a donné l'opportunité de réaliser un stage de recherche en 2022 dans le cadre du programme *REunion NOVative Research on cyclonic RISKs (ReNovRisk)* (un programme à l'initiative du CEMOI), où j'ai pu acquérir des bases solides en matières d'évaluations économiques des impacts cycloniques et une occasion à partir duquel j'ai pu commencer à rédiger la présente communication. Mes remerciements s'adressent également à Idris Fontaine (MCF du CEMOI) pour le temps qu'il m'a accordé et pour l'intérêt scientifique qu'il a manifesté, un tel article ne pouvait se concevoir sans ses précieux conseils. Le dernier et non le moindre, mes sincères reconnaissances vont auprès de la Région Réunion et l'Union Européenne (*Programme FEDER INTERREG 2021-2027*) pour leur soutien financier dans le cadre de ma thèse ; qui est notamment une continuité et donc une amélioration de ce qui a déjà été débuté lors du stage de recherche.

Annexes

Tableau 2 : Test de Robustesse des résultats (Modification de la valeur des seuils de vents cycloniques).

	LR (93/270)	Sens.Min1 (80/270)	Sens.Min2 (70/270)	Sens.Min3 (60/270)	Sens.Max1 (93/250)	Sens.Max2 (93/230)	Sens.Max3 (93/210)
$f_{ci\ moyen}$	1060 (1319)	1099,79 (1315)	1129,59 (1313)	1158 (1311)	1269 (1533)	1518 (1782)	1814 (2066)
F_i	18,6%	19,33%	19,85%	20,37%	22,31%	26,69%	31,89
		Sens.Min1 Max1 (80/250)	Sens.Min2 Max1 (70/250)	Sens.Min3 Max1 (60/250)			
$f_{ci\ moyen}$		1304 (1519)	1332 (1509)	1358 (1500)			
F_i		22,9%	23,41%	23,88%			
		Sens.Min1 Max2 (80/230)	Sens.Min2 Max2 (70/230)	Sens.Min3 Max2 (60/230)			

$f_{ci\ moyen}$		1548 (1752)	1570 (1731)	1592 (1712)	
F_i		27,21%	27,61%	27,99%	
		Sens.Min1 Max3 (80/210)	Sens.Min2 Max3 (70/230)	Sens.Min3 Max3 (60/210)	
$f_{ci\ moyen}$		1835 (2015)	1850 (1980)	1865 (1947)	
F_i		32,26%	32,53	32,79%	

Source : Auteure, Données TCE-Dat et VIIRS

Notes : les valeurs entre parenthèses représentent l'écart-type, les valeurs de $f_{ci\ moyen}$ (coût moyen par pixel) sont en US Dollars constant 2015, les valeurs de F_i sont exprimées en % de la valeur économique total.

Références bibliographiques

Article de revue :

Anglais:

Apel H , Merz B , Thieken A (2008) Quantification of uncertainties in flood risk assessment. *International Journal River Basin Manage*. V (6):149-162.

Berlemann M, Wenzel D (2018) Hurricanes, economic growth and transmission channels: Empirical evidence for countries on differing levels of development. *World Development*: 231-247.

Bertinelli L, Mohan P, Strobl E (2016) Hurricane damage risk assessment in the caribbean: An analysis using synthetic hurricane events and nightlight imagery. *Ecological Economics*: 135-144.

Bertinelli L, Strobl E (2013) Quantifying the local economic growth impact of hurricane strikes: An analysis from outer space for the Caribbean. *Journal of Applied Meteorology and Climatology* 52(8): 1688-1697.

Bhandari L, Roychowdhury K (2011) Night Lights and Economic Activity in India: A study using DMSP-OLS night time images. *Asia-Pacific Advanced Network* : 218-236.

Botzen W, Deschenes O,Sanders M (2019) The economic impacts of natural disasters: A review of models and empirical studies. *Review of Environmental Economics and Policy* 13(2):167-188.

Camargo S, Hsiang S (2015) Tropical cyclones: From the influence of climate to their socioeconomic impacts. *In* : Chavez M, Ghil M, Urrutia-Fucugauchi, J. (Eds.), *Extreme Events: Observations, Modeling, and Economics*. chapter 18. Wiley.

Chen X, Nordhaus W (2015) A test of the new viirs lights data set: Population and economic output in Africa. *Remote Sensing* 7(4):4937-4947.

Chen X, Nordhaus W (2011) Using luminosity data as a proxy for economic statistics. *Proceedings of the National Academy of Sciences* 108(21):8589-8594.

Done J, PaiMazumder D, Towler E, Kishtawal C (2018) Estimating impacts of North Atlantic tropical cyclones using an index of damage potential. *Climatic Change*: 561-573.

Elliott R, Strobl E, Sun P (2015) The local impact of typhoons on economic activity in china: A view from outer space. *Journal of Urban Economics*: 50-66.

Emanuel K (1987) The dependence of hurricane intensity on climate. *Nature*: 483-485.

Emanuel K (2011) Global warming effects on u.s. hurricane damage. *Weather, Climate, and Society* 3(4), 261-268.

Felbermayr G, Gröschl J (2014) Naturally negative: The growth effects of natural disasters. *Journal of development economics* : 92-106.

Freni G, La Loggia G, Notaro, V (2010) Uncertainty in urban flood damage assessment due to urban drainage modelling and depth damage curve estimation. *Water Science Technology*: 2979-2993.

Fontaine I, Garabedian S, Jammes, M. (2022) Short-term impact of tropical cyclones in Madagascar: Evidence from nightlight data. *Working Paper.*

Fontaine I, Garabedian S, Nortes-Martinez D, Veremes H et *al.* (2021) The current and future costs of tropical cyclones: a case study of La Réunion. *Mimeo Version*:1-35.

Gibson J, Olivia S, Boe-Gibson G (2020) Night lights in economics: Sources and uses. *Journal of Economic Surveys* 34(5):955-980.

Geiger T, Frieler K, Bresch D (2018) A global historical data set of tropical cyclone exposure (tce-dat).*Earth System Science Data* 10(1):185-194.

Ghosh T, Powell R, Elvidge C, Baugh K, Sutton P, Anderson S (2010) Shedding Light on the Global Distribution of Economic Activity.*The Open Geography* :148-161.

Gray M (1968) Global view of the origin of tropical disturbances and storms. *Mon. Wea Rev*: 669-700.

Hamid S, Kibria B.M, Gulati S, Powell M, Annane B, Cocke S, Pinelli J-P , Gurley K , Chen S-C (2010) Predicting losses of residential structures in the state of Florida by the public hurricane loss evaluation model.Statistical Methodology:552-573.

Héron D, Evan S, Pianezze J, Dauhut Th, Bioude J, Rosenlof K, Noel V, Bielli S, Barthe Ch , Cammas J(2020) Mesoscale simulations of Tropical cyclone Enawo (March 2017) and its impact on TTL water vapor. *Atmospheric Chimestry and Physics*:1-31.

Henderson J, Storeygard A, Weil N (2012) Measuring economic growth from outer space. *American Economic Review* 102(2):994-1028.

Hsiang S, Jina A (2014) The causal effect of environmental catastrophe on long-run economic growth: Evidence from 6,700 cyclones". *In* Technical report, National Bureau of Economic Research. NBER Working Paper N°20352: 1-68.

Jongman B, Kreibich H, Apel H, Barredo J, Bate P, Feyen L, Gericke A, Neal J, Aertsn H,Ward (2012) Comparative flood damage model assessment: towards a European approach.*Natural hazard and Earth System* Sciences:3733-3752.

Jordan M et Clayson C (2008) A new approach to using wind speed for prediction of tropical cyclone generated storm surge. *Geophysical Letters.*

Keola S, Andersson M, Hall O (2015) Monitoring economic development from space: using night time light and land cover data to measure economic growth. *World Development* 66(1): 322-334.

Knutson T, Camargo S, Chan J, Emanuel K, Ho C.-H., Kossin, J., Mohapatra, M., Satoh, M., Sugi, M., Walsh, K., & Wu, L. (2020): "Tropical cyclones and climate change assessment: Part ii: Projected response to anthropogenic warming", in Bulletin of the American Meteorological Society, 101(3), E303-E322.

Knutson T, McBride J, Chan J, Emanuel K, Holland G, Landsea C, Held I, Kossin J, Srivastava, Obersteiner M (2010) Tropical cyclones and climate change. *Nature Geoscience* 157-163.

Kousky C (2014) Informing climate adaptation: A review of the economic costs of natural disasters. *Energy Economics*: 576–592.

Kreibich H, Bubeck, P. (2013): "Natural Hazards: Direct Costs and Losses Due to the Disruption of Production Processes", in Global Assessment Report on Disaster Risk Reduction, 1-19.

Krichene H, Geiger T, Frieler K, Willner S, Sauer I, Otto C (2021) Long-term impacts of tropical cyclones and fluvial floods on economic growth–empirical evidence on transmission channels at different levels of development. *World Development*:1-48.

Kuleshov Y, Fawcett L, Qi B, Trewin D, Jones J, McBride,Ramsay H (2010) Trends 712 in tropical cyclones in the South Indian Ocean and the South Pacific Ocean. *Journal of Geophysical. Resources*.

Leroux M, Meister J, Mekies D, Dorla A (2018) A climatolofy of southwest indian ocean tropical systems: Their number, tracks, impacts, sizes empirical maximum potential intensity, and intensity changes. *Journal of Applied Meteorology and Climatology*: 1021-1041.

Masutomi Y, Iizumi T, Takahashi K, Yokozawa M (2012) Estimation of the damage area due to tropical cyclones using fragility curves for paddy rice in Japan. *Environmental Research Letters*: 1-9.

Mavume A (2008) Tropical cyclones in the south-west Indian Ocean: intensity changes, oceanic interaction and impacts.

McCord G, Rodriguez-Heredia M (2022) Nightlights and Subnational Economic Activity: Estimating Departmental GDP in Paraguay. *Remote Sensing*.

Mendelsohn R, Emanuel K, Chonabayashi S, Bakkensen L (2012) The impact of climate change on global tropical cyclone damage. *Nature climate change* 2(3): 205-209.

Meyer B, Becker N, Markantonis V, Schwarze R, van den Bergh J, Bouwer L,*, Bubeck P, Ciavola P, Genovese E, Green C, Hallegatte S, Kreibich H, Lequeux Q, Logar I, Papyrakis E, Pfurtscheller C, Poussin J, Przyluski8 V, Thieken A, Viavattene C (2013) Assessing the costs of natural hazards – state of the art and knowledge gaps. *Natural Hazard and System Science*:1351-1373.

Mohan P, Strobl E (2017) The short-term economic impact of tropical Cyclone Pam: an analysis using VIIRS nightlight satellite imagery. *International Journal of Remoting Sensing*:1-13

Mouquet P, Alexandre C, Rasolomamonjy J, Rosa J, Catry T, Révillion C, Rakotondraompiana S, Pennober G (2020) Sentinel-1 and Sentinel-2 time series processing chains for cyclone impact monitoring in South WestIndian Ocean. *In International Archives of Photogrammetry,Remote Sensing Spatial Information Sciences.*

Neumann C (1993) Global overview. Global guide to tropical cyclone forecasting.

Nordhaus W (2010) The economics of hurricanes and implications of global warming. *Climate Change Economics* 1(01):1-20.

Pistrika A, Tsakiris G, Nalbantis I (2013) Flood depth-damage Functions for built Environment. *Environmental Processes* 1:553-572.

Romali N , Ismail Z, Yusop Z (2015) Flood Damage Assessment: A review of Flood Stage-Damage Function Curve. *Springer Science + Business Media Singapore*.

Smith D (1994) Damage Estimation. Review of Urban Stage-Damage Curves and Loss Functions. *Water SA*:231-238.

Strobl E (2011) The economic growth of hurricanes: Evidence from US Coastal Counties. *The Review of Economics and Statistics* 93(2): 575-589.

Strobl E (2012) The economic growth impact of natural disasters in developing countries: Evidence from Hurricane strikes in Central American and Caribbean regions. *Journal of Development Economics*: 130-141.

Sutton P ,Costanza, R (2002) Global estimates of market and non-market values derived from nighttime satellite imagery, land cover, and ecosystem service valuation. *Ecological Economics* 41(3):509–527.

Tulet P ,Aunay B,Barruol G,Barthe C,Belon R,Bielli S, Bonnardot F,Bousquet O,Cammas J.-P,Cattiaux J, Chauvin F, Fontaine I, Fontaine F, Gabarrot F, Garabedian S, Gonzalez A, Join J.-L, Jouvenot F, Nortes-Martinez- D, Mékiès D, Mouquet P, Payen G, Pennober G, Pianezze J, Rault C, Revillion C, Rindraharisaona E , Samyn K, Thompson, Vérèmes H. (2021) Renovrisk: a multidisciplinary programme to study the cyclonic risks in the south-west indian ocean. *Natural Hazards*.

Ye M,Wu J,Liu W, He X , Wang,C (2020) Dependence of Tropical cyclone damage on maximum wind speed and socioeconomic factors. *Environmental Research letters*:1-11.

Rapports, documents de recherche.

Français et anglais :

Banque Mondiale (2022) : *L'urgence des réformes : Transformation économique et meilleure gouvernance au cœur de la lutte contre la pauvreté*. Mise à jour du Diagnostic-pays de Madagascar (P173774). Groupe de la Banque Mondiale.

EXPANSION (2019) : *Comesa et SADC, L'Agro-industrie comme tremplin*. In *Expansion*, Novembre-Décembre 2019.

IPCC (2019): *Special report on the ocean and cryosphere in a changing climate*. *In* WEYER, N. (Ed.), in it together: why less inequality benefits all?

JRC (2017): *Technical Reports, Tropical Cyclone Enawo: Post Event Report, Madagascar*. March 2017, TC-2017-000023-MDG.

PNUD (2018) *Rapport National sur le Développement Humain Madagascar.*

L'Observatoire Défense et Climat (2019) *Prospective de l'Océan Indien"*, Rapport d'étude (RE9), Mai 2019.

Chapitre 10

The current and future costs of tropical cyclones : a case study of La Réunion

Fontaine, Garabedian, Vérèmes

- ***Revue Économique***, en soumission, 2023
- ***Présentation :***
  Colloque ARUM, Paris, octobre 2022

RenovRisk – Impacts

The current and future costs of tropical cyclones: a case study of La Réunion *

Idriss Fontaine[†] — Université de La Réunion

Sabine Garabedian[‡] — Université de La Réunion

David Nortes-Martinez[§] — Université de La Réunion

Hélène Vérèmes[¶] — Université de La Réunion

April 2021

Document history:

April 2021 Mimeo version Idriss Fontaine

*Financial supports from the the European Fund for Economic and Regional Development (EFERD), the *Region Réunion* and the *Observatoire des Sociétés de l'Océan Indien* (OSOI) are gratefully acknowledged. For comments and insightful suggestions we thank Pascal Mouquet, Soline Bieli and Sylvie Malardel. We address a special thank to Kerry Emanuel for providing us the data of simulated cyclonic systems.

[†]Department of Economics (CEMOI), Université de La Réunion; E-mail: idriss-fontaine@univ-reunion.fr

[‡]Department of Economics (CEMOI), Université de La Réunion; E-mail: sabine.garabedian@univ-reunion.fr

[§]Department of Economics (CEMOI), Université de La Réunion; E-mail: david.nortes-martinez@univ-reunion.fr

[¶]Department of Atmospheric Physics (LACy, OSU-Réunion), Université de La Réunion; E-mail: helene.veremes@univ-reunion.fr

Contents

Abstract

In comparison to the current losses, what would be the variation of economic losses associated to tropical cyclones in the island of La Réunion in a warmer climate environment? This paper proposes an answer to this question by following a strategy based on two main steps. First, to proxy economic activity at a local level, we employ night light data available at a high level of resolution. Second, as historical data of tropical cyclones are of short length and probably uninformative about what would be the characteristics of future tropical cyclones, we rely on synthetic tropical cyclones generated under a "current" and "future" (and warmer) climate environment. By combining these two-input data, we find that economic losses due to tropical cyclones passing in the vicinity of La Réunion are likely to increase. Specifically, annual expected economic losses are estimated to amount to 0.36% of the economic value under a climate scenario similar to what have been observed currently against 0.69% under a future climate scenario. The return period of losses of 10% of total economic value decreases from 95 years to 49 years. Sensitivity analyses applied to check for the consistency of our baseline estimation show that our approach does not overestimate not underestimate the costs associated to tropical cyclones in this French overseas region. All in all, our finding suggests that policy designers should engage in adaptation policies in order to improve the resistance of goods to cyclonic winds and so reduce the total losses associated to such meteorological events.
Keywords: Tropical cyclone, costs, nightlight data, La Réunion.
JEL classifications: Q51, Q54, R12

1 Introduction

Tropical cyclones are often seen as one of the most natural destructive phenomena that an economy may face (Camargo & Hsiang, 2015). For instance, during the 2000-2009 period, the EMDAT database estimates that the total damages due to tropical cyclones amounts to approximately US$ 466 billion. Likewise, the total death tolls of tropical cyclones during this period was of 172 thousand people while approximately four million of people have been recorded as homeless in the wake of a passing tropical cyclone. There are now many evidence indicating that economic losses due to such meteorological events raise steadily from many decades (Cavallo et al., 2010; Grinsted et al., 2019). Perhaps even more worrying is the multiplication of evidence from the scientific literature indicating that climate change is likely to alter the frequency, the genesis, the spatial extent and the characteristics of the most extreme tropical cyclone events (Knutson et al., 2010; IPCC, 2019; Knutson et al., 2020). Combined with the fact that future economic and demographic growth would lead to an increase in people and asset exposure (Botzen et al., 2019), this tends to suggest that the future economic losses associated to tropical cyclones is likely to be higher.

Located in the South West Indian Ocean (SWIO, henceforth), a basin that records 11% of global cyclonic activity according to Leroux et al. (2018), the French overseas region of La Réunion is frequently threatened by cyclonic systems. The historical work of Mayer Jouanjean (2011) on the cyclonic events in La Reunion during the twentieth century shows that the island has experienced many disastrous events. Of course, the quality of infrastructure on the island has been greatly improved since then, but the referencing of events shows that, throughout the twentieth century, cyclones had a significant impact on the Reunionese society as a whole as well as in terms of damages. The cyclone of the "year" 1948 is perceived as the strongest since, according to the few existing measures at that time, the gusts of wind could have exceeded 300 km/h (Mayer Jouanjean, 2011). Other cyclonic events hurt La Réunion such as Jenny in 1962, Denise in 1966, Hyacinthe in 1980, Clotilda in 1987, Firinga in 1989 or Colina in 1993, each time causing significant damages and unveiling the vulnerability of the local population to such cyclonic events. More recently, the improvement of the measurement of the magnitude of tropical cyclones show that, in 2002, the half of the maximum wind speed generated by the tropical cyclone Dina on the Reunionese territory was higher than 186 km/h while the last quantile was was higher than 217 kmh. Quite surprisingly, given the threat posed by tropical cyclones on La Réunion, there is no comprehensive study providing an assessment of economic losses due to these events for this French overseas region. Such a study has however the potential to be of interest of policy makers to engage in adaptation policies as well as firms or economic agents as a whole. The purpose of this paper is to fill

this void.

Assessing the economic losses associated to tropical cyclones is however a difficult task as it faces conceptual as well as methodological challenges. From the conceptual side, the distinction between what the literature called the direct and indirect costs of tropical cyclones are not always easy (see Cavallo et al. (2010) or Kousky (2014) for detailed surveys). In this paper, we focus on the direct losses, namely the immediate physical destruction occurring in a wake of the event. Methodological challenges are twofold. First, historical data on tropical cyclones are of short length and high-quality observation are quite recent. Looking at past events is likely to be inappropriate since damaging cyclonic events, and even more the most extreme events, are still uncommon from a statistical viewpoint. Such an issue is probably more acute when the focus is on a particular and relatively small island, as it is the case in the present paper. Moreover, historical observations are likely to be uninformative about what would be the characteristics of tropical cyclones in a future and warmer climate environment. As a matter of fact, the future costs of tropical cyclones, but also the variation of future costs in comparison to what we call the contemporaneous costs, is a key indicator to engage in adaptation policy. Second, the extent of economic damages depends on many factors such as the physical characteristics of tropical cyclones themselves as well as the spatial distribution of economic assets over a given territory. Consequently, and even more in the case of a small island as La Réunion, it is requirement to objectively proxy the repartition of economic activity at a detailed spatial level (Bertinelli et al., 2016).

To overcome these two methodological issues we proceed as follows. Rather than relying on historical data, we follow a similar strategy than Hallegatte (2007), Emanuel (2011) or Bertinelli et al. (2016) (among others) and we resort on synthetic cyclonic systems generated by combining large-scale meteorological variables derived from climate models with a coupled ocean-atmosphere cyclonic system model. As many characteristics of cyclonic systems are "downscaled" from a given climate model, this method also allows us to overcome the second issue raised in the last paragraph. Thus, by considering two climate models, one for a climate environment similar to what have been observed during the last 30 years and the second one for a future and anticipated scenario of global warming, this methodology allows us to investigate to what extent future economic losses due to tropical cyclones will change in comparison to the contemporaneous economic losses. Then, to proxy economic activity and the spatial distribution of the economic value at a local level, we rely on nightlight brightness observed from satellite. This follows a new and flourishing literature that employ nightlight data as a proxy for economic activity to study various economic issues such as the measurement of economic activity in low-income countries (Chen & Nordhaus, 2011; Henderson et al., 2012; Chen & Nordhaus, 2015; Pinkovskiy & Sala-i Martin, 2016), the growth impact of natural

disasters (Bertinelli & Strobl, 2013; Elliott et al., 2015) or the recovery period following a disaster (Heger & Neumayer, 2019; Kocornik-Mina et al., 2020; Nguyen & Noy, 2019).[1]

Armed with these two-input data, we then compute the wind field profile over La Réunion of each simulated cyclonic system and translate them, using the well-known wind damage function of Emanuel (2011), into economic losses.[2] Our key findings is as follows. First, the average cost per cyclonic system circulating around La Réunion increases of about 89%, implying that localities concentrating more economic activities are likely to suffer more damages in the future. Second, our risk assessment, consisting in simulating 100,000 years of potential cyclonic events under both climate scenario, while keeping identical the average number of systems affecting La Réunion, shows that the proportion of years without damages decreases in the future. The magnitude of the average annual losses due to tropical cyclones increase from 0.36% to 0.69% of the economic value. Furthermore, for the same amount of total losses, the associated return period sharply decreases in a warmer climate environment. For instance, a total loss of 10% of the economic value is associated with a return period of 95 years in a contemporaneous climate environment against 49 years in a future and anticipated climate environment. Finally, sensitivity analyses based on changing parameters shaping our damage function or the frequency of future cyclones, indicate that our baseline estimates do not overestimate nor underestimate the losses and the variation of losses due to tropical cyclones in a future and warmer climate environment.

The outline of the paper is as follows. Section 2 provides some background about cyclonic activity in the SWIO and the economy of La Réunion. 3 presents the nightlight and tropical cyclone data used in this paper. Section 4 details the methodology and the underlying assumption associated to out baseline strategy. Section 5 presents our main results but also sensitivity analyses applied. Finally, section 6 concludes.

2 Background

2.1 Climatology of tropical cyclones in La Réunion

Tropical cyclones are natural atmospheric phenomena. According to Camargo & Hsiang (2015), they are considered as the most destructive natural disaster a socieconomic system may face. A cyclone can be defined as a large, organized systems of winds (driven by convective

[1] See the recent survey of Gibson et al. (2020), to have more information about how nightlight data has been used by economists.

[2] Other papers also employ the Emanuel (2011)' damage function either to measure economic losses or as a proxy of local destruction to be included in regressions. Examples include Bertinelli & Strobl (2013), Elliott et al. (2015), Sealy & Strobl (2017) or Mohan et al. (2018).

processes) that rotate around a center of low atmospheric pressure (Bobrowsky, 2013).[3] Tropical cyclones are associated with high speed winds that can be indeed very destructive. In the SWIO basin tropical systems are considered tropical cyclones when they reach maximum sustained wind speed (at 10 m above the surface) of 118 km/h . When the maximum sustained wind speed is above 63 km/h, they are labelled as tropical storms and tropical depressions when it is below 63 km/h. In case of extreme wind speeds, tropical cyclone can cause severe damage as well as total destruction of properties, buildings, crops or agricultural areas.

The SWIO basin represents 11% of the global cyclonic activity (Leroux et al., 2018) with about 9.7 observed tropical systems in average per year and among which 4.8 generate wind speeds that would characterize them as tropical cyclones[4]. The islands of the SWIO and countries along the east coast of Africa can suffer significant damages from the passage of cyclonic systems that can have significant health, economic and environmental consequences (Jury et al., 1993; Leroux et al., 2018). Although La Réunion has the resources to have an effective warning system to keep the population safe, the passage of La Réunion has a complex topography that makes it vulnerable to the hazards associated with tropical cyclones (Tulet et al., 2021).

By definition, the National Hurricane Center (NHC) considers a tropical cyclone to have landed (characterized as a "landfall cyclone" in the literature) when the center of the cyclone crosses the coast (NHC, 2019). Following this definition, all studies conclude that no tropical cyclone has landed on Reunion Island (Leroux et al., 2018; Weinkle et al., 2012) for the period they covered, i.e. from 1970 to 2016. This means that this situation is unprecedented and that no data could inform the passage of a tropical cyclone whose center would have touched the sides. Leroux et al. (2018) did not limit themselves with this landfall definition and differentiated tropical cyclones as falling into two categories: "direct impact" (meeting the NHC definition of a "landfall cyclone") or "threats" (the center of the cyclone passes within 100 km of the coast).[5] Although no tropical cyclone or tropical storm stage system has "directly" impacted La Reunion, there have been four threats between 1999 and 2016 (Leroux et al., 2018). These studies have focused on the passage of cyclones on or within 100 km of land, however, many examples in the SWIO have shown that a tropical cyclone whose center passed at a greater distance could have impacted territories economically and/or ecologically.

[3]Depending on the basin they are originated, these systems receive different names (Bobrowsky, 2013). They are called hurricanes in the North Atlantic and northeastern Pacific basins; typhoons in the northwestern Pacific basin and cyclones in the north Indian basin, the southwestern Pacific, in the southeastern as well as in the southwestern Indian basins and the Australian region.

[4]In term of magnitude, a "tropical cyclone" is equivalent to "hurricane" and "typhoon" used to described a given intensity of cyclonic systems in other basins.

[5]Here, the term "direct" impact should be understood with a physical perspective. Consequently, it is different to the notion of direct costs mentioned in the introduction. We however keep this terminology here because it is the most intuitive to understand the distinction introduced by Leroux et al. (2018).

Among them, we can mention Gamède in 2007 or Dumile in 2012 which passed as close as possible to La Réunion between 100 and 150 km. History has also shown that systems that did not reach the stage of a tropical cyclone can also induced significant damages. For instance, in 2018, at the stage of a strong tropical storm, Berguitta, passed by La Réunion and caused significant economic damages. Throughout this paper, we employ this "extended" definition to identify cyclonic systems that are the most likely to generate economic damages to La Réunion.

Leroux et al. (2018) was based on the best tracks of tropical storms in the SWIO obtained from the Regional Specialized Meteorological Center (RSMC) of La Réunion. Note, however, Leroux et al. (2018) did not take the RSMC wind criteria to categorize tropical systems. The best-track analyses of RSMC of Reunion Island provides 6-hour estimates of different parameters (storm location, minimum sea level pressure, maximum 10-m wind speed...). To have a measure of the average number of cyclonic systems circulating around La Réunion, we queried the same -but updated- database for the 1979-1980 season to 2018-2019 saison period to identify cyclonic systems (a minima strong tropical storm based on the specific terminology of RSMC to classify tropical systems) that had passed directly over the land or whose center would be located within 150 km of Reunion (coordinates chosen are 21.114533°S and 55.532062°E). The 150 km limit was chosen empirically to select the systems that probably impacted Reunion. We counted 19 systems (including 11 at the cyclone stage) whose center passed within 150 km of Reunion Island, but none of them formally landed. A significant number of systems have passed near the island of La Réunion. We notice that if the tropical cyclones arrive mainly by the north, they sometimes pass directly by the south. Their passage near La Réunion is done as well by the east as by the west. We can therefore expect that the risks presented are distributed differently on the island depending on the trajectory because there is a wide variety of trajectories. There are many patterns of passage of tropical systems in the vicinity of Reunion Island and, although the data archived at RSMC shows a long monitoring of cyclonic activity in the SWIO basin, the sample size appears to be too small to statistically assess the economic costs associated to the cyclonic risk.

2.2 The economy of La Réunion

The island of La Réunion is a former French colony. Just after Worl War II, in 1946, La Réunion obtained the status of French department and became a French oversea region in 1982. The 1970' decade corresponds to the economic take-off of the island. Between 1974 and 2008, its average annual growth rate was roughly equal de 5% (CEROM, 2004; Parain & Rivière, 2013). In 2018, the reference year in our study, the annual economic growth was lower (1.8%) and the output per capita of La Réunion was of 22,000 EUR. Overall, the strong

economic growth since 1970 was accompanied by an increase in the Human Development Index (HDI) which was estimated to 0.81 by Goujon & Hoarau (2015). However, despite such a good economic performance, the unemployment rate remains high (24%) while the employment and the participation rate are low (46% and 61%). Last but not least, the share of people living under the poverty threshold is sharply higher than the one observed in mainland France. In particular, 38.9% of Reunionese are under this threshold against 14.8% in mainland France (INSEE, 2019).[6]

The Reunionese economy has many specificities which broadly correspond to those of a small island economy. Specifically, the small size of its territory, which prevents the achievement of economies of scale, its insularity, the high distance between the island and mainland France, but also a relative specialization in services and tourism make it particularly vulnerable to shocks of exogenous nature, such as tropical cyclones (Croissant et al., 2019; Hoarau, 2019). The Reunionese economy is a "tertiary" economy where the role of services is largely dominant in the production of wealth. The added value of the service sector represents approximately 80% of total GDP. By contrast, the industrial and the agricultural sector contribute much less to total output. Specifically, the output share of the industrial sector amounts to 18% while the output share of the agricultural sector is about 2%. Such a repartition of economic activity within output is non-trivial for our study, because it is known that nocturnal brightness is a better proxy of the service and industrial sector than the agricultural one (Elliott et al., 2015; Gibson et al., 2020).

3 Data and methodology

3.1 Nightlight data

One prerequisite for our study is to objectively proxy economic activity at a local level. To do so, we follow an approach first used by Sutton & Costanza (2002) and further developed in Chen & Nordhaus (2011), Henderson et al. (2012), Chen & Nordhaus (2015), Bertinelli et al. (2016) or Gibson (2021) (among others) and we rely on nightlight brightness observed from satellite. As stressed in Gibson et al. (2020), night light data are growing in popularity among economists, especially in contexts where other data sources are either non-existent or presumed of poor quality. The appropriateness of nightlight data as a proxy for economic activity has been discussed in many studies and, in general, a strong positive relationship between the logarithm of GDP and the logarithm of the radiance value of nightlights is found

[6] According to the French National Institute of Statistics and Economic Studies, the poverty line in France by consumer unit was of 1063 EUR per month.

(Chen & Nordhaus, 2011; Henderson et al., 2012; Bertinelli & Strobl, 2013; Li et al., 2013). Against this background, it should be observed that nightlight data is not appropriate in capturing all types of economic activity. This is especially the case for rural activities which are often characterized by large unlit or low-lit areas (Gibson et al., 2020). *A priori*, such issues are not an important concern for our case study since the GDP of La Réunion relies more on the tertiary sector than the agricultural one. Finally, in the context of La Réunion, we are not aware of other data capturing the spatial distribution of economic activity so that nightlights are a relevant departure point.

In contrast to many papers of the economic literature (Bertinelli & Strobl, 2013; Elliott et al., 2015; Bertinelli et al., 2016) (among others), we use nighttime satellite images from the Day/Night Band (DNB) sensors of the Visible Infrared Imaging Radiometer Suite (VIIRS), on board the Suomi-National Polar-orbiting Partnership (S-NPP) instead of night lights data from the Defense Meteorological Satellite Program (DMSP). This choice is motivated by shortcomings of DMSP data, especially the existence of blurred images, geo-location errors and sensor saturation (Gibson et al., 2020). Furthermore, DMSP data are only available until 2013 and the original spatial resolution of picture are lower than the one of VIIRS.

For our study, our VIIRS input data are the 2018 daily nighttime data, also known as the "black marble" data, produced following the methodology of Román et al. (2018).[7] We aggregate daily data to annual data by employing a simple arithmetic average. The final resolution of cells of nocturnal brightness is of 0.004° (approximately 500 meters of horizontal resolution) implying that the entire territory of La Réunion is represented by approximately 10,000 pixels. Figure 1 shows the spatial distribution of night time brightness in La Reunion for our reference year, namely 2018. In the figure, unlit areas are depicted in black while the most lit areas turn from gray to white depending on the radiance value. Figure 1 shows that the most lit cells appear in areas near to the coast and especially in cities were economic activity is concentrated. This is especially true for the capital city of La Réunion, namely Saint-Denis, but also for the industrial area around the seaport. In contrast to the other parts of the island, the eastern part shows more unlit pixels, especially in area near to the volcano. Given the nature of our input data, we so implicitly assume, as Elliott et al. (2015), that unlit areas do not capture any economic activity. Table 1 report summary statistics associated to average nighttime light intensity in 2018. Approximately, 80% of cells show a radiance value lower than the average nightlight intensity of 21.75. Such a feature is confirmed by a positive skewness. The standard deviation of the distribution of nightlight intensity is twice larger than the mean and amounts to 56.62. The total nightlight brightness in 2018 is roughly of 273,084.

[7]The "black marble" products are freely available on adsweb.modaps.eosdis.nasa.gov

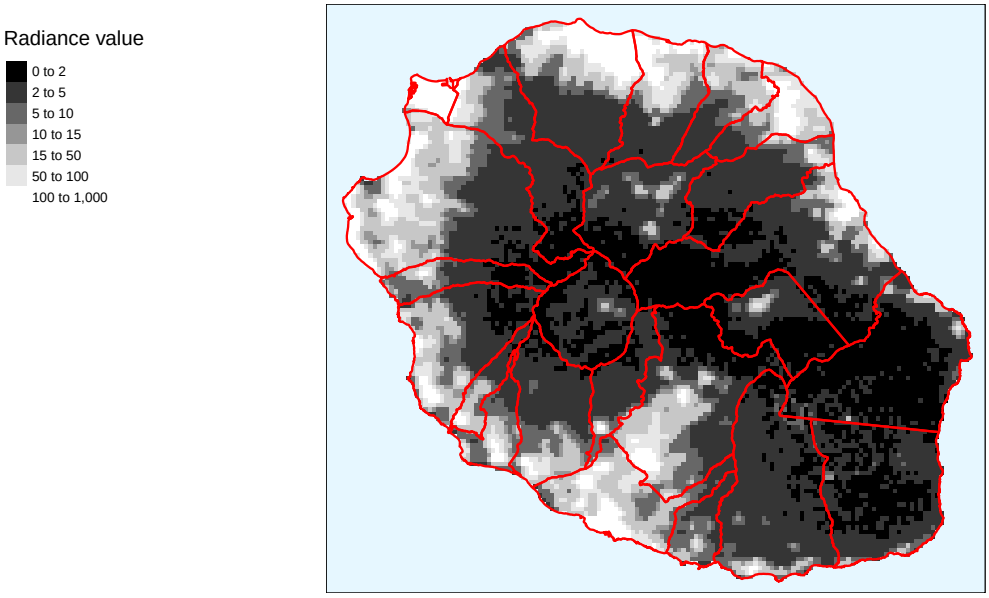

Figure 1: Mean value of daily night-light per pixel for La Réunion in 2008.
Sources: Black marble night light data (Román et al., 2018) and authors' own calcultations.

3.2 Tropical cyclone data

For a study of the economic costs and risk associated to tropical cyclones in La Réunion, relying on historical and observed events is likely to be problematic for at least two reasons. The first issue relies on the availability of historical data monitoring by RSMC. Indeed, when they exist, historical data are of short length and high-quality observations are recent since their records begin with the era of satellite observation. As stressed by Emanuel et al. (2008), in the southern hemisphere, the one which interested us here, good observations of cyclonic systems have been achieved only in the 1970s, namely when satellites coverage covers most of the earth's surface. In addition, even if historical data were of sufficient length using them for a risk analysis is challenging because the occurrence of extreme events is very uncommon from a statistical point of view, especially at an island level as La Réunion. The second shortcoming that accompanies the use of historical tropical cyclone data is that they are likely to be uninformative about what future cyclonic systems would be. In addition to the amount of historical costs, policy makers, but also economic agents as a whole, are likely to be interested in the future characteristics associated to tropical cyclones.

Anticipating what would be the future characteristics of tropical cyclones is however a challenging task, especially in a context of anthropogenic global warming that is likely to modify the genesis, the path but also the maximum intensity reached by cyclonic systems (Knutson et al., 2010; IPCC, 2019; Knutson et al., 2020). To achieve this challenging task,

	Night light intensity
Min.	0.00
Percentile 1%	1.01
Percentile 5%	1.47
Percentile 10%	1.65
Percentile 25%	2.05
Percentile 50%	3.11
Percentile 75%	12.38
Percentile 90%	55.81
Percentile 95%	106.03
Percentile 99%	315.90
Max.	975.09
Mean	21.75
Standard deviation	56.62
$\frac{\text{Standard deviation}}{\text{Mean}}$	2.60
Skewness	5.62
Total night light brightness	273084.2

Table 1: Summary statistics of average night light intensity in La Réunion in 2018.
Sources: Black marble nightlight products of Román et al. (2018) and authors' own calculation
Notes: Night light intensity is measured in nWatts cm^{-}2 sr^{-}1

several techniques have been employed. One approach, undertaken by Thompson et al. (2021), consists in studying how climatologically representative tropical cyclones could be damaging if a similar one would occur in the future. For the specific case of the cyclone Bejisa that affected La Réunion in 2014, the result suggests that future "Bejisa-like" cyclones would be more intense of about 6.5%.[8] The latitude at which this type of cyclone would reach their maximum lifetime intensity would be 2° further poleward but no substantial change was detected in the north-south trajectory that would mean that Reunion Island would be still impacted. However, Thompson et al. (2021) acknowledge that is is a requirement to reproduce this kind of projection for multiple cyclones, especially if one wants a measure of cyclonic risk. Here, we rely on another technique first pioneered in Emanuel (2006) and thereafter used by Hallegatte (2007), Emanuel et al. (2008), Emanuel (2011) or Bertinelli et al. (2016) (among others). This alternative approach consists in the construction of synthetic cyclonic systems generated by large-scale meteorological variables derived from climate models. More specifically, given many meteorological variables and a high-resolution coupled ocean-atmosphere cyclonic system model, synthetic systems are randomly launched

[8] Thompson et al. (2021) consider a scenario described by the IPCC Representative Concentration Pathways (RCP) 8.5 emissions and a 1.1–4.2° warming of the ocean surface by 2100.

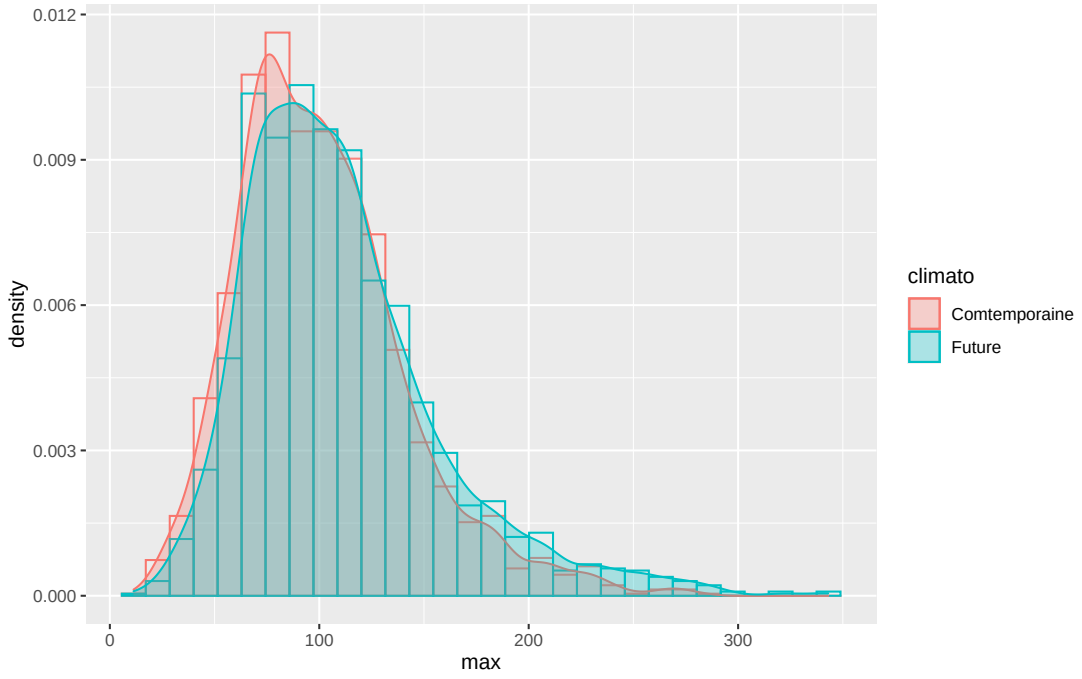

Figure 2: Contemporaneous and future averages of maximum wind speed per pixel.
Sources: Synthetic tropical cyclones (Emanuel, 2011) and authors' own calcultations.

in space and are assumed to develop according to the chosen climate condition. Some of them develop until reaching the level of tropical cyclones while others do not. By downscaling the characteristics of tropical cyclone, this technique allows to quantify the influence of climate on tropical cyclone activity. Furthermore, in addition to the appropriateness of the simulation of cyclonic systems by the coupled ocean-atmosphere cyclonic system models, this technique also benefits from the robust estimates of large-scale climate conditions from the climate model (Emanuel, 2011).[9] For our study, the use of synthetic cyclonic systems is motivated by two main reasons. First, it allows us to circumvent the problem that accompanies the use of historical data, especially their shortness and the inherent lack of extreme events. Second, as the technique can be employed under different climate models, it can also be used for climate models that anticipate the pattern of large-scale meteorological variables in a near future. Put differently, rather than using a climate model capturing contemporaneous condition, the method can also be implemented for a climate environment capturing future meteorological conditions under a given scenario of global warming. Consequently, relying on this technique allows us to compute the economic costs of "contemporaneous" tropical cyclone as well as those associated to "future" tropical cyclones as generated by a warmer climate environment.

[9] Emanuel et al. (2008) assess the ability of this method in reproducing historical cyclone climatology in the North Atlantic basin and find that it works remarkably well.

Synthetic TCs are generated using thermodynamic and kinematic statistics (Emanuel et al., 2006) based on recent historical climate data (or outputs from future scenario-based simulations) within a coupled ocean-atmosphere tropical storm model (Emanuel et al., 2008). The synthetic TCs are produced in three steps: genesis, tracks and intensity. Track points are initiated randomly (in space and time) with seeding warm-core vortices whose maximum wind speeds reach only 12 m.s-1. The tracks are calculated according to a beta-and-advection model (Holland, 1983) applied to the seed vortices, and the intensity is predicted using the CHIPS model (Emanuel et al., 2004). Seeds are considered to form tropical cyclones only when the vortex develops winds of at least of pre-defined threshold. A more detailed description of this technique can be found in Emanuel (2006) and (Emanuel et al., 2006, 2008)). Our study is based on two datasets of 2,000 synthetic TCs produced using this method for past and future conditions, respectively. Synthetic TCs were included in the dataset when they show maximum 1-min average maximum wind speeds of 21 m.s-1 when passing in a radius of 150 km around Reunion Island (exact coordinates of the center: 1.114533°S/ 55.532062°E). This distance of 150 km was chosen empirically; strong tropical storms and tropical cyclones whose center is located at this distance can potentially cause damage on Reunion Island. The past simulations are based on atmospheric and ocean conditions provided by the ERA5 reanalysis from 1980 to 2019. A reanalysis consists in reprocessing all the past observed data archived by ECMWF (European Centre for Medium-Range Weather Forecasts; including some observation data that had not been retrieved when the operational model was initially run) with a consistent (and upgraded) system. ERA5 combines vast amounts of historical observations into hourly global estimates of a large number of atmospheric, land and oceanic climate variables using advanced modelling and data assimilation systems. Compared to the former reanalysis (Dee et al., 2011), ERA5 shows a higher horizontal and temporal resolution and a better representation of tropical cyclones. The ERA5 dataset covering 1979 to present day is publicly available. The horizontal resolution is 31 km (versus 80 km for ERA-Interim) and the atmosphere is resolved using 137 levels (from the surface up to an altitude of 80 km). Future conditions are calculated by CNRM-CM6-1 which is an atmosphere-ocean coupled global climate model (Voldoire et al., 2019) that have been developed by the CNRM/CERFACS modelling group for CMIP Phase 6 (CMIP6) (Eyring et al., 2016). The CMIP (Couple Model Intercomparison Project) aims at better understanding past, current and future climate change in a multi-model context (Eyring et al., 2016). The CMIP provides standardized outputs from different models in order to facilitate model intercomparisons. CNRM-CM6-1 consists of several existing models designed independently and coupled through the OASIS-MCT software developed at CERFACS (Craig et al., 2017; **?**). The atmosphere is simulated with ARPEGE-Climat v6.3 global climate model (Roehrig et al., 2020) and the ocean with the NEMO ocean model v3.6 (Madec et al.,

2017). The surface fluxes are simulated with the numerical platform SURFEX (Masson et al., 2013) v8.0 and the sea-ice is represented by Gelato (Hunke and Dukowicz, 1997) v6.0. More details on the physical parameterizations can be found in Voldoire et al. (2017). Its native horizontal resolution for the atmosphere is 250 km and 100 km for the ocean. Thus, the future conditions are the outputs of the CNRM-CM6-1 model simulations calculated for the SSP-based (shared socioeconomic pathway; O'Neill et al. (2016)) scenario named ssp370 for the 2015-2100 period. The ssp370 scenario projects low action on climate mitigation and air pollutant emissions reduction. This scenario represents the medium to high end of the range of future forcing pathways (O'Neill et al., 2016). This scenario expects a radiative forcing of 7 W.m-2 in 2100 caused by the emissions. Then, using both historical and future track datasets will allow us to study the evolution of the losses due to tropical cyclones on La Réunion.

4 Methodology

The wind field of each synthetic TC is predicted using the CHIPS model (Emanuel et al., 2004, 2008). For each synthetic TC, CHIPS calculates the storm intensity and the radius of maximum wind along the track according to the potential intensity, the wind shear and the thermal stratification of the ocean given by the re-analysis and the climate model data. This a deterministic, coupled atmosphere-ocean, axisymmetric hurricane model. It should be noted nevertheless that the CHIPS model does not take into account topographic and baroclinic effects. CHIPS is computed into potential radius coordinates (i.e. two dimensions; radius and height) which means that the resolution is high/poor inside/outside of the eyewall. In order to accurately represent the increase and the decay of wind speed as a function of distance from the center of the tropical cyclone, we used the parametric wind model of Emanuel & Rotunno (2011) in the CHIPS model. Emanuel & Rotunno (2011) improved Emanuel et al. (2004)'s model for the outer part of the tropical cyclone eyewall by assuming a constant Richardson Number in the storm outflow. Details regarding the wind fields' calculation can be found in Emanuel et al. (2004), Emanuel et al. (2006) and Emanuel & Rotunno (2011). Once wind fields are estimated at the local level, the main challenge is to convert them into economic losses. In doing so, as the total dissipation of power of a cyclonic system (integrated over the lifetime of the event) increases as the cube of maximum wind speed, a natural first practice was to simply use the cubic value of maximum wind speed as a proxy for destruction (Emanuel, 2005). Furthermore, given that for wind speed of "low" intensity it is unlikely to observe significant damages, it was common to fix damages to 0 when wind speed is below a certain threshold (Strobl, 2011, 2012). However, and as noticed by Hallegatte (2007), one drawback of such indexes is that economic damages could infinitely increase in wind speed

even though the total amount of economic losses is bounded by the total economic value located at the surface of a given locality. To take into account this issue, we here follow the same strategy than Emanuel (2011) and we compute the following index of potential destruction f_{ci} that estimates the share of economic losses at a given cell c for event i:

$$f_{ci} = \frac{v_{ci}^3}{1 + v_{ct}^3} \tag{1}$$

with

$$v_{ci} = \frac{MAX\left(W_{ci} - \bar{W}, 0\right)}{W^* - \bar{W}}. \tag{2}$$

Where $\bar{W}$ is the minimum wind speed value above which economic damages are observed and W^* corresponds to the threshold at with half of the economic value of a given cell c is lost. Such an index of potential destruction captures three important features. First, the parameter $\bar{W}$ captures the fact that positive values of damages is produced only when maximum wind speed is above a certain threshold. Second, economic damages raises with the cubic power of maximum wind speed. Last but not least, for high level of wind, the index imposes that the fraction of total economic losses cannot exceed one. The choice of the two parameters in equation (2) is non-trivial as they shape the form our damage function. In the context of La Réunion, we however acknowledge that we lack of strong empirical evidence to choose these two parameter values. Indeed, insurance claim data are not publicly available and in recent years we lack of "intense" cyclonic systems so that post-cyclone satellite observations are uninformative. Consequently, we follow Elliott et al. (2015), and we set $\bar{W} = 93$ km/h and $W^* = 270$ km/h. The value of 93 km/h makes sense in the context of La Réunion as it is broadly consistent with the threshold at which the RSMC labelled a cyclonic system as a "strong tropical storm". In what concerns W^*, we check for the robustness of our results by varying it to ± 40 (see the robustness subsection below). Figure 3 displays our baseline index of potential economic lost. According to the constructed index, a maximum wind speed of 200 km/h is associated with an economic loss of about 16% while for a wind speed of 300 km/h the corresponding loss amounts to 58%, illustrating the non-linearity of economic damages in wind speed exposure. Overall, it should be observed that the shape of the damage function of Figure 3 is consistent with theoretical damage functions derived from the civil engineering literature, as those developed by Unanwa et al. (2000) or Vickery et al. (2006).

As noted by Emanuel (2011), this proxy of the share of economic losses is "highly idealized" in the sense that it only considers the maximum value of wind speed as an indicator of the hazards associated to tropical cyclones. We acknowledge that given the combination of low-pressure center and wind-induced sea waves, other hazards such as heavy rainfall,

landslides or storm surges are also likely to generate economic damages. However, and as observed by Jordan & Clayson (2008) or Haiyan et al. (2008), economic losses but also the magnitude of other hazards are all correlated, though not perfectly, with wind speed strength generated by cyclonic systems. A comprehensive study of the impact of the four main hazards associated to tropical cyclones, namely wind speed, heavy rainfall, landslides and storm surge on economic losses would require a specific damage function for each hazard. In contrast to wind speed, the modeling of inundation-induced or landslide-induced by tropical cyclone rainfall is more difficult. In the special case of La Réunion, we are not aware of studies that enable to establish a relationship between a given parameter of rainfall to inundations and economic losses. Finally, it should be mentioned that studies that collect post cyclone insurance data observe that the vast majority of insurance claim payments is due to wind speed rather than rainfall, landslide or storm surge (CCR, 2020). The combination of these evidence with the lack of materials in modeling economic damages related to other hazards, lead us to use wind speed as our main indicator of the magnitude of tropical cyclones.

Against this background, our damage function is used to translate wind speed into

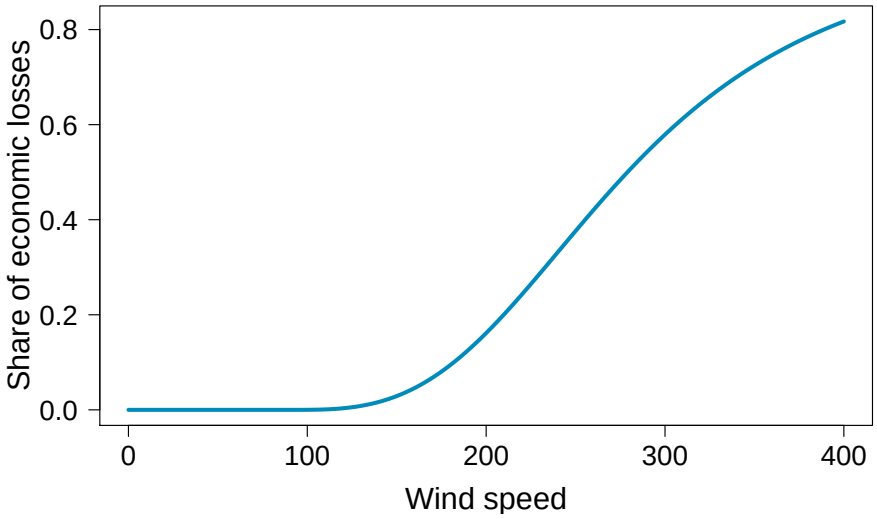

Figure 3: Index of the share of economic losses due to maximum wind speed.
Sources: Authors' own calcultations.
Notes: Wind speed is expressed in km/h.

economic damages for the "current" climate as well as the "future" one with the same spatial distribution of economic activity within La Réunion, namely the one computed from the daily night light data of 2018. Put differently, we employ the same damage function and the same distribution of economic activity for cyclonic systems generated under the contemporaneous and the future climate conditions. This implies two implicit assumptions. First, we assume

that the sensitivity of economic assets to wind speed does not change over time. This implicitly supposes that adaptation policy does not take place. Given this assumption, our estimation of the economic losses associated to tropical cyclone could be seen as an upper bound since adaptation policies are likely to reduce the costs of such meteorological events. Second, we do not forecast what would be economic activity in La Réunion in, for instance, 2100. Current knowledge points toward both a strong demographic and economic growth in La Réunion with, however, a large amount of uncertainty about the exact estimates of these variables in the future. We acknowledge that such features are likely to change the spatial distribution of economic activity within the island even if a significant part of the island's surface is protected for environmental reasons. Given this assumption, our estimation of economic losses could be seen as a lower bound since the anticipated evolution of economic growth is likely to increase the economic value located in the island.

5 Results

In this section, we present the results of our analyses in three steps. We first consider the two sets of 2,000 cyclonic systems to provide a detailed analysis of their cost and the spatial distribution of economic losses within the island. Then, we proceed to a simulation to provide annual statistics about what would be the contemporaneous and the future expected economic losses. Third, from these annual simulations, we apply a battery of robustness check. Third,

5.1 A look on simulated cost

We first compute, for each of the 4,000 synthetic cyclonic systems, and according to its generated wind field, whether it causes observable economic losses at the island level. In doing so, we combine equation ** and equation (1) together with the spatial distribution of the economic value of Figure 1. We derive total economic losses F_i at the island level for cyclonic event i, by applying the following formula:

$$F_i = \sum_{c=1}^{C} \frac{nl_c}{NL} \times f_{ci} \tag{3}$$

where, C corresponds to the total number of cells characterizing La Réunion in terms of night light, nl_c is the average brightness value of cell c in 2018 and $NL = \sum_{c=1}^{C} nl_c$ is the total "brightness" value observed in La Réunion in 2018. Table 2 reports summary statistics of total losses at the island level generated by tropical cyclones under "curent" and "future" climates.

Among the 2,000 contemporaneous cyclonic systems circulating within a circle of 150 km

radius around La Réunion, 48.88% generates no damage. The percentage of damaging tropical cyclones fall of 12.27% under the future climate scenario and 42.88% of events generates no damage. Significant economic losses, in the sense that they exceed 2% of the total economic value, appears between the 80th and the 90th percentiles of the loss's distribution for the anticipated weather of the 2070-2100 period while they appear later, between the 90th and the 95th percentiles, for weather similar to the 1984-2014 period. The proportion of damaging events exceeding 5% of the total economic value is also higher under the future climate scenario (7% against 4%, not shown in Table 2). The most severe tropical cyclones belonging to our sets of synthetic events under current climate generate a loss of 40.26% of the economic value against 67.75% under future climate. The average value of F_i under current climate conditions is of 0.76%. Under future climate conditions, the mean value of total economic losses due to tropical cyclone wind speed sharply increases, of almost 90%, and amounts to 1.43%. These simple descriptive statistics show that the destructiveness power of future tropical cyclones is higher than the one of current tropical cyclones.

	Contemporaneous	Future	Δ in %
% of TC with 0 damage	48.88	42.88	-12.27
Percentile 50%	0.00	0.00	–
Percentile 60%	0.00	0.01	–
Percentile 70%	0.03	0.10	–
Percentile 75%	0.08	0.24	–
Percentile 80%	0.19	0.55	–
Percentile 90%	1.15	2.76	–
Percentile 95%	3.76	7.66	–
Percentile 99%	17.44	31.76	–
Percentile 100%	40.26	67.75	–
Mean	0.76	1.43	89.56
Standard deviation	3.20	5.33	–
$\frac{\text{Standard deviation}}{\text{Mean}}$	4.21	3.73	–

Table 2: Summary statistics of TC losses generated by 2,000 contemporaneous and future cyclonic systems.

Sources: Black marble nightlight products of Román et al. (2018) and authors' own calculation

Notes: Damages ares expressed in percentage of the total brightness of La Réunion.

To illustrate the spatial distribution of economic losses within La Réunion, Figure 4 plots two maps each for a given climate environment. In these two maps, rather than reporting each element of the sum in equation (3), we multiply each of them by the total GDP value in 2018. Consequently, the scale of these maps can be interpreted in term of "output losses".[10]

[10]Rather than using GDP to obtain a monetary value of economic losses, a credible alternative option would be using total property values. However, such data does not exist in a consistent manner in the context

The average total losses, at the island level, associated to the two sets of tropical cyclones amounts respectively to 136 and 258 millions EUR. The spatial distribution of Figure 4 indicates that the most lit pixels are more likely to suffer from high economic damages. In particular, average economic losses per pixel higher than 100,000 euros are more frequent in Saint-Denis and around the industrial area next to the seaport. Furthermore, average economic losses per pixel are higher for synthetic cyclones simulated under the future climate scenario. Consistently, with our strategy, unlit areas as those located in the south east of the island show less economic damages.

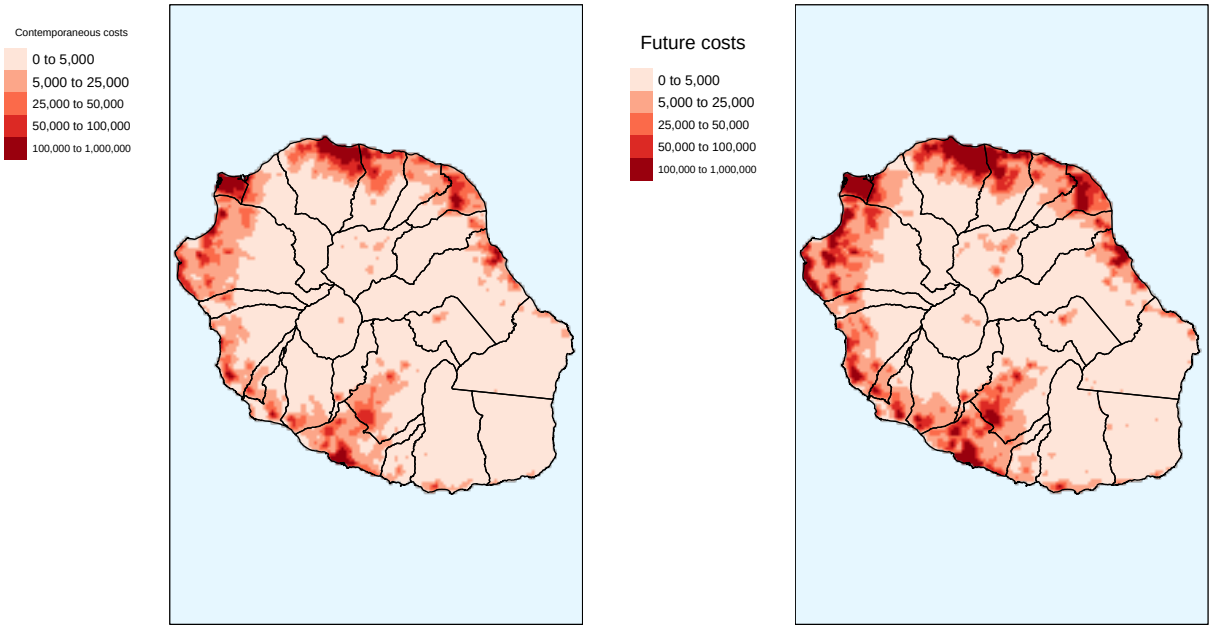

Figure 4: Contemporaneous and future average costs per pixel.
Sources: Black marble night light data (Román et al., 2018), synthetic tropical cyclones (Emanuel, 2011) and authors' own calcultations.

5.2 Annual probabilities

The analysis of subsection 5.1 though interesting as a first departure point lacks of economic interpretation since economic losses are expressed per cyclonic event without considering the

of La Réunion.

average number of cyclones per year. Consequently, to provide annual statistics about the risk associated to tropical cyclone in La Réunion, we run the following simulations. We produce a hypothetical year of tropical cyclone events by randomly sampling, according to a Poisson distribution, the number of cyclonic systems associated to a given year. In doing so, we fix the parameter of the Poisson distribution λ to 0.475 which corresponds to the average number of cyclonic systems circulating around 150 km of La Réunion per year during the 1979-2019 period (see also subsection 2.1).[11] We then randomly select among the corresponding set of cyclonic systems circulating around La Réunion, the previously chosen number of events associated to that year. For each of the selected cyclonic systems, we compute the total economic losses as in equation (3).[12] After the selection, the chosen event is replaced in the pool of selectable events. We repeat the experiment 100,000 times, letting us with potentially 100,000 years of tropical cyclone occurrence under both climate scenarios. We then consider that for each climate environment, the annual probability of drawing a hypothetical year is identical.

	Contemporaneous	Future	Δ in %
% years with 0 cost	78.50	76.30	-2.80
Percentile 80%	0.00	0.00	–
Percentile 90%	0.14	0.40	–
Percentile 95%	1.06	2.36	–
Percentile 99%	10.18	17.79	–
Percentile 100%	57.17	88.97	–
Mean	0.36	0.69	91.67
Standard deviation	2.30	3.84	–
$\frac{\text{Standard deviation}}{\text{Mean}}$	6.39	5.57	–
Return period of damage >0	5.00	4.00	–

Table 3: Summary statistics of annual cost generated 100,000 years of simulation of contemporaneous and future climates.
Sources: Black marble nightlight products of Román et al. (2018) and authors' own calculation
Notes: Damages ares expressed in percentage of the total brightness of La Réunion.

In Table 3, we report summary statistics of annual losses obtained by simulating 100,000 years of hypothetical years under current and future climate environments. Given the first row of this table, the annual probabilities of experiencing a damaging tropical cyclone is respectively of 0.215 and 0.237. These annual probabilities translate into return periods of five and four years, respectively. Put differently, under current climate (resp. future climate),

[11] In a Poisson distribution the parameter λ shapes the mean and the standard deviation of the distribution.
[12] In doing so, we assume that the losses due to tropical cyclone accumulate which could induce an upward bias to our estimates.

La Réunion should expect a damaging tropical cyclone to arise once every five years (resp. once every four years). In addition to the occurrence of a damaging tropical cyclone, the magnitude of the incurring losses is also of interest. In that respect, the bottom part of Table 3 reports the expected annual average losses. Thus, for a climate similar to what have been observed during the 1984-2014 period, the average annual losses are of 0.36%, while for an anticipated future climate this statistic is of 0.69%. Overall, the variation in expected annual losses between the two climate environment amounts to approximately 92% indicating that the risk associated with tropical cyclone wind speed would be sharply higher in a near future.

The two panels of Figure 5 complement our description of the expected annual average losses. The left panel reports in the y-axis the total annual losses while the x-axis reports the corresponding return periods. The right panel has the same y-axis but the x-axis rather corresponds to the associated probability loss. The figure of this panel so describes the probability that a given level of loss will be exceeded. When looking at the left panel of Figure 5 several comments are in order. First, the curve describing the future climate is always higher than the one describing the current climate. This is suggestive that return periods of events would be shorter under a warmer climate. Put differently, for the same amount of total cost, the associated return period is always higher for a climate environment similar to the current one. As an example, a total cost of 10% is associated with a return period of 95 years for a weather similar to the observed current one. For the anticipated climate scenario, the return period associated to such an event decreases of 46 years and amounts to 49 years.[13] Second, a closer look on the two curves suggests that for the same return period the associated total cost due to tropical cyclones is sharply higher under the future climate scenario. For instance, a 100-year return period event causes a total loss of economic value of about 10% under current climatology against 20% for the future climate. The gap in terms of total loss sharply increases before stabilizing at around 15 percentage points for return periods higher than 400 years. The second panel of Figure 5, by depicting the annual exceedance probability loss curve, reinforces the main message of our analysis. The curve representing the future climate being higher than the one representing the current one, for a given level of loss the associated probability is higher in the former case. For instance, the probability of observing economic losses higher than 10% is of 1% in a current climate environment against 2% for a warmer climate.

[13]The corresponding return period of an event generating a loss equivalent to the expected average annual loss is of 13 years under current climate and of 12 years under future climate.

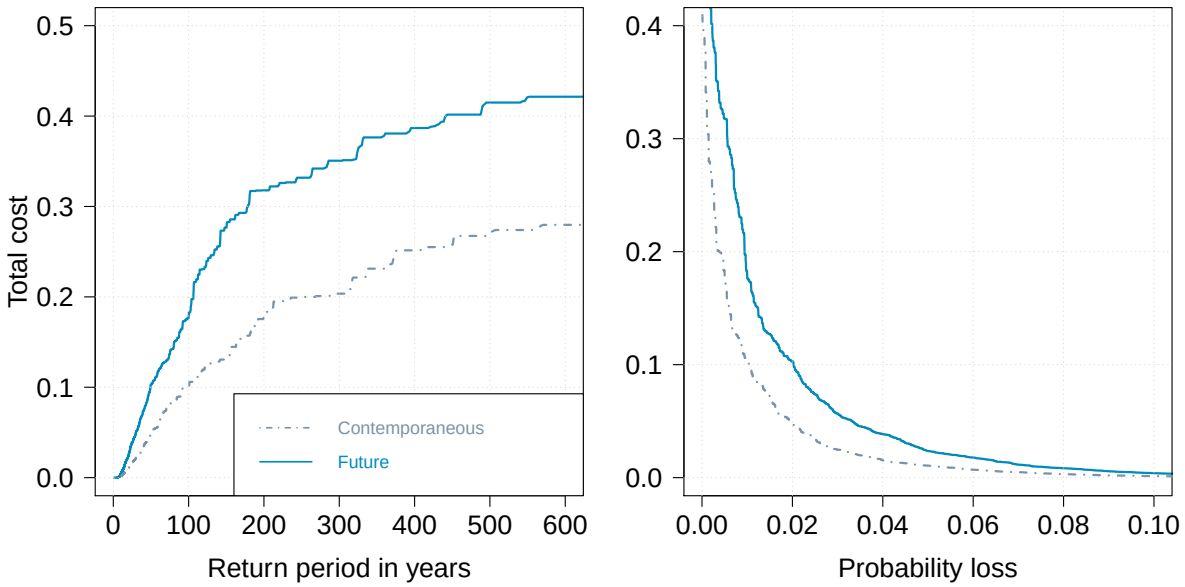

Figure 5: Return period and exceedance probability curves for current and future climate. *Sources*: Black marble night light data (Román et al., 2018), synthetic tropical cyclones (Emanuel, 2011) and authors' own calcultations.

5.3 Sensitivity analysis

Overall, our estimation of the costs due to tropical cyclones unveils that they are likely to increase in a future and warmer climate. As such a result could be sensitive to different modeling choice, we here check for its sensitivity along two dimensions. We first apply the same simulation of subsection 5.2 but we change the parameter value shaping the average number of cyclones per year in the future climate environment. Second, we modify the two parameters values of the damage function of equation (2). The following subsection details these alternative exercises and presents the associated results.

	Contemporaneous	Future	Sens. Future 1	Sens. Future 2	Sens. Future 3
% years with 0 cost	78.50	76.30	80.69	90.39	72.31
Percentile 80%	0.00	0.00	0.00	0.00	0.02
Percentile 90%	0.14	0.40	0.13	0.00	0.75
Percentile 95%	1.06	2.36	1.62	0.12	3.77
Percentile 99%	10.18	17.79	14.27	6.77	23.98
Percentile 100%	57.17	88.97	88.97	68.64	80.80
Mean	0.36	0.69	0.54	0.26	0.83
Standard deviation	2.30	3.84	3.44	2.39	4.25
$\frac{\text{Standard deviation}}{\text{Mean}}$	6.39	5.57	6.37	9.19	5.12
Return period of damage >0	5.00	4.00	5.00	10.00	3

Table 4: Summary statistics of annual cost generated 100,000 years of simulation of contemporaneous and future climates – Alternative values for λ.

Sources: Black marble nightlight products of Román et al. (2018) and authors' own calculation

Notes: Damages are expressed in percentage of the total brightness of La Réunion. In the simulation "Sens. future 1", λ is set to 0.375. In the simulation "Sens. future 2", λ is set to 0.175. In the simulation "Sens. future 3", λ is set to 0.575.

Changing λ In the simulations of the previous subsection, we choose a value of 0.475 for λ, namely the average number of cyclonic systems circulating around La Réunion per year under both climate environments. In doing so, we assume that the average occurrence of cyclones does not change with the expected global warming. Some evidence suggests that global warming is likely to alter the average number of cyclones downward while the magnitude of the most intense systems is likely to increase (IPCC, 2019; Cattiaux et al., 2020; Knutson et al., 2020).[14] In contrast, for the SWIO others evidence indicate that anthropogenic warming could modify the genesis and the path of cyclonic systems so that previously less exposed areas could be more exposed in the future (Cattiaux et al., 2020). For the special case of La Réunion, such path modifications could lead to a higher exposition in a warmer climate environement. Given those uncertainties we choose to keep the same average number of cyclones under both climate scenarios in our baseline estimates. In this sensitivity analysis, we relax this baseline assumption by considering three other scenarios for the future climate environment. In the first one, we follow conclusions drawn by Cattiaux et al. (2020) or Knutson et al. (2020) and we consider that the likelihood of having a cyclonic system close to La Réunion decreases. We take into account such a possibility be fixing $\lambda = 0.375$. The second scenario is in line with the first one, but we set λ to a lower value namely 0.175. Finally, in the third scenario, we rather follow suggestive evidence indicating that the future genesis of cyclones but also their future path imply that La Réunion would be more exposed. We consider this possibility by setting $\lambda = 0.575$. These three scenarios are respectively labeled "Sens. Future 1", "Sens. Future 2" and "Sens. Future 3" and Table 4 reports their summary statistics together with our baseline estimates while Figure 6 displays return period associated to each scenario.

As expected, in the first two scenarios the share of years experiencing no damage increases while it decreases when the average number of cyclones close to La Réunion is higher. The return periods of positive damages due to tropical cyclones is modified accordingly and amount to respectively five, ten and three years. In what concerns the expected annual costs of tropical cyclones, we witness that in scenario "Sens. Future 1" it is still higher, of about 50%, than what have been observed for a weather similar to the current period. The third scenario, the one anticipating the worse outcome in terms of exposure for La Réunion, is characterized by an increase in the expected average annual cost in comparison to the contemporaneous scenario as well as the future baseline scenario. More specifically, the expected annual cost of 0.83% corresponds to an increase of 130% (resp. 20%) in comparison to the baseline contemporaneous (resp. future) scenario. Overall, return period curves of Figure 6 are

[14] For the SWIO, Cattiaux et al. (2020) find that in a warmer climate environment, of about 2-k, the frequency of tropical cyclones should decrease of about 20% while their maximum lifetime intensity should increase. Moreover, they also find a poleward shift of tropical cyclone trajectory together with an increase of about one month of the cyclone season onset.

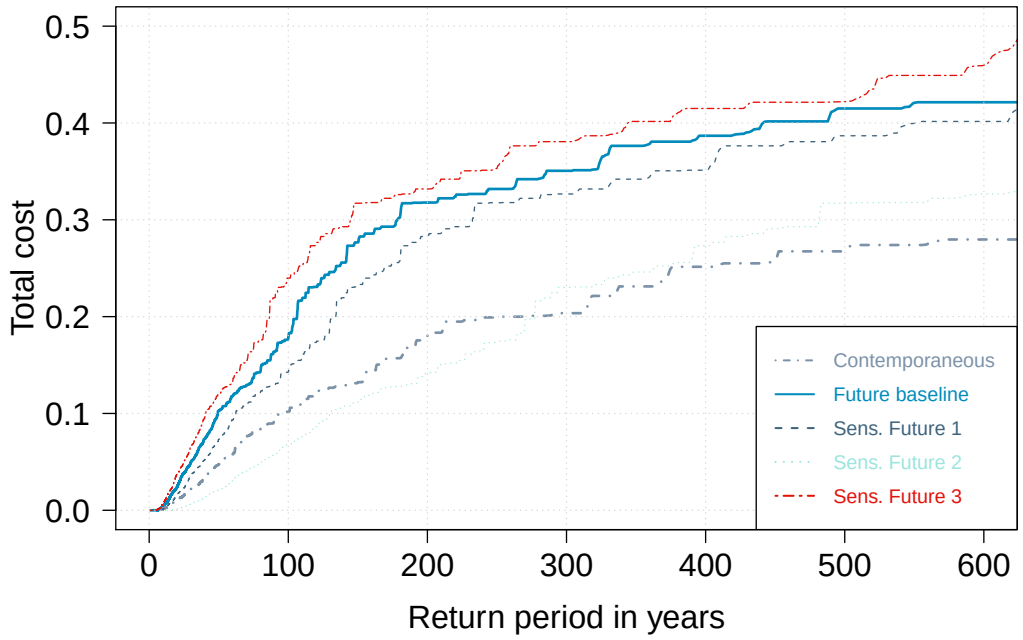

Figure 6: Return period for different calibration of the average number of cyclonic systems per year.
Sources: Black marble night light data (Román et al., 2018), synthetic tropical cyclones (Emanuel, 2011) and authors' own calcultations.
Notes: In the scenario labeled "Rob Furture 1" the parameter λ is set to 0.375. In the scenario labeled "Rob Furture 2" the parameter λ is set to 0.175.

consistent with these results. It further shows that total economic costs associated to a return period of 100 years are highest for the scenario "Sens. Future 3" and lowest for scenario "Sens. Future 2" our baseline scenario lying at the middle of these estimates. However, for return period of about 300 years, even the scenario "Sens. Future 2" is associated with higher total cost than our baseline contemporaneous scenario. This suggests that the possibility, though weak, of having extreme events is likely to be higher than what we could observe under current climate scenario. Finally, total costs of 10% of the economic value have a return period of 62, 131, and 41 years in scenarios "Sens. Future 1", "Sens. Future 2" and "Sens. Future 3", respectively. In the future baseline climate environment the corresponding return period amounts to 30 years.

To conclude, this sensitivity study shows that our baseline assumption about what future exposure of La Réunion would be does not overestimate the expected future costs. However, this analysis suggests that having an average cost lower than what we find for the current climate relies on an "irrealistic" scenario based on a very low average occurrence of cyclonic systems circulating close to La Réunion in a near future.

Changing $\bar{W}$ and $\bar{W}^*$ In the baseline estimate, we translate wind exposure at the cell level to damages by using the damage function f_{ci} of equation (1) and (2). This damage function implies a non-linear relationship between wind speed and economic damages. In this damage function, two parameters, namely $\bar{W}$ and W^*, are keys as they shape the damage function curve. In the baseline estimate, $\bar{W}$ is set to 93 km/h while W^* to 270 km/h. We here reconsider this choice by changing parameters one-by-one while keeping the second one to the baseline choice. Consequently, we re-run the baseline scenario four time by respectively fixing $\bar{W} = 130$ km/h, $\bar{W} = 50$ km/h, $W^* = 320$ km/h and $W^* = 240$ km/h. To save some space, we report summary statistics similar to those of Table 3 for each scenario in Tables 5 to 8 of Appendix A.

Overall, changes in parameters have the expected effect on the amount of economic losses. In particular, changing $\bar{W}$ has an incidence on the proportion of years experiencing no damages. Under current climate condition, when $\bar{W} = 130$, the share of years with no damage is of 91 against 78.50 in the baseline estimate. Accordingly, this share decreases when $\bar{W}$ is set to a low value (see Table 6). In contrast to $\bar{W}$, changing W^* has nearly no incidence on the proportion of years with no damage so that the return periods of having a year with losses due to cyclone are the same as the baseline scenario. However, changing W^*, namely the threshold for which half of the economic value is lost, impacts the magnitude of economic damages. As in Table 8, expected economic losses are the highest when W^* is low. In this scenario, for climate condition similar to what has been observed during the 1984-2014 period the expected economic losses is of 0.65% against 0.36% in our baseline estimates. Finally, another interesting feature of these four scenario relies on the fact that future economic losses increase respectively of 78.00%, 51.16%, 95.45% and 76.92%. Again, our baseline estimation of the variation of the economic losses falls inside the range obtained with the sensitivity study.

6 Conclusion

Using wind fields generated by synthetic tropical cyclones under a current as well as a future and warmer climate environment, we propose an estimation of the economic losses associated to tropical cyclones in La Réunion. We find that, comparatively to the expected current losses, future economic losses due to cyclonic systems are likely to increase, of about 90%, even if the spatial extent and the amount of economic activity are assumed unchanged. Sensitivity analyses applied to check for the robustness of our baseline estimation show that we do not overestimate nor underestimate the magnitude of the economic losses associated to tropical cyclones. Consequently, our paper suggests that policy designers should probably engage in

adaptation policies to reduce the disastrous nature of these meteorological events.

Our paper should be seen as a first step in the understanding the economic damages associated to tropical cyclones in La Réunion. In addition to the monetary losses, tropical cyclones are also associated with many non-tangible damages such as losses linked to the degradation of environmental goods or the loss of human life. Furthermore, our strategy only allows us to investigate the amount of direct losses without considering the potential indirect losses which could induce an interruption of economic activity. Such an issue, which could be analyzed through the lens of a computable general equilibrium model, are on our agenda for a future research but lies beyond the scope of the present paper.

References

Bertinelli, L., Mohan, P., & Strobl, E. (2016). Hurricane damage risk assessment in the caribbean: An analysis using synthetic hurricane events and nightlight imagery. *Ecological Economics*, 124, 135–144.

Bertinelli, L. & Strobl, E. (2013). Quantifying the local economic growth impact of hurricane strikes: An analysis from outer space for the caribbean. *Journal of Applied Meteorology and Climatology*, 52(8), 1688–1697.

Bobrowsky, P. T., Ed. (2013). *Encyclopedia of Natural Hazards*. Encyclopedia of Earth Sciences Series. Springer Netherlands.

Botzen, W. J. W., Deschenes, O., & Sanders, M. (2019). The economic impacts of natural disasters: A review of models and empirical studies. *Review of Environmental Economics and Policy*, 13(2), 167–188.

Camargo, S. J. & Hsiang, S. M. (2015). Tropical cyclones: From the influence of climateto their socioeconomic impacts. In M. Chavez, M. Ghil, & J. Urrutia-Fucugauchi (Eds.), *Extreme Events: Observations, Modeling, and Economics* chapter 18. Wiley.

Cattiaux, J., Chauvin, F., Bousquet, O., Malardel, S., & Tsai, C.-L. (2020). Projected changes in the southern indian ocean cyclone activity assessed from high-resolution experiments and cmip5 models. *Journal of Climate*, 33(12).

Cavallo, E., Powell, A., & Becerra, O. (2010). Estimating the direct economic damages of the earthquake in haiti*. *The Economic Journal*, 120(546), F298–F312.

CCR (2020). *Evolution du risque cyclonique en Outre-mer à horizon 2050*. Technical report, Caisse Centrale de Réassurance.

CEROM (2004). *"Une double transition presque réussie"*. Etudes cerom, CEROM.

Chen, X. & Nordhaus, W. (2015). A test of the new viirs lights data set: Population and economic output in africa. *Remote Sensing*, 7(4), 4937–4947.

Chen, X. & Nordhaus, W. D. (2011). Using luminosity data as a proxy for economic statistics. *Proceedings of the National Academy of Sciences*, 108(21), 8589–8594.

Craig, A., Valcke, S., & Coquart, L. (2017). Development and performance of a new version of the oasis coupler, oasis3-mct_3. 0. *Geoscientific Model Development*, 10(9), 3297–3308.

Croissant, Y., Garabedian, S., Issop, Z. M., & Hermet, F. (2019). Fragmentation mondiale de la production et différenciation de la demande dans un megc : proposition méthodologique. *Revue Economique*, 2019/7, 295–320.

Dee, D. P., Uppala, S. M., Simmons, A., Berrisford, P., Poli, P., Kobayashi, S., Andrae, U., Balmaseda, M., Balsamo, G., Bauer, d. P., et al. (2011). The era-interim reanalysis: Configuration and performance of the data assimilation system. *Quarterly Journal of the royal meteorological society*, 137(656), 553–597.

Elliott, R. J., Strobl, E., & Sun, P. (2015). The local impact of typhoons on economic activity in china: A view from outer space. *Journal of Urban Economics*, 88, 50 – 66.

Emanuel, K. (2005). Increasing destructiveness of tropical cyclones over the past 30 years. *Nature*, (436), 686–688.

Emanuel, K. (2006). Climate and tropical cyclone activity: A new model downscaling approach. *Journal of Climate*, 19(19), 4797 – 4802.

Emanuel, K. (2011). Global warming effects on u.s. hurricane damage. *Weather, Climate, and Society*, 3(4), 261–268.

Emanuel, K., DesAutels, C., Holloway, C., & Korty, R. (2004). Environmental control of tropical cyclone intensity. *Journal of the atmospheric sciences*, 61(7), 843–858.

Emanuel, K., Ravela, S., Vivant, E., & Risi, C. (2006). A statistical deterministic approach to hurricane risk assessment. *Bulletin of the American Meteorological Society*, 87(3), 299–314.

Emanuel, K. & Rotunno, R. (2011). Self-stratification of tropical cyclone outflow. part i: Implications for storm structure. *Journal of the Atmospheric Sciences*, 68(10), 2236–2249.

Emanuel, K., Sundararajan, R., & Williams, J. (2008). Hurricanes and global warming: Results from downscaling ipcc ar4 simulations. *Bulletin of the American Meteorological Society*, 89(3), 347–368.

Eyring, V., Bony, S., Meehl, G. A., Senior, C. A., Stevens, B., Stouffer, R. J., & Taylor, K. E. (2016). Overview of the coupled model intercomparison project phase 6 (cmip6) experimental design and organization. *Geoscientific Model Development*, 9(5), 1937–1958.

Gibson, J. (2021). Better night lights data, for longer*. *Oxford Bulletin of Economics and Statistics*.

Gibson, J., Olivia, S., & Boe-Gibson, G. (2020). Night lights in economics: Sources and uses1. *Journal of Economic Surveys*, 34(5), 955–980.

Goujon, M. & Hoarau, J.-F. (2015). "une nouvelle mesure du développement des économies ultramarines françaises à travers l'application de l'indicateur de développement humain "hybride" ". *Région et Développement*, (42-2015), 55–78.

Grinsted, A., Ditlevsen, P., & Christensen, J. H. (2019). Normalized us hurricane damage estimates using area of total destruction, 1900-2018. *Proceedings of the National Academy of Sciences*, 116(48), 23942–23946.

Haiyan, J., Halverson, J., Simpson, J., & Zipser, E. (2008). Hurricane rainfall potential derived from satellite observations aids overland rainfall prediction). *Journal of Applied Meteorology and Climatology*, 47, 944–959.

Hallegatte, S. (2007). The use of synthetic hurricane tracks in risk analysis and climate change damage assessment. *Journal of Applied Meteorology and Climatology*, 46(11), 1956 – 1966.

Heger, M. P. & Neumayer, E. (2019). The impact of the indian ocean tsunami on aceh's long-term economic growth. *Journal of Development Economics*, 141, 102365.

Henderson, J. V., Storeygard, A., & Weil, D. N. (2012). Measuring economic growth from outer space. *American Economic Review*, 102(2), 994–1028.

Hoarau, J.-F. (2019). *La vie chère en Outre-mer en phénomène structurel*. La lettre du CEMOI 20, Centre d'Economie et de Management de l'Océan Indien.

Holland, G. J. (1983). Tropical cyclone motion: Environmental interaction plus a beta effect. *Journal of the Atmospheric Sciences*, 40(2), 328–342.

INSEE (2019). *Bilan économique 2018, la croissance décroche*. INSEE Conjoncture 8, Institut National de la Statistique et des Etudes Economiques.

IPCC (2019). Special report on the ocean and cryosphere in a changing climate. In N. Weyer (Ed.), *In it together: why less inequality benefits all*: In press.

Jordan & Clayson (2008). A new approach to using wind speed for prediction of tropical cyclone generated storm surge). *Geophysical Letters*, 35.

Jury, M. R., Pathack, B., Wang, B., Powell, M., & Raholijao, N. (1993). A destructive tropical cyclone season in the sw indian ocean: January-february 1984. *South African Geographical Journal*, 75(2), 53–59.

Knutson, T., Camargo, S. J., Chan, J. C. L., Emanuel, K., Ho, C.-H., Kossin, J., Mohapatra, M., Satoh, M., Sugi, M., Walsh, K., & Wu, L. (2020). Tropical cyclones and climate change assessment: Part ii: Projected response to anthropogenic warming. *Bulletin of the American Meteorological Society*, 101(3), E303–E322.

Knutson, T., McBride, J., Chan, J., Emanuel, K., Holland, G., Landsea, C., Held, I., Kossin, J., Srivastava, A. K., & Obersteiner, M. (2010). Tropical cyclones and climate change. *Nature Geoscience*, (3), 157–163.

Kocornik-Mina, A., McDermott, T. K. J., Michaels, G., & Rauch, F. (2020). Flooded cities. *American Economic Journal: Applied Economics*, 12(2), 35–66.

Kousky, C. (2014). Informing climate adaptation: A review of the economic costs of natural disasters. *Energy Economics*, 46, 576–592.

Leroux, M.-D., Meister, J., Mekies, D., & Dorla, A.-L. (2018). A climatolofy of southwest indian ocean tropical systems: Their number, tracks, impacts, sizes empirical maximum potential intensity, and intensity changes. *Journal of Applied Meteorology and Climatology*, 57, 1021–1041.

Li, X., Xu, H., Chen, X., & Li, C. (2013). Potential of npp-viirs nighttime light imagery for modeling the regional economy of china. *Remote Sensing*, 5(6), 3057–3081.

Madec, G., Bourdallé-Badie, R., Bouttier, P.-A., Bricaud, C., Bruciaferri, D., Calvert, D., Chanut, J., Clementi, E., Coward, A., Delrosso, D., et al. (2017). Nemo ocean engine.

Mayer Jouanjean, I. (2011). *L'île de La Réunion sous l'œil du cyclone au XXème siècle. Histoire, Société, et catastrophe Naturelle.* Theses, Université de la Réunion.

Mohan, P. S., Ouattara, B., & Strobl, E. (2018). Decomposing the macroeconomic effects of natural disasters: A national income accounting perspective. *Ecological Economics*, 146, 1–9.

Nguyen, C. N. & Noy, I. (2019). Measuring the impact of insurance on urban earthquake recovery using nightlights. *Journal of Economic Geography*, 20(3), 857–877.

O'Neill, B. C., Tebaldi, C., Vuuren, D. P. v., Eyring, V., Friedlingstein, P., Hurtt, G., Knutti, R., Kriegler, E., Lamarque, J.-F., Lowe, J., et al. (2016). The scenario model intercomparison project (scenariomip) for cmip6. *Geoscientific Model Development*, 9(9), 3461–3482.

Parain, C. & Rivière, F. (2013). *"Approche comparée des évolutions économiques des Outre-mer français sur la période 1998-2010"*. Document de travail 131, Agence Française du Développement.

Pinkovskiy, M. & Sala-i Martin, X. (2016). Lights, Camera ... Income! Illuminating the National Accounts-Household Surveys Debate *. *The Quarterly Journal of Economics*, 131(2), 579–631.

Roehrig, R., Beau, I., Saint-Martin, D., Alias, A., Decharme, B., Guérémy, J.-F., Voldoire, A., Abdel-Lathif, A. Y., Bazile, E., Belamari, S., et al. (2020). The cnrm global atmosphere model arpege-climat 6.3: Description and evaluation. *Journal of Advances in Modeling Earth Systems*, 12(7), e2020MS002075.

Román, M. O., Wang, Z., Sun, Q., Kalb, V., Miller, S. D., Molthan, A., Schultz, L., Bell, J., Stokes, E. C., Pandey, B., Seto, K. C., Hall, D., Oda, T., Wolfe, R. E., Lin, G., Golpayegani, N., Devadiga, S., Davidson, C., Sarkar, S., Praderas, C., Schmaltz, J., Boller, R., Stevens, J., Ramos González, O. M., Padilla, E., Alonso, J., Detrés, Y., Armstrong, R., Miranda, I., Conte, Y., Marrero, N., MacManus, K., Esch, T., & Masuoka, E. J. (2018). Nasa's black marble nighttime lights product suite. *Remote Sensing of Environment*, 210, 113–143.

Sealy, K. S. & Strobl, E. (2017). A hurricane loss risk assessment of coastal properties in the caribbean: Evidence from the bahamas. *Ocean & Coastal Management*, 149, 42–51.

Strobl, E. (2011). The economic growth impact of hurricanes: Evidence from u.s. coastal counties. *The Review of Economics and Statistics*, 93(2), 575–589.

Strobl, E. (2012). The economic growth impact of natural disasters in developing countries: Evidence from hurricane strikes in the central american and caribbean regions. *Journal of Development Economics*, 97(1), 130 – 141.

Sutton, P. C. & Costanza, R. (2002). Global estimates of market and non-market values derived from nighttime satellite imagery, land cover, and ecosystem service valuation. *Ecological Economics*, 41(3), 509–527.

Thompson, C., Barthe, C., Bielli, S., Tulet, P., & Pianezze, J. (2021). Projected characteristic changes of a typical tropical cyclone under climate change in the south west indian ocean. *Atmosphere*, 12(2).

Tulet, P., Aunay, B., Barruol, G., Barthe, C., Belon, R., Bielli, S., Bonnardot, F., Bousquet, O., Cammas, J.-P., Cattiaux, J., Chauvin, F., Fontaine, I., Fontaine, F. R., Gabarrot,

F., Garabedian, S., Gonzalez, A., Join, J.-L., Jouvenot, F., Nortes-Martinez, D., Mékiès, D., Mouquet, P., Payen, G., Pennober, G., Pianezze, J., Rault, C., Revillion, C., Rindraharisaona, E. J., Samyn, K., Thompson, C., & Vérèmes, H. (2021). Renovrisk: a multidisciplinary programme to study the cyclonic risks in the south-west indian ocean. *Natural Hazards*.

Unanwa, C., McDonald, J., Mehta, K., & Smith, D. (2000). The development of wind damage bands for buildings. *Journal of Wind Engineering and Industrial Aerodynamics*, 84(1), 119–149.

Vickery, P. J., Skerlj, P. F., Lin, J., Twisdale, L. A., Young, M. A., & Lavelle, F. M. (2006). Hazus-mh hurricane model methodology. ii: Damage and loss estimation. *Natural Hazards Review*, 7(2), 94–103.

Voldoire, A., Decharme, B., Pianezze, J., Lebeaupin Brossier, C., Sevault, F., Seyfried, L., Garnier, V., Bielli, S., Valcke, S., Alias, A., et al. (2017). Surfex v8. 0 interface with oasis3-mct to couple atmosphere with hydrology, ocean, waves and sea-ice models, from coastal to global scales. *Geoscientific Model Development*, 10(11), 4207–4227.

Voldoire, A., Saint-Martin, D., Sénési, S., Decharme, B., Alias, A., Chevallier, M., Colin, J., Guérémy, J.-F., Michou, M., Moine, M.-P., et al. (2019). Evaluation of cmip6 deck experiments with cnrm-cm6-1. *Journal of Advances in Modeling Earth Systems*, 11(7), 2177–2213.

Weinkle, J., Maue, R., & Pielke, R. (2012). Historical global tropical cyclone landfalls. *Journal of Climate*, 25(13), 4729 – 4735.

Appendices

A Changing parameters of the damage function

	Contemporaneous	Future	Δ in %
% years with 0 cost	91.52	88.84	-2.80
75%	0.00	0.00	–
80%	0.00	0.00	–
90%	0.00	0.00	–
95%	0.02	0.27	–
99%	4.94	13.07	–
100%	48.36	86.08	–
Mean	0.18	0.42	133.33
Standard deviation	1.71	3.30	–
$\frac{\text{Standard deviation}}{\text{Mean}}$	9.50	7.86	–
Return period of damage >0	5.00	4.00	–

Table 5: Robustness - Summary statistics of annual cost generated 100,000 years of simulation of contemporaneous and future climates – $\bar{W} = 130$.

Sources: Black marble nightlight products of Román et al. (2018) and authors' own calculation

Notes: Damages are expressed in percentage of the total brightness of La Réunion.

	Contemporaneous	Future	Δ in %
% years with 0 cost	64.49	63.65	-1.30
60%	0.00	0.00	–
70%	0.02	0.04	–
75%	0.12	0.21	–
80%	0.38	0.64	–
90%	1.95	2.91	–
95%	4.68	7.14	–
99%	16.51	24.26	–
100%	64.96	91.19	–
Mean	0.86	1.30	51.16
Standard deviation	3.20	4.71	–
$\frac{\text{Standard deviation}}{\text{Mean}}$	3.72	3.62	–
Return period of damage >0	5.00	4.00	–

Table 6: Robustness - Summary statistics of annual cost generated 100,000 years of simulation of contemporaneous and future climates – $\bar{W} = 50$.

Sources: Black marble nightlight products of Román et al. (2018) and authors' own calculation

Notes: Damages are expressed in percentage of the total brightness of La Réunion.

	Contemporaneous	Future	Δ in %
% years with 0 cost	78.46	76.25	-2.82
75%	0.00	0.00	–
80%	0.00	0.00	–
90%	0.08	0.22	–
95%	0.60	1.35	–
99%	6.25	11.38	–
100%	37.57	63.08	–
Mean	0.22	0.43	95.45
Standard deviation	1.46	2.60	–
$\frac{\text{Standard deviation}}{\text{Mean}}$	6.64	6.05	–
Return period of damage >0	5.00	4.00	–

Table 7: Robustness - Summary statistics of annual cost generated 100,000 years of simulation of contemporaneous and future climates – $W^* = 320$.

Sources: Black marble nightlight products of Román et al. (2018) and authors' own calculation

Notes: Damages are expressed in percentage of the total brightness of La Réunion.

	Contemporaneous	Future	Δ in %
% years with 0 cost	78.46	76.25	-2.82
75%	0.00	0.00	–
80%	0.00	0.00	–
90%	0.29	0.82	–
95%	2.14	4.69	–
99%	18.58	30.35	–
100%	88.47	122.42	–
Mean	0.65	1.15	76.92
Standard deviation	3.78	5.83	–
$\frac{\text{Standard deviation}}{\text{Mean}}$	5.82	5.07	–
Return period of damage >0	5.00	4.00	–

Table 8: Robustness - Summary statistics of annual cost generated 100,000 years of simulation of contemporaneous and future climates – $W^* = 240$.

Sources: Black marble nightlight products of Román et al. (2018) and authors' own calculation

Notes: Damages are expressed in percentage of the total brightness of La Réunion.

Chapitre 11

Tropical Cyclones and Fertility : New Evidence from developing countries

Fontaine, Garabedian, Vérèmes

- ***Ecological Economics***, en révision, 2023
- ***Présentation :***
  Slice meeting, potsdam, Août, 2020
  Colloque AFSE, 69^{e}, Lille (visio), juin 2021
  Colloque JMA, 37^{e}, Annecy, juin 2021

Tropical Cyclones and Fertility: New Evidence from developing countries *

Idriss Fontaine†
Université de La Réunion

Sabine Garabedian‡
Université de La Réunion

Hélène Vérèmes§
Université de La Réunion

May 2023

*Financial supports from the the European Fund for Economic and Regional Development (FEDER-INTERREG), the *Region Réunion* and the *Observatoire des Sociétés de l'Océan Indien* (OSOI) are gratefully acknowledged. We would like to thanks Alexis Parmentier for his helpful comments.

†Department of Economics (CEMOI), Université de La Réunion EA13, France; E-mail: idriss-fontaine@univ-reunion.fr

‡Department of Economics (CEMOI), Université de La Réunion EA13, France; E-mail: sabine.garabedian@univ-reunion.fr

§Department of Atmospheric Physics (LACy), Université de La Réunion UMR 8105, CNRS, Météo-France, France; E-mail: helene.veremes@univ-reunion.fr

Abstract

Does exposure to tropical cyclones affect fertility? This paper tackles this question by constructing a panel dataset from geolocated microdata about mothers' fertility history along with wind field data generated by tropical cyclones hitting a sample of six developing during the 1985-2015 period. Using panel, we estimate the causal effect of tropical cyclone shocks on women's likelihood of giving birth. We find evidence that the effect of tropical cyclone exposure on motherhood is significantly negative. In particular, being exposed to a wind speed cyclone shock decreases the probability of giving birth by 2.6 points a year after exposure. We also find that the magnitude of the effect varies with the degree of cyclonic exposure associated to mother's living environment and to the number of children ever born. Alternative specifications of our baseline model provide further insights, as we find: i) a persistent effect of tropical cyclone shocks in the sense that we do not have evidence of any reversal effect, ii) that recent past exposures to cyclones is associated with a lower decrease in fertility when exposed and iii) no evidence of non-linearities in the effect. The estimated effect is shown to be robust when using alternative formulations of our baseline empirical model.
Keywords: Fertility, Tropical cyclone, Developing countries
JEL classifications: J13, O12, Q54, C23

1 Introduction

Evidence about the consequences of exposure to cyclonic systems at the individual level is still scarce (Anttila-Hughes & Hsiang, 2013). The lack of comprehensive microstudies, which could be explained by strong data requirements, leaves many questions unanswered, in particular how households reorganize their lives after being impacted by tropical cyclones. Exposure to tropical cyclones along with the associated destruction has the potential to induce high costs to households in terms of incomes, livelihoods, crop yields, assets, and loss of life. Arguably, it is likely that the micro-impacts of such adverse shocks are stronger in countries with almost inexistent institutional ways of coping, as is probably the case for developing countries (Dessy et al., 2019). In this context, households have the incentive to diversify their activities, and children often play a particular role within households (Banerjee & Duflo (2007), Banerjee & Duflo (2011)). They actively contribute to daily activities by, for example, caring for siblings or grandparents, participating in housework chores, and even sometimes directly participating in the labor market (Finlay, 2009).[1] In light of this, parents' decision to have children is probably altered after being affected by a tropical cyclone (Sellers & Gray, 2019). As a first piece of evidence, the data used in this paper show that 12% of women who have been exposed to cyclonic systems give birth the calendar year after the exposure compared to 19% for those who have not been exposed. Our paper therefore addresses the main following question: Does exposure to tropical cyclones causally impact fertility?

Understanding how households adjust after being exposed to adverse weather shocks such as tropical cyclones is of interest to researchers and policymakers alike, especially in the context of climate change that is expected to modify the frequency and intensity of tropical cyclones in the near future (IPCC (2019), Knutson et al. (2020)). However, the direction of these behavioral changes in terms of fecundity is *a priori* unclear from both a theoretical and empirical perspective. In theoretical models such as those of Finlay (2009), Pörtner (2014), and Dessy et al. (2019), the direction of the post-disaster decision ultimately depends on assumptions about the benefits and costs associated with children. Empirically, an increase in family size after a natural disaster was found by Nobles et al. (2015), Nandi et al. (2018), and Finlay (2009), whereas a fall was identified by Evans et al. (2010), Pörtner (2014), Davis (2017) and Norling (2022). Given the inconclusive nature of the previous studies, the issue of whether natural disasters affect fertility is still an open empirical question. The main goal of the paper is to rigorously establish the direction and magnitude of the causal effect of tropical cyclones on women's likelihood of giving birth when using high-resolution data on the true exposure to tropical cyclones experienced on the ground.

[1] Banerjee & Duflo (2011) and Finlay (2009) indicate that in the absence of insurance mechanisms, children's contributions may substitute for standard insurance and allow households to smooth consumption over time.

While previous studies exploring the effect of natural disasters on fertility mainly focus on earthquakes, it is likely that their results cannot be extrapolated to the case of cyclonic events. First, the macro-literature has shown that the consequences of natural disasters on economic growth are not identical for all kinds of disasters (Fomby et al. (2013), Felbermayr & Gröschl (2014)). We can therefore conjecture that the magnitude or even the direction of the effect may also be different for fertility depending on the type of natural disaster (Norling, 2022). Second, empirical studies on earthquakes mainly adopt a "one-event" approach by studying the fertility response after an earthquake shock of high intensity (Finlay (2009), Nobles et al. (2015), Nandi et al. (2018)). Although the measurement of a causal effect in these studies is undisputed, they do not consider variability in the degree of exposure, the magnitude of the disaster events or the existence of possible intensification effects. The database constructed here allows for the investigation of such issues.

We first begin by presenting a simple theoretical framework of parents decisions about fertility. The model developed, inspired by the works of Ranjan (1999), Finlay (2009) and Norling (2022), is employed to frame the discussion and the development of empirical model. In particular, three working assumptions about post-cyclone fertility responses are derived from the model. The first one suggests that after an adverse shock, such as an exposure to cyclones, the likelihood of fertility is expected to fall. The second one investigates the heterogeneous response of fertility for mothers living in cyclone prone areas and those living in non-prone area. In that respect, the model suggests that the former group should be less sensitive to cyclone shock. Finally, the third working assumption is about the response of fertility after an exposure to cyclones with respect to the number of children ever born. More specifically, the model suggests that post-cyclone response in terms of fertility is independent from the number of children ever born.

We draw on two main databases to provide empirical evidence for our research questions. We first exploit 14 waves of the Demographic and Health Survey (DHS) of six countries, namely Bangladesh, Cambodia, Dominican Republic, Haiti, Madagascar and the Philippines.[2] This cross-sectional household survey has several practical advantages for the issue at hand: it is nationally representative, has a large number of observations, and provides information about individuals' characteristics. In addition, the DHS includes the full fertility history of each woman interviewed together with detailed information about their geographic location. The second database used here is the Tropical Cyclone Exposure Database (TCE-DAT) of Geiger et al. (2018). This worldwide database provides high-resolution information about the wind field profile of more than 2,700 cyclonic systems, including 484 that made landfall on the six developing countries during the 1985-2015 period examined in this paper. By merging

[2]The choose of this DHS wave and the one of countries studied in this paper is guided by data requirements.

the geographic information of these two databases along with the fertility history of the DHS, we construct a panel data model in which we retrieve the tropical cyclone exposure of a given mother in a given year for the entire study period. The relationship between changes in tropical cyclone wind speed exposure and the female likelihood of giving birth is then examined by means of fixed effect regressions. In doing so, our panel reduced-form model has numerous advantages, since only a minimal set of assumptions is imposed.[3]

Our main empirical results can be summarized as follows. First, we can affirmatively respond to the abstract's question and to our first working assumption: exposure to tropical cyclone wind speed does indeed impact fertility. Our panel setup indicates that the direction of the effect is negative. The point estimate suggests that a tropical cyclone shock of a standard deviation magnitude, leads to a fall of 2.6 points in the probability of giving birth a year after exposure. Second, our baseline estimates then show that the causal effect of wind speed exposure depends on the degree of cyclonic exposure associated to the mother's living environment. In cyclone prone areas, the likelihood of giving birth decrease less. Third, the magnitude of the fall in fertility also depends on the number of children ever born since mothers with at least two children are much more likely to reduce their fertility after a cyclone than mother with no child. In a last step, we take advantage of the continuous nature of the wind speed variable together with the possibility of estimating models with more lags to refine the nature of the relationship between cyclonic exposure and fertility. In particular, we find i) a persistent effect of tropical cyclone shocks in the sense that we do not have evidence of any reversal effect, ii) that recent past exposure to cyclones is associated with a lower decrease in fertility when exposed and iii) no evidence of non-linearities in the causal effect. Overall, our results are estimated to be robust to other measures of tropical cyclone exposure and to several changes concerning sample restriction and/or the empirical specification.

Our paper is related to at least three strands of the economic literature. First, by merging spatially geolocated micro-data with weather variables, our paper is part of a new but flourishing body of literature that studies the effect of weather shocks on socioeconomic variables (e.g., Deschênes & Greenstone (2011), Kudamatsu et al. (2012), Anttila-Hughes & Hsiang (2013), Barreca et al. (2018), Dessy et al. (2019), Sellers & Gray (2019), Marchetta et al. (2019), Norling (2022). We contribute to this research by focusing on the effect of a specific weather variable, namely tropical cyclones, on fertility. Second, our paper contributes to the literature examining how households respond after an adverse event (e.g., Morduch (1995), Banerjee & Duflo (2007), Alam & Pörtner (2018)). Indeed, in developing countries, having

[3]First, the panel allows us to alleviate problems relating to omitted variables by fully controlling the individual and time fixed effects. Second, insofar as tropical cyclone exposure can be viewed as (quasi-)random, exploiting year-to-year variations in wind speeds experienced by inhabitants on the ground enables us to identify their causal effects.

children enables households to smooth their consumption over time. Thus, studying how households react to a cyclonic event that induces the loss of property, crops, and livelihoods allows us to contribute to the debate on how they respond to a cyclone shock. We add to this body of literature by providing evidence for six developing countries regularly threatened to tropical cyclones. Finally, our paper makes an important contribution to the literature on the effect of natural disasters on fertility. To the best of our knowledge, four comparable papers to our own focus on cyclonic events.[4] First, Evans et al. (2010) investigate how the fertility rate in US counties responds to storm advisories. They found that low-severity advisories are associated with a positive fertility effect, while high-severity advisories are associated with a negative effect. Second, Pörtner (2014) examines the effect of hurricane risks and shocks in Guatemala. He exploits cross-sectional data along with historical data about hurricane occurrences and finds a negative association between fertility and tropical cyclone exposure at the municipal level. Third, Davis (2017) exploits rainfall data as a measure of tropical cyclone exposure and observes that high levels of rainfall in Nicaraguan municipalities are associated with an increase in fertility. Fourth, Norling (2022) investigates how fertility responds to disasters in Africa and find that fertility is negatively associated to disasters. Our paper overcomes many of the problems associated with these four papers, since our panel setup alleviates concerns related to the unobserved heterogeneity of mothers. We rely on a measure of tropical cyclone exposure that is directly related to its physical intensity and destructiveness.[5] Furthermore, we investigate heterogeneity dimension with respect to the degree of cyclonic exposure of mother's living environment and the number of children ever born.

The roadmap of this paper is as follows. Section 2 presents some theoretical elements about fertility and natural disasters. Section 3 details the data used in the empirical analysis. Section 4 develops our econometric framework and discusses identification assumptions. Section 5 presents the results. Finally, section 6 provides the conclusions.

[4]Other papers focusing on the post-fertility effect of earthquakes are discussed in subsection 4.1.

[5]More specifically, Pörtner (2014) employs historical records ,Evans et al. (2010) use advisory data and Norling (2022) relies on the Emergency Events Database, a worldwide date known to be subject to several bias (Botzen et al., 2019).

2 Theoretical background

2.1 Economic theory on fertility

Theoretical models explaining fertility are based on the quality-quantity model first developed by Becker (1960), Mincer (1963), and Willis (1974) along with its subsequent extensions.[6] In general, the model environment considers a representative household that maximizes utility over consumption, the quantity of children, and their quality. The budget constraint is comprised of labor income, the benefits and costs associated with children and their education, and the interest gained from saving. Becker (1993) assumes that with increasing income, the demand for child quality increases disproportionately to child quantity. This produces an inverse relationship between income and fertility. In these models, a particular focus is given to education as an investment in human capital (Becker, 1992; Azarnert, 2006; Lee & Mason, 2010; Pörtner, 2014; Vogl, 2016).

Other extensions of the model explore the demand for children as a demand for insurance (Pörtner, 2001). This "risk-insurance" hypothesis supposes that in harsh poverty conditions, children function as a kind of generalized insurance against an uncertain future, with this insurance function constituting one of the main explanations of the high fertility (Cain, 1983; Robinson, 1986). The insurance strategy can derive from the number of children and their risk of death. Generally analyzed in the context of the demographic transition (Becker, 1992; Schultz, 1997; LeGrand et al., 2003; Doepke, 2005; Azarnert, 2006), some studies focus on the impact of mortality as a shock (Norling, 2022). The increase in fertility in response to expected future child mortality is also known as the "hoarding" effect. In models where mortality is stochastic and parents wish to preserve a certain number of children, the "hoarding" effect occurs when an increase in fertility occurs in response to the expected future mortality of children. If fertility is chosen sequentially, there is also a "replacement" effect: parents may condition their fertility decisions on the survival of previously born children (Doepke, 2005).

The insurance strategy can also come from on the uncertainty of expected future income (Ranjan, 1999; Pörtner, 2001). This uncertainty can occur in the labor market (Kreyenfeld, 2010, 2015; Hanappi et al., 2017). More recently, many studies have analyzed the link between uncertainty and fertility, especially in the context of economic recessions in developed countries.[7] The underlying argument of these studies is that greater uncertainty about future prospects will encourage couples to postpone and possibly forego childbearing altogether, because it involves an irreversible investment with long-term consequences on resources (Aassve et al., 2021). In this context, the aggregate fertility seems pro-cyclical over the

[6] The interested reader can refer to Schultz (1997) for a review of these extensions.
[7] The interested reader can refer to Aassve et al. (2021) or Sobotka et al. (2011) for a review.

business cycle[8] (Sobotka et al., 2011; Gozgor et al., 2021). This finding is also shown by Ranjan (1999) with a two-period stochastic model of fertility that takes into account the perceived uncertainty about future income. Finally, other works introduce the perception of uncertainty (or risk aversion) to explain fertility variations and show that at times of heightened uncertainty, risk-averse individuals will postpone childbearing more than risk lovers (Schmidt, 2008; Hofmann & Hohmeyer, 2013). Vignoli et al. (2020) propose a conceptual framework for the study of fertility decisions under uncertain conditions based on expectations and "experience".

2.2 Impact of natural disasters on fertility

Based on the literature on the determinants of fertility, some authors have explored the impact of natural shocks on fertility. They examine the meaning and magnitude of the potential impacts of natural disasters on fertility as well as the potential explanatory factors. Empirical evidence about the effect of natural disasters and, more generally, weather anomalies on fertility is mixed. The studies are primarily concerned with poor countries. In this way, most of the time, the occurrence of a natural disaster is modeled as an exogenous shift in labor income.[9] The first-order conditions associated with the maximization of household utility reveals that the desired number of children is chosen up to the point where the satisfaction obtained from an extra child equates to its opportunity cost.[10]

The positive impact can be explained by either the replacement effect or the insurance mechanism relating to income uncertainty. The replacement effect (or "hoarding" effect) is examined by Nobles et al. (2015) on the impact of Indian Ocean Tsunami in 2004 or by Nandi et al. (2018) on the earthquake in India in 2001. Finlay (2009) studies the insurance mechanism and argues that children can be used to smooth consumption over time. More precisely, she shows that fertility can increase after a disaster if and only if the benefit associated with children is higher than the cost of taking care of them. In the model of Dessy et al. (2019) for drought in Madagascar, an exogenous increase in labor market productivity has two opposite effects on the shadow price of an additional child. On the one hand, it increases the foregone income of women when they spend time out of the labor market to care for children. On the other hand, an income effect renders each additional child cheaper. Dessy

[8] This result can be nuanced as in the work of Buckles et al. (2021).

[9] In developing countries, this variation in income corresponds to the realization of labor productivity (in the agricultural sector) at the beginning of each period.

[10] The opportunity cost of the additional child is also known as the shadow price. In what follows, we use both terms interchangeably.

et al. (2019) assumes that the former prevails over the latter.[11] Sellers & Gray (2019) observes the same result for climate shocks (temperature and precipitation) where the reduction in the opportunity cost of having children (especially in rural areas) is the main driver of the fertility effect. Finally, for hurricane Cohan & Cole (2002) found a net increase of birth rate due to post-disaster family restructuring.

Skidmore & Toya (2002) study the impact of climatic disasters in 89 countries and finds a positive effect on economic growth but a negative impact on fertility. This negative impact can be explained, at least in part, by conjunctural (Lindstrom & Berhanu, 1999) and psychologic factors (Arnberg et al., 2011). Indeed, recent studies have shown that natural disaster or climate anomalies have a negative impact on fertility under certain circumstances. Thiede et al. (2022) emphasizes that climate exposure affects reproductive outcomes but only in specific locations and populations, with this heterogeneity underscoring the need to consider socioeconomic and environmental factors. More specifically, for cyclones, Berlemann & Wenzel (2018) showed a positive impact on fertility in low-income countries but a strong and significantly negative effect for countries with high levels of development. For the United States, Evans et al. (2010) found an increase in fertility for hurricanes of low severity, while severe tropical storms led to a decrease in fertility. The negative effect can also be explained by the increase in the opportunity cost of having children (Kochar, 1999; Evans et al., 2010; Alam & Pörtner, 2018; Berlemann & Wenzel, 2018; Norling, 2022) or by the uncertainties caused by the disaster shock (Davis, 2017; Pörtner, 2014; Wang et al., 2022).

Despite the underlying uncertainty assumption, few studies incorporate it explicitly. Pörtner (2014) differentiates between risk and shock variables. Risk represents the percentage probability of a hurricane occurring in a given year for each area, whereas shock is the number of cyclones experienced by a woman during her fertile period.[12] Pörtner (2014) finds that shock leads to a decrease in fertility, while the risk increases fertility for the households with land. [13] In the literature that uses theoretical models, (Finlay, 2009; Pörtner, 2014; Marchetta et al., 2019; Norling, 2022) integrate uncertainty in the evolution of income (that depends on the investment in education) in the decision to have children.

2.3 Theoretical model proposition

This subsection develops a model regarding parental decisions about fertility. The model environment has two periods. The household has utility in both periods but experiences

[11] Another reason based on more psychological factors is the fact that motherhood is a way to cope after an emotionally traumatic experience (Carta et al., 2012).

[12] More specifically, this is "the number of cyclones between the year the woman enters her fertility period (taken to be 15 years) and her 29th year or the survey year, whatever is first" (Pörtner, 2014).

[13] Pörtner (2014) also includes the effect of shock and risk on education.

some uncertainties about outcome in period 2 (Pörtner, 2014). The overall utility U of the household is the sum of utility in period 1 (U_1) and the expected utility of period 2 ($E(U_2)$):

$$U = U_1 + E(U_2)$$

In each period, the household receives utility from consumption of a general good c. In the utility function, we consider the log of consumption to obtain a diminishing marginal utility of consumption such that $U_1 = \ln(c_1)$ and $U_2 = \ln(c_2)$ (Finlay, 2009). The household budget constraint indicates that income from period 1 Y_1 is spent by consuming c_1 and by supporting the cost k of raising ever born children n_1. In period 2, the budget constraint is different. We assume that children born in period 1 contribute positively to household income wn_1, with $w > 0$. This new income supplements the income received in period 2 Y_2. The expenditure of period 2 is similar to that of period 1:

$$\begin{aligned} Y_1 &= c_1 + kn_1 \\ Y_2 + wn_1 &= c_2 + kn_2 \end{aligned}$$

Following Ranjan (1999), we assume that income in period 2 varies with probability.[14] So, the expected utility of period 2 depends on the probability of exposure to natural disasters λ in period 2. In the event of an adverse shock, we assume that income decreases by a quantity equal to δY_2 with $\delta \in [0, 1]$. Assuming an absence of intertemporal discounting and saving, the household can choose how many goods and children to have in each period to maximize a global additively separable utility function of the following form:

$$U = \ln(Y_1 - kn_1) + \lambda[\ln(Y_2(1-\delta) + wn_1 - kn_2)] + (1-\lambda)[\ln(Y_2 + wn_1 - kn_2)] \quad (1)$$

Let us now focus our discussion on the first-order condition with respect to the optimal number of children to have in period 2. The latter can be written as follows:

$$\frac{\partial U}{\partial n_2} = 0 \Leftrightarrow n_2 = \frac{Y_2\,(1 - \delta(1-\lambda)) + wn_1}{k} \quad (2)$$

The comparative statics of equation (2) informs us about the direction of the effect of a given parameter on the number of children to be born in period 2. With respect to the share of

[14] However, although Ranjan (1999) assumes that income increases with probability 1/2 and decreases with probability 1/2, we assume here that probability is a parameter between 0 and 1.

income loss due to the occurrence of an adverse event such as a cyclone δ, we obtain:

$$\frac{\partial n_2}{\partial \delta} = \frac{-(1-\lambda)Y_2}{k} < 0 \tag{3}$$

An increase in the amount of lost income has a negative incidence on fertility. This leads us to our first working assumption to be tested in empirical analysis:

> **Working assumption 1**: All else being equal, after an adverse shock such as the occurrence of a cyclone, the likelihood of motherhood is expected to fall.

Then, it may be interesting to compute the functional form of the derivative of (3) with respect to the probability of being exposed λ. Indeed, we cannot exclude that the effect of cyclonic exposure on motherhood depends on the degree of exposure of people living in the most exposed areas. The latter is written as:

$$\frac{\partial^2 n_2}{\partial \delta \partial \lambda} = \frac{Y_2}{k} > 0 \tag{4}$$

Given that the number of children is a decreasing function in the share of income loss, the positive sign of (4) indicates that n_2 decreases less in areas that are more frequently exposed to the disaster. Our second working assumption to test empirically is as follows:

> **Working assumption 2**: All else being equal, in cyclone prone areas, the sensitivity of fertility to cyclonic exposure is lower.

Finally, our data allow us to investigate if post-cyclone fertility depends on the presence of children ever born in the household. In the model, the derivative of (3) with respect to n_1 is thus:

$$\frac{\partial^2 n_2}{\partial \delta \partial n_1} = 0 \tag{5}$$

Consequently, our theoretical framework implies that the number of children to be born in period 2 after cyclone exposure is not related to the number of children born in period 1. Our third working assumption is as follows:

> **Working assumption 3**: All else being equal, the post-cyclone fertility response does not depend on the number of children ever born.

These three working assumptions will frame the development of our empirical results. Section 5 aims to provide an empirical response to these assumptions.

3 Empirical background and data

3.1 Demographic and Health Survey

Our primary source of micro-data about female fertility is the DHS of countries exposed to cyclones. The DHS is a series of cross-sectional surveys that is conducted approximately every 5 years. The DHS is generally conducted by the national institute of statistics and benefited from the technical and financial support of international institutions. For each phase of the DHS, a nationally representative sample of women aged from 15 to 49 years were interviewed. From these women, detailed information was collected about their sociodemographic (e.g., household composition, education level, number of children, household well-being) and health characteristics (e.g., infant mortality, nutritional practices, malaria prevalence, use of contraceptives). Among the broad range of information available in the DHS, we exploit the mother's fertility history in depth. This retrospective record allows us to retrieve information about the children's year of birth and gender or the women's age at childbirth. From this fertility history, we construct a panel dataset of women and define a binary variable to indicate whether a woman gave birth or not during a given year.

Let us now describe in further details the sample selection of the DHS, because it has important implications on the design of our empirical study. The sample of each DHS wave is a two-level stratified random sample. At the first level, the country territory is divided into thousands of clusters with a number of clusters being randomly selected.[15] At the second level, for each cluster selected at the first level, around 30 households were randomly chosen. The geographical information that we use to locate the women comes from the first-level selection. In particular, for each selected cluster, the data producer provides geographical information about its centroïd. However, to ensure the confidentiality of the selected households, the data producer does not provide the exact latitude and longitude of the cluster's centroïd but randomly displaces the actual location within a 2 (or 10) km radius in urban (or rural) areas. We then combine information about the cluster's location with information about tropical cyclones to retrieve the wind speed exposure experienced by inhabitants on the ground.

To conduct our research, we apply some restrictions to our sample. First, among all countries with DHS microdata, we first select those with a positive exposure to tropical cyclones. Second, given that the geographical information about cluster locations is essential, we exclude DHS' wave without geographic information. For the DHS with geographical information we exclude households living in clusters without exploitable coordinates.[16] Third,

[15] For instance in Madagascar, 285 clusters among 21,500 were selected for the 1997 phase of the DHS compared to 600 in 2008.

[16] Missing geographical information are due to i) inconsistencies in the reported geographic coordinates and ii) the incapacity of the data producer to access some clusters (ICF Macro (1998), ICF Macro (2010)).

as we use the retrospective data about mothers' fertility, we need to ensure that a given woman has been really exposed to a given tropical cyclone in a given year. To do so, we follow Kudamatsu (2012) and Anttila-Hughes & Hsiang (2013) by restricting our final sample to mothers declaring that they have always lived in their current home.[17] It should be observed that for some DHS' waves, information about the arrival in the current home is simply missing for all observations. As we believe that having knowledge about the residence of the mother is mandatory for our purpose, we select waves of DHS for which this information is recorded.[18] These restrictions leave us with a sample of six countries namely Banglasdeh, Cambodia, Dominican Republic, Haïti, Madagascar and Philippines.[19] Finally, as we iterate backwards to construct our panel database, we drop all records for which the mother's age is below the threshold of 15.[20]

Table 1 reports a selection of summary statistics. In our final sample, the total number of children per woman was 3.22, while the birth frequency was 17%. The average age at first childbirth was equal to approximately 20 years. Approximately, 23% of women reported having no education, while around 43% reported, at best, a level equivalent to primary education. This results in a relatively low number of years at school (around 3.5 years).

3.2 Macroeconomic context

Table 2 presents macroeconomic statistics for 2015 for the six countries that make up our sample.[21] We choose this year because the sample period studied in this paper ends in 2015. These statistics allow us to better understand the differences in the magnitude of the effects in our model.

The six countries included in our sample had more than 320 million people in 2015. The majority have a population density higher than the global average (57 inhabitants per km^2). Bangladesh and the Philippines are particularly populous, with 157 million and 103 million inhabitants, respectively. Given the smaller area of Bangladesh (147,630 km^2), it has a density

[17] In a robustness check, we relax this assumption (see Appendix C).

[18] Having no information about the arrival of the mother in the current home is problematic even if geographical information about cluster locations is available. In particular, one could attribute an exposure to a woman whereas she actually leaves elsewhere.

[19] Overall, we employ 14 waves of DHS. DHS waves used in this paper are: for Bangladesh waves IV and V, for Cambodia waves IV and V, for Dominican Republic wave V, for Haïti waves IV, V and VII, for Madagascar waves III and V, and for Philippines waves IV, V and VII.

[20] For instance, for a woman born in 1973 and aged 35 in 2008 at the time of the interview, we build annual records of her fertility from 1988. This woman enters the our dataset when she is 15 and her last record correspond to the year of the interview.

[21] These statistics are mainly from the World Bank (https://data.worldbank.org/. The HDI data comes from the UNDP (UNDP, 2016) and the EVI data comes from FERDi (https://ferdi.fr/en/indicators/a-retrospective-economic-vulnerability-index)

Variable	Sample mean
Mother's age	26.80
Mother's age at first birth	19.92
Mother's age at first marriage	18.68
Number of children	3.22
% of birth	0.17
Years of education	3.56
No education (in %)	0.23
Primary education (in %)	0.43
Secondary education (in %)	0.25
Tertiary education (in %)	0.09

Table 1: Sample mean of a selection of women's characteristics.
Sources: DHS and authors' own calculations.
Notes : Statistics are computed on a sample of 58653 women. The "% of birth" correspond to the frequency of birth once the panel is constructed.

of 1,213 inhabitants per km^2, making it one of the 10 most densely populated countries on the planet. Both the Philippines and Haiti also have high population densities, with 346 and 383 inhabitants per km^2, respectively, although the Philippines has a much larger area (300,000 km^2). Haiti and the Dominican Republic both have a population of about 10,500 inhabitants, although the territory of the latter is almost twice the area (27,750 vs. 48,670 km^2), thus resulting in its lower population density (215). Finally, Cambodia and Madagascar have lower population densities (87 and 43) due to their large territories, particularly Madagascar with 587,295 km^2. In most of these countries, their population growth rates are higher than the global rate of 1.2 births per 100,000 inhabitants . Madagascar has the highest population growth rate with 2.6 compared with rates between 1.2 and 1.7 births per 100,000 inhabitants for the five other countries.

Aside from the Dominican Republic, these countries are among the poorest on the planet. Madagascar is the poorest country included in the study, with GDP per capita of USD 1,508. Haiti, Bangladesh, and Cambodia have a per capita income between USD 2,935 and 4,217. Philippines has a higher per capita income of USD 7,123. However, the per capita income of the Dominican Republic is much higher compared with the other countries in the group, being USD 14,565 or twice that of the Philippines. A high proportion of the population in these countries lives below the poverty line. Indeed, the poverty headcount ratio at USD 3.65 a day as a percentage of the population is 92.4% for Madagascar, which is the poorest country.[22] Next, more than half of the population in Bangladesh and Haiti live below the

[22]For this indicator, we chose 2012, because this year has the most complete data, with the exception of

Variables	Bangladesh	Cambodia	DR	Haiti	Madagascar	Philippines
Demographic						
Pop. (in thousands)	157 830	15 417	10 405	10 563	24 850	103 031
Population growth	1.2	1.3	1.2	1.4	2.6	1.7
Area (in km^2)	147 630	181 040	48 670	27 750	587 295	300 000
Density	1 213	87	215	383	43	346
Economic and poverty						
GDP per capita	4217	3412	14565	2935	1508	7123
Annual GDP growth	6.6	7	6.9	2.6	3.1	6.3
PHR	51.6	–	14.3	58	92.4	34.6
Indicators of development						
HDI score	0.579	0.563	0.722	0.493	0.512	0.682
HDI rank	139	143	99	163	158	116
Total fertility rate	2.1	2.6	2.4	3.1	4.2	3
Birth rate	19.2	22.3	20.6	25.6	32.8	23.2
EVI	24.28	35.26	21.27	28.80	35.31	24.59

Table 2: Macroeconomic indicators.

Sources: World Bank, UNDP and FERDI.

Notes: DR stands for Dominican Republic. Density is measured as the number of people per km^2, GDP per capita is in USD in Purchasing Power Parity, PHR correspond to the Poverty headcount ratio in USD per day in % of population for 2012, 2016.

poverty line with 59.3% and 58% of the population, respectively. The poverty headcount ratio in the Philippines is similar to the world rate (32.7%) with 34.6%. Only the Dominican Republic has a better rate than the world rate with 14.3%. Thus, the Dominican Republic is clearly above the sample in terms of wealth. We may also draw attention to the wealth difference between the Dominican Republic and Haiti, which share the same island.

These countries are characterized by high but heterogeneous economic growth rates. Indeed, it is much higher than the world rate (3.1%) for Cambodia (7%), the Dominican Republic (6.9%), Bangladesh (6.6%), and the Philippines (6.3%), while it is equivalent for Madagascar (3.1%) and lower for Haiti (2.7%). The development indicators provide support to the economic data. Indeed, the human development index (HDI) places the six studied countries between 99th and 163rd place in the world rankings. More precisely, Haiti and Madagascar belong to the group of countries with low human development (<0.550), while Cambodia, Bangladesh, and the Philippines have medium human development (between 0.550 and 0.700). Only the Dominican Republic is in the high development group (>0.700).

To focus on birth, we may explore two indicators: the "total fertility rate" which represents the number of children that would be born to a woman if she were to live to the end of

Bangladesh, whose closest year is 2016, and Cambodia, for which this indicator is not available.

her childbearing years and bear children in accordance with age-specific fertility rates of the specified year, and the "crude birth rate", which indicates the number of live births per 1,000 midyear population. These two indicators show the strong birth dynamics in these territories. Madagascar has the highest rates with 4.2 and 32.8, respectively. For the total fertility rate, Haiti, the Philippines, and Cambodia also have a higher rate than the world rate (2.5), while Dominican Republic and Bangladesh have a lower rate. Finally, the birth rate in all these countries is higher than the global value (19.1), because the population is young and of reproductive age.

Finally, let us look at the economic vulnerability index (EVI) defined by the Committee for Development Policy of United Nations. The IVS aims to measure the structural vulnerability of developing countries resulting from the magnitude of shocks and exposure to shocks **??**. We see that the two most vulnerable countries are Madagascar and Cambodia, with scores of 35.31 and 35.26, respectively. Haiti has a score of 28.80. The Philippines and Bangladesh have an equivalent score of 24.59 and 24.28, although the Philippines has a more advanced level of development in terms of GDP and HDI. The Dominican Republic is also the least vulnerable country in the sample with a score of 21.27.

3.3 Tropical cyclone data and wind speed exposure

Tropical cyclones are natural atmospheric phenomena that develop mainly in tropical regions. A cyclone is a non-frontal synoptic scale system rotating clockwise in the Southern Hemisphere and counter-clockwise in the Northern Hemisphere. It is organized around a center of low atmospheric pressure called the eye, which is bounded by convective clouds that form an eye wall and precipitating spiral bands that wrap around it. This highly convective phenomenon is characterised by strong surface winds. Cyclonic systems are divided into several categories, according to the intensity of the associated winds (defined as the maximum speed of the wind at an altitude of 10 m, averaged over 10 min (except in the United States where it is averaged over 1 min). In this paper, we use the terms tropical systems, cyclonic systems, and tropical cyclones interchangeably to designate tropical systems of any magnitude.[23] The wind associated with cyclonic systems can thus cause severe damage. Some are listed by Tamura (2009)'s study according to wind speed thresholds. For instance, maximum 10-minute averaged winds of 90 km/h can damage roof tiles, while above 162 km/h, the constraints of the main frame of high-rise buildings exceed the elastic limit. The devastating effects of

[23]We however acknowledge that there are three classes of cyclonic phenomena. First, if the wind speed is less than 63 km/h, it is called a tropical depression. Second, between 63 and 117 km/h, it is called a tropical storm. Third, above 117 km/h, it is called a tropical cyclone in the Indian Ocean and the South Pacific, a hurricane in the North Atlantic and the North-East Pacific, or a typhoon in the North-West Pacific.

tropical cyclones mainly come from strong winds (CCR, 2020).[24]

3.3.1 TCE-DAT caracteristic

A prerequisite for our empirical study is a measure of wind speed exposure experienced by the population on the ground. As it is not possible to rely on weather ground station data at a detailed level in the context of the six developing countries under scrutiny here, we exploit the worldwide TCE-DAT of Geiger et al. (2018). To produce this database, Geiger et al. (2018) calculate an estimate of the lifetime's maximum surface wind speed at each spatial location (on a $0.1° \times 0.1°$ grid over land) for more than 2,700 landfalling cyclonic systems between 1950 and 2015. As the quality of data records resuired to compute wind speed is lower before 1980, we choose a cautious approach by placing our cut-off several years after 1980, namely in 1985.[25] The calculation is based on the International Best Track Archive for Climate Stewardship (IBTrACS) archive (Knapp et al., 2010), which contains all the information necessary for a wind field model such as that of Holland (1980) that is widely used in studies on the evaluation of the risks associated with the landfalling of tropical cyclones (Peduzzi et al., 2012). Geiger et al. (2018) implement the revised hurricane pressure-wind model of Holland (2008) in which the maximum surface wind speed W in $m.s^{-1}$ (for a given pixel)[26] at radial distance r of the center of a given cyclonic system is defined as follows:

$$W = \left(\frac{b_s}{\rho e} \Delta p \left(\frac{r}{r_m} \right) \right)^{0.5}, \tag{6}$$

where ρ is the surface air density in $kg.m^{-3}$, e the base of natural logarithms, and Δp the pressure drop at the cyclone center in hPa as a function of r and r_m (radius of maximum winds). Parameter b_s depends on Δp, the temporal intensity change in pressure, the absolute value of the latitude, and the tropical cyclone's translational speed. Further details on the development of the parametric equation of b_s can be found in Holland (2008). In addition to the wind field model in equation (6), Geiger et al. (2018) calculated a translational component multiplied by an attenuation factor (ratio between the tropical cyclone's center and the radius of maximum wind). The translational wind speed decreases with the distance from the cyclonic system's center, which is taken into account to provide more realistic estimates of

[24] CCR (2020) collect post-cyclone insurance data and find that the vast majority of insurance claim payments are due to wind speed rather than rainfall, landslides, or storm surges.

[25] Geiger et al. (2018) indicate that records are sometimes incomplete or of poor quality before the early 1980s. We confirm that the use of data since 1981 (the first available date for the rainfall variable in our econometric specification) has no incidence on the main message of the paper. Corresponding results are available upon request.

[26] For simplicity, we do not add an index to designate pixels.

wind exposure on the ground. To our knowledge, there is no other publicly available dataset from a ground weather station or remote sensing measurement covering the whole territory of Madagascar with a spatial resolution higher than $0.1° \times 0.1°$. This is the main reason why we decided to use the wind speed estimate calculated by Geiger et al. (2018).[27]

Table 3 and the barplot of Figure 1 show summary statistics about cyclonic exposure of clusters under scrutiny in this paper. Overall, 21.0% of our pairs of cluster-year observations experienced a positive wind speed exposure. Over our sample period, the mean number of exposures to cyclones was of 7.4. Given that the standard deviation of exposure frequency is approximately equal to its mean, the number of exposures by clusters is quite heterogenous. Thus, 11% of clusters were not exposed at all to cyclones. In Figure 2 these clusters are represented by the yellow part of each map. Looking at the top of the distribution, we observe that the top 10% of clusters were exposed at least 19 times over the 1985-2015 sample period. Given the nature of our empirical approach, such heterogeneity in the exposure of clusters is worth investigated because it creates within variations that could be explored by our panel fixed effect regressions. Let us now take a look on the profile of wind speed exposure generated at the surface. To do so, we now focus on DHS clusters when exposure is non-zero.[28] The average wind speed exposure during the 1985-2015 period is 93.5 km/h with a standard deviation of 32.2. Again, there is substantial heterogeneity in our sample insofar as 10% of clusters were exposed to tropical cyclones with wind speeds above 138.4 km/h. Observe that the maximum wind speed recorded during our sample period is 293.7 km/h. This extreme wind speed is due to Haiyan, one of the most severe phenomena that passed over Philippines. For illustrative purposes, we plot in Figure 2 the field of annual maximum wind speeds for the six countries belonging to our sample during the 1985-2015 period. It appears that exposure to cyclonic wind speed is the highest in Philippines especially at the north of this country. Then, Madagascar is the second country with the highest exposure. In particular, the north-east cost of the country is regularly threatened by tropical cyclones. Among the countries studied here, Bangladesh, Haiti and Dominican Republic have a wind speed exposure falling in the middle of distribution. Finally, the north east of Cambodia has a similar exposure as the three quoted countries but the other parts of the county appears to be less prone to be exposed to such a natural phenomenon.

[27]The dataset is referenced as Geiger et al. (2017) and is available at https://dataservices.gfz-potsdam.de/pik/showshort.php?id=escidoc:2387904.

[28]In doing so, we follow Elliott et al. (2015).

	Nb. of exposure	Wind speed	Rainfall	Temperature
Mean	7.40	93.50	19.00	25.60
Standard deviation	7.30	32.20	8.10	1.90
Min.	0.00	61.20	1.90	16.40
Percentile 1%	0.00	63.50	5.60	18.30
Percentile 5%	0.00	64.60	8.40	22.30
Percentile 10%	0.00	65.80	10.50	23.40
Percentile 25%	2.00	71.60	13.60	25.00
Percentile 50%	6.00	84.30	17.50	25.90
Percentile 75%	9.00	99.00	22.90	26.90
Percentile 90%	19.00	138.40	29.70	27.70
Percentile 95%	24.00	166.10	34.30	28.10
Percentile 99%	29.00	212.60	45.60	28.50
Max.	34.00	293.70	72.50	29.10
Observation	7,626			

Table 3: Summary statistics of weather variables for the DHS clusters during the 1981-2015 period.

Sources: DHS, TCE-DAT of Geiger et al. (2018), CHIRPS dataset of Funk et al. (2015), CRU dataset of Harris et al. (2014), and authors' own calculations.

Notes: Wind speed corresponds to the maximum wind speed experienced and is expressed in km/h. Rainfall corresponds to the cumulative precipitation over a year and is expressed in hundreds of millimeters. Temperature is the annual average temperature and is expressed in Celsius degrees. For the wind speed, summary statistics are computed only for non-zero cluster-year pairs.

3.3.2 Other weather data

Although our main focus is on the impact of tropical cyclone exposure on motherhood, we include two other weather variables in our analysis, namely rainfall and mean temperature. Their inclusion is meant to avoid noises due to the shared secular changes that might be correlated with tropical cyclone exposure. Our rainfall variable comes from the the Climate Hazards group InfraRed Precipitation with Stations (CHIRPS) dataset constructed by Funk et al. (2015). When constructing this dataset, Funk et al. (2015) combine ground station and satellite information to obtain high-resolution ($0.05° \times 0.05°$) gridded data. Concerning temperature, we use the updated worldwide gridded climate dataset of the Climate Research Unit (CRU) of the University of East Anglia (Harris et al., 2014). This dataset nevertheless has a lower resolution than that of CHIRPS, since it is available at 0.5° latitude/longitude grid cells. The last two columns of Table 3 report the univariate statistics of rainfall and mean temperature.

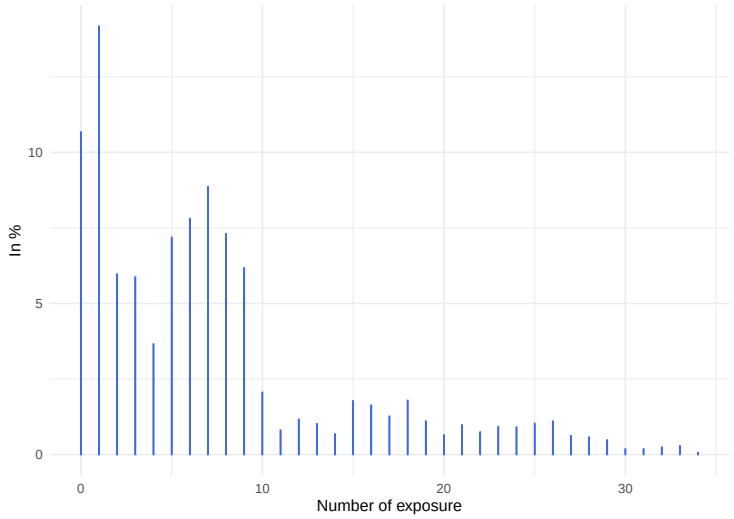

Figure 1: Distribution of cyclonic exposure experienced by DHS clusters (1981-2015).
Sources: DHS, TCE-DAT (Geiger et al., 2018), and authors' own calculations.

4 Empirical framework

4.1 Estimated equation

Our empirical strategy consists of estimating different versions of the following baseline model:

$$y_{itcv} = \sum_{l=1}^{L} \left(\beta_l^W \times W_{i,t-l} + \beta_l^R \times R_{i,t-l} + \beta_l^T \times T_{i,t-l} \right) + \mu_i + \eta_t + \theta_v + \alpha_c + u_{itcv} \quad (7)$$

Where i indexes a given woman, t a given year, and c a given cluster. The outcome of interest, namely y_{itc}, is a binary variable equal to one if mother i from country c living in cluster v gives birth in year t and zero otherwise. Given that y_{itcv} is dichotomous, we rely on a linear probability model. [29] In equation (7), β_l^j with $j \in [W, R, T]$ are coefficients to be estimated. Our main weather variable of interest corresponds to the tropical cyclone wind speed exposure W of woman i in year $t-1$ measured in kilometers per hour (km/h). We also include as controls two other weather variables: annual rainfall R expressed in hundreds of millimeters and annual land surface mean temperature T measured in Celsius degrees in $t-1$. We justify the inclusion of these two variables as an attempt to lessen the issues

[29] Such a practice is standard in the empirical literature dealing with dependent dichotomous variables in a panel setup (Anttila-Hughes & Hsiang (2013), Kudamatsu (2012), Kudamatsu et al. (2012)). In particular, it is well known that the incidental parameter problem complicates the estimation of panel models with fixed effects. In contrast to linear models, it is not possible to remove fixed effects with the traditional within transformation. Moreover, estimating them directly leads to biased estimates of all parameters (see also Wooldridge (2010) or Croissant & Millo (2018) for more details).

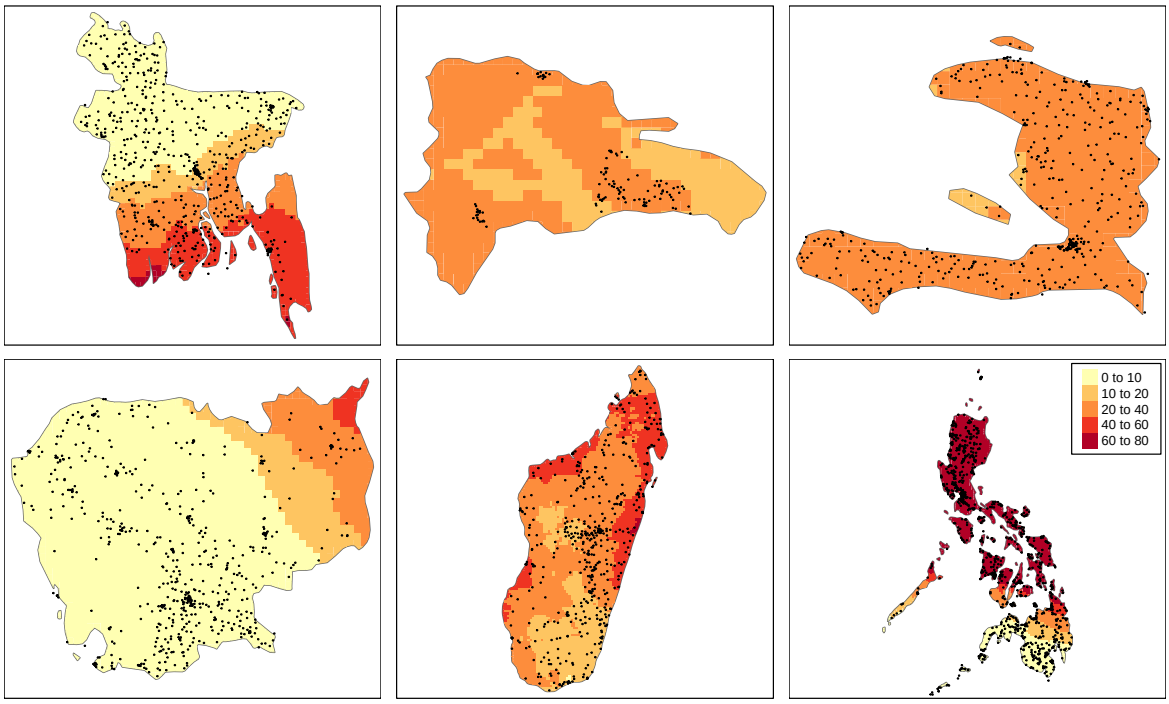

Figure 2: Mean of wind speed exposure (1980-2015)
Sources: DHS, TCE-DAT (Geiger et al., 2018), and authors' own calculations.
Notes: The dots of each panel correspond to cluster coordinates of the last wave of DHS used for each country. From the top-left to the bottom-right we have Bangladesh, Dominican Republic, Haïti, Cambodia, Madagascar and Philippines.

related to omitted variables. If there are correlations or shared secular changes among the weather variables, studying the impact of a weather variable in isolation could be problematic (Dell et al., 2014).[30] In the baseline model, we set $L = 1$ so that the three weather variables enter our model with a one period lag. We also consider the case where $L = 5$ so that each weather variable enters with up to five lags in sensitivity analysis (see subsection 5.2).[31] We include woman fixed effects μ_i to control for unobserved and time-invariant characteristics that could potentially affect women's likelihood of childbearing.[32] We also flexibly account for year-specific components shared by all women using a year fixed effect η_t. Their inclusion ensures that the relationship of interest can be identified from idiosyncratic shocks. We also

[30] In particular, it is arguable that the tropical cyclone exposure of a given spatial unit may be correlated with its surface temperature or rainfall level. In this respect, Hsiang (2010) finds that each additional Celsius degree in a country's local surface temperature is associated with a 9.36 km/h increase in local wind exposure in the Caribbean basin countries.

[31] As such model reveals that beyond one period, coefficients associated to lags of cyclonic exposure are significant but closer to zero, in the baseline we include only one lag.

[32] These unobserved factors could be the (time-invariant) preference of women to have a large family. Their preference can also be rationalized by emphasizing the opportunity cost of taking care of children. Women's more limited outside options in the labor market probably increase the opportunity cost of spending time in labor market activities, thus leading them to have more children and devote more time to their childrearing.

include cluster and country fixed effects θ_v and α_c to capture any unobserved characteristics that plausibly affect women's childbearing behavior at the "village" or the country level. Finally, u_{itcv} is the error term. Given the sampling design of the DHS surveys, we follow Abadie et al. (2017), while standard errors are clustered at the first-level sample selection to allow for any correlation of the error term u_{it} over time and space within each DHS cluster.

Our estimation of women's likelihood of giving birth mainly controls for weather-related variables. Two main arguments support this choice. First, control variables themselves should not be outcomes of weather-related variables (Dell et al., 2014). Let us take household income as an additional control variable.[33] In this case, we cannot exclude that it is also an outcome of cyclonic wind speed. Consequently, if a model includes income, then the estimated coefficient on wind speed would not capture its total net effect on fertility, because income can be written as a function of wind speed. Second, when adding control variables such as income, we may encounter an endogeneity problem. Specifically, we could argue that income has an effect on fertility, but we could also conjecture that fertility explains, at least in part, women's income.[34] This is the well-known reverse causation problem that leads to the introduction of a selection bias in the estimation of the income-related coefficient as well as other estimated coefficients in the model. Given these two arguments, we believe that the parsimonious model of equation (7) remains a relevant departure point. In doing so, our empirical model is able to unveil the true net effect of cyclonic wind speed (or the total effect) on women's likelihood of giving birth.

4.2 Identifying assumption

Insofar as fixed effects are included in equation (7), variables are expressed as deviations from the individual and temporal sample means (Croissant & Millo, 2018). Our identification emphasizes year-to-year variations in levels from the observed means. As a consequence, the fixed effect coefficients associated with wind speed could be interpreted as the impact of tropical shocks on women's probability of giving birth.

The main assumption used on to identify the causal effect of tropical cyclones on fertility is randomness in an individual's exposure. Being exposed to cyclonic systems can be viewed as (quasi-)random insofar as the formation of cyclonic systems in addition to their precise trajectories and magnitude are stochastic and difficult to predict. When they occur, tropical cyclones generate recognizable wind speeds of high magnitude hitting large spatial units

[33] Note that the construction of our panel data does not allow us to retrieve an income variable, because we mainly rely on the mothers' fertility history for which such information is not available.

[34] Similar problems could arise for variables such as education level, years of education, school dropout, participation in the labor market, and so on.

(quasi-)randomly so that inhabitants living in these areas experience the exposure, while those living in non-affected areas experience no exposure. We however acknowledge that some areas are more likely to be exposed by tropical cyclones so that the total effect on fertility could vary depending on the level of risk. We also consider this possibility by introducing such a heterogeneity dimension in our empirical analysis (see also section 5).

There are potentially two issues relating to the randomness of tropical cyclones, both of which are related to the ability of meteorologists to forecast the occurrence of tropical cyclones. Indeed, meteorologists have made substantial progress in forecasting the seasonal frequency of tropical systems (Klotzbach et al., 2019). Furthermore, it is now possible to forecast the occurrence of a tropical cyclone a few days before its landfall. From our point of view, this forecasting nevertheless has almost no incidence on our identification strategy, because our focus is on year-to-year variations. In particular, if seasonal forecasts have a higher predictive power, the year-to-year variations in tropical cyclone wind speed at a given spatial unit largely remains unpredictable for scientists and thus for inhabitants potentially concerned by tropical cyclones. Regarding short-run forecasting, it implicitly assumes that inhabitants living in areas threatened by a cyclonic system have perfect access to the information (by means of a radio, television, or newspaper). This could be not the case in the context of developing countries.Nevertheless, it is probable that important information about the occurrence of tropical cyclones circulates through other channels like people's social networks, so we cannot totally exclude the fact that individuals could engage in actions to protect their homes and livelihood or evacuate. These issues have some repercussions on the interpretation of our results. More specifically, the estimated effect could be viewed as the effect of tropical cyclone shocks after households engage in adaptive behaviors (if any). However, despite such behaviors, inhabitants cannot overcome all the negative effects of tropical cyclones, meaning that a degradation in their living environment is perceptible and may affect their decision to have children. Insofar as year-to-year variations in the exposure to tropical cyclones shocks are (quasi-)random, our reduced-form panel framework imposes relatively few identifying assumptions while ensuring a causative interpretation.

5 Results

This section presents the results obtained by estimating the econometric model detailed in the previous section. All estimations were made with the R software (R Core Team, 2019) using tools provided by the "`fixest`" package.[35]

[35]Details about the `fixest` package can be found via the following link: https://cran.r-project.org/web/packages/fixest/vignettes/fixest_walkthrough.html.

	(1)	(2)	(3)	(4)
Max. wind in $t-1$	-0.0659***	-0.0676***	-0.0784***	-0.0801***
	(0.0014)	(0.0014)	(0.0018)	(0.0018)
Max. wind in $t-1$ × Prone	–	–	0.0305***	0.0304***
	–	–	(0.0025)	(0.0025)
Rainfall in $t-1$	–	0.2001***		0.2029***
	–	(0.0154)	–	(0.0154)
Temperature in $t-1$	–	1.042***	–	0.7866***
	–	(0.2498)	–	(0.2524)
Observations	1,025,443	1,025,443	1,025,443	1,025,443

Table 4: Main regression results.

Sources: DHS, TCE-DAT of Geiger et al. (2018), CHIRPS dataset of Funk et al. (2015), CRU dataset of Harris et al. (2014), and authors' own calculations.

Notes: Significance levels: * 10%, ** 5%, *** 1%. Robust standard errors are in parentheses, adjusted for clustering at the DHS cluster level. All regressions include woman fixed effect, annual fixed effect, cluster fixed effect and country fixed effect. The term "Prone" refers to a dummy equal to one when the mother leaves in a village that was exposed to cyclone at least 10 times during the 1985-2015 period. Maximum wind speed is measured in km/h, rainfall in hundreds of millimeters and temperature in Celsius degrees.

5.1 Main results

5.1.1 Fertility response to cyclone shocks

Table 4 reports the regression results of the alternative estimations of equation (7). To see how the inclusion of controls for temperature and rainfall alter the results, we sequentially add both of them in columns (2) and (4).

Column (1) and (2) reports the results of a model with exposure to wind speed being measured by the maximum wind speed generated at the surface. These models show the negative impact of tropical cyclone wind speed shocks on mothers' likelihood of giving birth. The estimated relationship is consistently negative regardless the inclusion of controls for temperature and rainfall. In the model of column (2), a wind speed exposure shock in t equivalent to a standard deviation, namely 38.8 km/h, induces a fall of 2.6 points (38.8×-0.0676) in women's likelihood of giving birth in $t+1$.[36] Alternative specifications of the baseline empirical model, consisting in changing our sample restriction by including mothers who migrate or splitting the sample to consider two sub-periods do not change the qualitative nor the quantitative pattern of our baseline results. As a result, our empirical evidence provides an affirmative answer to our first working assumption.

[36] A similar metric shows that the probability of giving birth for mothers exposed to extreme wind speeds (e.g., 213 km/h), falls by about 14.4 points in the next calendar year.

Empirical evidence on working assumption 1:
Exposure to tropical cyclones does reduce the likelihood of motherhood.

5.1.2 Degree of exposure and fertility response to cyclone shocks

To further investigate the nature of the relationship between wind speed exposure and motherhood, in Appendix A we present country-by-country regressions. These regressions show that the qualitative pattern is the same for the six countries under scrutiny here: exposure to cyclones reduces the probability of giving birth. However, depending on the country, the quantitative patterns could differ substantially. Thus, countries such as Madagascar or the Philippines are those with the smallest effect. For instance, an extra exposure to wind speed reduce the probability of motherhood in $t+1$ of 0.0452 in Philippines and 0.0271 in Madagascar. By contrast, countries such as Haiti, Cambodia or Dominican Republic experience the highest effects in term of post-cyclone reduction in fertility. In Haiti, and extra exposure to cyclonic wind speed in t translates in a fall in the likelihood of having babies of 0.231. In comparison to Madagascar, the fertility response in Haiti is eight times higher. An interesting feature emerging from the comparison of country-by-country regressions is that the effect seems to be higher in countries least frequently exposed.[37] [38]

In columns (3) and (4) of Table 4, we further explore the link between the degree of exposure associated to cyclonic and fertility. As Figure 2 shows, clusters' exposure to tropical cyclones is quite heterogeneous. Summary statistics of Table 3 unveil that over our sample period, 10% of villages were exposed more than 19 times while 25% were exposed less than two times. Even after controlling for cluster fixed effects, it is still possible that the effect of cyclonic wind speed on motherhood depends on the degree of exposure and preparedness of people living in most exposed villages. We could imagine that mothers living in the most frequently exposed areas anticipate the higher probability of exposure when taking their decision about having babies. Thus, their response to a cyclone shock could be different from mothers living in non-prone areas. To investigate this issue, we interact wind speed exposure

[37] According to the TCE-DAT of Geiger et al. (2018), during the 1985-2015 sample period Haiti has been exposed to cyclones 23 times, Dominican Republic 24 and Cambodia 29. In contrast, Madagascar has been exposed 84 times and Philippines 284. Consequently, Bangladesh, with a number of exposure of 50, falls in the middle of the distribution.

[38] Another interesting feature emerging from Table 8 is about the magnitude of the effect for the two countries of the Hispaniola island, namely Haiti and the Dominican Republic. Haiti is much less developed than the Dominican Republic (see also Table 2). In the theoretical section, we highlight that the post-disaster responses of fertility could be related to the country's level of development. For Haiti and the Dominican Republic, it seems to be not the case. Indeed, even with two very different development levels, the fall in the probability of motherhood is of the same magnitude. Given that the level of exposure to cyclones of these two countries is similar, we could conjecture that, in this special case, the degree of exposure is more important in shaping the post-cyclone fertility response than the development level.

with a dummy equal to one if the village were exposed more than nine times to cyclonic systems during the sample period of our study.[39] We refer to these clusters as cyclone-prone areas. Coefficients associated to this model specification can be found in the last two columns of Table 4. Again, the inclusion of controls for temperature and rainfall do not alter the qualitative and the quantitative causal effect of wind speed exposure on motherhood. However, in these models, the coefficient β_1^W now captures the effect of wind speed exposure for mothers living in non-prone area. Compared to models of columns (1) and (2), the latter is higher. All else being equal, an exposure to cyclonic wind speed of one standard deviation size decreases the probability of having children by 3.11 points. The interaction term of wind speed with the dummy for cyclone prone area confirms what has been suggested previously. Overall, the decrease in the probability of giving birth after a cyclonic exposure is lower. For mothers living in the most exposed areas, the likelihood of giving birth decrease by 1.93 points for the same level of exposure.[40] Such a result suggests that the fertility response to a cyclone shock is sensitive to the degree of exposure associated to mother's environment. In that sense, our empirical results is in line with our second working assumption.

Empirical evidence on working assumption 2:
The fertility response to cyclone shocks depends on the degree of exposure associated to the mother's living environment: in cyclone prone areas, the likelihood of giving birth reduce less.

5.1.3 Children ever born and fertility response to cyclone shocks

As indicated before, the model of section 2.3 does not deliver a clear message about the post-disaster fertility response with respect to family size. Instead, the model suggest that the post-cyclone fertility response is independent of the number of children ever born. However, depending on the presence of children we could imagine that the post-cyclone response in terms of fertility could be different. The association between children ever born and future fertility is worth investigated empirically. Here, we wonder if the response of fertility to an adverse shock depends on past fertility. To consider this possibility, we run an alternative empirical model in which the exposure variable is interacted with dummies indicating the number of children ever born. More specifically, we consider three dummies for mothers having respectively one child at the time of the exposure, two children or more than two children. Corresponding results are reported in Table 5. It is noteworthy that as before the inclusion of rainfall and temperature does not alter the coefficient associated to cyclonic exposure. The first row of the corresponding table can be interpreted as the effect of cyclonic exposure on

[39] The number of nine correspond to the 75% percentile of the corresponding distribution (see also Table 3).
[40] The estimated effect in cyclone prone area is significantly different from the effect in non-prone area at the 1% level.

	(1)	(2)
Max. wind in $t-1$	-0.0298***	-0.0313***
	(0.0018)	(0.0018)
Max. wind in $t-1$ × Having 1 child	0.0139***	0.0133***
	(0.0024)	(0.0024)
Max. wind in $t-1$ × Having 2 children	-0.0372***	-0.0378***
	(0.0025)	(0.0025)
Max. wind in $t-1$ × Having >2 children	-0.1059***	-0.1063***
	(0.0023)	(0.0023)
Rainfall in $t-1$	–	0.2104***
	–	(0.0156)
Temperature in $t-1$	–	0.4174*
	–	(0.2504)
Observations	1,025,443	1,025,443

Table 5: Regression results depending on the number of children ever born.

Sources: DHS, TCE-DAT of Geiger et al. (2018), CHIRPS dataset of Funk et al. (2015), CRU dataset of Harris et al. (2014), and authors' own calculations.

Notes: Significance levels: * 10%, ** 5%, *** 1%. Robust standard errors are in parentheses, adjusted for clustering at the DHS cluster level. All regressions include woman fixed effect, annual fixed effect, cluster fixed effect, country fixed effect and controls for rainfall and temperature in $t-1$. Maximum wind speed is measured in km/h, rainfall in hundreds of millimeters and temperature in Celsius degrees.

fertility for mothers having no baby at the time of the exposure. The corresponding coefficient is negative for both specification of the empirical model. We consistently witness negative marginal effects for each of the interaction terms suggesting that the fall in the likelihood of giving birth after an exposure to cyclone is a robust pattern. However, it should be observed that, even if it remains negative, the estimated impact of cyclonic exposure is significantly lower for mothers having one child at the time of exposure. Thus, for a cyclonic wind speed shock in t equivalent to a standard deviation, the likelihood of having a baby in $t+1$ decreases by -0.70 point for mothers having one child against -1.21 point for those having no child. For mothers having two children (resp. more than two children) the corresponding fall in mothers' likelihood of having birth in $t+1$ is equal to 2.78 points (resp. 5.34 points).[41] As anticipated, the marginal effect of cyclonic exposure on fertility depends on the number of children ever born and in general mothers with a large number of children ever born reduces more their fertility. However, one of the particularity of our results is about mothers having one child the likelihood of motherhood seems to be less sensitive to cyclonic exposure. This quite puzzling feature could reflect mothers preference for having at least two children for those having already one child.

Empirical evidence on working assumption 3:
The fertility response to cyclone shocks depends on the number of children ever born: mothers with at least two children reduce more their fertility after a cyclone shock.

5.2 Further results

In this subsection, we propose an in-depth analysis to investigate three potential features of the causal effect. First, we estimate a specification to test the existence of non-linearities in the effect. Second, we test whether the negative causal effect depends on mothers' past exposure to cyclones. Three, we include more lags in the baseline model to verify whether the causal effect persists. The results of these alternative estimations are reported in Tables 7 and 6. Note that the study of other heterogeneity dimensions together with robustness checks, which consist of changing the sample or the wind speed variable, are respectively reported in Appendix B and C.

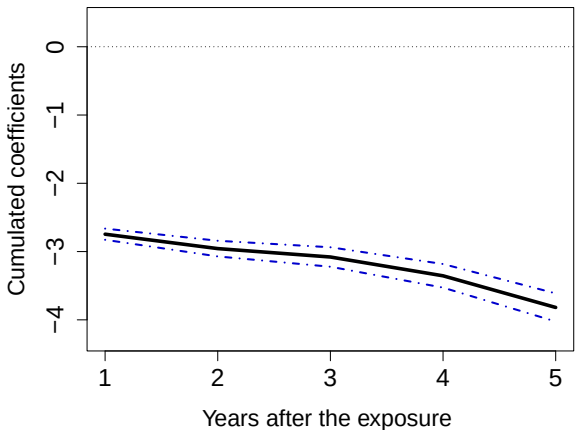

Figure 3: Cumulative effect of wind speed exposure on the likelihood of giving birth.
Sources: DHS, TCE-DAT of Geiger et al. (2018), CHIRPS dataset of Funk et al. (2015), CRU dataset of Harris et al. (2014), and authors' own calculations.
Notes: Black solid lines correspond to the cumulative sum of the estimated points, while blue error bands show the associated confidence intervals (at the 5% level of significance). The regression includes mother fixed effects (μ_i), time fixed effects (η_t), village fixed effects (θ_v), country fixed effects (α_c) controls for rainfall (from R_{t-1} to R_{t-5}) and mean temperature (from T_{t-1} to T_{t-5}).

5.2.1 Is the effect persistent over time?

In the baseline model, we include a lag of the exposure variable variable. Here, we reconsider the main specification by adding up to 5 lags of weather variables to the model.[42] The latter model allows us to investigate more precisely the medium-run effects of tropical cyclones on fertility. For illustrative purpose, we depict the cumulative effect of wind speed exposure on motherhood in Figure 3, while the coefficient values are provided in Table 11 of Appendix D.[43]

As shown in Figure 3, the effect of a tropical cyclone shock of one-standard deviation on the likelihood of giving birth persists over time. Furthermore, with a 5-year time frame, we do not observe any strong offsetting behavior, namely a strong positive effect of wind speed exposure for some lags. Table 11 of Appendix D shows that the estimated coefficients are all statistically negative. Exploring the distributed lag nature of this model, Figure 3 indicates that the cumulative effect of extra wind speed exposure amounts to $\sum_{l=0}^{L=5} \beta_l^W = -3.82$.[44]

[41] Each time, the estimated effect associated to the interaction term is significantly different from the effect for mothers having no children at the 1% level.

[42] Rainfall data are only available from 1981. We drop all observations prior to 1986, because it is not possible to obtain 5 lags of the rainfall variable before that year.

[43] We also illustrate the cumulative effects for rainfall and temperature shocks in Figures 4 and 5 of Appendix D.

[44] Regarding the other two weather variables, Figure 4 shows that when accounting for 5 lags, the negative effect of rainfall shocks persists during three years, whereas that of temperature shocks has a hump-shaped behavior.

	β_1^W	ω_1^W	ω_2^W	ω_3^W
Baseline	-0.0676***			
	(0.0014)			
Intensification	-0.0775***	0.0085***	0.0207***	0.0177***
	(0.0020)	(0.0024)	(0.0029)	(0.0027)

Table 6: Alternative specifications: Intensification.

Sources: DHS, TCE-DAT of Geiger et al. (2018), CHIRPS dataset of Funk et al. (2015), CRU dataset of Harris et al. (2014), and authors' own calculations.

Notes: Significance levels: * 10%, ** 5%, *** 1%. Robust standard errors are in parentheses, adjusted for clustering at the DHS cluster level. All regressions include, rainfall in $t-1$, temperature in $t-1$, as well as the four fixed effects. Maximum wind speed is measured in km/h, rainfall in hundreds of millimeters and temperature in Celsius degrees.

For the baseline row, we report the value of β_1^W.

Overall, extending the model to include more lags shows that the effect of tropical cyclone shocks has the potential to reduce permanently the probability of motherhood in the medium run as a non-reversal effect is observed.

5.2.2 Intensification mechanism

We now further test the hypothesis that the effect of cyclonic systems on female motherhood builds over time. Indeed, it is possible that the impact of a tropical cyclone shock in a given year t, as revealed by our panel estimate of equation (7), is magnified if the same woman has also been exposed to a tropical cyclone in the past few years (e.g., in $t-1$). Similar to Dell et al. (2014), we label this mechanism the intensification effect. We consider such a possibility by interacting wind speed exposure in a given period t with a dummy variable indicating that a given woman i has also been exposed to one, two or more than two tropical cyclones in the last 5 years before the exposure. Our set of dummy variables is denoted as $\tilde{W}_{i,t-l}$. The estimated equation now has the following form:

$$y_{itc} = \beta_1^W \times W_{i,t-1} + \beta_1^R \times R_{i,t-1} + \beta_1^T \times T_{i,t-1} + \sum_{j=1}^{J=3} \left(\omega_j^W \times \tilde{W}_{i,t-1}\right) + \mu_i + \eta_t + \theta_v + \alpha_c + u_{itcv}, \quad (8)$$

where ω_j^W are the parameters to be estimated and j the number of exposure during the past five years. Their interpretations differ from those of β_1^W. The latter corresponds to the effect of wind speed exposure in period $t-1$ on the current likelihood of motherhood. However, the second coefficient, namely ω_1^W, captures a different effect, namely the incremental effect of wind speed exposure on motherhood in period $t-1$ if the woman has additionally been exposed

	$\beta_1^{\tilde{w}^1}$	$\beta_1^{\tilde{w}^2}$	$\beta_1^{\tilde{w}^3}$	$\beta_1^{\tilde{w}^4}$	$\beta_1^{\tilde{w}^5}$	$\beta_1^{\tilde{w}^6}$
Baseline			-0.0676*** (0.0014)			
Non-linearities	-7.9307*** (0.1387)	-7.2436*** (0.2690)	-7.4471*** (0.4420)	-7.4507*** (0.5325)	-6.5088*** (0.7928)	-5.1767** (2.2655)

Table 7: Alternative specifications: Dummies for non-linearities.

Sources: DHS, TCE-DAT of Geiger et al. (2018), CHIRPS dataset of Funk et al. (2015), CRU dataset of Harris et al. (2014), and authors' own calculations.

Notes: Significance levels: * 10%, ** 5%, *** 1%. Robust standard errors are in parentheses, adjusted for clustering at the DHS cluster level. All regressions include, rainfall in $t-1$, temperature in $t-1$, as well as the four fixed effects. Maximum wind speed is measured in km/h, rainfall in hundreds of millimeters and temperature in Celsius degrees.

For the baseline row, we report the value of β_1^W.

to only one tropical cyclone during the five past years preceding the exposure. Consequently, the intensification parameters, namely ω_j^W, explore if the effect of a tropical cyclone shock depends on the pattern of previous shocks.

The last row of Table 6 explores the possibility of intensification effects by adding $\tilde{W}_{i,t-1}$ to the model. Overall, there is no evidence regarding the existence of an intensification mechanisms. The three ω_j^W are estimated to be significantly positive. This finding suggests that the impact of wind speed exposure in $t-1$ is dampened if between $t-2$ and $t-6$, the mother has also been exposed to tropical cyclones. Let us consider that before the exposure in $t-1$, the mother has been exposed to two tropical cyclones. In this case, the total effect of an extra wind speed exposure amounts to -0.0568 (namely, $\beta_1^W + \omega_2^W$).[45] All in all, the fact that the decrease in the probability of motherhood is lower for exposed mothers in a recent past echoes with the empirical evidence on working assumption 2: regularly exposed mothers appear to be less sensitive to cyclonic shock.

5.2.3 Non-linearities

Our baseline model implicitly assumes that the fertility response to tropical cyclone shocks is linear. However, the literature exploring the effect of weather shocks on economic variables often indicates that the effects are likely to be non-linear. In particular, Emanuel (2011) and Nordhaus (2010) suggest that damage due to tropical cyclones exponentially increases with the level of wind speed experienced on the ground. Despite such suggestions, it is not straightforward when other socioeconomic variables also respond non-linearly to wind

[45] For each coefficient, we check that the total effect is significantly different from β_1^W.

speed exposure, especially in a context when household micro-data is used. To reveal a possible non-linear relationship, we follow a non-parametric approach by breaking wind speed up into bins corresponding to the Saffir-Simpson scale. This approach has two main advantages. On the one hand, it is simple to implement. On the other, it is flexible and does not impose any functional forms on our wind speed explanatory variable. Hence, we construct six dummies equal to one when wind speed falls within the bin and zero otherwise. Specifically, $\tilde{w}_t^1 = 1(W_t \in [62; 118[)$, $\tilde{w}_t^2 = 1(W \in [118; 153[)$, $\tilde{w}_t^3 = 1(W \in [153; 177[)$, $\tilde{w}_t^4 = 1(W \in [177; 208[)$, $\tilde{w}_t^5 = 1(W \in [208; 251[)$, and $\tilde{w}_t^6 = 1(W \in [251; 300[)$.[46] We report the related results in Table 7.

Given the standard errors associated with point estimates, we cannot conclude that the post-fertility effect of the tropical cyclone shock is non-linear with maximum wind speeds. In particular, coefficients associated to the highest wind speed, namely $\beta_1^{\tilde{w}^6}$ is not significantly different from $\beta_1^{\tilde{w}^1}$. It should also be observed that coefficients' standard errors is increasing with the level of the Saffir-Simpson scale. This indicates that for the most extreme phenomenon the estimated effect between cyclonic exposure and fertility.[47] The linear approximation used in our baseline model appears as a relevant departure point.

6 Concluding remarks

The economic literature is still inconclusive about the direction of the effect of natural disasters on fertility. Theoretical models based on the quantity-quality approach of Becker (1960) as well as empirical estimates find both a positive and a negative association between the two phenomena. Given this disparity, our paper sought to respond to this question in the context of six developing countries regularly threatened by cyclonic systems. Our empirical strategy significantly improves the body of knowledge, because we exploit spatially geolocated household micro-data together with weather data that captures true cyclonic exposure at a high-resolution level (Geiger et al., 2018). Merging these two types of spatial data enables us to construct panel data to indicate whether a given mother gives birth in a specific period and whether she was exposed to cyclonic wind speeds. Our panel data allows us to retrieve the causal effect of tropical cyclone wind speed shocks while relying on a minimal set of identifying assumptions (Dell et al., 2014).

After presenting a theoretical model from which three working assumptions about the effect of cyclonic exposure and fertility are derived, we aim at providing empirical evidence

[46] Implicitly, the first bin $\tilde{w}_t^0 = 1(W_t \in [0; 62[)$ serves as reference in the regression.

[47] To further check the existence of a non-linear model, we run another regression with bins having the same amplitude. Again, we do not find any significant difference between coefficients associated to the highest and the lowest level of wind speed. Corresponding results are available upon request.

about these important questions. Improving the understanding of the links between cyclones and fertility is imperative in order to build appropriate public policy responses, particularly in poor countries. Our main results indicate that exposure to tropical cyclone wind speeds leads to a fall in the probability of giving birth, in line with the work of Pörtner (2014), Davis (2017), Norling (2022) but in contrast with the work of Cohan & Cole (2002), Hamilton et al. (2009), Evans et al. (2010) or Berlemann & Wenzel (2018). Heterogeneity analyses further suggest that the magnitude of the effect varies with the degree of exposure to cyclones associated to the household's living environment but also to the number of children ever born. First, in cyclone prone areas, the likelihood of giving birth reduce less, which suggests a process of adaptation in exposed populations. In that sense, our finding echoes with conclusions suggesting that human behaviors could adapt to climate change (Casey et al., 2019; Thiede et al., 2022). Second, mothers with at least two children reduce more their fertility after a cyclone shock. This result can also guide the design of public policies to respond to shocks by taking into account the family structure of the territory concerned, which could have an impact on demographic dynamics. Refinements of the main results indicate that the negative effect persists over time, while we find evidence that past exposure to cyclones imply a weaker decrease in fertility. However, our empirical model does not indicate non-linearities in the effect.

The panel estimates proposed in this paper are useful to highlight the fertility response to a tropical cyclone shock. In light of this, our estimates do not respond totally to how mothers adjust their fertility when the risk associated with tropical cyclones increases. This issue is of particular importance, since climate change has the potential to alter the frequency, genesis, spatial extent, and characteristics of the most extreme tropical cyclone events (Knutson et al., 2010; IPCC, 2019; Knutson et al., 2020). At this stage, even though our study found a negative response of fertility to cyclonic shocks, we cannot exclude the possibility that fertility could actually increase in response to tropical cyclone risks in the future. This is a further challenge for policy designers as climate change could also alter the opportunity cost of having babies. To deal with is, we believe that policy makers should engage in policies focusing the supply of family planning as well as those influencing the demand for fertility by reducing for instance household poverty and girl's school enrollment. We believe that such investigations could improve our understanding of the mechanisms explaining fertility behavior. This is, however, beyond the scope of this paper, although it is on our agenda for future research.

References

Aassve, A., Le Moglie, M., & Mencarini, L. (2021). Trust and fertility in uncertain times. *Population Studies*, 75(1), 19–36.

Abadie, A., Athey, S., Imbens, G. W., & Wooldridge, J. (2017). *When Should You Adjust Standard Errors for Clustering?* Working Paper 24003, National Bureau of Economic Research.

Alam, S. A. & Pörtner, C. C. (2018). Income shocks, contraceptive use, and timing of fertility. *Journal of Development Economics*, 131, 96 – 103.

Anttila-Hughes, J. & Hsiang, S. (2013). Destruction, disinvestment, and death: Economic and human losses following environmental disaster. *SSRN Electronic Journal*.

Arnberg, F. K., Eriksson, N.-G., Hultman, C. M., & Lundin, T. (2011). Traumatic bereavement, acute dissociation, and posttraumatic stress: 14 years after the ms estonia disaster. *Journal of traumatic stress*, 24(2), 183–190.

Azarnert, L. V. (2006). Child mortality, fertility, and human capital accumulation. *Journal of Population Economics*, 19, 285–297.

Banerjee, A. V. & Duflo, E. (2007). The economic lives of the poor. *Journal of Economic Perspectives*, 21(1), 141–168.

Banerjee, A. V. & Duflo, E. (2011). *Poor economics : a radical rethinking of the way to fight global poverty*. Public Affairs.

Barreca, A., Deschenes, O., & Guldi, M. (2018). Maybe next month? temperature shocks and dynamic adjustments in birth rates. *Demography*, 55, 1269–1293.

Becker, G. S. (1960). *An Economic Analysis of Fertility*, (pp. 209–240). Columbia University Press.

Becker, G. S. (1992). Fertility and the economy. *Journal of Population Economics*, 5(3), 185–201.

Berlemann, M. & Wenzel, D. (2018). Hurricanes, economic growth and transmission channels: Empirical evidence for countries on differing levels of development. *World Development*, 105, 231–247.

Bertinelli, L. & Strobl, E. (2013). Quantifying the local economic growth impact of hurricane strikes: An analysis from outer space for the caribbean. *Journal of Applied Meteorology and Climatology*, 52(8), 1688–1697.

Botzen, W. J. W., Deschenes, O., & Sanders, M. (2019). The economic impacts of natural disasters: A review of models and empirical studies. *Review of Environmental Economics and Policy*, 13(2), 167–188.

Buckles, K., Hungerman, D., & Lugauer, S. (2021). Is fertility a leading economic indicator? *The Economic Journal*, 131(634), 541–565.

Cain, M. (1983). Fertility as an adjustment to risk. *Population and Development review*, (pp. 688–702).

Carta, G., D'Alfonso, A., Colagrande, I., Catana, P., Casacchia, M., & Patacchiola, F. (2012). Post-earthquake birth-rate evaluation using the brief cope. *Journal of Maternal Fetal Neonatal Medecine*, 25(11), 2411–2414.

Casey, G., Shayegh, S., Moreno-Cruz, J., Bunzl, M., Galor, O., & Caldeira, K. (2019). The impact of climate change on fertility. *Environmental Research Letters*, 14(5), 054007.

CCR (2020). *Evolution du risque cyclonique en Outre-mer à horizon 2050*. Technical report, Caisse Centrale de Réassurance.

Cohan, C. L. & Cole, S. W. (2002). Life course transitions and natural disaster: marriage, birth, and divorce following hurricane hugo. *Journal of family psychology*, 16(1), 14.

Croissant, Y. & Millo, G. (2018). *Panel Data Econometrics with R*. John Wiley & Sons, Ltd.

Davis, J. (2017). Fertility after natural disaster: Hurricane mitch in nicaragua. *Population and Environment*, 4(38), 448–494.

Dell, M., Jones, B. F., & Olken, B. A. (2014). What do we learn from the weather? the new climate-economy literature. *Journal of Economic Literature*, 52(3), 740–98.

Deschênes, O. & Greenstone, M. (2011). Climate change, mortality, and adaptation: Evidence from annual fluctuations in weather in the us. *American Economic Journal: Applied Economics*, 3(4), 152–85.

Dessy, S., Marchetta, F., Pongou, R., & Tiberti, L. (2019). Fertility response to climate shocks. working paper or preprint.

Doepke, M. (2005). Child mortality and fertility decline: Does the barro-becker model fit the facts? *Journal of population Economics*, 18(2), 337–366.

Elliott, R. J., Strobl, E., & Sun, P. (2015). The local impact of typhoons on economic activity in China: A view from outer space. *Journal of Urban Economics*, 88, 50 – 66.

Emanuel, K. (2005). Increasing destructiveness of tropical cyclones over the past 30 years. *Nature*, (436), 686–688.

Emanuel, K. (2011). Global warming effects on u.s. hurricane damage. *Weather, Climate, and Society*, 3(4), 261–268.

Evans, R., Hu, Y., & Zhao, Z. (2010). The fertility effect of catastrophe: U.s. hurricane births. *Journal of Population Economics*, 23, 1–36.

Felbermayr, G. & Gröschl, J. (2014). Naturally negative: The growth effects of natural disasters. *Journal of Development Economics*, 111, 92 – 106. Special Issue: Imbalances in Economic Development.

Finlay, J. (2009). *Fertility Response to Natural Disasters The Case of Three High Mortality Earthquakes*. Policy Research Working Paper 4883, The World Bank.

Fomby, T., Ikeda, Y., & Loayza, N. V. (2013). The growth aftermath of natural disasters. *Journal of Applied Econometrics*, 28(3), 412–434.

Funk, C., Peterson, P., Landsfeld, M., Pedreros, D., Verdin, D., Shukla, S., Husak, G., Rowland, J., Harrison, L., Hoell, A., & Michaelsen, J. (2015). The climate hazards infrared precipitation with stations—a new environmental record for monitoring extremes. *Scientific Data*, 2(150066).

Geiger, T., Frieler, K., & Bresch, D. N. (2017). A global data set of tropical cyclone exposure (TCE-DAT). *GFZ Data Services*.

Geiger, T., Frieler, K., & Bresch, D. N. (2018). A global historical data set of tropical cyclone exposure (tce-dat). *Earth System Science Data*, 10(1), 185–194.

Gozgor, G., Bilgin, M. H., & Rangazas, P. (2021). Economic uncertainty and fertility. *Journal of Human Capital*, 15(3), 373–399.

Hamilton, B. E., Martin, J. A., Mathews, T., Sutton, P. D., & Ventura, S. J. (2009). The effect of hurricane katrina: births in the us gulf coast region, before and after the storm.

Hanappi, D., Ryser, V.-A., Bernardi, L., & Le Goff, J.-M. (2017). Changes in employment uncertainty and the fertility intention–realization link: An analysis based on the swiss household panel. *European Journal of Population*, 33, 381–407.

Harris, I., Jones, P., Osborn, T., & Lister, D. (2014). Updated high-resolution grids of monthly climatic observations – the cru ts3.10 dataset. *International Journal of Climatology*, 34(3), 623–642.

Hofmann, B. & Hohmeyer, K. (2013). Perceived economic uncertainty and fertility: Evidence from a labor market reform. *Journal of Marriage and Family*, 75(2), 503–521.

Holland, G. (1980). An analytic model of the wind and pressure profiles in hurricanes. *Monthly Weather Review*, (pp. 1212–1218).

Holland, G. (2008). A revised hurrican pressure-wind model. *Monthly Weather Review*, (pp. 3432–3445).

Hsiang, S. M. (2010). Temperatures and cyclones strongly associated with economic production in the caribbean and central america. *Proceedings of the National Academy of Sciences*, 107(35), 15367–15372.

ICF Macro (1998). *Madagascar Enquête Démographique et de Santé 1997*. Report, Institut National de la Statistique - INSTAT/Madagascar.

ICF Macro (2010). *Madagascar Enquête Démographique et de Santé 2008-2009*. Report, Institut National de la Statistique - INSTAT/Madagascar.

IPCC (2019). Special report on the ocean and cryosphere in a changing climate. In N. Weyer (Ed.), *In it together: why less inequality benefits all*: In press.

Klotzbach, P., Blake, E., Camp, J., Caron, L.-P., Chan, J. C., Kang, N.-Y., Kuleshov, Y., Lee, S.-M., Murakami, H., Saunders, M., Takaya, Y., Vitart, F., & Zhan, R. (2019). Seasonal tropical cyclone forecasting. *Tropical Cyclone Research and Review*, 8(3), 134 – 149. Special Issue for the 9th WMO International Workshop on Tropical Cyclones.

Knapp, K. R., Kruk, M. C., Levinson, D. H., Diamond, H. J., & Neumann, C. J. (2010). The international best track archive for climate stewardship (ibtracs). *Bulletin of the American Meteorological Society*, 91(3), 363–376.

Knutson, T., Camargo, S. J., Chan, J. C. L., Emanuel, K., Ho, C.-H., Kossin, J., Mohapatra, M., Satoh, M., Sugi, M., Walsh, K., & Wu, L. (2020). Tropical Cyclones and Climate

Change Assessment: Part II: Projected Response to Anthropogenic Warming. *Bulletin of the American Meteorological Society*, 101(3), E303–E322.

Knutson, T., McBride, J., Chan, J., Emanuel, K., Holland, G., Landsea, C., Held, I., Kossin, J., Srivastava, A. K., & Obersteiner, M. (2010). Tropical cyclones and climate change. *Nature Geoscience*, (3), 157–163.

Kochar, A. (1999). Smoothing consumption by smoothing income: Hours-of-work responses to idiosyncratic agricultural shocks in rural india. *The Review of Economics and Statistics*, 81(1), 50–61.

Kreyenfeld, M. (2010). Uncertainties in female employment careers and the postponement of parenthood in germany. *European sociological review*, 26(3), 351–366.

Kreyenfeld, M. (2015). Economic uncertainty and fertility. *Kölner Zeitschrift für Soziologie & Sozialpsychologie*, 67.

Kudamatsu, M. (2012). Has democratization reduced infant mortality in sub-saharan africa? evidence from micro data. *Journal of the European Economic Association*, 10(6), 1294–1317.

Kudamatsu, M., Persson, T., & Strömberg, D. (2012). *Weather and Infant Mortality in Africa*. CEPR Discussion Papers 9222, C.E.P.R. Discussion Papers.

Lee, R. & Mason, A. (2010). Fertility, human capital, and economic growth over the demographic transition. *European Journal of Population= Revue Europeenne de Demographie*, 26(2), 159.

LeGrand, T., Koppenhaver, T., Mondain, N., & Randall, S. (2003). Reassessing the insurance effect: A qualitative analysis of fertility behavior in senegal and zimbabwe. *Population and Development Review*, 29(3), 375–403.

Lindstrom, D. P. & Berhanu, B. (1999). The impact of war, famine, and economic decline on marital fertility in ethiopia. *Demography*, 36(2), 247–261.

Marchetta, F., Sahn, D. E., & Tiberti, L. (2019). The role of weather on schooling and work of young adults in madagascar. *American Journal of Agricultural Economics*, 101(4), 1203–1227.

Mincer, J. (1963). Market prices, opportunity costs, and income effects. *Measurement in economics*, (pp. 67–82).

Mohan, P. & Strobl, E. (2017). The short-term economic impact of tropical cyclone pam: an analysis using viirs nightlight satellite imagery. *International Journal of Remote Sensing*, 38(21), 5992–6006.

Morduch, J. (1995). Income smoothing and consumption smoothing. *Journal of Economic Perspectives*, 9(3), 103–114.

Nandi, A., Mazumdar, S., & Behrman, J. (2018). The effect of natural disaster on fertility, birth spacing, and child sex ratio: evidence from a major earthquake in india. *Journal of Population Economics*, 31, 267–293.

Nobles, J., Frankenberg, E., & Thomas, D. (2015). The effects of mortality on fertility: Population dynamics after a natural disaster. *Demography*, 52, 15–38.

Nordhaus, W. D. (2006). *The Economics of Hurricanes in the United States*. Working Paper 12813, National Bureau of Economic Research.

Nordhaus, W. D. (2010). The economics of hurricanes and implications of global warming. *Climate Change Economics*, 01(01), 1–20.

Norling, J. (2022). Fertility following natural disasters and epidemics in africa. *The World Bank Economic Review*, 36(4), 955–971.

Peduzzi, P., Chatenoux, B., Dao, H., Bono, A. D., Herold, C., Kossin, J., Mouton, F., & Nordbeck, O. (2012). Global trends in tropical cyclone risk. *Nature Climate Change*, 2, 289–294.

Pörtner, C. C. (2001). Children as insurance. *Journal of Population economics*, 14, 119–136.

Pörtner, C., C. (2014). *Gone With the Wind? Hurricane Risk, Fertility and Education*. Working paper, Seattle University.

R Core Team (2019). *R: A Language and Environment for Statistical Computing*. R Foundation for Statistical Computing, Vienna, Austria.

Ranjan, P. (1999). Fertility behaviour under income uncertainty. *European Journal of Population/Revue Européenne de Démographie*, 15, 25–43.

Robinson, W. C. (1986). High fertility as risk-insurance. *Population Studies*, 40(2), 289–298.

Schmidt, L. (2008). Risk preferences and the timing of marriage and childbearing. *Demography*, 45(2), 439–460.

Schultz, T. P. (1997). Chapter 8 demand for children in low income countries. volume 1 of *Handbook of Population and Family Economics* (pp. 349–430). Elsevier.

Sellers, S. & Gray, C. (2019). Climate shocks constrain human fertility in indonesia. *World Development*, 117, 357–369.

Skidmore, M. & Toya, H. (2002). Do natural disasters promote long-run growth? *Economic inquiry*, 40(4), 664–687.

Sobotka, T., Skirbekk, V., & Philipov, D. (2011). Economic recession and fertility in the developed world. *Population and development review*, 37(2), 267–306.

Strobl, E. (2011). The economic growth impact of hurricanes: Evidence from US coastal counties. *The Review of Economics and Statistics*, 93(2), 575–589.

Strobl, E. (2012). The economic growth impact of natural disasters in developing countries: Evidence from hurricane strikes in the central american and caribbean regions. *Journal of Development Economics*, 97(1), 130 – 141.

Tamura, Y. (2009). Wind-induced damage to buildings and disaster risk reduction. In *The Seventh Asia-Pacific Conference on Wind Engineering, November 8-12, 2009, Taipei, Taiwan*.

Thiede, B. C., Ronnkvist, S., Armao, A., & Burka, K. (2022). Climate anomalies and birth rates in sub-saharan africa. *Climatic Change*, 171(1-2), 5.

Vignoli, D., Bazzani, G., Guetto, R., Minello, A., & Pirani, E. (2020). Uncertainty and narratives of the future: A theoretical framework for contemporary fertility. *Analyzing contemporary fertility*, (pp. 25–47).

Vogl, T. S. (2016). Differential fertility, human capital, and development. *The Review of Economic Studies*, 83(1), 365–401.

Wang, Y., Gozgor, G., & Lau, C. K. M. (2022). Effects of pandemics uncertainty on fertility. *Frontiers in Public Health*, 10.

Willis, R. (1974). Economic theory of fertility behavior. In *Economics of the family: Marriage, children, and human capital* (pp. 25–80). University of Chicago Press.

Wooldridge, J. M. (2010). *Econometric Analysis of Cross Section and Panel Data*. The MIT Press.

Appendices

A Country-by-country regressions

	Bangladesh	Haïti	Cambodia	Madagascar	Philippines	Dominican Republic
	(1)	(2)	(3)	(4)	(5)	(6)
Max. wind in $t-1$	-0.0813***	-0.2314***	-0.2044***	-0.0271***	-0.0452***	-0.2392***
	(0.0056)	(0.0062)	(0.0075)	(0.0029)	(0.0022)	(0.0053)
Rainfall in $t-1$	-0.0783	0.2542***	-0.2107**	0.0352	0.0865***	-0.2156***
	(0.0746)	(0.0732)	(0.0912)	(0.0566)	(0.0290)	(0.0661)
Temperature in $t-1$	2.295	0.5763	-3.945	0.4324	4.893***	1.051
	(2.648)	(4.237)	(2.829)	(1.591)	(1.342)	(2.507)
Observations	70,266	184,742	185,876	166,238	187,823	230,498

Table 8: Country-by-country regression results

Sources: DHS, TCE-DAT of Geiger et al. (2018), CHIRPS dataset of Funk et al. (2015), CRU dataset of Harris et al. (2014), and authors' own calculations.

Notes: Significance levels: * 10%, ** 5%, *** 1%. Robust standard errors are in parentheses, adjusted for clustering at the DHS cluster level. All regressions include, woman fixed effect, annual fixed effect, cluster fixed effect and country fixed effect. Maximum wind speed is measured in km/h, rainfall in hundreds of millimeters and temperature in Celsius degrees.

B Exploring others heterogeneity dimensions

B.1 Differences in urban-rural

According to Kochar (1999), Evans et al. (2010), and Pörtner (2014), the occurrence of a cyclone modifies the shadow price of having an extra child, especially if couples live in areas that are more likely to be negatively impacted. In developing countries, a large share of the population lives in rural areas and depends on agricultural activities. As stressed by Dessy et al. (2019), the characteristics of economic life differ drastically in rural and urban areas. In rural areas, women contribute actively to agrarian activities, meaning that their labor supply is an important input of this production activity. By contrast, in urban areas, it is easier for women to diversify their activities, as they have greater employment opportunities in the service sector. Thus, in urban areas, women depend less on activities that may be damaged by tropical cyclone exposure unlike their rural counterparts engaged in agricultural activities. Consequently, it is likely that the opportunity cost of motherhood and raising children is less linked to tropical cyclone exposure in urban than in rural areas. To test this mechanism, we introduce another heterogeneity dimension into our econometric framework using interaction terms. We interact the wind speed variables with a dummy indicating if the household lives in a rural area.

The econometric model of column (1) of Table 9 show the corresponding estimates. Being exposed to tropical cyclone wind speed is associated with a greater decrease in the probability of giving birth in rural areas. The difference between the estimated marginal effects is significant.

	j = rural	j = low educated
Max. wind in $t-1$	-0.0614***	-0.0519***
	(0.0019)	(0.0016)
Max. wind in $t-1 \times (j=1)$	-0.0096***	-0.0279***
	(0.0023)	(0.0021)
Observations	1,025,443	1,025,443

Table 9: Cyclonic wind speed exposure for models including heterogeneity dimensions by interaction terms.

Sources: DHS, TCE-DAT of Geiger et al. (2018), CHIRPS dataset of Funk et al. (2015), CRU dataset of Harris et al. (2014), and authors' own calculations.

Notes: Significance levels: * 10%, ** 5%, *** 1%. Robust standard errors are in parentheses, adjusted for clustering at the DHS cluster level. All regressions include, rainfall in $t-1$, temperature in $t-1$, as well as the four fixed effects.

B.2 Differences by education

The last heterogeneity dimension that we explore involves interacting wind speed exposure with a dummy that indicates if the mother has a low level of education at the time of the interview. Indeed, we could conjecture that low-educated women have a greater chance of working in the agricultural sector compared to those with a high education level so that post-cyclone opportunity cost of having children could be higher. Correspond regression results are displayed in the second column of Table 9. As anticipated, the reduction in the likelihood of giving birth after a cyclone shock is higher of about 50% for mothers with a low level of education. More specifically, the total marginal effect amounts to 0.0798.

C Robustness analysis

Overall, the panel estimates presented in the main text reveal that a tropical cyclone shock leads to a significant fall in mothers' likelihood of giving birth. These findings could be sensitive to different choices when estimating the baseline model. To ensure that the main message of this paper holds true, we check for the robustness of our results along five dimensions: i) alternative formulations of the tropical cyclone variable, ii) the sample period, iii) the merging of geolocated data, iv) the inclusion of migrant mothers in our final sample, and v) the inclusion of cluster-specific time trends. Results of these alternative estimations are reported in Table 10.

Tropical cyclone variable An important robustness check is to establish whether the results are similar when alternative formulations of our measure of tropical cyclone exposure are used. We address this issue by considering two other measures of the tropical cyclone incidence.

More recently, rather than directly using the wind speed experienced by a given spatial unit, many papers construct ad-hoc indexes of potential destruction (also known as a damage function).[48] The reasoning behind such indexes follows Emanuel (2011). More specifically, below a certain threshold $\bar{W}$, it is unlikely that wind speed provokes substantial physical damage so that the level of physical destruction could be assumed to be zero. However, once the wind speed generated by the cyclonic system is above $\bar{W}$, the level of damage increases though in a non-linear fashion. To understand how such alternative measures of tropical cyclone exposure affect our conclusion, we run two other checks.

In the first one, we follow a similar strategy as Strobl (2012) and construct the following index of potential destruction:

$$D_{it} = W_{it}^{\lambda} \text{ if } W_{it} > \bar{W} \text{and zero otherwise} \tag{9}$$

When constructing D_{it}, two parameters are of importance, because they shape its functional form: λ, which corresponds to the parameter relating the maximum surface wind speed experienced to the level of damages, and $\bar{W}$, which is the threshold above which the level of destruction becomes perceptible. Different values of these two parameters have been proposed, although empirical evidence about them is scarce, especially for developing countries. In the US context, Emanuel (2005) suggests that the level of damage can be studied by the cubic value of the maximum wind speed at the surface. By contrast, Nordhaus (2006) suggests that

[48] Examples include Strobl (2011), Strobl (2012), Bertinelli & Strobl (2013), and Mohan & Strobl (2017).

destructiveness increases with the eighth power of maximum wind speed.[49] Concerning $\bar{W}$, Strobl (2012) and Bertinelli & Strobl (2013) set it to 177 km/h (the value above which a cyclonic system becomes category 3 on the Saffir-Simpson scale), while Mohan & Strobl (2017) select a value of 119 km/h (the value above which a cyclonic system becomes category 1 on the Saffir-Simpson scale). Without further evidence about these parameters, we choose $\lambda = 3$ as suggested by Emanuel (2005) and Strobl (2011), and we fix $\bar{W} = 93$ km/h as indicated by Emanuel (2011). Column (2) of Table 10 shows the results of this alternative estimation.

In the second check, we follow Emanuel (2011) and construct the following index f_{ct} to capture the proportion of damaged property:

$$f_{ct} = \frac{v_{ct}^3}{1 + v_{ct}^3} \tag{10}$$

with

$$v_{ct} = \frac{MAX\left(W_{ct} - \bar{W}, 0\right)}{W^* - \bar{W}}. \tag{11}$$

Where c denotes a cluster and W^* corresponds to the threshold at which half of buildings are damaged. Again, we lack strong empirical evidence when choosing an appropriate value for W^*. Here, as we fix $\bar{W}$ to 93 km/h, we set W^* to 166 km/h, namely the threshold of wind speed at which the RSMC of La Réunion labels a tropical system as "intense". Corresponding results are reported in column (3) of Table 10.

A closer inspection of columns (2)-(3) of Table 10 leads to a few comments. First, the qualitative patterns of our results are entirely preserved, since estimated coefficients for the two different measures of wind speed are all negative. Second, the observed quantitative patterns are broadly consistent with our baseline estimate, even if the non-linear nature of the wind speed variable of models has some interpretative incidence. Thus, for a level of destruction in $t-1$ equivalent to the standrad deviation of the damage function, the models of column (3) (resp. column (2)) indicates that a mother is 0.5 points (resp. 0.8) less likely to give birth in t. The negative effects are substantially higher when considering events with extreme wind speeds of 250 km/h. In particular, for such a level of exposure, the probability of motherhood falls by 6.1 points (resp. 12.8 points) for the index of potential destruction of equation (10) (resp. equation (9)). Regarding the use of a dummy variable, the model of column (2) suggests that being exposed to a tropical cyclone reduces the likelihood of childbearing by 28.97 points in t, 6.4 points in $t+1$, and 2.9 points in $t+2$.

Overall, the use of other measures of tropical cyclone exposure shows that our main result does not depend on the choice of the wind speed variable. The three alternative measures

[49] In the context of US coastal counties, Strobl (2011) uses an estimate of 3.17 for λ.

used in this section nevertheless have many limitations, since they either do not exploit the variability generated by W_{it} (model of column (2)) or rely on parameters for which the evidence is missing in the context of Madagascar (models of columns (3) and (4)). For this reason, our preferred specification directly uses the wind speed variable of Geiger et al. (2018).

	Baseline	Wind speed variable		With migrants	Sample period	
	(1)	(2)	(3)	(4)	(5)	(6)
β_1^W	-0.0676***	$-8.19e^{06}$***	-6.6639***	-0.0607***	-0.0666***	-0.0658***
	(0.0014)	($4.78e^{-07}$)	(0.4940)	(0.0010)	(0.0022)	(0.0019)
Obs.	1,025,443	1,025,443	1,025,443	1,785,137	526,822	498,621

Table 10: Alternative specifications: Robustness.

Sources: DHS, TCE-DAT of Geiger et al. (2018), CHIRPS dataset of Funk et al. (2015), CRU dataset of Harris et al. (2014), and authors' own calculations.

Notes: Significance levels: * 10%, ** 5%, *** 1%. Robust standard errors are in parentheses, adjusted for clustering at the DHS cluster level. All regressions include mother fixed effects (μ_i), time fixed effects (η_t), country fixed effects (α_c) cluster fixed effects (θ_v) controls for rainfall (R_{t-1}) and mean temperature (T_{t-1}).

The model of column (1) corresponds to the baseline model. The model of column (3) uses the index of potential destruction of equation (9) instead of the baseline wind speed variable. The model of column (3) uses the index of equation (10) instead of the baseline wind speed variable. The model of column column (4) corresponds to the estimation of the baseline estimate for a sample including migrant mothers. Results of columns (5) and (6) correspond to the models for the sample periods 1985-1997 and 1997-2015, respectively.

Sample restriction regarding migration In the main text, we present the results based on a sample of mothers who declared that they had always lived in their current home. We restrict our sample to non-migrant mothers to ensure that when iterating backwards, we retrieve only the true exposure to cyclones. Indeed, the risk when including migrant mothers is that cyclone exposure may be attributed to a woman who actually lived elsewhere at the time of the event. Furthermore, the DHS includes a variable that indicates the number of years of residence in the current home. However, as highlighted by Kudamatsu (2012), this declarative variable could be subject to a recall bias. For these two reasons, we exclude all migrant mothers in our baseline analysis. One potential pitfall of this sample restriction is that non-migrant and migrant mothers may differ with respect to the observable characteristics. In particular, we may suppose that non-migrant mothers are older than migrant mothers on average. In this robustness exercise, we consider another sample before re-estimating equation (7). In addition to non-migrant mothers, we include migrant mothers but keep only the observations after their arrival at their current home. Corresponding results can be found in column (4) of Table 10 and show no significant difference from the baseline estimates of the main text.

Sample period Implicitly, our baseline model assumes that the estimated effect is averaged over the entire sample under scrutiny. However, it is possible that the decision to have children changes over time. We address this possibility by separately estimating equation (7) for two sample periods. The first sample spans the 1985-1997 period, while the second one begins in 1985 and ends in 2015. Results are respectively reported in columns (5) and (6) of Table 10.

The main insight provided by these alternative panel estimations is that there is no significant difference in the causal effect of wind speed exposure among the two sub-periods.

D Model with 5 lags

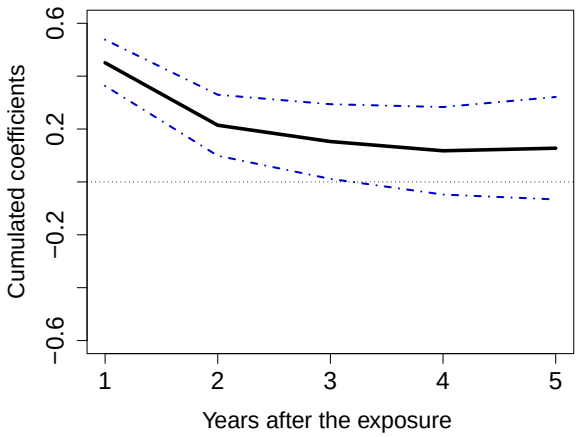

Figure 4: Cumulative effect of rainfall shocks on the likelihood of giving birth.
Sources: DHS, TCE-DAT of Geiger et al. (2018), CHIRPS dataset of Funk et al. (2015), CRU dataset of Harris et al. (2014), and authors' own calculations.
Notes: Black solid lines correspond to the cumulative sum of the estimated points, while blue error bands show the associated confidence intervals (at the 5% level of significance). The regression includes mother fixed effects (μ_i), time fixed effects (η_t), village fixed effects (θ_v), country fixed effects (α_c) controls for rainfall (from R_{t-1} to R_{t-5}) and mean temperature (from T_{t-1} to T_{t-5}).

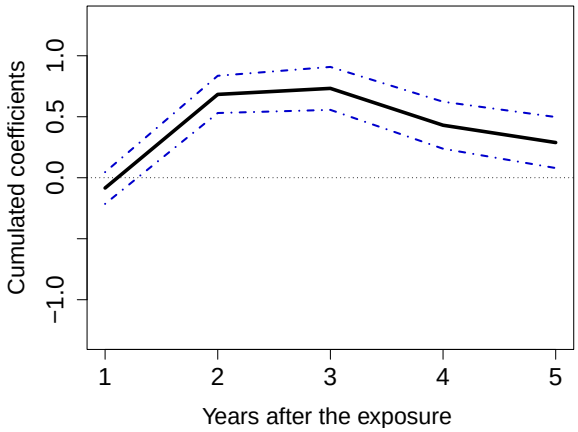

Figure 5: Cumulative effect of temperature shocks on the likelihood of giving birth.
Sources: DHS, TCE-DAT of Geiger et al. (2018), CHIRPS dataset of Funk et al. (2015), CRU dataset of Harris et al. (2014), and authors' own calculations.
Notes: Black solid lines correspond to the cumulative sum of the estimated points, while blue error bands show the associated confidence intervals (at the 5% level of significance). The regression includes mother fixed effects (μ_i), time fixed effects (η_t), village fixed effects (θ_v), country fixed effects (α_c) controls for rainfall (from R_{t-1} to R_{t-5}) and mean temperature (from T_{t-1} to T_{t-5}).

	β_1^W	β_2^W	β_3^W	β_4^W	β_5^W
Baseline	-0.0676***	-	-	-	-
	(0.0014)	-	-	-	-
Five lags	-0.0707***	-0.0054***	-0.0032***	-0.0071***	-0.0119***
	(0.0015)	(0.0012)	(0.0012)	(0.0012)	(0.0013)

Table 11: Alternative specifications: Varying the number of lags.

Sources: DHS, TCE-DAT of Geiger et al. (2018), CHIRPS dataset of Funk et al. (2015), CRU dataset of Harris et al. (2014), and authors' own calculations.

Notes: Significance levels: * 10%, ** 5%, *** 1%. Robust standard errors are in parentheses, adjusted for clustering at the DHS cluster level. All regressions include rainfall in $t-1$, temperature in $t-1$, as well as the four fixed effects. Maximum wind speed is measured in km/h, rainfall in hundreds of millimeters and temperature in Celsius degrees.

Conflict of interest statement:
The authors declare that they have no conflict of interest.

TEPP Working Papers 2021

21-1. On the heterogeneous impacts of the COVID-19 lockdown on US unemployment
Malak Kandoussi, François Langot

TEPP Working Papers 2020

20-8. COVID-19 mortality and health expenditures across European countries: The positive correlation puzzle
Serge Blondel, Radu Vranceanu

20-7. Measuring discrimination in the labour market
Emmanuel Duguet

20-6. The effects of age on educational performances at the end of primary school: cross-sectional and regression discontinuity approach applications from Reunion Island
Daniel Rakotomalala

20-5. Slowdown antitrust investigations by decentralization
Emilie Dargaud, Armel Jacques

20-4. Is international tourism responsible for the pandemic of COVID19? A preliminary cross-country analysis with a special focus on small islands
Jean-François Hoarau

20-3. Does labor income react more to income tax or means tested benefit reforms?
Michaël Sicsic

20-2. Optimal sickness benefits in a principal-agent model
Sébastien Ménard

20-1. The specific role of agriculture for economic vulnerability of small island spaces
Stéphane Blancard, Maximin Bonnet, Jean-François Hoarau

TEPP Working Papers 2019

19-8. The impact of benefit sanctions on equilibrium wage dispersion and job vacancies
Sebastien Menard

19-7. Employment fluctuations, job polarization and non-standard work: Evidence from France and the US
Olivier Charlot, Idriss Fontaine, Thepthida Sopraseuth

19-6. Counterproductive hiring discrimination against women: Evidence from French correspondence test
Emmanuel Duguet, Loïc du Parquet, Yannick L'Horty, Pascale Petit

19-5. Inefficient couples: Non-minimization of the tax burden among French cohabiting couples
Olivier Bargain, Damien Echevin, Nicolas Moreau, Adrien Pacifico

19-4. Seeking for tipping point in the housing market: evidence from a field experiment
Sylvain Chareyron, Samuel Gorohouna, Yannick L'Horty, Pascale Petit, Catherine Ris

19-3. Testing for redlining in the labor market
Yannick L'Horty, Mathieu Bunel, Pascale Petit

19-2. Labour market flows: Accounting for the public sector
Idriss Fontaine, Ismael Galvez-Iniesta, Pedro Gomes, Diego Vila-Martin

19-1. The interaction between labour force participation of older men and their wife: lessons from France
Idriss Fontaine

TEPP Working Papers 2018

18-15. Be healthy, be employed: a comparison between the US and France based on a general equilibrium model
Xavier Fairise, François Langot, Ze Zhong Shang

18-14. Immigrants' wage performance in the routine biased technological change era: France 1994-2012
Catherine Laffineur, Eva Moreno-Galbis, Jeremy Tanguy, Ahmed Tritah

18-13. Welfare cost of fluctuations when labor market search interacts with financial frictions
Elini Iliopulos, François Langot, Thepthida Sopraseuth

18-12. Accounting for labor gaps
François Langot, Alessandra Pizzo

18-11. Unemployment fluctuations over the life cycle
Jean-Olivier Hairault, François Langot, Thepthida Sopraseuth

18-10. Layoffs, Recalls and Experience Rating
Julien Albertini, Xavier Fairise

18-9. Environmental policy and health in the presence of labor market imperfections
Xavier Pautrel

18-8. Identity mistakes and the standard of proof
Marie Obidzinski, Yves Oytana

18-7. Presumption of innocence and deterrence
Marie Obidzinski, Yves Oytana

18-6. Ethnic Discrimination in Rental Housing Market: An Experiment in New Caledonia
Mathieu Bunel, Samuel Gorohouna, Yannick L'Horty, Pascale Petit, Catherine Ris

18-5. Evaluating the impact of firm tax credits. Results from the French natural experiment CICE
Fabrice Gilles, Yannick L'Horty, Ferhat Mihoubi, Xi Yang

18-4. Impact of type 2 diabetes on health expenditure: an estimation based on individual administrative data
François-Olivier Baudot , Anne-Sophie Aguadé,Thomas Barnay, Christelle Gastaldi-Ménager, Anne Fargot-Campagna

18-3. How does labour market history influence the access to hiring interviews?
Emmanuel Duguet, Rémi Le Gall, Yannick L'Horty, Pascale Petit

18-2. Occupational mobility and vocational training over the life cycle
Anthony Terriau

18-1. Retired, at last? The short-term impact of retirement on health status in France
Thomas Barnay, Eric Defebvre

TEPP Working Papers 2017

17-11. Hiring discrimination against women: distinguishing taste based discrimination from statistical discrimination
Emmanuel Duguet, Loïc du Parquet, Pascale Petit

17-10. Pension reforms, older workers' employment and the role of job separation and finding rates in France
Sarah Le Duigou, Pierre-Jean Messe

17-9. Healthier when retiring earlier? Evidence from France
Pierre-Jean Messe, François-Charles Wolff

17-8. Revisting Hopenhayn and Nicolini's optimal unemployment insurance with job search monitoring and sanctions
Sebastien Menard, Solenne Tanguy

17-7. Ethnic Gaps in Educational Attainment and Labor-Market Outcomes: Evidence from France
Gabin Langevin, David Masclet, Fabien Moizeau, Emmanuel Peterle

17-6. Identifying preference-based discrimination in rental market: a field experiment in Paris
Mathieu Bunel, Yannick L'Horty, Loïc du Parquet, Pascale Petit

17-5. Chosen or Imposed? The location strategies of households
Emilie Arnoult, Florent Sari

17-4. Optimal income taxation with composition effects
Laurence Jacquet, Etienne Lehmann

17-3. Labor Market Effects of Urban Riots: an experimental assessment
Emmanuel Duguet, David Gray, Yannick L'Horty, Loic du Parquet, Pascale Petit

17-2. Does practicing literacy skills improve academic performance in first-year university students? Results from a randomized experiment
Estelle Bellity, Fabrices Gilles, Yannick L'Horty

17-1. Raising the take-up of social assistance benefits through a simple mailing: evidence from a French field experiment
Sylvain Chareyron, David Gray, Yannick L'Horty

TEPP Working Papers 2016

16-8. Endogenous wage rigidities, human capital accumulation and growth
Ahmed Tritah

16-7. Harder, better, faster...yet stronger? Working conditions and self-declaration of chronic diseases
Eric Defebvre

16-6. The influence of mental health on job retention
Thomas Barnay, Eric Defebvre

16-5. The effects of breast cancer on individual labour market outcomes: an evaluation from an administrative panel
Thomas Barnay, Mohamed Ali Ben Halima, Emmanuel Duguet, Christine Le Clainche, Camille Regaert

16-4. Expectations, Loss Aversion, and Retirement Decisions in the Context of the 2009 Crisis in Europe
Nicolas Sirven, Thomas Barnay

16-3. How do product and labor market regulations affect aggregate employment, inequalities and job polarization? A general equilibrium approach
Julien Albertini, Jean-Olivier Hairault, François Langot, Thepthida Sopraseuth

16-2. Access to employment with age and gender: results of a controlled experiment Laetitia Challe, Florent Fremigacci, François Langot, Yannick L'Horty, Loïc Du Parquet, Pascale Petit

16-1. An evaluation of the 1987 French Disabled Workers Act: Better paying than hiring
Thomas Barnay, Emmanuel Duguet, Christine Le Clainche, Yann Videau

TEPP Working Papers 2015

15-10. Optimal Income Taxation with Unemployment and Wage Responses: A Sufficient Statistics Approach
Kory Kroft, Kavan Kucko, Etienne Lehmann, Johannes Schmieder

15-9. Search frictions and (in) efficient vocational training over the life-cycle
Arnaud Chéron, Anthony Terriau

15-8. Absenteeism and productivity: the experience rating applied to employer contributions to health insurance
Sébastien Ménard, Coralia Quintero Rojas

15-7. Take up of social assistance benefits: the case of homeless
Sylvain Chareyron

15-6. Spatial mismatch through local public employment agencies. Answers from a French quasi-experiment
Mathieu Bunel, Elisabeth Tovar

15-5. Transmission of vocational skills at the end of career: horizon effect and technological or organisational change
Nathalie Greenan, Pierre-Jean Messe

15-4. Protecting biodiversity by developing bio-jobs: A multi-branch analysis with an application on French data
Jean De Beir, Céline Emond, Yannick L'Horty, Laetitia Tuffery

15-3. Profit-Sharing and Wages: An Empirical Analysis Using French Data Between 2000 and 2007
Noélie Delahaie, Richard Duhautois

15-2. A meta-regression analysis on intergenerational transmission of education: publication bias and genuine empirical effect
Nicolas Fleury, Fabrice Gilles

15-1. Why are there so many long-term unemployed in Paris?
Yannick L'Horty, Florent Sari

TEPP Working Papers 2014

14-14. Hiring discrimination based on national origin and the competition between employed and unemployed job seekers
Guillaume Pierné

14-13. Discrimination in Hiring: The curse of motorcycle women
Loïc Du Parquet, Emmanuel Duguet, Yannick L'Horty, Pascale Petit

14-12. Residential discrimination and the ethnic origin: An experimental assessment in the Paris suburbs
Emmanuel Duguet, Yannick L'Horty, Pascale Petit

14-11. Discrimination based on place of residence and access to employment
Mathieu Bunel, Yannick L'Horty, Pascale Petit

14-10. Rural Electrification and Household Labor Supply: Evidence from Nigeria
Claire Salmon, Jeremy Tanguy

14-9. Effects of immigration in frictional labor markets: theory and empirical evidence from EU countries
Eva Moreno-Galbis, Ahmed Tritah

14-8. Health, Work and Working Conditions: A Review of the European Economic Literature
Thomas Barnay

14-7. Labour mobility and the informal sector in Algeria: a cross-sectional comparison (2007-2012)
Philippe Adair, Youghourta Bellache

14-6. Does care to dependent elderly people living at home increase their mental health?
Thomas Barnay, Sandrine Juin

14-5. The Effect of Non-Work Related Health Events on Career Outcomes: An Evaluation in the French Labor Market
Emmanuel Duguet, Christine le Clainche

14-4. Retirement intentions in the presence of technological change: Theory and evidence from France
Pierre-Jean Messe, Eva Moreno-Galbis, Francois-Charles Wolff

14-3. Why is Old Workers' Labor Market more Volatile? Unemployment Fluctuations over the Life-Cycle
Jean-Olivier Hairault, François Langot, Thepthida Sopraseuth

14-2. Participation, Recruitment Selection, and the Minimum Wage
Frédéric Gavrel

14-1. Disparities in taking sick leave between sectors of activity in France: a longitudinal analysis of administrative data
Thomas Barnay, Sandrine Juin, Renaud Legal

TEPP Working Papers 2013

13-9. An evaluation of the impact of industrial restructuring on individual human capital accumulation in France (1956-1993)
Nicolas Fleury, Fabrice Gilles

13-8. On the value of partial commitment for cooperative investment in buyer-supplier relationship
José de Sousa, Xavier Fairise

13-7. Search frictions, real wage rigidities and the optimal design of unemployment insurance
Julien Albertini, Xavier Fairise

13-6. Tax me if you can! Optimal nonlinear income tax between competing governments
Etienne Lehmann, Laurent Simula, Alain Trannoy

13-5. Beyond the labour income tax wedge: The unemployment-reducing effect of tax progressivity
Etienne Lehmann, Claudio Lucifora, Simone Moriconi, Bruno Van Der Linden

13-4. Discrimination based on place of residence and access to employment
Mathieu Bunel, Emilia Ene Jones, Yannick L'Horty, Pascale Petit

13-3. The determinants of job access channels: evidence from the youth labor market in France
Jihan Ghrairi

13-2. Capital mobility, search unemployment and labor market policies: The case of minimum wages
Frédéric Gavrel

13-1. Effort and monetary incentives in Nonprofit et For-Profit Organizations
Joseph Lanfranchi, Mathieu Narcy

The TEPP Institute

The CNRS **Institute for Theory and Evaluation of Public Policies** (the TEPP Institute, FR n°2024 CNRS) gathers together research centres specializing in economics and sociology:

- L'**Equipe de Recherche sur l'Utilisation des Données Individuelles en lien avec la Théorie Economique** (Research Team on Use of Individuals Data in connection with economic theory), **ERUDITE**, University of Paris-Est Créteil and University of Gustave Eiffel
- Le **Centre d'Etudes des Politiques Economiques de l'université d'Evry** (Research Centre focused on the analysis of economic policy and its foundations and implications), **EPEE**, University of Evry Val d'Essonne
- Le **Centre Pierre Naville** (Research on Work and Urban Policies), **CPN**, University of Evry Val d'Essonne
- Le **Groupe d'Analyse des Itinéraires et des Niveaux Salariaux** (Group on Analysis of Wage Levels and Trajectories), **GAINS**, University of Le Mans
- Le **Centre de Recherches en Economie et en Management**, (Research centre in Economics and Management), **CREM**, University of Rennes 1 et University of Caen Basse-Normandie
- Le **Groupe de Recherche ANgevin en Économie et Management** (Angevin Research Group in Economics and Management), **GRANEM**, University of Angers
- Le **Centre de Recherche en Economie et Droit** (Research centre in Economics and Law) **CRED**, University of Paris II Panthéon-Assas
- Le **Laboratoire d'Economie et de Management Nantes-Atlantique** (Laboratory of Economics and Management of Nantes-Atlantique) LEMNA, University of Nantes
- Le **Laboratoire interdisciplinaire d'étude du politique Hannah Arendt** – Paris Est, **LIPHA-PE**
- Le **Centre d'Economie et de Management de l'Océan Indien**, **CEMOI**, University of La Réunion

TEPP brings together 230 teacher-researchers and 100 doctoral students. It is both one of the main academic operators in the evaluation of public policies in France, and the largest multidisciplinary federation of research on work and employment. It responds to the demand for impact assessment of social programs using advanced technologies combining theoretical and econometric modeling, qualitative research techniques and controlled experiences.

www.tepp.eu

Chapitre 12

The effect of cyclone shocks on child marriage : Evidence from developing countries

Ba, Fontaine, Garabedian

- ***World Development***, en soumission, 2023
- ***Présentation :***
  Seminaire IRMAPE, ESC Pau Business School, 2022

The effect of cyclone shocks on child marriage: Evidence from developing countries *

Ba Mamoudou † Fontaine Idriss‡ Garabedian Sabine§

Abstract

The negative consequences of child marriage have been widely discussed in the literature. It is associated with poor outcomes in terms of education, health, and self-empowerment. In this study, we analyze geo-located household panel data combined with wind field data generated by ground-based cyclone systems to assess the impact of cyclone shocks on child marriage. We find that after negative cyclone shocks, in countries where dowry payments are common, child marriage is delayed in the sample of girls aged 12-18 to meet dowry payment requirements. We do not observe such reductions in marriage for girls of marriageable age. These results are robust to a number of robustness and sensitivity checks on other measures of ground wind speed. A thorough understanding of how marriage institutions work would be central to designing effective policies.

Keywords: Cyclone shocks; Child marriage; Developing countries

*We gratefully acknowledge the financial support from the European Fund for Economic and Regional Development (EFERD) and the *Region Réunion*.

†Research Engineer, CEMOI, University of Reunion, France. E. Mail :mamoudou.ba@univ-reunion.fr

‡Department of Economics (CEMOI), Université de La Réunion; E-mail: idriss-fontaine@univ-reunion.fr

§Department of Economics (CEMOI), Université de La Réunion; E-mail: sabine.garabedian@univ-reunion.fr

1 Introduction

The economic consequences of tropical cyclones in developing countries have recently received increased attention from development and policy researchers (Sekhri and Debnath, 2014; Takasaki, 2011; World Bank, 2021; WFP, 2022). In recent decades, the phenomenon has intensified with more destructive effects associated with considerable economic losses that are responsible for economic fluctuations at the national level. The situation is further accentuated due to the large increase in the population living in coastal areas (Bank and Nations, 2010). By their destructive nature, tropical cyclones pose a serious threat to the economy and lives of people in the short and long term in developing countries. There is a substantial literature on the relationship between tropical cyclones and economic growth (Elliott et al., 2015; Hsiang and Jina, 2014; World Bank, 2017). The consensus of the literature is that it is low-income countries that are severely affected by disasters due to the risk of exposure of their populations and their low adaptive capacity resulting from the lack of financial markets. For economies with a large agricultural sector, this problem is more pronounced. The lack of mechanisms leads rural households to adopt a wide range of individual responses to smooth their consumption over time and insure against future negative shocks (Hoogeveen et al., 2011). The consequences of natural shocks are most visible among women and children, the most vulnerable members, and result in high poverty, malnutrition, morbidity and domestic violence. The destruction of agricultural assets can lead to short-term responses that have long-term consequences for welfare development (Dessy et al., 2019).

Our article focuses on these short-term responses with an emphasis on child marriage, a coping mechanism commonly used after a natural disaster. According to the latest estimates from the United Nations Children's Fund (UNICEF), 21 percent of women worldwide are married before the age of 18. Child marriage is associated with very different demographic outcomes and economic opportunities for women and their children, with negative consequences for education, fertility, income, labor force participation, and decision making (World Bank, 2021; Unicef et al., 2014; Nguyen and Wodon, 2015). Although eliminating

child marriage is part of the Sustainable Development Goals and is prohibited by law in many developing countries, it remains relatively widespread in South Asia, sub-Saharan Africa, and the Caribbean. These regions also share high levels of exposure to natural disasters and weak climate change mitigation policies. There is very little data on the determinants of early marriage and how natural disasters affect the marriage behavior of women in developing countries, due to the scarcity of official and accurate data. For example, the only empirical studies on the topic are conducted by Corno et al. (2020), which found that rainfall variations have an impact on child marriage and that this effect depends on the direction of dowry payment at the time of marriage. Another study by Tsaneva (2020) revealed that climate variability affects child marriage through reduced income from agricultural production. However, the effects attributed to cyclonic events may be higher because of the significant economic losses to populations from the intensity of destruction resulting from their extreme and sudden nature. After the passage of a tropical cyclone, the context of household life could change radically because of the destruction of assets such as houses, agricultural production, livestock, etc. This situation can therefore change the behavior and timing of marriage of women and children. Families could lead to marry their daughters at a young age mainly for socio-economic and cultural reasons. In all cases, the reasons are generally similar across countries, and the direction of dowry payments depends on customs. In countries where dowry payments are common, adverse shocks may reduce the likelihood that children will marry, in part because the girl's family is unable to meet dowry requirements and honor payments.

To do this, we use two databases: the Demographic and Health Survey (DHS) and the Tropical Cyclone Exposure Database (TCE-DAT) from the Geiger et al. (2018). The advantage of the former is that it provides comprehensive information on individual household members' characteristics and accurate geographic information. The second provides geographic wind field information for over 2,700 cyclone systems worldwide with high accuracy over the period 1950-2015. By merging the geographic information from the DHS data history

and the tropical cyclone data (TCE-DAT), we obtain a panel of tropical cyclone exposure data for girls over the period 1981-2015. Applying a linear regression and controlling the model with fixed effects of education, religion, and geographic characteristics. We find that natural disasters are negatively associated with the probability that girls will marry between the ages of 12 and 17. The effect is not significant for girls aged 12-24. The dependence of household income on agriculture is the main possible vector through which natural shocks affect girls' marriage. In a downturn, households are unable to meet the demand for dowries, which reduces the likelihood of child marriage. This result further validates dependence on agriculture as a mechanism for the effect of cyclone shocks on child marriage.

This analysis makes an important contribution to the literature on the impact of cyclone shocks on child marriage and provides useful tools for policymakers and international organizations prioritizing marriage reduction in disaster-prone developing countries. These findings are also linked to a large parallel literature on metrological shocks and marriage behavior in developing countries. Recent empirical studies have highlighted the positive or negative effects of shocks on marriage behavior (e.g., Chowdhury et al., 2020; Asadullah and Wahhaj, 2019; Corno et al., 2016; Trinh and Zhang, 2021; Tsaneva, 2020). Authors have attempted to explain marriage behavior and weather events, which vary randomly over time in a given spatial area. Yet, none of these studies have addressed the potential impacts of cyclonic events on marriage behavior, despite the fact that tropical cyclones are the leading cause of economic losses due to natural disasters in these regions of the world (Dell et al., 2014; Bakkensen and Barrage, 2018; Krichene et al., 2021; Berlemann and Wenzel, 2018). To overcome these ambiguities, we propose an empirical approach that first estimates the impact of cyclones on the determinants of marriage while accounting for the weather variables used in previous studies. To our knowledge, this is the first and only study to quantify the effects of cyclone shocks on child marriage as a short-term coping strategy. We consider the causal effect of tropical cyclone shocks on the probability of child marriage as a function of individuals' random exposure to tropical cyclones and that the main channel through which

this impact occurs is agriculture on which farm incomes depend (Strobl, 2012a; Berlemann and Wenzel, 2018; Hsiang and Jina, 2014). By exploiting annual variations in wind speed experienced by individuals in the field, we identify their causal effects by controlling for individual and time fixed effects to mitigate problems of unobserved heterogeneity among girls. We use binary variables that correspond to wind speed intensity as a measure of tropical cyclone exposure on the ground. The study also sheds light on a still insufficiently understood area of economic strategies adopted by farm households to cope with the intensity of cyclone shocks. The study shows the differential effects on the marriage of adolescent girls and young women of marriageable age, and how households adapt by delaying early marriage to avoid the high cost of payments and the problems of regularizing endowments. This mechanism allows them to maintain a level of consumption in a post-cyclone period.

The remainder of the paper is organised as follows. Section 2 briefly presents an overview of the cyclone situation and resulting damages in developing countries. Section 3 presents the empirical model, defines the variables used and the data set employed. Section 4 reports the results and discusses the various implications of these results. Section 5 concludes.

2 Contextual background

2.1 The prevalence marriage in developing countries

The importance of child marriage today stems from the fact that it is part of developing countries' millennial Sustainable Development Goals (SDGs) for gender equality. Since 1980, more than half of these countries have passed laws prohibiting or limiting marriage before the age of 18 (Kim et al., 2013). According to Unicef et al. (2014), more than 700 million women alive today were married before they turned 18. South Asia is home to nearly half (42 percent) of the world's child marriages, with Bangladesh having the highest prevalence of child marriages in the world and India accounting for one-third of the global total respectively.

Although laws are in place in these countries, they often have little effect on the number of girls married before the age of 18, which has been steadily increasing for several decades. In Latin America and the Caribbean, among young women aged 20 to 24, 21.5 percent have married before the age of 18 (Unicef et al., 2022). For example, Haiti has a prevalence rate of 14.9 percent among this same population. In Eastern and Southern Africa, prevalence is 32 percent, with Madagascar having the highest prevalence (40 percent). The particularity of countries with a high prevalence of marriage is that they have a large rural population and that agriculture is the mainstay of the economy.

2.2 The effect of the cyclone destruction on economic activity

These regions are particularly exposed to natural disasters, but also in terms of the populations affected, since they are home to the poorest populations in the world. The damage caused by extreme natural disasters is becoming relatively important for several, and in particular tropical cyclones, whose intensity increases with time (Mendelsohn et al., 2012). More recently, to mention only a few countries affected by cyclones. For example, we have in the Southeast Asian region, the Philippines, were hit by the massive Typhoon Rai in 2022, which affected more than 7 million people and caused losses of $215 million in crops and farmland (about 420,000 hectares), $58 million in the fisheries sector, and $330 million in damage to homes, roads, power lines and water (OXFAM, 2022). In Timor Leste, Tropical Cyclone Seroja in April 2021 caused widespread flooding, landslides, damage to critical infrastructure, livestock, and crops, costing over $420 million. According to the report Learning from Tropical Cyclone Seroja: Building Disaster and Climate Resilience in Timor-Leste, losses in the agricultural sector are estimated at more than US$15.7 million, and losses at more than US$13.1 million. Total damage to the housing sector is estimated at US$ 60.3 million. Damage to roads and bridges is estimated at US$170 million (World Bank, 2021). In the Carabbian region, in 2008 alone, tropical storms and hurricanes caused losses estimated at 15 percent of the region's GDP. Nearly 50 percent of the damage and losses to the produc-

tive sectors were concentrated in the agricultural sector. In Haiti, Hurricane Matthew in 2016 caused coastal flooding, and the rainfall resulted in heavy flooding, landslides, and the destruction of much infrastructure, agricultural crops, and natural ecosystems. It inflicted damage and losses on Haiti estimated at the equivalent of 22 percent of GDP. It affected more than 2 million people, or about 20 percent of the Haitian population, mainly in the poorest regions of the country. The agriculture and housing/urban sectors were the hardest hit, with up to 90 percent of crops and livestock lost in some areas. Thousands of structures were damaged, and critical roads and bridges were washed away (World Bank, 2017).

2.3 Motivation

Overall economic performance influences marriage decisions and marriage markets, particularly in developing countries, where marriage is often regulated by traditional customary practices. Dowries are a key feature of the marriage market, being transfers of wealth between families at the time of marriage. Traditionally, financial transactions are made by the bride's family in the form of money or property that plays a key role in negotiating the marriage contract (Khanal and Sen, 2020). Financial transfers related to the dowry can often be several times the income of the bride's family. The timing and companions for the wedding are primarily decided by family members (Anukriti et al., 2022). Despite the fact that the majority of countries involved have passed a number of laws to delay the time of marriage for girls, the practice remains common in developing countries with harmful consequences. Much of the literature argues that it is associated with psychological, health, and educational risks such as low educational attainment, lower social status in their husband's family, low labor force participation, exclusion from household decision-making, and greater vulnerability to domestic violence (Arthur et al., 2018; Field and Ambrus, 2008; Parsons et al., 2015).

In recent decades, a number of research studies have identified some of the factors of child marriage, such as household socioeconomic status, cultural, religious, and social norms (An-

derson, 2007; Munshi, 2017; Nguyen and Wodon, 2015; Rao, 1993). From a socioeconomic perspective, poverty is considered a primary cause of child marriage in the majority of poor countries. Child marriage can be an important source of wealth and investment opportunities for poor families. In countries where dowry prevails, the amount of dowry depends not only on the wealth of the bride's family, but also on the social status and education of the groom that brides will be willing to pay for these qualities (Anderson, 2007; Munshi, 2017). Sometimes, brides must pay huge sums of money to acquire a husband, resulting in great vulnerability of the bride's parents (Botticini and Siow, 2003). However, this dowry voluntarism is often exacerbated by the high population growth experienced in these countries, leading to a surplus of women in the marriage market that is a major factor in speculation (Edlund, 2006; Rao, 1993). Despite the economic benefits that drive parents to marry off their daughters at a younger age, these benefits only serve the short-term interests of the daughters since most of these financial transactions are for current consumption rather than long-term investment.

From a sociocultural perspective, young brides are perceived as having greater sexuality and a longer fertility period (McNulty et al., 2016; Dhamija and Roychowdhury, 2020). Child marriage is strongly linked to traditional and religious beliefs in which marriage is often seen as a way to avoid premarital sex, which leads to family dishonor (Anderson, 2007; Nguyen and Wodon, 2015). Social and cultural norms determine the age at which girls are expected to marry or to whom she marries, negatively influence girls' education and women's participation in the labor market (Jensen and Thornton, 2003; Parsons et al., 2015). Although the practice of child marriage has been greatly reduced with the Sustainable Development Goals in developing countries, it remains commonly practiced after natural disasters (Lnu et al., 2020). The literature on cyclone disasters focuses primarily on the economic consequences at the global level (Strobl, 2012b; Hsiang and Jina, 2014; Krichene et al., 2021; World Bank, 2021, 2017). Research on how cyclones affect vulnerable groups is relatively less documented. Communities that rely on natural resources for food and livelihoods are extremely vulnera-

ble to climate change and its impacts. Natural disasters adversely affect people, especially the poor (Porter, 2012; Ba and Mughal, 2022). To ensure a good level of well-being in an environment marked by natural disasters, households adopt expenditure reduction choices related to food, health and education (Mottaleb et al., 2015). This rationing of expenditures is often less beneficial for women and children, whose ability to adapt to disasters is often limited by their socioeconomic status, localized social norms and practices (Asadullah and Wahhaj, 2019). Girls are considered burdens, deprived of any form of income generation and inheritance rights (Asadullah and Wahhaj, 2019; Chowdhury, 2004). Thus, households may resort to early child marriage as an individual coping strategy to ease short-term financial constraints. Frequent natural disasters such as cyclones may prompt households to rush or delay the marriage of their daughters according to customary norms. Transactions made at the wedding ceremony may alleviate financial constraints or save the dowry costs associated with marrying at a later age. In either case, it transfers the risk of wealth loss and reduces the economic burden of maintaining daughters during a period of resource scarcity after a disaster. As a result, the decision to marry or delay marriage is more likely to be made by households with low adaptive capacity.

3 Data and Descriptive statistics

3.1 Demographic and Health Survey

We use DHS surveys to analyze the effect of cyclones on the prevalence of child marriage in frequently affected countries. DHS surveys are provided by the U.S. Agency for International Development (USAID) and various international and national support partners. They collect data on household characteristics, health, and nutrition, and provide GPS coordinates of household clusters. The sample for each wave of DHS consists of a number of clusters containing a defined number of households that are randomly selected. Each selected cluster

provides geographic information about its centroid, the actual location of which is approximately ten kilometers away. During each phase of the survey, a questionnaire is administered to women aged 15-49, containing information such as marital status, education level, number of children. Data from each woman's marriage history allows us to retrieve retrospective information on the month, year and age at which the woman married. In our research, we apply certain restrictions to our sample. Among these, we use women's marriage history for all survey waves for which GPS coordinates were available at the time of the study. Clusters are composed primarily of villages for rural households or urban neighborhoods for urban households. To reduce the potential selection bias resulting from the omission of never-married women, we restrict our sample to only those women aged 25-49 at the time of the interview. We set the cut-off age for marriage at 12 years, although the minimum age in our sample is lower than 12 years to be consistent with the literature. This age is assumed to correspond to the age of first menstruation and the age at which girls are most likely to marry in developing countries (Maertens, 2013; Field and Ambrus, 2008). The main analysis is restricted to those who have always lived in the same place of residence to ensure that a given woman was exposed to a given shock in a given year (Kudamatsu, 2012). Among those exposed to tropical cyclones, the countries and survey waves selected after the above restrictions are Bangladesh (2000, 2004, 2007), Cambodia (2000, 2005), Haiti (2006, 2016), India (2014), Madagascar (1997, 2008), Philippines (2003, 2008, 2017), and Timor-Leste (2009, 2016). From this history, we construct a panel of data on women and define a binary variable indicating whether the woman is married or not in a given year. Ultimately, the women in our sample were born between 1957 and 1992 and live in rural areas. Table 1 shows the summary statistics of the individual sample, it has on average that women married after the age of 18. About 69.6 percent of women married between the ages of 12 and 24, and 28.1 percent of women married before the age of 18. We then combine household location information with tropical cyclone information to retrieve wind speed exposure experienced by residents in the field, but also rainfall and temperature location information. Finally, the

sample countries in this study were chosen because of their recurrent exposure to cyclonic disasters. They have large rural poor populations and a low degree of impact of climate change mitigation policies. Due to the lack of formal strategies to find a source of income diversification, it is likely that households take a step to reduce consumption expenditures by downsizing through child marriage.

Table 1: Summary statistics for the unique individual sample

Variable	Obs	Mean	Std. Dev.
Women's age	63,693	35.329	7.29
Years of education	63,667	4.986	5.074
Household members	63,693	5.761	2.445
Number of children 5 and under	63,693	0.818	0.974
Share of women married between 12 and 24	63,693	0.696	0.459
Share of women married between 12 and 17	63,693	0.281	0.449

3.2 Tropical cyclone and climatic data

To estimate the wind exposure of tropical cyclones, we rely on the TCE-DAT database of Holland (2008). Computational velocity estimates on a 0.1 × 0.1 degree grid covering the world's landmass for the period 1950 -2015. The TCE-DAT provides estimates of population and property exposure with sustained wind speeds of at least 34 knots (kn) over land (Knapp et al., 2010). These estimates reflect the intensity of exposure to the cyclonic wind by estimating the damage sustained or people affected Holland (2008). The choice of this basis has a significant advantage in combining the set of country panels affected by cyclonic disasters, measuring from exposure to wind speed experienced by affected populations on the ground robust in time and space. Geiger et al. (2018) calculate an estimate of the maximum surface wind speed over the lifetime of each spatial location for over 2,700 cyclonic systems that made landfall between 1950 and 2015. To construct this database, tropical cyclone exposure is calculated from tropical cyclone tracks generated using a wind field model Holland (2008). More precisely, they implement the revised hurricane pressure-wind model in which the maximum surface wind speed W in $m.s^{-1}$ (for a given pixel) at radial distance r of the center of a given cyclonic system is defined as follows:

$$C = \left(\frac{b_s}{\rho e} \Delta p \left(\frac{r}{r_m} \right) \right)^{0.5}, \tag{1}$$

where ρ is the surface air density in $kg.m^{-3}$, e the base of natural logarithms, and Δp the pressure drop at the cyclone center in hPa as a function of r and r_m (radius of maximum winds). Parameter b_s depends on Δp, the temporal intensity change in pressure, the absolute value of the latitude, and the tropical cyclone's translational speed. Further details on the development of the parametric equation of b_s can be found in Holland (2008). In addition to the wind field model in equation (1), Geiger et al. (2018) calculated a translational component multiplied by an attenuation factor (ratio between the tropical cyclone's center and the radius of maximum wind). The translational wind speed decreases with the distance from the cyclonic system's center, which is taken into account to provide more realistic estimates of wind exposure on the ground Fontaine (2018). [1] Thus, we define a binary variable that is equal to 1 when the winds on the ground are higher than 190 km/h and otherwise. This choice is based on the literature, which assumes that only cyclonic events producing intense winds are able to cause structural damage to crops and therefore affect agricultural income (Ouattara and Strobl, 2013).

To account for the correlation of tropical cyclone exposure with other weather variables in our analysis, we draw on the economic literature that exploits exogenous variations in local rainfall and temperature as a proxy for local economic conditions (Kaur, 2019; Shah and Steinberg, 2017; Dell et al., 2012). The basic idea of our empirical approach is to compare young women who have experienced different weather conditions at a given location and time are likely to be at high risk of marriage. Weather conditions significantly affect the overall economic performance of poor countries, while reducing the level of agricultural production, industrial production. These exogenous variations negatively affect crop yields in rural communities, and thus local economic development, and consequently the economic opportunities available to women, which in turn influences the timing of marriage.

Our precipitation data come from the Climate Hazards group Infrared Precipitation with Stations (CHIRPS) dataset combining ground station and satellite information with grid

[1] The dataset is referenced as Geiger et al. (2017) and is available at https://dataservices.gfz-potsdam.de/pik/showshort.php?id=escidoc:2387904.

resolution ($0.05° \times 0.05°$) (Funk et al., 2015). For temperature data, we use the updated Climate Research Unit (CRU) gridded global climate dataset from Harris et al. (2014) with a latitude/longitude grid of 0.5°. To control for weather, we consider average precipitation and temperature at the grid cell level, respectively. We also adapt an approach used by Corno et al. (2016) and define drought when calendar year precipitation is below the 15th percentile and flooding when it is above the 85th percentile of the annual precipitation distribution of a grid cell.

4 Empirical strategy

4.1 Person-year panel dataset

We assume that cyclone shocks affect women's marriage before and after age 18 differently. To create a person-year panel dataset for each woman aged 12-24, we use Cox proportional hazards models (Currie and Neidell, 2005; Corno et al., 2020). In this new panel, each woman contributes a number $(t_m - t_0 + 1)$ of observations to the data, after marriage she is removed from the data. The duration t_0 is the risk age at which a woman is likely to marry for the first time, and t_m is the age at which she first marries. We merge these individual data with our cyclonic wind, rainfall, and temperature data at the year level. Table 2 presents summary statistics for the person-year panel dataset between the ages of 12 and 24 for each woman, combined with data on hurricane winds, rainfall, and temperature (Table 2). For example, 7.2 percent of the women were married, 24 percent of which were married before the age of 18. Overall, 15.2 percent of women were exposed to cyclones. On average, wind speed, rainfall and temperature are 14km/h, 1700mm and 24 degrees respectively.

Table 2: Summary statistics of survival data*

Variable	Obs	Mean	Std.Dev.
Women's age	763,600	34.560	6.997
Years of education	763,343	5.194	5.1205
Household members	763,600	5.739	2.437
Number of children 5 and under	763,600	0.829	0.978
Age at first marriage	608,651	19.542	4.473
Share of women married between 12 and 24	516,373	0.078	0.269
Share of women married between 12 and 17	491,335	0.032	0.176
Drought (1/0)	763,600	0.142	0.349
Dummy (1 if Rainfall> 85e percentile)	763,600	0.146	0.353
Cyclone (1 if wind speed >190 km/h)	637000	0.003	0.056
Rainfall	746,645	1725.427	811.060
Temperature	745,416	23.877	4.427
Max wind speed	746,645	13.445	34.028

* Survival data: panel data obtained by historical recall from age 12 to 24 if the observation is of each woman vector is available in the data, i.e. before marriage.

Source: Author's calculations using DHS data.

4.2 Empirical specification

In this section, we base the variation in the velocity of each cyclone year across girls' locations on the probability that girls will be married by age 18 by estimating the following linear probability model:

$$M_{igkt} = C_{gkt-1}\alpha_1 + W_{gkt-1}\alpha_2 + \eta_{t+}\omega_g + \epsilon_k + \xi_{igkt-1} \tag{2}$$

The dependent variable, M_{igkt} , is a binary variable (1/0) in the year the child gets married. C_{ikt-1} is the binary variable that takes the value one when the cyclone wind speed is greater than 190 km/h at location g in the previous year in which the woman is born in

year k at age t. α_1 is the main coefficient of cyclone shocks on the probability of marriage[2]. W_{gkt-1} is a vector of controls for extreme weather conditions, i. e., drought, which is defined when precipitation is below the 15th percentile, and a binary variable that indicates heavy precipitation when it is above the 85th percentile of the distribution. η_t and ω_g are respectively an age fixed-effect dummy variable and time-invariant unobservable local characteristics, such as the fixed effects of year of birth, education and religion.

The main indicator used to report the prevalence of child marriage is the percentage of individuals who were married for the first time before the age of 18 for women aged 12 to 17 or 12 to 24 when they reported being married. We exclude cases where they were in a relationship because cohabitation, while presenting the same rights issues as marriage, is not common in the countries studied. The default variable of interest is the binary variable of cyclonic wind speed above 190 km/h on the ground defined earlier. Its coefficients capture how cyclonic shocks affect the probability of marrying before age 18. Consistent with the initial prediction that in the South Asian country and some countries in the Americas, the culture of dowry payment is predominant. The coefficient is expected to be negative, indicating that an adverse shock decreases the probability of child marriage.

4.3 Spillovers and potential threat

In this study, the first identification strategy is to locate the location of women's residence at the time of climate shocks. Unfortunately, the DHS data do not provide information on the timing of rainfall shocks and the location of marriage. However, the DHS data do contain geographic cluster information, which designates a village in rural areas and towns or districts in urban areas as necessary. To cope with the timing of the shock, we match these geographic data to the metrological data. For the marriage location constraint, the main challenge is to address the problem of virilocality, a known practice according to social

[2]We use as an alternative variable for the robustness of the results, Simpson's index which is a commonly used index in the literature and the damage function defined by Emanuel (2011).

norms that girls move away from their parents at the time of marriage (Levine and Kevane, 2003). To do so, we include only women who reported living in the same place of residence throughout their lives. This choice has an advantage of reducing measurement uncertainties related to individual and family migration and destination in response to rainfall shocks, although this bias is negligible since the majority of married women remain in the same geographic area as their parents or are within a short distance. Because we use grid surface level weather information, these rural migration distances are relatively short, so coefficient estimates are unlikely to be affected. Another concern in our study is related to measurement errors in the recall of age and year of marriage. Once gain, these are negligible given the validity of the age variables as a whole in the DHS data (Corno et al., 2020; Pullum, 2006).

We focus on shocks related to cyclone wind speed on the probability of being married at age 18. In order to control for correlation between cyclone-related shocks and other weather shocks, we include precipitation and temperature levels in the same grid cell. Our panel exploits the causal exogenous variation of cyclones over time in a given spatial area on the risk of early marriage. Reverse causality is unlikely to be a major issue. In a clustering model context, the most pressing econometric challenge to estimating 1 from the cross-sectional equation in (2) is potential omitted variable bias. In other words, the correlation between the metrological variables and other observed characteristics that may influence the outcome. Indeed, the effects of cyclones may be associated with certain determinants of marriage decisions. For example, some populations in certain regions may have a greater capacity to respond to cyclone disasters than others due to the endowment of adequate infrastructure and economic opportunities or post-cyclone response measures. In a context of limited employment in rural areas, the ability to be resilient to shocks will depend on the individual characteristics of each woman. If these characteristics are not properly captured in the control variables, estimates of the effect of cyclone winds could be biased. Therefore, in equation (2), we include fixed effects expressed as deviations from the individual and time

sample means (Croissant and Millo, 2018)[3]. This allows us to interpret the fixed effects coefficients associated with wind speed as the impact of tropical shocks on the probability of being married. Another point of discussion concerns the exposure of populations to cyclonic events. Indeed, cyclones are considered by nature as local events and the associated damages depend on the population density and the concentration of activities (Naguib et al., 2022; Hsiang, 2010). Exposure varies exogenously depending on the timing, location, and wind speed intensity of cyclones (Hsiang, 2010). All of these are unpredictable and stochastic from year to year, conditioned by the average weather and climate conditions of each country (e.g., Eskander and Barbier, 2022; Naguib et al., 2022; Eskander and Barbier, 2022; Pugatch, 2019; Berlemann and Wenzel, 2018). To absorb these effects, we include country, year and grid fixed effects. Thus, this process allows us to assume that the shock is exogenous and uncorrelated with other unobserved factors influencing the marriage decision, and thus identify the causal effect of cyclones (Hsiang and Jina, 2014).

[3]However, because there are other time-varying factors that cannot be accounted for using only fixed effects, it is possible that the conditional independence assumption is violated. To address this, we perform an Oster (2019) test for all main regressions. These tests show that the effect is determined solely by the observed factors.

5 Findings

5.1 Main results

Table 3 presents the results of the estimated coefficients of equation (1). It shows that the effect of adverse cyclone shocks measured by wind speed on the timing of marriage of young women aged 12-24. All regression specifications include grid cell fixed effects. The effect is not significant before and after controlling for individual and cohort time effects. The question of introducing such variables is whether there are other omitted variables that would render the coefficients insignificant or whether these estimates represent only causal effects. In contrast to Corno et al. (2020), we find that cyclone shocks do not have a negative impact on women aged 12-24 years. In other words, young women exposed to winds above 190 km/h are not likely to marry. To confirm this result, we also test the effect on the sample of women aged 18-24, and again the results remain insignificant (Table A1). This is because the timing of marriage and the choice of a husband are most often decided by the girl's parents or family members (Chowdhury, 2004; Asadullah and Wahhaj, 2019). Marriageable girls are not only a burden to consumption, they are also considered a dishonor to the family, which puts additional pressure on their parents. The intuition behind this result is that when girls are of marriageable age, they are only willing to postpone their marriage if they anticipate lower prices in the future. Given the extremely difficult context, this postponement is more costly in the future than it is today, which could explain the insignificant effect of the shock on older young women.

Table 4 presents the partial results of the estimates of the probability of marrying before age 18 regressed on the binary variable of cyclone wind speed greater than 190 km/h for the sample of young women aged 12-17 years. The results show that cyclone shocks are negatively and significantly associated with the probability of getting married. The estimated coefficients are 0.012 and 0.017 points, respectively, and are both significant at the 1 percent level. In effect, the estimated coefficients show that a shock is associated with a decrease

Table 3: Effect of cyclone on get married

VARIABLES	(1) Get married	(2) Get married	(3) Get married	(4) Get married	(5) Get married	(6) Get married
Cyclone (1/0)	-0.00288	-0.00922	-0.00280	-0.00427	-0.00288	-0.00875
	(0.0207)	(0.0212)	(0.0207)	(0.0212)	(0.0207)	(0.0216)
Birth Year FE	No	Yes	No	No	No	Yes
Religion FE	No	No	Yes	No	No	Yes
Education FE	No	No	No	Yes	No	Yes
Country FE	No	No	No	No	Yes	Yes
Observations	430,471	430,471	430,449	430,336	430,471	430,314
Adjusted R-squared	0.019	0.021	0.019	0.023	0.019	0.025

Notes: Our dependent variable is a dummy variable equal to 1 if the woman married at the age corresponding to the age observation of 12 to 24. The cyclone variable is a dummy variable that equals 1 if the lag of the wind speed is greater than or equal to 190km/h. We control for the fixed effects of year of birth, years of schooling, religion, country, and mesh (coefficients not shown). Standard errors are shown in parentheses; ***, **, * represent significance at the 1%, 5%, 10% level, respectively.

Source: Authors' calculations using DHS data.

in the probability of marrying in each estimate without and with additional control for individual and time fixed effects. The results also show that the estimated effect coefficients remain similar if we introduce the religion and country fixed effect (0.012 point significant at the 1 percent level). However, the effect is relatively more significant with the introduction of the birth year cohort fixed effect, with an estimated coefficient of 0.015 point (Table 4, column 5). By introducing all fixed effects, the estimated coefficient increases to 0.017 point. Women experiencing cyclonic winds greater than 190km/h between the ages of 12 and 17 in t have a 1.7 point less likely to be married in t+1 (columns 4, p<001). As the average annual risk of marriage for young women aged 12 to 17 is equal to 0.052, the approximate effect is 0.336.

In addition, we include extreme precipitation variables, such as drought and heavy precipitation, which are likely to have a negative impact on agricultural productivity (Corno et al., 2020; Tsaneva, 2020)[4]. The purpose is to see whether extreme precipitation conditions alter the results, while sequentially adding individual and time fixed effects as we did

[4]The results remain similar with the introduction of the mean temperature in the regression (Table A2 in appendix.

previously. The results remain similar but slightly higher (Table 5, columns 1-6). These results are consistent with Corno et al. (2016) showing that droughts reduce child marriage in India due to cultural traditions favoring dowry payments. These findings are coherent with the main idea that in developing countries where agriculture is the main activity, a negative shock negatively affects agricultural productivity and thereby farm income. Thus, child marriage could serve as a short-term insurance mechanism for farm households facing crop failure and asset losses due to the shock of a natural event. In societies where dowry payments are practiced, households with young daughters will tend to delay marriage in order to obtain financial benefits to improve their welfare. Furthermore, Trinh and Zhang (2021) has shown that adverse shocks in India have a negative impact on household welfare, as families are unable to meet dowry requirements, resulting in a lower incidence of child marriage. Unlike the studies mentioned above, drought does not have a significant effect on child marriage. This reflects the context of the countries in our sample that are islands or have large coastal areas that, because of their humid tropical climate, are less prone to long droughts (Fung et al., 2020).

Table 4: Effect of cyclone on Child marriage

VARIABLES	(1) chilmarr	(2) chilmarr	(3) chilmarr	(4) chilmarr	(5) chilmarr	(6) chilmarr
Cyclone (1/0)	-0.0123**	-0.0158***	-0.0123**	-0.0154***	-0.0123**	-0.0177***
	(0.00532)	(0.00573)	(0.00532)	(0.00594)	(0.00532)	(0.00625)
Birth Year FE	No	Yes	No	No	No	Yes
Religion FE	No	No	Yes	No	No	Yes
Education FE	No	No	No	Yes	No	Yes
Country FE	No	No	No	No	Yes	Yes
Observations	248,827	248,827	248,818	248,748	248,827	248,739
Adjusted R-squared	0.046	0.047	0.046	0.050	0.046	0.052

Notes: Our dependent variable is a dummy variable that equals 1 if the child married before age 18. The cyclone variable is a dummy variable that equals 1 if the lag of the wind speed is greater than or equal to 190km/h. We control for the fixed effects of year of birth, years of schooling, religion, country, and mesh (coefficients not shown). Standard errors are shown in parentheses; ***, **, * represent significance at the 1%, 5%, 10% level, respectively.

Source: Authors' calculations using DHS data.

Table 5: Inclusion of extreme weather variables

VARIABLES	(1) chilmarr	(2) chilmarr	(3) chilmarr	(4) chilmarr	(5) chilmarr	(6) chilmarr
Cyclone (1/0)	-0.0125**	-0.0160***	-0.0125**	-0.0155***	-0.0125**	-0.0178***
	(0.00535)	(0.00578)	(0.00535)	(0.00597)	(0.00535)	(0.00628)
Drought (1/0)	-0.00721	-0.00720	-0.00730	-0.00684	-0.00721	-0.00703
	(0.00736)	(0.00749)	(0.00735)	(0.00773)	(0.00736)	(0.00784)
Dummy (Rainfall> $85e$ percentile)	-0.00290	-0.00130	-0.00264	-0.00157	-0.00290	-0.00113
	(0.00451)	(0.00449)	(0.00460)	(0.00455)	(0.00451)	(0.00457)
Birth Year FE	No	Yes	No	No	No	Yes
Religion FE	No	No	Yes	No	No	Yes
Education FE	No	No	No	Yes	No	Yes
Country FE	No	No	No	No	Yes	Yes
Observations	248,827	248,827	248,818	248,748	248,827	248,739
Adjusted R-squared	0.046	0.047	0.046	0.050	0.046	0.052

Notes: Our dependent variable is a dummy variable that equals 1 if the child married before age 18. The cyclone variable is a dummy variable that equals 1 if the lag of the wind speed is greater than or equal to 190km/h. We control for the fixed effects of year of birth, years of schooling, religion, country, and mesh (coefficients not shown). Standard errors are shown in parentheses; ***, **, * represent significance at the 1%, 5%, 10% level, respectively.

Source: Authors' calculations using DHS data.

5.2 Alternative model

5.2.1 Saffir-Simpson index

To verify the non-linearity of our basic model, we implicitly assume that damage increases exponentially with the level of wind speed. Tropical cyclones are indeed characterized by intense winds, which cause physical damage on the ground (Eskander and Barbier, 2022; Naguib et al., 2022). To this end, we adopt the Saffir-Simpson scale, a simple functional form of wind speed often used in the literature. The advantage of this index is that it does not account for the possibility of other cyclone-related impacts, such as storm surge and rainfall-induced flooding (Berlemann and Wenzel, 2018; Pugatch, 2019). The categories of the scale range from 1 to 5 according to their maximum speed. Thus, depending on the thresholds adopted, these five categories represent a tropical depression, a cyclonic system, a tropical storm, an intense cyclone and a very intense cyclone, respectively. Each variable takes the value one when the wind speed is included in the category and zero otherwise. We introduce weather variables to capture the destruction effect of economic losses attributed to these events. The results show that the Simpson index measures corresponding only to the intense cyclone and the very intense cyclone are negative and significant on girls' probability of marriage (Table 6). Girls experiencing an intense cyclone between the ages of 12 and 17 have a 0.019 probability of not being married. Young women who have been exposed to an intense cyclone between the ages of 12 and 17 have a 0.039 point less likely to be married. These results are in line with the position of Ouattara and Strobl (2013), who suggest that significant damage only occurs when a cyclone reaches a strength of three or more on the Simpson scale. Thus, the high winds associated with these two categories can cause considerable structural damage to crops and thus affect farm income.

Table 6: Effect of cyclone categorization on Child marriage

VARIABLES	(1) chilmarr	(2) chilmarr	(3) chilmarr	(4) chilmarr	(5) chilmarr	(6) chilmarr
Simpson index = 1	0.0135	0.00988	0.0135	0.0130	0.0135	0.00948
	(0.0122)	(0.0126)	(0.0122)	(0.0121)	(0.0122)	(0.0123)
Simpson index = 2	-0.000198	-0.00399	-0.000249	0.00202	-0.000198	-0.00163
	(0.0128)	(0.0132)	(0.0128)	(0.0133)	(0.0128)	(0.0136)
Simpson index = 3	-0.00117	-0.00552	-0.000998	-0.00336	-0.00117	-0.00709
	(0.0158)	(0.0159)	(0.0158)	(0.0165)	(0.0158)	(0.0165)
Simpson index = 4	-0.0139**	-0.0166**	-0.0140**	-0.0181***	-0.0139**	-0.0198***
	(0.00622)	(0.00677)	(0.00622)	(0.00604)	(0.00622)	(0.00653)
Simpson index = 5	-0.0339**	-0.0392**	-0.0341**	-0.0376**	-0.0339**	-0.0392**
	(0.0162)	(0.0196)	(0.0162)	(0.0163)	(0.0162)	(0.0196)
Drought (1/0)	-0.00681	-0.00685	-0.00692	-0.00629	-0.00681	-0.00647
	(0.00727)	(0.00745)	(0.00725)	(0.00765)	(0.00727)	(0.00782)
Dummy (Rainfall> 85e percentile)	-0.00530	-0.00288	-0.00510	-0.00399	-0.00530	-0.00277
	(0.00420)	(0.00413)	(0.00427)	(0.00421)	(0.00420)	(0.00420)
Birth Year FE	No	Yes	No	No	No	Yes
Religion FE	No	No	Yes	No	No	Yes
Education FE	No	No	No	Yes	No	Yes
Country FE	No	No	No	No	Yes	Yes
Observations	300,266	300,266	300,254	300,175	300,266	300,163
Adjusted R-squared	0.037	0.039	0.037	0.042	0.037	0.043

Notes: Our dependent variable is a dummy variable that equals 1 if the child married before age 18. The Simpson index variable takes the value one when the wind speed is included in the wind speed category and zero otherwise. We control for the fixed effects of year of birth, years of schooling, religion, country, and mesh (coefficients not shown). Standard errors are shown in parentheses; ***, **, * represent significance at the 1%, 5%, 10% level, respectively.

Source: Authors' calculations using DHS data.

5.2.2 Damage function

To further establish the robustness of our results, we use a different alternative measure of people's exposure to tropical cyclones to determine the presence of an intensification mechanism. The intensity of tropical cyclones has particularly important economic consequences that households adopt their short-term strategies to cope with. Due to the fact that tropical cyclones are immediate natural disasters, their direct effects occur immediately after impact (Strobl, 2012b; Rakotobe et al., 2016). To capture the short-term dynamics, we used as a general indicator of potential damage from tropical storms. Thus, we are able to estimate the amount of property damage caused by a tropical storm as a function of the physically felt wind speed (Elliott et al., 2015; Emanuel, 2011). To capture these aspects, we use the index, f, proposed by Emanuel (2011), which assumes that the fraction of property damaged varies with the cubic power of the ground wind speed :

$$f = \frac{V_n^3}{1 + V_n^3}$$

Where f is the fraction of the property value lost depending on the wind speed function:

$$V_n = \frac{Max[(V - \overline{V}), 0]}{V_h - \overline{V}}$$

Following Elliott et al. (2015) and Zhou and Zhang (2021), we consider a damage function that produces only positive values and establish an arbitrary threshold $\overline{V}$=119 below which we assume no damage exists. We then define V_h as the threshold at which half of the property is damaged and set it at 278 km/h. The results show that the proportion of damaged property significantly reduces the probability of marriage for females aged 12 to 17 years after the introduction of fixed effects (Table 7). Finally, an additional cyclone dummy variable is defined which is equal to 1 if exposure to a wind speed in t-2 is greater than or

equal to 190km/h. Table A3 in the Appendix shows that girls who experience a wind speed greater than 190 km/h in t-2 between the ages of 12 and 17 have a probability of 0.021 of not being married in t. Overall, the robustness of our results to different sets of controls supports the causal effect of hurricane shocks on the probability of child marriage.

Table 7: Effect of cyclone damage on Child marriage

VARIABLES	(1) chilmarr	(2) chilmarr	(3) chilmarr	(4) chilmarr	(5) chilmarr	(6) chilmarr
Cyclone damage	-0.0562	-0.0845**	-0.0563	-0.0737*	-0.0562	-0.0974**
	(0.0384)	(0.0413)	(0.0384)	(0.0391)	(0.0384)	(0.0410)
Drought (1/0)	-0.00341	-0.00360	-0.00351	-0.00258	-0.00341	-0.00322
	(0.00720)	(0.00741)	(0.00719)	(0.00764)	(0.00720)	(0.00780)
Dummy (Rainfall> 85e percentile)	-0.00292	-0.00154	-0.00269	-0.00146	-0.00292	-0.00144
	(0.00406)	(0.00414)	(0.00414)	(0.00410)	(0.00406)	(0.00422)
Birth Year FE	No	Yes	No	No	No	Yes
Religion FE	No	No	Yes	No	No	Yes
Education FE	No	No	No	Yes	No	Yes
Country FE	No	No	No	No	Yes	Yes
Observations	300,353	300,353	300,341	300,262	300,353	300,250
Adjusted R-squared	0.036	0.038	0.036	0.041	0.036	0.042

Notes: Our dependent variable is a dummy variable that equals 1 if the child married before age 18. Our cyclone variable is the fraction of property damaged as a function of the cubic power of the ground wind speed. We control for the fixed effects of year of birth, years of schooling, religion, country, and mesh (coefficients not shown). Standard errors are shown in parentheses; ***, **, * represent significance at the 1%, 5%, 10% level, respectively.

Source: Authors' calculations using DHS data.

5.3 Discussion

Since the responsibility for arranging and paying for their children's marriages rests with the parents, they begin saving for dowries as soon as their daughters are born (Chowdhury et al., 2020). In the context of a general lack of credit and insurance markets, their ability to save for dowry depends solely on farm income. According to the theory, most dowries in the competitive market are compensatory payments to the families of the bride and groom, rather than a willingness on the part of parents to bequeath resources to their daughters (Anukriti et al., 2022; Sekhri and Debnath, 2014; Anderson, 2007). In other words, the dowry is essentially a bride price rather than a simple inheritance. In societies where dowry prevails, norms and institutions privilege men (Sekhri and Debnath, 2014). When faced with this income shock, households are more likely to reduce saving in advance for their daughters' dowries because of their variable consumption and low resilience to shocks, which can exacerbate behavioral biases ((Karlan et al., 2014; Anderson, 2007). The destruction of agricultural and non-agricultural assets by natural disasters could affect women's dowry rights and parental investment in children over time. After a cyclone, households may decide to delay their daughters' marriages due to financial hardship in order to meet their dowry payment commitments. This decision would then have a negative effect on the likelihood of children marrying. These results are similar to those of Corno et al. (2020) and Tsaneva (2020), who observed that rainfall variation has a negative impact on marriage in countries where dowry custom prevails. In contrast to these previous studies, the non-significant effect on older girls in our case could be explained by a marriage compression effect based on the fact that in a growing population. As men's preferences are skewed toward younger girls, there will be relatively few men to marry in the marriage market for marriage-age girls. Thus, the cost of delaying a woman's marriage beyond a certain age requires additional financing that further reduces livelihoods. Social pressures on parents with older daughters do not encourage parents to delay marriage despite their financial difficulties (Chowdhury et al., 2020). Another possible explanation could be that households alter their labor decisions to

mitigate income variability related to adverse weather events. Child labor is still relatively common in rural areas of various poor countries, especially on family farms (Shah and Steinberg, 2017). Agricultural labor is often traded on spot markets, allowing women and children to work for short-term wages (Branco and Féres, 2021). Because older girls can work as day laborers, they can leave home to work if wages are high, reducing the effect of the shock on farm income after a catastrophic event, and hence the delay in marriage for households with older girls.

We recognize, however, that such a conclusion would need to be confirmed by other empirical studies that ideally observe the use of child marriage as a coping strategy in the face of cyclone shocks and other unobserved parameters inherent in the cyclone phenomenon.

6 Conclusion

Cyclones cause economic losses, which lead significantly to food insecurity. These impacts are exacerbated by economic factors such as poverty and food insecurity, social and cultural norms, making them more vulnerable to current and future extreme weather events. This situation is also exacerbated by the lack of a comprehensive policy to manage the agricultural sector, which is the main driver of the rural economy. These issues represent a significant challenge for national and international organizations in developing countries. Using unique geo-located household data combined with wind field data generated by cyclonic systems, we generated cyclonic wind intensity indicators on the ground to assess annual variations in a cell grid. We found that during cyclonic events, wind speed does not significantly affect the probability of marriage for girls aged 12-24 years. This suggests that households do not rely on marriage of marriage-age girls as part of their short-term coping strategies to deal with a cyclone event. However, wind speed has negative and significant effects on the probability of marriage for girls aged 12-17. It is possible that struggling farm households delay their daughter's marriage in order to meet dowry payment deadlines to protect their consumption after a cyclone event. These results are robust to a number of robustness and sensitivity checks on the ground wind speed definitions used. Moreover, repeated household exposure to cyclone shocks leads to the depletion of productive assets of agricultural households, accelerating the dynamics of social inequality and reduced welfare in rural communities. However, the evidence we have does not allow us to provide a definitive answer on the true nature of the decision to delay girls' marriage. For this, additional empirical evidence is needed to shed new light on the relationship between cyclone disasters and child marriage, the prevalence of which still remains significant in poor countries. Finally, the intensity of tropical cyclones is expected to increase in the future due to rising sea surface temperatures caused by increasing levels of greenhouse gases in the atmosphere. This could lead to an increase in direct damage from high winds and substantially change the behavior of households to long-term shocks. Thus, future studies should address the impact of cyclone intensity and

how significant damage could alter the magnitude of outcomes in these regions.

References

Anderson, S. (2007). The economics of dowry and brideprice. *Journal of economic perspectives*, 21(4):151–174.

Anukriti, S., Kwon, S., and Prakash, N. (2022). Saving for dowry: Evidence from rural india. *Journal of Development Economics*, 154:102750.

Arthur, M., Earle, A., Raub, A., Vincent, I., Atabay, E., Latz, I., Kranz, G., Nandi, A., and Heymann, J. (2018). Child marriage laws around the world: Minimum marriage age, legal exceptions, and gender disparities. *Journal of women, politics & policy*, 39(1):51–74.

Asadullah, M. N. and Wahhaj, Z. (2019). Early marriage, social networks and the transmission of norms. *Economica*, 86(344):801–831.

Ba, M. and Mughal, M. (2022). Weather shocks, coping strategies and household well-being: Evidence from rural mauritania. *The Journal of Development Studies*, 58(3):482–502.

Bakkensen, L. and Barrage, L. (2018). Climate shocks, cyclones, and economic growth: bridging the micro-macro gap. Technical report, National Bureau of Economic Research.

Bank, W. and Nations, U. (2010). *Natural hazards, unnatural disasters: the economics of effective prevention*. The World Bank.

Berlemann, M. and Wenzel, D. (2018). Hurricanes, economic growth and transmission channels: Empirical evidence for countries on differing levels of development. *World Development*, 105:231–247.

Botticini, M. and Siow, A. (2003). Why dowries? *American Economic Review*, 93(4):1385–1398.

Branco, D. and Féres, J. (2021). Weather shocks and labor allocation: Evidence from rural brazil. *American Journal of Agricultural Economics*, 103(4):1359–1377.

Chowdhury, F. D. (2004). The socio-cultural context of child marriage in a bangladeshi village. *International Journal of Social Welfare*, 13(3):244–253.

Chowdhury, S., Mallick, D., and Chowdhury, P. R. (2020). Natural shocks and marriage markets: Fluctuations in mehr and dowry in muslim marriages. *European economic review*, 128:103510.

Corno, L., Hildebrandt, N., and Voena, A. (2016). Weather shocks, age of marriage and the direction of marriage payments. Technical report, Working Paper.

Corno, L., Hildebrandt, N., and Voena, A. (2020). Age of marriage, weather shocks, and the direction of marriage payments. *Econometrica*, 88(3):879–915.

Croissant, Y. and Millo, G. (2018). *Panel Data Econometrics with R*. John Wiley & Sons, Ltd.

Dell, M., Jones, B. F., and Olken, B. A. (2012). Temperature shocks and economic growth: Evidence from the last half century. *American Economic Journal: Macroeconomics*, 4(3):66–95.

Dell, M., Jones, B. F., and Olken, B. A. (2014). What do we learn from the weather? the new climate-economy literature. *Journal of Economic Literature*, 52(3):740–98.

Dessy, S., Marchetta, F., Pongou, R., and Tiberti, L. (2019). Fertility response to climate shocks. working paper or preprint.

Dhamija, G. and Roychowdhury, P. (2020). Age at marriage and women's labour market outcomes in india. *Journal of International Development*, 32(3):342–374.

Edlund, L. (2006). The price of marriage: net vs. gross flows and the south asian dowry debate. *Journal of the European Economic Association*, 4(2-3):542–551.

Elliott, R. J., Strobl, E., and Sun, P. (2015). The local impact of typhoons on economic activity in china: A view from outer space. *Journal of Urban Economics*, 88:50–66.

Emanuel, K. (2011). Global warming effects on u.s. hurricane damage. *Weather, Climate, and Society*, 3(4):261–268.

Eskander, S. M. and Barbier, E. B. (2022). Long-term impacts of the 1970 cyclone in bangladesh. *World Development*, 152:105793.

Field, E. and Ambrus, A. (2008). Early marriage, age of menarche, and female schooling attainment in bangladesh. *Journal of political Economy*, 116(5):881–930.

Fontaine, I. (2018). L'effet causal du nombre d'enfants sur l'offre de travail des mères : le cas de la france métropolitaine et de ses départements d'outre-mer. *Revue Economique*, 69(5):869–898.

Fung, K., Huang, Y., and Koo, C. (2020). Assessing drought conditions through temporal pattern, spatial characteristic and operational accuracy indicated by spi and spei: case analysis for peninsular malaysia. *Natural Hazards*, 103(2):2071–2101.

Funk, C., Peterson, P., Landsfeld, M., Pedreros, D., Verdin, D., Shukla, S., Husak, G., Rowland, J., Harrison, L., Hoell, A., and Michaelsen, J. (2015). The climate hazards infrared precipitation with stations—a new environmental record for monitoring extremes. *Scientific Data*, 2(150066).

Geiger, T., Frieler, K., and Bresch, D. N. (2017). A global data set of tropical cyclone exposure (TCE-DAT). *GFZ Data Services*.

Geiger, T., Frieler, K., and Bresch, D. N. (2018). A global historical data set of tropical cyclone exposure (tce-dat). *Earth System Science Data*, 10(1):185–194.

Harris, I., Jones, P., Osborn, T., and Lister, D. (2014). Updated high-resolution grids of monthly climatic observations – the cru ts3.10 dataset. *International Journal of Climatology*, 34(3):623–642.

Holland, G. (2008). A revised hurrican pressure-wind model. *Monthly Weather Review*, pages 3432–3445.

Hoogeveen, J., Van Der Klaauw, B., and Van Lomwel, G. (2011). On the timing of marriage, cattle, and shocks. *Economic Development and Cultural Change*, 60(1):121–154.

Hsiang, S. M. (2010). Temperatures and cyclones strongly associated with economic production in the caribbean and central america. *Proceedings of the National Academy of Sciences*, 107(35):15367–15372.

Hsiang, S. M. and Jina, A. S. (2014). The causal effect of environmental catastrophe on long-run economic growth: Evidence from 6,700 cyclones. Technical report, National Bureau of Economic Research.

Jensen, R. and Thornton, R. (2003). Early female marriage in the developing world. *Gender & Development*, 11(2):9–19.

Karlan, D., Ratan, A. L., and Zinman, J. (2014). Savings by and for the poor: A research review and agenda. *Review of Income and Wealth*, 60(1):36–78.

Kaur, S. (2019). Nominal wage rigidity in village labor markets. *American Economic Review*, 109(10):3585–3616.

Khanal, K. and Sen, R. (2020). The dowry gift in south asia: An institution on the intersection of market and patriarchy. *Journal of Economic Issues*, 54(2):356–362.

Kim, M., Longhofer, W., Boyle, E. H., and Nyseth Brehm, H. (2013). When do laws matter? national minimum-age-of-marriage laws, child rights, and adolescent fertility, 1989–2007. *Law & Society Review*, 47(3):589–619.

Knapp, K. R., Kruk, M. C., Levinson, D. H., Diamond, H. J., and Neumann, C. J. (2010). The international best track archive for climate stewardship (ibtracs). *Bulletin of the American Meteorological Society*, 91(3):363–376.

Krichene, H., Geiger, T., Frieler, K., Willner, S., Sauer, I., and Otto, C. (2021). Long-term impacts of tropical cyclones and fluvial floods on economic growth–empirical evidence on transmission channels at different levels of development. *World Development*, 144:105475.

Kudamatsu, M. (2012). Has democratization reduced infant mortality in sub-saharan africa? evidence from micro data. *Journal of the European Economic Association*, 10(6):1294–1317.

Levine, D. and Kevane, M. (2003). Are investments in daughters lower when daughters move away? evidence from indonesia. *World Development*, 31(6):1065–1084.

Lnu, A., Kwon, S., Prakash, N., et al. (2020). Saving for dowry: Evidence from rural india. Technical report, The World Bank.

Maertens, A. (2013). Social norms and aspirations: age of marriage and education in rural india. *World Development*, 47:1–15.

McNulty, J. K., Wenner, C. A., and Fisher, T. D. (2016). Longitudinal associations among relationship satisfaction, sexual satisfaction, and frequency of sex in early marriage. *Archives of sexual behavior*, 45(1):85–97.

Mendelsohn, R., Emanuel, K., Chonabayashi, S., and Bakkensen, L. (2012). The impact of climate change on global tropical cyclone damage. *Nature climate change*, 2(3):205–209.

Mottaleb, K. A., Mohanty, S., and Mishra, A. K. (2015). Intra-household resource allocation under negative income shock: A natural experiment. *World Development*, 66:557–571.

Munshi, S. (2017). 'arranged'marriage, education, and dowry: A contract-theoretic perspective. *Journal of Economic Development*, 42(1):35.

Naguib, C., Pelli, M., Poirier, D., and Tschopp, J. (2022). The impact of cyclones on local economic growth: Evidence from local projections. *Economics letters*, 220:110871.

Nguyen, M. C. and Wodon, Q. (2015). Global and regional trends in child marriage. *The Review of Faith & International Affairs*, 13(3):6–11.

Oster, E. (2019). Unobservable selection and coefficient stability: Theory and evidence. *Journal of Business & Economic Statistics*, 37(2):187–204.

Ouattara, B. and Strobl, E. (2013). The fiscal implications of hurricane strikes in the caribbean. *Ecological Economics*, 85:105–115.

OXFAM (2022). *Philippines hit by over half a billion dollars in damages from Typhoon Rai; farming and fishing hardest hit - Philippines*. OXFAM.

Parsons, J., Edmeades, J., Kes, A., Petroni, S., Sexton, M., and Wodon, Q. (2015). Economic impacts of child marriage: a review of the literature. *The Review of Faith & International Affairs*, 13(3):12–22.

Porter, C. (2012). Shocks, consumption and income diversification in rural ethiopia. *Journal of Development Studies*, 48(9):1209–1222.

Pugatch, T. (2019). Tropical storms and mortality under climate change. *World Development*, 117:172–182.

Pullum, T. W. (2006). *An assessment of age and date reporting in the DHS surveys, 1985-2003*, volume 5. Macro International.

Rakotobe, Z. L., Harvey, C. A., Rao, N. S., Dave, R., Rakotondravelo, J. C., Randrianarisoa, J., Ramanahadray, S., Andriambolantsoa, R., Razafimahatratra, H., Rabarijohn, R. H., et al. (2016). Strategies of smallholder farmers for coping with the impacts of cyclones: A case study from madagascar. *International journal of disaster risk reduction*, 17:114–122.

Rao, V. (1993). Dowry 'inflation'in rural india: A statistical investigation. *Population Studies*, 47(2):283–293.

Sekhri, S. and Debnath, S. (2014). Intergenerational consequences of early age marriages of girls: Effect on children's human capital. *The Journal of Development Studies*, 50(12):1670–1686.

Shah, M. and Steinberg, B. M. (2017). Drought of opportunities: Contemporaneous and long-term impacts of rainfall shocks on human capital. *Journal of Political Economy*, 125(2):527–561.

Strobl, E. (2012a). The economic growth impact of natural disasters in developing countries: Evidence from hurricane strikes in the central american and caribbean regions. *Journal of Development economics*, 97(1):130–141.

Strobl, E. (2012b). The economic growth impact of natural disasters in developing countries: Evidence from hurricane strikes in the central american and caribbean regions. *Journal of Development Economics*, 97(1):130 – 141.

Takasaki, Y. (2011). Targeting cyclone relief within the village: kinship, sharing, and capture. *Economic Development and Cultural Change*, 59(2):387–416.

Trinh, T.-A. and Zhang, Q. (2021). Adverse shocks, household expenditure and child marriage: evidence from india and vietnam. *Empirical economics*, 61(3):1617–1639.

Tsaneva, M. (2020). The effect of weather variability on child marriage in bangladesh. *Journal of International Development*, 32(8):1346–1359.

Unicef et al. (2014). *Ending child marriage: Progress and prospects*. Unicef.

Unicef et al. (2022). *Child marriage-UNICEF Data Warehouse*. Unicef.

WFP (2022). *WFP Madagascar Cyclone Response Update (As of 24 March 2022) - Madagascar*. UN World Food Programme (WFP).

World Bank, W. B. (2017). *Rapidly Assessing the Impact of Hurricane Matthew in Haiti*. World Bank.

World Bank, W. B. (2021). *Timor-Leste: Rebuilding After Cyclone Seroja Will Be Costly but Offers Opportunities to Strengthen Disaster Resilience*. World Bank.

Zhou, Z. and Zhang, L. (2021). Destructive destruction or creative destruction? unraveling the effects of tropical cyclones on economic growth. *Economic Analysis and Policy*, 70:380–393.

7 Appendices

Table A1: Effect of the cyclone on get married using a sample of women aged 18-24.

	(1)	(2)	(3)	(4)	(5)	(6)
VARIABLES	Get married	Get married	Get married	Get married	Get married	Get married
Cyclone (1/0)	0.0156	-0.00156	0.0154	0.0146	0.0156	0.00388
	(0.0624)	(0.0652)	(0.0624)	(0.0600)	(0.0624)	(0.0622)
Drought (1/0)	-0.000108	-0.00777	-0.000266	-0.00434	-0.000108	-0.00934
	(0.0262)	(0.0257)	(0.0262)	(0.0248)	(0.0262)	(0.0245)
Dummy (1 if Rainfall> 85e percentile)	-1.85e-05	0.000750	0.000284	-0.000170	-1.85e-05	0.00182
	(0.00922)	(0.00926)	(0.00945)	(0.00897)	(0.00922)	(0.00904)
Birth Year FE	No	Yes	No	No	No	Yes
Religion FE	No	No	Yes	No	No	Yes
Education FE	No	No	No	Yes	No	Yes
Country FE	No	No	No	No	Yes	Yes
Observations	181,644	181,644	181,631	181,588	181,644	181,575
Adjusted R-squared	0.022	0.028	0.023	0.029	0.022	0.036

Notes: Our dependent variable is a dummy variable equal to 1 if the woman married at the age corresponding to the age observation of 12 to 24. The cyclone variable is a dummy variable that equals 1 if the lag of the wind speed is greater than or equal to 190km/h. We control for the fixed effects of year of birth, years of schooling, religion, country, and mesh (coefficients not shown). Standard errors are shown in parentheses; ***, **, * represent significance at the 1%, 5%, 10% level, respectively.

Source: Authors' calculations using DHS data.

Table A2: Effect of cyclone on Child marriage

VARIABLES	(1) chilmarr	(2) chilmarr	(3) chilmarr	(4) chilmarr	(5) chilmarr	(6) chilmarr
Cyclone (1 /0)	-0.0135**	-0.0171***	-0.0135**	-0.0169***	-0.0135**	-0.0190***
	(0.00549)	(0.00591)	(0.00549)	(0.00623)	(0.00549)	(0.00641)
Drought (1/0)	-0.00907	-0.00913	-0.00914	-0.00892	-0.00907	-0.00894
	(0.00717)	(0.00727)	(0.00718)	(0.00759)	(0.00717)	(0.00769)
Dummy (1 if Rainfall> 85e percentile)	-0.00734	-0.00565	-0.00714	-0.00660	-0.00734	-0.00522
	(0.00480)	(0.00470)	(0.00491)	(0.00488)	(0.00480)	(0.00485)
Temperature	0.00573	0.0117*	0.00599	0.0101*	0.00573	0.0122*
	(0.00560)	(0.00665)	(0.00559)	(0.00565)	(0.00560)	(0.00663)
Birth Year FE	No	Yes	No	No	No	Yes
Religion FE	No	No	Yes	No	No	Yes
Education FE	No	No	No	Yes	No	Yes
Country FE	No	No	No	No	Yes	Yes
Observations	238,062	238,062	238,054	237,994	238,062	237,986
Adjusted R-squared	0.024	0.027	0.024	0.029	0.024	0.031

Notes: Our dependent variable is a dummy variable that equals 1 if the child married before age 18. The cyclone variable is a dummy variable which is equal to 1 if the wind speed exposure in t-2 is greater than or equal to 190km/h. We control for the fixed effects of year of birth, years of schooling, religion, country, and mesh (coefficients not shown). Standard errors are shown in parentheses; ***, **, * represent significance at the 1%, 5%, 10% level, respectively.

Source: Authors' calculations using DHS data.

Table A3: Effect of cyclone on Child marriage

VARIABLES	(1) chilmarr	(2) chilmarr	(3) chilmarr	(4) chilmarr	(5) chilmarr	(6) chilmarr
Cyclone (1/0)	-0.0129***	-0.0187***	-0.0130***	-0.0162***	-0.0129***	-0.0217***
	(0.00441)	(0.00528)	(0.00441)	(0.00569)	(0.00441)	(0.00617)
Drought (1/0)	-0.000981	-0.00113	-0.00109	-0.00123	-0.000981	-0.00169
	(0.00697)	(0.00735)	(0.00694)	(0.00720)	(0.00697)	(0.00760)
Dummy (1 if Rainfall> 85e percentile)	-0.00689	-0.00491	-0.00659	-0.00574	-0.00689	-0.00459
	(0.00450)	(0.00442)	(0.00459)	(0.00453)	(0.00450)	(0.00451)
Birth Year FE	No	Yes	No	No	No	Yes
Religion FE	No	No	Yes	No	No	Yes
Education FE	No	No	No	Yes	No	Yes
Country FE	No	No	No	No	Yes	Yes
Observations	278,659	278,659	278,650	278,588	278,659	278,579
Adjusted R-squared	0.027	0.029	0.027	0.032	0.027	0.034

Notes: Our dependent variable is a dummy variable that equals 1 if the child married before age 18. The cyclone variable is a dummy variable which is equal to 1 if the wind speed exposure in t-2 is greater than or equal to 190km/h. We control for the fixed effects of year of birth, years of schooling, religion, country, and mesh (coefficients not shown). Standard errors are shown in parentheses; ***, **, * represent significance at the 1%, 5%, 10% level, respectively.

Source: Authors' calculations using DHS data.

Chapitre 13

Effets économiques d'un choc spatialisé et évaluation des politiques de compensation : le cas d'un MEGC appliqué au cyclone tropical Dina à La Réunion

Mamboundou, Garabedian, Fontaine

- ***Revue Économique***, en soumission, 2023

RenovRisk – Impacts

Effets économiques d'un choc spatialisé et évaluation des politiques de compensation : le cas d'un MEGC appliqué au cyclone tropical Dina à La Réunion

Mamboundou Pierre[1], Garabedian Sabine[2], Fontaine Idriss[3]

Résumé

L'accroissement du risque cyclonique commande d'évaluer les impacts économiques indirects des cyclones afin d'y faire face. A cet effet, nous construisons un modèle d'équilibre général calculable (MEGC) dynamique récursif, calibré sur l'économie de La Réunion pour analyser les effets économiques indirects spatialisés du cyclone DINA de 2002. Cette analyse qui intègre deux scénarii de choc basés sur l'intensité et sur la récurrence cyclonique ainsi que trois politiques d'atténuation montre que les chocs cycloniques se diffusent à l'ensemble de l'économie par l'accroissement des prix. Il en découle une diminution de la compétitivité des branches et de la demande domestique. Les résultats suggèrent que pour atténuer ces chocs cycloniques, une politique d'investissement au prorata des dommages sectoriels a plus d'efficacité qu'un réinvestissement dans les secteurs intensifs en valeur ajoutée ou qu'un investissement dans les secteurs d'entrainements.

Classification JEL: C68, Q54, O11, E6

Remerciement : Ce travail a été réalisé avec le ssoutien financiers du Fonds européen de développement économique et régional (FEDER).

[1] Ecole d'Ingénieurs de PURPAN, E-mail: pierre.mamboundou@purpan.fr
[2] Laboratoire CEMOI, Université de La Réunion; E-mail: sabine.garabedian@univ-reunion.fr
[3] Laboratoire CEMOI, Université de La Réunion; E-mail: idriss-fontaine@univ-reunion.fr

1. Introduction

Dans le contexte de réchauffement climatique actuel, l'adaptation aux catastrophes naturelles constitue une problématique majeure. En effet, en même temps que la hausse des températures, l'accroissement du niveau des mers et la perturbation des écosystèmes, on observe une recrudescence des catastrophes naturelles de types cyclones, sécheresses, inondations (Mavume et al., 2009 ; Banholzer et al., 2014 ; Bindoff et al., 2019 ; Knuston et al., 2020). Ce processus fragilise davantage les territoires exposés que sont les économies insulaires et les pays en développement (Tullet et al., 2020 ; IPCC 2022) comme cela l'a été mentionné encore récemment lors de la COP27. C'est le cas des territoires ultramarins français tel que La Réunion qui est située au cœur d'un des bassins cycloniques le plus actif au monde (Leroux et al., 2018, Tulet et al., 2021), qui détient la période de retour des cyclones de catégorie 4 la plus courte par rapport aux autres départements d'Outre-Mer (CCR 2020) et qui a été historiquement le théâtre de plusieurs évènements cycloniques (Jenny en 1962, Denise en 1966, Hyacinthe en 1980, Clotilda en 1987, Firinga en 1989, Colina en 1993, Dina en 2002, Gamède en 2007, Bejisa en 2014 (Jouanjean 2011). Ce contexte géo-climatique particulier couplé à une situation économique difficile caractérisée par un niveau de pauvreté et de chômage élevé (INSEE, 2018), rend nécessaire la réalisation d'études des effets économiques des cyclones à La Réunion, dans l'optique d'aiguiller les pouvoirs publics sur les politiques permettant de s'y adapter.

Bien que l'analyse des impacts économiques des catastrophes naturelles fasse l'objet d'une attention croissante depuis une dizaine d'année, leur évaluation demeure encore assez peu étudiée dans la littérature. Globalement, l'analyse des impacts de ces catastrophes naturelles, peuvent traiter d'une part des répercussions « naturelles » qui regroupent les dommages directs c'est-à-dire observés au moment de la catastrophe (Kahn 2005 ; Kellenberg et Mobarak 2008), des dommages indirects c'est-à-dire les changements dans l'activité économique après la catastrophe (Kousky 2016 ; Zander et al., 2020 ; Rahman et al., 2022). D'autre part, elles peuvent traiter des outils déployés par les pouvoirs publics pour faire face avec efficacité à ces dommages (Wittwer et Griffith 2011, Rose et al., 2011, Xie et al., 2014). En termes de méthode, les répercussions naturelles directes sont généralement évaluées à l'aide d'une fonction de dommage qui permet de lier un niveau de destruction à la force de l'aléa climatique (Emanuel 2011 ; Bertinelli et al., 2016 ; Dinan 2017 ; Botzen et al., 2019). Cette destruction peut être estimée en valeur monétaire ou en proportion d'une valeur économique d'ensemble. Les répercussions naturelles indirectes peuvent quant à elles, être étudiées à travers des modèles économétriques qui reposent généralement sur des régressions des variables

agrégées mesurées au niveau des pays telles que les montants des dommages monétaires, le nombre de morts, l'évolution de l'emploi, des inégalités, du bien-être, etc. (Skidmore et Toya 2002 ; Hsiang 2010 ; Anttila-Hughes et Hsiang 2013 ; Estrada et al., 2015 ; Kousky 2016 ; Rahman et al., 2022 ; Zander et al., 2020 ; Fontaine et al., 2021 ; Tovar Reanos 2021). Cependant ces modèles ne permettent ni d'identifier les canaux de transmission des catastrophes à l'ensemble de l'économie, ni d'analyser les effets des politiques d'atténuation et / ou d'adaptation (Hallegate 2008 ; MacKenzie et al., 2012 ; Koks et Thissen (2016), Botzen et al., 2019). Le recours aux modèles d'Equilibre général Calculable (MEGC) permet de pallier ces deux dernières limites puisqu'ils retracent les canaux par lesquels les désastres naturels se répercutent à l'économie et peuvent modéliser des politiques d'adaptation (Narita 2010 ; Washida et al. 2014 ; Sassi 2014 ; Wittwer et Griffith 2011 ; Rose et al., 2011 ; Xie et al., 2014 Okuyama et Santos 2014 ; Rose et Liao 2005 ; Botzen et al., 2019). Toutefois, ces modèles ne sont pas toujours spatialisés ce qui peut apparaitre comme une limite. Nous proposons donc une approche originale qui repose sur un MEGC dynamique récursif calibré sur une matrice de comptabilité sociale (MCS) de 2016 dont l'activité économique a été spatialisée. A partir de cette situation de référence, nous menons une analyse en deux temps. Dans le premier, nous appliquons une fonction de dommages cycloniques sectoriels et spatialisés permettant de comparer les répercussions naturelles d'un cyclone de forte intensité (scénario I) à celles liées à la récurrence de quatre cyclones d'intensité plus faible (scénario R). Le scénario d'intensité simule les impacts du cyclone DINA de 2002 à la fois pour des considérations empirique et méthodologique. En effet, sur le plan empirique, s'il ne s'agit pas du système le plus important que La Réunion ait connu, il s'agit d'un évènement qui a touché l'ensemble du territoire. Sur le plan méthodologique, il s'agit d'un cyclone ayant été traité par la méthode BOGUS qui permet d'avoir des champs de vents spatialisés tenant compte de la topographie du territoire a un niveau très fin. Dans le second temps, nous simulons trois politiques d'intervention des pouvoirs publics afin d'explorer leurs effets potentiels dans les deux cas de figures. Ces politiques reposent sur un investissement public dans les différents secteurs d'activités au prorata des dommages constatés (scénario IT-PRD), dans les secteurs à forte valeur ajoutée (IT-VA), ou dans les secteurs dits d'entrainement c'est-à-dire ceux dont les produits sont les plus demandés en consommations intermédiaires (IT-CI). Les résultats suggèrent, qu'un plan d'investissement basé sur le montant des dommages observés permet d'atténuer les effets lorsqu'il repose sur un investissement public dans les différents secteurs d'activités au prorata des dommages constatés. La suite de cet article est organisée comme suit : La section 2 présente les caractéristiques du cyclone DINA que nous utilisons comme cyclone de référence dans cette

analyse. Dans la section 3, nous explicitons le cadre méthodologique et les données mobilisées. Les sections 4 à 6 présentent les simulations et discutent les résultats obtenus alors que la dernière section est consacrée aux remarques conclusives.

2. Eléments contextuels

Cette étude vise à analyser les effets économiques du passage d'un cyclone de type DINA (2002) sur l'économie de La Réunion d'aujourd'hui (représentée par la MCS de 2016 étant l'année la plus récente disponible pour les comptes publics consolidés). Ce choix est justifié par le fait que c'est le dernier évènement cyclonique caractérisé par des intensités extrêmes en termes de vent générés et, qu'il pourrait survenir avec une période de retour de 34 ans (CCR 2020).

2.1. L'économie de La Réunion

La Réunion est une île de 2512 Km² pour 850 000 habitants dont le PIB par habitant s'élevait à 21 171 euros en 2016. L'activité économique du territoire est synthétisée dans la MCS calibrée sur l'année 2016 qui contient dans sa version initiale 20 secteurs d'activités et autant de produits, trois agents économiques représentatifs (les agents privés qui regroupent les ménages, les entreprises et les institutions sans but lucratif au service des ménages), le gouvernement et le reste du monde, ainsi que deux facteurs de production. L'analyse de la MCS révèle une économie dominée par les secteurs tertiaires, qui contribuent pour près de 75% au PIB, et relativement plus intensive en valeur ajoutée (55%). Plus précisément, la branche des services d'enseignement et de santé est celle qui contribue le plus au PIB (25%), suivie de l'immobilier (14,8%), puis de l'administration publique (10%). Ces secteurs moteurs de l'économie ont par ailleurs une production plus intensive en valeur ajoutée avec respectivement 81,7% pour l'immobilier, 78,4% pour de l'enseignement et la santé, et 74,7% pour l'administration publique (voir Tableau 1).

Tableau 1 - Structure de production des principaux secteurs

Secteur intensif en VA	Part de la VA dans la production	Poids dans la VA totale	Secteur intensif en CI	Part des CI dans la production	Poids dans les CI totales
Immobilier	81,7%	14,8%	Sucre et rhum	79,7%	2,4%
Enseignement et santé	78,4%	25%	Electricité et l'eau	69,5%	6,8%

Administration publique	74,7%	10%	Agroalimentaire	64,5%	8,8%
Autres services	66,6%	4%	Construction	63,2%	13,3%
Services administratifs	56,8%	3,4%	Transport	63,2%	8,1%
Agriculture	52%	1,8%	Industrie manufacturière	54,8%	14,2%

Au total, ce sont 8 des 20 secteurs qui ont une production intensive en valeur ajoutée. Dès lors, ces derniers seront relativement plus sensibles à des chocs sur l'offre des facteurs de production. Au sein de ces secteurs intensifs en valeur ajoutée, on observe que la masse salariale domine le capital. En effet, seules quatre branches sont intensives en capital (immobilier 94%, agriculture 65,9%, information et communication 57,2%, finance et assurance 51,8%). Concernant le commerce extérieur, La Réunion importe plus qu'elle n'exporte. Toutefois, 90% des importations sont concentrées dans trois types de biens : les produits manufacturiers (70% des importations totales), les produits agroalimentaires (15,52%) et les produits de la cokéfaction et du raffinage (6,52%). Les exportations quant à elles, ne pèsent que 1,8% de la production totale.

2.2.Le cyclone DINA : caractéristiques et impacts à la Réunion

Le choix du cyclone tropical DINA de 2002 s'appuie sur des considérations empirique et méthodologique. Sur le plan empirique, il s'agit du dernier évènement cyclonique extrême par son intensité. En effet, DINA a engendré des vents violents sur l'ensemble du territoire mais surtout sur la façade Nord-Ouest et dans les hauteurs de l'île. On note par ailleurs que les vents ayant le nombre d'occurrences le plus important (150) durant ce cyclone avaient une vitesse d'un peu plu de 150Km/h (voir Figure 1).

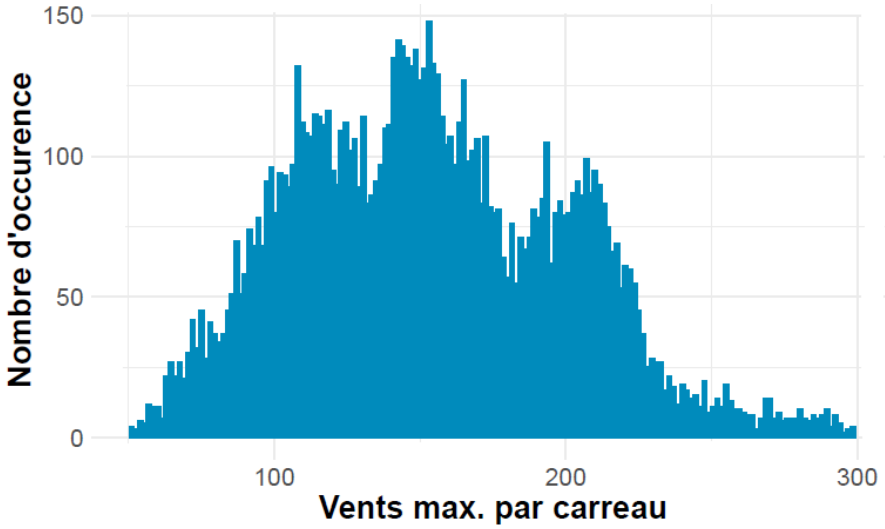

Figure 1: Estimation des vents maximums par carreau

A l'échelle du territoire, ces vents sont répartis de façon hétérogène. Comme le montre la figure 2, les communes de Saint Denis, Le Port, Saint Paul et Trois Bassins ont concentré les vents les plus forts (compris entre 190 Km/h et 220 Km/h) alors que le Sud-Est a été exposé à des vents relativement moins intenses.

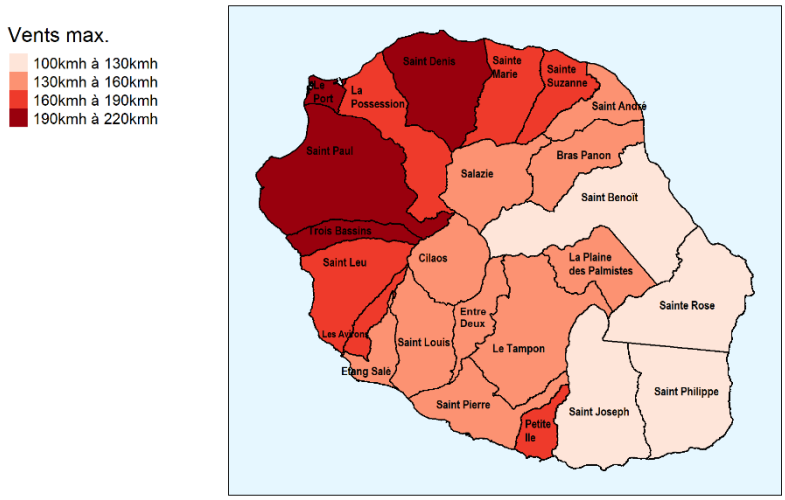

Figure 2: Estimation des vents maximums d'un cyclone de type DINA à partir de BOGUS

L'inégale exposition du territoire aux vents d'un cyclone de type DINA laisse entrevoir une inégale répartition des dommages. Or, cette hétérogénéité spatiale des dommages est rarement prise en compte dans l'analyse des impacts économiques indirects des catastrophes naturelles (Botzen et al., 2019). Pourtant les chocs cycloniques ayant des impacts spatialisés différents, il parait nécessaire d'appréhender cette dimension afin d'apprécier les répercussions d'un tel

phénomène dans sa globalité et ainsi permettre de mieux structurer la réponse des pouvoirs publics à ce type d'évènement.

3. Le modèle et ses caractéristiques

L'originalité de ce travail réside dans la proposition d'une méthodologie hybride reposant sur des fonctions de dommages appliquées à une valeur économique spatialisée pour évaluer les effets directs couplé à un MEGC pour analyser les effets indirects et les politiques d'atténuation.

3.1. La spatialisation de l'activité économique

La première étape vise à répartir l'activité économique sur le territoire pour évaluer quels sont les secteurs économiques (et donc quelle valeur économique associée) présents dans les différentes communes qui seront potentiellement touchés par les fonctions de dommages directs. Cette spécification sectorielle est indispensable pour prendre en compte l'hétérogénéité sectorielle des impacts d'une catastrophe naturelle (Carerra et al., 2014, Borgomeo et al., 2018 ; Garcia-Léon et al., 2021). Cependant, à notre connaissance, seuls Shugrue et al., (2020) mobilisent une démarche ayant le même objectif dans le cadre de l'analyse des effets d'un cyclone sur l'activité urbaine. Pour ce faire, nous mobilisons deux sources de données : des données sur le recensement agricole (fichier RA 2016) pour le secteur agricole et les données du fichier FARE Réunion (INSEE 2016) pour les autres secteurs d'activité. Concernant le secteur agricole, nous avons utilisé les surfaces cultivées par commune pour ventiler la valeur économique agricole de la MCS sur l'ensemble du territoire. Concernant les autres secteurs, nous avons déterminé la part que représente chaque secteur d'activité dans l'activité économique communale à partir des chiffres d'affaires déclarés des entreprises au sein des communes où elles mènent leur activité. A partir de cette part, nous avons ventilé les valeurs agrégées de la MCS pour obtenir une répartition spatialisée de l'activité économique sur l'ensemble du territoire (voir figure 3).

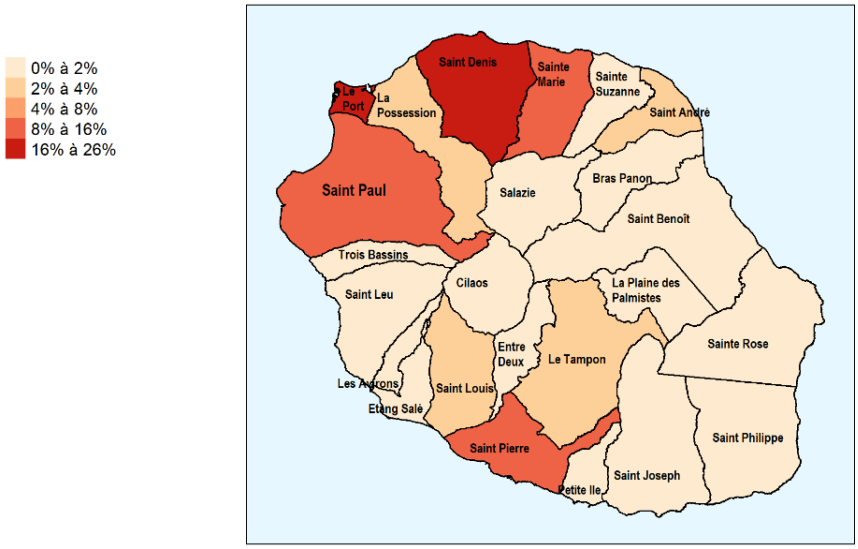

Figure 3: Répartition de l'activité économique sur le territoire

Il en ressort que les communes de Saint-Denis (25,59%), le Port (19,57%) et Saint-Pierre (10,49%) concentrent plus de 55% de l'activité économique. A l'inverse, l'Entre-Deux (0,17%), la Plaine des Palmistes (0,11%), Saint Philippe (0,18%), Sainte-Rose (0,10%), Salazie (0,15%), les Trois-Bassins (0,14%) et Cilaos (0,16%) ne concourent qu'à 1,01% de la richesse créée sur le territoire. Cette décomposition sectorielle nous permet d'appliquer des coefficients de destruction communaux différenciés selon deux critères. D'une part, selon la force des vents auquel la commune est exposée (voir partie 3.2) et d'autre part, selon la structure de l'activité économique de chaque commune. Cela nous permettra d'obtenir des pertes économiques sectorielles à l'échelle communale qui, une fois agrégées correspondront au montant des dommages sectoriels pour l'ensemble du territoire.

3.2. Application d'une fonction de dommage

La deuxième étape consiste à calculer les coefficients de destruction à travers l'utilisation d'une fonction de dommage. Ces coefficients de destruction permettent d'évaluer les pertes économiques en fonction de la force des vents pour chaque commune du territoire sur la base de sa structure économique. Pour cela, nous avons estimé d'une part, les champs de vents qui ont touché chaque commune et d'autre part, le niveau de pertes économiques propres à chaque secteur d'activité.

L'estimation des champs de vents du cyclone à l'échelle des différentes communes a été réalisée à travers la méthode dite de « BOGUS » développée par Vérémès et al., (2020) qui

comprend les caractéristiques topographiques[4] (terrains montagneux, plaines, plateaux, bandes côtières) du territoire à une échelle fine.[5]

Le niveau de pertes économiques est ensuite obtenu par l'application de fonctions de dommage qui consiste à calculer un indice de destruction à partir de la moyenne de la vitesse maximale des vents par commune (Emanuel 2011, Meyer et al., 2013). Or, la difficulté repose ici sur le fait que les dégradations liées à l'exposition aux vents ne sont pas linéaires (Meyer et al., 2013 ; Hsiang et al., 2017, Bretschger et Pattakou 2019). Cette non-linéarité découle du fait que d'une part l'accroissement de la vitesse du vent ne génère pas des dégradations proportionnelles et d'autre part, du fait que les objets n'ont pas la même résistance face à l'intensité des vents. Nous avons retenu l'approche de Fontaine et al. (2021) inspirée des travaux de Bertinelli et al., (2016), Emanuel (2011) ou encore Boose (2004) qui propose la fonction de dommage définie par l'équation 1 ci-dessous :

$$f_{ci} = \frac{v_{ci}^3}{1 + v_{ct}^3}$$

Avec :

$$v_{ci} = \frac{MAX\ (W_{ci} - \bar{W}^*, 0)}{W^* - \bar{W}}$$

Dans ces expressions, f_{ci} désigne l'indice de perte économique pour un espace en fonction de l'évènement cyclonique i, $\bar{W}$ la valeur minimale de la vitesse du vent au-dessus de laquelle une perte économique est observée et, W^* le seuil à partir duquel la moitié de la valeur économique d'une cellule donnée est totalement détruite. Cet indice de destruction permet de capturer trois caractéristiques importantes. La première liée au paramètre $\bar{W}$ transcrit le fait que les valeurs positives des dommages économiques ne se produisent que lorsque le vent enregistré dépasse un certain seuil. La seconde traduit le fait que les dommages économiques augmentent avec la puissance cubique de la vitesse maximale du vent. La troisième porte sur le fait que pour des vents forts, l'indice impose que la fraction de la perte économique totale ne puisse pas dépasser 1. Le choix des paramètres W^* et $\bar{W}$ dans l'équation est donc important, car ils façonnent la forme de notre fonction de dommage. Cependant, dans le cadre de La Réunion, il n'y a pas d'études empiriques permettent de calibrer la valeur de ces deux paramètres. Cependant nous

[4] La prise en compte des informations topographiques est déterminante pour estimer l'exposition réel au sol, notamment à La Réunion ou le relief est escarpé.

[5] Les estimations des vents générés par cette méthode ont été comparées avec les données réelles relevées des cyclones DINA et BEJISA permettant ainsi sa validation empirique. Pour plus de détails techniques, le lecteur intéressé peut se référer au papier de Vérèmes et al., (2020).

avons supposé que le secteur agricole était plus vulnérable au vent de tel sorte que pour les activités agricoles nous retenons $\overline{W}$ fixé à 70 km/h et W^* à 120 Km/h afin que le montant des dommages totaux corresponde[6] à la valeur déclaré dans le rapport préfectoral (2022). Pour les autres secteurs, nous retenons les valeurs $\overline{W}$ fixé à 93 km/h et W^* à 270 Km/h proposés par Emanuel (2011) ou Eliott et al., (2015).

L'application des fonctions de dommage a alors permis de déterminer des pertes économiques globales de 16,78% de la valeur économique du territoire en différentiant l'impact selon les communes. Ainsi, comme le montre la figure 4, la façade Nord-Ouest est la plus impactée avec une concentration des pertes économiques les plus importantes dans les communes de Saint-Denis (59,91%), du Port (14,52%) et de Saint-Paul (12,36%).

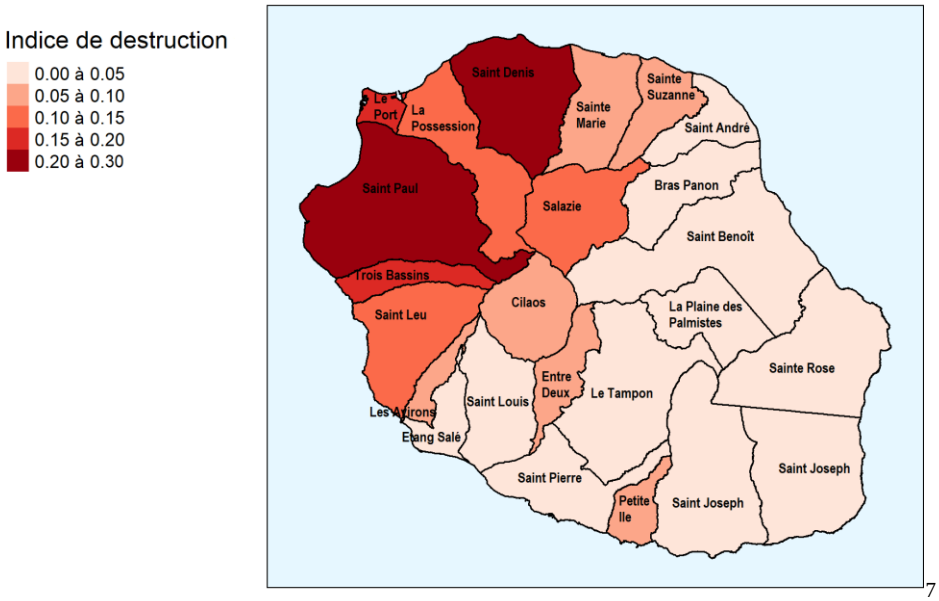

[7]

Figure 4: Indice des pertes économiques communales générées par DINA

Lorsqu'on analyse les pertes économiques en fonction des types d'activités (voir tableau 2), on s'aperçoit que les communes sont là aussi impactées de façon différente. En effet, les dommages agricoles les plus importants sont localisés dans les communes du Tampon, de Saint-Paul et de Saint-Leu avec des pertes économiques de respectivement 16,12%, 12,66% et 10,22%. Les pertes économiques non agricoles sont quant à elles plus importantes dans les communes de Saint-Denis (63,86%), du Port (15,49%) et de Saint-Paul (12,34%).

[6] Nous avons obtenu ces seuils par tâtonnement.
[7] Le coefficient 0.10 correspond à une destruction de 10% de l'activité économique dans la commune

Tableau 2 – Evaluation des dommages agricoles et non agricoles

Nom des communes	Valeur de destruction agricole	Indice de destruction agricole en %	Valeur de destruction non agricole	Indice de destruction non agricole en %	Valeur de destruction totale	Indice de destruction totale en %
Les Avirons	1075,04	0,67	83,10	0,00	1158,81	0,05
Bras-Panon	2998,94	1,88	457,95	0,02	3458,78	0,14
Entre-Deux	250,66	0,16	19,51	0,00	270,33	0,01
L'Etang-Salé	1798,68	1,13	1283,81	0,05	3083,62	0,12
Petite-île	6122,50	3,84	112,99	0,00	6239,33	0,25
La Plaine des Palmistes	1516,90	0,95	2,53	0,00	1520,38	0,06
Le Port	284,74	0,18	366564,47	**15,49**	366849,38	**14,52**
La Possession	490,47	0,31	19391,77	0,82	19882,55	0,79
Saint-André	11996,35	7,53	28807,17	1,22	40811,05	1,62
Saint-Benoît	9657,78	6,06	8129,30	0,34	17793,14	0,70
Saint Denis	2015,84	1,26	1511608,33	**63,86**	1513625,44	**59,91**
Saint-Joseph	6777,77	4,25	500,27	0,02	7282,29	0,29
Saint-Leu	16293,57	**10,22**	4536,16	0,19	20839,95	0,82
Saint-Louis	6023,00	3,78	1308,97	0,06	7335,75	0,29
Saint-Paul	20177,16	**12,66**	292055,06	**12,34**	312244,88	**12,36**
Saint Pierre	15830,00	9,93	32883,69	1,39	48723,62	1,93
Saint-Philippe	3536,11	2,22	39,24	0,00	3577,57	0,14

Sainte-Marie	8125,61	5,10	87237,65	3,69	95368,36	3,77
Sainte-Rose	4445,34	2,79	50,74	0,00	4498,86	0,18
Sainte-Suzanne	8244,97	5,17	7591,91	0,32	15842,04	0,63
Salazie	1396,37	0,88	66,84	0,00	1464,09	0,06
Le Tampon	25688,58	**16,12**	4052,69	0,17	29757,39	1,18
Les Trois-Bassins	4402,13	2,76	227,19	0,01	4632,08	0,18
Cilaos	230,18	0,14	51,55	0,00	281,88	0,01
Total	159378,71	100,00	2367062,89	100,00	2526541,60	100,00

Source : Résultats des auteurs tirés de l'application de la fonction de dommage

3.3. Les autres spécificités du modèle EGC

La troisième étape est d'inclure le montant des dommages dans un modèle EGC qui permettra d'évaluer les effets indirects dans l'ensemble de l'économie via les interdépendances de marché. Le modèle que nous avons construit est un modèle dynamique récursif, inspiré des hypothèses du modèle GetRUN-NRJ de Garabedian (2020), Croissant *et al.* (2020) et du modèle PEP 1-t de Décaluwé et al. (2013). Il retrace l'ensemble des interactions entre les agents économiques et les variables économiques de l'économie au travers des 20 secteurs d'activités des trois types d'agents économiques représentatifs que sont le gouvernement, les agents privés et le reste du monde. Concernant la dynamique récursive du modèle, elle suppose qu'à chaque période un nouvel équilibre est calculé en se basant sur les résultats obtenus à la période précédente. Ainsi, en l'absence de choc exogène, les variables de l'économie évoluent grâce au taux d'accroissement de la population qui est fixé à 0,5% (INSEE 2019). En outre, l'accumulation du capital contribue également à lier les différentes périodes entre elles. De façon pratique, le stock de capital de la période *t* dépend du stock de capital déprécié de la période précédente auquel s'ajoute les nouveaux investissements en capital réalisés ($IND_{(k,j,t-1)}$).

L'une des spécificités du modèle est l'intégration du choc cyclonique et des stratégies de réponse à ce dernier. Rappelons que conformément à la littérature (Narita 2010 ; Wittwer et Griffith 2011 ; Wasida et al. 2014 ; Xie et al., 2014), les catastrophes naturelles peuvent être modélisées dans ce type de modèle au travers d'un coefficient de dommage dans la fonction de

valeur ajoutée ou dans celle du stock de capital. Considérant que les dommages liés aux cyclones sont majoritairement des destructions physiques des actifs, nous adoptons l'approche retenue par Wittwer et Griffith 2011, Rose et al., 2011, Xie et al., 2014. De façon pratique, nous introduisons dans la fonction d'accumulation du capital de chaque secteur une variable de dommage cyclonique « $CD_{j,t}$ ». De ce fait, l'offre de capital disponible à la période t pour produire dépendra de l'effet du dommage cyclonique sur le stock de capital déprécié, auxquels s'ajoute le volume des nouveaux investissements réalisés à la période « $t-1$ ». $CD_{j,t}$ correspond au niveau de dommages pour chaque secteur en pourcentage du PIB. Pour tenir compte des effets de l'intervention des pouvoirs publics qui est basée sur un accroissement des investissements, nous introduisons le volume des nouveaux investissements publics consentis pour faire face aux dommages cycloniques « $IND_{\_DENV(k,j,t-1)}$ » dans l'équation d'accumulation du capital. Ce volume d'investissements publics nouveaux découle du budget d'investissement public qui est alloué à chaque secteur d'activité pour faire face à la catastrophe.

$$KD._{fx(k,j,t)} = (1 - CD_{j,t-1}) * KD_{k,j,t-1} * (1 - \delta_{(k,j)}) + IND_{(k,j,t-1)} + IND_{\_DENV(k,j,t-1)}$$

En outre, en suivant l'approche de Blanchflower et Oswald (1995), la modélisation du marché du travail se fait en considérant l'existence du chômage qui est introduit grâce à une courbe des salaires modifiant la fonction d'offre de travail tel qu'il suit :

$$LS_{l,t} = \sum_{j} LD_{l,j,t} / (1 - UR_{l,t})$$

Dans cette expression, $LS_{l,t}$ désigne l'offre de travail, $LD_{l,j,t}$ la demande en facteur travail exprimée par les différents secteurs et $UR_{l,t}$ le taux de chômage. Les indices l, j, t représentent respectivement les types de main d'œuvre, les secteurs d'activités et les périodes. Dès lors, l'évolution du salaire réel ($W_{l,t}$) va désormais être influencée par celle du chômage.

$$W_{l,t} = A_l * UR_{l,t}^{\epsilon} * PIXCON\ (t)$$

4. Présentation des scénarii et discussion des résultats

A partir du modèle construit nous avons évalué les répercussions naturelles dans le premier ensemble des scénarios en regardant si les effets indirects sont plus importants dans le cas d'un choc unique de forte intensité ou dans le cas d'une récurrence de chocs de plus faible intensité. Pour cela, nous comparons le scénario d'« intensité » (IT) caractérisé par la simulation d'un choc unique dont les dommages directs équivalent à ceux d'un cyclone de type

DINA à un scénario de « récurrence » (IR) caractérisé par quatre évènements cycloniques identiques à un intervalle de deux ans et dont la somme des dommages équivaut au choc d'intensité. Dans le second ensemble, nous investiguons l'efficacité des politiques de soutien en simulant trois scénarios (pour IT et IR). Le premier scénario (scénario •-PRD[8]) repose sur un investissement public dans les différents secteurs affectés au prorata des dommages constatés ; le deuxième scénario (scénario •-VA), repose sur un investissement orienté vers les secteurs à forte valeur ajoutée ; enfin, le troisième scénario (scénario •-CI) repose sur un investissement orienté vers les secteurs dits d'entrainement c'est-à-dire ceux dont les produits sont les plus demandés en consommations intermédiaires. Les simulations sont faites sur 10 ans (10 périodes) et les résultats analysés à court terme correspondent à ceux de la période qui suit la survenue du choc cyclonique et à long terme, ceux de la 10ème période.

4.1. Les répercussions naturelles

4.1.1. Impacts macroéconomiques

Les résultats macroéconomiques nous permettent d'effectuer des comparaisons exclusivement en moyenne ou à long terme car les effets du choc de récurrence concernent une intensité quatre fois moindre que le choc d'intensité, donc non comparables à court terme, tandis que la somme des dommages des deux scénarios est équivalente ce qui permet leur comparaison à long terme et en moyenne.

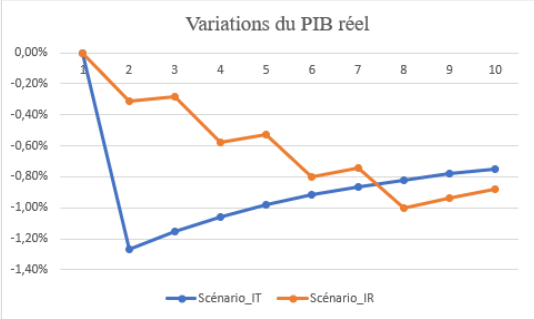

Figure 5 : Variations du PIB réel sur la période

Nous pouvons constater sur le tableau 3 et la figure 5, que la baisse du PIB réel à long terme est plus importante lors de chocs récurrents de faible intensité que lors d'un choc de forte intensité (-0,75% pour IT vs -0,88% pour IR). Or, les effets moyens vont dans le sens inverse avec une baisse de 0,95% dans le scénario IT contre 0,67% dans IR. Cette tendance s'explique d'une part par les délais de reprise qui sont courts entre le dernier choc du scénario IR (qui a

[8] Les politiques d'ajustement étant testées dans le cas des scénarios d'intensité et de récurrence, le symbole • peut prendre les valeur IT ou IR.

lieu à la septième période) et le moment retenu pour l'analyse à long terme qui correspond à la dixième période ; et d'autre part par le fait que l'ampleur des effets négatifs à court terme du scénario IT sur la demande, les coûts de production réduit davantage les capacités productives des secteurs sur la période que dans le scénario IR.

Tableau 3 - Effets sur les variables macroéconomiques en %

Variables	**Choc d'intensité (IT)**		**Choc de récurrence (IR)**	
	LT	Moyenne	LT	Moyenne
PIB Réel	**-0,75%**	**-0,95**	**-0,88**	**-0,67**
Ind. prix conso.	1,11	1,57	1,38	1,12
Dem. domestique	-1,36	**-1,63**	-1,16	**-0,85**
Offre de capital	-1,69	-1,81	-1,76	-1,22
Production totale	-1,05	-1,27	-1,19	-0,88
Taux de chômage	0,36	1,29	0,94	1,07
Exportations	-2,41	-3,05	-2,80	-2,15
Importations	2,04	2,53	2,35	1,76

Source : Résultats des auteurs tirés du MEGC

Bien que l'ampleur des effets soit différente, les canaux de propagation des chocs semblent similaires dans les deux scénarios. En effet, cette baisse du PIB réel est consécutive à la raréfaction du capital productif utilisé par les différentes branches pour produire, ce qui favorise l'accroissement des coûts de production. Cette situation va favoriser une diminution de la demande locale en biens et services du fait de la hausse des prix et renforcer l'effet négatif observé sur la production. En effet, la hausse des prix affecte à la fois les biens finaux et les biens intermédiaires. Il en résulte une contraction de la demande domestique globale (-1,63% dans IT et de -0,85% dans IR sur la période). Par ailleurs, la contraction de l'activité productive entraine un accroissement du chômage qui détériore la situation des agents privés.

Concernant le commerce extérieur, la hausse des prix domestiques entraine un accroissement de la demande des biens importés. Cette tendance renforce la dépendance aux partenaires commerciaux extérieurs et ce principalement pour les produits alimentaires. Du côté des exportations, on observe une tendance baissière qui résulte à la fois de la réduction de la production des filières locales mais aussi de la hausse des prix. Cette dernière engendre une perte de compétitivité par rapport aux concurrents internationaux qui se traduit par une baisse de la demande à l'export des produits locaux.

4.1.2. Impacts sectoriels et communaux

En plus des dynamiques sectorielles observées au niveau macroéconomique, notre modèle nous permet d'appréhender les dynamiques sectorielles communales. L'analyse sectorielle montre qu'une baisse de la production des différents secteurs qui entraine une contraction de leur demande en facteurs de production. Pour ce qui est du capital, sa demande diminue pour l'ensemble des branches (tant dans le scénario IT que IR). Cette situation s'explique par la hausse du coût d'utilisation du capital sur la période suite à sa raréfaction. Pour y faire face, les secteurs réduisent majoritairement leur demande en capital et une minorité le substitue davantage par du travail. C'est essentiellement le cas pour les secteurs immobilier et éducation-action sociale (voir Annexe 1) dont les demandes en travail augmentent en moyenne respectivement de 7,22% et de 0,91% en IT et de 3,76% et 0,58% en IR. En ce qui concerne les dynamiques sectorielles communales présenté sur le tableau 4, nous observons que les communes les plus affectées sont Saint-Denis (59,91%), Le Port (14,52%) et Saint-Paul (12,35%) qui concentrent plus de 86% des dommages. Ces résultats sont assez préoccupants dans la mesure où ces communes contribuent pour 60% de l'activité économique. Les secteurs du commerce et de l'action sociale y sont par ailleurs les plus affectés.

Tableau 3 - Impacts sectoriels dans les communes les plus affectées

Communes	Secteur 1	Secteur 2	Secteur 3	Secteur 4
Saint-Denis	Immobilier (30,46%)	Education, Action sociale (24,54%)	Commerce (10,03%)	Information (9,15%)
Le Port	Education, Action sociale (26,61%)	Commerce (20,92%)	Construction (12,57%)	Manufacture (9,53%)
Saint-Paul	Education, Action sociale (34,34%)	Commerce (9,51%)	Immobilier (8,37%)	Construction (8,83%)

Source : Résultats des auteurs

Dans les 3 communes les plus affectées, les secteurs de l'éducation-action sociale, du commerce, de l'immobilier et de la construction sont ceux qui sont les plus affectés. Ces résultats, mis en relief avec la structure de l'économie locale présentée par la MCS, permettent de mieux appréhender l'ampleur des chocs. En effet, on relève que les secteurs de l'éducation et l'action sociale, l'immobilier et la construction qui sont parmi les plus impactés concentrent à eux trois près de 45% de la valeur ajoutée et 30% des consommations intermédiaires à la base.

De ce fait, une attention particulière à ces secteurs dans le cadre des politiques d'atténuation pourrait s'avérer utile pour relancer efficacement l'activité économique.

4.1.3. La situation des agents économiques

L'analyse de la situation des agents économiques résumée dans le tableau 5 laisse apparaître deux grandes tendances.

Tableau 5 - Impacts sur les agents en %

Variables	Choc d'intensité (IT)		Choc de récurrence (IR)	
	LT	Moyenne	LT	Moyenne
Revenu RDM	0,80	**1,03**	0,94	**0,72**
Epargne RDM	1,07	1,37	1,26	0,96
Revenu gouv.	0,75	0,95	0,88	0,66
Revenu AP	1,72	2,38	2,13	1,07
Conso. AP	-0,48	-0,73	-0,64	-0,54

Source : Résultats des auteurs tirés du MEGC.

La première tendance concerne les agents qui « tirent profit » du choc cyclonique, soit le reste du monde et le gouvernement. Pour ce qui est du reste du monde, il bénéficie d'un accroissement de son revenu de 1,03% en moyenne après un cyclone intense et de 0,72% après des cyclones récurrents grâce à l'augmentation des importations et la diminution des exportations. Cette tendance favorise par ailleurs une hausse de son épargne. Pour ce qui est du gouvernement, c'est la hausse des importations et surtout des taxes liées à ces dernières qui lui permet d'accroître son revenu.

Concernant les agents privés locaux, ils peuvent être classés dans la seconde tendance c'est-à-dire celle de ceux qui sont fragilisés par les chocs cycloniques. En effet, bien que le choc cyclonique entraine une hausse de leur revenu stimulé par d'une part la hausse du prix du capital et d'autre part celle des salaires du fait de la hausse de la demande de travail dans certains secteurs, leur consommation diminue. Cette contraction de la consommation résulte d'une hausse plus importante des prix à la consommation comparativement à celle de leurs revenus.

4.2. Implications économiques des politiques d'atténuation

Etant donné que le choc cyclonique conduit à une destruction du capital, la réponse des pouvoirs publics pour en atténuer les effets pourraient reposer sur un accroissement des

investissements en capital. A cet effet, ces investissements pourraient se faire au prorata des dommages constatés dans chaque secteur (ce qui correspond à une logique assurancielle) ou en fonction d'objectifs économiques plus opportunistes visant à modifier la structure de l'économie locale. C'est pourquoi, nous retenons et analysons trois politiques d'atténuation.
La première (scénario -PRD), repose sur un investissement public dans les différents secteurs affectés au prorata des dommages constatés. Dans la seconde (scénario -VA), nous faisons l'hypothèse d'un investissement orienté vers les secteurs à forte valeur ajoutée. Enfin, dans la troisième, on postule que le gouvernement met l'accent sur les secteurs dits d'entrainement (scénario -CI).

Les résultats des politiques simulées permettent d'observer une tendance similaire face à l'atténuation d'un cyclone intense ou de cyclones récurrents. Dans les deux cas de figure, aucune des politiques envisagées ne permet au PIB réel de rattraper la tendance du BAU comme le montre la figure 6.

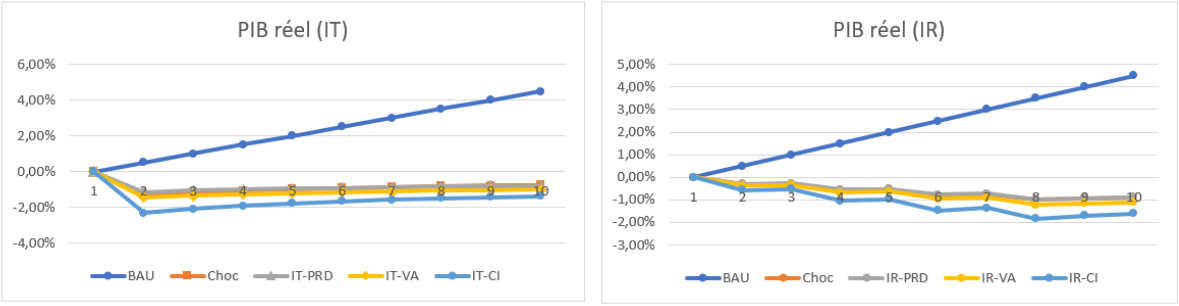

Figure 6: Evolution du PIB réel

Toutefois, on note que seule la politique d'investissement au prorata des dégâts (•-PRD) atténue davantage les effets négatifs observés sur le PIB réel dans les deux scénarios. Cette dynamique résulte de l'impact positif de cette mesure sur les prix locaux. En effet, le surplus d'offre de capital disponible qui provient des investissements réalisés entraine une diminution des coûts de production des secteurs. On observe alors une baisse des prix à la consommation (voir figure 7) par rapport aux scénarios de choc qui, cumulée à la hausse des revenus du travail des agents privés permet d'atténuer la baisse de la consommation sans pour autant renverser sa tendance baissière.

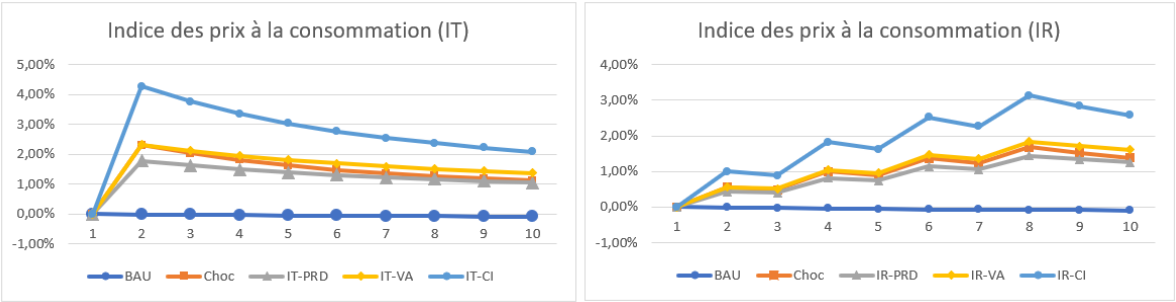

Figure 7 : Variation de l'indice des prix à la consommation

En ce qui concerne l'emploi, la figure 8 montre que les politiques d'investissement au prorata des dommages et celle tournée vers les secteurs intensifs en valeur ajoutée (•-PRD et •-VA) sont les seules qui atténuent la hausse du chômage.

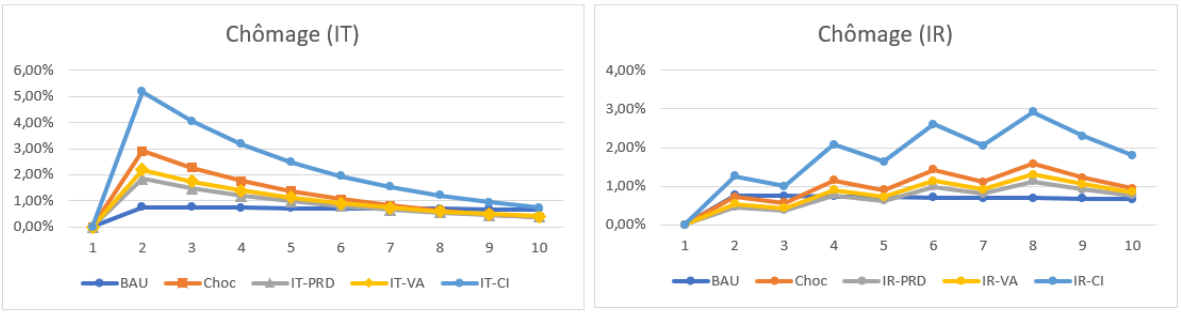

Figure 8: Variation du chômage

L'amélioration en termes d'emploi résulte de l'impact de ces mesures sur le prix du travail par rapport au capital, ce qui favorise une hausse de la demande de travail des branches et insuffle une hausse des salaires. La comparaison des effets sur l'emploi de la politique d'investissement au prorata des dommages avec celle basée sur un investissement dans les secteurs intensifs en valeur ajoutée montre que c'est la compensation au prorata des dégâts qui a les effets positifs les plus importants sur l'emploi. Cette tendance découle du fait qu'avec un investissement vers les secteurs intensifs en valeur ajoutée, la baisse des coûts du capital se fait plus rapidement, ce qui pousse les secteurs à moins substituer du travail par du capital. L'inverse est observé dans le cadre de la politique d'investissement au prorata des dégâts où la persistance d'un prix du capital relativement plus élevé incite les branches à recourir à plus de travail.

5. Conclusion

De par sa situation géographique et du fait du réchauffement climatique, La Réunion fait face à un accroissement de son exposition au risque cyclonique qui rend pertinente l'analyse des effets économiques des cyclones sur l'économie locale dans leur dimension directe mais

aussi indirecte. Le modèle d'équilibre général calculable dynamique calibré sur l'économie de La Réunion permet ainsi d'évaluer les impacts économiques indirects spatialisés d'un cyclone de type DINA. Le choix du cyclone DINA s'explique par le fait que c'est le dernier évènement cyclonique caractérisé par des intensités extrêmes dont la modélisation des vents a pu être réalisée en tenant compte de la topologie du territoire. Nous avons alors testé deux scénarii de choc. Le premier, retrace un choc d'intensité correspondant à un évènement cyclonique ayant les mêmes caractéristiques que DINA. Le second est un choc de récurrence équivalant à quatre cyclones se produisant à intervalle de deux ans et dont la somme des dommages correspond à ceux du choc d'intensité. Pour calibrer ces simulations, nous avons dans un premier temps spatialisé la valeur économique de la MCS sur l'ensemble des communes. Ensuite, nous avons déterminé les dommages économiques directs du cyclone DINA au niveau de chaque commune grâce à des fonctions de dommage. Enfin, les dommages ont été rapportés à la structure économique de chaque commune puis compilés afin d'obtenir les pertes économiques sectorielles totales. Ce choix méthodologique a l'avantage d'obtenir des montants de dommages sectoriels qui soient spatialisés.

Les résultats macroéconomiques et sectoriels montrent que le canal des prix est celui par lequel se diffuse l'onde de choc à toute l'économie. En effet, la hausse du prix du capital, va entrainer un accroissement des coûts de production et conduire à une réduction des productions. Il en découle une augmentation des prix des consommations qui vont induire une contraction de la demande. Ces résultats rejoignent ceux déjà observés dans l'évaluation d'autres phénomènes naturels extrêmes dans d'autres contextes (Xie et al., 2014, Rose et al., 2016, Garcia-Léon et al., 2021, Zhang et al., 2021). En outre, l'analyse des politiques d'intervention montre qu'une stratégie d'atténuation adaptée peut reposer sur un investissement public en capital. Toutefois, cette option ne produit pas les mêmes effets selon que le l'investissement se fasse au prorata des dommages ou soit ciblé sur des secteurs intensifs en valeur ajoutée ou en consommations intermédiaires. Dans le cas d'espèce, seul un investissement au prorata des dégâts permet d'atténuer les effets négatifs observés. Néanmoins, cette atténuation n'est pas de nature à rattraper la tendance du BAU. En outre, la robustesse de ces résultats a été vérifiée par des tests de sensibilité qui ont conforté la tendance des résultats.

Pour les pouvoirs publics, l'enseignement majeur à tirer de cette analyse porte sur le fait que face à des cyclones intenses ou récurrents, la stratégie de réponse à adopter pour relancer l'économie peut se baser sur des politiques d'investissement tournées vers les secteurs les plus impactés. Il faut toutefois que les ressources mobilisées soient supérieures aux coûts des dommages pour relancer durablement l'activité économique.

Bibliographie

Anttila-Hughes, J. K., and S. M. Hsiang. 2013. Destruction, disinvestment, and death: economic and human losses following environmental disaster. Available at SSRN: https://ssrn.com/ abstract¼2220501 or http://dx.doi.org/10.2139/ ssrn.2220501.

Arndt, C., Strzepeck, K., Tarp, F., Thurlow, J., Fant, C., & Wright, L. (2011). Adapting to climate change: an integrated biophysical and economic assessment for Mozambique. Sustainability Science, 6(1), 7-20.

Banholzer, S., Kossin, J., & Donner, S. (2014). The impact of climate change on natural disasters. In Reducing disaster: Early warning systems for climate change (pp. 21-49). Springer, Dordrecht.

Barros, V. R., Field, C. B., Dokken, D. J., Mastrandrea, M. D., Mach, K. J., Bilir, T. E., ... & White, L. L. (2014). Climate change 2014 impacts, adaptation, and vulnerability Part B: regional aspects: working group II contribution to the fifth assessment report of the intergovernmental panel on climate change. In Climate Change 2014: Impacts, Adaptation and Vulnerability: Part B: Regional Aspects: Working Group II Contribution to the Fifth Assessment Report of the Intergovernmental Panel on Climate Change (pp. 1-1820). Cambridge University Press.

Bertinelli, L., Mohan, P., & Strobl, E. (2016). Hurricane damage risk assessment in the Caribbean: An analysis using synthetic hurricane events and nightlight imagery. Ecological Economics, 124, 135-144.

Bielli, S., Barthe, C., Bousquet, O., Tulet, P., & Pianezze, J. (2021). The Effect of Atmosphere–Ocean Coupling on the Structure and Intensity of Tropical Cyclone Bejisa in the Southwest Indian Ocean. Atmosphere, 12(6), 688.

Bindoff, N. L., Cheung, W. W., Kairo, J. G., Arístegui, J., Guinder, V. A., Hallberg, R., ... & Williamson, P. (2019). Changing ocean, marine ecosystems, and dependent communities. IPCC special report on the ocean and cryosphere in a changing climate, 477-587.

Blanchflower, D. G., & Oswald, A. J. (1995). An introduction to the wage curve. Journal of economic perspectives, 9(3), 153-167.

Borgomeo, E., Vadheim, B., Woldeyes, F. B., Alamirew, T., Tamru, S., Charles, K. J., ... & Walker, O. (2018). The distributional and multi-sectoral impacts of rainfall shocks: Evidence from computable general equilibrium modelling for the Awash Basin, Ethiopia. Ecological Economics, 146, 621-632.

Bosello, F., R. J. Nicholls, J. Richards, R. Roson, and R. S. J. Tol. 2012. Economic impacts of climate change in Europe: sea-level rise. Climatic Change 112:63–81.

Botzen, W. W., Deschenes, O., & Sanders, M. (2020). The economic impacts of natural disasters: A review of models and empirical studies. Review of Environmental Economics and Policy.

Caisse Centrale de Réassurance (2020). Rapport « Evolution du risque cyclonique en outre-mer à horizon 2050 »

Carrera, L., G. Standardi, F. Bosello, and J. Mysiak. 2015. Assessing direct and indirect economic impacts of a flood event through the integration of spatial and computable general equilibrium modelling. Environmental Modelling & Software 63:109–22.

Carrera, L., Standardi, G., Bosello, F., & Mysiak, J. (2015). Assessing direct and indirect economic impacts of a flood event through the integration of spatial and computable general equilibrium modelling. *Environmental Modelling & Software*, *63*, 109-122.

Croissant, Y., Garabedian, S., Issop, Z. M., & Hermet, F. (2020). Fragmentation mondiale de la production et différenciation de la demande dans un MEGC: proposition méthodologique. *Revue économique*, *71*(4), 597-621.

Dinan, T. (2017). Projected increases in hurricane damage in the United States: the role of climate change and coastal development. Ecological Economics, 138, 186-198.

Emanuel, K. (2011). Global warming effects on US hurricane damage. Weather, Climate, and Society, 3(4), 261-268.

Estrada, F., W. J. W. Botzen, and R. Tol. 2015. Economic losses from US hurricanes consistent with an influence from climate change. Nature Geoscience 8:880–84.

Felbermayr, G., and J. Gro¨schl. 2014. Naturally negative: the growth effects of natural disasters. Journal of Development Economics 111:92–106.

Fontaine, I., Garabedian, S., Nortes-Martinez, D., & Vérèmes, H. (2021). Tropical Cyclones and Fertility: New Evidence from Madagascar. https://hal.archives-ouvertes.fr/hal-03243455/

Galochet, M., Longuépée, J., Morel, V., Petit, O., & JOLLIVET, P. D. M. (2008). L'environnement. Discours et pratiques interdisciplinaires, Arras, Artois Presses Université, 21-33.

Garabedian S., Narindranjanahary A., Ricci O., & Selosse S, S. (2020). A macroeconomic evaluation of a carbon tax in overseas territories: A CGE model for Reunion Island. Energy Policy, 147, 111738.

García-León, D., Standardi, G., & Staccione, A. (2021). An integrated approach for the estimation of agricultural drought costs. Land Use Policy, 100, 104923.

Haddad, E. A., & Teixeira, E. (2015). Economic impacts of natural disasters in megacities: The case of floods in São Paulo, Brazil. Habitat International, 45, 106-113.

Hallegatte, S. 2008. An adaptive regional input–output model and its application to the assessment of the economic cost of Katrina. Risk Analysis 28:779–99.

Hoeppe, P. 2016. Trends in weather related disasters – consequences for insurers and society. Weather and Climate Extremes 11:70–79.

Hsiang, S. M. 2010. Temperatures and cyclones strongly associated with economic production in the Caribbean and Central America. Proceedings of the National Academy of Sciences of the United States of America 107:15367–72.

Hsiang, S., R. Kopp, A. Jina, J. Rising, M. Delgado, S. Mohan, D.J. Rasmussen, R. Muir-Wood, P. Wilson, M. Oppenheimer, K. Larsen, and T. Houser. 2017. "Estimating economic damage from climate change in the United States",Science 3566345: 1362–9.

Jouanjean, I. M. (2011). L'île de La Réunion sous l'œil du cyclone au XXème siècle. Histoire, Société, et catastrophe Naturelle (Doctoral dissertation, Université de la Réunion).

Kahn, M. E. 2005. The death toll from natural disasters: the role of income, geography and institutions. Review of Economics and Statistics 87:271–84.

Kellenberg, D. K., and A. M. Mobarak. 2008. Does rising income increase or decrease damage risk from natural disasters? Journal of Urban Economics 63:788–802.

Knutson, T., Camargo, S. J., Chan, J. C., Emanuel, K., Ho, C. H., Kossin, J., ... & Wu, L. (2020). Tropical cyclones and climate change assessment: Part II: Projected response to anthropogenic warming. Bulletin of the American Meteorological Society, 101(3), E303-E322.

Koks, E. E., and M. Thissen. 2016. A multiregional impact assessment model for disaster analysis. Economic Systems Research 28:429–49.

Kousky, C. 2014. Informing climate adaptation: a review of the economic costs of natural disasters. Energy Economics 46:576–92.

Kousky,2016. Impacts of natural disasters on children. Future of Children 26:73–92.

Kunreuther, H., & Michel-Kerjan, E. (2007). Climate change, insurability of large-scale disasters and the emerging liability challenge.

Leroux, M. D., Wood, K., Elsberry, R. L., Cayanan, E. O., Hendricks, E., Kucas, M., ... & Yu, Z. (2018). Recent advances in research and forecasting of tropical cyclone track, intensity, and structure at landfall. Tropical Cyclone Research and Review, 7(2), 85-105.

MacKenzie, C. A., J. R. Santos, and K. Barker. 2012. Measuring changes in international production from a disruption: case study of the Japanese earthquake and tsunami. International Journal of Production Economics 138:293–302.

Maharaj, S., Mycoo, M., Nalau, J., & Wairiu, M. (2022). IPCC Sixth Assessment Report (AR6): Climate Change 2022-Impacts, Adaptation and Vulnerability: Regional Factsheet Small Islands.

Mavume, A. F., Rydberg, L., Rouault, M., & Lutjeharms, J. R. (2009). Climatology and landfall of tropical cyclones in the south-west Indian Ocean. Western Indian Ocean Journal of Marine Science, 8(1).

Météo France (2002). Synthèse des évènements : DINA, cyclone tropical intense (22 et 23 janvier 2002) http://www.risquesnaturels.re/pdf/EVENEMENTS_HISTORIQUES/evenement_historique_Dina.pdf

Meyer, V., Becker, N., Markantonis, V., Schwarze, R., van den Bergh, J. C., Bouwer, L. M., ... & Viavattene, C. (2013). Assessing the costs of natural hazards–state of the art and knowledge gaps. Natural Hazards and Earth System Sciences, 13(5), 1351-1373.

Ministère de l'écologie et du développement durable (2002). Cyclone dina a la Réunion les 22 et 23 janvier 2002 : Caractérisation, conséquences et retour d'expérience. https://cgedd.documentation.developpement-durable.gouv.fr/documents/Affaires-0003877/2002-0036-01.pdf

Narita, D., R. S. J. Tol, and D. Anthoff. 2010. Economic costs of extratropical storms under climate change: an application of FUND. Journal of Environmental Management 53:371–84.

Okuyama, Y., and J. R. Santos. 2014. Disaster impact and input-output analysis. Economic Systems Research 26:1–12.

Rahman, M. S., Andriatmoko, N. D., Saeri, M., Subagio, H., Malik, A., Triastono, J., ... & Yusuf, Y. (2022). Climate disasters and subjective well-being among urban and rural residents in Indonesia. Sustainability, 14(6), 3383.

Reaños, M. A. T. (2021). Floods, flood policies and changes in welfare and inequality: Evidence from Germany. Ecological Economics, 180, 106879.

Rose, A., and D. Wei. 2013. Estimating the economic consequences of a port shutdown: the special role of resilience. Economic Systems Research 25:212–32.

Rose, A., and S.-Y. Liao. 2005. Modeling regional economic resilience to disasters: a computable general equilibrium analysis of water service disruptions. Journal of Regional Science 45:75–112.

Rose, A., I. Sue Wing, D. Wei, and A. Wein. 2016. Economic impacts of a California tsunami. Natural Hazards Review 17(2):1–12.

Sassi, M. (2011). L'évaluation monétaire des dommages du risque naturel d'inondation en région PACA : une analyse à l'aide d'un modèle d'équilibre général calculable. Revue dEconomie Regionale Urbaine, (4), 627-650.

Shibusawa, H., Yamaguchi, M., & Miyata, Y. (2009). Evaluating the impacts of a disaster in the Tokai region of Japan: a dynamic spatial CGE model approach. Studies in Regional Science, 39(3), 539-551.

Shughrue, C., Werner, B. & Seto, K.C. Global spread of local cyclone damages through urban trade networks. Nat Sustain 3, 606–613 (2020). https://doi.org/10.1038/s41893-020-0523-8

Skidmore, M., and H. Toya. 2002. Do natural disasters promote long-run growth? Economic Inquiry 40:664–87.

Tulet, P., Aunay, B., Barruol, G., Barthe, C., Belon, R., Bielli, S., ... & Vérèmes, H. (2021). ReNovRisk: a multidisciplinary programme to study the cyclonic risks in the South-West Indian Ocean. Natural Hazards, 107(2), 1191-1223. https://doi.org/10.1007/s11069-021-04624-w

Warner, K., Ranger, N., Surminski, S., Arnold, M., Linnerooth-Bayer, J., Michel-Kerjan, E., ... & Herweijer, C. (2009). Adaptation to climate change: Linking disaster risk reduction and insurance. United Nations International Strategy for Disaster Reduction, Geneva.

Washida, T., Yamaura, K., & Sakaue, S. (2014). Computable general equilibrium analyses of global economic impacts and adaptation for climate change: the case of tropical cyclones. International Journal of Global Warming, 6(4), 466-499.

Wittwer, G., & Griffith, M. (2011). Modelling drought and recovery in the southern Murray-Darling basin. Australian Journal of Agricultural and Resource Economics, 55(3), 342-359.

Xie, W., Li, N., Wu, J. D., & Hao, X. L. (2014). Modeling the economic costs of disasters and recovery: analysis using a dynamic computable general equilibrium model. Natural Hazards and Earth System Sciences, 14(4), 757-772.

Zander, K. K., Wilson, T., & Garnett, S. T. (2020). Understanding the role of natural hazards in internal labour mobility in Australia. Weather and Climate Extremes, 29, 100261.

Zhang, H., Liu, C., & Wang, C. (2021). Extreme climate events and economic impacts in China: A CGE analysis with a new damage function in IAM. Technological Forecasting and Social Change, 169, 120765.

Annexe 1

Tableau A - Impacts sur la production et la demande de travail en %

Secteurs	Choc d'intensité (IT)				Choc de récurrence (IR)			
	Production		Demande travail		Production		Demande travail	
	LT	Moy	LT	Moy	LT	Moy	LT	Moy
Agriculture	-1,55	-1,61	-0,46	-1,84	-1,59	-2,00	-1,09	-0,94
Pêche	-0,47	-0,57	0,05	-0,59	-0,51	-0,68	-0,25	-0,28
Extraction	-2,87	-3,35	-3,27	-5,30	-3,10	-4,04	-4,30	-3,06
Industrie agro-alimentaire	-1,74	-2,17	-1,70	-2,73	-1,94	-2,58	-2,21	-1,57
Industrie sucre - rhum	-1,05	-1,29	-0,80	-1,65	-1,17	-1,54	-1,22	-0,92
Manufacture	-2,19	-2,84	-2,17	-3,71	-2,50	-3,36	-2,93	-2,11
Electricité, Gaz & Eau	-0,47	-0,58	-0,11	-0,51	-0,52	-0,69	-0,30	-0,26
Construction	-0,87	-1,14	-0,37	-1,06	-1,00	-1,34	-0,70	-0,56
Commerce	-0,56	-0,68	0,39	0,08	-0,62	-0,81	0,27	0,11
Transport	-1,27	-1,66	-1,09	-1,87	-1,46	-1,96	-1,47	-1,06
Hébergement	-0,37	-0,40	-0,01	-0,26	-0,38	-0,49	-0,13	-0,13
Information	-0,97	-1,20	0,15	-1,01	-1,09	-1,44	-0,35	-0,44
Finance	-0,74	-0,94	0,20	-0,66	-0,84	-1,12	-0,17	-0,27
Immobilier	-0,97	-1,64	2,51	**7,22**	-1,30	-1,88	4,68	**3,76**
Service technologique	-0,91	-1,19	-0,55	-1,24	-1,05	-1,41	-0,89	-0,68
Service aux administrations	-0,82	-1,06	-0,43	-1,03	-0,93	-1,25	-0,72	-0,56
Administration publique	0,00	0,00	0,00	0,00	0,00	0,00	0,00	0,00
Education et action sociale	-0,13	-0,16	0,86	**0,91**	-0,15	-0,19	0,92	**0,58**
Autres services	-0,34	-0,39	-0,05	-0,23	-0,36	-0,48	-0,14	-0,12

Source : Résultats des auteurs tirés du MEGC

Chapitre 14

Tropical Cyclones and Economic Growth : The Importance of Considering Small Island Developing State

Sivatharsan Kulanthaivelu

- ***Revue d'Économie Politique***, en révision, 2023
- ***Présentation :***
  Colloque AFSE, 70^{e}, Dijon, juin 2022

Tropical Cyclones and Economic Growth: The Importance of Considering Small Island Developing States

Eric Kulanthaivelu*

September 2022

Abstract

A number of empirical studies have explored the short and long-run economic relationship between tropical cyclones and national growth rates, but no general conclusion can be drawn from them so far. While negative effects are found in samples of exposed countries worldwide, cyclone shocks also show no significant influence in other national-level analyses. Using cross-country panel datasets for 83 affected nations between 1970 and 2015, this paper further investigates this issue by distinguishing a sub-group of nations which is particularly exposed to cyclonic risk and characterized by structural factors of economic vulnerability: Small Island Developing States (SIDS). To capture tropical cyclones' overall impact on economic activity, a set of exogenous climatic indicators is built by combining physical intensity data with information on exposed areas. A negative and persistent impact is found for the sub-group of SIDS, while no effect is observed for other countries irrespective of their level of development. On impact, an additional km/h of intensity over a SIDS reduces *per capita* GDP growth by 0.016 percentage point, and this negative effect accumulates to -0.024 percentage point 15 years later. In contrast, more local approaches are suggested for non SIDS. The estimated negative impact in SIDS appears to be driven by an increased dependence on foreign economic conditions, insufficient reconstruction capacities and difficulties to implement adaptation policies.

Keywords: Natural disasters; Cyclones; Growth; Economic impacts; Environmental risk; Small Island Developing States
JEL classification: O44; Q54; Q56; R11

*University of Reunion Island, Centre d'Economie et de Management de l'Océan Indien. 15 avenue René Cassin, 97400, Saint-Denis Cedex 9, La Réunion
E-mail: eric-sivatharsan.kulanthaivelu@univ-reunion.fr

1 Introduction

Tropical cyclones are arguably one of the most damaging and threatening natural disasters for human systems. Among other examples, Cyclone Bhola, which struck East Pakistan (present-day Bangladesh) on 12-13 November 1970, remain known as the world's deadliest storm to ever devastate a coastal area with an estimated death toll of between 300,000 to 500,000 people. More recently, the 2005 Hurricane Katrina caused the displacement of approximately 650,000 people and destroyed more than 200,000 homes along the US Gulf Coast. In a context of intensified global climate change, with highly expected alterations in frequency and intensity of storm events (Knutson & al., 2010; IPCC, 2019), these climate-related shocks may become a serious source of economic fluctuations in coming years and it is of considerable importance to assess their impact on economic activity.

Several empirical studies have already addressed this question from short-run to long-run, but conclusions vary depending on the scale chosen. While Felbermayr & Gröschl (2014) or Krichene & al. (2021) find evidence of negative and persistent effects of tropical cyclones on economic growth using universal datasets, Strobl (2011) or Zhou & Zhang (2021) show that these extreme events are not disruptive enough to be reflected in national economic growth rates in the US or in Hong-Kong respectively. Hence, this paper exploits key dimensions across which one might expect the economic impact of cyclone shocks to be heterogeneous. First, since cyclone events are primarily localized along coastal areas, they may only affect a reduced share of national economies. Even though massive losses can be generated locally, it is not obvious how cyclone events can shift aggregate output growth patterns. Apart from the geographic dimension, another aspect to consider is the level of development. In the more general framework of natural disasters, developing countries are almost always found to be more adversely affected than advanced economies (Kahn, 2005; Noy, 2009; Fomby & al., 2013). Moreover, developing countries tend to have agricultural-based economies and may thus experience stronger effects from weather shocks such as cyclone events. In fact, cyclones can trigger a number of catastrophes like floods or landslides, potentially causing losses of crops that spread to the rest of the economy. The combination of these two factors brings to light a sub-group of countries: Small Islands Developing States (SIDS). SIDS are today the focus of many political and scientific debates. These countries are characterized by a broad spectrum of structural factors of vulnerability regarding environmental risk, and their existence is even threatened by climate change's impact (IPCC, 2019). Storm events may constitute a bigger threat to SIDS due to their smallness, insularity, limited domestic market and remoteness for some of them (Briguglio, 1995). Since their total area is small relative to other countries, the risk exposure is more homogeneous compared to a larger country, and thus, it is likely that their entire economy is concerned by these shocks. As tropical cyclones can represent a national concern in SIDS, local governments arguably have a greater ability to respond nationally in the aftermath of the catastrophes. However, SIDS have, on average, higher levels of public debt than other developing countries, which restricts space for fiscal stimulus post-disaster (OECD, 2018).

Using a worldwide database of 83 nations affected during the period 1970-2015, this paper aims to capture the overall effects of storm shocks on national economic growth. To do this, geophysical and meteorological data sources are used to construct exogenous and accurate measures of cyclone intensity, precipitation and temperature for each country

during the sample period.[1] As stated above, it is relevant to control for local climatic parameters that can increase tropical cyclones' intensity, or trigger various natural disasters. All these measurements are built in accordance with the definition of vulnerability in IPCC (2019), namely, physical intensity and degree of exposure at national scale are combined. The empirical framework follows Dell & al. (2012) and is based on earlier work in Bond, Leblebicioglu, & Schiantarelli (2010). It consists in a distributed lag model. To preview the paper's results, after having recovered the persistent negative effect found elsewhere in the literature for a worldwide sample (Krichene & al., 2021), the sub-group of SIDS is distinguished and results are reanalysed. Splitting the initial sample in such a way provides novel results. Consistent evidence for quasi-constant growth losses from short- to long-run is found for SIDS. On impact, an additional km/h of intensity over a SIDS decreases growth by 0.016 percentage point, and these growth losses accumulate to -0.024 percentage point after 15 years. However, as for non SIDS, when these countries are considered as a group, in no case are the results significant: cyclone events do not appear to be economically important enough to affect national economic growth rates irrespective of their level of development. Local approaches should be privileged for the latter sub-group of countries, focusing fundamentally on regions that are exposed and vulnerable to tropical cyclones.

To further explore the results obtained for SIDS, transmission mechanisms are analysed with a focus on economic and physical channels. The existing empirical literature usually proceeds through the study of cyclones' impacts on economic or non-economic growth determinants, or estimate whether these determinants mitigate or amplify the observed output growth losses (Mohan & al., 2018; Krichene & al., 2021). Instead, this paper first investigates the effects on an outcome variable that is specifically designed to characterize SIDS' economic vulnerability: the degree of dependence to foreign economic conditions (Briguglio, 1995). Then, effects on *per capita* investment growth and on construction sector GDP growth are examined to study SIDS' ability to recover and rebuild after the disaster. Lastly, growth effects of tropical cyclones are studied for the most frequently exposed SIDS. This last analysis allows to study the adaptive capacities of SIDS. Results show that SIDS' dependence to foreign markets is amplified for five years after a cyclone strike, but also that their recovering capacities are limited as no effect is detected on *per capita* investment or on construction sector GDP growth. Finally, growth losses are not attenuated for those that are the most frequently exposed, which reveals a lack of adaptability to tropical cyclones. These transmission channels results suggest the existence of poverty traps at least in frequently exposed SIDS, as the latter are unable to rebuild entirely between each disaster event and constantly remain in a stage of reconstruction (Hallegate & Dumas, 2009).

This paper contributes to several strands of the literature. First, by distinguishing SIDS, it investigates a source of heterogeneity existing in worldwide samples when studying national growth responses to cyclone shocks. Findings shed light on the differentiated impact for those combining small country size as well as lower level of development. Then, it contributes to debates upon maximum lag choice to study cyclones' long-run effects. While other studies choose to employ 5 lags (Felbermayr & Gröschl, 2014), 15 lags (Krichene & al., 2021),

[1] Using physical characteristics of weather events is opposed to economic-based indicators such as death toll, total amount of damages etc., which are subject to reverse causality bias and other sources of endogeneity coming from exploitable data sources. See Felbermayr & Gröschl (2014) for a detailed discussion.

this paper rather demonstrates that this choice is not crucial since coefficients associated to lagged variables are rarely statistically significant. However, as for the worldwide panel or SIDS, cumulative growth losses are always negative and significant, meaning that the negative contemporaneous impact is not counteracted either in future response periods. Third, it contributes to the literature on SIDS, and particularly their economic resilience and adaptive capacities when facing tropical cyclones. To date, this paper is the first one to estimate causal effects of a natural disaster with a focus on SIDS economies, even though their increased exposure and vulnerability to environmental risk relative to other countries is commonly admitted.

The remainder of the paper proceeds as follows. Section 2 describes the data sources used in the analysis. Section 3 details the construction of weather intensity measurements and presents the estimation strategy. Section 4 examines main findings and checks for their robustness. Transmission mechanisms are discussed in section 5, and section 6 concludes.

2 Data

2.1 Cyclone data

The raw data on cyclone events come from the *Tropical Cyclone Exposure Database* (TCE-DAT; Geiger & al., 2018), which provides consistent country-event-level data on cyclone intensity and exposure from 1950 to 2015. TCE-DAT filters 2713 landfalling tropical cyclones with at least 34 knots ($\approx$ 63 km/h) wind speed and sustained at least one minute from the widely used *International Best Track Archive for Climate Stewardship* (IBTrACS; Knapp & al., 2010). Since the IBTrACS data only identify geographic coordinates of each tropical cyclone's eye, the wind field model proposed by Holland (2008) is subsequently applied in order to get an overall cyclone trajectory and intensity at 0.1° latitude x 0.1° longitude grid cell level for each event recorded in the database. A cyclone is considered as landfalling if at least one grid cell of a country is affected by the simulated wind field. This means that for a given country, all the storms that affect neighbouring countries are considered as long as they passes by near enough to be felt. Figure 1 presents the average wind speed for all tropical cyclone events across years at pixel level for two tropical cyclone basins: South West Pacific/South East Indian Ocean and North Atlantic/North East Pacific. This figure provides support for IPCC (2019) as it shows that the exposure to cyclonic risk is unequal between countries, especially between small and large ones. It highlights the existence of fluctuations in annual mean cyclone wind speed within countries. In fact, tropical cyclones lose their strength as they get deeper in lands, which is due to an increasing surface roughness and frictions. When making landfall, tropical cyclones are deprived of their main source of energy which corresponds to water. Alternatively, this figure shows that tropical cyclones can cover large distances and can even affect countries located outside tropical cyclones' latitude lines. In such case, tropical cyclones progressively transform into extratropical cyclones, sometimes called mid-latitude cyclones. The latter meteorological phenomena have different physical properties than tropical cyclones, but are still characterized by low pressure centres and can also bring strong damages *via* storm surges, landslides, extreme winds, heavy rain etc. Since this paper aims to capture the overall effects of tropical cyclones, the sub-group

of countries affected by extratropical cyclones that were initially tropical cyclones is also included in the sample. More specifically, the included extratropical cyclones are only those that are the consequence of a prior tropical cyclone formation. In addition to information on exposed land and local wind speed intensity, the dataset provides gridded estimates of exposed population, which is used to study the robustness of main results presented in section 4.

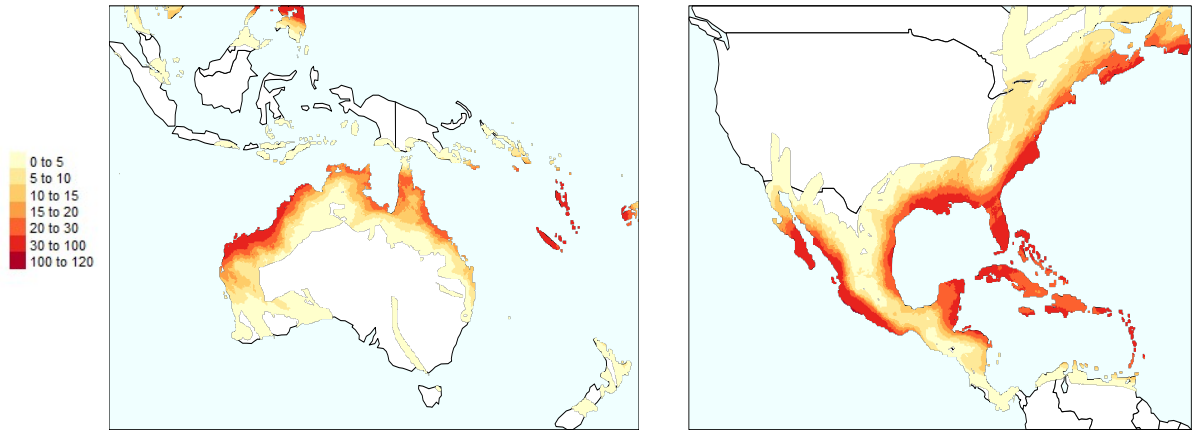

Figure 1: Annual average maximum wind speed (in km/h) from 1950 to 2015 at pixel level for two tropical cyclone basins : South West Pacific Ocean and South East Indian Ocean basin (left-hand side) and North Atlantic and North East Pacific basin (right-hand side).
[Color should be used]

The 83 nations included in the study have all faced at least one cyclone event during the sample period and are mainly distributed across five tropical cyclone basins as defined by the World Meteorological Organization: South West Indian Ocean (9.6 %), Arabian Sea and Bay of Bengal (13.3 %), North West Pacific (8.4 %), North Atlantic and North East Pacific (32.5 %), South West Pacific and South East Indian Ocean (19.3 %). Remaining nations (16.9 %) constitute a group mostly affected by extratropical cyclones.

2.2 Temperature and precipitation data

As cyclone events can trigger a great number of hazards when making landfall, and their intensity can be linked with local atmospheric conditions, including additional climatic variables appears to be particularly relevant in this study. Temperature and precipitation correspond to such climatic controls. Both of these parameters are correlated with cyclone events, exogenously determined and can affect annual growth rates (Dell & al., 2012). Data on precipitation and temperature levels were obtained from the *Climatic Research Unit gridded Time Series* database (CRU TS; Harris & al., 2020), which provides monthly estimates derived from land-based weather station observations. Total monthly precipitation data are recorded in millimetres and temperatures are measured in °Celsius. Both of these variables are collected at 0.5° latitude x 0.5° longitude resolution. As in TCE-DAT, the gridded data are then matched to each corresponding country-year level. Data are available from 1901 to 2019.

Detailed national summary statistics for sample nations are presented in Appendix Table A.1. Philippines, Japan and China are most affected by cyclone events, with more than three cyclones per year in the period 1950 - 2015 and the most frequently hit SIDS are Bahamas, followed by Cuba and Vanuatu with around one cyclone per year. Moreover, a comparison of the annual wind speed relative to the exposed surface and the level of rainfall gives support for Haiyan & al. (2008) as they are positively related.

2.3 Economic data

Information on *per capita* GDP and other GDP components that are used in section 5 come from the *United Nations Statistics Division* (UNSD, 2020). UNSD database provides data without gaps for the baseline panel of 83 countries from 1970 to 2015.[2] While the main results focus on *per capita* GDP growth, data on imports and exports of goods and services, GDP, gross capital formation and sectoral GDP for the construction industry are exploited for the analysis of transmission mechanisms. All values are recorded from National Accounts in constant 2015 prices in US Dollars and reported by international or national statistical services.[3]

3 Methodology

This section examines the empirical framework chosen for analysing the impact of storm shocks on economic growth. The measure of cyclone intensity at country-year level is entirely based on physical characteristics of the disaster and is designed to be in line with the definition of vulnerability suggested by the IPCC (2014). Vulnerability relates the intensity of a specific natural disaster with its effects on natural and human systems given the specific exposure. Thus, it is important to combine information on wind speed intensities with spatial aspects of the question. As argued by Skidmore & Toya (2002), the impact of a given natural disaster on the economy of a country depends on the disaster's intensity and is relative to the overall size of the country. Hence, cyclone events are measured as a spatially-weighted average of the maximum sustained wind speed over all pixels in a country. This normalization approach is also in line with Nordhaus (2006) as it aims to determine the average effect of storms on an average pixel for a given country. Finally, this measurement method is quite similar to the one established by Hsiang & Jina (2014) and provides an estimate of a cyclone's average intensity in a randomly selected unit of land for each country. It can be expressed as follows for each country i and year t:

$$\overline{Cyc}_{i,t} = \frac{\sum_{p} \max_{p}\{Wind_{p,i,t}\} * Area_{p}}{LandSize_{i,t}}$$

$Wind_{p,i,t}$ are the local wind speed estimates in km/h for each pixel p, and $Area_p$ the exact area of pixel p in km^2 measured with respect to the corresponding latitude and longitude

[2]Except for the nations created after 1970 and included in the sample, *i.e.* Russia, Timor-Leste and Yemen.

[3]`https://unstats.un.org/unsd/snaama/Downloads`

values, and $LandSize_{i,t}$ are total areas reported in the *World Development Indicators* (WDI) database of the World Bank.

In addition, one might notice that the pixel level wind speed is selected as the maximum wind speed value felt each year as in Felbermayr & Gröschl (2014), irrespective of the number of cyclone events identified during this year. Regarding this methodological choice, it can be argued that since the replacement of destroyed capital needs more than one year to be effective, the occurrence of less devastating cyclones within the same year is considered as negligible. Appendix Table A.3 examines regional statistics for this indicator over equally split time intervals of the sample period. It shows that the North West Pacific and South West Pacific/South East Indian Ocean tropical cyclone basins have both a long-lasting greater exposure. Countries located outside tropical cyclone basins have the lowest values on average, which is explained by a lower frequency of events.

As the effects of cyclone events on economic activity depend on local climatic conditions, annual measures for temperature and precipitation are also constructed. These measures bring pertinent climatic control variables linked with storms as pointed out by Dell & al. (2014). The average annual temperature ($\overline{Temp}_{i,t}$) is measured in °Celsius and is based on monthly temperature records for each country while the annual precipitation level ($Prec_{i,t}$) is the yearly sum of monthly precipitation levels recorded in millimeters. Table 1 examines the fluctuations between countries for these three input variables during the sample period. The maximum average value for the cyclone intensity measurement is reached by Philippines (105.3 km/h), while Tanzania has the lowest (0.002 km/h). The latter country has only one cyclonic year identified in the database. Vanuatu is the SIDS having the highest average cyclone intensity value with 74.1 km/h during the period 1970-2015. The hottest country in the sample is Somalia, with an average temperature of 27.3°C over the sample period, and the coldest is Canada with an average temperature of -4.9°C. Finally, the highest average annual rainfall level from 1970 to 2015 is recorded for Dominica with 3602.1mm per year, and the driest nation is Saudi Arabia with an average rainfall level of 75.1mm. This table further stresses that SIDS face higher average storm intensities than other countries.

Table 1: Descriptive statistics

	Min.	Max.	Median	Mean	Std Dev.
$\overline{Cyc}_{i,.}$	0.002	105.3	5.8	16.0	21.1
SIDS	*1.6*	*74.1*	*29.1*	*28.1*	*16.5*
Non SIDS	*0.002*	*105.3*	*2.4*	*9.6*	*20.5*
$\overline{Temp}_{i,.}$	-4.9	27.3	24.7	21.5	7.4
$Prec_{i,.}$	75.1	3602.1	1613.3	1605.4	862.5

Notes: Average values within countries from 1970 to 2015. Cyclone intensity measurement is in km/h, temperature in degrees Celsius, and precipitation in millimeters.

From the immediate to the long-term perspective, the dynamic adjustment path of the exogenous and scale-invariant predictor of cyclone events on *per capita* GDP growth rate

($g_{i,t}$) is analysed controlling for country-level climatic conditions and usual country and year fixed effects (μ_i and η_t, respectively). In the spirit of Dell & al. (2014), and to a lesser degree Krichene & al. (2021), no economic control variables are included so that correlations with the dependent variable and further over-controlling issues are avoided. The equation of interest is based on the model developed in Dell & al. (2012) in the context of weather shocks. More specifically, it takes the form of a distributed lag model and it is given by:

$$g_{i,t} = \alpha + \sum_{j=0}^{L} \beta_j \overline{Cyc}_{i,t-j} + \sum_{j=0}^{L} \gamma_j \overline{Temp}_{i,t-j} + \sum_{j=0}^{L} \delta_j Prec_{i,t-j} + \mu_i + \eta_t + \varepsilon_{i,t} \tag{1}$$

Where $\varepsilon_{i,t}$ denotes the white noise error term and $g_{i,t} \equiv \dfrac{y_{i,t} - y_{i,t-1}}{y_{i,t-1}}$, with $y_{i,t}$ *per capita* GDP.

Following the approach of Noy (2009), one important feature of the model is the inclusion of a temporal weight for $j = 0$ to the cyclone measurement so that the immediate impact is captured with more accuracy. In fact, it seems reasonable to assume that the earlier the cyclone occurs in a given year, the bigger its impact in the same year. This choice is crucial as the immediate impact is likely to drive future periods' responses. For $j = 0$, the cyclone indicator can therefore be rewritten:

$$\overline{Cyc}_{i,t} = \frac{\sum\limits_{p} \max\limits_{p}\{Wind_{p,i,t}\} * Area_p * \dfrac{(12 - m_p)}{12}}{LandSize_{i,t}}$$

With m_p the month in which the cyclone occurred in pixel p.

This paper ultimately analyses the marginal cumulative effect of cyclone events. For a given lag horizon L, it is defined by:

$$\Omega_l = \sum_{j=0}^{l} \beta_j, l \in [\![0; L]\!] \tag{2}$$

In order to increase comparability with the existing literature, the baseline lag structure chosen in the marginal cumulative effect analysis follows Krichene & al. (2021) and is fixed at 15 years. As argued by Greene (2003), it is better including too many than too few lags, since irrelevant extra lags would just be estimated as noise. Still in line with this distributed-lag literature, in what follows, the immediate effect of tropical cyclones (*i.e.* the year that they occur, β_0) and the cumulated effect (Ω_L, with lag horizon $L > 0$) are separately estimated. As pointed by Dell & al. (2012), the summation of cyclone coefficients corresponds to the growth effect of the weather shock.

The baseline specification in equation (1) and the associated immediate and marginal cumulative effects can be estimated using standard ordinary least squares (OLS) procedure. However, a deeper exploration of the data reveals the presence of outliers that influence the OLS estimator. In the present context, only growth rates' outliers must be considered as the latter can be driven by external economic shocks unrelated with natural disasters. In fact, extreme values of the climatic variables are determined by the nature, *i.e.* purely exogenous. Hence, overall impact of cyclone events must be captured given other socioeconomic shocks

occurring the same year. In this study, many points are likely to be affected in such a way: among others, high growth rates observed for Ireland in 2015 or Zimbabwe in 2009 are mainly due to changes in fiscal policies, while some negative growth rate points like Timor-Leste in 1999 or Yemen in 2015 are linked with political conflicts. These examples of influential observations are a source of serious concern as they can distort estimates obtained from OLS by providing excessive importance to extreme residual values. To cope with this issue, Li's (1985) robust regression is used. It downweights influential observations based on residual values.[4] This robust estimation technique has been used in a variety of topics such as financial economics (Kaplan & Zingales, 1997), political economy (Acemoglu & al., 2019), labor economics (Acemoglu & Restrepo, 2020) or international trade (Amiti & Wei, 2009), but the importance of using outlier-robust regression in the context of estimating causal effects of storm events on economic growth has been firstly underlined by Krichene & al. (2021). In the more general framework of natural disasters, Cavallo & al. (2013) conclude that no significant effect is found on economic growth once strong socioeconomic disruptions following natural disasters are controlled for.[5]

4 Empirical Results

The effect of cyclone events on economic growth is first measured for the entire set of cyclone-prone countries using a robust estimation technique based on equation (1).[6] Then, separate analyses for SIDS and non SIDS are conducted by adding an interaction term with a dummy variable to the main model. This revised model corresponds to:

$$g_{i,t} = \alpha + \sum_{j=0}^{L} \beta_{j,1} \overline{Cyc}_{i,t-j} + \sum_{j=0}^{L} \beta_{j,2} \left(\overline{Cyc}_{i,t-j} \times SIDS \right) + \sum_{j=0}^{L} \gamma_j \overline{Temp}_{i,t-j} + \sum_{j=0}^{L} \delta_j Prec_{i,t-j} + \mu_i + \eta_t + \varepsilon_{i,t} \tag{3}$$

Across all estimations, standard errors are computed using the pseudovalues approach designed for robust regressions as in Street & al. (1988).

4.1 Measuring the impact of cyclone events on economic growth

4.1.1 World base estimations

Table 2 presents results from estimating equation (1) without lag, with one lag, five lags, ten lags or fifteen lags. Estimates for each corresponding marginal cumulative effect are also showed on the bottom row of the table. Figure 2 plots the time path of cumulative effect on *per capita* GDP growth from a cyclone strike at time 0 together with its corresponding 90 % confidence intervals, for $L = 15$. The line $y = 0$ represents the counterfactual trajectory of

[4] See Appendix B for further details and statistics on influential observations.

[5] In particular, they refer to the Islamic Iranian Revolution of 1979 occurring at the dawn of the 1978 earthquake, and the Sandinista Nicaraguan Revolution of 1979 following the earthquake of 1972.

[6] On average, each country is observed 31 years. 62 observations out of 2556 are dropped with the robust estimation technique. Different parameter calibrations which downweight observations less drastically are tested in Appendix B and produce similar results.

the economy if the cyclone event had not occurred. On the year when the disaster occurs, one additional km/h of wind speed intensity over a country decreases growth by 0.013 percentage point. Across all lag horizon choices, the null hypothesis that cyclones have no immediate effect on growth is rejected at the 1% level. Focusing on the case when $L = 15$, the estimated long-run cumulative effect is also found to be significantly negative: growth losses accumulate to -0.029 percentage point after 15 years. Put another way, these estimates imply that a one standard deviation ($\sigma_{\overline{Cyc}_{i,t}} = 35.1$) increase in the cyclone measurement is associated with a reduction in growth of 1.0 percentage point 15 years later. On the global scale, economic growth is found to be sensitive to cyclone events as the sum of significant coefficients progressively declines over 15 years after a strike and remains below the counterfactual trajectory. This first result is well in line with the existing literature as it provides another evidence for a negative and persistent effect of cyclone events on economic activity for a worldwide sample (Felbermayr & Gröschl, 2014; Krichene & al., 2021).

Table 2: Regression results, world sample.

	No lag	1 lag	5 lags	10 lags	15 lags
	(1)	(2)	(3)	(4)	(5)
$\overline{Cyc}_{i,t}$	-0.00012***	-0.00013***	-0.00014***	-0.00014***	-0.00013***
	(0.00004)	(0.00004)	(0.00004)	(0.00004)	(0.00004)
$\overline{Cyc}_{i,t-1}$		0.00004**	0.00003	0.00003*	0.00001
		(0.00002)	(0.00002)	(0.00002)	(0.00002)
$\overline{Cyc}_{i,t-2}$			-0.00001	-0.00002	-0.00002
			(0.00002)	(0.00002)	(0.00002)
$\overline{Cyc}_{i,t-3}$			-9.17e-06	-0.00002	-0.00003
			(0.00002)	(0.00002)	(0.00002)
Observations	3676	3676	3356	2956	2556
Adjusted R^2	0.25	0.25	0.27	0.29	0.32
Marginal cumulative effect (Ω_L)	-0.00012***	-0.00009**	-0.00011**	-0.00020***	-0.00029***
	(0.00004)	(0.00004)	(0.00005)	(0.00007)	(0.00009)

Notes: Outlier-robust regression estimates. Standard errors incorporating the Street & al. (1988) correction are in parentheses. Time and country fixed effects, as well as temperature and precipitation controls are included in all specifications, but not reported in the table.
Significance levels : *** 1 % ; ** 5 % ; * 10 %.

4.1.2 Distinguishing Small Island Developing States

Historically, special challenges faced by island developing countries have been raised and discussed at the United Nations since 1972, but the group of SIDS was recognized and founded later at the 1992 United Nations Conference on Environment and Development held in Rio de Janeiro, Brazil.[7] SIDS are located in the Caribbean Sea and the Atlantic, Indian and Pacific Oceans and are inherently characterised by a wide amount of social, economic and environmental issues. In fact, SIDS are particularly exposed to natural disasters and to further climate change impacts such as sea level rise. Here, the focus is on SIDS' economic vulnerability in the wake of cyclone events. The above descriptive statistics already suggest that SIDS face higher average cyclone intensities than non SIDS (Table 1).

[7] `https://www.un.org/ohrlls/content/about-small-island-developing-states`

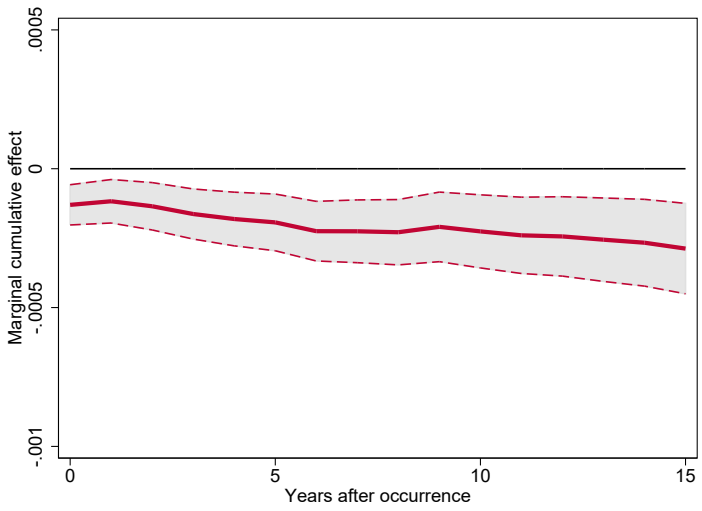

Figure 2: Measures of the marginal cumulative effects over fifteen years of cyclone events on *per capita* GDP growth for the world sample [Color should be used]

Notes: Estimations with outlier-robust regression. Standard errors are computed using the Street & al. (1988) correction. Shaded areas represent the associated 90 % confidence intervals.

Distinguishing the SIDS from the rest of the worldwide sample seems to be of great interest for geographical, economic, or political reasons. First of all, tropical cyclones may constitute a bigger threat to SIDS due to their smallness, insularity, limited domestic market and remoteness for some of them. The occurrence of a cyclone event can devastate coastal zones, which are intensely exploited for tourism and marine-related activity (Briguglio, 1995). Then, the smallness of their exploitable area poses a natural obstacle for economic diversification, which in turn weakens reconstruction capacities after a cyclone strike. As domestic production is often limited to a narrow range of goods, SIDS are strongly dependent to international trade and are sensitive to economic fluctuations abroad. In the end, this leads to higher per unit costs of production dedicated to rebuilding work, and this over-dependence on foreign exchanges is emphasized by extended supply schedules due to their frequent exclusion from major maritime and air routes. Besides, SIDS often rely on larger states in their political decisions and some aspects of public administration, which can undermine the efficiency in investment strategies or restructuring issues. All in all, the main sample is composed of 29 SIDS: 55% of them are located in the North Atlantic and North East Pacific tropical cyclone basin, 31% in the South West Pacific and South East Indian Ocean basin, 7% in the South West Indian Ocean basin, and the 7% remaining are located outside tropical cyclone basins.

Table 3 reports the results from estimating equation (3), while Figure 3 examines the cumulative effects with $L = 15$ for SIDS and non SIDS. Altogether, SIDS and non SIDS form a partition of the set of sample nations. Splitting the sample in such a way reveals the existence of a differential impact, and hence, that national growth responses obtained with the worldwide base mask some heterogeneity. The estimated immediate effect of one additional km/h of cyclone intensity is to decrease growth rates in SIDS by -0.016 percentage

point, and this negative effect accumulates to -0.024 percentage point after 15 years.[8] The estimated growth penalty for one standard deviation increase in the cyclone indicator is of 0.85 percentage point after 15 years. Cumulative effects from short-run to long-run are almost of same magnitude. Such quasi-constant slope is explained by the fact that most of the lagged values cannot be distinguished from 0. More specifically, it indicates that SIDS manage to avoid an intensification of negative effects, but do not manage to counteract them either. Moreover, it is worthy to note that minor signs of mitigation are detected shortly after period 1 and after period 8, but these impulses are not sufficiently strong to embrace any recovery to the pre-disaster trend. The null hypothesis that cyclone events do not affect growth rates in SIDS in the year that they occur is rejected at the 1% level across all lag choices. In contrast, when non SIDS are considered as a group, point estimates tend to show they experience an increased growth in the short-run, which plummets in the long-run, but these results are not statistically significant and no conclusion can be drawn from them.

One can argue that these negative effects observed for SIDS are driven by their development level. In fact, it is well-established in the literature on natural disasters and economic growth that poorer nations tend to experience stronger effects than richer ones (Rasmussen, 2004; Toya & Skidmore, 2007; Noy, 2009; Fomby & al., 2013). As such, Appendix D provides complementary estimations for the subset of developed countries and non SIDS developing countries.[9] No effects are found for either of those particular sub-groups of non SIDS countries.

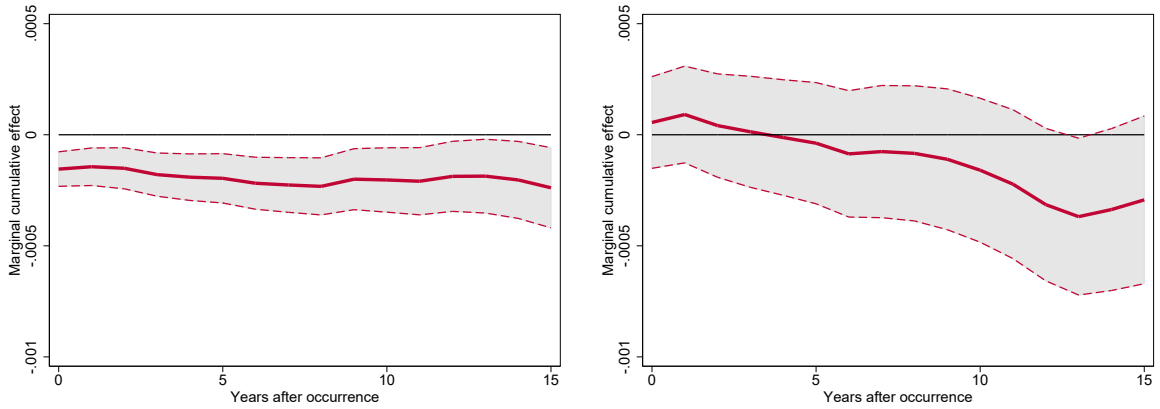

Figure 3: Measures of the marginal cumulative effects over fifteen years of cyclone events on *per capita* GDP growth for Small Island Developing States (right-hand side), and the world sample excluding Small Island Developing States (left-hand side). [Color should be used]

Notes: Estimations with outlier-robust regression. Standard errors are computed using the Street & al. (1988) correction. Shaded areas represent the associated 90 % confidence intervals.

[8]Detailed marginal effects coefficients for all estimations in subsection 4.1 are presented in Appendix C

[9]Developed countries are defined as in the *World Economic Outlook 2000* database of the International Monetary Fund, and correspond to Australia, Canada, Hong Kong, France, Iceland, Ireland, Japan, New Zealand, Norway, Portugal, Republic of Korea, Singapore, Spain, United Kingdom, United States.

Table 3: Regression results, models distinguishing Small Island Developing States.

	No lag	1 lag	5 lags	10 lags	15 lags
	(1)	(2)	(3)	(4)	(5)
$\overline{Cyc}_{i,t}$	0.00012	0.00010	0.00010	0.00005	0.00006
	(0.00011)	(0.00011)	(0.00011)	(0.000012)	(0.00013)
$\overline{Cyc}_{i,t-1}$		0.00007	0.00005	0.00005	0.00004
		(0.00004)	(0.00004)	(0.00005)	(0.00004)
$\overline{Cyc}_{i,t-2}$			-0.00001	-0.00003	-0.00005
			(0.00004)	(0.00005)	(0.00005)
$\overline{Cyc}_{i,t-3}$			0.00003	-7.26e-06	-0.00003
			(0.00004)	(0.00005)	(0.00005)
$\overline{Cyc}_{i,t} \times SIDS$	-0.00028**	-0.00027**	-0.00025**	-0.00022*	-0.00021
	(0.00012)	(0.00011)	(0.00012)	(0.00013)	(0.00013)
$\overline{Cyc}_{i,t-1} \times SIDS$		-0.00004	-0.00003	-0.00002	-0.00003
		(0.00004)	(0.00005)	(0.00005)	(0.00005)
$\overline{Cyc}_{i,t-2} \times SIDS$			3.57e-06	-0.00002	0.00004
			(0.00005)	(0.00005)	(0.00005)
$\overline{Cyc}_{i,t-3} \times SIDS$			-0.00005	-0.00002	-5.46e-07
			(0.00005)	(0.00005)	(0.00005)
Observations	3676	3676	3356	2956	2556
Adjusted R^2	0.25	0.25	0.27	0.29	0.32
Marginal cumulative effect (Ω_L) in SIDS	-0.00016***	-0.00014***	-0.00018***	-0.00022***	-0.00024**
	(0.00004)	(0.00005)	(0.00006)	(0.00008)	(0.00011)
Marginal cumulative effect (Ω_L) in non SIDS	0.00012	0.00017	0.00019	-0.00003	-0.00029
	(0.00011)	(0.00011)	(0.00015)	(0.00018)	(0.00022)

Notes: Outlier-robust regression estimates. Standard errors incorporating the Street & al. (1988) correction are in parentheses. Time and country fixed effects, as well as temperature and precipitation controls are included in all specifications, but not reported in the table.
Significance levels : *** 1 % ; ** 5 % ; * 10 %.

4.2 Robustness checks

This subsection presents a variety of robustness checks and proceeds in three steps. First, robustness to alternative cyclone measures is considered following the existing literature. Then, main results' sensitivity to changes in weights is examined. And finally, alternative panel specifications are investigated.

4.2.1 Alternative cyclone measures

Baseline estimations rely on a measure of cyclone that combines intensity and share of exposed land. Intensity is measured as the maximum wind speed observed at pixel level, and this point is questioned in two ways. In the context of Atlantic hurricanes landfalling along the U.S. Gulf and East Coasts, Emanuel (2011) introduced a threshold value for wind speed below which no property damage is likely to occur. This threshold value is equal to 50 knots ($\approx$ 92.6 km/h), and is calculated from insurance data in the US. It is embedded in the previously built cyclone measurement by only keeping cyclone events during which at least one pixel is hit by winds strictly greater than 92 km/h. Additionally, in the spirit of Krichene & al. (2021), a second index based on the exposed land and omitting the wind speed intensity dimension is examined. The latter measurement corresponds to a cyclone occurrence index relative to the exposed surface.

Table 4 reports the results from regressing these alternative cyclone measures on *per capita* GDP growth using equation (3) and the outlier-robust estimator. Results are broadly

consistent with previous findings as restricting to "damaging cyclones" only or omitting the wind speed parameter both exhibit larger effects. These larger point estimates are explained by a higher mean value for all identified cyclone events with the former indicator, and an equal consideration between cyclones of low and high wind speed intensity with the latter index. The persistent negative effect of cyclone events on economic growth in SIDS is also confirmed, but the cumulative effect is now statistically insignificant in final periods with the cyclone occurrence index when $L = 15$.[10] As for non SIDS, there is still no tangible evidence of any immediate or cumulative impact on national growth rates.

Table 4: Regression results using alternative cyclone measurements

	SIDS (1)	Non SIDS (2)
Weight = exposed land		
$\overline{Cyc}_{i,t} \times \mathbb{1}_{\{\exists\ pixel\ p\ \mid\ Wind_{p,i,t}>92km/h\}}$		
Immediate effect, $L = 0$	-0.00019***	0.00006
	(0.00004)	(0.00011)
Marginal cum. effect, $L = 1$	-0.00017***	0.00011
	(0.00005)	(0.00011)
Marginal cum. effect, $L = 5$	-0.00021***	0.00009
	(0.00006)	(0.00014)
Marginal cum. effect, $L = 10$	-0.00031***	-0.00009
	(0.00008)	(0.00018)
Marginal cum. effect, $L = 15$	-0.00036***	-0.00034
	(0.00011)	(0.00023)
$\mathbb{1}_{\{\overline{Cyc}_{i,t}>0\}}$		
Immediate effect, $L = 0$	-0.01453***	0.01642
	(0.00457)	(0.01199)
Marginal cum. effect, $L = 1$	-0.01295***	0.02134*
	(0.00500)	(0.01273)
Marginal cum. effect, $L = 5$	-0.01768***	0.03292**
	(0.00688)	(0.01618)
Marginal cum. effect, $L = 10$	-0.01853**	0.01015
	(0.00957)	(0.02071)
Marginal cum. effect, $L = 15$	-0.01164	-0.02525
	(0.01263)	(0.02575)

Notes: Estimations with outlier-robust regression. Standard errors incorporating the Street & al. (1988) correction are in parentheses. Time and country fixed effects as well as temperature and precipitation controls are included in all specifications, but not reported in the table.
Significance levels : *** 1 % ; ** 5 % ; * 10 %.

[10] Detailed results are available upon request.

4.2.2 Alternative weights

Table 5 reconsiders the main specification by applying alternative weights to the cyclone measurement. Firstly, instead of scaling the indicator by the share of exposed land, another strand of the TCE-DAT is exploited with population-weights. For each cyclone event recorded in the database, TCE-DAT provides spatially explicit population data at 0.1° x 0.1° resolution based on the *History Database of the Global Environment* v3.2 (HYDE; Klein Goldewijk & al., 2017).[11] The use of such weight constitutes a strong complement to the above results for two plausible reasons: it might be the case that a cyclone affect a wide area but sparsely populated, meaning that it does not affect an economically dynamic area. Analogously, a sparsely populated area could also be endowed with a high level of physical capital or natural resources (*e.g.* industrial or agricultural areas). In both cases, the intensity of the cyclone event and its trajectory within a given country remain unrelated to the intensity of economic activity at pixel level. In a second phase, the assumption that the immediate impact depends on the month in which the cyclone occurs is relaxed as it may be driving future responses and the successive adjustment path. As a final step, an extension of this monthly weight up to 3 years after the cyclone strike is also analysed. In fact, the main specification assumes that a cyclone event occurring in January and another one occurring in December with the same trajectory and intensity are given an equal weight after period 0, which can seem simplistic since in the former case, reconstruction processes and resilience can be more advanced than in the latter case.

Examining for alternative weights continues to show substantial negative effects in SIDS. Results appear slightly larger in magnitude when using population-weights, slightly lower when removing the period 0 temporal weight, and remain of same magnitude with an extension of the latter weight until lag 3. Concerning non SIDS, using population-weights or removing temporal weight now shows significant negative cumulative effect in the very long-run. However, the latter results should be interpreted with caution since statistically significant values are highly sensitive to specification and only occur in final periods.

4.2.3 Alternative panel specifications

Thus far, results obtained for SIDS are consistent with the neoclassical growth theory in the very short-run as it predicts an immediate negative impact on economic growth and a slight recovery one period later. The growth loss is often explained by the potential destruction of capital stock or employment caused by the disaster. Then, after the occurrence of the disaster, theory predicts a gradual return to stable steady state level of output *per capita* and thus, a temporary increase in growth.[12] Accordingly, results' sensitivity is further analysed by including some determinants of growth to the main specification. However, as

[11] HYDE provides decennial values up to 2000, and annual values afterwards. Thus, annual population data before 2000 are recovered with linear interpolation.

[12] Concerning this specific point, several interpretations can be found in the literature. The expected positive effect in growth is mainly explained by budgetary impulses intending to replace the destroyed capital stock. Among others, Skidmore & Toya (2002) argue that disasters stimulate innovation while Caballero & Hammour (1994) or Crespo Cuaresma & al. (2008) support that the faster growth is related to the replacement of the destroyed physical capital, potentially old and outdated, by newer and more efficient equipment.

Table 5: Regression results using alternative weighting specifications.

	SIDS	Non SIDS
	(1)	(2)
Weight = exposed population		
Immediate effect, $L = 0$	-0.00017***	0.00002
	(0.00004)	(0.00010)
Marginal cum. effect, $L = 1$	-0.00016***	0.00006
	(0.00005)	(0.00010)
Marginal cum. effect, $L = 5$	-0.00021***	0.00007
	(0.00006)	(0.00013)
Marginal cum. effect, $L = 10$	-0.00027***	-0.00026
	(0.00009)	(0.00016)
Marginal cum. effect, $L = 15$	-0.00035***	-0.00048**
	(0.00011)	(0.00020)
No monthly weight at period 0		
Immediate effect, $L = 0$	-0.00008***	0.00002
	(0.00002)	(0.00004)
Marginal cum. effect, $L = 1$	-0.00005*	0.00009
	(0.00003)	(0.00006)
Marginal cum. effect, $L = 5$	-0.00010**	0.00011
	(0.00005)	(0.00010)
Marginal cum. effect, $L = 10$	-0.00016**	-0.00006
	(0.00008)	(0.00014)
Marginal cum. effect, $L = 15$	-0.00020**	-0.00034*
	(0.00010)	(0.00020)
Monthly weight extended until lag 3		
Immediate effect, $L = 0$	-0.00016***	0.00012
	(0.00004)	(0.00011)
Marginal cum. effect, $L = 1$	-0.00013***	0.00020
	(0.00005)	(0.00013)
Marginal cum. effect, $L = 5$	-0.00018***	0.00023
	(0.00007)	(0.00016)
Marginal cum. effect, $L = 10$	-0.00021**	3.36e-06
	(0.00009)	(0.00020)
Marginal cum. effect, $L = 15$	-0.00025**	-0.00028
	(0.00011)	(0.00024)

Notes: Estimations with outlier-robust regression. Standard errors incorporating the Street & al. (1988) correction are in parentheses. Time and country fixed effects, as well as temperature and precipitation controls are included in all specifications, but not reported in the table.
Significance levels : *** 1 % ; ** 5 % ; * 10 %.

recalled by Dell & al. (2014), one should be cautious when including control variables that are themselves outcomes of cyclone events as it will induce an "over-controlling problem". The addition of economic control variables can prevent from estimating the true net effect of cyclone events on output as cyclones surely have an impact on these variables, which in turn impact the dependent variable.[13] To limit this concern, lagged values of control variables are used. Following Solow (1956) but also Mankiw & al. (1992) and Islam (1995), logarithmic lagged values of *per capita* GDP, population, *per capita* investment and trade openness are

[13]Economic controls can therefore be considered as "bad controls" (Angrist & Pischke, 2009).

included to the main model. According to the Solow growth model, the lagged value of *per capita* GDP captures the rate of convergence towards the steady state.[14] Table 6 reports the results from this change in specification in column 3. It also shows results from a regression that includes region × year and SIDS × year fixed effects in column 2. Columns 4 and 5 re-estimate equation (1) with a sample restricted respectively to SIDS and non SIDS only. To ease comparisons, main results presented in Table 3 are repeated in column 1.

With additional control variables (column 3), cumulative effects' significance are lessened for SIDS. In the case when $L = 15$, estimates become non-significant after period 8 for SIDS, and are statistically significant after period 10 for non SIDS. The magnitude of these coefficients also varies: the time path of the effects in SIDS becomes a straight line. Three core aspects are highlighted by this result. It confirms the exogeneity of the cyclone indicator as estimates are of same magnitude given 95% confidence bands. Then, it confirms that lag structures are not particularly influential and short-term effects are most decisive. Third, the negative sign associated with the lagged value of *per capita* GDP shows that the economy is still converging towards its steady state level after the cyclone strike. Point estimates from column 2 and column 3 and are fairly comparable in terms of statistical significance for both sub-samples. Estimates are once again non-significant for SIDS in the very long-run with the 15 lags model. Results reported for non SIDS are intermittently significant in final periods when including additional fixed effects, but across all different lag specifications, the estimated coefficient for period 0 remains non-significant. These results for non SIDS are consistent with previous findings as statistical significance varies widely across specifications and does not provide a sufficient basis for any general conclusion. Finally, running regressions separately for SIDS and non SIDS sub-samples does not change the results either, even though the standard errors increase in column 4 as the number of observations is greatly reduced. As additional specification checks, Appendix Table E.1 reports regressions when keeping the same number of observations than the baseline specification with $L = 15$, while Table E.2 re-estimates equation (3) when all the countries affected by extratropical cyclones only are excluded from the sample.[15] In no case are the estimates significant for non SIDS, while results remain in line with those obtained above for SIDS.

5 An Increased Economic Vulnerability for Small Island Developing States

Previous estimations infer a persistent negative growth effect of tropical cyclones in SIDS and suggest further investigation on the underlying mechanisms leading to this result. It is proved that national growth effects are heterogeneous across countries, especially for those combining small size and lower development level such as SIDS. This may be explained by structural factors of vulnerability such as the concentration of activity over a reduced surface or the lack of spatial heterogeneity in terms of cyclone exposure at national scale.

[14] In case of convergence, the estimated coefficient should be negative. See Acemoglu (2007) for a detailed discussion.

[15] This set of countries corresponds to Algeria, Canada, France, Iceland, Ireland, Morocco, Norway, Portugal, Russia, Spain, and United Kingdom.

Table 6: Regression results using alternative panel specifications.

	Main Model Specification (1)	Additional Fixed Effects (2)	Additional Control Variables (3)	Sample restricted to SIDS only (4)	Sample restricted to non SIDS only (5)
Model with no cyclone lag: immediate effect					
$ln(GDP\ per\ capita)_{i,t-1}$			-0.01216***		
			(0.00312)		
$\overline{Cyc}_{i,t}$	0.00012	0.00019	0.00008	-0.00019***	0.00012
	(0.00011)	(0.00012)	(0.00011)	(0.00005)	(0.00010)
$\overline{Cyc}_{i,t} \times SIDS$	-0.00028**	-0.00034***	-0.00024**		
	(0.00012)	(0.00013)	(0.00012)		
$ln(Population)_{i,t-1}$			0.02637***		
			(0.00424)		
$ln(Trade\ Openness)_{i,t-1}$			0.00752***		
			(0.00187)		
$ln(Investment\ per\ capita)_{i,t-1}$			0.00393**		
			(0.00185)		
Observations	3676	3676	3629	1285	2391
Adjusted R^2	0.25	0.30	0.28	0.16	0.31
Immediate effect in SIDS	-0.00016***	-0.00015***	-0.00016***	-0.00019***	-
	(0.00004)	(0.00005)	(0.00004)	(0.00005)	
Model with 1 cyclone lag:					
Marginal cumulative effect in SIDS	-0.00014***	-0.00013***	-0.00013***	-0.00016***	-
	(0.00005)	(0.00005)	(0.00004)	(0.00006)	
Marginal cumulative effect in non SIDS	0.00017	0.00025*	0.00014	-	0.00017
	(0.00011)	(0.00013)	(0.00012)		(0.00011)
Model with 5 cyclone lags:					
Marginal cumulative effect in SIDS	-0.00018***	-0.00012*	-0.00013**	-0.00018**	-
	(0.00006)	(0.00007)	(0.00006)	(0.00008)	
Marginal cumulative effect in non SIDS	0.00019	0.00035**	0.00010	-	0.00015
	(0.00015)	(0.00016)	(0.00015)		(0.00013)
Model with 10 cyclone lags:					
Marginal cumulative effect in SIDS	-0.00022***	-0.00017*	-0.00013*	-0.00021*	-
	(0.00008)	(0.00009)	(0.00008)	(0.000011)	
Marginal cumulative effect in non SIDS	-0.00003	0.00017	-0.00016	-	-0.00006
	(0.00018)	(0.00020)	(0.00018)		(0.00016)
Model with 15 cyclone lags:					
Marginal cumulative effect in SIDS	-0.00024**	-0.00015	-0.00013	-0.00017	-
	(0.00011)	(0.00011)	(0.00010)	(0.00015)	
Marginal cumulative effect in non SIDS	-0.00029	-0.00050**	-0.00045**	-	-0.00032
	(0.00022)	(0.00025)	(0.00022)		(0.00020)

Notes: Outlier-robust regression estimates. Standard errors incorporating the Street & al. (1988) correction are in parentheses. Time and country fixed effects, as well as temperature and precipitation controls are included in all specifications, but not reported in the table. Additional fixed effects model refers to the inclusion of Region × Year and SIDS × Year fixed effects.
Significance levels : *** 1 % ; ** 5 % ; * 10 %.

In what follows, economic and physical channels are explored. First, SIDS' degree of dependence with international markets after a cyclone strike is analysed. Then, effects on their rebuilding capacities are examined using *per capita* investment and sectoral GDP growth for construction industry. According to neoclassical growth theory, *per capita* investment is fundamental to explain the absence of sustained recovery. Finally, the adaptive behavior of SIDS to tropical cyclones is analysed by repeating the main specification on those most frequently exposed to this shock.

5.1 Exposure to foreign economic conditions

Given the particularity of SIDS' geographical situation and economic issues, it is important to study the transmission channels using indicators that are specifically designed for this subgroup of countries. In this sense, Briguglio (1995) developed an index based on major sources rendering SIDS economies vulnerable to forces outside their control, *i.e.* their small size, remoteness, insularity and proneness to natural disasters. To take advantage of this work, the main empirical strategy (equation (3)) is first applied to one of the variables included in this index: the degree of exposure to foreign economic conditions, which is calculated as the mean volume of exports and imports relative to GDP. Mathematically, it is expressed as follows:

$$Exposure_{i,t} = \frac{Imports_{i,t} + Exports_{i,t}}{2 * GDP_{i,t}}$$

The relevance of using this dependent variable additionally lies in the fact that previously observed negative effects on economic activity might be triggered by a negative effect on a combination of determinants of growth, and not necessarily by distinct impacts on each of them.

Figure 4 plots the cumulative growth response of Briguglio's (1995) economic exposure indicator with $L = 15$. On impact, the dependence of SIDS economies to foreign exchanges is significantly increased. After the strike, this dependence remains increased for 5 years, with point estimates significant at the 10% level for period 0 and 5, and at the 5% level for all periods between 1 and 4. One additional km/h of cyclone intensity is associated with 0.03 percentage point increase of economic exposure growth five years after a cyclone strike. Thus, the negative immediate effect observed on economic growth and the absence of subsequent recovery in the short-run is linked with this result as SIDS are strongly dependent on foreign exchange earnings or on importation of basic supplies that cannot be produced domestically. This increase of economic vulnerability is emphasized by additional results on the impact on tourism receipts growth reported in Appendix Figure F.1. These additional results suggest that tourism receipts growth, which represents one of SIDS' main source of revenue is, on impact, negatively affected by cyclone strikes. Losses of tourism receipts persists in the short-run as the cumulative effect remains significant up to five years after a strike.[16]

5.2 Hurdles to recover

The main panel methodology is then applied to explore the effects of tropical cyclones on *per capita* investment growth as well as sectoral GDP growth for construction industry. *Per capita* investment is at the forefront of growth theories. For instance, according to the Solow-Swan model, it brings on capital accumulation, while in an endogenous growth framework, it stimulates technological progress. In such models, when a storm destroys a share of capital stock, the economy may return to its steady state by raising *per capita* investment growth. As for construction sector, it is found to be positively impacted in other world base, regional, national-level analyses (Hsiang & Jina, 2014; Hsiang, 2010; Zhou

[16]However, as the data on tourism receipts are extracted from the WDI database, which is an alternative economic data source, the number of observations is drastically diminished.

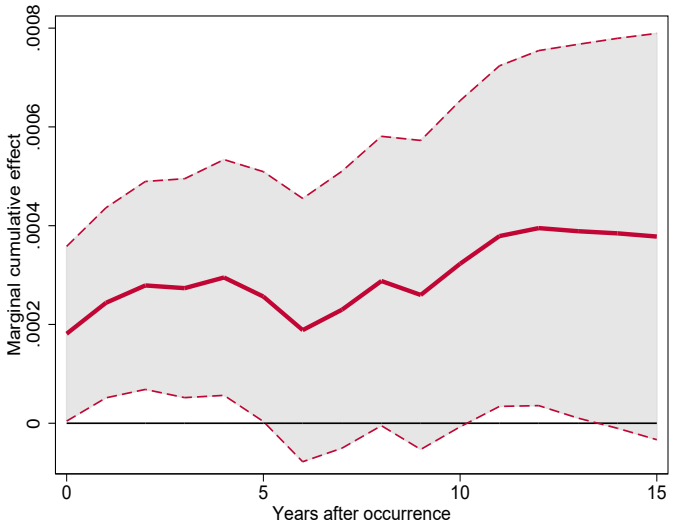

Figure 4: Measures of the marginal cumulative effects over fifteen years of cyclone events on Briguglio's (1995) economic exposure index growth for Small Island Developing States. [Color should be used]

Notes: Estimations with outlier-robust regression. Standard errors are computed using the Street & al. (1988) correction. Shaded areas represent the associated 90 % confidence intervals.

& Zhang, 2021), or even in local single event studies (Vigdor, 2008). In particular, it is used to bring evidence for a creative destruction scenario, as damages from cyclones trigger opportunities for reconstruction.

Results are presented in Figure 5, and show consistency with previous findings on *per capita* GDP growth. Point estimates are almost always non-significant for both variables, suggesting that institutional responses brought after a storm shock are limited in SIDS. The absence of immediate and cumulative increase in *per capita* investment growth can be explained by their incapacity to increase their debt level to finance reconstruction and implement a clear-cut recovery plan. In 2015, SIDS had, on average, greater debt-to-GNI ratio than other developing countries (OECD, 2018). These higher levels of public debt limits fiscal scope for governments to make appropriate investments for risk mitigation, or more generally for development. This point is further investigated in Appendix Figure F.2, where the absence of any significant effect (immediate and cumulative) of tropical cyclones on SIDS' debt-to-GDP ratio is demonstrated.[17] No positive shift in investment growth patterns also suggests that cyclones may be a factor of deterrence for private investors. Interpreting with previous result obtained in section 4.2.3 when lagged value of *per capita* GDP is included in the model, the Solow growth model predicts that convergence towards the steady state is maintained but not accelerated after a cyclone strike. Reaching the steady state is simply delayed in time. Then, findings on construction sector growth suggest that SIDS' reconstruction capacities are low. The obtained results differ from those observed

[17]However, as the data are once again extracted from WDI database, the number of observations is still drastically diminished.

in the existing literature as no significant positive effect is found for 15 years.[18] SIDS' narrow resource base might explain the absence of leap in construction sector growth. Such incapacity to positively respond in the aftermath of a tropical cyclone might, in turn, lead to shoddy or incomplete rebuilding work between each disaster event.

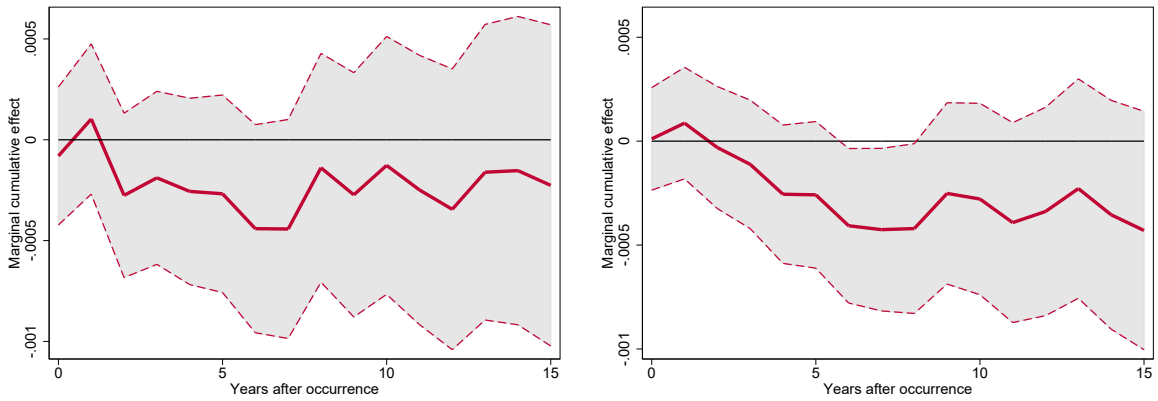

Figure 5: Measures of the marginal cumulative effects over fifteen years of cyclone events on *per capita* investment growth (left-hand side) and construction industry growth (right-hand side) for Small Island Developing States.[Color should be used]
Notes: Estimations with outlier-robust regression. Standard errors are computed using the Street & al. (1988) correction. Shaded areas represent the associated 90 % confidence intervals.

5.3 Lack of adaptability

SIDS' ability to adapt to cyclone events is examined by distinguishing those that are more prone to these hazards. A SIDS is considered as frequently hit if it has known an above median number of cyclone events among the entire set of SIDS from 1950 to 2015. This median threshold corresponds to 0.44 cyclone per year. No significant difference in means is found between most frequently hit SIDS' and other SIDS' *per capita* GDP, meaning that those that are most frequently hit are not the poorer countries. Figure 6 presents marginal cumulative effects of one additional km/h of intensity shock on frequently hit SIDS' economic growth. Estimates of short- to long-term impacts are larger in magnitude for SIDS if they are repeatedly hit by cyclones. The absence of enhanced growth dynamics suggest that SIDS struggle to implement adaptation policies. In fact, one might expect that countries that are more prone to disasters have more incentives to invest in mitigating measures, so that the economic impact is reduced *in fine*. The obtained results rather demonstrate the increasing difficulties to restrain losses for frequently affected SIDS. This point is even more concerning in regard to alterations expected in tropical cyclones' frequency, intensity or duration due to climate change (IPCC, 2019). The present results combined with those on *per capita* investment and construction industry growth additionally infer the risk of poverty traps due

[18] Although Hsiang (2010) finds a positive impact using a sample of Carribean and Central American countries, which is mostly composed of SIDS, these countries only represent about 50% of the present sample. Other small islands like those located in the Pacific for instance, are often more isolated than other countries, which increases even more their lack of domestic economic production (Tisdell, 2007).

to cyclone strikes, and this risk is even greater when the frequency of storm events is high. The more a SIDS is hit by tropical cyclones, the more it is unable to fully rebuild between each catastrophe. These SIDS may end up remaining in a continuous stage of reconstruction (Hallegate & Dumas, 2009).

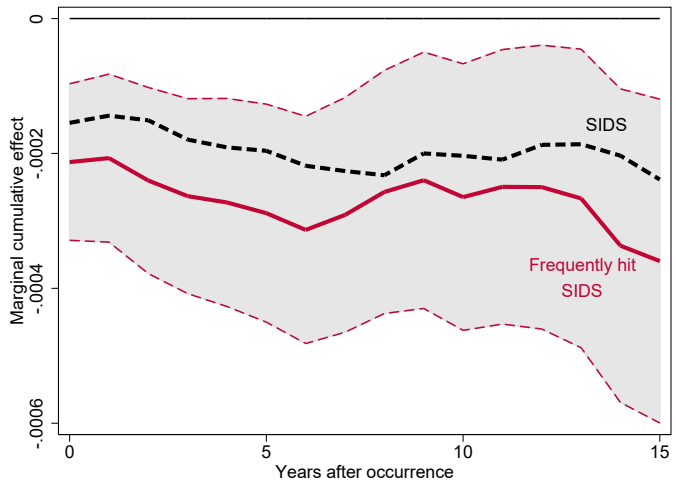

Figure 6: Measures of the marginal cumulative effects over fifteen years of cyclone events on *per capita* GDP growth for frequently hit Small Island Developing States. [Color should be used]
Notes: Estimations with outlier-robust regression. Standard errors are computed using the Street & al. (1988) correction. Shaded areas represent the associated 90 % confidence intervals obtained for frequently hit states. Black dashed line correspond to the estimations for Small Island Developing States (SIDS), identical to those expressed in section 3.

6 Concluding remarks

This paper investigates the impact of cyclone events on economic growth for 83 nations during the period 1970-2015. First, a set of exogenous weather indicators is built at the pixel level using geophysical and meteorological datasets. Results on worldwide basis confirm those already existing in the literature as negative immediate and persistent effects are found over 15 years on economic activity. Then, a special focus is made on SIDS, which are of particular interest as they are expected to be more vulnerable to natural disasters, especially due to their small size and low level of development. Beyond an inequality of exposure to tropical cyclones between SIDS and non SIDS, evidence is brought for differentiated impact between these two groups of countries. Tropical cyclones are found to increase SIDS' economic vulnerability, whereas they show to be not disruptive enough to be reflected in non SIDS' national growth rates irrespective of their level of development. This differential impact may come from the fact that, in a SIDS, the entire economy and population are likely to be concerned by these shocks. In contrast, in a non SIDS, this might not be the case and the present study provides support for more micro-scaled research, eventually at county or regional level as in Strobl (2011). Non SIDS may have only small parts of their respective territories that are highly vulnerable to tropical cyclones, and our results suggest that conducting subnational level

analyses would be far more adequate in these countries. All in all, a one km/h increase of cyclone intensity over a SIDS is responsible for a 0.024 percentage point cumulative growth loss 15 years later. Expressed differently, a one standard deviation increase in the cyclone intensity indicator is associated with a 0.85 percentage point cumulative loss of national growth 15 years later.

Short-term results obtained for SIDS appear very robust and are in line with basic predictions of the neoclassical growth model as an immediate negative effect is observed due to destruction of a share of the capital stock, followed by a slight recovery explained by the convergence towards a stable steady-state. However, in no case response curves outperform the counterfactual scenario when no disaster occurs. Very long-run cumulative effects estimates are more noisy given the specification, but still remain significant at least 8 years after a cyclone strike across all methods employed here. Additionally, it is proved that conclusions are not altered by the maximum lag length choice as long-run economic losses remain of same magnitude as time goes by. Related propagation mechanisms are documented through economic and physical channels. First, a specific vulnerability variable designed for SIDS is exploited: the extent of exposure to foreign economic conditions (Briguglio, 1995). Cyclone events are found to increase SIDS' dependence to foreign markets in the short-run, which counteracts the first signs of recovery triggered at period 1 and maintains the adverse impacts observed on economic growth. Then, further investigation on investment *per capita* and sectoral GDP growth for construction industry also sheds light on their low reconstruction capacities and difficulties to pin down crucial investment decisions at national scale. This second strand of results also suggests that SIDS' debt constraints are tight, preventing them from implementing a proper fiscal stimulus plan following a storm. Finally, adaptation issues are discussed by evaluating growth impacts on most frequently affected share of SIDS. Hurdles to adopt mitigating measures are detected, and adaptive capacities are found to be limited as growth losses are not attenuated by cyclone frequency. More importantly, this last result contributes to debates over future impacts of climate change and warns on SIDS' potential destiny. Policy implications regarding the urge to invest in economic preparedness or early warning systems shall emerge from this study.

The study of all possible underlying mechanisms deserves more exploration and further impact evaluations are needed to fully understand the inferred growth loss. This article is intended to inform on SIDS' specific vulnerability to cyclone risks, but several other aspects remain to be explored like migrations, aid surges, or remittances. These three output variables are essential to maintain SIDS' consumption levels and can display significant responses even though investment is unaffected. The impact on transport costs, another variable of vulnerability suggested by Briguglio (1995) to stress SIDS' remoteness and insularity, could also be estimated. Last but not least, GDP poorly explains impacts on populations' welfare, purchasing power or inequality which seem to be of equal importance regarding the resilience after a cyclone shock. This first set of findings should trigger the opportunity for further empirical and theoretical research.

References

Acemoglu, D. (2007). *Introduction to Modern Economic Growth.* Princeton University Press.

Acemoglu, D. Naidu, S., Restrepo, P. & Robinson, J. A. (2019). Democracy Does Cause Growth. *Journal of Political Economy.* 127(1), 47-100.

Acemoglu, D., & Restrepo, P. (2020). Robots and jobs: Evidence from US labor markets. *Journal of Political Economy*, 128(6), 2188-2244.

Albala-Bertrand, J. M. (1993). Political Economy of Large Natural Disasters. *Oxford: Clarendon Press.*

Amiti, M., & Wei, S. J. (2009). Service offshoring and productivity: Evidence from the US. *World Economy*, 32(2), 203-220.

Angrist, J. D., & Pischke, J. S. (2009). *Mostly harmless econometrics: An empiricist's companion.* Princeton university press.

Beaton, A. E. & Tukey, J. W. (1974). The Fitting of Power Series, Meaning Polynomials, Illustrated on Band-Spectroscopic Data. *Technometrics*, 16, 147-185.

Belsley, D. A., Kuh, E., & Welsch, R. E. (1980). Regression diagnostics: Identifying influential data and sources of collinearity. *Wiley Series in Probability and Mathematical Statistics.*

Bond, S., Leblebicioğlu, A., & Schiantarelli, F. (2010). Capital accumulation and growth: a new look at the empirical evidence. *Journal of Applied Econometrics, 25* (7), 1073-1099.

Botzen, W. W., Deschenes, O., & Sanders, M. (2019). The economic impacts of natural disasters: A review of models and empirical studies. *Review of Environmental Economics and Policy*, 13(2), 167-188.

Briguglio, L. (1995). Small island developing states and their economic vulnerabilities. *World Development*, 23(9), 1615-163.

Caballero, R. J., & Hammour, M. L. (1994). The Cleansing Effect of Recessions. *American Economic Review*, 84, 1350-1368.

Cavallo, E., Galiani, S., Noy, I. & Pantano, J. (2013). Catastrophic Natural Disasters and Economic Growth. *The Review of Economics and Statistics*, 95, issue 5, p. 1549-1561.

Cook, R. D. (1977). Detection of Influential Observations in Linear Regression. Technometrics. *American Statistical Association.* 19 (1): 15–18. doi:10.2307/1268249

Cook, R. D. & Weisberg, S. (1982). Residuals and Influence in Regression. *New York: Chapman and Hall.*

Crespo Cuaresma, J., Hlouskova, J., & Obersteiner, M. (2008). Natural disasters as creative destruction? Evidence from developing countries. *Economic Inquiry*, 46(2), 214-226.

Dell, M., Jones, B. F., & Olken, B. A. (2012). Temperature Shocks and Economic Growth: Evidence from the Last Half Century. *American Economic Journal: Macroeconomics*, 4(3), 66–95.

Dell, M., Jones, B. F., & Olken, B. A. (2014). What do we learn from the weather? The new climate-economy literature. *Journal of Economic Literature*, 52(3), 740-98. Emanuel, K. (2011). Global warming effects on U.S. hurricane damage. *Weather Clim Soc*, 3(4), 261–268.

Felbermayr, G., & Gröschl, J. (2014). Naturally negative: The growth effects of natural disasters. *Journal of Development Economics*, 111, 92–106.

Fomby, T., Ikeda, Y. & Loayza, N., (2013). The growth aftermath of natural disasters. *Journal of Applied Econometrics*, 28(3), 412–434.

[dataset] Geiger, T., Frieler, K., & Bresch, D. N. (2018). A global historical data set of tropical cyclone exposure (TCE-DAT). Earth Syst. Sci. Data, 10, 185–194, https://doi.org/10.5194/essd-10-185-2018.

Goodall, C. (1983). M-estimators of location: An outline of the theory. In Understanding Robust and Exploratory Data Analysis, ed. D. C. Hoaglin, C. F. Mosteller, and J. W. Tukey, 339–431. New York: Wiley.

Greene, W.H. (2003) Econometric Analysis. 5th Edition, Prentice Hall, Upper Saddle River.

Haiyan, J., Halverson, J., Simpson, J. & Zipser, E. (2008). Hurricane 'rainfall potential' derived from satellite observations aids overland rainfall prediction. *Journal of Applied Meteorology and Climatology*, 47, 944–959.

Hallegatte, S. & Dumas, P. (2009). Can natural disasters have positive consequences? Investigating the role of embodied technical change. *Ecological Economics*, 68(3), 777–786.

Hamilton, L. C. (1991a). srd1: How robust is robust regression? Stata Technical Bulletin 2: 21–26. Reprinted in Stata Technical Bulletin Reprints, vol. 1, pp. 169–175. College Station, TX: Stata Press.

Hamilton, L. C. (1992). Regression with Graphics: A Second Course in Applied Statistics. Belmont, CA: Duxbury.

Harris, I., Osborn, T.J., Jones, P. et al. (2020). Version 4 of the CRU TS monthly high-resolution gridded multivariate climate dataset. Sci Data 7, 109.

Holland, G. (2008). A revised hurricane pressure–wind model. *Monthly Weather Review*, 136(9), 3432-3445.

Hsiang, S. M. (2010). Temperatures and Cyclones strongly associated with economic production in the Caribbean and Central America. *Proceedings of the National Academy of Sciences*, 107(35), 15367–15372.

Hsiang, S. M., & Jina, A. S. (2014). The causal effect of environmental catastrophe on long-run economic growth: Evidence from 6,700 cyclones. *National Bureau of Economic Research*.

Huber, P. J. (1964). Robust estimation of a location parameter. *Annals of Mathematical Statistics*, 35, 73–101.

IPCC (2014). Climate Change 2014: Synthesis Report. Contribution of Working Groups I, II and III to the Fifth Assessment Report of the Intergovernmental Panel on Climate Change [Core Writing Team, R.K. Pachauri and L.A. Meyer (eds.)]. IPCC, Geneva, Switzerland, 151 pp.

IPCC (2018). Global warming of 1.5°C. An IPCC Special Report on the impacts of global warming of 1.5°C above pre-industrial levels and related global greenhouse gas emission pathways, in the context of strengthening the global response to the threat of climate change, sustainable development, and efforts to eradicate poverty [V. Masson-Delmotte, P. Zhai, H. O. Pörtner, D. Roberts, J. Skea, P.R. Shukla, A. Pirani, W. Moufouma-Okia, C. Péan, R. Pidcock, S. Connors, J. B. R. Matthews, Y. Chen, X. Zhou, M. I. Gomis, E. Lonnoy, T. Maycock, M. Tignor, T. Waterfield (eds.)]. In Press.

IPCC (2019). IPCC Special Report on the Ocean and Cryosphere in a Changing Climate [H.O. Pörtner, D.C. Roberts, V. Masson-Delmotte, P. Zhai, M. Tignor, E. Poloczanska, K. Mintenbeck, A. Alegria, M. Nicolai, A. Okem, J. Petzold, B. Rama, N.M. Weyer (eds.)]. In press.

Islam, N. (1995). Growth empirics: a panel data approach. *The quarterly journal of economics*, 110(4), 1127-1170.

[dataset] Knapp, K. R., Kruk, M. C., Levinson, D. H., Diamond, H. J., & Neumann, C. J. (2010). The international best track archive for climate stewardship (IBTrACS) unifying tropical cyclone data. *Bulletin of the American Meteorological Society*, 91(3), 363-376.

Kaplan, S. N., & Zingales, L. (1997). Do investment-cash flow sensitivities provide useful measures of financing constraints? *The quarterly journal of economics*, 112(1), 169-215.

[dataset] Klein Goldewijk, K., Beusen, A., Doelman, J., & Stehfest, E. (2017). Anthropogenic land use estimates for the Holocene – HYDE 3.2, *Earth System Science Data*, 9(2), 927–953.

Knutson, T.R., Mcbride, J., Chan, J., Emanuel, K., Holland, G., Landsea, C., Held, I., Kossin, J.P., Srivastava, A.K. & Sugi M. (2010). Tropical cyclones and climate change. *Nature Geoscience*, 3, 157–163.

Krichene, H., Geiger, T., Frieler, K., Willner, S. N., Sauer, I., Otto, C. (2021). Long-term impacts of tropical cyclones and fluvial floods on economic growth – Empirical evidence on transmission channels at different levels of development. *World Development*, Volume 144, 105475.

Li, G. (1985). Robust regression. *In Exploring Data Tables, Trends, and Shapes*, ed. D. C. Hoaglin, C. F. Mosteller, and J. W. Tukey, 281–340. New York: Wiley.

Loayza, N. V., Olaberría, E., Rigolini, J., & Christiaensen, L. (2012). Natural disasters and growth: Going beyond the averages. *World Development*, 40(7), 1317–1336.

Mankiw, N. G., Romer, D. & Weil, D. (1992). A Contribution to the Empirics of Economic Growth. *Quarterly Journal of Economics*, 107, 407–437.

Nordhaus, W. D. (2006). Geography and macroeconomics: New Data and new findings. *Proceedings of the National Academy of Sciences*, 103 (10).

Noy, I. (2009). The macroeconomic consequences of disasters. *Journal of Development Economics*, 88, 221–231.

OECD (2018), Making Development Co-operation Work for Small Island Developing States, *OECD Publishing*, Paris, https://doi.org/10.1787/9789264287648-en.

Raddatz, C. (2007). Are External Shocks Responsible for the Instability of Output in Low-Income Countries? *Journal of Development Economics*, 84, 155–187.

Raddatz, C. (2009). The Wrath of God: Macroeconomic Costs of Natural Disasters. *World Bank policy research working paper*, 5039.

Rasmussen, T.N. (2004). Macroeconomic implications of natural disasters in the Caribbean. *IMF Working Paper*, WP/04/224.

Romer, C. D. & Romer, D. H. (2010). The Macroeconomic Effects of Tax Changes: Estimates Based on a New Measure of Fiscal Shocks. *The American Economic Review*, 763–801.

Solow, R. (1956). A Contribution to the Theory of Economic Growth. *The Quarterly*

Journal of Economics, 70(1), 65-94.

Strobl, E. (2011). The economic growth impact of hurricanes: Evidence from US coastal counties. *Review of Economics and Statistics*, 93(2), 575-589.

Strobl, E. (2012). The economic growth impact of natural disasters in developing countries: Evidence from hurricane strikes in the Central American and Caribbean regions. *Journal of Development Economics*, 97(1), 130-141.

Skidmore, M. & Toya, H. (2002). Do Natural Disasters Promote Long-Run Growth? *Economic Inquiry*, 40(4), 664–687.

Street, J. O., Carroll, R. J., & Ruppert, D. (1988). A note on computing robust regression estimates via iteratively reweighted least squares. *The American Statistician, 42*(2), 152-154.

Tisdell, C. A. (2007): "Globalization and the Economic Future of Small Isolated Nations, Particularly in the Pacific", in: Prasad, Biman L.; Roy, Kartik C. (eds): *Globalization and the Economic Future of Small Isolated Nations, Particularly in the Pacific.* New York: Nova Science Publishers, 4-21

Toya, H. & Skidmore, M. (2007). Economic development and the impacts of natural disasters. *Economics Letters*, 94(1), 20-25.

Vigdor, J. (2008). The economic aftermath of Hurricane Katrina. *Journal of Economic Perspectives*, 22(4), 135-54.

Zhou, Z., & Zhang, L. (2021). Destructive destruction or creative destruction? Unraveling the effects of tropical cyclones on economic growth. *Economic Analysis and Policy*, 70, 380-393.

APPENDIX

A Additional descriptive statistics

Table A.1: National Summary Statistics for Sample Nations

Country	ISO	Average values from 1950 to 2015				
		Annual Cyclone Windspeed (by exposed land, in km/h)	Annual Number of Cyclones	Annual Mean Temperature (in °C)	Annual Precipitation Level (in mm)	Classification
Algeria	DZA	0.0	0.0	22.8	87.7	
Antigua & Barbuda	ATG	42.4	0.6	26.2	2363.9	SIDS
Australia	AUS	4.8	1.8	21.8	528.4	
Bahamas	BHS	62.1	1.0	25.1	1310.6	SIDS
Bangladesh	BGD	13.3	0.7	25.1	2573.7	
Barbados	BRB	33.7	0.4	26.3	2154.6	SIDS
Belize	BLZ	26.6	0.4	25.6	2195.5	SIDS
Brazil	BRA	0.0	0.0	25.2	1760.5	
Brunei	BRN	0.6	0.0	27.1	2787.6	
Cambodia	KHM	4.6	0.6	27.1	1890.9	
Canada	CAN	1.2	1.1	-5.0	530.3	
Cape Verde	CPV	18.5	0.4	23.5	418.5	SIDS
China	CHN	4.1	3.7	7.3	626.6	
Colombia	COL	0.2	0.2	24.7	2601.9	
Comoros	COM	10.9	0.1	25.8	1664	SIDS
Costa Rica	CRI	1.8	0.1	25.1	2883.2	
Cuba	CUB	38.7	1.0	25.5	1360.9	SIDS
Dominica	DMA	44.6	0.6	22.5	3602.1	SIDS
Dominican Republic	DOM	29.9	0.6	24.7	1418.7	SIDS
El Salvador	SLV	2.5	0.1	24.7	1732.2	
Fiji	FJI	26.8	0.4	24.6	2697.9	SIDS
France	FRA	0.2	0.1	11.2	859.6	
Grenada	GRD	24.8	0.2	26.9	1545.3	SIDS
Guatemala	GTM	9.1	0.4	23.7	2716.9	
Guinea	GIN	0.1	0.0	26.0	1685.3	
Guinea-Bissau	GNB	1.2	0.0	27.0	1636.5	SIDS
Haiti	HTI	34.1	0.5	25.1	1441.1	SIDS
Honduras	HND	14.9	0.5	23.8	1964.1	
Hong Kong SAR China	HKG	86.9	1.6	22.9	2264.3	
Iceland	ISL	3.6	0.1	2.2	1009.1	
India	IND	4.1	1.2	23.9	1069.7	
Indonesia	IDN	0.3	0.3	26.0	2743.4	
Iran	IRN	0.0	0.0	17.7	214.7	
Ireland	IRL	8.6	0.2	9.6	1145.5	
Jamaica	JAM	29.4	0.4	25.2	2092.0	SIDS
Japan	JPN	77	3.7	11.5	1694.2	
Laos	LAO	15.0	1.4	23.0	1820.8	
Madagascar	MDG	16.2	0.9	22.9	1471	
Malawi	MWI	0.0	0.0	22.2	1137.8	
Malaysia	MYS	0.6	0.1	25.7	2947.3	
Mauritius	MUS	28.2	0.4	22.7	1973.1	SIDS
Mexico	MEX	14.7	2.4	21.4	742.4	
Montserrat	MSR	41.2	0.5	25.3	2632.6	SIDS
Morocco	MAR	0.5	0.0	17.4	330.2	

Table A.2: National Summary Statistics (continued)

Country	ISO	Average values from 1950 to 2015				
		Annual Cyclone Windspeed (by exposed land, in km/h)	Annual Number of Cyclones	Annual Mean Temperature (in °C)	Annual Precipitation Level (in mm)	Classification
Mozambique	MOZ	2.5	0.3	24.1	1015	
Myanmar (Burma)	MMR	4.4	0.5	23.2	2092.6	
New Caledonia	NCL	38.8	0.8	22.3	1481.6	SIDS
New Zealand	NZL	1.6	0.1	10.6	1720.3	
Nicaragua	NIC	10.1	0.4	25.2	2357.2	
North Korea	PRK	6.7	0.4	6.0	1051.4	
Norway	NOR	0.2	0.0	1.9	1129.3	
Oman	OMN	1.8	0.2	25.8	95.0	
Pakistan	PAK	0.4	0.1	20.5	298.6	
Panama	PAN	1.6	0.0	25.6	2666.8	
Papua New Guinea	PNG	1.2	0.3	25.3	3129.4	SIDS
Philippines	PHL	105.1	4.3	26.0	2412	
Portugal	PRT	0.4	0.1	15.5	840.4	
Puerto Rico	PRI	36.4	0.5	25.5	2122.3	SIDS
Russia	RUS	0.1	0.5	-4.7	460.3	
Samoa	WSM	16.3	0.2	27.1	3024.8	SIDS
Saudi Arabia	SAU	0.0	0.0	25.1	74.5	
Singapore	SGP	1.8	0.0	26.8	2581.7	SIDS
Solomon Islands	SLB	17.5	0.5	25.7	3023.8	SIDS
Somalia	SOM	0.5	0.1	27.2	267.5	
South Africa	ZAF	0.0	0.0	18.1	483.4	
South Korea	KOR	40.1	1.2	11.9	1414.6	
Spain	ESP	0.7	0.1	13.7	620.1	
Sri Lanka	LKA	4.8	0.2	27.1	1705.2	
St. Kitts & Nevis	KNA	38.0	0.5	24.7	2188.6	SIDS
St. Lucia	LCA	36.3	0.5	25.7	2402.2	SIDS
St. Vincent & Grenadines	VCT	33.7	0.4	27.0	1614.2	SIDS
Tanzania	TZA	0.0	0.0	22.6	1032.4	
Thailand	THA	2.7	0.7	26.5	1628	
Timor-Leste	TLS	1.3	0.0	25.3	1443.2	SIDS
Tonga	TON	23.2	0.3	25.5	1972.6	SIDS
Trinidad & Tobago	TTO	11.6	0.1	25.9	1781	SIDS
United Kingdom	GBR	3.5	0.2	8.8	1248	
United States	USA	3.4	1.8	8.9	736.2	
Vanuatu	VUT	53	1.0	24.1	2785.3	SIDS
Venezuela	VEN	0.4	0.2	25.6	1877.2	
Vietnam	VNM	35.6	2.3	24.6	1812.2	
Yemen	YEM	0.4	0.1	24.0	158.1	
Zimbabwe	ZWE	0.5	0.0	21.4	685.4	

Table A.3: Regional Summary Statistics for the cyclone intensity measurement $\overline{Cyc}_{i,t}$

Region/cyclone basin	Average values		
	1970-1985	1985-2000	2000-2015
Arabian Sea and Bay of Bengal	1.88	6.35	4.74
North Atlantic and North East Pacific	18.23	20.02	22.12
North West Pacific	35.36	43.46	29.54
South West Indian Ocean	8.28	12.43	11.46
South West Pacific and South East Indian Ocean	18.08	29.07	22.27
Other regions	2.49	2.53	2.92

B Outlier-robust regression

Outlier-robust regression reveals to be of crucial importance in case of estimations with data contaminated by extreme values. As a matter of fact, OLS estimations assume that errors are *i.i.d* with standard normal distribution and thus, the presence of influential points can greatly deteriorate the efficiency of the estimation and generate misleading estimates. A wide range of robust regression techniques can be used, whether for detecting influential observations or estimating the coefficients of the robust regression. Table B.1 presents usual indicators in influential observations detection: the *studentized residual*, the *Cook's distance* D, defined by Cook (1977), the *leverage score* and two indicators based on successive row deletions defined by Belsley, Kuh & Welsh (1980), $DFBETA$ and $DFFITS$, computing respectively the change in estimated coefficients and in fit for each observation i when i is excluded from the sample. All of these indicators are estimated using the main identification strategy.

The outlier-robust regression corresponds to a so-called *M-estimation* and is described by Hamilton (1991a, 1992). M-estimators are designed to deal with dependent variable outliers (Y-outliers), unlike bounded-influence methods which deal with both dependent and independent variable outliers (X-outliers and Y-outliers). In this study, it seems reasonable to believe that protecting also against X-outliers would be absurd since the occurrence of a cyclone event, extreme temperatures or strong levels of precipitation is purely determined by the nature. Hence, the estimation of the outlier-robust regression is based on absolute residuals analysis and proceeds as follows. Firstly, a screening based on Cook's distance D is made and observations with $D > 1$ are dropped in order to eliminate gross outliers, as suggested by Cook & Weisberg (1982). Then, it calculates the set of weights to be attributed to each observations in the final regression by combining two weighting procedures: Huber weights (Huber, 1964) and biweights (Beaton & Tukey, 1974). These two weighting functions are complementary since Huber weighting shows weaknesses when dealing with severe outliers and biweighting can fail to converge or can have multiple solutions (Li, 1985).

Without loss of generality, in a cross-sectional case, let $e_i = y_i - X_i\hat{\beta}$ be the residual of the i^{th} observation and $M = med(|e_i - med(e_i)|)$ the median absolute deviation from the median residual. Huber weighting provides:

$$w_i = \begin{cases} 1 & \text{if } |e_i| \leq 2M \\ 2M/|e_i| & \text{otherwise} \end{cases}$$

And the smoothly decreasing biweight function, calculated after Huber weights converge iteratively below a tolerance threshold (fixed by default at 0.01) is given by:

$$w_i = \begin{cases} [(1 - (e_i/7M)^2]^2 & \text{if } |e_i| \leq 7M \\ 0 & \text{otherwise} \end{cases}$$

This biweight threshold of 7 is called *tune*. Goodall (1983) states that the performance remains correct with a tune comprised between 6 and 12. Thus, a lower tuning constant implies a more drastic downweighting. In this study, none of the observations reach the

threshold for Cook's distance D and 62 observations (out of 2556 observations) are muted by biweighting. Increasing the tuning constant diminishes the number of excluded observations and has barely no effect on the estimated coefficients and their respective statistical significance (Figures B.2 and B.3).

Table B.1: Influential observations statistics

	Observations	Min.	Median	Max.	Mean	Standard Dev.
Studentized res.	2556	-9.94	0.04	14.7	0.0001	1.01
Leverage points	2573	0.05	0.06	0.14	0.06	0.02
DFFITS	2556	-2.61	0.01	3.53	-0.00001	0.26
DFBETA($\overline{Cyc}_{i,t}$)	2556	-0.32	-0.00002	0.63	$-4.96 * 10^{-6}$	0.02
Cook's distance D	2556	$4.51 * 10^{-11}$	0.00008	0.07	0.0004	0.002

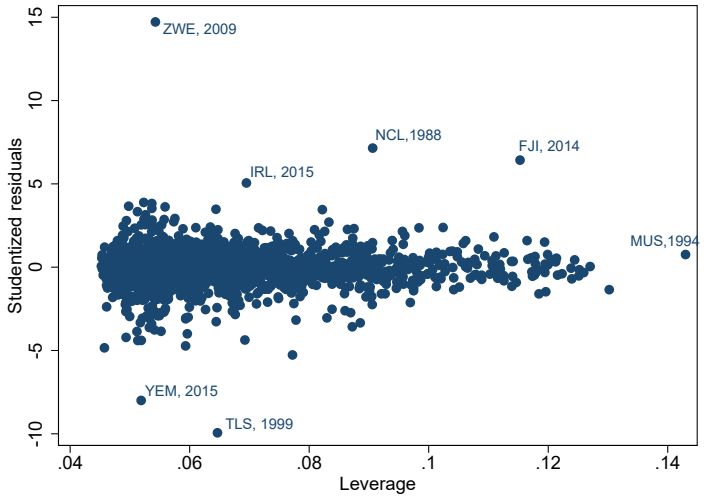

Figure B.1: Influential observations analysis. [Color should be used]
Notes: The graph presents studentized residuals (Y-axis) calculated for each observation included in the main outlier-robust regression specification, plotted against their respective leverage point estimate (X-axis).

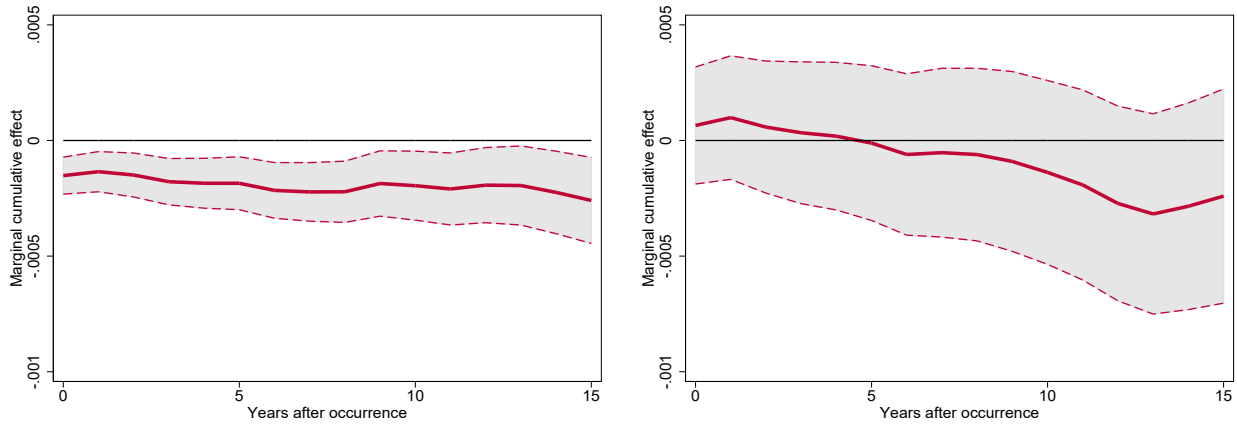

Figure B.2: Measures of the marginal cumulative effects over fifteen years of cyclone events on *per capita* GDP growth for the sample SIDS (left-hand side) and non SIDS (right-hand side). [Color should be used]
Notes: Outlier-robust regression with tuning constant fixed at 9. Shaded areas represent the 90 % confidence intervals. 83 countries, $\overline{T} = 31$, 2556 observations (including 29 observations with weight 0).

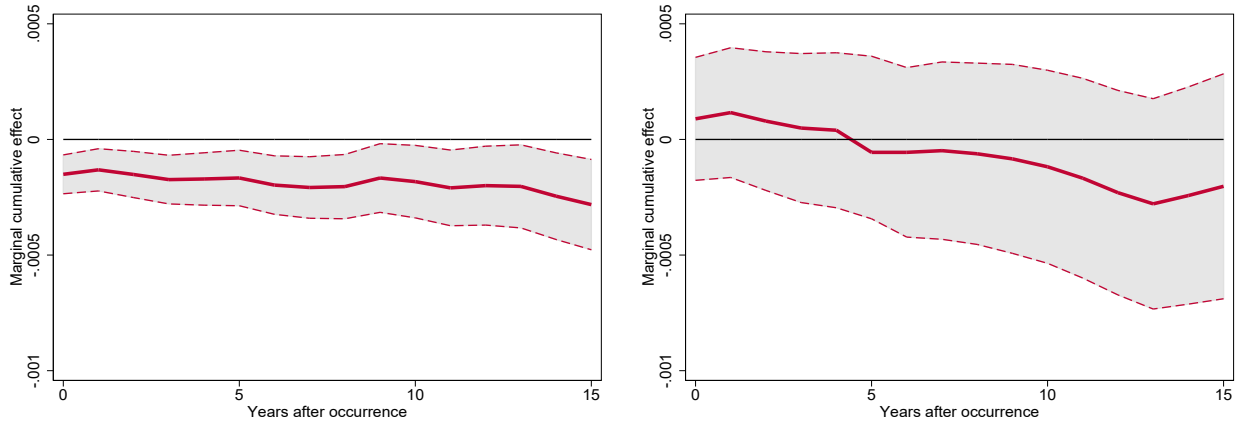

Figure B.3: Measures of the marginal cumulative effects over fifteen years of cyclone events on *per capita* GDP growth for the sample SIDS (left-hand side) and non SIDS (right-hand side). [Color should be used]
Notes: Outlier-robust regression with tuning constant fixed at 12. Shaded areas represent the 90 % confidence intervals. 83 countries, $\overline{T} = 31$, 2556 observations (including 10 observations with weight 0).

C Detailed coefficients for main estimations

Table C.1: Impact of cyclone events on *per capita* GDP growth. Detailed marginal cumulative coefficients with $L = 15$.

	World	SIDS	Non SIDS
Immediate effect, year 0	-0.00013***	-0.00016***	0.00006
	(0.00004)	(0.00005)	(0.00013)
Marginal cum. effect, 1 year	-0.00012**	-0.00014***	0.00009
	(0.00005)	(0.00005)	(0.00013)
Marginal cum. effect, 2 years	-0.00013***	-0.00015***	0.00004
	(0.00005)	(0.00006)	(0.00014)
Marginal cum. effect, 3 years	-0.00016***	-0.00018***	0.00001
	(0.00005)	(0.00006)	(0.00015)
Marginal cum. effect, 4 years	-0.00018***	-0.00019***	-0.00001
	(0.00005)	(0.00006)	(0.00016)
Marginal cum. effect, 5 years	-0.00019***	-0.00020***	-0.00004
	(0.00006)	(0.00007)	(0.00017)
Marginal cum. effect, 6 years	-0.00023***	-0.00022***	-0.00009
	(0.00007)	(0.00007)	(0.00017)
Marginal cum. effect, 7 years	-0.00023***	-0.00023***	-0.00008
	(0.00007)	(0.00007)	(0.00018)
Marginal cum. effect, 8 years	-0.00023***	-0.00023***	-0.00008
	(0.00007)	(0.00008)	(0.00018)
Marginal cum. effect, 9 years	-0.00021***	-0.00020**	-0.00011
	(0.00008)	(0.00008)	(0.00019)
Marginal cum. effect, 10 years	-0.00023***	-0.00020**	-0.00016
	(0.00008)	(0.00008)	(0.00020)
Marginal cum. effect, 11 years	-0.00024***	-0.00021**	-0.00022
	(0.00008)	(0.00009)	(0.00020)
Marginal cum. effect, 12 years	-0.00024***	-0.00019**	-0.00032
	(0.00009)	(0.00009)	(0.00021)
Marginal cum. effect, 13 years	-0.00025***	-0.00019*	-0.00037
	(0.00009)	(0.00010)	(0.00022)
Marginal cum. effect, 14 years	-0.00027***	-0.00020**	-0.00034
	(0.00010)	(0.00010)	(0.00022)
Marginal cum. effect, 15 years	-0.00029***	-0.00024**	-0.00029
	(0.00010)	(0.00011)	(0.00023)
Observations	2494	2494	2494
Adjusted R^2	0.32	0.32	0.32

Notes: Estimations with outlier-robust regression. Standard errors incorporating the Street & al. (1988) correction are in parentheses. Time and country fixed effects as well as temperature and precipitation controls are included in all specifications, but not reported in the table.
Significance levels : *** 1 % ; ** 5 % ; * 10 %.

D Impact of cyclone events on *per capita* GDP for other subgroups of the world sample

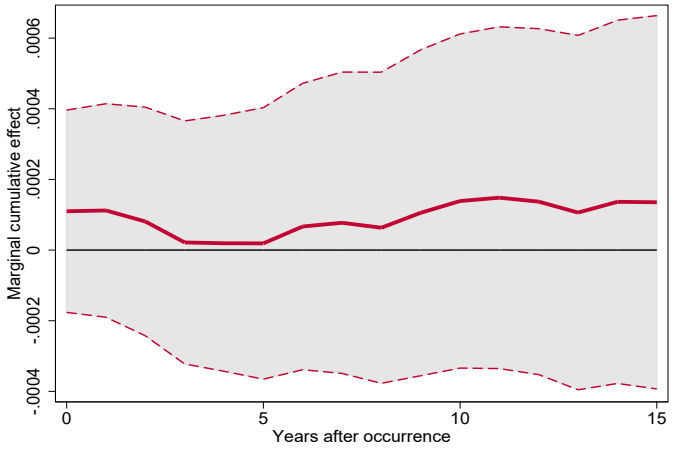

Figure D.1: Measures of the marginal cumulative effects over fifteen years of cyclone events on *per capita* GDP growth for the sample of developing countries excluding SIDS. [Color should be used]
Notes: Developing countries are defined as in the World Economic Outlook reports, 2000 (International Monetary Fund). Estimations with outlier-robust regression. Standard errors are computed using the Street & al. (1988) correction. Shaded areas represent the associated 90 % confidence intervals.

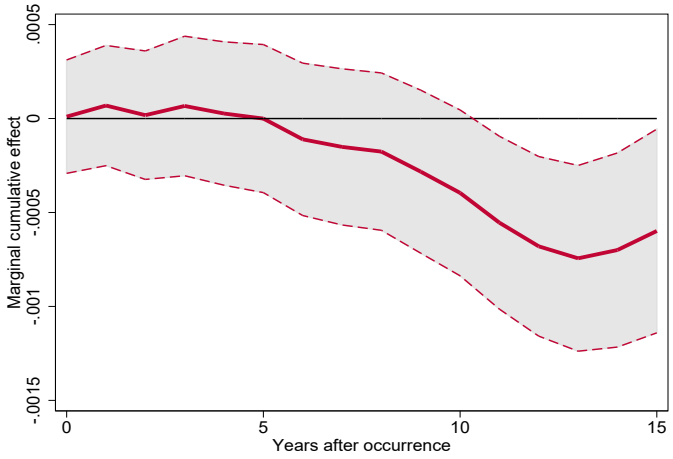

Figure D.2: Measures of the marginal cumulative effects over fifteen years of cyclone events on *per capita* GDP growth for the sample of developed countries.[Color should be used]
Notes: Developed countries are defined as in the *World Economic Outlook 2000* database (International Monetary Fund). Estimations with outlier-robust regression. Standard errors are computed using the Street & al. (1988) correction. Shaded areas represent the associated 90 % confidence intervals.

E Additional robustness checks

Table E.1: Regression results using alternative lag structures and keeping the same number of observations as the main model (2494).

	SIDS	Non SIDS
	(1)	(2)
Immediate effect, $L = 0$	-0.00016***	0.00002
	(0.00005)	(0.00012)
Marginal cumulative effect, $L = 1$	-0.00015***	0.00006
	(0.00005)	(0.00013)
Marginal cumulative effect, $L = 5$	-0.00020***	-0.00005
	(0.00007)	(0.00016)
Marginal cumulative effect, $L = 10$	-0.00019**	-0.00015
	(0.00008)	(0.00019)

Notes: Estimations with outlier-robust regression. Standard errors incorporating the Street & al. (1988) correction are in parentheses. Time and country fixed effects, as well as temperature and precipitation controls (same number of lags as the cyclone indicator) are included in all specifications. This restriction implies that the sample period is limited to 1985-2015.
Significance levels : *** 1 % ; ** 5 % ; * 10 %.

Table E.2: Regression results using a sample that excludes countries affected by extratropical cyclones only.

	SIDS	Non SIDS
	(1)	(2)
Immediate effect, $L = 0$	-0.00016***	0.00012
	(0.00004)	(0.00012)
Marginal cumulative effect, $L = 1$	-0.00015***	0.00016
	(0.00005)	(0.00013)
Marginal cumulative effect, $L = 5$	-0.00021***	0.00007
	(0.00007)	(0.00013)
Marginal cumulative effect, $L = 10$	-0.00023***	0.00001
	(0.00009)	(0.00019)
Marginal cumulative effect, $L = 15$	-0.00026**	-0.00027
	(0.00011)	(0.00025)

Notes: Estimations with outlier-robust regression. Standard errors incorporating the Street & al. (1988) correction are in parentheses. Time and country fixed effects, as well as temperature and precipitation controls are included in all specifications. This restriction excludes Algeria, Canada, France, Iceland, Ireland, Morocco, Norway, Portugal, Russia, Spain, and United Kingdom.
Significance levels : *** 1 % ; ** 5 % ; * 10 %.

F Channels: additional estimations

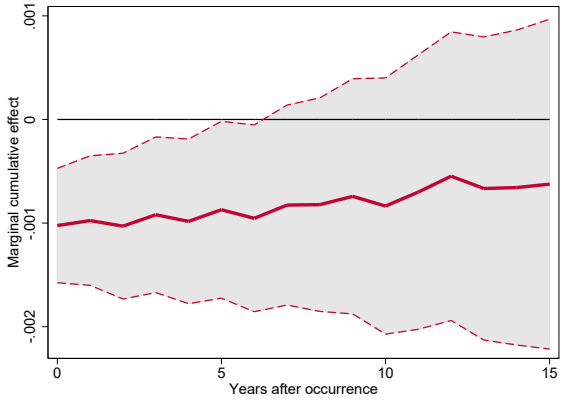

Figure F.1: Measures of the marginal cumulative effects over fifteen years of cyclone events on tourism receipts growth (measured in constant 2015$) for Small Island Developing States.[Color should be used]

Notes: N=1270. Data on tourism receipts come from the *World Development Indicators* database of the World Bank. Estimations with outlier-robust regression. Standard errors are computed using the Street & al. (1988) correction. Shaded areas represent the associated 90 % confidence intervals.

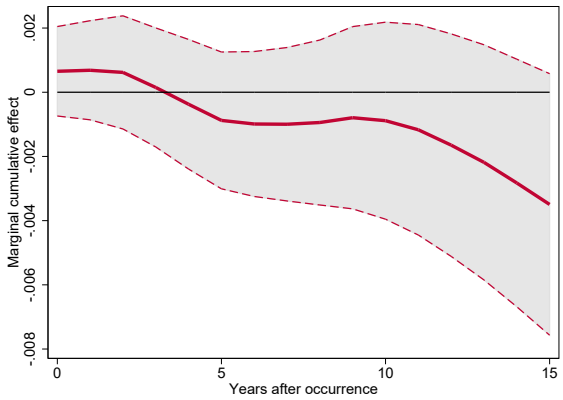

Figure F.2: Measures of the marginal cumulative effects over fifteen years of cyclone events on the logarithm of debt-to-GDP ratio for Small Island Developing States.[Color should be used]

Notes: N=701. Data on debt-to-GDP ratio come from the *World Development Indicators* database of the World Bank. Estimations with outlier-robust regression. Standard errors are computed using the Street & al. (1988) correction. Shaded areas represent the associated 90 % confidence intervals.

Chapitre 15

The impact of tropical cyclones on income inequality in the U.S. : an empirical analysis

Sivatharsan Kulanthaivelu

- ***Ecological Economics***, en soumission, 2023
- ***Présentation :***
  Colloque European Economics and Finance Society, Berlin, juin 2023

The impact of tropical cyclones on income inequality in the U.S.: an empirical analysis

Eric Kulanthaivelu*

January 2023

Abstract

Despite a growing number of studies on the effects of tropical cyclones on economic growth, not much is known about their effects on income inequality. This paper addresses this question by using a panel data set of U.S. counties affected during the period 2010 - 2019. It exploits geophysical information to construct the disaster intensity predictor, and shows that storm shocks significantly decrease local income inequality levels in the year that they occur. A close study of the composition effects reveals several interesting patterns. First, the immediate impact is driven by the two lowest quintiles, and to a lesser extent, the top quintile of the income distribution. Second, the beneficial effects on income inequality are stabilized in the short-run and the frequency of events is a crucial parameter to consider as repeatedly exposed counties exhibit larger responses after a cyclone strike than their rarely exposed counterparts. Finally, among others, this study stresses the importance of social safety nets in counteracting tropical cyclones' adverse income distributional effects.

Keywords: Natural disasters; Tropical cyclones; Income inequality; Economic impacts; Environmental risk

JEL classification: Q54; O15; D63

*University of Reunion Island, Centre d'Economie et de Management de l'Océan Indien. 15 avenue René Cassin, 97400, Saint-Denis Cedex 9, La Réunion
E-mail: eric-sivatharsan.kulanthaivelu@univ-reunion.fr

1 Introduction

With a total cost for weather and climate disasters in the U.S. rising to record levels in recent years according to the National Oceanic and Atmospheric Administration, contributing to debates on socio-economic impacts in the wake of these events has never been more pressing for economists. This paper specifically focuses on tropical cyclones, which are arguably the most deadly and destructive ones, and their effects on income inequality in the U.S. context.

Recent literature has brought substantial evidence of negative effects of these extreme events on economic growth at worldwide scale (Krichene & al., 2021; Kunze, 2021), or locally as in Strobl (2011) with negative impacts stressed in a U.S. panel cross-county study. While evaluating growth effects of tropical cyclones represents the dominant empirical approach, other externalities generated by these disasters barely remain unexplored. Among potential externalities, income inequality might be one of the most concerning. In fact, beyond the increasing attention it received from researchers, income inequality has also become a public concern ever since the Occupy Wall Street movement in New York in 2011, which has then been emulated worldwide (*e.g.* yellow vests protests in France since 2018, the Chilean social outburst from 2019 to 2021 etc.). Moreover, as expressed by Karim & Noy (2016), the direct impact of natural disasters must go further than analysing cross-country distribution of costs and economic activity, and effects across households with various income levels within a country could bring worthwhile insights into the literature.

There are reasons to believe that U.S. local income inequality patterns can be altered by cyclone shocks. First, a number of studies stress how hurricanes can affect local labor markets (Belasen & Polachek, 2009; Coffman & Noy, 2012; Deryugina, 2017; Groen & al., 2020). Then, Fothergill & Peek, (2004) claim that the poor are more vulnerable to natural disasters in the United States, and more specifically due to their place and type of residence, the quality of building construction, or social exclusion. In addition to the differential impact between low- and rich-income populations, income inequality can be impacted by how people or governments cope with such extreme events, and to what extent the associated risk is shared within the population. As a matter of fact, tropical cyclones, and more generally natural disasters, are surely a source of socio-economic disruptions. In the social resilience theory, the concept of panarchy (Allen & al., 2014) states that these disturbances

of wealth and power can have sizeable effects on inequality levels *via* the management of economic recovery processes and subsequent political decisions taken by the public authorities. In order to mitigate the adverse effects of tropical cyclones, reallocation of resources and redistribution mechanisms are triggered either between affected and non-affected areas, or within affected areas. For instance, government disaster and non-disaster related aid programs can be seen as a transfer from one taxpayer to another (Kousky, 2014). Natural disasters can therefore influence public sector corruption (Yamamura, 2014), but also social cohesion and societal trust (Toya & Skidmore, 2014) which can, in turn, affect inequalities within populations of a same country.

All this being said, however, having expectations on whether natural disasters and income inequality are positively or negatively associated is a very arduous task. As argued by Keerthiratne & Tol (2018), on the one hand, poor households possess little that can be lost to a natural disaster, unlike wealthier ones who are endowed with much more material assets. Business owners are likely to face an adverse income shock resulting from business interruptions, which are either due to direct damages or indirectly due to a break in the supply chain, whereas low-skilled or unskilled labourers may not go through a monthly wage decline as they may quickly find new opportunities in the construction sector or expand their income sources. On the other hand, poor households are more likely to live with irregular income, and thus, are more subject to losses compared to rich ones. Besides, results reported in the literature are mixed and reveal to greatly depend on the country studied or the scale chosen. Using the 2008 Vietnam Household Living Standard Survey, Bui & al. (2016) find that natural disasters increased national income inequality. In the Bangladeshi case, Abdullah & al., (2016) find a decrease in regional income inequality in the Sundarbans after Cyclone Aila in 2009. Yamamura (2015) concludes on a short-run increasing effect of natural disasters on income inequality using a worldwide panel data set, but no longer-term effect. Feng & al. (2016) state that the 2008 Sichuan earthquake in China had no effect on income inequality, even though the average income of households dropped substantially. Keerthiratne & Tol, (2018) find a beneficial effect of natural disasters on Sri Lankan income inequality levels between 1990 and 2013 using household survey data. More recently, in the German case, Reaños (2021) simulates expected flood damages under multiple fiscal scenarios and suggests that, overall, floods increase income inequality. Finally, as for studies carried out in the U.S., anticipating the direction of the relationship reveals to

be even more tricky. First, while some single-event studies suggest that hurricaines are negatively associated with earnings in the short-run but positively associated in the long-run (Groen & al., 2020), other longitudinal studies on a series of hurricane events either find a positive relationship (Belasen & Polachek, 2009) or no significant effect (Deryugina, 2017). Then, in a more general study on natural disasters, Pleninger (2022) exploits the Current Population Survey and concludes on a negative effect of disaster strikes on middle shares of the income distribution in U.S. counties, which translates into an absence of effect on the Gini index. This study proposes, to date, the empirical exercise that is the most related to ours within the existing literature. We argue that the present paper constitutes a strong complement to these results as we focus on one type of natural disasters, namely tropical cyclones, and thereby offer a perspective to unravel the heterogeneity in these general results. In fact, natural disasters might differ by their outcomes on an economy. For instance, droughts are considered as the deadliest catastrophes worldwide from 1970 to 2019 while tropical cyclones are the costliest ones (World Meteorological Organization, 2021). In addition, some types of disasters such as floods or landslides might be the consequence of prior tropical cyclone formations, and thus, losses due to natural disasters might be the result of cumulative processes. Accordingly, the magnitude of a natural disaster's impact on an economy undoubtedly depends on its characteristics, especially its intensity. By properly considering the latter dimension, we hope that the present study will make a significant contribution to the literature on this topic.[1]

To characterise the distributional effects of tropical cyclones, we exploit a geophysical data set in order to build a physical measure of disaster intensity. In this paper, tropical cyclone shocks consist of a two-pronged approach as it considers the intensity of storm events in terms of wind speed and the exposure within each county using the share of exposed population. Tropical cyclones' effects can be felt over large areas surrounding their centre, and thus, their spatial structure and movements are estimated with an appropriate wind field model. Information on their overall trajectory are

[1]Pleninger (2022) uses a dummy variable to express the occurrence of at least one natural disaster during a year, and evaluates the effect of "severe" disasters by restricting to those that resulted in at least 10 death among the population during a given year. However, this definition of severity might raise reverse causality bias concerns, as some studies suggest that human costs are negatively correlated with GDP per capita (Kahn, 2005; Felbermayr & Gröschl, 2014). As inequality levels are relatively high in the United States compared to other developed countries, it is likely that the deadliest disasters mainly occurred in poorest areas. To overcome this issue, Noy (2009) recommends to express the intensity of disasters by using only physical indicators.

provided with respect to their exact latitude and longitude coordinates. Our measures of income inequality come from detailed household-level data from the American Community Survey (ACS) 1-year estimates, available from 2010 to 2019. This data set allows us to consider different inequality measures (share of the bottom 60% of aggregate household income, share of the two lowest quintiles, share of the lowest quintile, share of the top quintile, share of the top 5% of the distribution, Gini index) to test whether tropical cyclones have redistributive effects at the county scale. All in all, we obtain an unbalanced panel of 540 counties, which were all affected by storm events from 2010 to 2019. Our key empirical exercise consists of dynamic panel data regressions which include year and county fixed effects to control for common time trends, institutional differences across counties or their geographical location. Given the shortness of our panel and a fairly large number of counties, we use a two-step system GMM approach (Arellano & Bover, 1995; Blundell & Bond, 1998). Our results are noteworthy as we provide evidence that tropical cyclones reduce income inequality in the year that they occur. Further exploration indicates that the two lowest quintiles of the income distribution, and to a lesser degree the top quintile, are those driving this favorable impact. Then, we conclude that income inequality does not decrease further one year after the cyclone strike, but the contemporaneous impact is not counteracted either in following years as the cumulative impact after two years remains negative and significant, with almost same magnitude. This result additionally shows that having already experienced an increase in intensity one or two years before is beneficial, as introducing lags to the baseline equation intensifies tropical cyclones' contemporaneous effect on income inequality. In a final extension, we address the issue of transmission mechanisms. In line with Deryugina (2017), but also Pleninger (2022), this investigation suggests the presence of post-disaster spending adjustments in favor of the poorest as well as capital income losses for higher income groups. Lastly, one can rightly think that, as tropical cyclones are a major threat to physical capital, analysing their effects on wealth inequality might also be of great importance. In this regard, as wealth accumulation mainly depend on earned income and is not only determined by the stock of assets owned at some point in time, the issue of how the income inequality effects can be measured seems to be a preliminary question to be solved. Hence, we believe that our results constitute a first step in the direction of wealth inequality concerns, but also in determining what kind of policies or income sources within quintiles can more accurately explain how these extreme

weather events impact income inequality. Yet, this paper contributes to make the link between Strobl's (2011) local negative growth impact of tropical cyclones and the positive relationship found between income inequality and economic growth in the U.S. by Rubin & Segal (2015).

The remainder of the paper is organised as follows. Section 2 introduces the data. More specifically, it discusses the construction of our cyclone intensity measurement as well as income inequality measures, and provides descriptive statistics. Section 3 describes the estimation strategy, presents the main results on the impact of tropical cyclone shocks on local income inequality, and considers a series of robustness checks. Section 4 analyses more deeply the distributional effects, documents on timing effects and studies how the impact shifts given exposure levels. This section also discusses potential channels through which tropical cyclones affect income inequality. Section 5 concludes.

2 Data

In this section, we first describe the data set on tropical cyclone records as well as the construction of the county-by-year cyclone intensity measurement. Then, we present the American Community Survey, the set of local income inequality measures and other economic variables extracted from it for the purpose of this paper.

2.1 Cyclone data

2.1.1 The Tropical Cyclone Exposure Database

Data on cyclone events in the U.S. are taken from *Tropical Cyclone Exposure Database* (TCE-DAT; Geiger & al., 2018), with an extension up to 2019 kindly provided by the research team upon request. TCE-DAT is a comprehensive historical data set on each landfalling tropical cyclone event worldwide from 1950 to 2019. To meet the needs of this paper, we only retain those affecting the U.S. at some point of their trajectory. TCE-DAT first compiles data from the *International Best Track Archive for Climate Stewardship* (IBTrACS; Knapp & al., 2010), which is released publicly by the *National Climatic Data Center of the National Oceanic and Atmospheric Administration*

(NOAA). For each cyclone centre (called the "eye"), IBTrACS reports information on latitude and longitude position, wind speed, surface air pressure and trajectory (*via* 6-hourly observations). These information are then used as input in Holland's (2008) widely used wind field model in order to get an overall cyclone trajectory and intensity at 0.1° latitude x 0.1° longitude grid cell level for each event recorded in the IBTrACS database with wind speeds of at least 34 knots ($\approx$ 63 km/h) and sustained at least one minute. A cyclone is considered as landfalling if at least one grid cell of the U.S. is affected by the simulated wind field. This means that even storms for which the eye does not make landfall but still passes by near enough the U.S. coasts to be felt are included in the data set. All in all, TCE-DAT identifies 314 cyclone events during the period 1950 - 2019, and among them, 46 occurred during our period of study (2010 - 2019).

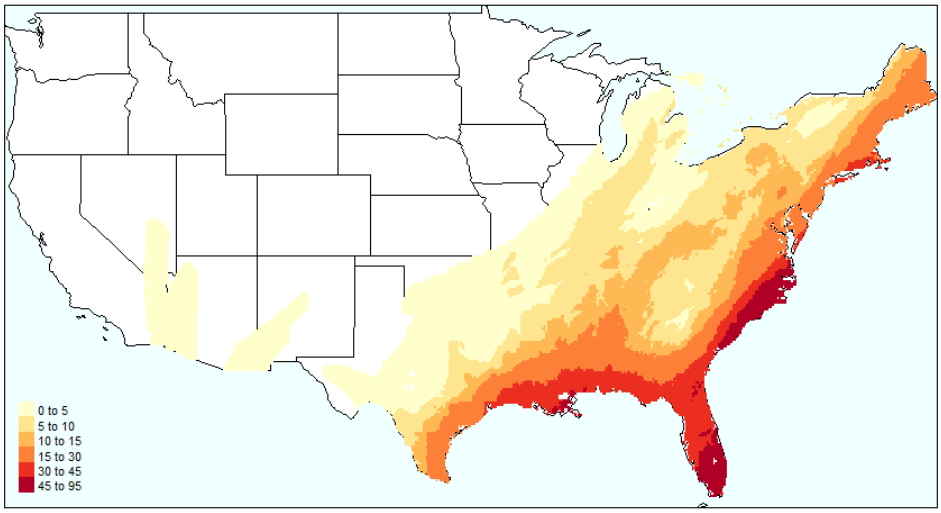

Figure 1: Yearly average wind speed intensity (in km/h) in the contiguous U.S. between 1950 and 2019

[Color should be used]

Figure 1 maps the yearly average wind speed felt at pixel level in the contiguous U.S. from 1950 to 2019. Storms are more intense along coastal areas, and lose their power once they get deeper in lands because of increasing frictional forces and the loss of storms' main source of energy which is water. This map also illustrates the existence of strong inequality in terms of exposure within the country. As a matter of fact, Florida is the most frequently hit state of the U.S., with 118 cyclone

events between 1950 and 2019, while Kansas has only been affected once during the same period (Figure 2).

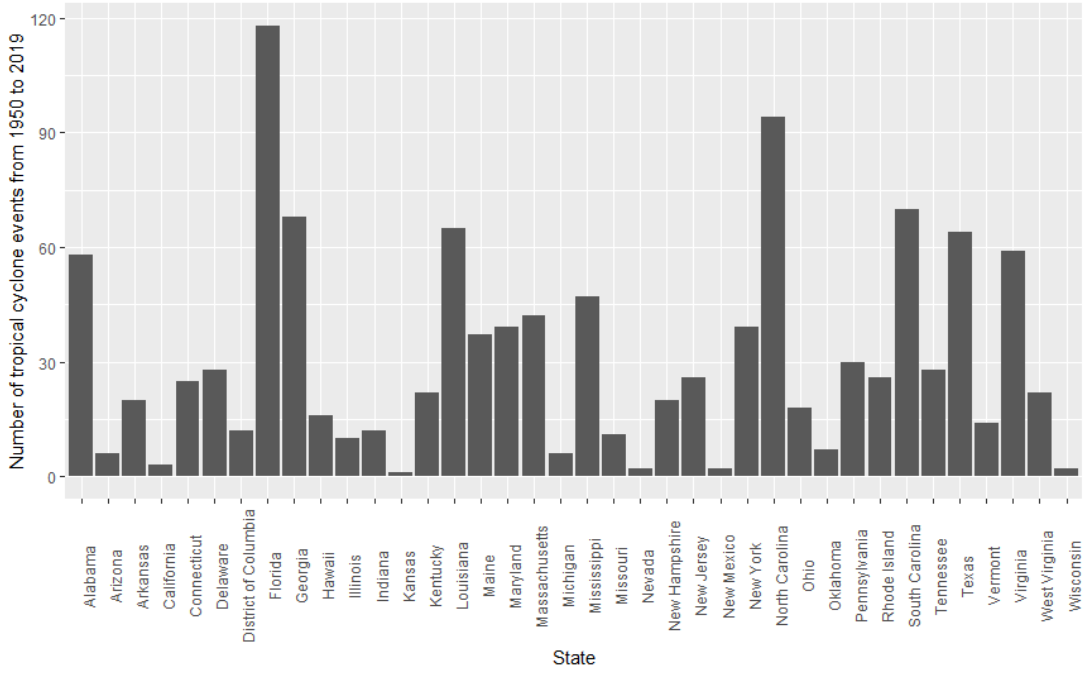

Figure 2: Number of storm events in the U.S., by state, between 1950 and 2019

2.1.2 Physical measure of cyclone intensity

TCE-DAT's pixel-event level data are rescaled and brought to county-year level in order to fit with our cross-county panel data framework. Since our purpose is to assess counties' vulnerability regarding income inequality, it is essential to consider the levels of exposure within each county in addition to local wind speed estimates. To do this, we exploit another strand of the data set, which is the gridded estimates of exposed population. In the end, this makes us able to build a physical measure of cyclone intensity. This scale-free indicator can be expressed as follows:

$$\overline{Cyc}_{c,t} = \frac{\sum_{p=1}^{P_c} \max_{s \in \{1,\dots,S_{p,c,t}\}} \{Wind_{p,s,c,t}\} \left(\frac{12 - m_{p,s}}{12}\right) Exposed\ Population_{p,t}}{Total\ Population_{c,t}} \tag{1}$$

where $Wind_{p,s,c,t}$ is the wind speed recorded in pixel p, for storm s that struck county c in year t. $Exposed\ Population_{p,t}$ corresponds to the estimated population in pixel p and reported in TCE-

DAT, while $Total\ Population_{c,t}$ is the number of inhabitants in county c during year t as estimated in the American Community Survey (1-year estimates). Following the approach of Noy (2009), we also include a temporal weight $(12 - m_{p,s})/12$, with $m_{p,s}$ the month in which the storm occurred. This additional feature enables to capture the contemporaneous impact with more accuracy as a cyclone that strikes in the early months of a given year has arguably a bigger impact in the same year than another one - with same intensity - occurring some months later. This monthly weighting is all the more important since tropical cyclones mostly occur in the second part of the year.

One might notice that the pixel level wind speed is selected as the maximum wind speed value felt in each year t, irrespective of the number of cyclone events $S_{p,c,t}$ identified within each pixel for the given year as in Felbermayr & Gröschl (2014). Regarding this methodological choice, it can be argued that since the replacement of destroyed capital needs more than one year to be effective, the occurrence of less devastating cyclones within the same year is considered as negligible.

In sum, this indicator corresponds to a population-weighted average of the maximum sustained wind speed over all pixels P_c contained in county c. Such normalisation approach is in line with Nordhaus (2006) as it aims to determine the average effect of storm events on an average pixel for a given county. To a slightly lesser extent, using such a population-weighted disaster measure can also help to capture where the economic activity is more intense. This measurement is quite similar to the one established by Hsiang & Jina (2014) and can be thought as an estimate of a cyclone's average intensity in a randomly selected unit of land for each county, or the value of a given cyclone's intensity if this one had struck the county homogeneously across all its locations.

Last but not least, this class of indicators must be distinguished from economic-based indicators such as death toll, total amount of damages etc., which are subject to reverse causality bias and other sources of endogeneity coming from exploitable data sources.[2] Our physical disaster measure must also be differentiated from damage functions, which are assumed to be non-linear in wind speed. Even if it physically makes sense that damages can sharply increase with wind speed because of a subsequent energy dissipation blowout, finding a true damage function reveals to be unmanageable. In fact, while Nordhaus (2006) suggests that the relationship between wind speed and damages

[2]See Felbermayr & Gröschl (2014) for a detailed discussion.

in the U.S. is around the eighth power, Strobl (2011) finds a coefficient around three.[3] To date, no general consensus emerges on this question and wide range of possibilities for the wind speed to damage correlation coefficient can exist. Moreover, an ultimate issue with a damage function approach revolve around the fact that most existing disaster loss data sets ignore indirect losses or damages to non-market goods and services (Kousky, 2014). As most data on losses generated by disasters probably underestimate their overall economic cost, we choose to rely on a physical storm measure based on local wind speed intensity. Tropical cyclones' damaging effects on physical capital can lead to infrastructure failures and business interruptions which, in turn, affect local labor markets and alter income inequality.

2.2 Macroeconomic data

2.2.1 The American Community Survey

Our income inequality data come from the American Community Survey (ACS), 1-year estimates. The ACS is a nation-wide survey maintained by the U.S. Census Bureau and provides social, economic, housing and demographic data every year. In the 1-year survey, information are collected almost every day of the calendar year from a very large sample that represents the U.S. civilian population, and among geographic areas with at least 65 000 inhabitants. For the purpose of this paper, we extract the shares of quintiles of aggregate household income as well as the Gini index of income inequality to construct our primary measures of local inequality. Data are available from 2010 to 2019. Aggregate income corresponds to the sum of all types of income considered in the ACS: wage or salary, self-employment, interest, dividends, net rental income, royalty income, or income from estates and trusts, social security or railroad retirement, supplemental security, public assistance, retirement, survivor, or disability, and all other periodic income other than earnings (unemployment compensation etc.). At household level, income is measured as the sum of householder's income and those of all other individuals' aged 15 and above who were members of the household at the time the interview was conducted. The Gini index is calculated from the household income distribution.[4]

[3] Using a non-statistical methodology, Emanuel (2005) also finds a cubic relationship in the U.S. case.

[4] For further details, see the subject definitions in `https://www.census.gov/programs-surveys/acs/technical-documentation/code-lists.html`

2.2.2 Measures of income inequality

Hence, given the availability of household income data, the ACS allows us to study the behavior of income inequality. Based on Kuznets & Jenks (1953) or Kuznets (1955), we focus on the following measures: the share of the bottom 60% of the aggregate income distribution, the share of the two lowest quintiles, the share of the lowest quintile, the share of the top quintile and the share of the top 5% of the distribution. Top income shares have a fairly different income composition than bottom ones, and are often of particular interest in studies on income inequality (Atkinson, Piketty & Saez, 2007). In addition, we also consider the Gini index, which remains a widely used synthetic indicator and explains the extent to which household income is equally allocated or deviates from a purely proportionate distribution.

2.2.3 Other macroeconomic variables

In order to provide understanding of the transmission channels through which tropical cyclones can affect local income inequality, we exploit more macroeconomic variables coming from the ACS. In particular, we are interested in employment shares for populations respectively below and above the poverty line, and several components of aggregate income. For the former class of variables, the ACS' poverty thresholds are determined in accordance with three criteria: the size of family, the number of children, and, for one- and two- person families, the age of the householder. As for income components, we make a distinction between wage and salary income, and earnings which includes both wage and salary income as well as self-employment income. Then, we also extract information on interest, dividends, net rental income or income obtained from estates and trusts, which serves as a proxy for capital income. Finally, we include the data on other types of income, which is constructed with answers to the section "any other sources of income received regularly such as Veterans' (VA) payments, unemployment compensation, child support or alimony" appearing in the survey form. In what follows, this residual type of income is considered as a proxy for the amount unemployment benefits perceived by households. As a matter of fact, it seems reasonable to assume that the amount of VA, child support or alimony benefits are unrelated to the occurrence of a tropical cyclone.

2.3 Descriptive statistics

Table 1 provides summary statistics for our unbalanced panel of 540 counties which were all, at least once, affected by a storm from 2010 to 2019. The strongest cyclone event recorded during the sample period is hurricane Irene, which struck the East Coast of the U.S. in August 2011. According to our cyclone intensity indicator, York county in Virginia records the highest average wind speed value of the sample with 144.04 km/h during Irene, followed by Richmond in New York (136.83 km/h), and Hudson in New Jersey (136.82 km/h) during the same catastrophe. Income inequality statistics also show a great dispersion within the sample and across counties. Kendall county in Illinois has the lowest Gini coefficient of the sample, with 0.33 in 2019, while the highest level of inequality is recorded for Putnam in Tennessee (0.63 in 2013). Kendall (Illinois) reveals to be the county with lowest income inequality as measured by all our set of inequality metrics. Putnam (Tennessee) shows the highest level of inequality across all metrics, except when analysing the share of the first quintile and the share of the two lowest quintiles, for which either Lowndes (Georgia) or New York (New York) have respectively the lowest value.

Table 1: Summary Statistics (N = 5335)

	Mean	Std. Dev.	Min.	Max.
$\overline{Cyc}_{c,t}$	6.13	14.88	0	144.04
Gini index	0.45	0.04	0.33	0.63
Bottom 60% share of aggregate income	27.95	2.64	17.13	37.05
Bottom 40% share of aggregate income	12.76	1.63	6.63	18.94
First quintile's share of aggregate income	3.60	0.66	0.52	5.92
Fifth quintile's share of aggregate income	48.63	3.35	37.69	64.83
Top 5% share of aggregate income	20.69	3.09	12.35	40.99
Share of employed population below poverty level	4.04	1.87	0.47	18.33
Share of employed population above poverty level	54.78	6.53	20.09	76.45
Wage or salary income (logged)	22.11	1.03	20.30	25.78
Interest, dividends or net rental income (logged)	19.22	1.20	15.59	23.17
Earnings (logged)	22.18	1.03	20.34	25.82
Other types of income (logged)	18.47	0.90	15.80	21.97

3 Effects of tropical cyclones on income inequality

In this section, we investigate whether U.S. local income inequality patterns from 2010 to 2019 varied with tropical cyclone shocks. We first discuss the model specification and the estimation methodology. Then, we present our baseline results for different income inequality measures.

3.1 Econometric specification

We opt for a dynamic panel data regression approach:

$$y_{c,t} = \gamma y_{c,t-1} + \beta \overline{Cyc}_{c,t} + \mu_c + \lambda_t + \varepsilon_{c,t} \tag{2}$$

where the subscripts c and t represent county and year, respectively. y is the income inequality measure, and $\overline{Cyc}_{c,t}$ corresponds to our population-weighted average of cyclone intensity as introduced in the previous section. μ_c denotes unobserved county-specific effects, and λ_t represents time-specific effects and captures common shocks across periods. ε is an independent and identically distributed (i.i.d.) error term with mean 0 and finite variance.

As we are in a context of a small and wide panel data set, *i.e.* a limited number of time periods and a large number of exposed counties, the estimation of (2) using the within-group estimator is undoubtedly inappropriate (Nickell, 1981). Besides, most existing studies consider tropical cyclones as strictly exogenous, which is debatable. In fact, even though the exact timing and trajectory of a storm cannot be exactly predicted in advance, the frequency and intensity of such a catastrophe and its impact in a given county can be correlated with unobserved variables such as the practice of local people (Bui & al., 2014), the influence of human-induced climate change (IPCC, 2022), or local economic preparedness. The latter point is crucial as the likelihood, or propensity, of a county to be exposed and adversely affected by a hazard is one major feature that characterises its intrinsic vulnerability (Cutter, 1996; IPCC, 2022). To deal with both of these issues and avoid statistical shortcomings, we estimate the model using the generalized method of moments (GMM) procedure designed for dynamic panel specifications. Introduced by Holtz-Eakin, Newey, & Rosen (1988), and subsequently enhanced by Arellano & Bond (1991), Arellano & Bover (1995) and Blundell & Bond

(1998), these estimators consist in using previous observations of explanatory and lagged dependent variables as internal instruments in order to cope with the aforementioned endogeneity biases. As stated above, we also relax the assumption that tropical cyclones are strictly exogenous, that is, these extreme events are henceforth considered as unrelated to current disturbances but can be influenced by past ones.

We follow Arellano & Bover (1995) and Blundell & Bond (1998) and use the two-step system GMM estimator. This estimator corrects potential biases of the difference GMM estimator previously developed by Arellano & Bond (1991), especially when weak instruments are generated by persistent series. This procedure relies on a system of two regression equations, one is the first-differenced version of equation (2) to control for unobserved county-specific effects and the other one is the equation (2) in levels. The inclusion of this second equation, and thus of additional moment conditions, improves the precision of the estimator. Both equations are simultaneously estimated but distinctly instrumented. Instruments of the difference equation correspond to lagged levels of the explanatory variables, while the equation in levels is instrumented by the lagged differences of these variables. Under the resulting assumption that the correlation between the dependent variable and county fixed effects is time-invariant, the two-step system GMM procedure renders consistent and efficient estimates of the parameters of interest.

3.2 Results

One underappreciated issue behind the usage of system GMM method concerns instrument proliferation (Roodman, 2009). As a matter of fact, explanatory variables are instrumented separately for each time period, and the potential set of instruments for the difference equation grows quadratically with the number of time periods T. A large instrument count can overfit instrumented variables, and ultimately generate biased two-step estimates. It also weakens the Hansen J test of overidentifying restrictions, which tests for the instruments' joint validity. A high instrument count relative to the number of groups underestimates the statistic.[5] To cope with this, we limit the number of lags of each instrumenting variable to two. In addition, we also run Arellano-Bond tests

[5]For the J test, H_0 corresponds to a validation of the set of over-identifying restrictions. Thus, accepting the null hypothesis provides support to the model.

of serial correlation applied to the error term in differences.[6]

Table 2: System GMM regression of income inequality on cyclone intensity.

	Bottom 60% share of aggregate income	Bottom 40% share of aggregate income	Gini index	First quintile's share of aggregate income	Fifth quintile's share of aggregate income	Top 5% share of aggregate income
	(1)	(2)	(3)	(4)	(5)	(6)
$y_{c,t-1}$	0.055*	0.027	0.048	0.064**	0.032	0.011
	(0.031)	(0.031)	(0.030)	(0.030)	(0.031)	(0.027)
$\overline{Cyc}_{c,t}$	0.006***	0.004***	-0.00008***	0.001***	-0.006***	-0.001
	(0.002)	(0.001)	(0.00002)	(0.0004)	(0.002)	(0.003)
Observations	4795	4795	4795	4795	4795	4795
Number of counties	540	540	540	540	540	540
Number of instruments	57	57	57	57	57	57
Arellano-Bond test for AR(1) in first-differences	0.00	0.00	0.00	0.00	0.00	0.00
Arellano-Bond test for AR(2) in first-differences	0.96	0.87	0.36	0.34	0.33	0.34
Hansen test of overidentifying restrictions	0.33	0.77	0.28	0.56	0.08	0.04

Notes: All regressions are two-step system GMM. Standard errors clustered by counties and incorporating the Windmeijer (2005) correction are in parentheses. Time fixed effects are included in all specifications, but not reported in the table.
Significance levels : *** 1% ; ** 5% ; * 10%.

Results of the baseline model are presented in Table 2. Overall, we find an immediate negative impact of tropical cyclones on income inequality, which seems to be driven by the poorest quintiles for whom the share of aggregate income rises compared to those at the top of the distribution. The share of the bottom 60% one raises by 0.006 percentage point for each additional km/h of cyclone intensity, while the share of the lowest 40% of the distribution increases by 0.004 percentage point. Both of these results are significant at the 1% level. This beneficial effect on income inequality is emphasised by the decrease observed in the Gini coefficient, which is our synthetic index. Each km/h increase in wind speed exposure over a county diminishes local Gini index by 0.00008, and this point estimate is significant at the 1% level. Put another way, a one standard deviation increase in the cyclone indicator ($\sigma_{\overline{Cyc}_{c,t}} = 14.9$) decreases the Gini coefficient by 0.001. As for the top income groups' share of income, the J test is rejected at the 10% level for the top quintile and at the 5% level for the top 5% and no conclusion can be drawn for them. These findings are consistent with the results reported in previous studies. More specifically, Strobl (2011) shows that hurricanes have a negative impact on economic growth in the U.S. at county level, and Rubin & Segal (2015) conclude that growth and income inequality are positively associated in the U.S..

Our main results are stable across a variety of robustness checks. To start with, in Appendix A, we check the robustness of these estimates to more drastic cuts in instrument count by "collapsing"

[6]Model specification is supported when the null hypothesis of the test is rejected for first-order serial correlation (*i.e.* presence of correlation), and accepted for second-order correlation.

them. We also re-estimate our model with a difference GMM method. In fact, losses of statistical significance when bringing our system GMM estimations back to difference GMM would suggest the presence of endogeneity biases (Roodman, 2009). We finally check the validity of our results when withdrawing the lagged dependent variable from equation (2) and thereby using a fixed effects estimator. In no case are the results altered by these changes in estimators, except for the impact on the bottom 60%'s share of income when collapsing instruments: the null hypothesis of the J test becomes rejected at the 5% level. Results on the top quintile and the top 5%'s share of income when using the static model stress the absence of impact on the richest households, even though we find statistical significance for the former with a difference GMM approach or with collapsed instruments.

Secondly, in Appendix B, we present the estimates obtained when some features of our cyclone indicator are modified. Choosing the percentage of exposed population as disaster proxy in the spirit of Krichene & al. (2020) or Keerthiratne & Tol (2018), removing monthly weighting, or simply using maximum wind speed levels over each areas as Felbermayr & Gröschl (2014) does not change the results either. Once again, the top quintile intermittently shows statistically significant negative point estimates. Interestingly, removing the wind speed component leads to stronger effects, while these are lessened in the both other cases. Hence, these results further underlines the importance of the choice of the metric in the magnitude and significance of the effects.

Thirdly, we check whether our results hold when including additional meteorological or economic control variables to equation (2), namely, temperature and precipitation, or income per capita growth and the share of poor households in the county (Appendix C). Across both extensions, we find that tropical cyclones and income inequality are still negatively associated, with almost similar point estimates of the disaster, but slightly varying statistical significance. The effect on the first quintile is now insignificant, though with a p-value lightly above 10%. Furthermore, it is interesting to notice the positive relationship between temperature and inequality. This point surely deserves further exploration in another study. The positive correlation between economic growth and income inequality is also verified within the present sample (coefficient of 0.016 for the Gini index, significant at the 10% level). However, our results cannot fully provide support for Rubin & Segal (2015): even though we find no link between economic growth and low-income shares, J tests

are rejected at the 10% level for the top quintile's share of income and at the 1% level for the top 5% of the distribution.

As a last step, in Appendix D, we consider robustness to alternative samples. First, our main specification is repeated on a balanced sample, *i.e.* where all the counties are present in the sample for the entire 2010 - 2019 period. Estimates remain almost unchanged in terms of magnitude, but standard errors slightly increase, probably due to the fact that the amount of data in the model is reduced. Then, we expand the panel to include all the counties that were ever affected during the period 1950 - 2019. In fact, given the fat tailed nature of the tropical storms distribution presented in section 2, one can argue that our baseline sample may not be representative of the entire sample of counties actually exposed to cyclonic risk. It is likely that for many counties storms represent very rare events, but still devastating at some point in their history. All the counties that have not experienced a storm during our sample period of 10 years can even be thought as a pertinent control group, as they all remain potential targets and concerned by this issue, even though they were unaffected during this specific time period. Reconsidering the sample in such a way continues to show substantial negative effects on income inequality, with very few change compared to the baseline results. Finally, we pursue our controls for potential selection biases and re-run the analysis with the entire set of U.S. counties that are included in the ACS 1-year. The newly included 287 counties which were unaffected during the sample period can again be considered as quasi-control group whereas counties of the baseline sample are treated one. Under this last framework, coefficients are smaller in magnitude but signs and statistical significance remain barely unchanged.

4 Disentangling composition effects

Thus far, our estimates stress that counties hit by a tropical cyclone experience a contemporaneous decrease in income inequality. In what follows, this result is further explored by bringing some extensions to equation (2). Firstly, we investigate the influence of each income quintiles in the above results. Then, we include additional lags of cyclone intensity to the main model and examine the impact of these extreme weather events over time. Finally, components of aggregate income are disaggregated and shares of employed population below and above the poverty level are analysed

so that transmission mechanisms can be studied.

4.1 Which quintiles lead the contemporaneous effect?

In the baseline results, shares of bottom income quintiles are summed and studied as a whole in order to be consistent with the existing literature (Kuznets, 1955). Instead, this subsection explores the distinct impact across all quintiles and additionally if there is a monotonic behavior among bottom ones, *i.e.* if $\beta_i \leq \beta_j, \forall$ *quintile* $i <$ *quintile* $j <$ *quintile* 4, which would suggest a labor income effect. Table 3 shows the results. We find only partial evidence of a monotonic ordering of the effect as the coefficient associated to the second quintile is larger than the first one's, but results are invalid for the third and fourth quintiles (Hansen tests rejected at the 5% level).[7] Hence, the first and second quintiles, and probably to a lesser extent as it is only intermittently significant across our estimations, the top quintile are those triggering the immediate decrease in income inequality observed on more aggregate indices. This table also suggests that shares of aggregate income in the middle of the distribution are unaffected by tropical cyclone events. These findings are partially consistent with Pleninger (2022) who demonstrates that income losses are increasing for higher income groups in the aftermath of hurricanes or storms.[8] Middle income groups may go through some income losses, but in the end, these losses do not translate into a significant loss in their aggregate income shares. However, as point estimates are not significant for the top 5% income share, our results shed light on the heterogeneous impact across top income share levels.[9]. This slight difference in results with Pleninger (2022) probably stems from the pooling of storms and hurricanes in the present paper, and from the fact that our indicator captures the intensity of phenomena.

[7]The absence of impact on these two quintiles is confirmed by estimations using a static fixed effects model, with which point estimates are insignificant. These additional results are available upon request.

[8]In particular, she shows that the top decile of the income distribution experiences, on average, significant losses that are more than 10 times larger than that of individuals between the 40th and 90th percentile of the distribution after a storm. Average losses following a hurricane are more than 4 times larger but point estimates are insignificant for the top decile group.

[9]This conclusion is supported by Cordoba & Uliczka (2021), who suggest that the 2005 Hurricane Katrina had a positive impact on the top 1% income share in Louisiana.

Table 3: System GMM regression of income inequality on cyclone intensity.

	First quintile's share of aggregate income	Second quintile's share of aggregate income	Third quintile's share of aggregate income	Fourth quintile's share of aggregate income	Fifth quintile's share of aggregate income
	(1)	(2)	(3)	(4)	(5)
$y_{c,t-1}$	0.064**	0.038	0.052*	-0.022	0.032
	(0.030)	(0.029)	(0.031)	(0.030)	(0.031)
$\overline{Cyc}_{c,t}$	0.0013***	0.0026***	0.0020***	-0.00069	-0.0061***
	(0.0004)	(0.0006)	(0.0008)	(0.00088)	(0.0023)
Observations	4795	4795	4795	4795	4795
Number of counties	540	540	540	540	540
Number of instruments	57	57	57	57	57
Arellano-Bond test for AR(1) in first-differences	0.00	0.00	0.00	0.00	0.00
Arellano-Bond test for AR(2) in first-differences	0.29	0.90	0.72	0.19	0.33
Hansen test of overidentifying restrictions	0.56	0.60	0.02	0.03	0.08

Notes: All regressions are two-step system GMM. Standard errors clustered by counties and incorporating the Windmeijer (2005) correction are in parentheses. Time fixed effects are included in all specifications, but not reported in the table.
Significance levels : *** 1% ; ** 5% ; * 10%.

4.2 Is there any lasting impact?

Another extension that can be made is to examine the persistence of the effects using a series of cyclone intensity measurement lags. As the contemporaneous impact is captured according to the month in which the storm occurred, we extend and adapt this monthly weighting to each additional lag that is included in the augmented version of equation (2). We introduce up to two time lags, and their respective time weights correspond to $\frac{12+(12-m_{p,s})}{24}$ and $\frac{24+(12-m_{p,s})}{36}$, with $m_{p,s}$ as defined in (1).

Table 4 presents results from estimating equation (2) with two lags of the cyclone intensity measurement together with the cumulative impact through years, which is calculated by summing the coefficient of the contemporaneous cyclone variable and those of its lags.[10] Across all our income inequality measures except for the first quintile or the top 5% where the validity of the model is rejected, we do not find evidence of any intensification, nor attenuation of the impact beyond the year of the cyclone strike as none of the lags' point estimates are significant. This means that the immediate decrease in income inequality is stabilized in the short-run. This point is emphasised by the cumulative effect analysis: the sum of the coefficients is negative and significant after two years, with almost similar magnitude.

Alternatively, by adding lags to the model, we also address the issue of how the frequency of events influences the results. Controlling for past experiences of tropical cyclones over the last

[10] In line with the distributed-lag literature, the immediate effect of tropical cyclones (*i.e.* the year that they occur, section 3) and the cumulated effect (with lag horizon $L > 0$) are separately estimated (Greene, 2003).

Table 4: System GMM regression of Gini index of income inequality on cyclone intensity, including additional lags.

	Bottom 60% share of aggregate income	Bottom 40% share of aggregate income	Gini index	First quintile's share of aggregate income	Fifth quintile's share of aggregate income	Top 5% share of aggregate income
	(1)	(2)	(3)	(4)	(5)	(6)
$y_{c,t-1}$	0.119***	0.136***	0.085**	0.169***	0.063*	0.029
	(0.046)	(0.050)	(0.039)	(0.042)	(0.036)	(0.029)
$\overline{Cyc}_{c,t}$	0.009***	0.006***	-0.00009***	-0.003***	-0.007**	0.004
	(0.002)	(0.001)	(0.00003)	(0.0008)	(0.003)	(0.004)
$\overline{Cyc}_{c,t-1}$	-0.0007	-0.0006	2.62e-06	-0.0007***	0.0002	-0.002
	(0.0009)	(0.0006)	(0.00001)	(0.0003)	(0.001)	(0.002)
$\overline{Cyc}_{c,t-2}$	-0.0002	-0.0002	5.36e-07	-0.0002	-0.00003	-0.001
	(0.0007)	(0.0004)	(0.00001)	(0.0002)	(0.001)	(0.001)
Observations	4255	4255	4255	4255	4255	4255
Number of counties	540	540	540	540	540	540
Number of instruments	93	93	93	93	93	93
Arellano-Bond test for AR(1) in first-differences	0.00	0.00	0.00	0.00	0.00	0.00
Arellano-Bond test for AR(2) in first-differences	0.73	0.25	0.43	0.07	0.35	0.51
Hansen test of overidentifying restrictions	0.14	0.16	0.30	0.00	0.12	0.05
Sum of all cyclone intensity coefficients	0.008***	0.005***	-0.00009**	0.002***	-0.007*	0.0006
	(0.003)	(0.002)	(0.00004)	(0.0009)	(0.004)	(0.005)

Notes: Both regressions are two-step system GMM. Standard errors clustered by counties and incorporating the Windmeijer (2005) correction are in parentheses. Time fixed effects are included in both specifications, but not reported here.
Significance levels : *** 1% ; ** 5% ; * 10%.

two years leads to larger contemporaneous effects. This additional interpretation of the results offers thoughtful insights regarding counties' adaptive capacity. On the one hand, in accordance with Rubin & Segal (2015), as growth and income inequality are positively associated in the U.S., our results suggest that the larger effects on income inequality might be triggered by greater local economic losses in counties where tropical cyclones occur frequently. In particular, as the income of top income groups is more sensitive to growth than that of lower income groups, the greater reduction in income inequality might be explained by greater income losses in top income groups. On the other hand, to limit the adverse effects on the poorest, counties that are repeatedly hit are more likely to implement disaster mitigating measures than their counterparts that are rarely affected. In the latter subgroup of counties, storm events may not constitute a sufficient base-level risk to implement specific disaster-related redistributive policies, or to undertake public investments in risk mitigation (Schumacher & Strobl, 2011; Kousky, 2014). These stronger reductions in income inequality may also arise from the role of coordination and transfers between people, which increases in communities that are repeatedly exposed to storms (Zylberberg, 2010).[11]

[11] Within the same strand of the literature, Yamamura (2010) suggests that frequency of natural disasters fosters social capital in Japan.

4.3 Exploring transmission mechanisms

This last extension pertains to get a better understanding of the channels through which tropical cyclones lead to such redistribution of income. To do so, we quantify the effects of tropical cyclones on different components of aggregate income. It is well known that there is heterogeneity across households in terms of their primary sources of income. Even though most households derive their income from labor, low income groups mainly rely on transfer income while top income groups receive a larger portion of income from their wealth than others (Pleninger, 2022). As such, we distinctly analyse the effects on the logarithm of earnings, wage and salaries, capital income, which is defined here by the aggregate amount of interest, dividends or net rental income perceived by households, and other types of income. As explained in section 2, in this particular context, the aggregate amount of other types of income extracted from the ACS corresponds to a reasonable proxy for unemployment benefits. On top of this, we also investigate the effects on the share of employed population respectively below and above the national poverty level to help us discern the effects observed on labor income. Finally, a dynamic specification is rejected for these dependent variables, and thus, we use a standard panel fixed effects estimator.

Table 5 outlines the results of these regressions. Point estimates for aggregate earnings and wage or salary are statistically insignificant. However, the employment rate of population below national poverty threshold substantially decreases in the year a tropical cyclone occurs, while the employment rate for those above the poverty line is not significantly affected. This means that, even though the sample of individuals below poverty level does not exactly coincide with the two lowest quintiles of the aggregate income distribution, poorest individuals experience salary losses for after a storm shock. To explain the gains for the bottom quintiles in shares, our results provide support for a transfer payments channel as other sources of income - *i.e.* unemployment benefits - are positively affected by tropical cyclones (+0.1% increase for an additional km/h of tropical cyclone intensity, significant at the 1% level). Notwithstanding the fact that the amount of unemployment benefits does not outweight their lost wages, this compensation seems to be enough to increase the aggregate shares of bottom quintiles in comparison with the higher groups of the distribution for which aggregate income shares is either unchanged or reduced. Finally, we find evidence of capital income losses in the wake of cyclone events: each additional km/h of wind speed intensity decreases

the aggregate level of capital income by 0.2%. Most of these losses can arguably be attributed to the top quintile of the distribution. In fact, the share of capital income in total income is increasing for higher income groups, meaning that lowest income groups receive no capital income and middle income ones mainly rely on earnings but also derive a small share of their income from capital as they include small business owners (Pleninger, 2022). As tropical cyclones represent a major threat to physical capital, the losses for the top quintile in shares estimated above might be a consequence of the decrease in aggregate capital income that they mainly receive compared to other income groups. As for the top 5% of the distribution, it is likely that they experience larger capital losses than those with income between the 80th and 95th percentile. Yet, as their share of aggregate income is not affected by tropical cyclones, these losses might be compensated by other income sources or might not represent a significant share of their total income.

These findings can also be linked with those presented in last subsection. As income inequality levels do not substantially rise back after the year of occurrence, the obtained results may be explained by the persistent increase in some income components such as transfer payments or social safety net programs observed in the aftermath of hurricanes in the U.S. (Deryugina, 2017). Indeed, the government's response to a catastrophe is not only limited to direct disaster aid programs, and non-disaster related transfers such as income maintenance payments, unemployment insurance and public medical benefits also increase due to the subsequent recession. This paper's baseline results stress a crucial role played by the two first quintiles in the estimated decrease in income inequality, and these two quintiles are precisely those benefitting the most from social benefits. They are also more likely to be in need after a cyclone strike (Fothergill & Peek, 2004). It also suggests that the top quintile does not recover from its losses in aggregate income shares in the short-run, meaning that the replacement of destroyed capital takes more than two years to offset the losses in shares and be fully efficient.

5 Conclusion

Recent debates have brought the impact of climate related disasters to the forefront of policy issues, either across or within countries. This paper tries to bring some fresh perspective on

Table 5: Results for regressing employment shares and income types on cyclone intensity

	Share of employed pop. below the poverty level (1)	Share of employed pop. above the poverty level (2)	Earnings (logged) (3)	Wage or salary income (logged) (4)	Interest, dividends or rental income (logged) (5)	Other sources of income (logged) (6)
$\overline{Cyc}_{c,t}$	-0.002**	0.003	0.00007	0.00006	-0.002**	0.001***
	(0.0008)	(0.002)	0.00007	0.00007	0.001	0.0003
Observations	5335	5335	5335	5335	5275	5335
Number of counties	540	540	540	540	540	540
Adjusted R^2	0.11	0.27	0.44	0.44	0.05	0.21

Notes: Panel fixed effects estimator. Robust standard errors clustered by counties are in parentheses. Time and county fixed effects are included, but not reported in the table.
Significance levels : *** 1% ; ** 5% ; * 10%.

this topic and addresses the question of tropical cyclones' effects on income inequality in the U.S. After having built a physical measure of tropical cyclone intensity which fits with a cross-county panel data framework, we show that such disasters decrease contemporaneous levels of local income inequality. This finding is well in line with the already observed negative effects of hurricanes on counties' economic growth (Strobl, 2011), and the positive links between economic growth and income inequality in the U.S. (Rubin & Segal, 2015).

In a next step, we further examine the mechanisms that might explain this immediate effect. First, the two lowest quintiles and to a lesser extent the top quintile of aggregate household income distribution appear to be those driving this result. Even though they derive a larger portion of their income from capital compared to lower income groups, the impact on the top 5% income share is insignificant. However, the impact is perhaps different across top income share levels, and focusing on the top 1% income share for instance can be of particular interest in our context (Cordoba & Uliczka, 2021). Unfortunately, we could not find the latter measurement in the ACS. Then, the investigation of timing effects indicates that the immediate effect seems to be persistent over time. The study of marginal cumulative effects concludes on an immediate impact that translates into an overall negative effect two years after the catastrophe. Hence, this result also documents the effects of tropical cyclones according to how past experiences of such disasters vary across counties. We find evidence of a larger decline in income inequality for those that are repeatedly hit. Counties with lower exposure to cyclonic risk may not find enough incentives to set automatic stabilizers operating in the aftermath of tropical cyclone events. These counties may have many other equally risky issues vying for their attention (Posner, 2006) compared to others where the occurrence of a

natural disaster can represent a more focusing event, and thereby leading to more investments in mitigation or to altruist behaviors by political leaders (Kousky, 2014). Accordingly, local quality of governments and their capacity to react to natural disasters might also be determinant.

In a final extension brought to our main model, we try to quantify the impact of tropical cyclones on employment rates given poverty status as well as on various sources of aggregate income. The differential composition of households' income can be particularly relevant in explaining the distributional consequences of tropical cyclones on aggregate household income shares. While transfer income is a particularly important component of low income households, top income groups derive a greater share of total income from capital compared to other groups (Pleninger, 2022). We show that tropical cyclones negatively impact the poorest individuals' employment rate, but the underlying labor income losses are compensated by social insurance. In the mean time, the top quintile of the distribution experiences capital income depletion which explains, at least partly, its losses in aggregate shares. However, to better understand this income composition mechanism, further study on these extreme weather events' effects on distinct types of income specifically received by households with different levels of wealth seems warranted.

Hence, our results somehow shed light on the efficiency of policy actions undertaken by governments, or other public institutions to counteract the adverse income effects on the poorest households. In fact, the persistent effect observed on our income inequality measures combined with such an income composition effect provide further support for Deryugina (2017) who demonstrates the crucial role of transfer payments in mitigating hurricane shocks. As suspected by Keerthiratne & Tol (2018), this depletion in income inequality levels might stem from the fact that poor individuals do not possess a high level of physical capital, and thus, losses can be disproportionate across the income distribution. Regarding this point, it would also be interesting to examine to what extent the substitution effect from physical capital to human capital due to natural disaster risk observed in Skidmore & Toya (2002) is reflected in our results. Finally, the influence of internal migration in the aftermath of the catastrophe might constitute another key factor that explains our main result: Strobl (2011) shows that negative growth effects of hurricanes are partly due to the move of relatively richer people from affected counties in the wake of the hurricane. As only a reduced share of the U.S. economy is exposed to cyclonic risk, these phenomenons may not have much of

an impact on a more macro scale. Yet, it can be said that they play a role in shaping the income inequality trends across local areas.

References

Abdullah, A. N. M., Zander, K. K., Myers, B., Stacey, N., & Garnett, S. T. (2016). A short-term decrease in household income inequality in the Sundarbans, Bangladesh, following Cyclone Aila. *Natural Hazards, 83*(2), 1103-1123.

Allen, C. R., Angeler, D. G., Garmestani, A. S., Gunderson, L. H., & Holling, C. S. (2014). Panarchy: Theory and Application (Nebraska Cooperative Fish & Wildlife Research Unit).

Arellano, M., & Bond, S. (1991). Some tests of specification for panel data: Monte Carlo evidence and an application to employment equations. *The review of economic studies, 58*(2), 277-297.

Arellano, M., & Bover, O. (1995). Another look at the instrumental variable estimation of error-components models. *Journal of econometrics, 68*(1), 29-51.

Atkinson, A. B., Piketty, T., & Saez, E. (2011). Top incomes in the long run of history. *Journal of economic literature, 49*(1), 3-71.

Belasen, A. R., & Polachek, S. W. (2009). How disasters affect local labor markets the effects of hurricanes in Florida. *Journal of Human Resources, 44*(1), 251-276.

Blundell, R., & Bond, S. (1998). Initial conditions and moment restrictions in dynamic panel data models. *Journal of econometrics, 87*(1), 115-143.

Bui, A. T., Dungey, M., Nguyen, C. V., & Pham, T. P. (2014). The impact of natural disasters on household income, expenditure, poverty and inequality: evidence from Viet-

nam. *Applied Economics, 46*(15), 1751-1766.

Coffman, M., & Noy, I. (2012). Hurricane Iniki: measuring the long-term economic impact of a natural disaster using synthetic control. *Environment and Development Economics, 17*(2), 187-205.

Cordoba, G. F., & Uliczka, N. (2021). The Impact of Hurricane Katrina on Income Inequality: A Synthetic Control Analysis (No. 6). Graduate School of Economics and Management, Tohoku University.

Cutter, S. L. (1996). Vulnerability to environmental hazards. *Progress in human geography, 20* (4), 529-539.

Deryugina, T. (2017). The fiscal cost of hurricanes: Disaster aid versus social insurance. *American Economic Journal: Economic Policy, 9*(3), 168-98.

Emanuel, K. (2005). Increasing destructiveness of tropical cyclones over the past 30 years. *Nature, 436*(7051), 686-688.

Felbermayr, G., & Gröschl, J. (2014). Naturally negative: The growth effects of natural disasters. *Journal of development economics, 111*, 92-106.

Feng, S., Lu, J., Nolen, P., & Wang, L. (2016). The effect of the Wenchuan earthquake and government aid on rural households. *IFPRI book chapters*, 11-34.

Fothergill, A., & Peek, L. A. (2004). Poverty and disasters in the United States: A review of recent sociological findings. *Natural hazards, 32*(1), 89-110.

Geiger, T., Frieler, K., & Bresch, D. N. (2018). A global historical data set of tropical cyclone exposure (TCE-*DAT). Earth System Science Data, 10*(1), 1 85-194.

Greene, W.H. (2003) Econometric Analysis. 5th Edition, Prentice Hall, Upper Saddle River.

Groen, J. A., Kutzbach, M. J., & Polivka, A. E. (2020). Storms and jobs: The effect of hurricanes on individuals' employment and earnings over the long term. *Journal of Labor Economics, 38*(3), 653-685.

Harris, I., Osborn, T.J., Jones, P. et al. Version 4 of the CRU TS monthly high-resolution gridded multivariate climate dataset. *Sci Data* 7, 109 (2020). https://doi.org/10.1038/s41597-020-0453-3

Holland, G. (2008). A revised hurricane pressure–wind model. *Monthly Weather Review, 136*(9), 3432-3445.

Holtz-Eakin, D., Newey, W., & Rosen, H. S. (1988). Estimating vector autoregressions with panel data. *Econometrica: Journal of the econometric society,* 1371-1395.

Hsiang, S. M., & Jina, A. S. (2014). The causal effect of environmental catastrophe on long-run economic growth: Evidence from 6,700 cyclones (No. w20352). National Bureau of Economic Research.

IPCC, 2022: *Climate Change 2022: Impacts, Adaptation, and Vulnerability.* Contribution of Working Group II to the Sixth Assessment Report of the Intergovernmental Panel on Climate Change [H.-O. Pörtner, D.C. Roberts, M. Tignor, E.S. Poloczanska, K. Minten-

beck, A. Alegría, M. Craig, S. Langsdorf, S. Löschke, V. Möller, A. Okem, B. Rama (eds.)]. Cambridge University Press. In Press.

Kahn, M. E. (2005). The death toll from natural disasters: the role of income, geography, and institutions. *Review of economics and statistics, 87*(2), 271-284.

Karim, A., & Noy, I. (2016). Poverty and natural disasters—a qualitative survey of the empirical literature. *The Singapore Economic Review, 61(01),* 1640001.

Keerthiratne, S., & Tol, R. S. (2018). Impact of natural disasters on income inequality in Sri Lanka. *World Development, 105,* 217-230.

Knapp, K. R., Kruk, M. C., Levinson, D. H., Diamond, H. J., & Neumann, C. J. (2010). The international best track archive for climate stewardship (IBTrACS) unifying tropical cyclone data. *Bulletin of the American Meteorological Society, 91*(3), 363-376.

Kousky, C. (2014). Informing climate adaptation: A review of the economic costs of natural disasters. *Energy economics, 46,* 576-592.

Krichene, H., Geiger, T., Frieler, K., Willner, S. N., Sauer, I., & Otto, C. (2021). Long-term impacts of tropical cyclones and fluvial floods on economic growth–Empirical evidence on transmission channels at different levels of development. *World Development, 144,* 105475.

Kunze, S. (2021). Unraveling the effects of tropical cyclones on economic sectors worldwide: direct and indirect impacts. *Environmental and Resource Economics, 78*(4), 545-569.

Kuznets, S., & Jenks, E. (1953). Shares of upper income groups in savings. In *Shares*

of upper income groups in income and savings (pp. 171-218). NBER.

Kuznets, S. (1955). Economic Growth and Income Inequality. *The American Economic Review, 45*(1), 1–28. http://www.jstor.org/stable/1811581

Nickell, S. (1981). Biases in dynamic models with fixed effects. *Econometrica: Journal of the econometric society*, 1417-1426.

Nordhaus, W. D. (2006). The economics of hurricanes in the United States. *National Bureau of Economic Research Working Paper Series, n°12813*

Noy, I. (2009). The macroeconomic consequences of disasters. *Journal of Development economics, 88*(2), 221-231.

Pleninger, R. (2022). Impact of natural disasters on the income distribution. *World Development, 157*, 105936. Posner, R. A. (2005). Efficient responses to catastrophic risk. *Chi. J. Int'l L., 6,* 511.

Reaños, M. A. T. (2021). Floods, flood policies and changes in welfare and inequality: Evidence from Germany. *Ecological Economics, 180*, 106879.

Roodman, D. (2009). A note on the theme of too many instruments. *Oxford Bulletin of Economics and statistics, 71*(1), 135-158.

Roodman, D. (2009). How to do xtabond2: An introduction to difference and system GMM in Stata. *The stata journal, 9*(1), 86-136.

Rubin, A., & Segal, D. (2015). The effects of economic growth on income inequality in the US. *Journal of Macroeconomics, 45,* 258-273.

Schumacher, I., & Strobl, E. (2011). Economic development and losses due to natural disasters: The role of hazard exposure. *Ecological Economics, 72,* 97-105.

Skidmore, M., & Toya, H. (2002). Do natural disasters promote long-run growth? *Economic inquiry, 40*(4), 664-687.

Strobl, E. (2011). The economic growth impact of hurricanes: Evidence from US coastal counties. *Review of Economics and Statistics, 93*(2), 575-589.

Toya, H., & Skidmore, M. (2014). Do natural disasters enhance societal trust? *Kyklos, 67*(2), 255-279.

WMO, 2021: Atlas of mortality and economic losses from weather, climate, and water extremes (1970–2019). WMO-1267, 89 pp., `https://library.wmo.int/index.php?lvl=notice_display&id=21930#.YubOcnZBzIU.`

Windmeijer, F. (2005). A finite sample correction for the variance of linear efficient two-step GMM estimators. *Journal of econometrics, 126*(1), 25-51.

Yamamura, E. (2010). Effects of interactions among social capital, income and learning from experiences of natural disasters: A case study from Japan. *Regional Studies, 44*(8), 1019-1032.

Yamamura, E. (2014). Impact of natural disaster on public sector corruption. *Public Choice,*

161(3), 385-405.

Yamamura, E. (2015). The impact of natural disasters on income inequality: analysis using panel data during the period 1970 to 2004. *International Economic Journal, 29*(3), 359-374.

Zylberberg, Y. (2010). Do tropical typhoons smash community ties? Theory and Evidence from Vietnam. ⟨*halshs-00564941*⟩

APPENDIX

A Alternative estimators

Table A.1: Results for regressing income inequality on cyclone intensity: alternative estimators.

	Bottom 60% share of aggregate income (1)	Bottom 40% share of aggregate income (2)	Gini index (3)	First quintile's share of aggregate income (4)	Fifth quintile's share of aggregate income (5)	Top 5% share of aggregate income (6)
Two-step system GMM, using the "collapse" option						
$\overline{Cyc}_{c,t}$	0.006***	0.004***	-0.00006***	0.001***	-0.005**	-0.001
	(0.001)	(0.001)	(0.00002)	(0.0004)	(0.002)	(0.002)
Observations	4795	4795	4795	4795	4795	4795
Number of counties	540	540	540	540	540	540
Number of instruments	28	28	28	28	28	28
Arellano-Bond test for AR(1) in first-differences	0.00	0.00	0.00	0.00	0.00	0.00
Arellano-Bond test for AR(2) in first-differences	0.41	0.72	0.80	0.40	0.77	0.36
Hansen test of overidentifying restrictions	0.05	0.34	0.36	0.41	0.26	0.08
Two-step difference GMM						
$\overline{Cyc}_{c,t}$	0.005***	0.004***	-0.00006***	0.001***	-0.004**	0.001
	(0.001)	(0.001)	(0.00002)	(0.0004)	(0.002)	(0.003)
Observations	4255	4255	4255	4255	4255	4255
Number of counties	540	540	540	540	540	540
Number of instruments	39	39	39	39	39	39
Arellano-Bond test for AR(1) in first-differences	0.00	0.00	0.00	0.00	0.00	0.00
Arellano-Bond test for AR(2) in first-differences	0.88	0.81	0.53	0.85	0.37	0.41
Hansen test of overidentifying restrictions	0.27	0.63	0.45	0.65	0.33	0.25
Static panel data model: fixed effects estimator						
$\overline{Cyc}_{c,t}$	0.003***	0.002***	-0.00003*	0.001***	-0.003	0.001
	(0.001)	(0.0008)	(0.00002)	(0.0004)	(0.002)	(0.002)
Observations	5335	5335	5335	5335	5335	5335
Number of counties	540	540	540	540	540	540
Adjusted R^2	0.04	0.03	0.05	0.03	0.05	0.05

Notes: Standard errors clustered by counties are in parentheses. For the panel fixed effects estimator, we compute robust standard errors. For the difference and system GMM, standard errors incorporate the Windmeijer (2005) correction. Time fixed effects are included in all specifications, but not reported in the table.

Significance levels : *** 1% ; ** 5% ; * 10%.

B Alternative cyclone metrics

Table B.1: Results for regressing income inequality on cyclone intensity: alternative cyclone metrics.

	Bottom 60% share of aggregate income (1)	Bottom 40% share of aggregate income (2)	Gini index (3)	First quintile's share of aggregate income (4)	Fifth quintile's share of aggregate income (5)	Top 5% share of aggregate income (6)
% *Population exposed*$_{c,t}$	0.150***	0.106***	-0.002***	0.038***	-0.158**	-0.028
	(0.048)	(0.032)	(0.001)	(0.015)	(0.070)	(0.082)
Observations	4795	4795	4795	4795	4795	4795
Number of counties	540	540	540	540	540	540
Number of instruments	57	57	57	57	57	57
Arellano-Bond test for AR(1) in first-differences	0.00	0.00	0.00	0.00	0.00	0.00
Arellano-Bond test for AR(2) in first-differences	0.89	0.97	0.38	0.29	0.37	0.34
Hansen test of overidentifying restrictions	0.42	0.74	0.27	0.51	0.09	0.02
$\overline{Cyc}_{c,t}$ without monthly weight	0.002***	0.002***	-0.00002**	0.0006***	-0.002*	0.0004
	(0.0006)	(0.0004)	(9.61e-06)	(0.0002)	(0.0009)	(0.001)
Observations	4795	4795	4795	4795	4795	4795
Number of counties	540	540	540	540	540	540
Number of instruments	57	57	57	57	57	57
Arellano-Bond test for AR(1) in first-differences	0.00	0.00	0.00	0.00	0.00	0.00
Arellano-Bond test for AR(2) in first-differences	0.72	0.94	0.50	0.33	0.48	0.39
Hansen test of overidentifying restrictions	0.69	0.90	0.50	0.68	0.23	0.10
$\overline{Wind}_{c,t}$	0.002***	0.001***	-0.00002**	0.0004***	-0.001	0.0009
	(0.0005)	(0.0003)	(7.79e-06)	(0.0001)	(0.0007)	(0.0008)
Observations	4795	4795	4795	4795	4795	4795
Number of counties	540	540	540	540	540	540
Number of instruments	57	57	57	57	57	57
Arellano-Bond test for AR(1) in first-differences	0.00	0.00	0.00	0.00	0.00	0.00
Arellano-Bond test for AR(2) in first-differences	0.54	0.81	0.63	0.43	0.58	0.47
Hansen test of overidentifying restrictions	0.51	0.81	0.57	0.41	0.24	0.33

Notes: All regressions are two-step system GMM. Standard errors clustered by counties and incorporating the Windmeijer (2005) correction are in parentheses. Time fixed effects are included in all specifications, but not reported in the table.
Significance levels : *** 1% ; ** 5% ; * 10%.

C Additional controls

In these complementary estimations, a distinction is made between meteorological controls and economic controls. Meteorological controls refer to the average annual temperatures (measured in °Celsius), and total annual precipitation levels (measured in mm). Data were obtained from the *Climatic Research Unit gridded Time Series* database (CRU TS v4.05; Harris & al., 2020), which provides monthly estimates derived from land-based weather station observations for the period 1901 to 2019. However, CRU TS data are recorded at 0.5° latitude x 0.5° longitude resolution, which makes us unable to match them to all the sample counties. For the same reasons as those listed for our cyclone intensity measurement, these local climatic variables are considered as not strictly exogenous in the estimation. Then, economic controls correspond to income per capita growth (measured in constant 2019 dollars) and the logarithm of the share of poor households. These data come from the ACS (1-year estimates) and are plausibly endogenous. Accordingly, we use these control variables' lagged values. Households with total income in the last 12 months below an appropriate poverty threshold are classified as poor, and poverty threshold are defined as in section 2.

Table C.1: Results for regressing income inequality on cyclone intensity: additional controls.

	Bottom 60% share of aggregate income	Bottom 40% share of aggregate income	Gini index	First quintile's share of aggregate income	Fifth quintile's share of aggregate income	Top 5% share of aggregate income
	(1)	(2)	(3)	(4)	(5)	(6)
Meteorological controls						
$\overline{Cyc}_{c,t}$	0.005**	0.003**	-0.00006*	0.0009	-0.005	0.001
	(0.002)	(0.001)	(0.001)	(0.0006)	(0.003)	(0.004)
$Precipitation_{c,t}$	-0.0002	-0.0001	2.91e-06	0.00005	0.0002	0.00003
	(0.0002)	(0.0001)	(3.66e-06)	(0.020)	(0.0003)	(0.004)
$\overline{Temp}_{c,t}$	-0.085***	-0.042**	0.001***	-0.015*	0.158***	0.125***
	(0.031)	(0.019)	(0.0004)	(0.008)	(0.040)	(0.036)
Observations	1975	1975	1975	1975	1975	1975
Number of counties	223	223	223	223	223	223
Number of instruments	48	48	48	48	48	48
Arellano-Bond test for AR(1) in first-differences	0.00	0.00	0.00	0.00	0.00	0.00
Arellano-Bond test for AR(2) in first-differences	0.82	0.62	0.82	0.59	0.66	0.65
Hansen test of overidentifying restrictions	0.28	0.44	0.70	0.56	0.74	0.82
Economic controls						
$\overline{Cyc}_{c,t}$	0.005***	0.003**	-0.00007**	0.0008	-0.006**	-0.002
	(0.002)	(0.001)	(0.00003)	(0.0006)	(0.003)	(0.003)
$\Delta ln(income\ per\ capita)_{c,t}$	-0.811	-0.386	0.016*	-0.009	1.886**	2.102**
	(0.572)	(0.298)	(0.009)	(0.126)	(0.855)	(1.040)
$ln(share\ of\ poor\ households)_{c,t}$	-0.048	0.007	0.002	0.065	0.203	0.151
	(0.251)	(0.159)	(0.004)	(0.075)	(0.340)	(0.394)
Observations	4255	4255	4255	4255	4255	4255
Number of counties	540	540	540	540	540	540
Number of instruments	44	44	44	44	44	44
Arellano-Bond test for AR(1) in first-differences	0.00	0.00	0.00	0.00	0.00	0.00
Arellano-Bond test for AR(2) in first-differences	0.30	0.71	0.95	0.67	0.68	0.25
Hansen test of overidentifying restrictions	0.46	0.84	0.17	0.30	0.07	0.01

Notes: Both regressions are two-step system GMM with collapsed instruments. Standard errors clustered by counties and incorporating the Windmeijer (2005) correction are in parentheses. Time fixed effects are included in all specifications, but not reported in the table.
Significance levels : *** 1% ; ** 5% ; * 10%.

D Alternative samples

Table D.1: Results for regressing income inequality on cyclone intensity: alternative samples.

	Bottom 60% share of aggregate income (1)	Bottom 40% share of aggregate income (2)	Gini index (3)	First quintile's share of aggregate income (4)	Fifth quintile's share of aggregate income (5)	Top 5% share of aggregate income (6)
Balanced panel						
$\overline{Cyc}_{c,t}$	0.007***	0.004***	-0.00008***	0.001***	-0.007***	-0.002
	(0.002)	(0.001)	(0.00002)	(0.0004)	(0.002)	(0.003)
Observations	4743	4743	4743	4743	4743	4743
Number of counties	527	527	527	527	527	527
Number of instruments	57	57	57	57	57	57
Arellano-Bond test for AR(1) in first-differences	0.00	0.00	0.00	0.00	0.00	0.00
Arellano-Bond test for AR(2) in first-differences	0.99	0.44	0.49	0.18	0.56	0.37
Hansen test of overidentifying restrictions	0.24	0.44	0.31	0.28	0.11	0.06
Panel extended to all counties ever affected between 1950 and 2019						
$\overline{Cyc}_{c,t}$	0.006***	0.004***	-0.00006***	0.001***	-0.005**	-0.0003
	(0.002)	(0.0009)	(0.00002)	(0.0004)	(0.002)	(0.002)
Observations	5571	5571	5571	5571	5571	5571
Number of counties	627	627	627	627	627	627
Number of instruments	57	57	57	57	57	57
Arellano-Bond test for AR(1) in first-differences	0.00	0.00	0.00	0.00	0.00	0.00
Arellano-Bond test for AR(2) in first-differences	0.83	0.91	0.46	0.40	0.51	0.39
Hansen test of overidentifying restrictions	0.24	0.63	0.25	0.37	0.08	0.06
Panel extended to all U.S. counties						
$\overline{Cyc}_{c,t}$	0.004***	0.003***	-0.00005**	0.001**	-0.003	0.001
	(0.001)	(0.001)	(0.00002)	(0.0005)	(0.002)	(0.002)
Observations	7328	7328	7328	7328	7328	7328
Number of counties	827	827	827	827	827	827
Number of instruments	57	57	57	57	57	57
Arellano-Bond test for AR(1) in first-differences	0.00	0.00	0.00	0.00	0.00	0.00
Arellano-Bond test for AR(2) in first-differences	0.22	0.63	0.65	0.24	0.34	0.82
Hansen test of overidentifying restrictions	0.12	0.35	0.52	0.17	0.17	0.04

Notes: All regressions are two-step system GMM. Standard errors clustered by counties and incorporating the Windmeijer (2005) correction are in parentheses. Time fixed effects are included in all specifications, but not reported in the table.
Significance levels : *** 1% ; ** 5% ; * 10%.